Durham University

Durham E-Theses

A petrographic, structural and geochemical study of the alkaline igneous rocks of the motzfeldt centre, south Greenland

Colin Bradshaw

How to cite:

Bradshaw, Colin (1988) A petrographic, structural and geochemical study of the alkaline igneous rocks of the motzfeldt centre, south Greenland. Doctoral thesis, Durham University.

Use policy

The full-text may be used and/or reproduced, and given to third parties in any format or medium, without prior permission or charge, for personal research or study, educational, or not-for-profit purposes provided that:

- a full bibliographic reference is made to the original source
- a https://etheses.durham.ac.uk/id/eprint/6446/ is made to the metadata record in Durham E-Theses
- the full-text is not changed in any way

The full-text must not be sold in any format or medium without the formal permission of the copyright holders.

Please consult the full Durham E-Theses policy for further details.

Academic Support Office, The Palatine Centre, Durham University, Stockton Road, Durham, DH1 3LE
e-mail: e-theses.admin@durham.ac.uk Tel: +44 0191 334 6107
https://etheses.durham.ac.uk

A Petrographic, Structural and Geochemical Study of the Alkaline Igneous Rocks of the Motzfeldt Centre, South Greenland.

by

Colin Bradshaw. BSc (Hons). FGS.

The Graduate Society

The copyright of this thesis rests with the author. No quotation from it should be published without his prior written consent and information derived from it should be acknowledged.

Thesis submitted for the degree of Doctor of Philosophy at the Department of Geological Sciences, University of Durham.

1988

- 4 OCT 1989

Abstract

The Motzfeldt Centre (1310 +/- 31 MY) is one of four Gardar alkaline igneous Centres belonging to the Igaliko Nepheline syenite Complex, South Greenland. Motzfeldt is a multiphase, high-level intrusive ring-centre comprised principally of nepheline syenite and emplaced in the Proterozoic Julianehåb granite and the overlying Gardar volcano-sedimentary succession.

The Centre commenced with the intrusion of three poorly centralised satellitic intrusions of syenite, pulaskite and nepheline syenite, collectively known as the Geologfjeld Formation. These are partly truncated by concentric, multiple intrusions comprising the Motzfeldt Ring Series whose steep-sided contacts dip outwards and individual nepheline syenite units young inwards. On the basis of field relations, petrography and geochemistry the Ring Series is further subdivided into the Motzfeldt Sø and Flinks Dal Formations, and a number of minor intrusions collectively termed the Hypabyssal Series. The results of field surveys, carried out during two summer field seasons, are presented on a 1:50,000 geological map. The petrography and field relations are described for 16 distinct, plutonic and hypabyssal rock units which range in lithology from larvikite to lujavrite. These represent at least 10 separate intrusive episodes and show a remarkable array of rock textures, mineralogical and geochemical features.

170 whole-rock (XRF), 33 Rare earth element (INAA) and over 300 mineral (EDS) geochemical analyses are presented. These show that the syenite/nepheline syenite lithologies in Motzfeldt can be subdivided chemically and mineralogically into the three groups: 'hypoalkaline', alkaline and peralkaline. The geochemical features of the various units are evaluated and elemental behaviour discussed. The data is additionally assessed, using non-parametric statistics, as a means of discriminating between the units. A number of units which have proved difficult to separate in the field are established to be geochemically distinct, whilst others are shown to be very closely associated. The peralkaline, pegmatite rich, silica saturated outer and upper margins of the Motzfeldt Sø Formation and its associated microsyenite sheet sequences, host extensive economic reserves of Nb, Ta, Zr, U, Th and LREE. The evolution of these mineralised zones is discussed and the importance of country rock (+ water) — magma interaction emphasised.

Recent works have helped clarify the magmatic development of the Gardar Province. Here emphasis has been placed on the structural evolution of the Gardar with the aim of complementing these works. The Gardar represents a prolonged (c.200 MY), cyclic period of limited, passive intracontinental extension. Crustal thinning facilitated the rise, along deep fracture zones, of magmas generated by higher thermal gradients. In response to regional, sinistral shear stresses, ENE extensional fractures and associated dyking developed. In addition, crustal decoupling occurred along several parallel WNW-ESE sinistral strike-slip faults. Motzfeldt and other ring centres of the Gardar are preferentially located at the intersections of these zones of weakness.

Contents

Title Page i
Abstract ii
Contents iii
List of Figures and Tables viii
List of Plates xi
List of Enclosures, Declaration and Copyright xvi
Acknowledgements xvii
Frontispiece xx

PART ONE - INTRODUCTION

Chapter 1 - The Motzfeldt Centre and its geological setting

1.1 Geographical location 1
1.2 Topography and climate 1
1.3 Geological setting 2
1.3.1 The Archean Gneiss Complex 2
1.3.2 The Ketilidian Basement 3
1.3.3 The Gardar Period 3
i. Eriksfjord Formation 4
ii. Gardar Dykes 4
iii. Central Complexes 5
iv. Gardar chronology 6
v. Structure of the province 6

Chapter 2 The Project

2.1 History of Previous Research 8
2.2 Current Research 9
2.3 Fieldwork and aims of the Project 10

PART TWO - THE ROCK UNITS

Chapter 3 - Introduction to the Rock Units and Country Rock

3.1 Geological summary, from previous studies 11
3.2 Revised geological nomenclature 12
3.3 Classification of Motzfeldt rock types 13
3.4 Mineralogical features 15
3.4.1 Introduction 15
3.4.2 Olivine 15
3.4.3 Pyroxene 16
3.4.4 Amphibole 17
i. The hypoalkaline syenites 18
ii. The alkaline and peralkaline rocks 18
3.4.5 Feldspar and Biotite 19
3.5 The structure and country rock 21
3.5.1 Introduction 21

3.5.2 Country rock 21
3.5.3 Contact relations 22
i. The roof contact 22
ii. The internal contacts 23
3.5.4 Faulting 23

Chapter 4 - The Geologfjeld Formation (GF)

4.1 Introduction 25
4.2 GF-Geologfjeld Syenite 26
4.2.1 Rock character and structure 26
4.2.2 Field observations 26
i. NE Motzfeldt 26
ii. NW Motzfeldt 28
4.2.3 Petrographic features 28
4.3 GF-Pulaskite 30
4.3.1 Rock character and structure 30
4.3.2 Field observations 30
4.3.3 Petrographic features 30
4.4 GF-The Nepheline Syenite 31
4.4.1 Rock character and structure 31
4.4.2 Field observations 31
4.4.3 Petrographic features 31
4.5 Sodalite nepheline syenite 32

Chapter 5 - The Motzfeldt Sø Formation (MSF)

5.1 Introduction 35
5.2 MSF-Marginal arfvedsonite syenite 35
5.2.1 Rock character and structure 35
5.2.2 Field observations 36
i. NE Motzfeldt 36
ii. SE Motzfeldt 37
iii. NW Motzfeldt 38
iv. SW Motzfeldt 38
5.2.3 Petrographic features 38
5.3 MSF-Altered syenite 40
5.3.1 Rock character and structure 40
5.3.2 Field observations 41
i. SE Motzfeldt 41
ii. E Motzfeldt 42
iii. NE Motzfeldt 43
iv. C Motzfeldt 43
v. NW Motzfeldt 44
vi. SW Motzfeldt 45
5.3.3 Petrographic features 45
5.4 MSF-Peralkaline Microsyenite Suite 46
5.4.1 Rock character and structure 46
5.4.2 Field relations 46
i. Intrusive relations of NE Motzfeldt 46

ii. Internal sheet and pegmatite segregations 47
iii. Intrusive relations of SE Motzfeldt 48
5.4.3 Petrographic features 48

5.5 MSF-Nepheline syenite 50
5.5.1 Rock character and structure 50
5.5.2 Field observations 51
i. SE Motzfeldt 51
ii. C Motzfeldt 51
iii. S Motzfeldt 53
iv. SW Motzfeldt 53
5.5.3 Petrography 54

Chapter 6 The Flinks Dal Formation (FDF)

6.1 Introduction 56
6.2 FDF-Porphyritic nepheline syenite/microsyenite 56
6.2.1 Rock character and structure 56
6.2.2 Field observations 57
i. SE Motzfeldt 57
ii. S Motzfeldt 58
iii. C Motzfeldt 59
6.2.3 Petrographic features 62

6.3 FDF-Foyaite 65
6.3.1 Rock character and structure 65
6.3.2 Field observations 66
i. SE Motzfeldt (transgessive type) 66
ii. S Motzfeldt (transgressive type) 67
iii. SW Motzfeldt (transgressive type) 67
iv. C Motzfeldt (central type) 68
v. S Motzfeldt (central type) 68
6.3.3 Petrographic features 69
i. Central FDF-Foyaite 69
ii. Transgressive FDF-Foyaite 69

6.4 FDF-Nepheline syenite 70
6.4.1 Rock character and structure 70
6.4.2 Field observations 71
6.4.3 Petrographic features 72

Chapter 7 - The Ring-dykes and Sheet-intrusions

7.1 Introduction 73
7.2 Laminated alkali syenite 73
7.2.1 Rock structure and character 73
7.2.2 Petrographic features 74

7.3 Laminated porphyritic syenite 76
7.3.1 Rock character and structure 76
7.3.2 Field observations 78
i. SE Motzfeldt 78
ii. NE Motzfeldt 78

7.3.3 Petrographic features 80

7.4 Poikilitic arfvedsonite microsyenite 81
7.4.1 Rock character and structure 81
7.4.2 Petrographic features 82

7.5 Other minor-intrusions 82
7.5.1 Introduction 82
7.5.2 Larvikite ring-dyke 83
7.5.3 Lujavrite 83

PART THREE - GEOCHEMISTRY AND EVOLUTION

Chapter 8 - Geochemistry and Mineralisation

8.1 Geochemical features 85
8.1.1 Introduction 85
8.1.2 Geochemical range and overall characteristics 86
8.1.3 The nepheline syenites 89
i. Introduction 89
ii. Geochemical variation between the Formations 91
8.1.4 The syenites 93
i. Introduction 93
ii. GF-Geologfjeld syenite vs. GF-Pulaskite 93
iii. Laminated porphyritic vs. Poikilitic arfvedsonite syenites 94
iv. Laminated alkali syenite vs. Laminated porphyritic syenite 95
v. Laminated porphyritic syenite vs. MSF-Marginal syenite 96
8.1.5 Rare-earth elements 98

8.2 Economic mineralisation 102
8.2.1 Introduction 102
8.2.2 Distribution of the mineralisation 102
8.2.3 Evolution of the mineralised zones 103

Chapter 9 - Tectonic and Magmatic evolution

9.1 Tectonic control 109
9.1.1 Introduction 109
9.1.2 Lineaments 109
9.1.3 Gardar rifting 110
9.1.4 Continental tectonic setting 112
9.2 Magmatic development 115

PART FOUR - CONCLUSIONS

Chapter 10 - Concluding Remarks

10.1 Introduction 119
10.2 Field interpretation 119
10.2.1 New nomenclature 120
10.2.2 The Geologfjeld Formation 120
10.2.3 The Motzfeldt Sø Formation 121
10.2.4 The Flinks Dal Formation 122

10.2.5 The Hypabyssal Series 124
10.3 Mineralogical and Geochemical conclusions 125
10.3.1 Mineralogy 125
10.3.2 Geochemistry 127
10.3.3 Economic mineralisation 129
10.4 Structure and faulting 130
10.5 Geological summary and chronology 131

APPENDIX ONE - PUBLISHED WORK AND OTHER PROJECTS

1.1 Publications 135
1.1.1 Uranium exploration in South Greenland. 135
1.1.2 Geological and radiometric mapping of the Motzfeldt Centre, South Greenland. 143
1.1.3 Geological and radiometric mapping of the Igaliko Complex, South Greenland. 144
1.1.4 New extensive Th-Zr-NB-REE mineralisation in the Motzfeldt Centre, South Greenland as outlined by airborne gamma-spectrometric survey. 145
1.1.5 The alkaline rocks of the Motzfeldt Centre; progress report on the 1984 field season. 150
1.2 Additional Projects 153
1.2.1 Paul Nicholson 153
1.2.2 Joan Nichols 155

APPENDIX TWO - FIELD INFORMATION

2.1 Members of the SYDURAN 1982 expedition 158
2.2 Members of the PYROCHLORE 1984 expedition 159
2.3 Field statistics 160
2.3.1 Field work accomplished 160
2.3.2 Camp site information 161
2.4 The Motzfeldt samples; facts and figures 163
2.4.1 Sample quantity, variation and usage 163
2.4.2 lithological coding 164
2.4.3 Sample locations and distribution 164

APPENDIX THREE - WHOLE ROCK GEOCHEMISTRY

3.1 X-ray fluorescence spectroscopy 165
3.1.1 Sample preparation 165
3.1.2 Operating conditions 167
a. Major elements 167
b. Trace elements 168
3.1.3 Notes on the geochemical tables 169

APPENDIX FOUR - MINERAL GEOCHEMISTRY

4.1 Electron-probe microanalysis 170
4.1.1 Preparation and operating conditions 170
4.1.2 Mineral calculations 171
4.1.3 Notes on the microprobe tables 173

REFERENCES 174

List of Figures and Tables

Fig 1.2.1 Motzfeldt regional divisions

Fig 1.3.1 Gardar geology

Fig 1.3.2 Gardar chronology

a. Chronological scheme for the Gardar Province b. Distribution of Garar ages

---

Fig 2.3.1 Camp site locations

a. Camp locations of earlier surveys b. C. Bradshaw camp locations

---

Fig 3.2.1 New Motzfeldt nomenclature

Table 3.2.2 Guide to symbols used throughout this thesis

Fig 3.3.1 Alkalis vs Silica Plot - all units

a. (Na_2O+K_2O) / SiO_2 - plot (all units) b. Nomeclature from Cox et. al. (1979)

Fig 3.3.2 Alkalis vs Silica Plot - Formations, a. to d.

Table 3.3.3 Motzfeldt Classification Table

Fig 3.3.4 Silica saturation vs peralkalinity plot

Table 3.3.5 Nepheline syenite distinguishing features

Fig 3.4.1 Pyroxene trends (Ca - Fe^2+Mn - Na), all units

a. all units b. Nomenclature c. Formation trends d. Comparitive trends

Fig 3.4.2 Pyroxene trends (Ca - Fe^2+Mn - Na), Formations. a. to d.

Fig 3.4.3 Pyroxenes Element / (Na-Mg), all units

a. Fe^2 b. Mn c. Fe^3 d. Ti

Fig 3.4.4 Pyroxenes Element / (Na-Mg), all units

a. Si b. Al c. Ca d. Zr

Fig 3.4.5 Amphibole classification tables (all units), a. to c.

Fig 3.4.6 Amphibole trends, (Mg - Ca - Na), Formations. a. to d.

Table 3.4.7 Amphibole characteristics

Table 3.4.8 Typical Motzfeldt Amphiboles

Table 8.1.1 Motzfeldt geochemical range

Table 8.1.2 Geochemical changes between alkaline groups

Fig 8.1.3 Hypoalkaline vs Alkaline vs Peralkaline

a. Saturated b. Undersaturated

Table 8.1.4 Geochemical correlation - fresh rocks

Table 8.1.5 Geochemical correlation - altered rocks

Fig 8.1.6 Element vs Peralkalinity Index (PI)

a. MgO b. TiO_2 c. P_2O_5

Fig 8.1.7 Element vs Peralkalinity Index (PI)

a. CaO b. Ba c. Sr

Fig 8.1.8 Element vs Peralkalinity Index (PI)

a. Y b. Fe_2O_3T c. MnO

Fig 8.1.9 Element vs Peralkalinity Index (PI)

a. Na_2O b. Al_2O_3 c. K_2O

Fig 8.1.10 Element vs Peralkalinity Index (PI)

a. SiO_2 b. Pb c. Zn

Fig 8.1.11 Element vs Peralkalinity Index (PI)

a. Rb b. U c. Th

Fig 8.1.12 Element vs Peralkalinity Index (PI)

a. Nb b. Zr c. La

Table 8.1.13 Incompatible element comparisons

Fig 8.1.14 Incompatible element spidergrams

a. GF-Nepheline syenite, MSF-Nepheline syenite, FDF-Porph. nepheline syenite

b. S Qôroq, N Qôroq, Khibina

Fig 8.1.15 Incompatible element spidergrams

a. Lovozero, Ilimaussaq

b. Motzfeldt - Hypoalkaline, alkaline, peralkaline (mean values from Table 8.1.2)

Table 8.1.16 The Motzfeldt-Nepheline syenite

a. Majors, traces and CIPW norms b. Rare earth elements c. Mean $\sum$Trace element contents of the rock units

Fig 8.1.17 Geochemical range - nepheline syenites

Fig 8.1.18 Pie diagrams (trace elements) of the various nepheline syenite units

Fig 8.1.19 Nepheline syenite - discrimination plots

a. Ba/Rb vs K/Rb FDF-Foyaites (transgressive & central) b. Zr/La vs Zr for MSF and FDF nepheline syenites

Fig 8.1.20 Syenites - comparison plots

a. Geologfjeld Formation normalised against Laminated alkali syenite

b. Laminated porphyritic syenite and poikilitic arfvedsonite microsyenite normalised against Laminated alkali syenite

Fig 8.1.21 Geologfjeld Formation - geochemical trends

a. Zr vs K/Rb b. Ba v K/Rb

Fig 8.1.22 Hypabyssal Series - discrimination plots

a. Zr vs Nb b. Ba/Rb vs Pb/Sr

Fig 8.1.23 Peralkaline syenite - discrimination plots

a. Zr vs Ba b. Ca/Ba vs PI (all units)
Fig 8.1.24 REE spidergrams (chondrite normalised)
a. Geologfjeld Formation b. Motzfeldt Sø Formation
Fig 8.1.25 REE spidergrams (chondrite normalised)
a. Flinks Dal Formation b. Hypabyssal Series
Fig 8.1.26 REE spidergrams (Rock and chondrite normalised)
a. Mineral/rock plots b. Mineralised and fresh rocks compared (chondrite)
Fig 8.1.27 Total REE - Motzfeldt range

Fig 8.2.1 Distribution of the Mineralisation - Th radiometric grid map
Fig 8.2.2 Distribution of the Mineralisation - $_{e}$U radiometric grid map
Fig 8.2.3 Evolution of the Mineralisation

Fig 9.1.1 The major strike-slip faults of the Gardar Province
Fig 9.1.2 Theoretical wrench faulting in clay
Fig 9.1.3 Extensional tectonic settings

Table 10.5.1 Motzfeldt chronology
Fig 10.5.2 Motzfeldt intrusive sequence
Fig 10.5.3 Motzfeldt intrusive sequence continued.

Tables in Appendicies

Table A2.1 Members of the SYDURAN 1982 expedition
Table A2.2 Members of the PYROCHLORE 1984 expedition
Table A2.3 Field Statistics a. SYDURAN b. PYROCHLORE
Table A2.4 Camp site information - SYDURAN 1982
Table A2.5 Camp site information - PYROCHLORE 1984
Table A2.6 Lithological codes numbers for the Motzfeldt units

Table A3.1 XRF - Operating conditions
Table A3.2 Whole-rock geochemical analysis
Table A3.3 Rare-earth element analysis

Table A4.1 Mineral calculations
Table A4.2 Pyroxene - Electron-micrprobe analysis
Table A4.3 Amphibole - Electron-microprobe analysis
Table A4.4 Feldspar - Electron-micrprobe analysis
Table A4.5 Biotite - Electron-microprobe analysis

List of Plates

Frontispiece

View east over Motzfeldt Sø to the cliffs of SE Motzfeldt.

PART ONE - INTRODUCTION

Plate 1.1 a. View south overlooking the mountains of the Motzfeldt Centre. (NJGP.84.C.01.31).

b. Sketch of the photograph above, showing the regional divisions of the area.

Plate 1.2 a. High summer in "Harry's Dal", S Motzfeldt. (NJGP.84.C.12.10).

b. Camp 13 (alt. 1220 m) becoming engulfed in a blanket of cloud. (CB.84.C.09.24).

Plate 1.3 a. The mountains of SE and E Motzfeldt after recent snowfall. (CB.84.C.10.30).

b. View ENE of the ampitheatre-like ridge surrounding Camp 13 (alt. 1220 m), S Motzfeldt. (CB.84.C.08.22).

Plate 1.4 a. View SE over the area of NE Motzfeldt occupied by the GF-syenites comprising the N Motzfeldt 'satellite'. (CB.82.C.05.24).

b. Lunch stop. The 1700 m. mountains of S Motzfeldt loom in the background (CB.82.C.14.22).

PART TWO - ROCK UNITS AND FIELD RELATIONS

Plate 3.1 a. EF-Quartzite. NE Motzfeldt. Showing cross-bedding and ripple marks. (CB.82.C.06.01).

b. EF-Siltstone. NE Motzfeldt. Probably lacustrine sediment with medium and fine layers. (CB.82.C.06.03).

Plate 3.2 a. Volcanic plug. NE Motzfeldt. (CB.82.C.05.32).

b. EF-Conglometrate. NE Motzfeldt. (CB.82.C.13.02).

Plate 3.3 a. EF-Basalt/agglomerate raft in MSF-Altered syenite E Motzfeldt. The raft is over 400 m in length and 100 m thick. (CB.82.C.05.06).

b. Trachytic raft in FDF-Nepheline syenite. C Motzfeldt. (CB.82.C.09.15).

Plate 3.4 a. View SW across the south end of Motzfeldt Sø . (CB.84.C.07.08).

b. View NE from C Motzfeldt across the glacier Avanardleq to the mountain of Geologfjeld, NE Motzfeldt. (CB.82.C.13.17).

Plate 3.5 a. View north across Motzfeldt Sø to NE Motzfeldt. (CB.84.C.07.10).

b. View NW, showing the northern tip of SE Motzfeldt (foreground), NE and C Motzfeldt (middle) and NW Motzfeldt (background). (CB.82.C.02.04).

Plate 3.6 a. View E along Flinks Dal with the mountains of NE Motzfeldt in the distance. (CHE.62.C.01.37).

b. View north of the area around Camp 2 in SE Motzfeldt. (CB.82.C.01.26).

Plate 3.7 a. The west facing cliffs of SE Motzfeldt. (NJGP.84.C.15.16).

b. Sketch showing the concentric ring structure of the syenite units as seen in the photograph above. (Drawing by Joan Nichols).

Plate 3.8 a. View NW from C Motzfeldt across Qôrqup sermia to NW Motzfeldt and Mellemlandet. (CB.82.C.09.13).

b. View ESE across Qôrqup sermia to the northern tip of C Motzfeldt. (CB.84.C.02.17).

Plate 3.9 a. View west from E Motzfeldt along Sermia qiterdleq and across Motzfeldt Sø . (CB.82.C.04.17).

b. View WNW showing the plateau area of NE Motzfeldt with the Flinks Dal fault zone in the foreground. (CB.82.C.04.10).

Plate 3.10 a. View north showing 'lower Flinks Dal' , SW Motzfeldt (foreground) and C Motzfeldt (west) beyond. (CB.84.C.04.32) & (CB.84.C.04.31).

Plate 3.11 a. Panoramic view of NE and SE Motzfeldt. Viewed from C Motzfeldt.

b. Geological structure of the view above.

Field Plates

Plate 4.2 a. Geologfjeld syenite. NE Motzfeldt (Storeelv). Typical example. (CB.82.C.07.24).

b. Geologfjeld syenite. NW Motzfeldt. Heterogeneous variety from roof zone. (CB.84.C.12.14).

Plate 4.2 a. GF-Geologfjeld syenite. NE Motzfeldt. Strongly 'baked' variety with up to 10% interstitial nepheline. Near MSF contact? (CB.84.C.03.23).

b. GF-Pulaskite (NM1). NE Motzfeldt. Typical example. (CB.82.C.05.17).

Plate 4.3 a. GF-Nepheline syenite (NM2). NE Motzfeldt. Typical variety, showing characteristic pegmatitic segregations. (CB.82.C.10.11).

b. GF-Nepheline syenite (NM2). NE Motzfeldt. Close up showing similar modal mineralogy of the coarse patches and the finer matrix. (CB.83.C.01.20).

Thin section Plates

Plate 4.4 a. GF-Geologfjeld syenite. NE Motzfeldt. (304160). P.L. 9mm.

b. GF-Pulaskite. NE Motzfeldt. (58352) P.L. 5mm.

Plate 4.5 a. GF-Nepheline syenite. NE Motzfeldt. (304055). X.P. 9mm.

b. As above P.L.

Field Plates

Plate 5.1 a. MSF-Marginal syenite (SM1). NE Motzfeldt. Typical red euhedral, 'blocky' feldspars with arfvedsonite matrix. (CB.82.C.05.27).

b. MSF-Marginal syenite (SM1). NE Motzfeldt. Example showing mafic/felsic phase layering. (CB.82.C.05.26).

Plate 5.2 a. MSF-Marginal syenite (SM1). NE Motzfeldt. Example showing mafic rich clot-like segregations. (CB.83.C.10.14).

b. MSF-Altered syenite (SM1). C Motzfeldt (north). Variety showing altered nepheline and fluorite vein. (CB.83.C.01.21).

Plate 5.3 a. MSF-Altered syenite (SM1). NE Motzfeldt. Very altered variety from the 'hot' zone of the unit. Yellow-ochre staining and metallic (Fe-Mn?) coatings are characteristic. (CB.83.C.02.16).

b. MSF-Altered syenite (SM1). NW Motzfeldt. Typical example of the red feldspathic syenite with very coarse pegmatitic patches. (CB.84.C.12.17).

Plate 5.4 a. MSF-Altered syenite (SM1). E Motzfeldt. Massive pegmatite with giant alkali-amphibole crystals. (TT.84.C.01.10).

b. MSF-Altered syenite (SM1). SE Motzfeldt. Sinuously banded pegmatite/microsyenite. (CB.82.C.09.30).

Plate 5.5 a. MSF-Altered syenite/MSF-Nepheline syenite contact. View WNW-ESE of the northern tip of C Motzfeldt. (T.T).

b. GF-Geologfjeld syenite/MSF-Altered syenite contact where viewed WNW-ESE with Qôrqup sermia in the background. (CB.84.C.12.15).

Plate 5.6 a. Peralkaline microsyenite suite. NE Motzfeldt (Storeelv). The whole cliff side is cut by thin microsyenite sheets. (CHE. 82).

b. Peralkaline microsyenite suite. NE Motzfeldt. Closer view of Camp 9 with microsyenite sheets beyond.

Plate 5.7 a. Peralkaline microsyenite. NE Motzfeldt (CB.83.C.01.08).

b. Peralkaline microsyenite. NE Motzfeldt (Storeelv). As above showing variation in texture. (CB.84.C.03.20).

Plate 5.8 a. Peralkaline microsyenite. NE Motzfeldt (Storeelv). Typical porphyritic, banded, mesotypic microsyenite. (CB.82.C.10.32).

b. Peralkaline microsyenite. NE Motzfeldt (Storeelv). Showing the common association of blue equigranular microsyenite net veined by porphyritic microsyenite similar to above.

Plate 5.9 a. MSF-Nepheline syenite (SM1). SE Motzfeldt. Characteristically pale coloured, subhedral granular and containing grey or red nepheline. (CB.82.C.03.17).

b. MSF-Nepheline syenite (SM1). SE Motzfeldt. Example showing the characteristic weathering by granular disintegration. (CB.82.C.03.18).

Plate 5.10 a. MSF-Nepheline syenite (SM1). SE Motzfeldt. Very coarse pegmatite. (CB.82.C.01.18).

b. MSF-Nepheline syenite (SM1). SE Motzfeldt. Massive pegmatite vein (running diagonally across picture). (CB.84.C.06.23).

Thin section plates

Plate 5.11 a. MSF-Marginal arfvedsonite syenite. NE Motzfeldt. (304052). X.P. 5mm.

b. As above P.L.

Plate 5.12 a. MSF-Altered syenite. NE Motzfeldt. (304053). P.L. 9mm.

b. MSF-Altered syenite. NE Motzfeldt. (297652). P.L. 5mm.

Plate 5.13 a. PMS-Peralkaline microsyenite. NE Motzfeldt. (304120). X.P. 5mm.

b. As above. P.L.

Plate 5.14 a. PMS-Peralkaline microsyenite. NE Motzfeldt. (304185). X.P. 5mm.

b. As above. P.L.

Plate 5.15 a. MSF-Nepheline syenite. SE Motzfeldt. (304003). X.P. 9mm.

b. As above P.L.

Field Plates

Plate 6.1 a. FDF-Porphyritic nepheline syenite (SM2). SE Motzfeldt. Typical example containing distinctive dark grey porphyry xenoliths. (CB.82.C.03.21).

b. FDF-Porphyritic nepheline microsyenite (SM2). SE Motzfeldt. Example close to the MSF contact and containing angular MSF-Nepheline syenite xenoliths. (CB.82.C.15.33).

Plate 6.2 a. FDF-Porphyritic nepheline microsyenite (SM4). C Motzfeldt, Flinks Dal (east). (CB.84.C.05.27).

b. FDF-Porphyritic nepheline syenite (SM4). C Motzfeldt (north). Example from the contact zone. (CB.82.C.09.07).

Plate 6.3 a. FDF-Porphyritic nepheline microsyenite (SM2). SE Motzfeldt. Intruded by FDF-Foyaite containing xenoliths of coarse MSF-Nepheline syenite. (CB.82.C.02.16).

b. FDF-Foyaite (SM3). SE Motzfeldt. The foyaite clearly intruding MSF-Nepheline syenite. (CB.82.C.02.19).

Plate 6.4 a. FDF-Foyaite (SM3). SE Motzfeldt. Coarse grained foyaite with tabular feldspars, poikilitic amphibole, grey sodalite and red nepheline. (CB.82.C.03.20).

b. FDF-Foyaite (SM4). S Motzfeldt. Showing the characteristic 'framework' of feldspars. (CB.84.C.08.28).

Plate 6.5 a. FDF-Foyaite (SM4). S Motzfeldt ("Harry's Dal"). Enclosed is a xenolith of coarse and blocky MSF- Nepheline syenite. (CB.84.C.11.07).

b. FDF-Foyaite (SM3). SE Motzfeldt. Foyaite showing flow lineation around a MSF-Nepheline syenite xenolith. (CB.84.C.06.10).

Plate 6.6 a. FDF-Foyaite (SM3). SE Motzfeldt. Showing cyclic mafic layering. (CB.82.C.01.05).

b. FDF- Foyaite (SM4). S Motzfeldt. ('The Wall'). Similar development of asymmetric, cyclic phase layering as above. (CB.84.C.08.26).

Plate 6.7 a. FDF-Foyaite (SM4). S Motzfeldt. Large scale benching in the Foyaite, seen in the east facing cliffs of "Harry's Dal". (CB.84.C.10.32).

b. FDF-Foyaite (SM4) C. Motzfeldt (west). The Central Foyaite corresponding to above, N of the Flinks Dal Fault.

Plate 6.8 a. FDF-Nepheline syenite (SM5). C Motzfeldt (Flinks Dal). Typical example. (CB.84.C.05.10).

b. FDF-Nepheline syenite (SM5). C Motzfeldt. (Flinks Dal). Shows partially developed feldspar lamination.

Thin section plates

Plate 6.9 a. FDF-Porphyritic nepheline microsyenite. C Motzfeldt. (304101). X.P. 9mm.

b. As above. P.L.

Plate 6.10 a. FDF-Foyaite. SW Motzfeldt. (326113). X.P. 9mm.

b. As above. SW Motzfeldt. (326114). P.L. 9mm.

Plate 6.11 a. FDF-Nepheline syenite. C Motzfeldt. (272490). X.P. 9 mm.

b. As above P.L.

Field plates

Plate 7.1 a. Laminated alkali syenite. NE Motzfeldt ('Lejr elv'). Example showing poikilitic amphibole and weakly laminated feldspar tablets. (CB.82.C.07.25).

b. West facing cliffs of NE Mozfeldt. Three seperate sheets of Laminated alkali syenite are visible. (CHE 1982).

Plate 7.2 a. Laminated porphyritic syenite. NE Motzfeldt (Storeelv). Strongly porphyritic-seriate variety. (CB.84.C.03.35).

b. Laminated porphyritic syenite. NE Motzfeldt (Storeelv). Densly phyric variety. (CB.84.C.03.24).

Plate 7.3 a. Laminated porphyritic syenite. Intruding lam. alkali syenite. (CB.84.C.10.03).

b. Laminated alkali syenite enclosing blocks of MSF syenite, NE Motzfeldt. (CB.82.C.07.34).

Plate 7.4 a. A dyke of Laminated porphyritic syenite showing flow differentiation and an aphyric margin. NE Motzfeldt ('Lejr elv'). (CB.82.C.08.22).

b. Dykes of Laminated porhyritic syenite cutting pink syenite of the Geologfjeld Formation. NE Motzfeldt (Storeelv). (CB.84.C.03.08).

Plate 7.5 a. Poikilitic arfvedsonite microsyenite. SE Motzfeldt. Sheet cutting red MSF-altered syenite and grey Laminated porphyritic syenite. View W-E (CHE.82.).

b. Poikilitic arfvedsonite microsyenite. SE Motzfeldt. Typical example. (CB.83.C.01.15).

Plate 7.6 a. Larvikite (SM5*). From the ring-dyke in C Motzfeldt (west).

b. Alkali gabbro. C Motzfeldt. From the composite giant dyke.

Thin section plates

Plate 7.7 a. Laminated alkali syenite. NE Motzfeldt. (304097). X.P. 9mm.

b. As above P.L.

Plate 7.8 a. Laminated porphyritic syenite. NE Motzfeldt. (304090). X.P. 9mm.

b. As above. P.L.

Plate 7.9 a. Poikilitic arfvedsonite microsyenite. SE Motzfeldt. (304033). P.L. 5mm.

b. MSF-Marginal syenite. NE Motzfeldt. (304710). P.L. 5mm.

Plate 7.10 a. Larvikite. Ring-dyke. C Motzfeldt (west). (272454). X.P. 9mm.

b. As above P.L.

List of Enclosures

Enc.1

Geological map of the Motzfeldt Centre. 1:50 000 scale

Enc.2

Sample location map 1:50 000. Durham specimens collected by C.H. Emeleus, W.T. Harry, A.P. Jones and C. Bradshaw.

Enc.3

Guide to symbols used throughout this thesis.

Enc.4

Motzfeldt - showing regional divisions and locality names

Declaration

The content of this thesis is the original work of the author (other people's work, where included is acknowledged by reference). It has not been previously submitted for a degree at this or any other university.

Copyright

The copyright of this thesis rests with the author. No quotation from it should be published without his prior written consent and information derived from it should be acknowledged.

Acknowledgements

Preface

This study was made possible by the award of a N.E.R.C./C.A.S.E. Research Studentship, instigated through collaboration between the Greenland Geological Survey (GGU) and Dr C.H. Emeleus of the University of Durham. The work has involved the close co-operation of GGU with the author enjoying two field seasons in Greenland (1982 & 1984) and several working visits to GGU in Copenhagen. In addition several other academic establishments have played key roles in this study and are acknowledged separately below.

University of Durham

Grateful thanks are extended to Dr C.H. Emeleus for his supervision, scientific reasoning and his common sense. Thanks to to Professor J.F. Dewey for making available the facilities in the Geology Department and for his infectious enthusiasm for research. Accumulation of geochemical data has played a large part of this work. In this regard, thanks go to Dr A. Peckett, Dr J.G. Holland and Mr R Hardy their guidance and use of the microprobe, XRF and XRD. Mr P. Laverick (Paul) is gratefully acknowledged for his work in wet geochemical techniques as well as his considerable help in data preparation and processing. Rock thin-sections and microprobe sections were expertly prepared by the 'men downstairs' (workshop), namely; Mr G. Randall and Mr R. Lambert. For photographic work thanks go to Mr J. Nielsen, Mr G. Dresser and Mr A. Carr. I extend my thanks to Mr A Reid of the Drawing Office for his work and instructive advice. Whilst computing I have benefited from the advice of numerous geophysicists for which I express my gratitude. In particular I thank Mr M.J. Smith for his programming skills. Mr G. Ruth is thanked for the use of the microprocessor facilities in G2. My thanks are extended to Mrs L. Mines, Mrs C. Blair and Miss N.E. Bruce for their professional secretarial help. For most of this thesis my handwriting has been converted into the typed form by Miss. N.E. Bruce to whom I am very grateful. My sincere thanks are extended to Mr D. Asbery and Miss G. Whale (Grace) who together play such an integral role in the day to day life of this department. Mr. Asbery has magician-like powers of always being able to help and has never let me down yet. Mr D. Schofield is thanked for his caligraphic skills, as used in some diagrams of this work. Thanks to all past and present in the 'hard rock' lab (Rm. 202), for many useful discussions and good company. I am grateful to all the members of the academic staff who have influenced my geological thinking through discussion and seminars throughout my time at Durham.

Greenland Geological Survey (GGU)

I am indebted to the Director of the Greenland Geological Survey, Dr M. Ghisler for allowing me the facilities and logistic support of GGU. Considerable financial investment has been outlayed during the exploration of the Motzfeldt Centre from which the author has benefited. In particular the superb contoured 1:10,000 orthophoto base maps provided by GGU considerably improved the quality of the field survey and is here acknowledged by the author. Without the co- operation of GGU this research would not have been possible.

In Greenland, logistical support was entirely provided by GGU and members of the SYDURAN and PYROCHLORE teams. GGU provided the field equipment, the excellent food boxes, sample transportation, generous helicopter time and the overall back-up support. Mr J. Lau is gratefully acknowledged for his services as Base camp manager (1982 & 1984) and my gratitude is extended to the helicopter pilots for their courageous and skillful flying.

Special thanks are extended to Mr T. Tukiainen (Tapsa) with whom I have enjoyed particularly close collaboration during this study. Tapsa has provided me with data, maps, diagrams and geochemical plots all proving invaluble to this work. Moreover, the trace element data used in this study have been processed by Tapsa at GGU using the raw counts derived from the Durham XRF machine. This is a very time consuming task, and the author is extremely grateful. In addition, I express my gratitude to Tapsa and his late wife Arja for their kind and generous hospitality during my visits to Copenhagen. Also thanks go to Mrs I. Rytved for her logistic help during the frequent correspondance between Tapsa and myself.

Thanks go to all the members of the 1982 SYDURAN (South-Uranium) expedition led by Dr A. Armour-Brown and Mr T. Tukiainen. During the 1982 field season I worked mainly with Mr J. Ohberg to whom I express my sincere thanks for his help and companionship. Thanks also to Mr A. Pratt and Mr K. Hansen for their temporary assistance in the field.

Thanks are also extended to all members of the 1984 PYROCHLORE expedition led by Dr L.M. Larsen and Mr L. Thorning. The structural chapter of this work has benefited greatly from discussion with Dr A. Armour-Brown and Mr P. Nyergaard.

University of Edinburgh

Thanks are extended to Dr G. Fitton and Mrs D. James who allowed me the facilities and instructed me in the use of the fusion- bead preparation at Edinburgh. They also generously ran the samples and provided me with an excellent set of major element data for which I am very grateful. Discussion with Professor B. Upton and Dr D. Stephenson about the Gardar Province has been very rewarding and I thank them both for their very useful reprints. Thanks go to all mentioned for making my stay at Edinburgh an enjoyable one.

University of Manchester

Thanks go to Mr T. Hopkins and Mr D. Plant for their hospitality, permission and instruction in the use of the Manchester Microbrobe. The data derived from this machine has been used extensively in this study.

Sunderland Polytechnic

Thanks are extended to Mr D. Hall and the students Miss J. Nichols (Joan) and Mr P. Nicholson (Paul).

University of Munich

Thanks are extended to the Professor G. Morteani and Mr B. Kronimus for their hospitality during my visit to Munich. In particular the generous hospitality of Mr B. Kronimus and his wife during my stay is gratefully acknowledged.

University of Berlin

Dr. P. Möller is thanked for providing the REE data on my Motzfeldt samples.

Hancock Museum, Newcastle

Thanks go to the Staff at the Hancock for allowing me use of their computer and other facilities during the latter stages of this work.

Personal

My thanks are extended to my parents for their practical and financial support during this work and to Mr and Mrs Cawthorne for their generous hospitality. Finally I would like to thank Miss G. Cawthorne (Gillie) who has given me invaluable support and encouragement during this work as well as helping enormously with proofing, typing, drawing and countless other vital and time consuming tasks, for which I am most grateful.

FRONTISPIECE.



"The general appearance of the Igaliko batholite mountains differs from that of the Ilimausak batholite. They are higher and steeper. Boldly and precipitously they tower above the sea, and attain to large altitudes, there being, as a rule no beach."

N.V. Ussing 1912.

PART ONE

INTRODUCTION

Chapter 1

The Motzfeldt Centre and its geological setting.

1.1 Geographical location

The Motzfeldt Centre is situated in S Greenland approximately 10 km E from the main airport-town of Narssarssuaq. The Centre outcrops over a roughly oval shaped area of about 255 km^2 (c.20 km E-W x c.15 km N-S) and occupies much of the high, barren, mountainous region between Qôroq and the Inland Ice (Fig 1.2.1).

1.2 Topography and climate.

The mountains of Motzfeldt rise from sea level to a general plateau level of between 1100 and 1500 m with summits reaching 1900 m. The area is deeply dissected by ice eroded valleys, hanging tributary glaciers and at low elevations, wide (2 km) main-valley glaciers that flow westward from the Inland ice. This topography provides an excellent three dimensional view of the structure within the Motzfeldt Centre.

The syenite of the complex is easily distinguished from the surrounding crystalline basement by virtue of its pale-grey or red stained colour, scarcity of vegetation and characteristic development of scree. Unlike the surrounding 'granite' the syenite weathers readily by frost wedging and granular distintergration to form a rather mobile regolith which makes it difficult for plants to become established. Much of the high ground is concealed by a 'blanket' of angular blocks or 'plateau talus', derived from the in situ mechanical weathering of the syenite bedrock. Permanent-snow covers the very high ground and extensive fans of scree conceal the lower slopes of the steep valleys. However, stream gullies, polished roché-moutonées and cliff faces provide good exposures. In addition, many of the huge, precipitous cliff faces (although inaccessible) show remarkably clear geological relationships (Plates 3.4 to 3.11).



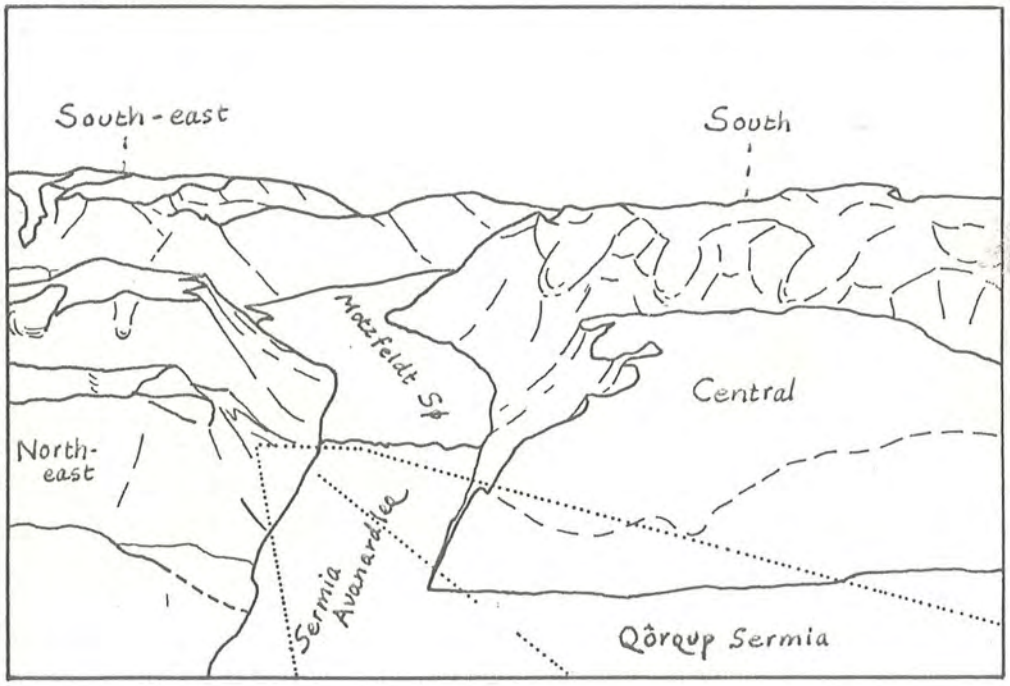
Plate 1.1

a.

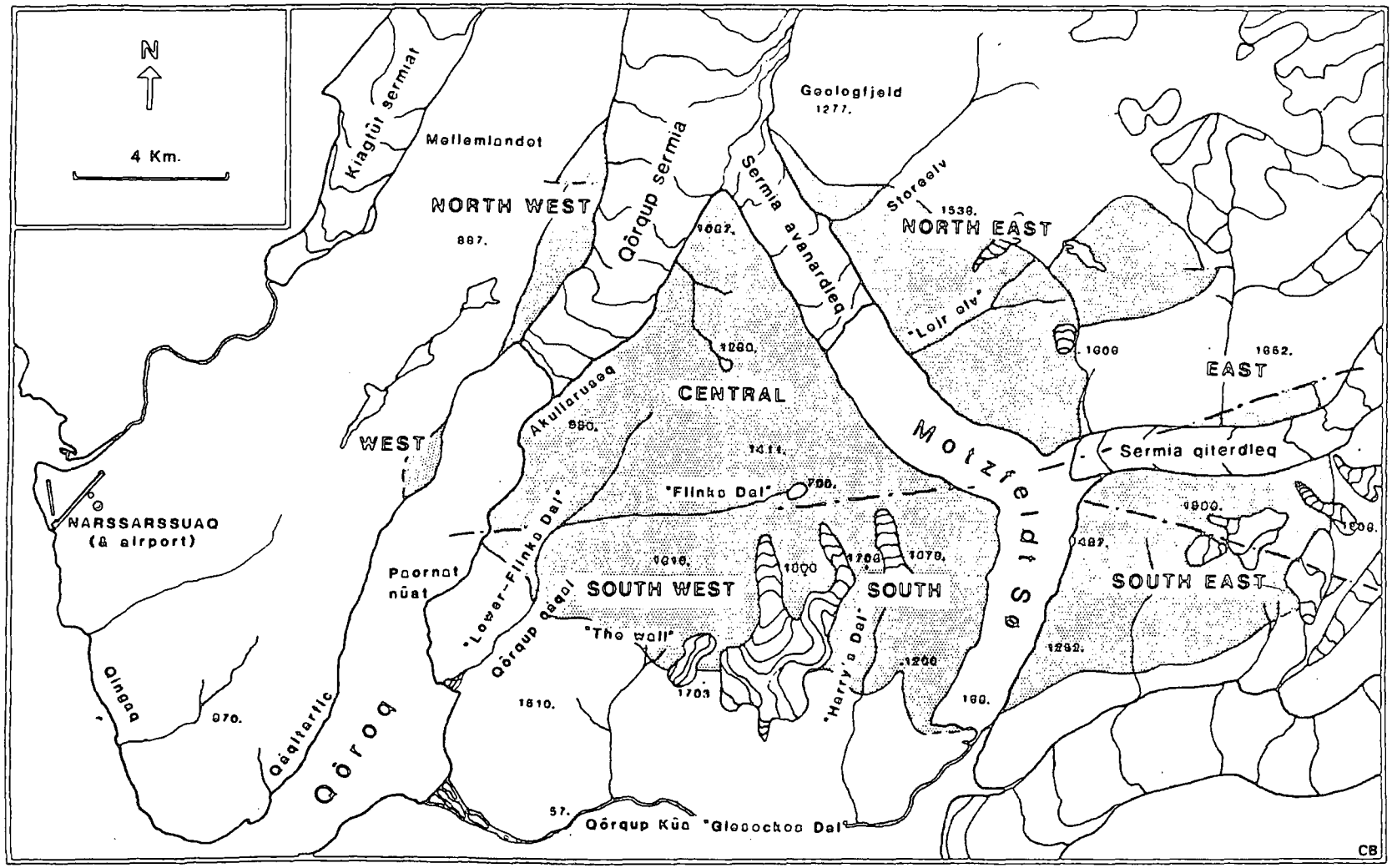


View south overlooking the mountains of the Motzfeldt Centre. Photograph taken from the SAS DC8, June 29th 1984. (NJGP.84.C.01.31).

b.



Sketch of the photograph above, showing the regional divisions of the area. (see also Fig.2).



Topography and regional divisions of the Motzfeldt Centre.

Motzfeldt regional divisions Fig 1.2.1

The 'intrusion' derives its name from the prominent and central (11 km x 3 km) boomerang-shaped ribbon lake, known as Motzfeldt Sø (alt. 168 m). The lake is surrounded by spectacular cliffs and forms the terminus of the glaciers, Sermia Avarndleq and Sermia Qiterdleq. Together they form a natural barrier between the mountains of SE, NE, and C Motzfeldt. Fig 1.2.1, illustrates these and the other main topographical features of Motzfeldt and also introduces the nomenclature ascribed to the natural divisions of the area. This nomenclature will be used throughout the text.

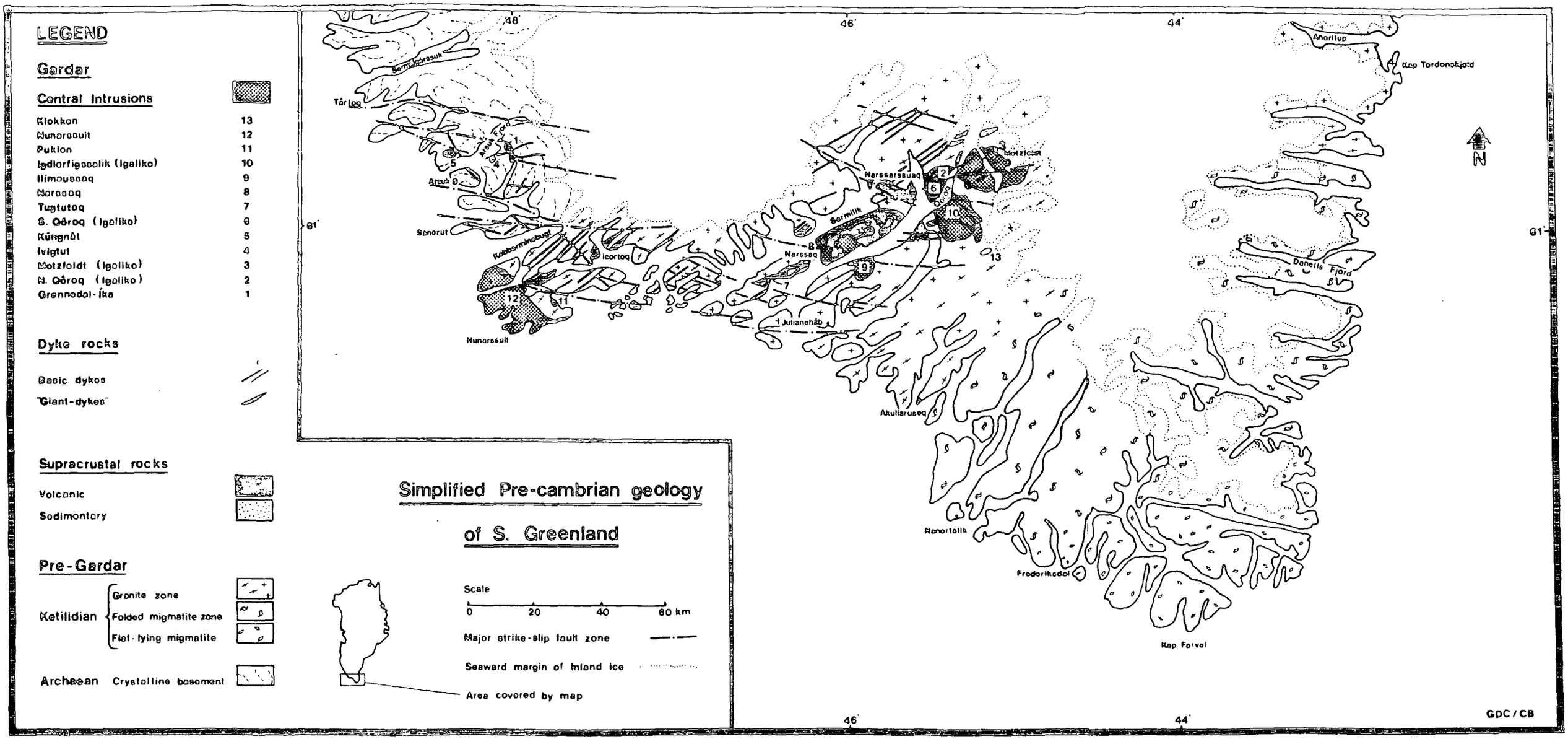
Whilst working on the Centre more than one third of the total time was lost due to the effects of bad weather (Table A2.3, Appendix Two); this was equally divided between periods of rain/snow, fog and violent 'Fohn' winds. The Fohn winds usually followed fine, clear, sunny spells and often had a devastating effect on the field camps. Fog could prove a hinderance at all elevations. Low in the valleys, early morning mist and fog is common. Most serious however, is the thick cloud which frequently mantled and enveloped the plateau level (1100-1500 m), (Plate 1.2b). The cloud could often persist for up to four days and on occasion precipitate deep snow (Plate 1.2a). Mosquitoes and black fly were a great nuisance in the low ground of NW Motzfeldt.

1.3 Geological Setting

The geology of S Greenland may be broadly divided into three parts (Fig 1.3.1) all of Precambrian age; 1) crystalline 'basement' rock of the Archean gneiss complex (c.2500 MY); 2) Proterozoic 'basement' rock comprising the Ketilidian mobile belt (c.1850 - 1400 MY); and 3) lava, sediment and intrusive rock of the Gardar Period (c.1320 - 1120 MY).

1.3.1 The Archean Gneiss Complex

The Archean gneiss complex extends from Itivdleq to Ivigtut on the west coast and from Gyldenløves Fjord to Mogens Heinesen Fjord on the east (Bridgwater et al., 1976). Only in the region between Târtoq, Arsuk and Qôrnoq (GGU Map sheet: Ivigtut 61


LEGEND
Gardar
Central Intrusions
Klokkon 13
Nunarssuit 12
Puklon 11
Igdlerfigaalik (Igaliko) 10
Ilimaussaq 9
Narssaq 8
Tugtutoq 7
S. Qôroq (Igaliko) 6
Kûngnât 5
Ivigtut 4
Motzfeldt (Igaliko) 3
N. Qôroq (Igaliko) 2
Grønnedal-Ika 1
Dyke rocks
Basic dykes
"Giant-dykes"
Supracrustal rocks
Volcanic
Sedimentary
Pre-Gardar
Ketilidian
Granite zone
Folded migmatite zone
Flat-lying migmatite
Archaean Crystalline basement
Simplified Pre-cambrian geology
of S. Greenland
Scale
0 20 40 60 km
Major strike-slip fault zone
Seaward margin of inland ice
Area covered by map
48°
46°
44°
61°
Tårtog
Sammisôrasuk
Arsuk Fjord
Arsuk Ø
Sønerut
Kobbermineburg
Igortoq
Narssaq
Julianehåb
Nunarssuit
Motzfeldt
Narssarssuaq
Qôroq
Ilimaussaq
Kûngnât
Akuliaruseq
Anoritup
Kap Tordenskjold
Danells Fjord
N
Ikinortalik
Frederikhaab
Kap Farvel
GDC/CB

V.1 SYD) is Archean gneiss the exposed basement to Gardar intrusions. These intrusions include the central complexes of Kûngnât, Ivigtut and Grønnedal-Ika and several generations of lamprophyric, basaltic and trachytic dykes. The Archean basement in the area displays complex inverted folding and is interpreted as belonging to a major nappe structure plunging ESE to SE around Arsuk Fjord (Berthelsen & Henriksen, 1975., pp 29-32). The WNW- ESE metamorphic fabric is almost at right angles to that of the adjacent Ketitlidian basement. The Gardar dykes however, cut the Archean/Ketilidian contact without any significant shift in trend.

1.3.2 The Ketilidian Basement

The Ketilidian Mobile Belt occupies the region between Qôrnoq in the west, Ikermit in the east, and Kap Farvel in the south (Allaart, 1976). Within the Mobile belt, four zones are distinguished each approximately 100 km wide and trending SW-NE (Fig 1.3.1). Most of the Gardar intrusions are confined to the central granite zone, which consists of granite-gneiss, granite, diorite and a central belt of late intrusive orogenic granite, adamellite and monzonite. The granite zone is essentially synonymous with Allaart's (1964) extended usage of the much used term 'Julianehåb Granite'. However, because the Ketilidian country rocks encompassing Motzfeldt are of such variable lithology, the term Julianehåb Formation will be used in this study, and is synonymous with Allaart's (1976) Granite Zone.

1.3.3 The Gardar Period

The Gardar lasted from c.1320 to c.1120 MY and is characterised by continental sediment/volcanic sequences, dyke injection and emplacement of predominantly 'salic' alkaline central complexes. During the Gardar Period, S Greenland was contiguous with N America and Northern Europe, forming a vast Proterozoic land mass or 'supercontinent' (Piper, 1982). Much of this land mass was subjected to intracontinental rifting and associated volcanism, but only the Gardar Province accomodates such an extraordinary

variety of alkaline igneous rock types and rare mineral species. Many geologists have been attracted to the area and a number of geological reviews have been published (eg; Upton, 1974 ; Emeleus & Upton, 1976 ; Upton & Emeleus 1987)

i. The Eriksfjord Formation

The early Gardar is represented by a thick (> 3.5 km) interbedded sequence of continental clastic sediments, pyroclastics and lavas, known as the Eriksfjord Formation (Poulsen, 1964). The sequence lies unconformably on rocks of the Julianehåb Formation and accumulated whilst active horst-graben faulting was in progress (Stewart, 1964). The sediments consist largely of medium to fine-grained white to grey or red quartzite, but arkosic and silty varieties do occur. Intercalated with the sediments and constituting approximently 50% of the supracrustal succession are three thick sub-aerial volcanic sequences. These include the Mussartût, Ulukasik and Ilimaussaq (youngest) Volcanic Members (Poulsen, 1964). They comprise predominantly mildly-alkaline olivine basalt and hawaiite, although monchiquitic and carbonatitic varieties have been described (Stewart, 1970). Trachytic flows, although subordinate, do occur higher in the sequence near Ilimaussaq (Stewart, 1964) and with phonolite are common as xenolithic rafts in the syenites of the Motzfeldt Centre (Jones, 1980). It has been noted that successive eruptive sequences in the Eriksfjord Formation show a general tendency to become more evolved with time (Upton & Emeleus, 1987), however the apparent geographical correlation between differentiated lava and later syenitic intrusive centres is of significance (Larsen & Tukiainen, 1985).

ii. The Gardar Dykes

ENE and NE trending dykes abound over most of the Gardar Province. These form several distinct swarms and amount to crustal dilation in excess of 3 km (Upton & Blundell, 1978). Although, the early Mid-Gardar 'brown dykes' (BD0s) trend WNW-ESE, subsequent dykes (BD1 to BD3) shifted anticlockwise toward the dominant Late Gardar SW- NE trend (Berthelsen & Henriksen, 1975). The Gardar dykes are remarkably varied in size, lithology and chemical composition. Basic and intermediate types predominate,

although lamprophyric and carbonatitic varieties are not uncommon. Recent mapping, in fact has shown the latter to be considerably more abundant than previously reported (Pearce, 1988; Upton & Fitton, 1985). Two important dyke varieties in the province include the 'big feldspar' and 'Giant dykes'. The former are characterised by high proportions (up to 80%) of megacrysts or inclusions of plagioclase, anorthosite or gabbroic anorthosite. Detailed accounts of the inclusions by Bridgwater (1967) and Bridgwater and Harry (1968), emphasise the wide distribution of the dykes throughout the Gardar Province and suggest that wide areas are underlain by a substantial layer of anorthositic rock. The 'Giant dykes' (Upton et al., 1985) although invariably containing a gabbroic component can occur as composite gabbro-syenite (and even nepheline syenite) bodies, often with well-developed layered structures. (Upton & Fitton, 1985; Upton et. al. 1985) Commonly, the dykes bifurcate into smaller dolerite dykes, and therefore represent local 'swellings' within the regional ENE swarms of basic dykes (Emeleus & Upton, 1976).

iii. The Central Complexes

Ten central complexes within the Gardar Province embrace nearly 200 MY of igneous activity between c.1320 MY and c.1120 MY. The complexes, with perhaps the exception of Nunarssuit comprise predominantly undersaturated or oversaturated felsic rock types, which include many varieties of nepheline syenite, syenite and granite. They are generally high level, passively emplaced, multiple intrusions that have steep-sided, ring dyke or ring stock form. The individual intrusive units have trangressive internal and external contacts and display a host of layered igneous structures (Upton, 1961; Parsons, 1979; Parsons & Butterfield, 1981; Parsons & Becker, 1987; Sørensen & Larsen, 1987). The Motzfeldt Centre is one of four intrusive ring centres that comprise the Igaliko Nepheline Syenite Complex (Emeleus & Harry, 1970). Associated with this Centre and with many of the other Central complexes are smaller satellitic stocks, late partial ring dykes (often gabbroic) and hypabyssal sheet intrusions. It seems reasonable to assume that many of the central complexes are of subvolcanic type. The Motzfeldt Centre in particular has

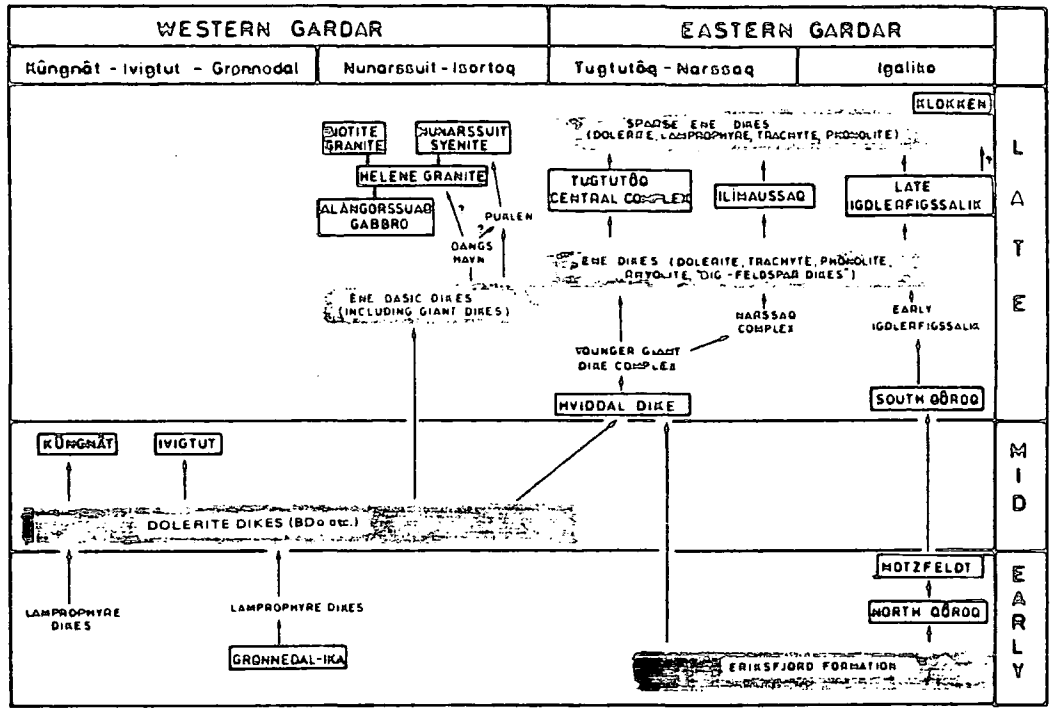
an exposed sequence of high-level plutonic, hypabyssal and volcanic rock types which together represent a full igneous cycle.

iv. Gardar chronology

The chronology of the Gardar Period has been well documented by Blaxland et al., 1978 and is summarised in this work in Figs 1.3.2a and 1.3.2b (both from Blaxland et al., op.cit.) Field relationship data between the dykes, central complexes and the supracrustal succession together with Rb-Sr isochron age data have been used as the basis of a threefold chronological division into Early, Mid and Late Gardar times (Blaxland et al., 1978; Upton & Blundell, 1978). In a recent review by Upton and Emeleus (1987) the authors have confirmed the cyclic nature of the Gardar igneous activity. They suggest that each division corresponded to a single cycle of activity which commenced with a large scale uprise of basic magma during phases of crustal attenuation. This magma gave rise to the plateau-type lavas and major dyke swarms. Each cycle terminated during decreasing tensional stresses with the emplacement of the central complexes (Upton & Blundell, 1978). Although there are three main cycles, the central complex emplacement culminated in two main phases, one at c.1290 MY (Early Gardar) and the other at c.1150 MY (Late Gardar), (Fig 1.3.2a). This distribution is also shown by the four intrusive ring centres that comprise the Igaliko nepheline Syenite Complex (Emeleus & Harry, 1970). The early centres of Motzfeldt and N Qôroq are very similar in composition (augite syenite - nepheline syenite) to the later Centres of S Qôroq and Igdlerfigssalik despite the 120 MY age gap. It is remarkable that all of the centres were emplaced at a very similar structural level in the crust despite their considerable age differences.

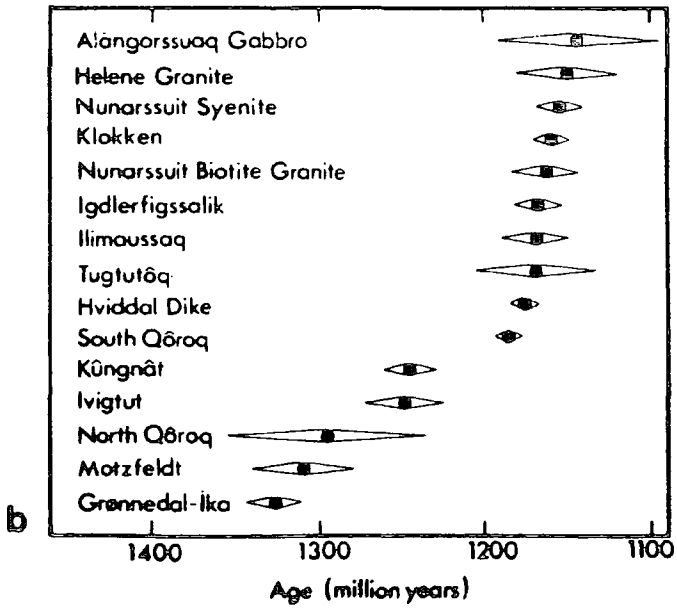
v. Structure of the Province

The Gardar Period was characterised by intense and prolonged faulting, which has played a major role in controlling sedimentation and magmatic activity (see also Chapter 9). The Province is cut by major, roughly parallel, WNW-ESE sinistral strike-slip faults



Chronological scheme for the Gardar Province.

The arrow indicates that the top event is known to be younger than the bottom event on field or isotopic evidence. a box indicates a Rb–Sr isochron age (after Blaxland et. al., 1978).



Distribution of Gardar ages. Errors are indicated at 2σ level (from Blaxland et. al., 1978).

(Fig 9.1.1). These are associated with a subordinate conjugate set trending NW and NE which have minor dextral offsets.

Although, igneous rocks of the Gardar Province are found across the whole of S Greenland (Bridgewater & Gormsen, 1969) most of the dykes and central complexes are found concentrated about two ENE trending axial regions, namely the Nunarssuit - Isortoq zone and the Tugtutôq - Ilimaussaq zone (Fig 1.3.1). Geophysical measurements have also shown the Tugtutôq - Ilimaussaq zone to be associated with a gravity 'high' of 300 *gu* amplitude, 30 km wide and elongated ENE-WSW (Blundell, 1978). This Blundell interpreted as an underlying basic mass, some 50 km long and 35 km wide, lying from 3 to 5 km below the surface to at least 10 km depth. This structure is comparable with the axial 'highs' associated with other continental rift systems and was suggested by Upton and Blundell (1978) to be analogous with the deep portions of the Southern Kenya rift. The Gardar dykes within each axial zone show distinct compositional differences (Upton & Emeleus, 1987). Although, both contain giant dykes and associated salic differentiates, the Tugtutôq - Ilimaussaq zone has a far higher proportion of dykes of intermediate composition. Moreover, the basic dykes of this zone have consistantly higher contents of Ba, Sr, LREE and Nb than basic dykes of the Nunarssuit - Isotoq zone (Upton & Emeleus, op. cit.). This divided chemistry is probably a manifestation of the different sub-surface crustal structure below each zone, as depicted by the gravity survey of Blundell, 1978. Elsewhere in the Province, trachytic and phonolitic dykes occur in local SW-NE swarms, especially in the regions adjacent to the major central complexes (eg; Grønnedal-Ika & Igaliko). The central complexes are significantly located most frequently where the ENE 'axial' zones are intersected by the WNW-ESE strike-slip faults. Although the latest fault movement is taken up by the strike slip structures, the evidence suggests that movement has taken place repeatedly along these faults throughout Gardar time (Henriksen, 1960; Stephenson, 1976a). The fault system therefore must play a fundemental role in controlling the distribution and development of the Gardar igneous activity (see Chapter 9).

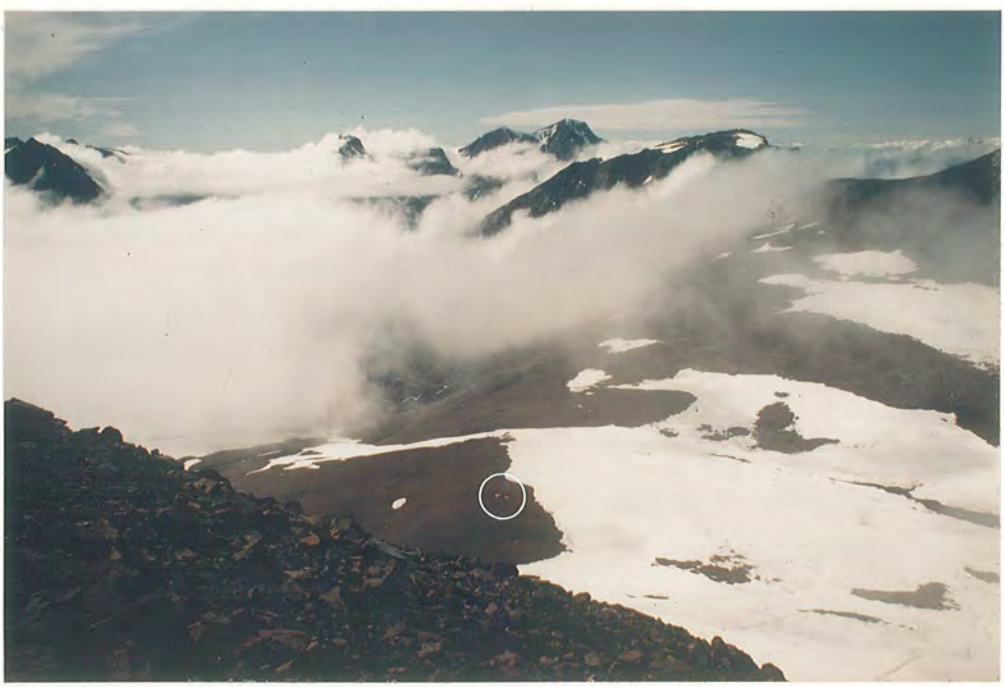
Plate 1.2

a.



High summer in "Harry's Dal", S Motzfeldt. Temporary snow can be a great hinderance to geological work. View north, with Camp 14 (alt. 1162 m) in the foreground. (NJGP.84.C.12.10).

b.



Camp 13 (alt. 1220 m) becoming engulfed in a blanket of cloud. In the background the 1700 m peaks of Igdlerfígssalik stand above the cloud level. (CB.84.C.09.24).

Plate 1.3

a.

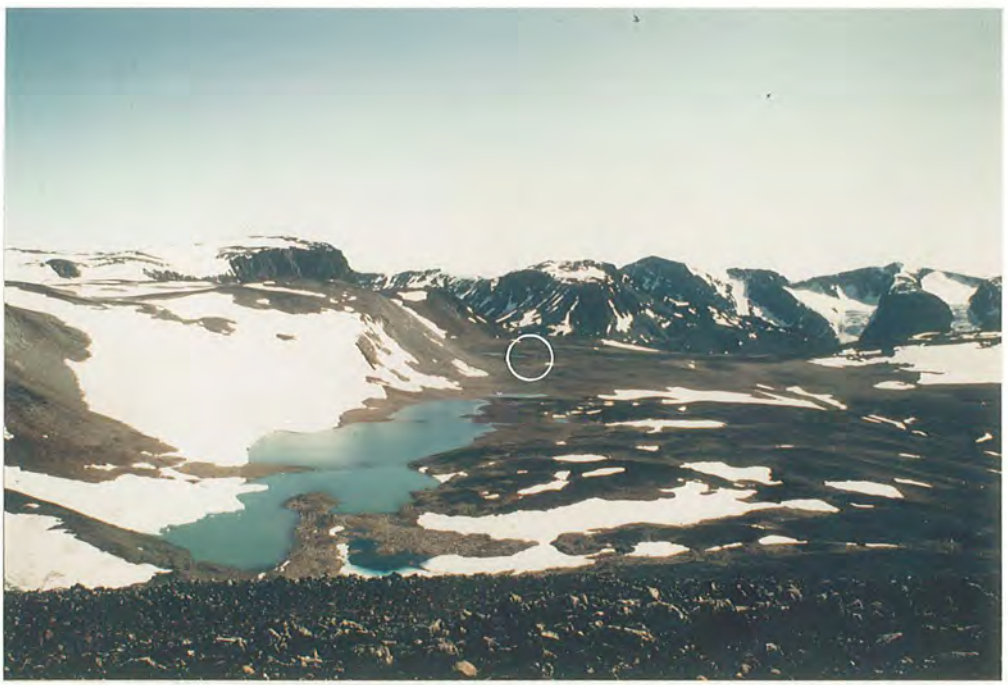


The mountains of SE and E Motzfeldt after recent snowfall. The snow line is at c.800 m altitude. View ENE from S Motzfeldt across Motzfeldt Sø (CB.84.C.10.30).

b.



View ENE of the amphitheatre-like ridge surrounding Camp 13 (alt. 1220 m), S Motzfeldt. The tents are just visible in the lower centre of the photograph. This area became known as 'The Wall'. (CB.84.C.08.22).



a.

View SE over the area of NE Motzfeldt occupied by the GF-syenites comprising the N Motzfeldt 'satellite'. The orange tent of Camp 4 (alt. 1192 m) is just visible beside two small lakes in the centre of the picture. (CB.82.C.05.24).



b.

Lunch stop. The 1700 m mountains of S Motzfeldt loom in the background (CB.82.C.14.22).

Chapter 2 - The Project

2.1 History of Previous Research

Ussing (1912) was aware of the very large tracts of syenite and nepheline syenite that comprise the Igaliko Syenite Complex; "The lofty mountains north, south and east of the Koroq Fjord belong to a large batholite which is indicated here as the Igaliko batholite." Unfortunately, due to lack of time at his disposal (fourteen days) and the inevitable bad weather Ussing was unable to reach the Motzfeldt Centre... "The eastern parts of the district being difficult of approach have not been surveyed." The considerable extent and distribution of syenite of the Motzfeldt Centre only became obvious when the Greenland Geological Survey (GGU) carried out a number of helicopter flights over the area between Igaliko and the Inland Ice during the latter part of the 1950's. This reconnaissance initiated a general geological survey of the Igaliko Complex during the field seasons of 1961, 1962 and 1963. This survey was carried on out behalf of GGU by C.H. Emeleus (University of Durham) and W.T. Harry (University of St. Andrews), the results and geological map being published in 1970 (Emeleus & Harry, 1970). Emeleus and Harry spent several weeks in Motzfeldt during 1962 and 1963 establishing eight field camps (Fig 2.3.1a). Of all the Igaliko Centres, Motzfeldt received the least coverage, mainly because of its large size, the extreme topography and its relative remoteness. Large areas of S and SE Motzfeldt in particular were not visited during their survey.

Each individual Centre of the Complex has subsequently been studied in more detail by various postgraduate research students at the University of Durham, (D. Stephenson, S Qôroq 1973; A.D. Chambers, N Qôroq 1976; M. Powell (also Leeds Univ.), Igdlerfigssalik, 1976; and A.P. Jones, Motzfeldt, 1980). During the summers of 1977 and 1979, Jones spent several weeks in Motzfeldt, mapping and sampling. He established three camp sites, two in C Motzfeldt and one in the SW ('Lower Flinks Dal'), (Fig 2.3.1a). Studying the samples he collected and those collected by Emeleus and Harry, Jones described in

detail the petrography, mineralogy and geochemistry of the various established units of the Centre. Jones also added further field data to the original map of Emeleus and Harry, 1970.

Motzfeldt was further surveyed during the summers of 1979 and 1980 as part of the GGU-South Greenland Uranium Exploration Project (SYDURAN), (Armour-Brown, Tukiainen & Wallin, 1980, 1981 & 1982). A team led by T. Tukiainen (GGU) concentrated on the Motzfeldt Centre and carried out reconnaissance airborne-radiometric surveys, drainage geochemical sampling and limited geological field work. The results showed that large areas of reddened syenite in the NE, E and SE contained highly elevated U and Th values. The new findings suggested the Centre may contain economic potential and there was a necessity for a major geological reappraisal of the Centre (Tukiainen, 1981).

2.2 Current Research

A detailed geological and radiometric mapping programme of the Motzfeldt Centre commenced in 1982 as part of the extended SYDURAN project under the Danish Ministry of Energy's Research Programmes of 1981 and 1982 (Armour-Brown, Tukiainen & Wallin, 1982; Armour-Brown et. al. 1983). As a member of the SYDURAN team, the author, with the assistance of Mr J. Ohberg (GGU), carried out the geological mapping, while the U-Th mineralisation was investigated by T. Tukiainen using detailed helicopter-borne gamma spectrometer equipment and additional field surveys (Bradshaw & Tukiainen, 1983). The radiometric survey proved to be invaluable not only for mineral exploration but also as an aid to the geological mapping (Tukiainen, Bradshaw & Emeleus., 1984).

The Nb and Ta (Pyrochlore) potential, discovered in the area during 1982 prompted further exploration and in 1984 the GGU-PYROCHLORE project was instigated. This project is funded by the EEC's Resources and Raw Materials Programme and the Geological Survey of Greenland. The venture involves collaboration between German geologists namely; Prof. G. Morteani and Mr B. Kronimus, University of Munich, (geochemistry

and petrography of Pyrochlore-bearing syenites); Dr P. Möller, University of Berlin (Geochemistry of REE); Dr D. Ackerman, University of Kiel, (electron probe investigations) and GGU geologists; Mr T. Tukiainen (mineralisation and exploration); Dr L.M. Larsen (petrochemistry) and Mr L. Thorning, (Geophysical investigations). All members took part in field surveys during the summer of 1984. The detailed mapping programme in the Motzfeldt Centre which commenced in 1982 with the SYDURAN Project was continued during 1984 by the author (with NERC financial support) in conjunction with the members of the PYROCHLORE project.

2.3 Fieldwork and aims of the Project

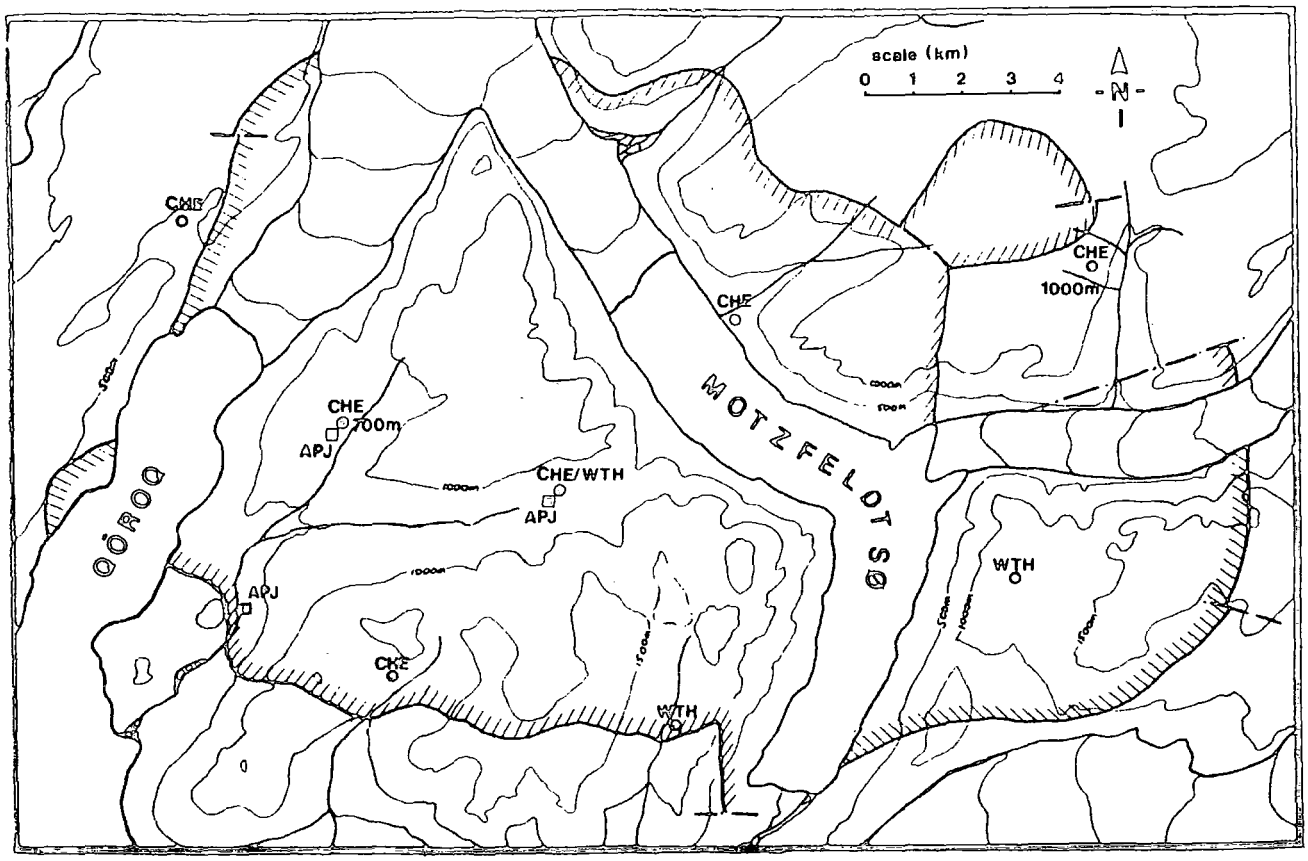
The aim of the study was to develop a detailed geological reappraisal of the Motzfeldt Centre and thereby, provide a reliable reference framework for economic evaluation, exploration and continued geological research. To fulfill this aim the author has spent a total of sixteen field weeks in the Motzfeldt area during the summers of 1982 and 1984 (see Appendix Two, Field Statistics). Work was carried out on foot from each of nineteen established campsites (sixteen different camps, see Fig 2.3.1b), [1] although occasional helicopter support proved invaluable for reconnaissance of the more inaccessible areas (Plate 1.4b). Mapping was undertaken using high quality 1:10,000 contoured orthophoto maps and 1:50,000 stereopair aerial photographs.

In addition to the rock samples already available from previous collections of CHE, WTH and APJ, 480 samples were collected by the author. Currently, 1025 Motzfeldt specimens are 'housed' at Durham and have been used extensively in supporting petrographic and geochemical studies.

[1] for grid references see Tables A2.4 and A2.5, Appendix Two

Camp site locations

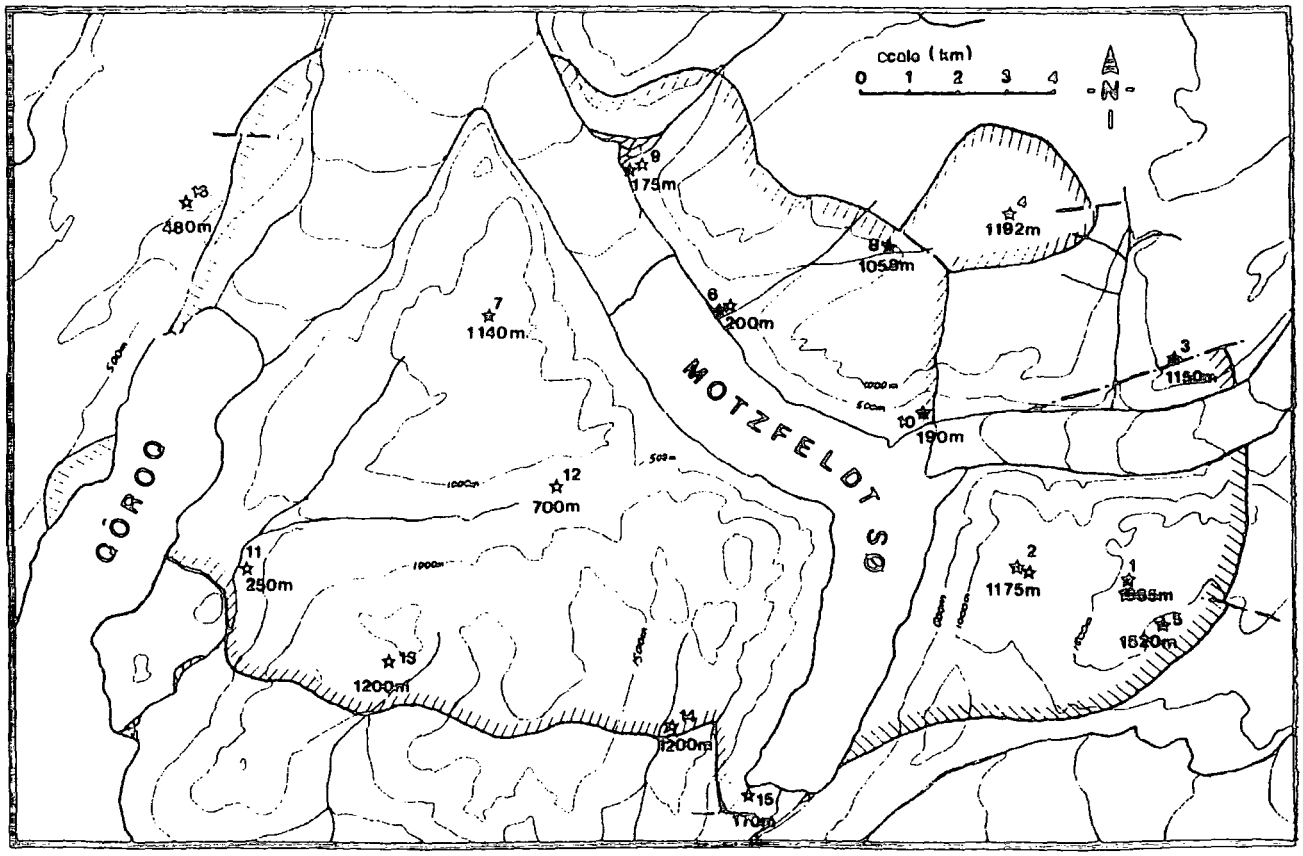
Fig 2.3.1



a. Camp locations of earlier surveys:-

A.P.Jones: ⊡ 1977; □ 1979.

C.H.Emeleus & W.T.Harry: ○ 1962; ○ 1963.



b. C. Bradshaw camp locations: ☆ SYDURAN 1982; ★ PYROCHLORE 1984.

PART TWO

THE ROCK UNITS

Chapter 3 - Introduction

3.1 Geological summary, from previous studies

The Motzfeldt Centre (1310+/-31 MY) is one of four alkaline Centres belonging to the Igaliko Nepheline Syenite Complex, S Greenland (Emeleus & Harry, 1970). Motzfeldt is a multiphase, high level intrusive Ring Centre emplaced in the 'basement' Proterozoic Julianehåb Formation and overlying Gardar supracrustal succession. Although the bulk of the rocks comprising the Centre are syenites and nepheline syenites, lesser units range from syenogabbro to lujavrite (Jones, 1980). Emeleus and Harry (1970) distinguished five major bodies of syenite and nepheline syenite (SM1 to SM5) and showed that these units followed the classic ring intrusion pattern of internally overlapping, circular or arcuate bodies that young inwards (See enclosure Enc.1). Whether we now see a ring-dyke or a stock-like body depends on the current level of erosion. Two 'satellite' intrusions, cut by the Ring Centre, were also described. These include a composite body in NE Motzfeldt (NM1 & NM2) and a poorly known syenite in SE Motzfeldt - the East Motzfeldt Syenite. The Centre was shown to be cut by two large dykes of alkali- gabbro and syenogabbro composition, a suite of 'late' microsyenite sheets (NE Motzfeldt) and numerous dykes belonging to the late Gardar regional swarm. Jones (1980) showed conclusively that certain strongly foliated and banded medium grained syenites on the S side of Flinks Dal were not large rafts of metasomatically altered gneiss (cf. Emeleus & Harry. op. cit.) but late intrusive bodies of lujavrite composition, to which he assigned the notation SM6. In addition, Jones emphasised the petrological similarity between the marginal facies of the nepheline syenite SM5 and the Syenogabbro[1] ring dyke. To indicate this relationship he renamed the dyke with the notation SM5*.

[1] which he showed to be larvikitic

3.2 Revised geological nomenclature

Comprehensive field surveys associated with this study (see Appendix Two) made it possible to further subdivide the established units and establish a number of previously undescribed rock units. Moreover, it was apparent that the major syenite units (NM1/2 and SM1 to SM6 of Emeleus and Harry, 1970; Jones, 1980) could, from field and petrographical evidence, be divided into three main 'families' or Formations. On this basis a new scheme of nomenclature was proposed (Bradshaw & Tukiainen, 1983) which incorporates these divisions, known respectively as the Geologfjeld Formation, Motzfeldt Sø Formation and Flinks Dal Formation. This scheme, modified following discoveries during the 1984 field season, is shown on Table 3.2.1 correlated with the previously established SM notation for ease of reference. The scheme was proposed because of its flexibility in allowing the addition of new field data. Thereby, previously undescribed units and new subdivisions of established units, discovered during the GGU-Syduran and GGU-Pyrochlore surveys (and in any future mapping surveys) can be included without confusing changes in the SM notation of Emeleus and Harry, 1970. Further, the syenites of the Motzfeldt Sø and Flinks Dal Formations, although distinct episodes of magmatic activity follow a common focus of intrusion and together comprise the main plutonic ring structure known as the Motzfeldt Ring Series (Bradshaw & Tukiainen, 1983). Many minor intrusions are also associated generically with each Formation and by using the appropriate prefix (ie, MSF or FDF) this can be indicated.

In the following text, when individual members are discussed, the Formation to which they belong is indicated as an abbreviated prefix.

Where:

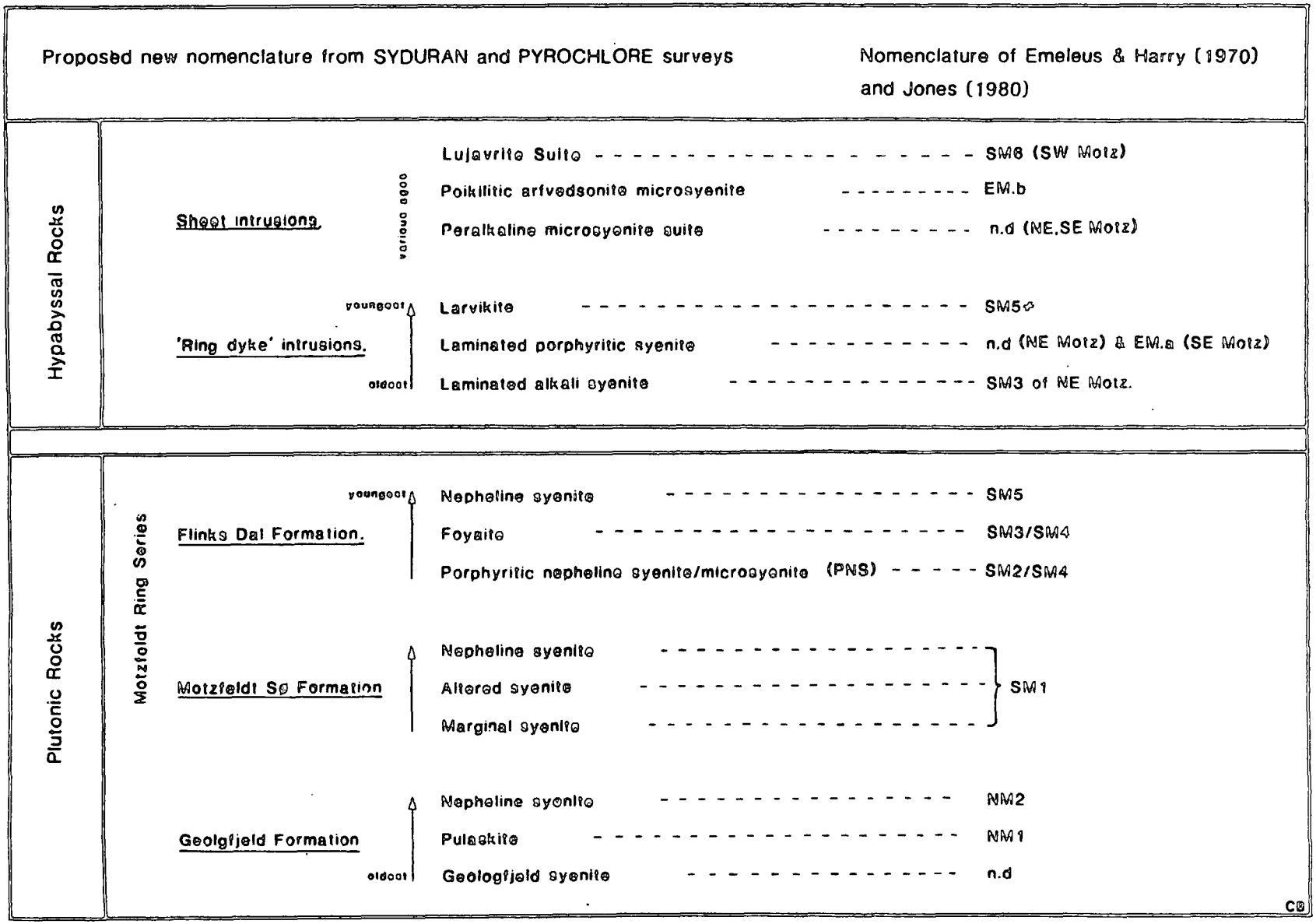
FDF = Flinks Dal Formation.

MSF = Motzfeldt Sø Formation.

GF = Geologfjeld Formation.

EF = Eriksfjord Formation.

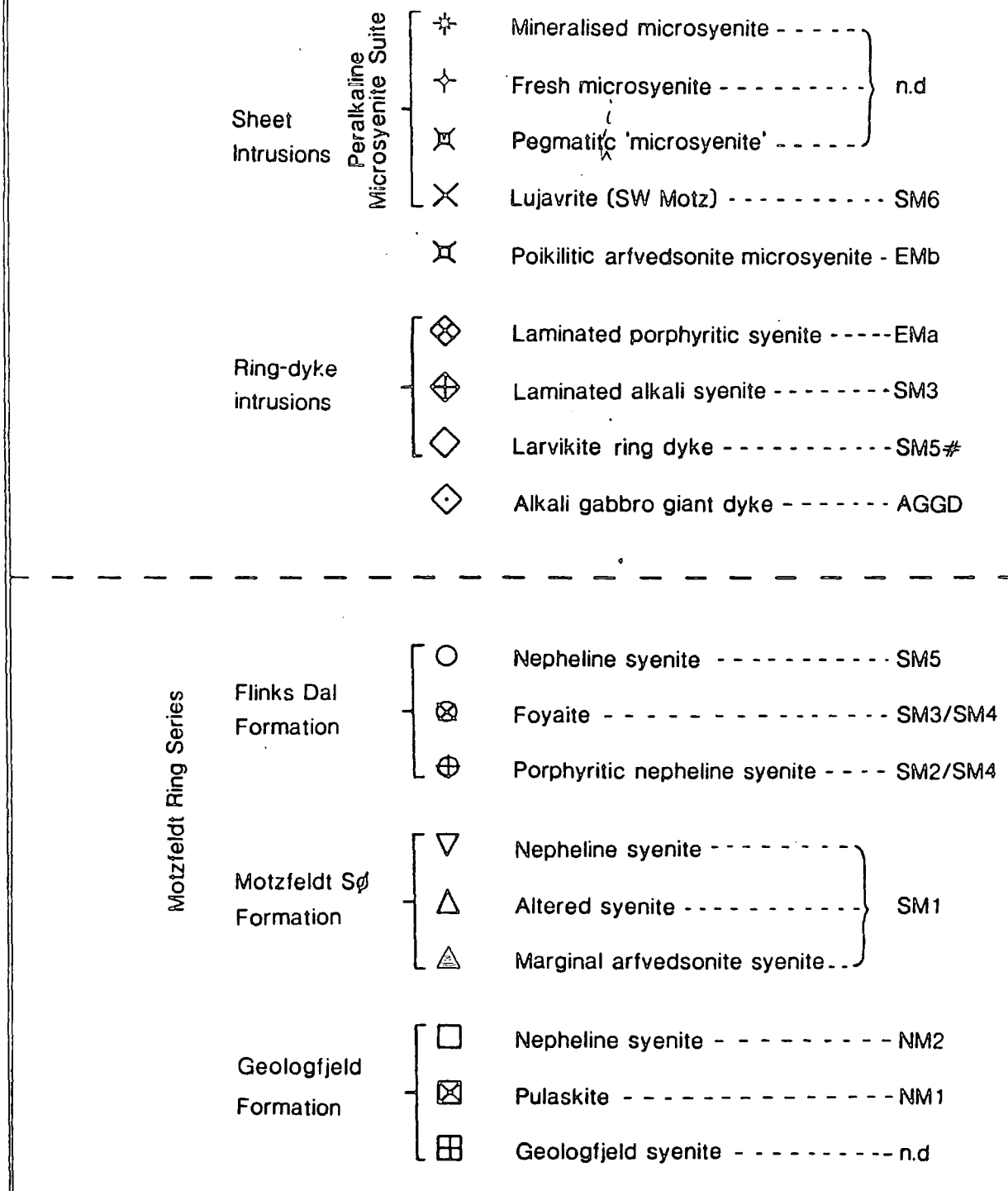
JF = Julianehåb Formation.



n.d = not previously described

Table 3.2.1

Guide to symbols used thoughout this thesis



The previous nomenclature of Emeleus & Harry (1970) and Jones (1980) is shown for reference.

CB

Table 3.2.2 shows symbols used to represent the units of the Centre. These symbols are used in all the geochemical figures throughout this thesis: Geologfjeld Formation units - square, Motzfeldt Sø Formation - triangular and the Flinks Dal Formation - circular. The ring dykes have diamond shaped symbols and the sheet intrusions are represented by stars.

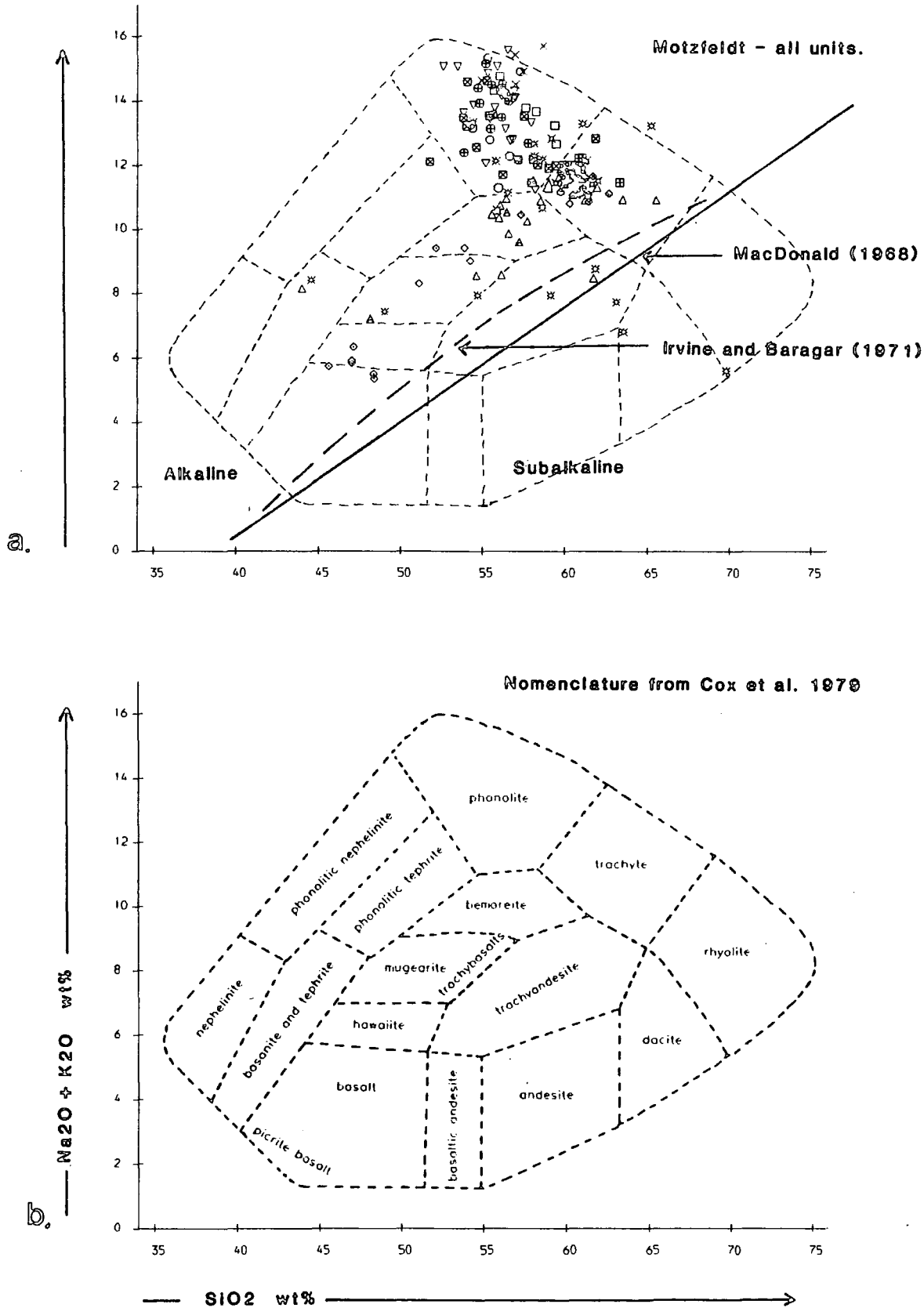
The photographs have a number of different scale markers with sizes as follows: Knife - 7 cm; Lens caps - 5 cm; 1 pound coin - 2 cm; Wooden hammer, shaft - 35 cm, head - 10 cm; Estwing hammer, shaft - 27 cm, head - 15 cm.

3.3 Classification of the Motzfeldt syenites and nepheline syenites

The alkaline rocks comprising the Motzfeldt Centre represent strongly differentiated members of the Alkali olivine basalt (sodic) Series (of; Irvine and Baragar, 1971), and are typical subvolcanic igneous rocks produced by intracratonic magmatic processes. The full range of rock types from the above series is represented by the cross- cutting Gardar dykes and overlying lavas in the area. Carbonatite dykes in the area are also more abundant than previously recognised (Pearce & Emeleus, 1985). Although, the intrusive rocks of the Motzfeldt Centre range from larvikite to lujavrite, they are predominantly phonolitic and trachytic in composition. (Fig 3.3.1 & Fig 3.3.2). Oversaturated syenites do occur where magmatic interaction with the surrounding country rock (gneisses & quartzites) has taken place. On the basis of the petrography and geochemistry of the different units (this study) a broad three fold classification may be applied (see Table 3.3.3). The different syenites (*sensu lato*) may be divided on the basis of their alkalinity. The Peralkalinity Index (Na_2+K_2O/Al_2O_3; mol. props) used for this purpose not only reflects the degree of differentiation but also strongly indicates the geochemical and mineralogical features which can be expected in the rock (see section 8.1.2) In addition, further subdivision into undersaturated/saturated types is used. However the major 3-fold division of mineralogical characteristics is still applicable. Hypoalkaline units are the least evolved varieties in Motzfeldt and as the name suggests they are 'deficient' in alkalis relative to alumina, as shown by the dominance of calcic mafic minerals. Syenites (*sensu*

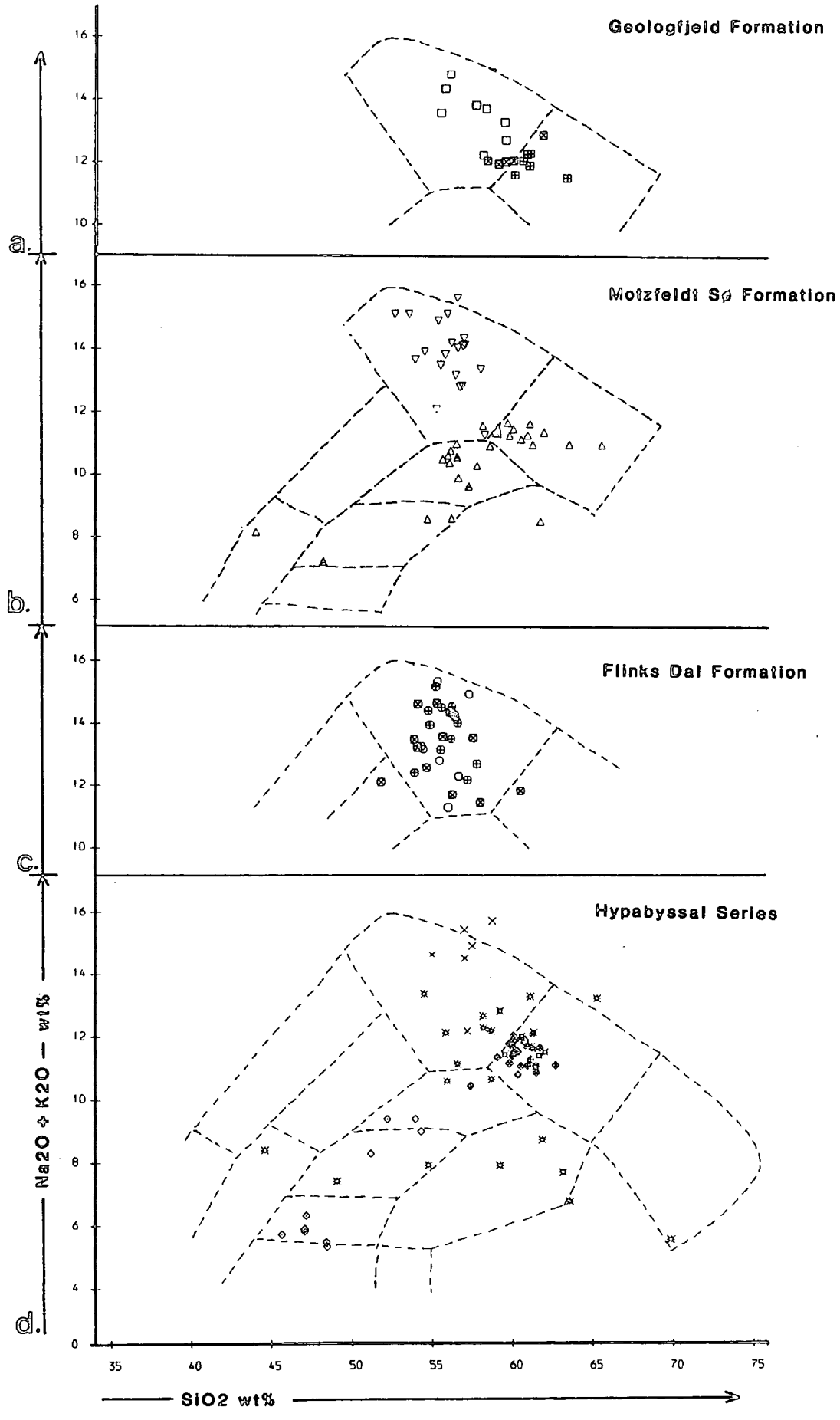
Alkalis vs Silica Plot - All units

Fig 3.3.1



Alkalis vs Silica Plot - Formations

Fig 3.3.2

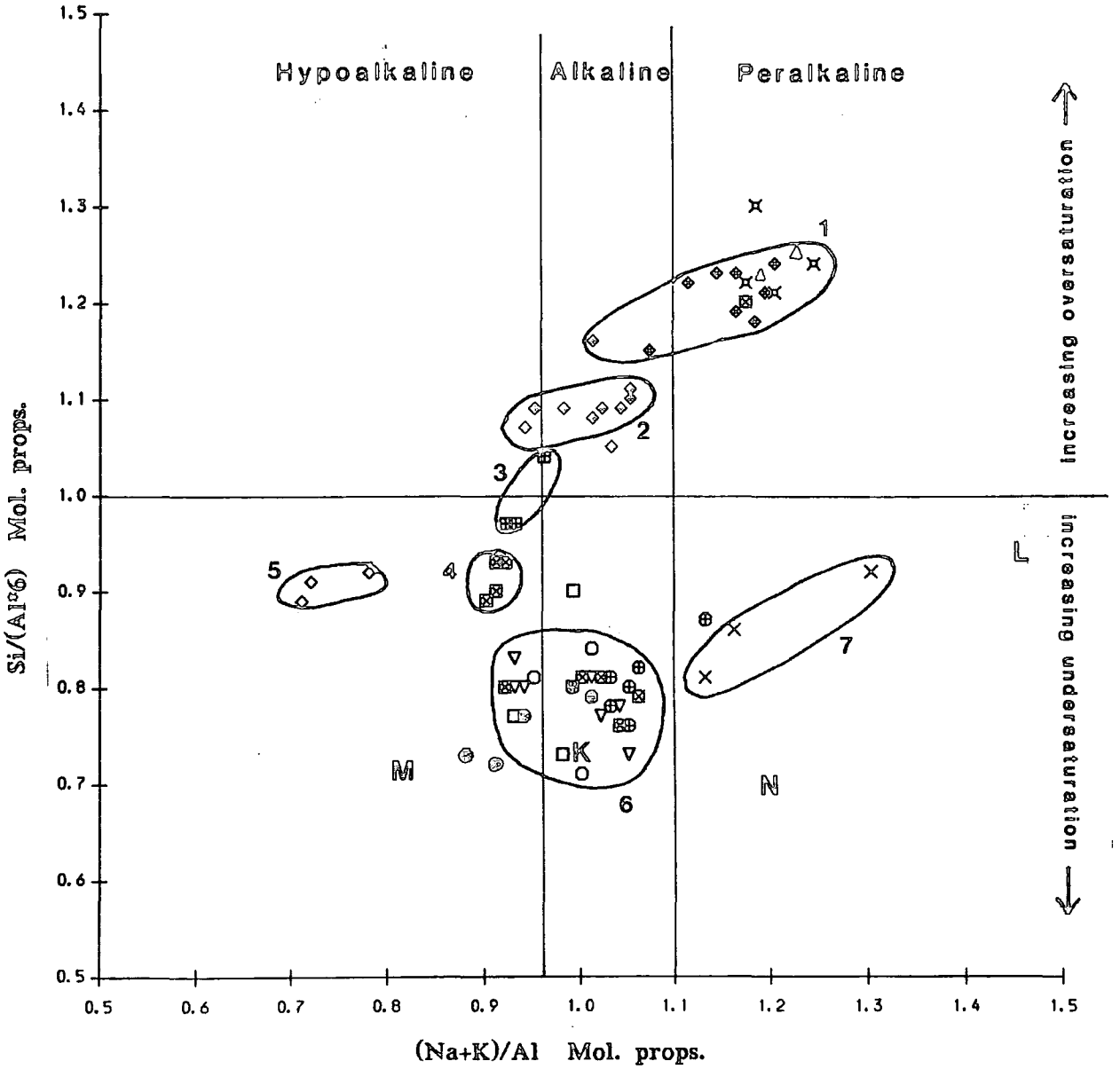


Motzfeldt Classification Table

Table 3.3.3

HYPOALKALINE		ALKALINE		PERALKALINE	
Saturated	Undersaturated (Miaskitic)	Saturated	Undersaturated (khibinitic or intermediate)	Saturated	Undersaturated (Agpaitic)
Na+K/AL <0.95	Na+K/AL <0.95	Na+K/Al ≥0.95 <1.1	Na+K/Al ≥ 0.95 <1.1	Na+K/Al ≥ 1.1	Na+K/Al ≥ 1.1
Often K > Na	Often K > Na	Na > K	Na > K	Na > K	Na > K
Na+k:Al:Si = (<1):1:6	(<1):1:(<6)	~1 : 1 : 6	~1 : 1 : (<6)	(>>1) : 1 : 6	(>>1) : 1 : (<6)
high in Ca Ba Sr low in Zr Nb Th U REE low in F Cl		mixed chemistry mod. to high conc. of incompatible elements low to high in F,Cl		High Zr Nb Be REE Zn Th U High F Cl Low in Ba Sr (except 414)	
Occasional Ca-anorthoclase cores in alkali-feldspars. Predominantly calcic pyriboles ie, Hastingsitic hornblende, Hastingsite and Ferro-edenite. Pyroxenes include Salite-Ferrosalite. Apatite, Fe-TI oxides, Sphene, Zircon, occasional Fayalite. Synneusis texture prominant in mafic minerals and oxides. Breakdown minerals and secondary alteration poorly developed. Zoning weak to mod. Ca-al silicate accessories occasionally present. Pegmatite rare. Mineralisation absent.		Mixed mineralogy:- Zoning usually strong. Miaskitic affinities to early cumulus minerals but peralkaline type inter-cumulus. However dominantly Na-Ca Pyriboles. Na-Ca amphiboles = Kataphorite to Ferrorichterite, with occassional Ferro-edenite core, Arf. rim. Na-Ca pyroxines = aeg-augite/aeg-hedenbergite bright green rims usual. Eudialyte, Rinkite/Lavenite minerals occasional accessories in undersaturated types. Aenigmatite, zircon, pyrochlore accesssory in sat. varieties. Fe-Ti oxides mantled by biotite. Interstitial sodalite and analcite fairly common. Secondary breakdown products and exsolution textures well developed.		Poor in Fe-Ti Oxides, Aenigmatite common. Na-pyriboles predominate; eg, Arfvedsonite, Aeg-Hedenbergite & Aegirine. Fluorite common. Albite abundant. Eudialyte, Rinkite/Lavenite minerals and other unidentified rare-metal silicates usual in undersaturated varieties. Local development of economic concentrations of Pyrochlore, Zircon and Thorite in saturated/oversaturated types. Skeletal relics of early mafic minerals and resorbed-sutured margins to mafics common. Albitisation often profound in mineralised varieties.	
GF-Geologfield syenite.	GF-Pulaskite. Occasional Mafic bands in cumulate sequences of the GF, MSF & FDF Nepholine syenites.	Lam. alkali syenite MSF-Altered syenite (some areas) Nepheline free vars.	Most Nepheline syenites from all Formations are predominantly of this type	Altered members of the PMS. Poik. Arf. Microsyenite Laminated Porph. syenite	Undersaturated members of PMS Lujavrite of SW Motzfeldt.

Silica saturation vs Peralkalinity Fig 3.3.4



LEGEND

1 = Peralkaline (arfvedsonite) syenites, 414, 644, 724 & (733 not shown).
2 = Alkali (kataphorite) syenites, 634 & (423 not shown).
3 = Hypoalkaline (hastingsite) syenites, 314.
4 = Hypoalkaline (hastingsite) Pulaskites, 324.
5 = Larvikites, 624.
6 = Nepheline syenites, 334,434,514,524,525, & 534.
7 = Lujavrites, 714.
M = Miaskite, Vishnevogarsk (Ronenson, 1966).
K = Average foyaite, Khibina (Gelakhov, 1967).
N = Average Naujaite, Ilimaussaq (Gerasimovsky, 1969).
L = Average aegirine Lujavrite, Ilimaussaq (Gerasimovsky, 1969).

Nepheline syenite distinguising features

Table 3.3.5

NEPHELINE SYENITE UNIT	DOMINANT COLOUR	DOMINANT TEXTURE	GRAIN-SIZE
FDF-Nepheline syenite	pink-grey	subhedral-equigranular occ. cumulitic	very coarse
FDF-Foyaite(C & T)	grey/grey-blue /pink	foyaitic/ cumulitic	coarse
FDF-Porph. neph. sy.	blue-grey/grey	porphyritic/ foyaitic (laminated)	fine-medium-coarse
MSF-Nepheline syenite	pink	subhedral equigranular/ pegmatitic	coarse (aplitic-massive peg.)
GF-Nepheline syenite	grey/pink	euhedral equigranular (intersertal) drusy pegmatitic	coarse (very coarse peg)

stricto) and 'miaskitic' nepheline syenites are included in this group. Alkaline rock types show a relative balance of alkalis and alumina. They represent the predominant rock type in Motzfeldt and include alkali syenites (saturated) and khibinitic (intermediate) nepheline syenites. Peralkaline rocks are the most evolved rocks in Motzfeldt, they are represented by arfvedsonite syenites/microsyenites and agpaitic lujavrites.

It is important to note there are no abrupt physical and chemical boundaries between the three, and therefore the chemical delimitations used in Table 3.3.3 should be for guidance only and not used in isolation.

The plot Si/(Al x 6) v PI (Fig 3.3.4) shows clearly, in terms of alkalinity and silica saturation the distribution of of the main rock units of Motzfeldt (excluding mineralised and pegmatitic samples). Combined with Table 3.3.3 this plot may be used to classify the rock types, from which inferences can be made about the the trace element (see Chapter 8) and mineralogical features which might be expected. Fig 3.3.4 also shows the tendency for most of the major units of nepheline syenite in Motzfeldt to fall in the same general compositional area. Indeed they are virtually indistinguishable using only their major element compositition and basic mineralogy. Fortunately however, rock colouration, grain size and textural differences do occur, and when used in combination with field-relations, make it possible to discriminate between the units (but not always). Five main textures commonly occur in the syenites, namely; porphyritic, pegmatitic, equigranular, foyaitic and cumulitic. Table 3.3.5 lists the definitive textural features (hand-specimen scale) of the main nepheline syenite units. The nomenclature developed for use in Motzfeldt (Bradshaw & Tukiainen, 1983; Bradshaw, 1985; also section 3.2 this work) has attempted to utilize these differences as much as possible with the aim of simplifying future field surveys.

3.4 Some mineralogical features of the Motzfeldt units

3.4.1 Introduction

A great deal of research has been carried out on the mineralogical trends, particularly of the ferromagnesian silicates of the Gardar Province and the various alkaline centres of the Igaliko Nepheline Syenite Complexes (eg. Chambers, 1976; Jones, 1980, 1985; Jones and Peckett, 1980; Powell, 1976, 1978; Larsen, 1976, 1977; Stephenson, 1972, 1973, 1974; Stephenson & Upton, 1982; Parsons, 1979, 1981; Pearce, 1988; and others).

Jones (1980, 1985) has gone into considerable detail regarding these trends in Motzfeldt and it is therefore unnecessary to repeat the detail here. The 'Petrographic features' sections of the following Rock Unit Chapters indicate the mineralogical characteristics of the individual units. Here the mineralogical aspects of the rock units as a whole are introduced.

New microprobe data are tabulated in Appendix Four, for the mineral groups Pyroxene (A4.2), Amphibole (A4.3), Feldspar (A4.4), and Biotite (A4.5). Most of the rock groups in Motzfeldt are covered, although in this work analyses have been concentrated on the 'new' rock units eg. GF-Geologfjeld syenite, and those little analysed by Jones (1980), with the aim that both works combined might provide a good spectrum of data for all of the Motzfeldt rock units. In the preceding section, the Motzfeldt syenites and nepheline syenites were broadly divided into three main groups; 'hypoalkaline', alkaline and peralkaline. These are related through progressive fractional crystallisation and although the division is based on rock chemistry (PI) the mineral assemblages of the different groups reflect these divisions in their own general chemical characteristics (see Table 3.3.3).

3.4.2 Olivine

Olivine is only an important constituent in the larvikite ring-dyke of Central Motzfeldt and the lardalitic margin of the FDF-Nepheline syenite to which it is considered to be related (Jones, 1980). Small rounded olivine crystals (c.3 mm) do occur in the fine

grained (chilled) varieties of the FDF-Porphyritic nepheline syenite and the partial ring-dyke of Laminated porphyritic syenite. Coarser varieties of these units however, only occasionally contain larger (up to 5 mm) corroded and highly stained olivines. The basic, lower horizons of the cumulate FDF-Foyaite sequence contain yellow fayalitic olivines in modal concentrations up to 10%. In the field these are easily recognised by their strongly rusted appearance. Olivine was not discovered from petrographically similar (although not cumulate) rocks of the Motzfeldt Sø Formation which is probably a reflection of the higher H_2O content and fo_2 of this unit, where:

$$3Fe_2SiO_4 + O_2 = 2Fe_3O_4 + 3SiO_2. \quad \text{or:}$$

$$NaAlSi_3O_8 + \tfrac{1}{4}O_2 + \tfrac{1}{2}Fe_2SiO_4 = \tfrac{1}{2}Al_2O_3 + NaFeSi_2O_6 + \tfrac{1}{2}SiO_2 \quad \text{(Ewart, 1981)}$$

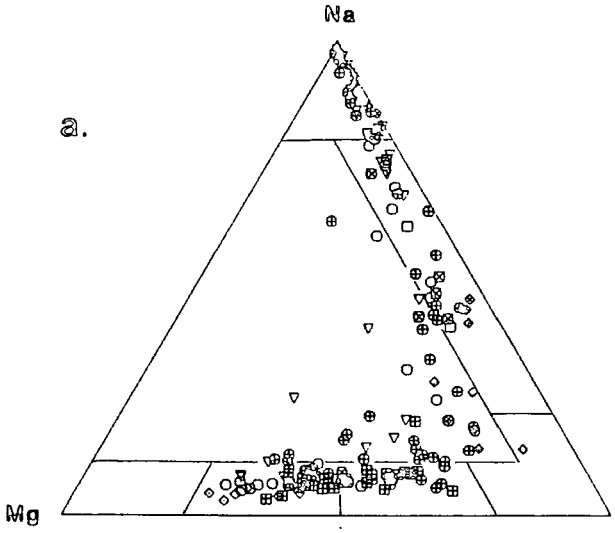
3.4.3 Pyroxene

The pyroxenes of Motzfeldt are displayed here in terms of Mg -(Fe^2 + Mn) - Na (atom%) (Fig 3.4.1 & Fig 3.4.2). Early cumulus pyroxenes are of salite and ferrosalite compositions, which tend to be pale lilac and pale apple green in thin section, respectively. These are commonly rimmed by bright green aegirine-hedenbergite or amphibole and then a second generation of aegirine-hedenbergite or aegirine. This quite distinct paucity of compositions between ferrosalite and aegirine-hedenbergite (see Fig 3.4.2 and Figs 3.4.3 & 3.4.4) [1] probably represents the increased importance of amphibole crystallisation, at this stage (Larsen, 1976; Jones, 1980). The series of scatter plots of elemental concentration (atom%) versus (Na-Mg) shows how early evolution can be expressed in terms of Mg^2 - Fe^2 substitution in $CaMgSi_2O_6$ to $CaFeSi_2O_6$ with concomitant decreasing Al and Ti and increasing Mn + Si. However, unlike in the Ilimaussaq Intrusion (Larsen, 1976) or many of the oversaturated rocks of the Gardar (eg. Stephenson and Upton, 1982), hedenbergite is not reached, and the pyroxene trend is influenced by increasing Na and Fe^3. The pyroxenes of the MSF-Nepheline syenite are noticeably less Mg depleted than those of the Flinks Dal Formation before becoming enriched in the acmite component, (Fig 3.4.2). Larsen(1976) postulated low fO_2 conditions (and low

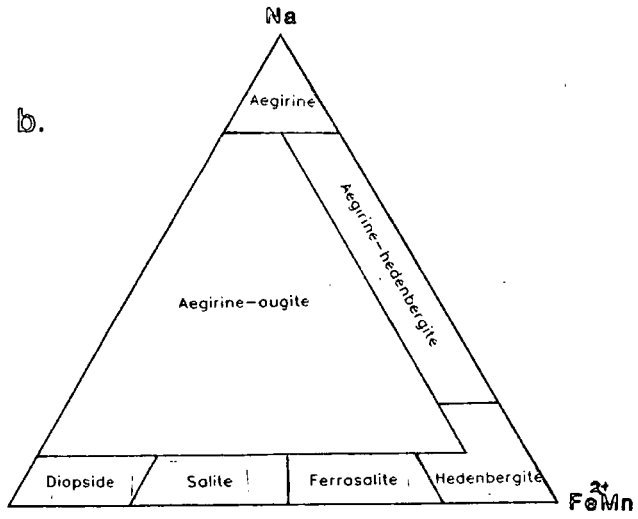
[1] hedenbergite = 0.0 Na-Mg

Pyroxene trends (Ca-Fe2+Mn-Na), all units

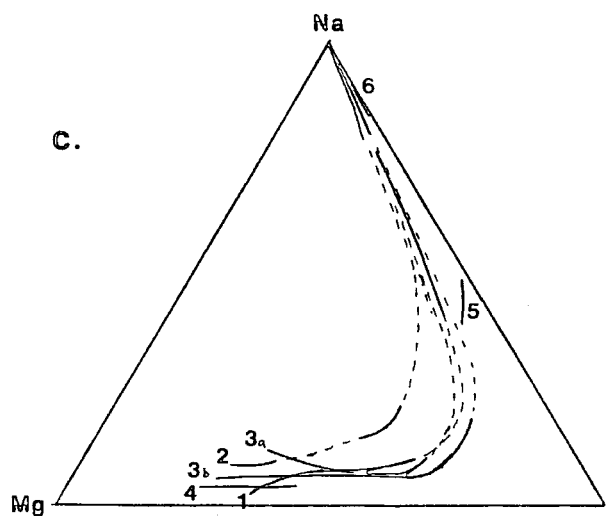
Fig 3.4.1



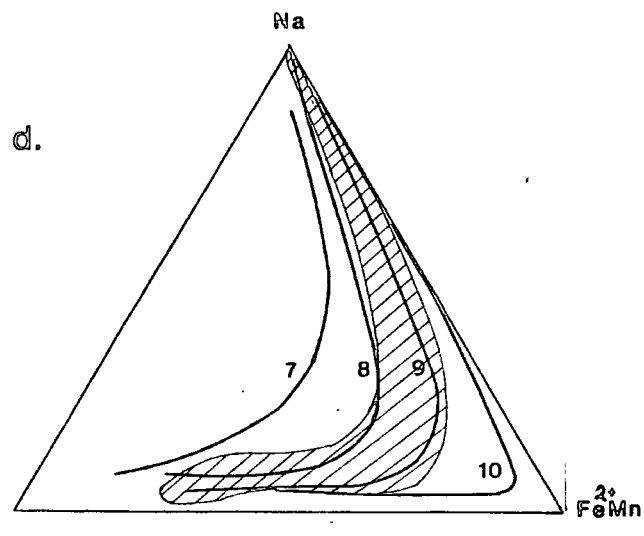
All units



Nomenclature
(from Jones 1980)



Formation trends



Provincial trends compared

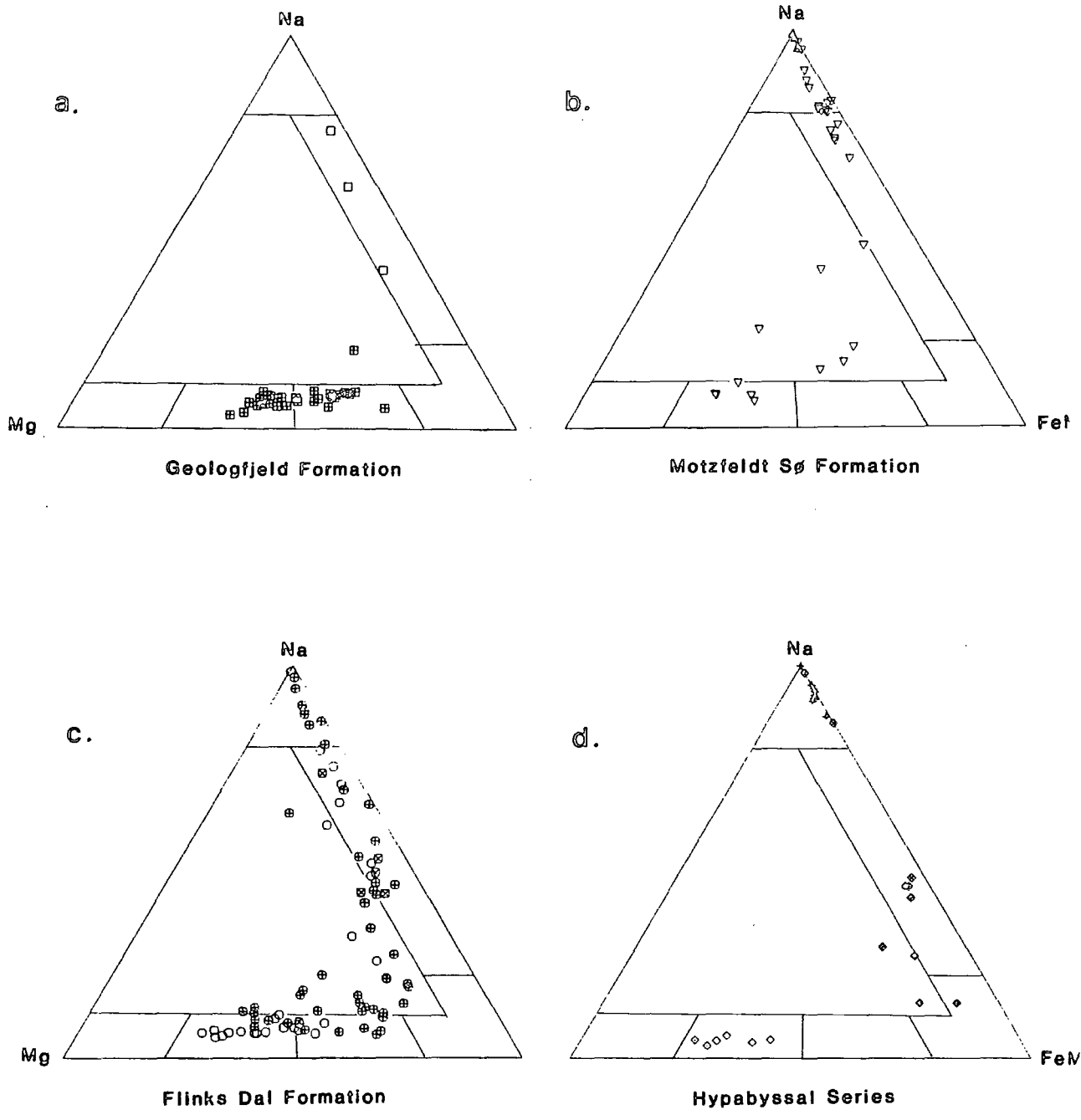
a. Motzfeldt pyroxene analyses plotted in terms of Diopside-Hedenbergite-Acmite (atomic percent).

b. Nomenclature used throughout this work, taken from Jones, (1980, pp.93-94).

c. A comparison of the Motzfeldt pyroxene trends, shown by individual units or formations: where 1 = Geologfjeld Formation; 2= Motzfeldt Sø Formation; 3a= Flinks Dal Formation - PNS; 3b= Flinks Dal Formation - NS; 4= Alkali-gabbro/Larvikite; 5= Laminated porphyritic syenite; 6= Peralkaline microsyenite.

d. A comparison of the pyroxene trends shown by different centres of the Gardar Province. Data from Uganda included for reference. Where, 7= Uganda (Tyler & King, 1967); 8= S. Qôroq (Stephenson, 1972); 9= N. Qôroq (based on Chambers, 1976); 10= Ilimaussaq (Larsen, 1976); ▨ = Loci of Motzfeldt samples.

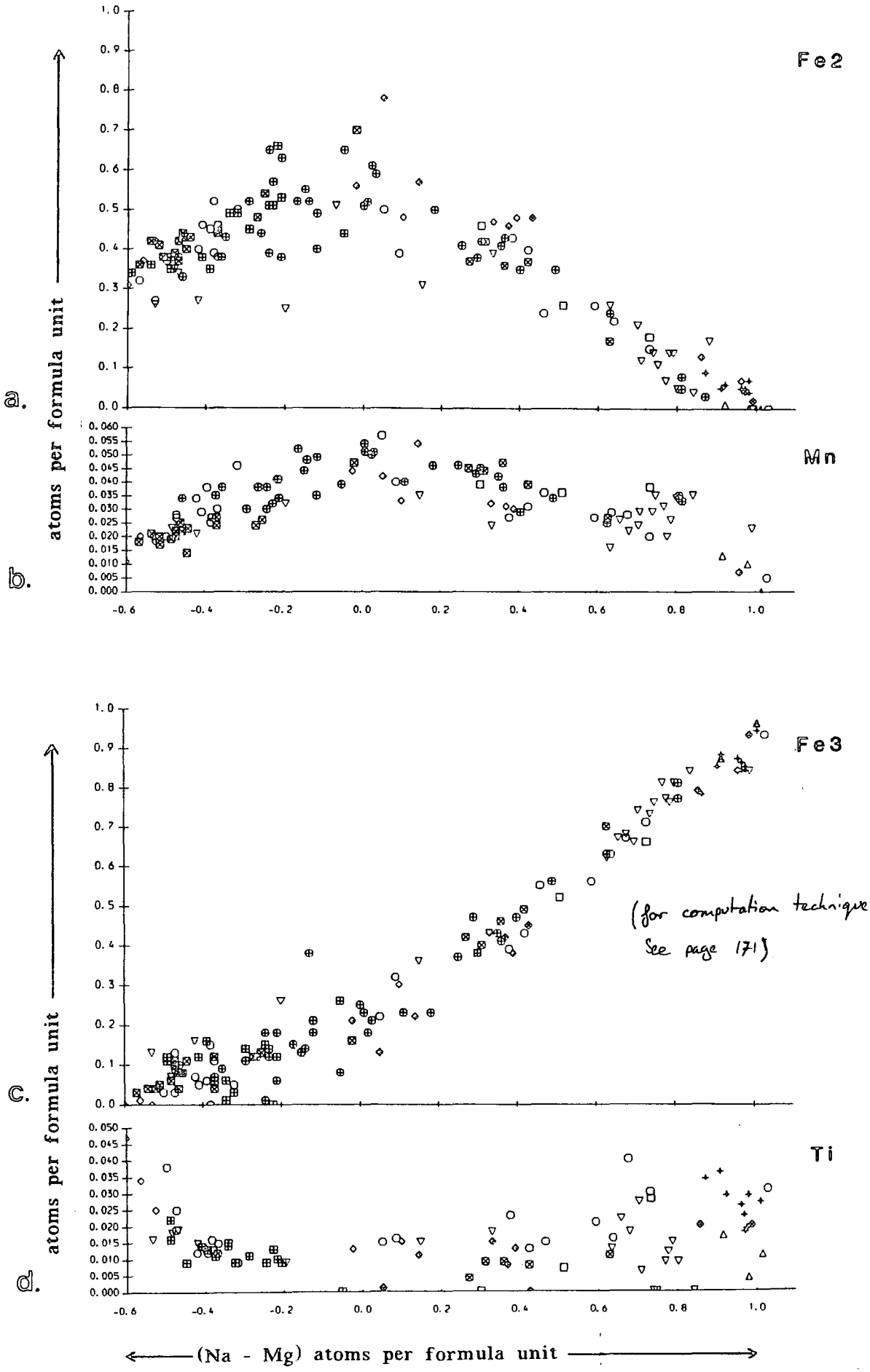
Pyroxene trends (Ca-Fe2+Mn-Na), Formations Fig 3.4.2



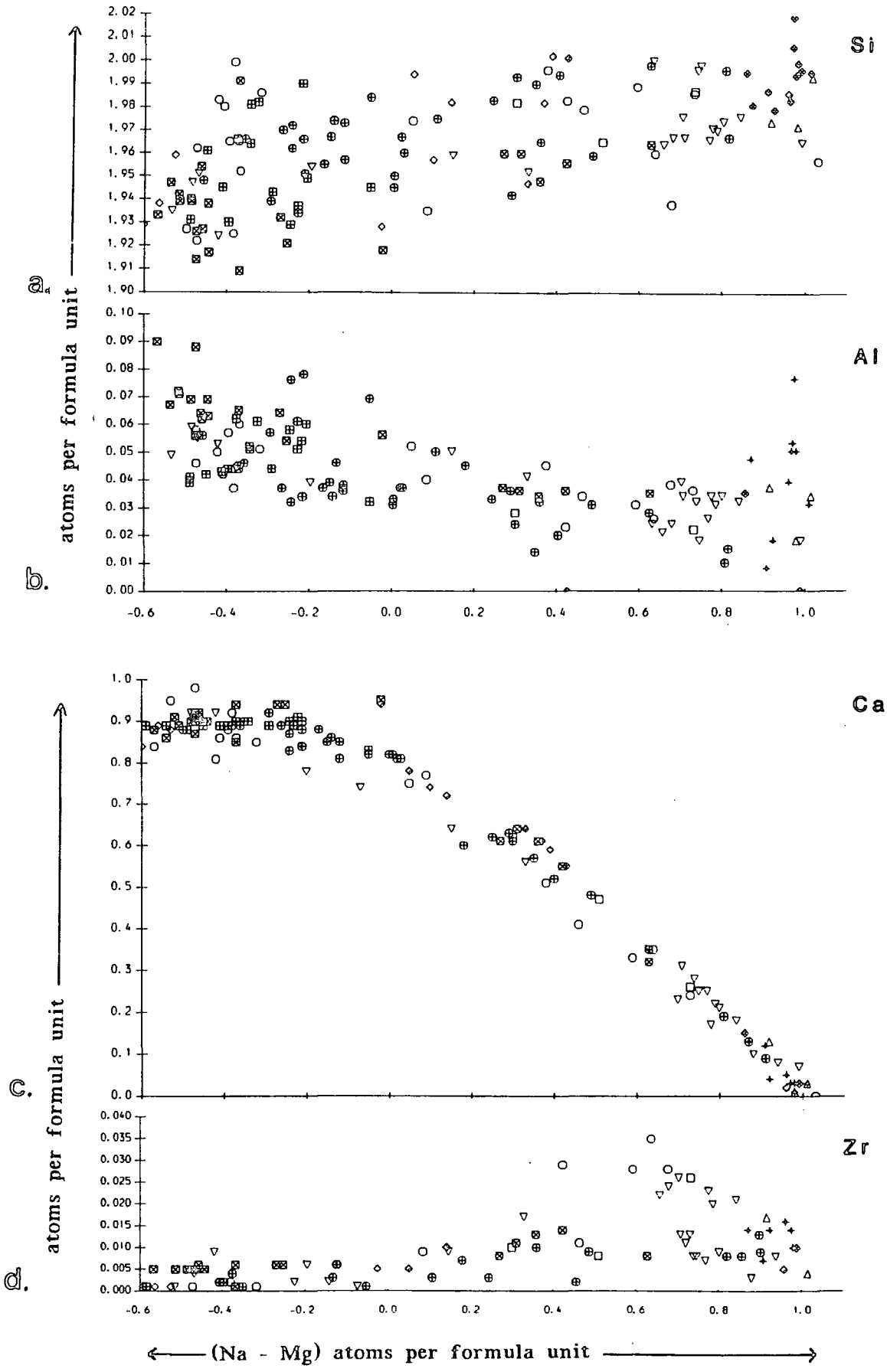
Motzfeldt pyroxene analyses plotted in the system
Diopside - Hedenbergite - Acmite (atomic percent)

Pyroxenes Element/(Na-Mg), all units

Fig 3.4.3



Pyroxenes Element/(Na-Mg), all units Fig 3.4.4



initial MgO) to explain extreme enrichment of Fe^2 and Mn in Ilimaussaq. Conversely, therefore, higher fo_2 in the Motzfeldt Sø Formation compared to the Flinks dal Formation would explain the aforementioned trend and be consistent with the field evidence (Chapter 5).

With an increase in the acmite component ($NaFe^3Si_2O_6$), there is a general increase of Si, Ti, and Zr with declining Al, Fe^2, Mn, Mg and Ca (Figs 3.4.3 & 3.4.4) with trends from this study being virtually identical to those shown by Jones (1980 and 1985).

High levels of Zr (up to 6.9 wt%) were discovered in aegirines present in the peralkaline intercumulus of the FDF-Foyaite (transgressive type) (Jones, 1980; Jones & Peckett, 1980). The substitution invoked being:

$$(Fe, Mg)^{2+} + Zr^{4+} = 2Fe^{3+}$$

The Zr concentrations analysed in this work show a general increase with fractionation (Na-Mg) but with increasing scatter toward the Na rich varieties (Fig 3.4.3). Jones and Peckett (1980) noted this scatter even on a hand specimen scale and concluded that small pockets of residual intercumulus melt would represent largely isolated chemical environments which could often be Zr rich (Dietrich, 1968; Siedner, 1965; Watson, 1979).

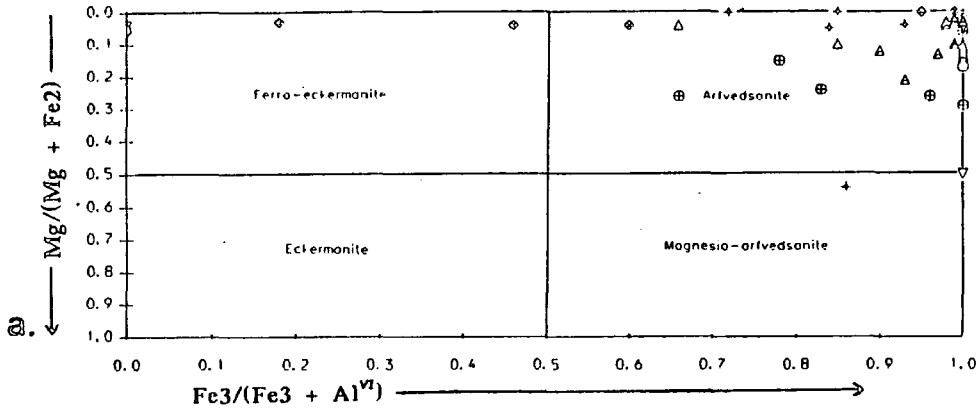
3.4.4 Amphiboles

Members of the Amphibole group are present as intercumulus minerals in all rock units and are the most abundant mafic minerals in Motzfeldt. The threefold classification, based on peralkalinity, which is used here for the syenites of Motzfeldt is strongly reflected by the characteristic amphibole in each group. Using Leake's nomenclature (1978), these include calcic, sodic-calcic and sodic amphiboles respectively (Table 3.4.7). Optically these stages are easily recognised by the change in dominant colour from brown through green to shades of blue (Chambers, 1976; Jones, 1980). Of the crystals analysed from Motzfeldt all but 3 have $Mg/(Mg + Fe^2) < 0.5$ (Fig 3.4.5). All amphiboles from Motzfeldt are $\sum$Fe rich with Fe_2O_3 + FeO ranging from c.18 wt% to c.35 wt% (Table A4.3). The

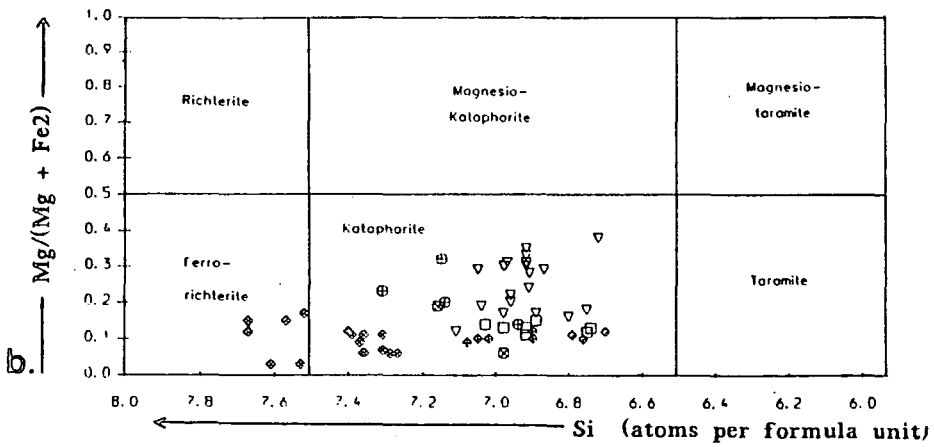
Amphibole classification tables

Fig 3.4.5

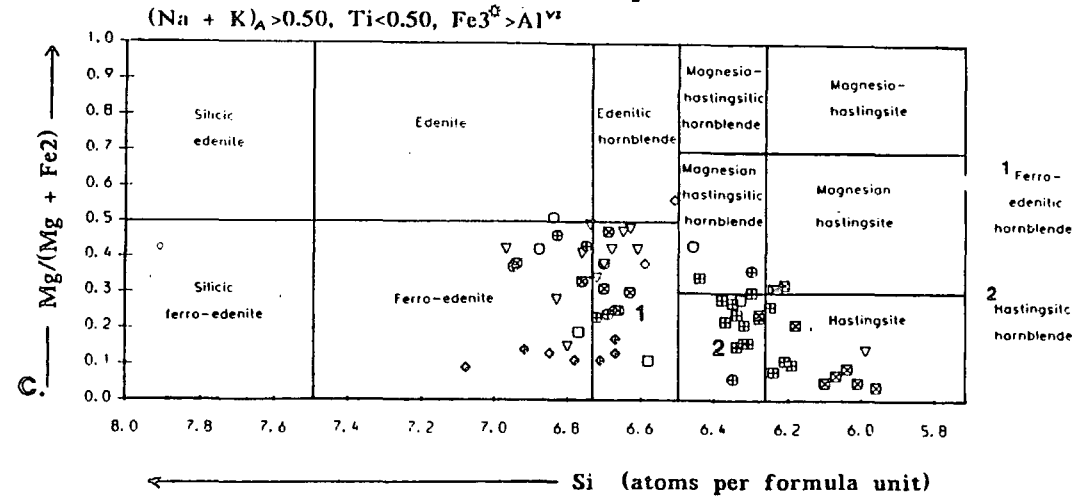
Alkali amphiboles $Na_B > 1.34$ $(Na + K)_A > 0.50$



Sodic-calcic amphiboles $(Ca + Na)_B > 1.34$, $0.67 < Na_D < 1.34$ $(Na + K)_A > 0.50$

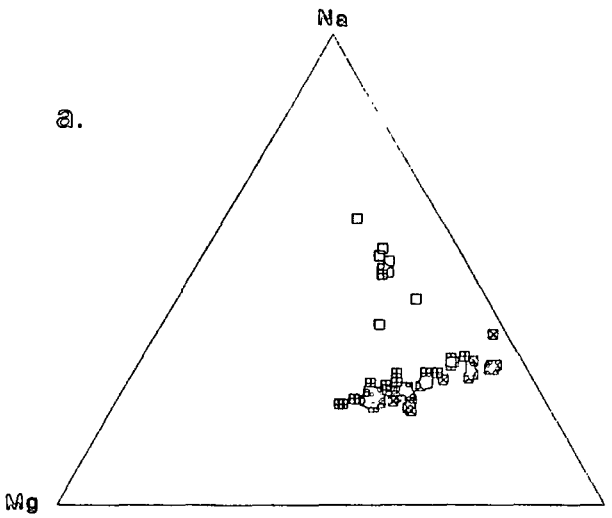


Calcic amphiboles $(Ca + Na)_B > 1.34$ $Na_B < 0.67$
$(Na + K)_A > 0.50$, $Ti < 0.50$, $Fe3^{\star} > Al^{VI}$

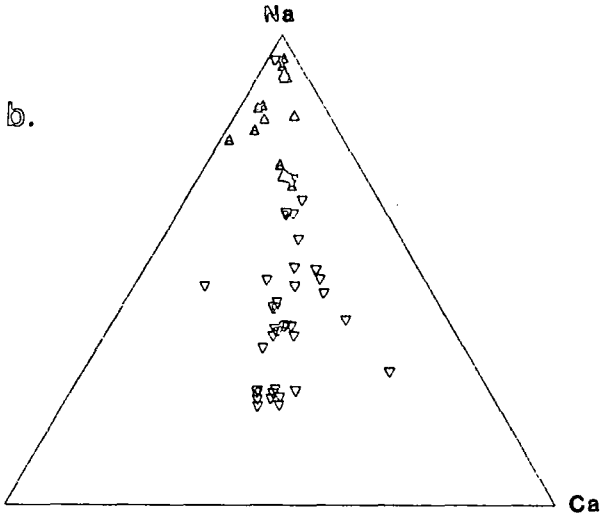


* Due to possible error in Fe3 determination all amphiboles are assumed to comply with this condition.

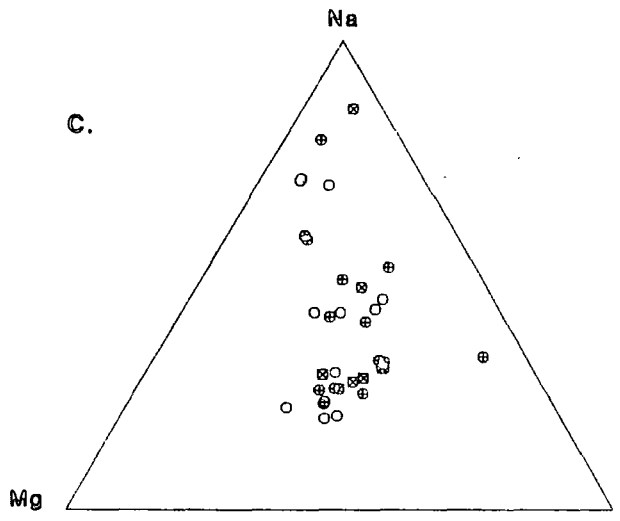
Amphibole trends (Mg-Ca-Na), Formations Fig 3.4.6



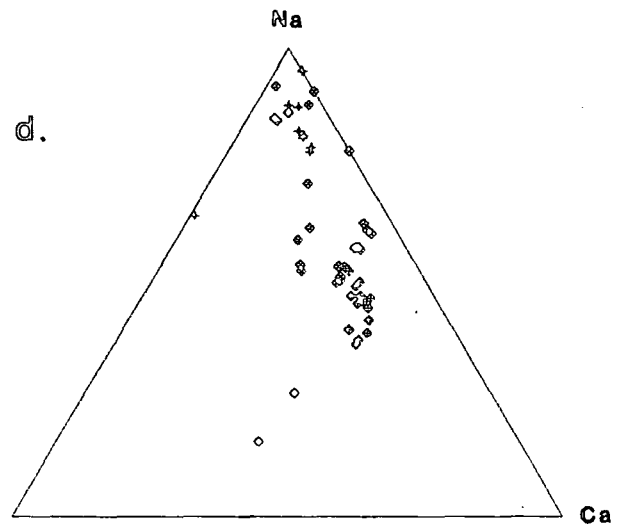
Geologfjeld Formation



Motzfeldt Sø Formation



Flinks Dal Formation



Hypabyssal Series

Motzfeldt amphibole analyses plotted in the system
Na - Mg - Ca (atomic percent).

amphiboles analysed from the different Motzfeldt units are plotted on the classification diagrams (Hawthorne, 1981; modified from Leake, 1978) in Fig 3.4.5.

i. Hypoalkaline Syenites

The amphibole typical of this syenite variety is deep red-brown to staw coloured hastingsite or hastingsitic hornblende. Traditionally these amphiboles would be classified as barkevikite (Deer et. al., 1964). Reclassification of these barkevikites by Rock and Leake, (1984) using the IMA nomenclature of Leake 1978 gave Hastingsitic compositions. These distinctive red-brown hastingsitic amphiboles are common in augite-syenites/syenites throughout the Igaliko Province (Table 3.4.8a).

Chemically the hastingsites differ from the more evolved amphiboles in Motzfeldt in that the dominant substitution is $Mg^C \Longleftrightarrow Fe^C$ and not $Ca^B + Al^T \Longleftrightarrow Na^B + Si^T$. Infact Ca, Na and K remain consistently steady (Fig 3.4.6a) whilst Si concentrations drop toward the rims[2]. The hastingsites are relatively early crystallising phases (higher temperature) and therefore the concomitant crystallisation of feldspar probably plays an important role in buffering the concentration of alkalis entering into the amphibole structure. The prolonged crystallisation of alkali-feldspar (with little or no feldspathoid) also explains the drop in Si as it causes the intercumulus residuum to become progressively silica undersaturated.

ii. Alkaline and peralkaline rocks

In the alkaline and peralkaline rocks the amphibole is predominantly interstitial to the earlier formed feldspar (and often nepheline) crystals. The alkalis with aluminium and calcium play an important role in the dominant substitution $Ca^B + Al^T \Longleftrightarrow Na^B + Si^T$. In addition Fe continues to increase at the expense of Mg. In the nepheline syenites the typical (primary) amphibole sequence is ferro-edenitic hornblende $\Longrightarrow$ ferro-edenite $\Longrightarrow$ kataphorite. The peralkalinity of the rock largely determines which of these phases is

[2] quite the reverse trend to most other Motzfeldt amphiboles

Table of typical characteristics of Motzfeldt amphiboles

	UNDERSATURATED	SATURATED	
Brown	Hastingsite	Hastingsitic hornblende	HYPOALKALINE
Green	**(Ferro-edenitic hornblende)** Kataphorite	**(Ferro-edenite)** Kataphorite (Ferro-richterite)	ALKALINE
Blue	Arfvedsonite	Arfvedsonite	PERALKALINE

(brackets indicate subordinate phase)

Table 3.4.8 (overleaf)

a. b. & c. Tables of typical Motzfeldt amphibole values divided into Hypoakaline, alkaline and peralkaline groups.

Data from Ilimaussaq (Larsen, 1976), Kûngnât (Kung) (Upton and Stephenson, 1982) and Deer, Howie and Zussman (1963) are tabled for comparative purposes.

Nomenclature from Leake (1978) and Rock & Leake (1984). See Appendix Four for key to code names.

Typical Motzfeldt Amphiboles Table 3.4.8

a. Table of amphiboles typical of the hypoalkaline group

Element (wt%)	Motz 304160	Motz 304051	NQ 59758	Ilim 1507522	Kung 126868	DHZ No.3
SiO2	39.57	39.56	39.63	38.90	38.95	40.88
TiO2	2.75	3.65	3.31	2.23	1.47	0.22
Al2O3	9.33	10.66	10.24	10.31	9.60	11.04
Fe2O3T	24.18	25.11	23.47	27.66	29.32	24.97
MnO	1.09	0.68	0.76	0.46	0.62	1.32
MgO	4.88	3.65	5.24	2.72	2.05	5.92
CaO	10.33	11.11	10.95	10.61	10.40	10.46
Na2O	2.65	2.57	2.84	2.59	2.69	3.75
K2O	1.50	1.68	1.53	1.67	1.49	0.78
Name	H-Hb	Has	H-Hb	H-Hb	H-Hb	H-Hb (Na Mg)

b. Table of amphiboles typical of the alkaline group

Element (wt%)	(<—Motz—326092 —>) core	Int	Rim	DHZ(56) No.3	Ilim 91980
SiO2	43.13	42.97	42.94	48.87	42.78
TiO2	2.72	2.89	3.01	1.72	1.32
Al2O3	7.21	5.97	6.22	3.86	4.81
Fe2O3T	22.30	29.27	28.62	24.00	33.47
MnO	0.82	1.18	1.12	1.52	0.67
MgO	6.55	2.64	2.68	6.13	0.52
CaO	10.48	8.33	6.23	5.02	6.89
Na2O	3.43	4.29	5.46	6.52	4.64
K2O	1.53	1.77	1.78	1.03	1.71
Name	FEdHb	FEd	kat	Kat	kat

c. Table of amphiboles typical of the peralkaline group

Element (wt%)	Motz 304758	Motz 304052	(Motz 304185) Core	Rim	DHZ(57) No.11	Ilim 91980
SiO2	47.97	48.76	46.99	48.14	48.41	47.07
TiO2	0.96	0.73	0.81	0.86	1.32	0.54
Al2O3	2.18	1.63	3.09	2.57	1.81	2.50
Fe2O3T	26.89	30.98	33.34	34.18	~34.00	34.00
MnO	1.46	1.04	1.14	1.00	0.75	0.61
MgO	4.64	1.92	0.91	0.91	0.06	0.13
CaO	3.25	2.88	2.69	1.91	1.18	1.85
Na2O	7.46	7.44	7.64	8.09	7.34	7.75
K2O	1.58	1.59	1.55	1.55	1.52	1.70
Name	Arf	Arf	Arf	Arf	Arf	Arf

dominant. Most commonly green kataphorite encloses (as a reaction rim) corroded and resorbed pale red-brown ferro- edenitc cores. (Table 3.4.8b).

Whilst arfvedsonite occurs as small (< 1 mm) late-stage (secondary) minerals in many of the alkaline rocks, the peralkaline types contain primary crystals up to 20 mm in length (eg, 304052). These commonly display a pleochroic scheme from very deep blue to pale straw-yellow and are often mantled by secondary aegirine (eg, 304185), (Table 3.4.8c).

3.4.5 Feldspar and Biotite

A number of electron-microprobe analyses were taken from these minerals[3] (A4.4 and A4.5). They have proved of little discriminatory value because of their narrow range of compositions and in the case of the feldspars, perthitic nature.

Petrographically the feldspars occur in several different forms, which are described for each rock type in the following rock-unit chapters. Essentially, all are 'hyposolvus' alkali-feldspars (Tuttle & Bowen, 1958) showing varying degrees of unmixing and have bulk compositions of roughly equal proportions Na and K (mol% K - Na - Ca). Cryptoperthites, microperthites and coarse patch-perthites all occur in Motzfeldt (nomenclature from Parsons, 1978). Very commonly the feldspars show cryptoperthitic (sometimes braided) cores with 'coarser' microperthitic texture toward the rims (see Brown, Becker & Parsons, 1983). The Laminated alkali syenite is notable in that feldspar laths which were poikilitically enclosed by amphibole are generally cryptoperthitic whereas those 'outside' are coarsely perthitic. This suggests the importance of late-stage fluid interaction as postulated by Parsons (1978, 1980), Parsons & Becker (1986). The peralkaline rocks of Motzfeldt particularly the Lujavrites and those belonging to the MSF-Peralkaline microsyenite suite contain prominant patch-perthites with microcline generally occupying the core of the crystal. Analyses of these feldspars (A4.4, crystal nos. 123 & 124) show how pure these 'end-member' compositions can be. The only rock-type measured

[3] spot analyses only

by the author to contain significant amounts of Ca in the the feldspar was the hypoalkaline GF-Pulaskite (c.5 mol% in K - Na - Ca). Jones (1980), had previously shown that Ca-rich cores occurred not only in SM5* (larvikite ring-dyke) but also in the SM5 (FDF-Nepheline syenite). In all cases the whole-rock REE normalised data show positive Eu anomalies (see Chapter 8).

Biotite is found usually as rims to opaque oxides or in matted swathes associated with the breakdown of amphibole crystals. 'Metasomatic' biotite occurs as coppery flakes in trachytic supracrustal rafts contained in FDF-Nepheline syenite of C Motzfeldt and is developed in syenites adjacent to enclosed rafts of Julianehåb granite (ie, near Camp 15, S Motzfeldt). For geochemical considerations see Jones (1980).

3.5 Introduction to the structure and country rock

3.5.1 Introduction

The Motzfeldt Centre is a high-level, nested pluton. In plan view the Centre only partially displays the 'typical' ring pattern of outcrop. This is because at present the centre is exposed close to the complex roof zone of the intrusion. Deep glaciers, however, have in places, dissected the area to approximately 1.5 to 2 km below the roof surface. The Centre was emplaced passively. Large scale block subsidence, directly related to transtensional stresses in the region (see Part Four) facilitated the rise and accumulation of the alkaline magmas. This accumulation took place at the Julianehåb Formation/Eriksfjord Formation unconformity. The sequence of Plates (3.4 to 3.11) show the overall structure of the area and the general relationships between the rock units

3.5.2 Country rock

This study has placed little emphasis on the country rocks surrounding and occurring as xenoliths within the Centre, and therefore for detailed description the reader is referred to previous studies by Emeleus and Harry, 1970; Jones, 1980 and more recently, Larsen and Tukiainen (1985).

Jones (1980), suggested that the units are part of the Ilimaussaq Volcanic Member (Poulson, 1964). Larsen and Tukiainen (1985), however have correlated the *in situ* section of Eriksfjord Formation around Motzfeldt, (which essentially consists of a lower sequence of sandstone, resting unconformably on the Julianehåb Formation with an upper sequence of mixed sandstone and volcanic rocks rich in agglomerates), with the Majut Sandstone Member and Mussartût Volcanic Member respectively (Poulson 1964). The latter is characterised by the occurrence of carbonatites and ultramafic volcanics, and indeed the first and largest intrusion of the Motzfeldt Ring Series, the Motzfeldt Sø Formation, contains many basic and carbonatitic rafts (Plate 3.3a), see also chapter 5). The outer regions of this Formation (MSF-Altered syenite) also display signs of interaction with the quartzites. Most outer areas are unusually high in silica with some showing clear

granoblastic quartz (eg, 304068) and others interstitial free-quartz. The later intrusions of the Flinks Dal Formation similarly contain great subhorizontal supracrustal rafts, up to 3 km in length. These however are predominantly of trachyte and phonolite composition, and the surrounding nepheline syenites show little or no interaction with quartz bearing rocks. From this it is concluded that the Motzfeldt Sø Formation incorporated through subsidence, stoping and assimilation, most of the Majut and Mussartût members, while the Flinks Dal Formation members penetrated beyond the Motzfeldt Sø Formation roof and into a higher supracrustal sequence. If the Eriksfjord Formation succession was reduced in this eastern region[1] then this higher sequence is almost certainly part of the Ilimaussaq Volcanic Member (as suggested by Jones (1980) on trace element geochemical considerations), which was proportionally lower in sandstone and higher in more evolved lavas. Jones (op. cit.) also noted the geochemical similarity between the evolved lavas and the plutonic units of Motzfeldt and suggested a generic relationship. The Motzfeldt Centre may therefore be yet another example of a pluton intruding into its own ejecta (cf: Myers 1975).

3.5.3 Contact relations

The outstanding three-dimensional exposure of Motzfeldt exhibits dramatically many of the roof and internal contact relations (Plates 3.3 to 3.11). Many of these features can be compared with those described by workers in the great batholiths of the Andes (eg. Knox, 1974; Pitcher, 1977; Cobbing et. al. 1981). Unfortunately, because Motzfeldt is exposed around its roof zone, there is little indication of the elusive 'floors' to the intrusive units (cf; Buddington, 1959) although detailed study at low elevations in Motzfeldt, S of the Flinks Dal Fault may prove to be very informative.

i. The external roof

The roof contact is convex upward and penetrates into the Eriksfjord Formation in central parts of the pluton (Plate 3.5) but remains roofed by the Julianehåb Formation

[1] as envisaged by Jones, (1980)

along its flanks (Plate 3.4) The greatest thickness of *in situ* Eriksfjord Formation in contact with the Centre is c.800 m and is exposed in the 1696 m cliff in NE Motzfeldt (Plate 3.5) The supracrustal rocks at this position however are dipping SW at c.45° and therefore, this rotated block gives an unusually large thickness. The c.300 m of Eriksfjord Formation which is in contact with the Motzfeldt Sø Formation in NE Motzfeldt on the 1487 m hill probably gives a more reliable figure for the maximum penetration above the planar surface.

ii. The Internal contacts

Internal contacts between the syenite units are invariably sharp, outwardly dipping and steep to very steep. Accidental inclusions are abundant and are good indicators of younging. Chilled margins occur in units of the Flinks Dal Formation whereas an increase in pegmatitic development is a characteristic of the external contacts of the Geologfjeld and Motzfeldt Sø Formations. Detailed contact relations between the units are discussed more fully in the following chapters. Of note however, are the two complex roof zones of NE Motzfeldt and SW Motzfeldt. In both cases the roof is of an earlier syenite. In NE Motzfeldt the Motzfeldt Sø Formation is partially roofed and walled by the Geologfjeld Formation, which is itself roofed by the Julianehåb Formation. The subsidence related to the emplacement of the Motzfeldt Sø Formation has repeatedly fractured the GF-Geologfjeld Syenite along subhorizontal planes which parallel its own roof contact. As this block foundered the sequence of fractures was utilised by the vast number of microsyenite sheets (over 100 individuals) which were extended from the volatile rich Motzfeldt Sø Formation (Plate 3.11). In SW Motzfeldt it is suggested that a similar situation may have developed involving lujavrite sheets which extend from the Flinks Dal Formation into the older neighbouring MSF-Nepheline syenite.

3.5.4 Faulting

Faulting in the Motzfeldt region occurred in response to left-lateral wrench stresses which affected the whole of the Gardar Province (see Chapter 9). The structures present are strikingly similar to those predicted using clay models in left-lateral, simple shear,

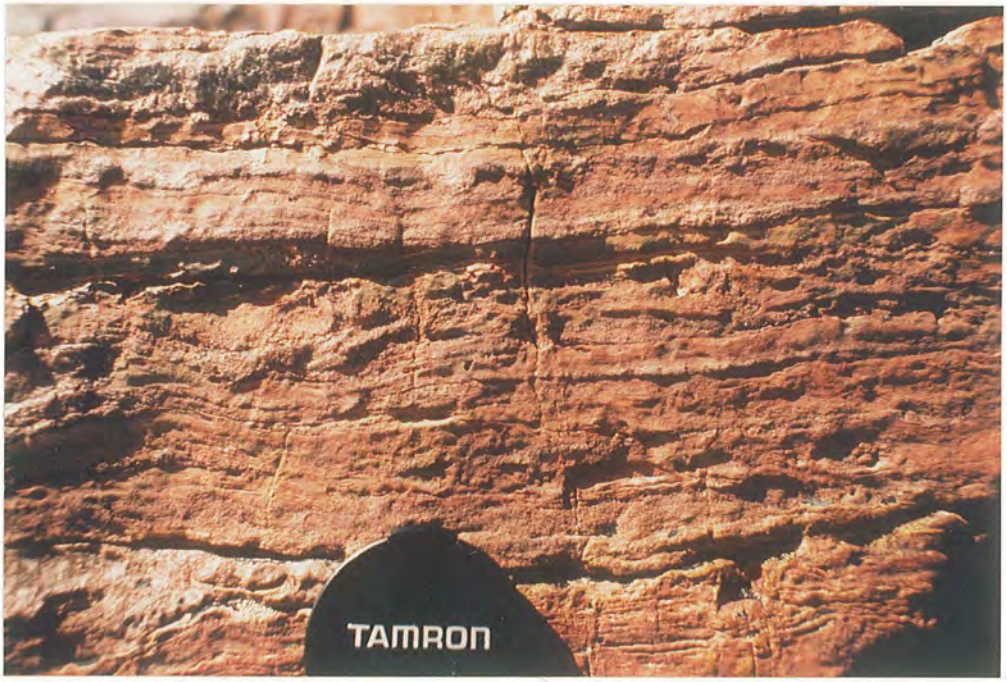
stress regimes (Wilcox et al., 1973; Fig 9.1.2). Bisecting the Centre, is the sinistral strike-slip Flinks Dal Fault. Approximately 6 km of lateral movement has been demonstrated along this fault (Tukiainen, 1981; Bradshaw, 1985). On a regional scale this fault is an arm of the major strike-slip structure referred to in Part Four as the Qagssiarssuk Fault, which extends through South Qôroq, the Qagssiarssuk region and across the whole Gardar Province (Fig. 9.1.1). Vertical movement along the Flinks Dal Fault is at least 400 m (probably, 700 m), downthrow to the N (cf: Jones, 1980). This is indicated by the elevation of the Julianehåb Formation/Eriksfjord Formation unconformity which is found generally above 1700 m S of the fault and at approximately 1300 m to the N. Furthermore, investigations of the Flinks Dal Formation units (this work, Chapter 6) on either side of the fault in C Motzfeldt, also confirm this movement. In the SE the South East Motzfeldt Fault (Tukiainen, 1986b) is a WNW-ESE sinistral, strike-slip fault which is an arm of the Flinks Dal Fault. Movement is in the order of 1 km (horizontal left-lateral) and 100 to 200 m downthrow to the N. On a theoretical model of left-lateral wrench faulting (Fig 9.1.2) the South East Motzfeldt Fault and the Flinks Dal Fault represent secondary synthetic shear and synthetic shear faults respectively and are exactly the structures predicted from simple shear conditions (see also Stephenson, 1976a). Associated with this stress system, both theoretically and in Motzfeldt are ENE-antithetic shear faults which have relatively small (< 100 m) dextral displacements (if any). In Motzfeldt these faults, although representing minor displacements have had a profound effect on the topography of the area, and are depicted now by numerous linear 'v'-shaped valleys.

a.



EF-Quartzite. NE Motzfeldt. Showing cross-bedding and ripple marks. (CB.82.C.06.01).

b.



EF-Siltstone. NE Motzfeldt. Probably lacustrine sediment with medium and fine layers, infilled mud cracks and occasional graded beds. (CB.82.C.06.03).

Plate 3.2

a.



Volcanic plug. NE Motzfeldt. The plug intrudes EF-quartzite and contains sub-rounded blocks of basalt, quartzite and granitic rocks in a coarse tuffaceous matrix. (CB.82.C.05.32).

b.



EF-Agglomerate. NE Motzfeldt. Well rounded blocks of quartzite predominate. (CB.82.C.13.02).

a.

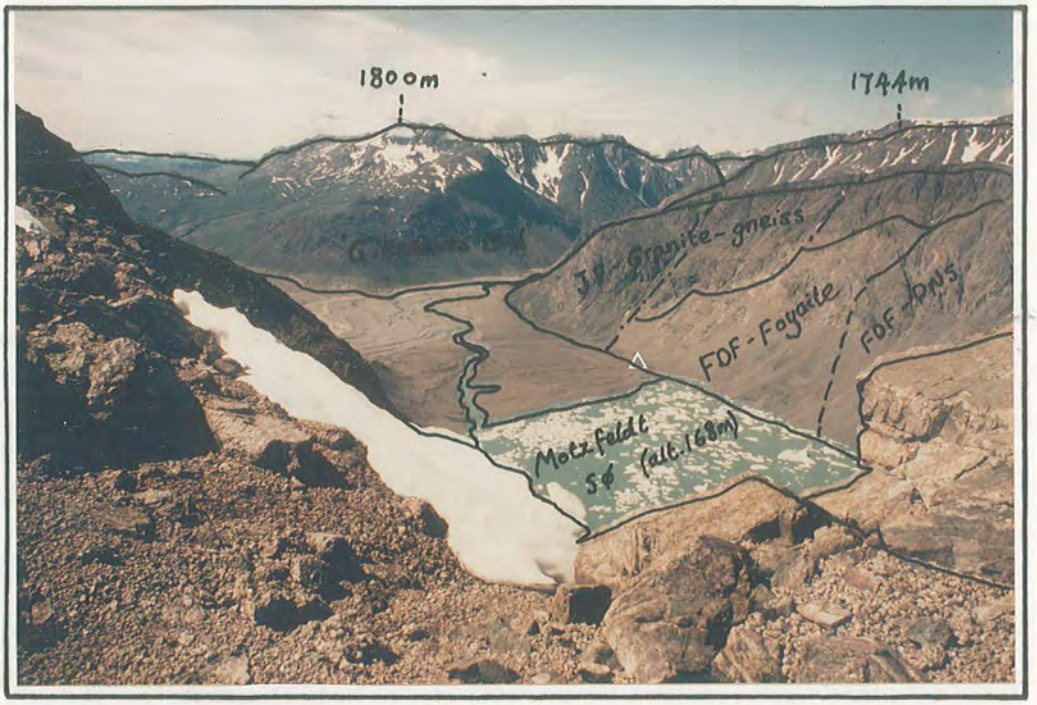


EF-Basalt/agglomerate raft in MSF-Altered syenite E Motzfeldt. View N of cliff face overlooking Sermia qiterdleq. Only the upper half of the raft is shown. The raft is over 400 m in length and 100 m thick. (CB.82.C.05.06).

b.



Trachytic raft in FDF-Nepheline syenite. C Motzfeldt. Close view showing net veining and brecciation by syenite material. (CB.82.C.09.15).



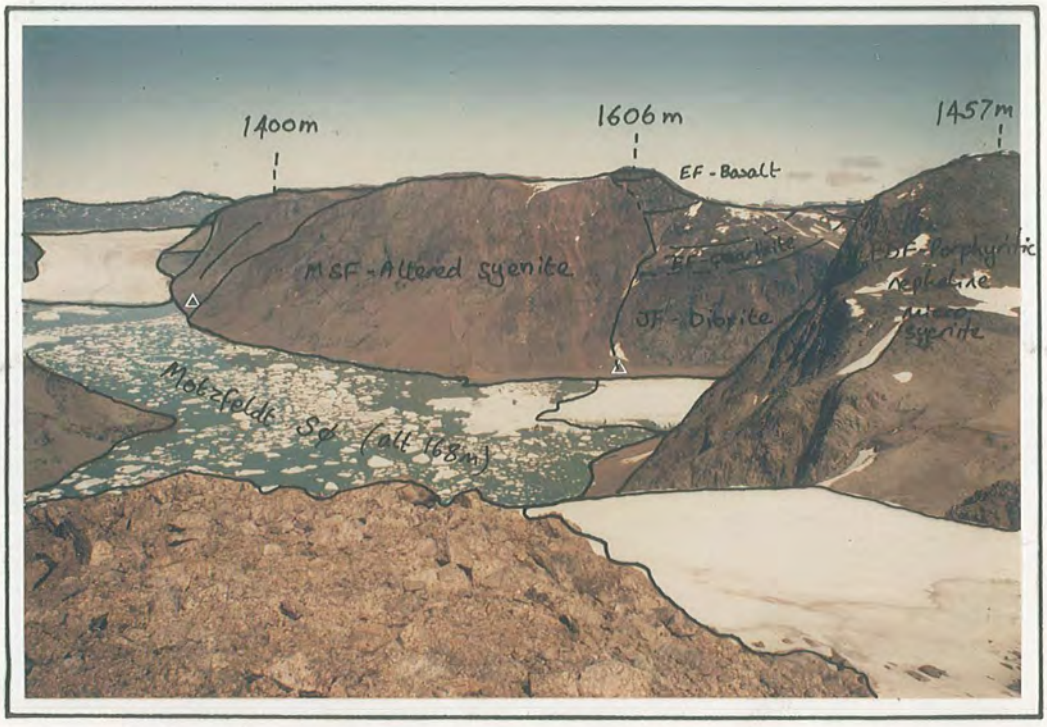
a.

View SW across the south end of Motzfeldt Sø, showing the west facing cliffs of S Motzfeldt and 'Gieseckes Dal' beyond. (CB.84.C.07.08).



b.

View NE from C Motzfeldt across the glacier Avanardleq to the mountain of Geologfjeld, NE Motzfeldt. (CB.82.C.13.17).



a.

View north across Motzfeldt Sø to NE Motzfeldt. The glaciers Avanardleq (left) and Qiterdleq (right) terminate and calve into Motzfeldt Sø. Camp 10 was situated on the marginal moraine of Qiterdleq, centre right of photograph. (CB.84.C.07.10).



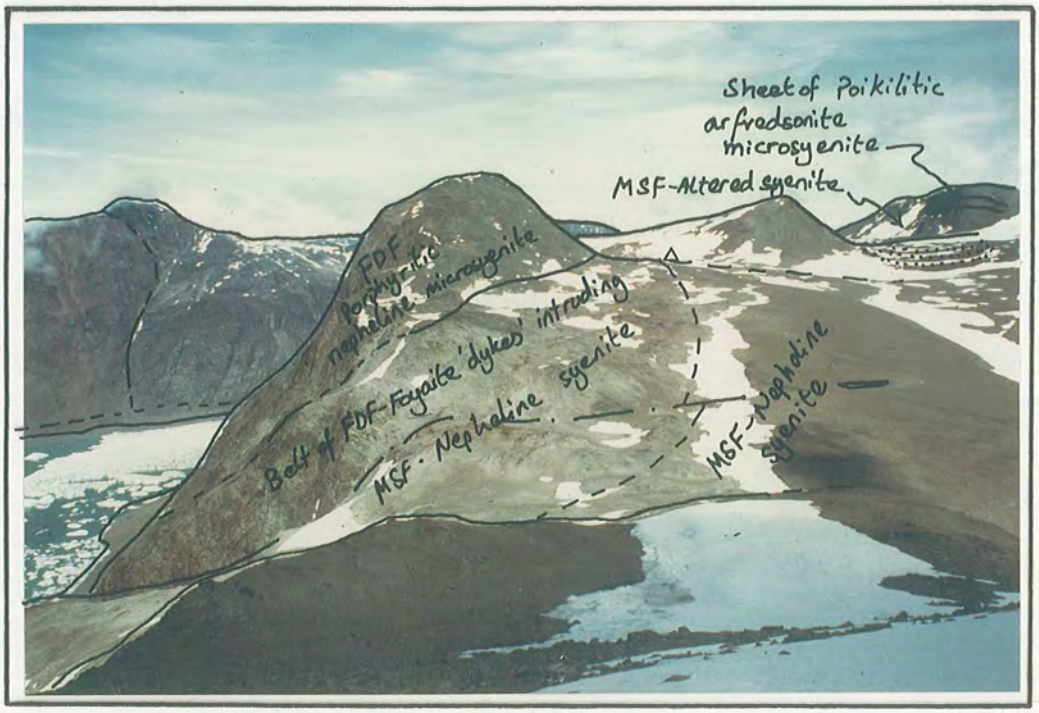
b.

View NW, showing the northern tip of SE Motzfeldt (foreground), NE and C Motzfeldt (middle) and NW Motzfeldt (background). (CB.82.C.02.04).



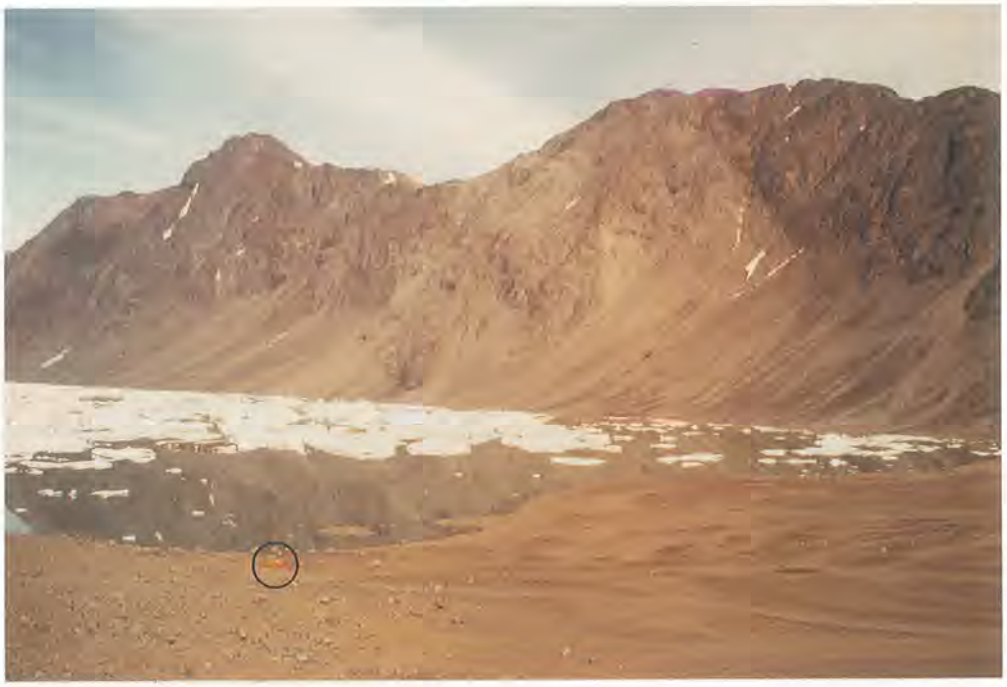
a.

View E along Flinks Dal with the mountains of NE Motzfeldt in the distance. Camp 12 (alt. 750 m) was situated beside the lake seen in the centre of the photograph. (CHE.62.C.01.37).



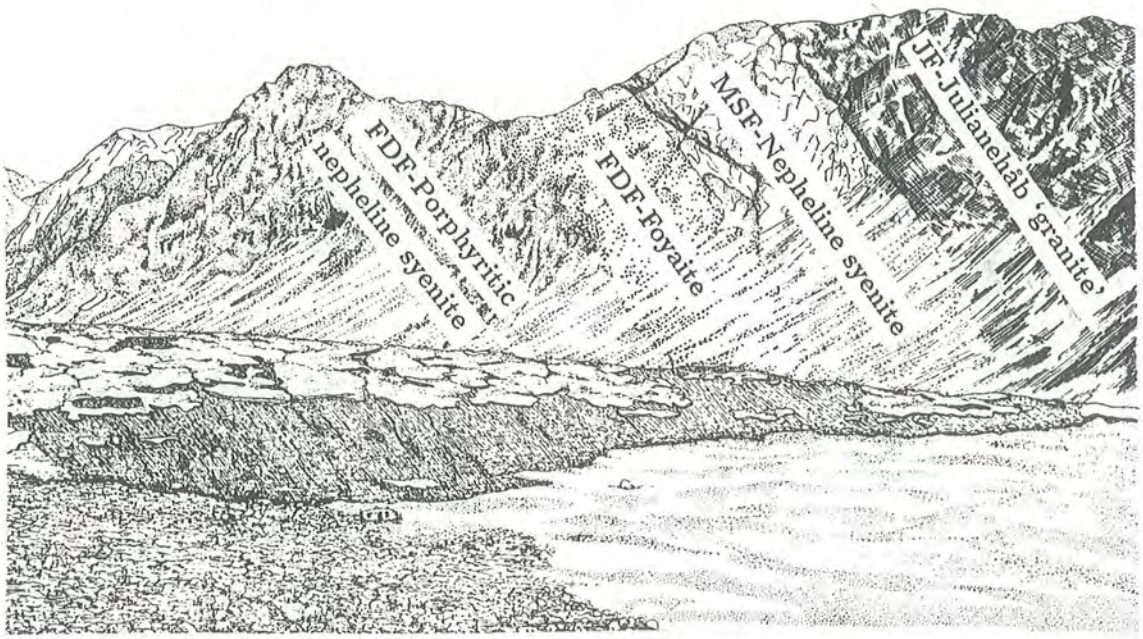
b.

View north of the area around Camp 2 in SE Motzfeldt. The camp (alt. 1175 m) was situated at the northern end of the plateau. (CB.82.C.01.26).



a.

The west facing cliffs of SE Motzfeldt. Viewed from the south end of Motzfeldt Sø. Camp 15 (alt. 180 m) in the foreground. (NJGP.84.C.15.16).



b.

Sketch showing the concentric ring structure of the syenite units as seen in the photograph above. The cliff section is approximately 6 km long and 1 km to 1.3 km high. (Drawing by Joan Collins).

a.

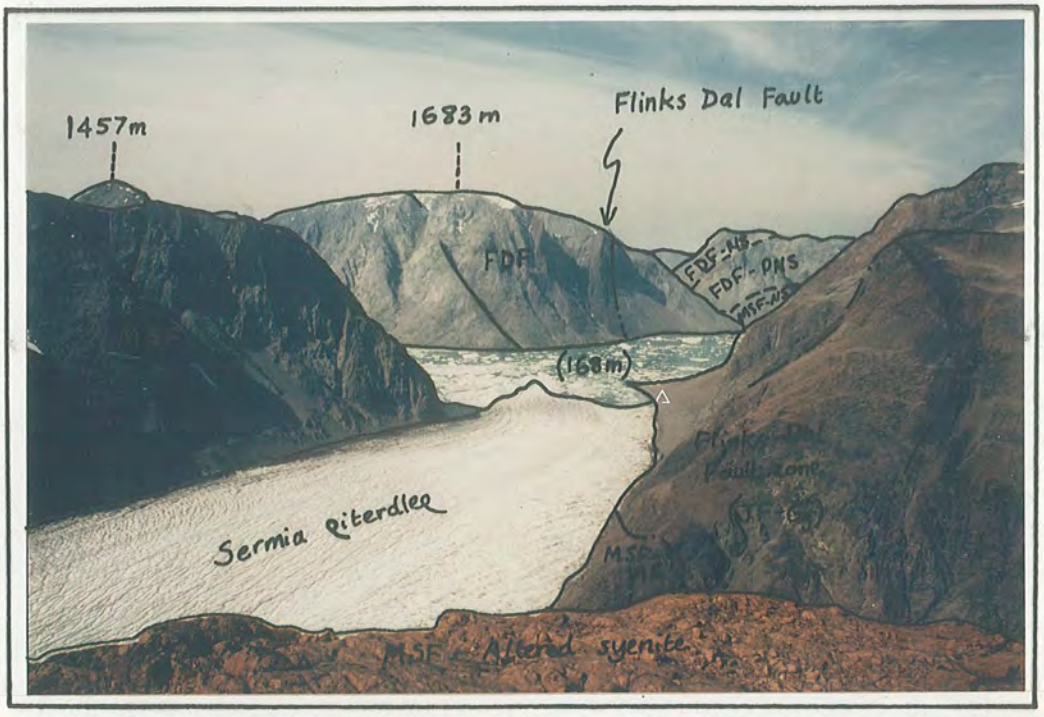


View NW from C Motzfeldt across Qôrqup sermia to NW Motzfeldt and Mellemlandet. Camp 17 (alt. 490 m) was situated beside the lake seen left of centre in the picture. (CB.82.C.09.13).

b.

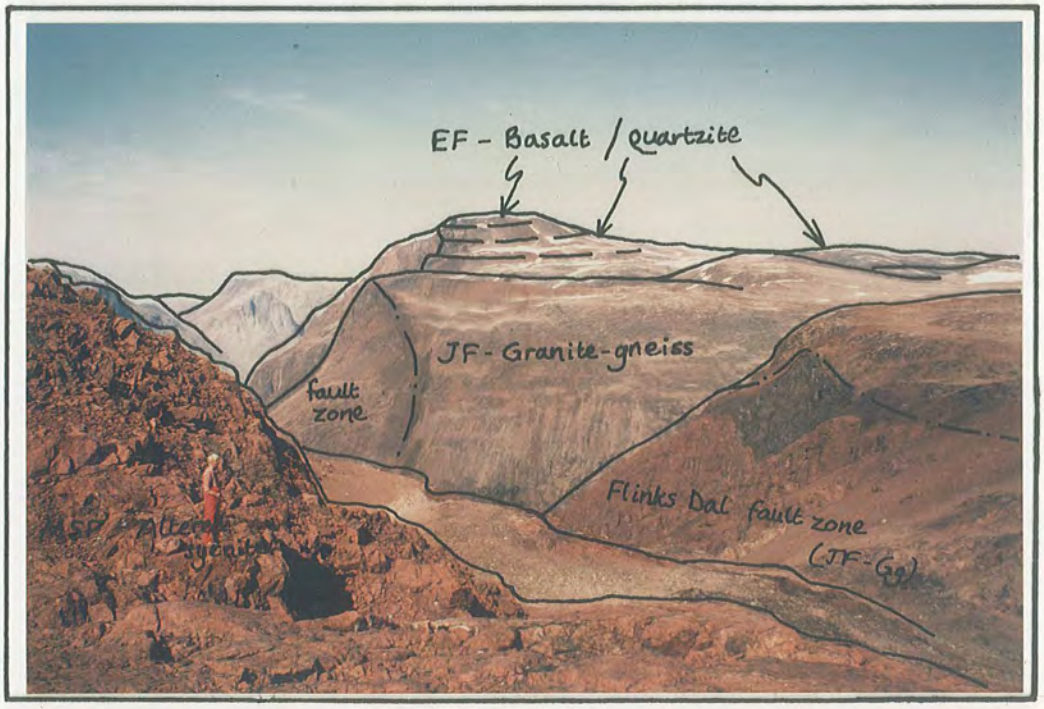


View ESE across Qôrqup sermia to the northern tip of C Motzfeldt. (CB.84.C.02.17).



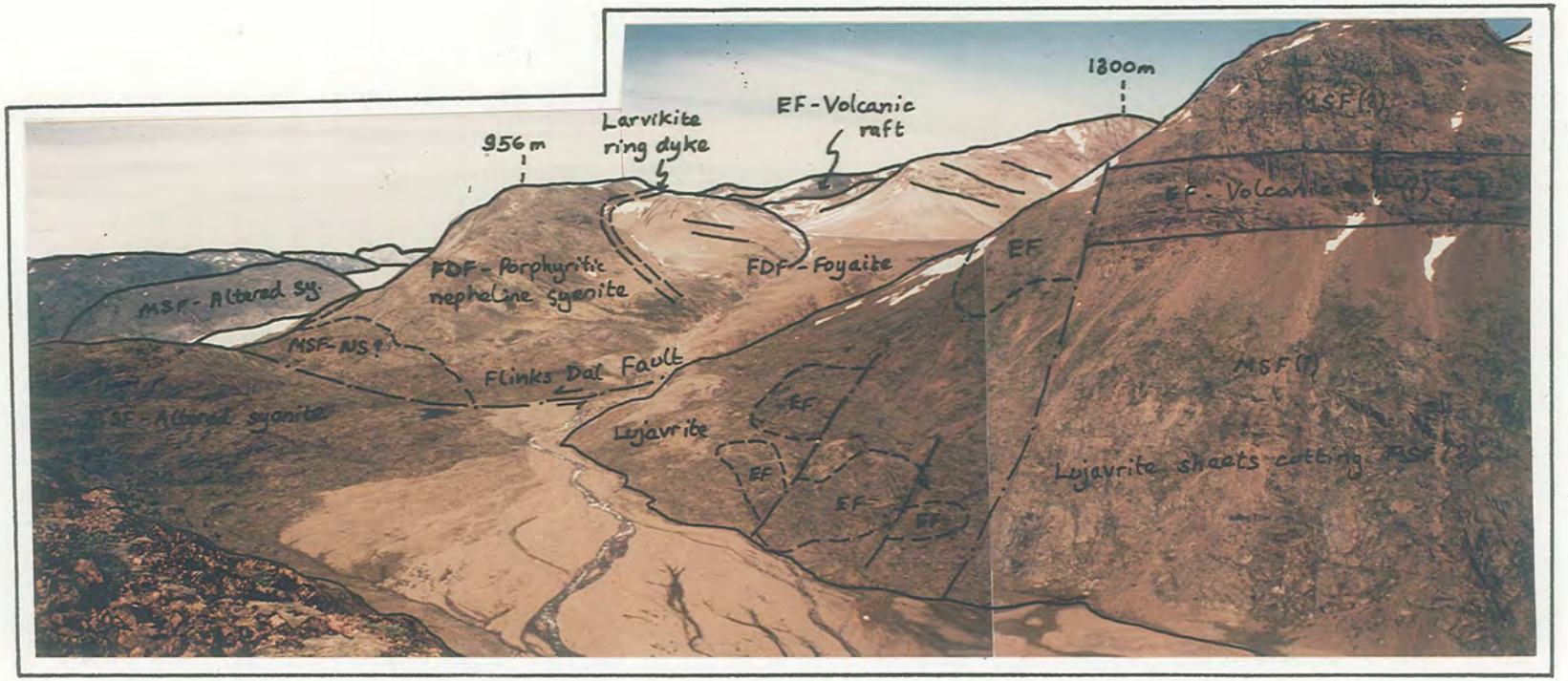
a.

View west from E Motzfeldt along Sermia qiterdleq and across Motzfeldt Sø. The mountains of S Motzfeldt are in the distance. (CB.82.C.04.17).



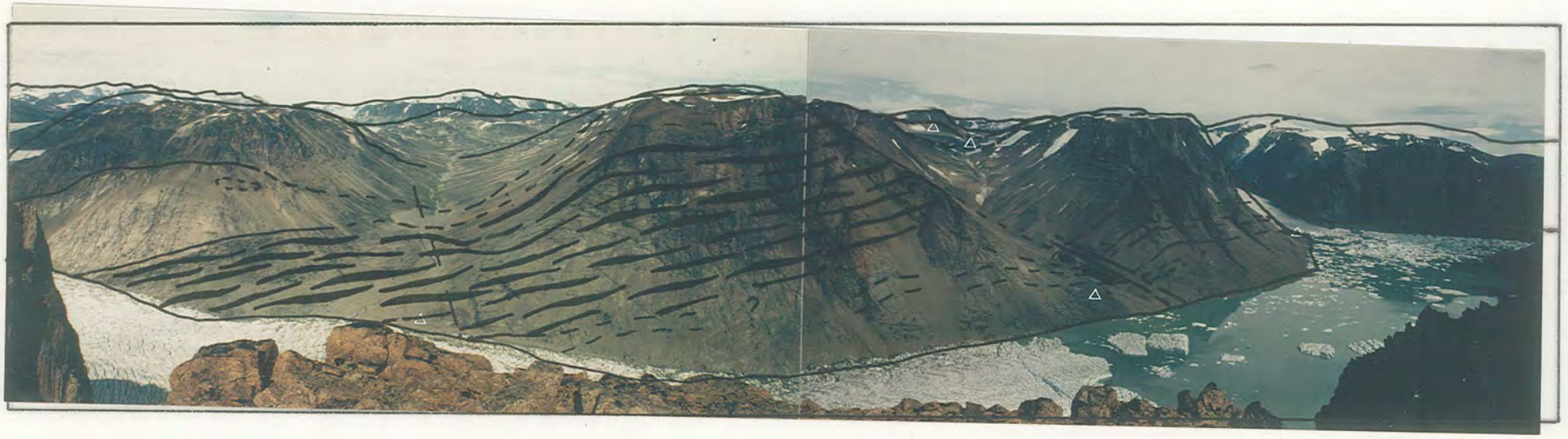
b.

View WNW showing the plateau area of NE Motzfeldt with the Flinks Dal fault zone in the foreground. The geologist is standing on red MSF-altered syenite. (CB.82.C.04.10).



View N showing 'lower Flinks Dal' (foreground) and C Motzfeldt (west) beyond. Camp 11 (alt. 255 m) can be seen in the low-middle of the picture. (CB.84.C.04.32) and (CB.84.C.04.31).

Plate 3.10



Panoramic view of NE and SE Motzfeldt viewed E from C Motzfeldt showing clearly the great valleys of Storeelv and 'Ljer elv'. The authors camp sites in NE Motzfeldt are indicated.

Plate 3.11

Chapter 4 - The Geologfjeld Formation

4.1 Introduction

The Geologfjeld Formation comprises a group of syenites (*sensu lato*) which represent the earliest plutonic intrusive members of the Motzfeldt Centre. They are satellite intrusions which pre-date the main ring-centre units known as the Motzfeldt Ring Series. The Formation includes the satellite of 'North Motzfeldt syenites'; NM1 and NM2 of Emeleus and Harry (1970) and the Geologfjeld syenite of Bradshaw and Tukiainen (1983). The Formation is divided into 3 members, each more undersaturated than the last, namely (oldest to youngest); **GF-Geologfjeld syenite, GF-Pulaskite** and **GF-Nepheline syenite**. Characteristically the members are white to pale-grey in colour and host very little radioactive mineralisation. All have been truncated by the younger syenites of the Motzfeldt Ring Series, which geographically separates the Geologfjeld syenite from the North Motzfeldt Satellite. It seems probable that these syenite bodies were originally part of the same, roughly concentric, internally overlapping, multiple intrusion. Although the Formation now occupies an area totalling some 20 km^2, an area of at least equal size was probably removed by the emplacement of the Motzfeldt Sø Formation. The petrography and geochemistry of the GF-Geologfjeld syenite is very similar to the GF-Pulaskite. They are unequivocally closely related and may in fact belong to the same syenite body, now 'cored' out (and consequently separated) by the GF-Nepheline syenite. They are also the least evolved major intrusions in Motzfeldt and are classified here as hypoalkaline syenites (see section 3.3). The chemistry is typified by the predominance of Ca - amphiboles and pyroxenes, low concentrations of incompatible elements and high levels of Ba and Sr. The GF-Nepheline syenite although more evolved (alkaline), still contains relatively low concentrations of incompatible elements[1] with mean values roughly half those found in the nepheline syenites of the Motzfeldt Sø and Flinks Dal Formations (see section 8.1.4).

1. Compared to other Motzfeldt units

Thus the Geologfjeld Formation is physically and chemically distinct from the main igneous phase the Motzfeldt Ring Series.

4.2 The Geologfjeld Syenite

4.2.1 Rock character and structure (Plates 4.1 & 4.2a)

The syenite is striking in appearance by virtue of its pale white-grey colour and its small and large scale homogeneity (cf: samples 304160 and 304159). The rock is a very coarse, subhedral granular syenite composed essentially of alkali feldspar, calcic amphibole and pyroxene with accessory Fe-Ti oxide and apatite. The rock is silica saturated and hypoalkaline. Mafic minerals occur as clot-like 'corona' aggregates 5 to 10 mm in size and commonly show signs of high temperature alteration. The mafic minerals are evenly distributed throughout the rock and comprise c.20% of the mode. The coarse, bladed feldspars are subhedral, randomly oriented and up to 3 cm in length.

The GF-Geologfjeld syenite now occupies an area of approximately 12 km^2 and consists of a 'sheet-like' body some 500 m thick. This body dips 25-30° NE and is sandwiched between the roofing Julianehåb Formation above and the undercutting Motzfeldt Sø Formation below.

The bulk of the syenite unit is very coarse and extremely homogeneous. Radioactive mineralisation is very low except where contaminated by younger intrusions. The unit in NE Motzfeldt has been intruded by a vast swarm of microsyenite sheets belonging to the Motzfeldt Sø Formation (Plate 3.11).

4.2.2 Field Observations.

i. NE Motzfeldt.

The syenite composes much of the ground between the valleys of Storeelv and Lejr elv. In the S facing cliffs of Storeelv the Geologfjeld syenite is roofed by granite-gneiss of the Julianehåb Formation. This contact is clearly exposed, convex upward and dips 25-30° NE (Plate 3.4b). Southward from Storeelv the syenite caps a high mountainous

WSW-ENE ridge that rises to 1482 m. Eastward along this ridge the unit is roofed by EF-quartzites and basalts. The S facing cliffs of this ridge provide an excellent (although inaccessible) cross-section through the Geologfjeld Formation/Julianehåb Formation and Geologfjeld Formation/Motzfeldt Sø Formation contacts, (Tukiainen, 1985, Fig. 3.a). The pale syenites of the Geologfeld Formation are clearly truncated downwards by the intrusion of the younger red syenites of the Motzfeldt Sø Formation. These red syenites extend farther E than the GF rocks and are themselves roofed by the Eriksfjord Formation succession. The Geologfjeld Formation/Motzfeldt Sø Formation contact dips roughly 30° NE. In the W facing cliffs between Storeelv and Lejr elv, overlooking Motzfeldt Sø , this relationship is hidden by the very thick (> 500m) sequence of sheet intrusions which comprise the MSF-Peralkaline Microsyenite Suite. The 'type' GF-Geologfjeld syenite is best exposed in the south facing cliffs of Storeelv and above the topmost microsyenite sheets of the Peralkaline Microsyenite Suite (Plate 3.4b). Within the sheet sequence the screens of Geologfjeld syenite show varying degrees of alteration (cf. 304172 & 304146). The extent of this alteration is dependent upon the composition of the adjacent microsyenite (see section 5.4). Where these effects are only slight, pale blue cores and pink rims to the feldspars depict clear zonal variation (eg, 304153). Mafic minerals are also distinctly 'fuzzy' in appearance. Very thin screens of syenite show a hard 'baked' character (eg, 304750) whereas others commonly display varying degrees of brittle micro- fracturing. The exact position of the Geologfjeld Formation/Motzfeldt Sø Formation contact in the area around camp 9, is unresolved. However, examination of the lower levels of the Geologfjeld syenite in this area show that the 'type' rock grades rapidly downwards from a coarse, homogeneous nepheline-free syenite through a zone approximately 20 m wide of pink-brown syenite with nepheline (Plate 4.2a), into a pink-brown feldspar laminated variety also with conspicuous (c.10%) nepheline. The westward extent of this syenite is obscured by the ring dyke of laminated Porphyritic syenite.

ii. NW Motzfeldt

The Geologfjeld syenite is of restricted occurrence. A narrow wedge (< 600m wide) is roofed by Julianehåb granite to the north and is clearly truncated by syenites of the Motzfeldt Sø Formation to the South. The Geologfjeld Formation/Motzfeldt Sø Formation contact is well exposed in places and is found to be sharp (Plate 5.5b) with several pegmatitic apophyses extending into the Geologfjeld syenite. The rocks exhibit contrasting weathering behaviours; near the contact the Motzfeldt Sø Formation is red coloured, competent and durable, whereas the paler Geologfjeld syenite is friable due to brittle microfractured feldspars and the altered character of the mafic minerals. Although the older syenite is stained over a 10 m zone, the characteristic white colour of the Geologfjeld syenite is rapidly resumed away from the contact (Bradshaw, 1985). This suggests that the rock was consolidated and therefore essentially impervious to the volatile phase that hematised, altered and mineralised the syenite of the Motzfeldt Sø Formation. (Tukiainen et al., 1984). Due to the close proximity of the Julianehåb Formation roof the syenite in NW Motzfeldt displays a patchy variation in grain size (Plate 4.1b). Commonly developed are coarse lenses up to 50 cm in size. The increase in grain size is gradational with no change in mineralogical composition (cryptic changes have not been investigated). Although, pegmatitic segregations are not fully developed, it is clear that this contact region was one of relative volatile enrichment.

4.2.3 Petrographic features (Plate 4.4a)

This is an homogeneous, leucocratic, subhedral-granular rock consisting of very coarse, equigranular mesoperthite/antiperthite and medium to coarse, clustered mafic minerals. Randomly oriented subhedral alkali feldspar (c. 10 x 6 x 4 mm) forms the greater part of the rock. A coarse interlocking mesoperthitic texture is always apparent, comprising clear lamellar twinned albite with subordinate slightly turbid microcline. The latter, which often displays fine-scale cross- hatch twinning, occurs not only intimately interwoven with the albite, but as rounded, irregular 'relics' upto 3 mm in size within the

large feldspar crystals. Crystal boundaries are commonly sutured and embayed and often seem to have partially corroded adjacent amphibole crystals. Late-stage albitisation therefore appears to have played an important role. Small (< 0.5 mm) altered nepheline occurs occasionally (less than 2%) as discrete irregular blebs in the feldspar. The feldspar chemistry in the norm (Table A3.2) gives a bulk composition of An 4.2, Ab 51.4, Or 44.4. This is probably a good approximation, except that the An content is too high due to the high Al content of the amphibole. The mafic minerals display synneusis texture and commonly show corona structure. The early formed subhedral clinopyroxenes (3 to 5 mm in length) are zoned salites and ferrosalites, coloured very pale mauve and pale apple green respectively. Slight pleochroism in these shades is usual. Calcic amphibole is present in amounts roughly equal to those of pyroxene (5 to 10%), occuring as individual subhedra up to 6mm in length, or more commonly as subhedral grains mantling and enveloping the pyroxene, oxide and apatite. The distinctive deep red-brown to pale yellow-brown pleochroic scheme is very consistent throughout the unit. Strong zonation, both optical and chemical, is restricted to the outer margins of the crystals where the colour changes to a deep green or deep green-brown. The amphiboles are very similar to those described by Ussing (1912) as barkevikite from the augite syenite of Ilimaussaq which were later renamed kaersutite by Fergusson (1969). Using Leake's nomenclature these 'barkevikites' prove to be predominantly deep red-brown hastingsitic hornblendes with deep green hastingsite rims (Fig 3.4.5c).

Apatite is the earliest formed mineral and is a consistent accessory occuring as small (0.1 to 1mm) individual prisms, enclosed almost exclusively within mafic clusters. Fe-Ti oxide similarly is closely associated with the clusters. Grains vary considerably in size: from 0.1 mm to 3 mm. All sizes may be mantled by amphibole but only the smallest appear enclosed by pyroxene. Rounded, iron-stained and corroded psueodomorphs after olivine are rare. Where the syenite has been thermally affected by later intrusion (eg, 304146) deep-brown to yellow-brown biotite has developed. This forms matted swathes around the oxide and amphibole, and granular aggregates confined within the amphibole. Green chlorite is associated occurring around and along fractures of the less altered

pyroxene. Sphene has occasionally developed with the concurrent break down of Fe-Ti oxide and Ca-amphibole. The feldspar shows finely disseminated sericitic alteration and extremely sutured crystal boundaries.

4.3 GF-Pulaskite

4.3.1 Rock character and structure (Plate 4.2b)

The rock is medium-coarse grained, subhedral granular, pale grey to white in colour and is typically massive and homogeneous. Mafic minerals occur as stout prisms 3 to 10 mm in length and are evenly distributed throughout the rock (15%). Randomly oriented, subhedral-blocky feldspars up to 10mm in length comprise the bulk of the rock. The individual feldspar crystals are difficult to distinguish but commonly have pale translucent cores and milky white rims. In thin section, analcite is a common (5 to 10%) interstitial accessory mineral.

4.3.2 Field observations.

Because this unit is largely cored-out by the GF-Nepheline syenite, their combined field relationships are described in section 4.4.2.

4.3.3 Petrographic Features (Plate 4.4b).

This rock is extremely similar petrographically to the GF-Geologfjeld syenite differing mainly in the increased amount of feldspathoid present. In the samples analysed normative nepheline content is always between 5 and 10%. The feldspathoid in the mode may be either analcite alone or analcite and nepheline. Analcite occurs as clear, fresh interstitial crystals, 0.4 to 3 mm in size, which may be isotropic or, as is more frequent, have very low, deep grey (often anomalous) birefringence. In one sample examined, (58352) analcite is found surrounding a euhedral but altered nepheline and is clearly a later phase. Nepheline is always rare and it is difficult to determine whether the analcite is its replacement or a separate late- primary or secondary phase. Interestingly, specimen 58352 also contains a large (3 mm) isolated crystal of idocrase.

4.4 GF-Nepheline syenite

4.4.1 Rock character and structure (Plate 4.3)

This pale, pink to grey syenite is characterised by the consistent development of small, coarse grained drusy patches in a medium grained matrix. The coarse areas, 2 to 10 cm in diameter, contain randomly oriented euhedral tabular feldspars up to 5 cm in length, interstitial dark minerals (15%) and abundant red to white nepheline (25%). The medium grained equigranular matrix is of similar texture and composition.

4.4.2 Field observations.

The combined outcrop of the two units GF-Pulaskite and GF- Nepheline syenite is oval in plan with a long axis of 8 km running SW-NE and a NW-SE short axis approximately 6 km in length. The GF- Nepheline syenite comprises the bulk of the outcrop and has 'cored out' the earlier GF-Pulaskite, restricting it to a marginal band some 200 to 600 m wide. The GF-Nepheline Syenite is abruptly truncated westward by the syenites of the Motzfeldt Sø Formation. This relation is clearly exposed (although inaccessible) in the south facing cliffs, on the E side of the small triangular glacier 1300 m SE from Camp 8. The contact is sharp dipping very steeply (75-80°) E striking approximately NNW-SSE. The arcuate band of GF-Pulaskite is reached approximately 1.3 km E of Camp 9. The GF-Nepheline syenite/GF- Pulaskite contact is generally poorly exposed but is marked by a distinct arcuate valley, concave westward. The contact is best exposed, on the 1233 m hill 1.2 km SE of Camp 4. The nepheline syenite becomes dense, medium-coarse grained and poor in nepheline (eg, 304048). The characteristic 'drusy' texture is not developed, mafic minerals remain small in size (< 2 mm) and occasional phenocrysts of feldspar can be seen. The unit sends aplitic veins into the adjacent pulaskite. The GF-Pulaskite/Julianehåb Formation contact occurs as a positive ridge feature approximately 600 m farther E. Close to its outer contact, the pulaskite becomes inhomogeneous and develops coarse pegmatitic patches with localised red staining. In addition, the diorites of the Julianehåb Formation, near this contact have suffered extensive, although local

fenitisation and are intruded by veins and apophyses of pulaskite (ie, 350 m E of Camp 4).

750 m E of Camp 4 the GF-Nepheline syenite contains prominent red-brown rafts (c. 30 x 20m) of trachytic lavas and agglomerates belonging to the Eriksfjord Formation.

This whole area occupied by the GF-Pulaskite and GF-Nepheline syenite (Plate 1.4a) is well summarised by Emeleus and Harry (1970) .. ."The ground occupied by the North Motzfeldt syenites is high but generally undulating. An exception to this is the prominent hill (1300 m) within NM.2 which rises several hundreds of metres above the sea of boulders derived from the *in situ* disintegration of the syenites."

4.4.3 Petrographic features (Plate 4.5)

The primary minerals found in the rock include perthitic alkali feldspar (c.55%), nepheline (c.25%), Na-Ca amphibole (c.10%) and Na-Ca clinopyroxene (c.5%). Accessories include analcite, small amounts of Fe-Ti oxide, apatite and fluorite with the secondary minerals gieseckite and biotite.

Texturally the rock is consistent, having a coarse subhedral-'intergranular' character. Discrete, randomly oriented, lamellar feldspar crystals (c.6 x 3 x 2 mm) form a framework to the rock, with mafic minerals and nepheline confined to interstitial areas. No laminated foyaitic texture is developed, instead however, rounded pegmatitic segregations are common and characteristic (see also field description). The feldspars are perthitic and show well developed simple twins. Individual crystals are distinct and 'lath'-like, commonly over 6 mm in length. Unlike the alkali-feldspar which is cloudy in plane polarising light the equant nepheline subhedra are generally clear although often partially altered to a white micaceous mineral (gieseckite). The crystals range in size from 2 to 5 mm, are evenly distributed, and are often 'sub-ophitic' to the earlier formed feldspar. Mafic minerals tend to occur as isolated, poorly formed subhedra less than 3mm is size. The ratio of pyroxene to amphibole may vary from specimen to specimen, however the latter is normally dominant. In common with all nepheline syenites from the Motzfeldt Centre, the

mafic mineral content shows a wide range of composition and very strong zonation. The pyroxene may be zoned from very pale mauve/pale green ferrosalite to dense grass-green aegirine-hedenbergite, however it is the latter pyroxene which dominates. In addition, less common green aegirine is found as small late crystals. The dominant amphibole is a very deep green to brownish-green katophorite with subhedral crystals ranging from 1 to 4 mm in size. Some crystals have paler brownish cores of ferroedenite.

4.5 Sodalite nepheline syenite (Formation uncertain)

This rock was originally discovered in 1982 in SE Motzfeldt (Bradshaw & Tukiainen, 1983) and was thought to be a remanent of a satallitic stock belonging to the Geologfjeld Formation. Subsequent field work has shown this to be unlikely (Bliksted, 1984 - GGU: field notes) and that the rock 'body' belongs to the MSF-Altered syenite.

As the name suggests the rock is characterised by the presence of primary and conspicuous sodalite (Photos 3 & 4 of Bradshaw & Tukiainen, 1983). The rock is subhedral, equigranular, medium-coarse grained and of pale pink-grey colour. It is comprised of pale grey-blue sodalite approximately 4 mm in width, red nepheline (3 to 5 mm), alkali mafic minerals (3 to 6 mm), and alkali feldspar (4 to 8 mm) in length. The modal volume proportions are about 15,12,10 and 60% respectively.

The rock is remarkably fresh[1] and forms an *in situ* exposure of limited extent (c.40 m x 10 m) at an altitude of 1510 m, 0.8 km SW of the 1739 m peak. The syenite appears to be truncated upwards at an altitude of 1550 m by the cross-cutting, suhorizontal, Poikilitic arfvedsonite microsyenite sheet (Bradshaw & Tukiainen, 1983). Laterally the exposure is very limited and the exact relationships are unknown. Bliksted (1984 - GGU: field notes) found evidence, in loose blocks, that the rock gradually merges into the adjacent MSF-Altered syenite.

This small but lithologically remarkable 'body' therefore represents a Cl rich pocket of magma which somehow remained largely unaffected by the deuteric/hydrothermal

[1] particularly for that area of Motzfeldt
Fresh in the sense – not mineralised

alteration which stained and mineralised the surrounding rocks of the area. The rock probably belongs to the Motzfeldt Sø Formation and not the Geologfjeld Formation (cf: Bradshaw & Tukiainen, 1983).

a.



Geologfjeld syenite. NE Motzfeldt (Storeelv). Typical example. Very coarse, homogeneous and white in colour. Boulder 35 cm tall. (CB.82.C.07.24).

b.



Geologfjeld syenite. NW Motzfeldt. Heterogeneous variety from roof zone. (CB.84.C.12.14).

a.



GF-Geologfjeld syenite. NE Motzfeldt. Strongly 'baked' variety with up to 10% interstitial nepheline. Near MSF contact? (CB.84.C.03.23).

b.



GF-Pulaskite (NM1). NE Motzfeldt. Typical example, coarse, white and homogeneous. Interstitial analcite/nepheline difficult to distinguish in hand specimen. (CB.82.C.05.17).

a.

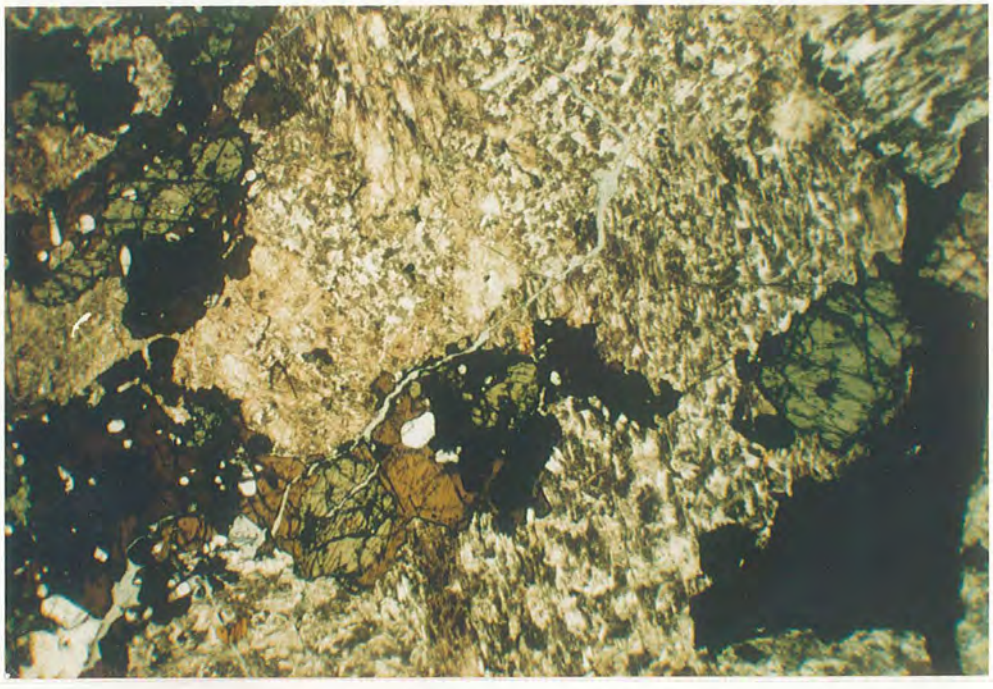


GF-Nepheline syenite (NM2). NE Motzfeldt. Typical variety, showing characteristic pegmatitic segregations. (CB.82.C.10.11).

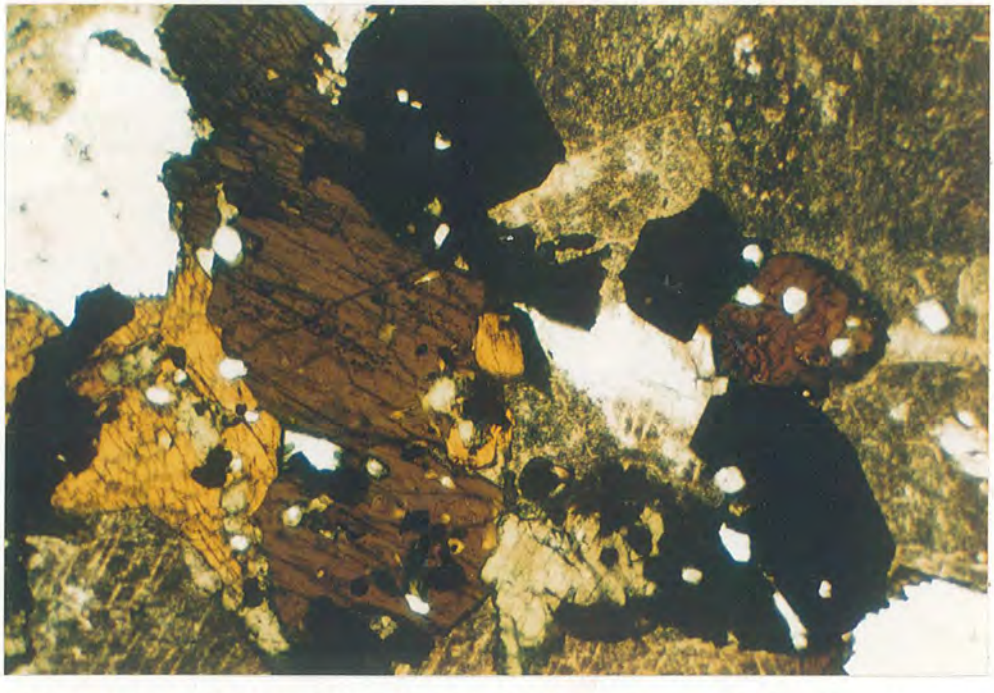
b.



GF-Nepheline syenite (NM2). NE Motzfeldt. Close up showing similar modal mineralogy of the coarse patches and the finer matrix. (CB.83.C.01.20).

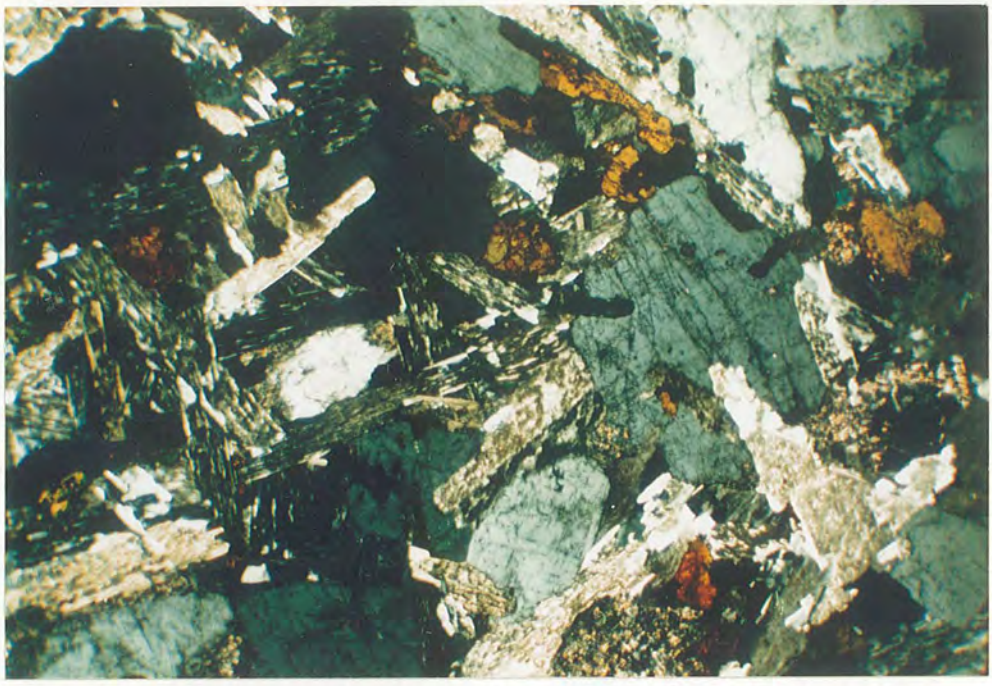


GF-Geologfjeld syenite. NE Motzfeldt. (304160). Mesoperthite and mafic clusters comprising pale green salite/ferrosalite, brown hastingsitic hornblende/hastingsite, magnetite and small clear apatite crystals. P.L. 9 mm.

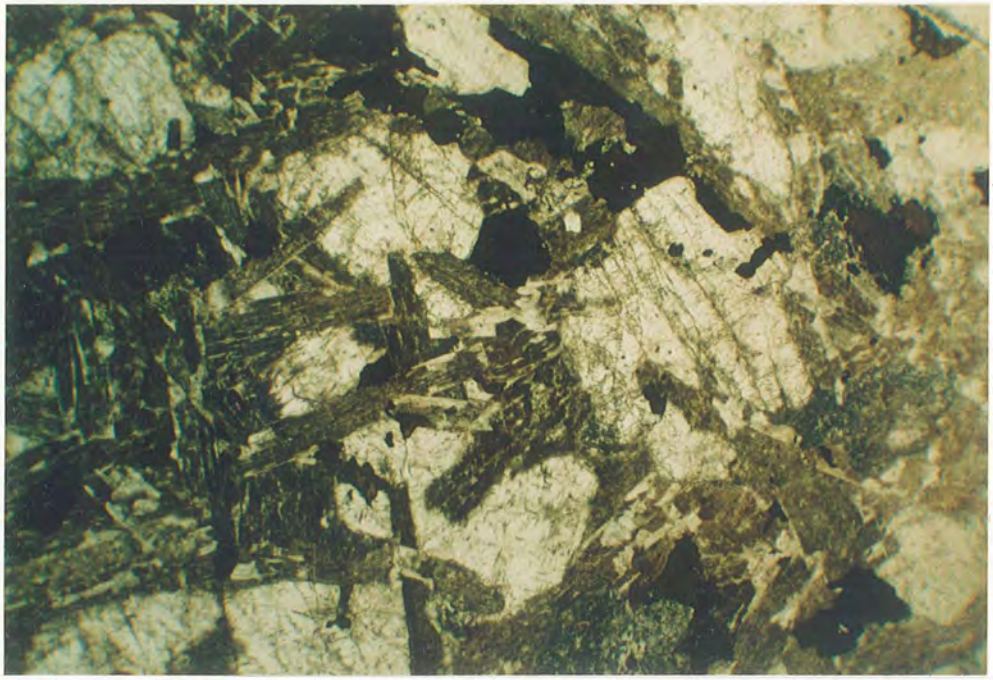


GF-Pulaskite. NE Motzfeldt. (58352). Mafic cluster similar to above but closer view. The clear mineral right of centre is analcite which makes up 5 to 10% mode of the rock. P.L. 5 mm.

Plate 4.5



GF-Nepheline syenite. NE Motzfeldt. (304055). X.P. 9mm.



As above. P.L. Mafic minerals include dark-green katophorite and grass-green aegirine-hedenbergite. Feldspar laths and equant nepheline subhedra are easily distinguished.

Chapter 5 - The Motzfeldt Sø Formation

5.1 Introduction

This Formation comprises the major syenite body (SM1) of Emeleus and Harry (1970) and is the first intrusive phase of the Motzfeldt Ring Series. GGU-SYDURAN field mapping enabled the unit to be further divided (Bradshaw & Tukiainen, 1983). Three concentric members are described and include an outermost **MSF-Marginal arfvedsonite syenite,** an **MSF-Altered syenite** and an inner fresh **MSF-Nepheline syenite.** The MSF-Marginal syenite and in particular the MSF-Altered syenite host extensive radioactive mineralisation and have therefore been subject to detailed investigations by the SYDURAN and PYROCHLORE teams. (Armour-Brown, Tukiainen & Wallin, 1982; Tukiainen, 1986c). Within the fresh Nepheline syenite, however, mineralisation is largely restricted to fracture zones extending from the altered areas. Although the Formation is subdivided, the members belong to a single major intrusion of alkaline to peralkaline trachyte/phonolite composition and are the products of combined, *in situ* differentiation, country rock assimilation, and later deuteric/hydrothermal modification (Tukiainen, Bradshaw & Emeleus, 1984).

5.2 Marginal arfvedsonite syenite

5.2.1 Rock character and structure (Plates 5.1 to 5.2a)

This peralkaline rock is very distinctive, essentially comprising 'brick' shaped (and coloured), red, euhedral alkali feldspar (c.10 x 3 x 2 mm) and blue-black interstital anhedral to euhedral arfvedsonite. Coarse mafic banding develops where the amphibole matrix varies in modal % per layer (Plate 5.1a). The mafic modal % ranges from 10 to 60% within the unit. Within the more felsic bands feldspars form the framework and the amphibole is restricted to the interstitial areas. In the mafic rich bands, amphibole occurs as euhedral prismatic crystals, 3 to 6 mm in length, showing the same preferred

orientation as the feldspars (304052). Both phases are laminated parallel to the mafic mineral banding. In areas where the exposure is good the lamination is clearly parallel to the Formation's outer contact and therefore may be the product of congelation accumulation of crystals against the chamber wall or roof (Bradshaw & Tukiainen, 1983).

The MSF-Marginal syenite represents a discontinuous outermost facies to the Motzfeldt Sø Formation and comprises an outer band, generally less than 500 m wide which is particularly well developed at high elevations in NE Motzfeldt. In NW Motzfeldt and at low elevations in the NE and SE the marginal syenite occurs within the coarse MSF-Altered syenite as discontinuous patches of varying size.

4.2.2 Field Observations

i. NE Motzfeldt

The marginal syenite is very well developed in a band approximately 300 m broad on the high ridge between the peaks 1443 m and 1487 m. Unfortunately only loose blocks are found, but they display very clear mafic layering (Plate 5.1b). The outer contact with EF- Quartzite to the E, is steep but poorly exposed. The EF-Quartzite shows little sign of disturbance or alteration. The MSF-Marginal syenite is also well exposed in a stream gully, 500 m S of Camp 8. The rock there (eg, 304165) shows moderate feldspar lamination (E dip 085°/345° strike) but poorly developed mafic banding. The feldspars are brick shaped, euhedral, red in colour and tightly packed (c 10 x 6 x 5 mm). The interstitial arfvedsonite (subhedral-anhedral) is accompanied by conspicuous rounded fluorite grains (1-2 mm). This rock grades rapidly westward into the coarse, red, feldspathic, hetrogeneous MSF- Altered syenite. Both the ridge and stream gully provide excellent profiles across the outer margins of the Motzfeldt Sø Formation. The Marginal/Altered syenite contact is gradational but rapid over a zone of several metres, where the marginal rock quickly becomes feldspathic, hetrogeneous and very coarse.

From Camp 10, at the western margin of Sermia Qiterdleq, the Motzfeldt Sø Formation/Julianehåb Formation contact can be examined at low elevations. The marginal 'facies' is poorly developed. Here the red syenites are similar in mineralogy but have an irregular patchy texture with small arfvedsonite-rich clots 2 to 5 cm in size. Low in the cliff face the syenite extends two, 3 m wide apophyses 50 m into the basement rock (diorite). The offshoots display distinct pegmatitic banding and mineral lamination, characteristic of the marginal facies. Sample 304710 is taken from a medium grained mafic rich band comprising subhedral alkali feldspar and subhedral to euhedral, prismatic black amphibole (40%) 2-3 mm in length. Fluorite is a common accessory.

ii. SE Motzfeldt

It was thought that much of the high ground of this area was underlain by MSF-Marginal syenite (Bradshaw & Tukiainen, 1983). More recent observations however have confirmed the widespread occurrence in the area of the Laminated porphyritic syenite (Bradshaw, 1985) which is extremely similar in hand specimen (see chapter 7). For instance, 3 km due S from Camp 2, a steep sided stream gully running NNW-SSE was thought to provide a clear section through the outer margins of the Motzfeldt Sø Formation. An arfvedsonite syenite forms a 500 m broad outer band in contact with Julianehåb basement gneiss. The feldspars are clearly laminated (eg, 304028), and dip steeply S. Foliation in the gneiss also follows the same trend. Large (20 x 25 m) stoped blocks of gneiss occur enclosed within the syenite in this area. Accessory quartz commonly occurs in the marginal syenite and has almost certainly been derived from the adjacent Julianehåb gneisses. However, in the high gound to the E of this area a PYROCHLORE field team (1984) found a massive country rock raft enclosed by similar arfvedsonite syenite. Above this raft the syenite was pale grey coloured and fresh, whereas below it was the typical[1] brick red colour. It was suggested that the pale grey rock had been protected by the raft from the upward migration of hydrothermal fluids which had so affected the rest of the unit (Bliksted, pers. comm. 1984). While this may still hold true, after investigation it

[1] typical of MSF-Marginal arfvedsonite that is

became clear that the grey rock was unquestionably the Laminated porphyritic syenite and identical to examples found further N in SE Motzfeldt, 1.5 km NE from Camp 2 (see section 7.3.2) as well as in NE Motzfeldt beside Camps 6 and 9. Further field investigations are necessary to determine the relative extent of the two arfvedsonite syenites in the area.

iii. NW Motzfeldt

The MSF-Marginal syenite is only partially developed in this area. The rock plays a subordinate role to the coarse feldspathic altered syenite and forms a discontinuous outer band to the Formation. Locally, however the characteristic texture and mineralogy of the MSF-Marginal syenite are very well developed. A good example is found 2.5 km NE of Camp 16, where the rock (eg, 326651), close to the outer contact is a medium-coarse grained, mesotype, arfvedsonite syenite with laminated euhedral feldspars. Inwards, this rock grades (within 100 m) to a coarse feldspathic and pegmatitic syenite.

iv. SW Motzfeldt

Red tightly laminated syenite does occur near the outer contact in this area (eg, 326033, 1.5 km SSE of Camp 11). This rock, the 'Brown syenite' of Jones, (1980) needs further investigation as he showed it to have an intrusive relationship with the adjacent syenites.

5.2.3 Petrographic Features (Plate 5.11)

The rock is typically medium to coarse grained, mesotypic and consists essentially of subhedral to euhedral arfvedsonite (25 - 60%) and euhedral to subhedral antiperthitic alkali feldspar (70 - 35%). The usual accessory minerals include, in order of abundance, fluorite, zircon, aenigmatite or opaque oxides and pyrochlore. In addition, very occasional crystals of Na pyroxene may be present. It has been previously suggested that the

rock is a product of congelation accumulation and crystallisation against the roof and sides of the chamber (Bradshaw & Tukiainen, 1983). In the field the rock may show distinct mineral lamination and also mineral layering on a 10 cm scale (See Plate 5.1b). The texture of the rock varies between these mineral layers. In feldspar rich bands the subhedral arfvedsonite is peripheral or occasionally subophitic to the well formed, laminated brick-shaped feldspar and ranges in size from 1 to 3 m. In mafic rich bands the arfvedsonite is subhedral to euhedral and 2 to 4 mm in length. The crystals are elongated and may show moderate to strong mineral lamination, which is invariably concordant with, and parallel to both the accompanying feldspars and the overall mineral banding (eg, 304052). Optically the arfvedsonite shows very little colour zoning which reflects their small within-crystal chemical variation (Fig 3.4.5a; Table A4.3). The pleochroic scheme and absorption are always intense and may be deep green to yellow green (eg, 304052) or very deep blue green to green (eg, 304165). Where complete extinction is seen the angle is small (0-3°) and birefringence almost completely masked by the body colour. A common feature to all sections examined is the resorbed and embayed or feather-like habit of amphibole when juxtaposed to feldspar. In addition, isolated islets of amphibole surrounded by albite are common and are in optical continuity with the nearby parent crystal. Thus suggesting a replacement origin for the antiperthite due to wholesale albitisation. The antiperthite itself is dominantly albite which shows striking lamellar twinning and is colourless and fresh in plane light. The K-feldspar occurs within the albite as coarse beads or patches often interlocking, and is easily distinguishable because of its lack of twinning and its mass of red powdery inclusions in plane light. The feldspar is characteristically brick shaped (bladed) 5 to 10 mm in length and is consistently larger than the accompanying amphibole. Fluorite can make up between 5 and 10% of the rock, occuring as very small inclusions in the amphibole or as equant isolated crystals 1 to 2 mm in diameter. Very occasionally tiny pyrochlore crystals which extend radiating fractures can be seen enclosed by the fluorite. Zircon is common (1-3%), forming very distinctive isolated euhedra 0.1 to 0.3 m. Pale yellow-brown isotropic

pyrochlore of similar size is less common. Red aenigmatite occurs sporadically (< 2%) as 1 mm anhedra and is always associated with the amphibole.

5.3 MSF-Altered Syenite

5.3.1 Rock character and structure (Plates 5.2b & 5.5)

The MSF-Altered syenite is characterised by its inhomogeneity. A consistent feature however, is the red colour. The syenite shows a whole range of textures from aplitic to pegmatitic and may be hololeucocratic to mesotypic. Typically the rock is alkaline to peralkaline in character, and silica saturated. Free quartz may occur near to the outer contact whereas nepheline (mainly altered) bearing varieties occur frequently near the fresh MSF-Nepheline syenite contact (eg, 304778). The rock is usually coarsely feldspathic with many very coarse pegmatitic patches. The MSF- Altered syenite occupies a broad ring outcrop (average 3 km in width) near the outer margin of the Motzfeldt ring series. SYDURAN mapping has shown the unit to be particularly complex with a broad radial zonation being apparent (Bradshaw & Tukiainen, 1983). Furthermore, the unit hosts a vast complex of pegmatite and microsyenite 'sheets'. This 'sheeted' complex known as the MSF-Peralkaline Microsyenite Suite extends from NE to SE Motzfeldt. Its overall cupola shape across this area possibly reflects the original 'bell-jar' shape of the original intrusion. Within the MSF-Altered syenite the 'sheets' exist as pegmatitic/aplitic, sub-horizontal segregations (Plate 5.4). That is, they do not have sharp intrusive relationships but rather undulating and concordant contacts. These sheet segregations are normally between 1 and 10 m wide and may be laterally consistent over several kilometres. They increase in frequency with elevation within the unit, but are still well developed some 1.5 km below the roof in the N and S facing cliffs of Sermia Qiterdleq (E. Motzfeldt). Where the sheet- segregations extend beyond the unit, and into older syenite (eg, NE Motzfeldt) or country rock (eg, SE. Motzfeldt) they form swarms of sub-horizontal sheets and are clearly intrusive (see section 5.4). Also contained within the

unit are huge quantities of EF-Supracrustal material. Much of the EF-Basalts and EF-Pyroclastic succession remain as raft material, whereas the EF-Quartzite has been largely assimilated. This influx of siliceous material has caused wholesale silica saturation (and in places oversaturation) of the magma in this unit. Moreover, connate water derived from the Eriksfjord Formation has probably played a major part in the development of the pegmatite and the extensive hydrothermal alteration (see Chapter 8). The MSF-Altered syenite has been of particular interest to the SYDURAN and PYROCHLORE teams because it hosts the majority of U-Th-Zr-Nb-Ta-REE mineralisation in Motzfeldt (Tukiainen, Bradshaw & Emeleus, 1984; Tukiainen et. al. 1984).

5.3.2 Field Observations

i. SE Motzfeldt

2 km SE of Camp 2, red stained syenite is encountered on the lower slopes of the W facing ridge. The coarse brick red syenite is heterogeneous, with red aplitic lenses bordered by pegmatite a common feature. These lenses range in size from a few cms to 1 m. Much of the local loose block debris is stained and sheared with black grey Fe/Mn oxide coatings. Similar rocks are encountered 100 m E from the 1402 m peak (1.5 km NE of Camp 2). Here MSF-Altered syenite occurs in shear zones which extend from the main MSF-Altered syenite body into the MSF-Nepheline syenite. The high radioactive counts of these zones indicate that mobilisation of mineralised fluids has probably been facilitated along late stage stress systems within the unit. Moraine of the adjacent plateau glacier which is almost totally composed of red stained MSF-Altered syenite also has many 'hot' red equigranular microsyenite veins with dark grey aphyric centres (1 to 20 cm wide) (eg, 304032). These veins gave radioactive counts up to 8x the background level. A notable feature of the W facing ridge of the 1739 m peak (viewed from the W) is what appears to be very large ($\geq$ 20 m) pale coloured blocks or rafts. Adventurous field work by a PYROCHLORE team showed these blocks to be pale trachytic lavas from the Eriksfjord Formation (Blikstead, pers. comm.). Sinuously banded microsyenites and

syenites (Plate 5.4) were discovered on a helicopter reconnaissance to the NE margin of SE Motzfeldt at the foot of the N facing 1768 m cliffs (altitude 600 m). The rocks are very distinctive with coarse pegmatite and mafic mineral layering that dips approximately 20 degrees SW. The mafic phases include dark mica and black amphibole, the latter often poikilitic. The feldspar occurs as small bladed crystals (3-5 mm) laminated parallel to the layering. This syenite also occupies ground at low elevations on the opposite side of Qiterdleq glacier in E Motzfeldt.

The MSF-Altered syenite of the high ground around 'Humbug-Brae' in northern SE Motzfeldt contains many xenolithic rafts of EF- Supracrustal. These include dark conspicuous metasomatised tuffs and agglomerates (up to 300 m in length), carbonatitic knolls and EF- Quartzite. (The latter is restricted in occurrence to these very high levels in the magma chamber). The area is particularly rich in radioactive minerals and has consequently been studied in detail by the PYROCHLORE team (Tukiainen, 1986c; Morteani et. al., 1986). In the high ground S of the SE Motzfeldt fault the MSF-Altered syenite is largely obscured by the sub-horizontal sheet of Poikilitic arfvedsonite microsyenite.

ii. E Motzfeldt

The red altered syenite forms the ridge (alt. 1100 m) that runs adjacent and roughly parallel to Qiterdleq glacier. The rock is massive, extremely feldspathic and coarse. Sporadic white fluorite crystals (1-2 cm) are frequent and white quartz is a common accessory at high elevations in this area. In fact quartz veining is very much in evidence near the eastern contact with the JF- Julianehåb granite, 150 m SSE of Camp 3. The most noteable feature along this ridge is the occurence of dark-green mafic metasomatised blocks of volcanic rock. These fragments cover a distance of approximately 100 m along the centre of the ridge. However, on helicopter reconnaissance of the S facing cliffs of this ridge the fragments could be clearly seen to belong to a huge supracrustal raft some 400

m in length and 100 m deep. The raft is dipping at about 65° W and is enclosed and partially fragmented by the MSF-Altered syenite (Plate 3.3a).

iii. NE Motzfeldt

Best exposure of this unit occurs along the upper reaches of the stream valley of Ljer elv and the adjacent ridges. The heterogeneous syenite found on the ridge between the peaks 1443 m and 1487 m (3.5 km W of Camp 4) is particularly altered, with Fe-Mn coated irregular mafic areas consistently present (eg, 304053). The background radioactive count of these syenites is approximately 4x that of the MSF-Nepheline syenite and locally can be over 10x. Syenite of similar texture and degree of alteration occupies the E margin of the cliffs N of Camp 10 (eg, 304722). Again the radioactivity count is high and the Fe-Mn oxide coatings abundant. A yellow ochreous alteration is also characteristic. Westward the rock passes gradually into a coarse more homogeneous, less altered syenite with less radioactive mineralisation. Exposures of the altered nepheline syenite unit in the 'Ljer elv' valley display rocks of variable character. Above 800 m elevation the red syenites are coarse and often pegmatitic (eg, 304140 & 304145). Below, the rocks become more finely grained and often show distorted mineral layering. Narrow (1-3 cm) radioactive veins abound and cut the stream section (dip 80° W/330° strike).

The MSF-Altered syenite near Camp 6 and close to Motzfeldt Sø , is very coarse, feldspathic and relatively fresh. This is probably due to the low elevation (c.200 m) and large distance from the units outer contact (c. 4 km). However, sub-horizontal mineralised shear zones (0.5 - 1 m) and narrow (1-3 cm) radioactive veins are abundant in the area. The latter have the same general trend as those mentioned in the last paragraph.

iv. C Motzfeldt (north).

In this area the red MSF-Altered syenite has a distinct 'colour' contact with the fresh pale MSF-Nepheline syenite (Plate 5.5a). No change in lithology or any evidence

of a separate intrusive event was detected. The MSF-Altered syenite has well developed pegmatitic bands and lenses and has low radioactive mineralistion. Airborne - spectrom etry data indicates that the radioactive mineralisation increases at the eastern margin of this area, a trend shown by the unit throughout the eastern half of the Centre (Tukiainen, Bradshaw & Emeleus, 1984).

v. NW Motzfeldt.

The MSF-Altered syenite is extremely well exposed in this area and its brick red colour makes the unit easy to distinguish, even from large distances (Plates 3.5b & 3.8a). The rock is very heterogeneous, with textures ranging from pegmatitic to medium grained. The bulk of the rock however, is generally very coarse, red, subhedral and granular (Plate 5.3b). Essential components are red alkali feldspar and black amphibole. Subordinate white or purple fluorite, green pyroxene (often fibrous) and zircon are all often visible in hand specimen. The outer contact with the JF-Granite gneiss is very sharp. The green-grey gneisses are reddened and partially fenitised over a 10 m contact zone. The red staining of the MSF-Altered syenite is accompanied by radioactive mineralisation. Consequently the unit in NW Motzfeldt is clearly distinguished from the neighbouring country rock by its elevated radioactive emissions, as shown by the airborne radiometric survey (Figs 8.2.1 & 8.2.2)

2.5 km S of Camp 16, sinuously banded syenites outcrop on a small peninsula on the northern shores of Qôroq (Emeleus & Harry, 1970. Fig. 8, pp25). Although the author has not visited this outcrop there are many textural similarities between this rock and the banded pegmatite/microsyenite sequences found at equally low elevation exposures of NE, E and SE Motzfeldt. 3 km NE of Camp 16 the Altered syenite intrudes GF-Geologfjeld syenite, leaving a wedge shaped outcrop (< 600 m wide) of the older syenite (see section 4.2). Because the GF-Geologfjeld syenite in this area is heterogeneous in texture and has a red stained appearance near the Motzfeldt Sø Formation contact it

can be difficult to distinguish. The GF-Geologfjeld syenite however, unlike the MSF-Altered syenite is generally friable, easily weathered and comprises brittle feldspars and altered dark minerals.

vi. SW Motzfeldt

Red stained and coarsely feldspathic syenites are located in this area near the outer contact with the Juliainehåb Formation, 1 km NW of Camp 11. This and the syenite comprising much of the 456 m hill W of Camp 11 is tentatively ascribed to the MSF-Altered syenite. The latter contains much pegmatite and microsyente as well as high levels of radioactivity.

5.3.3 Petrographic Features (Plate 5.12)

This unit is directly related petrologically and chemically, to the MSF-Marginal syenite into which it grades. Mineralogically there are many similarities, but in texture they differ considerably. The altered syenite is extremely heterogeneous due to the effects of a high volatile content and the incorporation of a large amount of country rock material. The rock is very coarse, often very feldspathic with ubiquitous pegmatitic/aplitic segregations. Locally very high concentrations of pyrochlore, zircon and numerous other Nb/Zr/REE minerals occur. For detailed descriptions of these, and of this unit as a whole, the reader is referred to the works of T. Tukiainen (1985a; 1985b; 1985c; 1986a; 1986b; 1986c).

5.4 MSF-Peralkaline Microsyenite Suite

5.4.1 Rock character and structure (Plate 5.6 to 5.8)

As discussed in section 5.3, this complex suite is genetically related to the MSF-Altered syenite and as such has been studied in detail by the GGU-PYROCHLORE team (Tukiainen, 1986c; Morteani, et. al. 1986) and was also the MSc project study of G Schwartz (University of Copenhagen). Consequently only a general description will be given here.

The Suite developed within the MSF-Altered syenite as late stage volatile/magma segregations, akin to the Lujavrite development of Ilimaussaq (Ferguson, 1964). Similarly, the suite is profoundly enriched in 'residual' elements Zr-Nb-TH-U-Be-LREE. The quantity of microsyenite/pegmatite material is vast, making up at least c. 400 m in thickness and stretching a distance of over 15 km.

5.4.2 Field relations

The suite may be conveniently described in the following three situations.

i. Intrusive relations of NE Motzfeldt.

The MSF-Peralkaline Microsyenite Suite is very well exposed and easily accessible from Camp 10 in the valley of Storeelv (Plate 5.6). In this area the sheets have a general dip of 20 to 40° toward the NNE and intrude the GF-Geologfjeld syenite. The sheets range in thickness from 1 to c.20 m and comprise a total thickness of over 400 m. Within the unit as a whole, the frequency of the sheets increases upwards until they make up over 80% of the bulk outcrop. Screens of white GF-Geologfjeld syenite remain, and in nearly all cases are remarkably competent laterally, even when very thin (ie, < 1 m). The sheets also dip noticeably at much the same angle and orientation of the JF-Julianehåb Granite roof contact with the GF- Geologfjeld syenite (Plate 3.4b). It seems

likely therefore that the sheets have been passively emplaced during the foundering of the GF- Geologfjeld syenite in response to the emplacement of the Motzfeldt Ring Series. Texturally the microsyenites of this area are varied and complex. Four principal varieties occur, although they are often intimately associated: 1, Porphyritic banded microsyenite (leucocratic and mesotypic varieties eg, 304181/304182, Plates 5.7 and 5.8a; 2, Blue-grey equigranular microsyenite (eg, 304177, Plate 5.8b); 3, Coarse pegmatite (eg, 304179); and 4, Iron-stained equigranular microsyenite. Usuall y, the first three above are closely associated, often in layered sequence. Within most of the banded microsyenites small (< 3 mm) albite laths form a matrix which is strongly laminated parallel to the layering. Many sheets also show net-veining of the blue-microsyenite by the porphyritic leucocratic type (Plate 5.8b). This is probably due to volatile separation in a system similar to that envisaged by Jahns and Burnham, (1969) to explain aplite/pegmatite sequences. They postulate that the rock becomes water saturated after crystallisation of the fine-grained microsyenite (or aplite) and when combined with the heat of crystallisation retrograde boiling would occur and thus create a separate aqueous phase which if confined could disrupt and break up the early formed portions.

The iron-stained microsyenite sheets can be seen in a N facing gully wall 100 m S of Camp 10. They belong to a later generation of activity than the other microsyenite sheets and cut not only these but also the Laminated porphyritic syenite ring-dyke which outcrops in the area. Although the narrow screens of GF-Geologfjeld syenite are unquestionably 'baked' and in places fractured by the minor intrusions they remain largely unaffected by any pervasive volatile and mineralising activity. Therefore the alteration/mineralisation of the sheets would seem deuteric and contemporaneous with their intrusion.

ii. Internal sheet and pegmatite segregations

The type areas for examining 'sheet segregations' developed within the MSF-Altered syenite are the N and S facing cliffs of Sermia Qiterdleq. The sheets range from massive

pegmatite bands containing huge arfvedsonite crystals up to 1 m in length (Plate 5.4a) to sinuous and diffuse bands of alternating pegmatite and aplite sequences (Plate 5.4b). The sheets are often siliceous, and loose blocks of such material found on the S side of Qiterdleq contain conspicuous molybdenite (Tukiainen, pers. comm.) It has been noted that the sheets at low elevations are relatively low in radioactive mineralisation compared to those above 1400 m in the same area (Tukiainen, 1986b). Highly mineralised quartz-microsyenite comprises some 50% of the high ground in the northern part of SE Motzfeldt (N of the SE Motzfeldt Fault). This region beside 'Humbug Brae' has been described as a major area of roof- collapse (Bradshaw & Tukiainen, 1983) and is one of the most economically important regions of Motzfeldt. The 'roof' zone contains large rafts of EF-supracrustal rock (see section 5.3) and, unusually EF-Quartzite and JF-Juliainehab granite blocks are preserved. The microsyenite has been silicified by the assimilation of this crustal material and now contains numerous poikiloblasts of quartz (eg, 304068). The rock is medium grained, equigranular and pinkish to dark red-brown in colour. In sheared areas the colour is a dark-violet.

iii. Intrusive relations of SE Motzfeldt

A c.200 m thick swarm of microsyenite sheets extend SE from the Humbug Brae area and extend into the JF-Julianehåb granite, for over 2 km. The sheets form a spectacular and economically important sheeted sequence in the SE facing granite-gneiss cliffs 2 km E of Camp 5 (see Tukiainen, 1986b, p.50).

5.4.3 Petrographic features (Plate 5.13 & 5.14)

In NE Motzfeldt, by far the most abundant sheets are the leucocratic to mesotypic, porphyritic peralkaline microsyenites. They are similar petrographically to the MSF-Marginal syenite (see section 5.2.3), particularly to the banded microsyenites which make up the apophyses near Camp 10 (cf: 304711 and 304158). Essentially the rock comprises square to rounded poikilocrysts of arfvedsonite (5 to 10 mm) in a matrix of trachytoid

alkali-feldspar (< 2 mm in length). Usually, but not always the rock also contains psuedomorphed poikilocrysts (similar in size to the arfvedsonite) made up of aggregates of aegirine, carbonate, micaceous material +/- sphene, zircon and unidentified REE minerals. Rounded, phenocrysts of analcite , 3 to 10 mm in diameter (usually altered to geiseckite; Plate 5.15) or euhedral nepheline (usually altered to zeolites) of similar size occur in the undersaturated varieties. Secondary aegirine is invariably present, normally at the expense of the arfvedsonite. The rocks contain fluorite and an extremely complex array of accessory minerals. Because of their economic potential, these have been studied in detail by the PYROCHLORE team (Tukiainen, 1986c). The peralkaline microsyenites contain very high values of incompatible elements and microprobe investigations by the PYROCHLORE team have identified the following accessory minerals from the sheets in NE Motzfeldt; Eudialyte, zircon (several generations from different forms), bastnasite, pyrochlore and many unidentified (or unnamed!) Zr-REE silicates. Most of these minerals appear at the expense and wholesale breakdown of the eudialyte crystals (Tukiainen, 1986b;1986c). Zircon occurs in unusually complex forms in the sheets. Backscattered electron imagery has discovered different within-crystal generations of zircon (Tukiainen, 1986b). Moreover, the zircon appears as rounded metamict colloform grains, mauve-brown in colour, 0.5 to 2 mm in size (eg, 304158). These are also intimately associated with REE-carbonate (Tukiainen, 1986b).

The groundmass consists of bladed alkali-feldspars (patch-perthites) with turbid cores and clear albitic rims. They penetrate the poikilocrysts without any change in size or perthitic character. Simple and lamellar twinning forms are common. Aegirine is developed to a varying degree at the contacts between these feldspars and the arfvedsonite crystals.

Although, the sheet sequence in the NE displays a profound suite of textural types, they are basically variants of the mineralogical scheme described here.

The internal microsyenite sheet-segregations are very similar in mineralogy to the MSF-Altered syenite (see section 5.3.3) but with pronounced aplitic and pegmatitic texture. The intrusive types of SE Motzfeldt and the sheet-segregations in the area around Sermia Qiterdleq generally show evidence of crustal contamination. Commonly developed, particularly in the sheets of Sermia Qiterdleq (S side) are large (3-10 mm) plates of ferruginous biotite (eg, 304115), whereas granoblastic quartz comprises upto 30% of the mode in the intrusive microsyenite of the Humbug Brae area, SE Motzfeldt. Unlike the microsyenites of NE Motzfeldt the incompatible elements are commonly found in complex oxides, though silicates and carbonates do occur. Accessory minerals identified include; pyrochlore, zircon, thorite, monazite, columbite, bastnasite, Nb-bearing Fe-Ti oxides, Nb-bearing Fe-oxides and Nb-bearing Ti-oxides (Tukiainen, 1986b).

5.5 MSF-Nepheline syenite

5.5.1 Rock character and structure (Plates 5.9 & 5.10)

This syenite outcrops over a large area and displays a range of textures and mineralogies. Pegmatite (a constant feature of high elevation exposures) and coarse blocky granular weathering are characteristic. The unit forms the inner 'band' of the Motzfeldt Sø Formation. This band ranges in width from a 750 m to 1.5 km in C and SE Motzfeldt respectively. The original size of the unit is unknown as its interior has been 'cored' out by the intrusion of syenites comprising the Flinks Dal Formation. Typically the MSF- Nepheline syenite is a coarse grained, subhedral granular syenite composed predominantly of stout bladed feldspars, generally large (c. 10 x 6 x 4 mm) and randomly oriented. Nepheline is abundant, comprising approximately 30% of the mode, where equant subhedral crystals 5 to 12 mm in size occur evenly distributed throughout the rock. The dark minerals cluster to form mafic 'clots' of subhedral to anhedral crystals. The 'clots' are evenly distributed and comprise approximately 15% of the mode. Pegmatitic patches are abundant ranging from fist-sized vugs to irregular 'pods' (Plate 5.10a), to major sheet like bodies (Plate 5.11b & Fig 14, Emeleus & Harry, 1970).

5.5.2 Field Observations

i. SE Motzfeldt

The MSF-Nepheline syenite is well exposed in the plateau like area around Camp 2. The unit outcrops over a broad strip of ground approximately 1.5 km wide that curves concave toward the centre of the intrusion. The syenite is bounded inwardly by the FDF-Porphyritic nepheline syenite body, and outwardly by the MSF-Altered syenite. Erosion has exposed the unit from elevations of 1300 m in the N to below 900 m in the S. This easily weathered rock comprises most of the southward sloping plateau with much of the outcrop being blanketed by plateau- talus derived *in situ* (see Plate 3.6b). Other than pegmatite, the rock is homogeneous with no apparent internal structure. Pegmatite, however, abounds and large pod-like bodies occur over the whole area. A typical example occurs 1.5 km N of Camp 2 at 1270 m, near the cliff edge. Radiating clusters of aegirine-augite are striking and may be 5 to 40 cm in length (eg, 304014). Massive euhedral feldspar crystals (5 to 40 cm) are also common, together with red altered nepheline euhedra (3 to 8 cm) and less abundant dark mica. Purple fluorite is also commonly associated and, significantly, the larger pegmatite bodies generally emit higher radioactive 'counts' than the surrounding rock.

ii. C Motzfeldt

a. Eastern region (Upper Flinks Dal)

MSF-Nepheline syenite was discovered in this region on the N side of the Flinks Dal Fault in 1984 (Bradshaw, 1985). Location of the FDF/MSF contact, 2.25 km ENE of Camp 12 (see Chapter 6 for further details), confirmed the approximately 6 km sinistral offset along the Flinks Dal fault (Tukiainen, Bradshaw & Emeleus, 1984). The MSF-Nepheline syenite is similar to the rock descibed in SE Motzfeldt.

b. Northern region

The MSF-Nepheline syenite outcrops as a curving, 700 m wide band which trends NW across the area. As in SE Motzfeldt, the unit is inwardly bounded by the FDF-Porphyritic nepheline syenite and outwardly by MSF-Altered syenite. Excellent exposure enables the colour differences between the units of the Motzfeldt Ring Series to depict their structural relationship clearly (Plate 3.8b). The pale pink-grey MSF-Nepheline syenite is easily distinguished from the red MSF-Altered syenite and the blue-grey FDF-Porphyritic nepheline syenite. Unlike in SE Motzfeldt, the FDF-Foyaite does not intrude along the Flinks Dal Formation/Motzfeldt Sø Formation boundary.

c. Western region

North of the Flinks Dal Fault and 1.2 km NW of Camp 11, the c.440 m hill consists of coarse, highly pegmatitic and heterogeneous nepheline syenite. From the field evidence this rock is considered to be MSF-Nepheline syenite. To the S the unit is truncated by the Flinks Dal Fault and to the N and E by the Flinks Dal Formation. The resulting triangular patch of heterogeneous nepheline syenite forms a small spur extending into Qôroq Fjord. This spur can be linked to a similar small resistant headland 2 km NNE, which, on investigation (1984; helicopter reconnaissance) was shown to be also of coarse heterogeneous nepheline syenite. The bay in between, consists of the preferentially eroded FDF-Porphyritic nepheline syenite. These discoveries mean that the Motzfeldt Sø Formation completely encloses the Flinks Dal Formation in Motzfeldt and therefore gives a more symmetrical ring-intrusion shape to the Centre (Bradshaw, 1985). This interpretation corresponds well with the airborne- radiometric grid map of Tukiainen, Bradshaw & Emeleus,(1984) as shown on Fig 8.2.1.

iii. NE Motzfeldt

MSF-Nepheline syenite is not clearly developed in this area. In the area around Camp 6 the Motzfeldt Sø Formation is coarse feldspathic, pale coloured and nepheline free. The

characteristic red staining of the MSF-Altered syenite is only weakly developed although there are a large number of pegmatite sheets, 'radioactive' shear zones and mineralised veins. Earlier work has proposed that the low elevation of the area around Camp 6 (Ljer elv) explains the absence of nepheline. Recent field evidence in the area, however suggests that the rock does not become increasingly undersaturated upward and that it should be ascribed to the MSF-Altered syenite unit (cf; Tukiainen, Bradshaw & Emeleus, 1984). It is the author's opinion that partial assimilation and modification of syenite blocks from the nearby Geologfjeld Formation have played an important role in determining the petrological character of these syenites. Interestingly, nepheline-bearing syenites were found during the 1984 season, at low elevations (400 m) approximately 2 km SE of Camp 6 (Larsen, L.M. pers. comm.). The rock is partially altered and not typical of the MSF-Nepheline syenite.

iv. S Motzfeldt

Although no *in situ* occurrence of this unit exists in the area, a very large raft (c.300 m wide) of nepheline syenite was discovered in 1984 (Bradshaw, 1985). The 'raft', located in the high ground of 'Harry's Dal', 2 km NNE of Camp 14, is contained within and pervaded by the central FDF-Foyaite. The neighbouring FDF-Porphyritic nepheline syenite in the area also contains many cm-scale xenoliths of the MSF- Nepheline syenite.

v. SW Motzfeldt

Although the rocks of this area are poorly understood the field and radiometric evidence suggests that this area is largely comprised of MSF-Nepheline syenite (Tukiainen, Bradshaw & Emeleus, 1984). The area is further complicated however by many intrusions of FDF-Foyaite (transgressive type), lujavrite (Jones, 1980) and microsyenite sheets. Moreover, much of the high ground around Camp 13 is unfortunately made up of loose talus material, very little being *in situ* outcrop. FDF-Foyaite blocks are abundant and display strong cumulate textures. Blocks of subhedral equigranular syenites do occur

however (eg, 326121) which are very similar in hand specimen to the type MSF-Nepheline syenite of SE Motzfeldt. In addition, lujavrites and subhorizontal microsyenite sheets cut the N and W facing cliffs of this area. They extend laterally to the 'HY' contact zone of Jones (1980) some 6.5 km eastwards. Whilst, minor intrusions are abundant and almost characteristic of the Motzfeldt Sø Formation they are almost completely absent in the well established units of the Flinks Dal Formation. Moreover, Jones (1980) showed a genetic relationship between the lujavrites and the Flinks Dal Formation (SM4) so these may well be intrusive offshoots from that Formation.

5.5.3 Petrographic Features (Plate 5.15).

This rock, where not pegmatitic is coarse, homogeneous, subhedral and roughly equigranular. Perthitic alkali feldspar (60%), nepheline (25%) and Na-Ca mafics (15%) are the essential minerals. Accessories include sodalite apatite and iron ore. A host of secondary minerals may be developed. These are due to the effects of the later intrusion of the Flinks Dal Formation, and also to the active volatile phase, (enriched in incompatible elements) which has greatly affected the Motzfeldt Sø Formation. Secondary minerals include, biotite, iron ore, sphene, gieseckite Na mafic minerals fluorite, pyrochlore, zircon and/or complex Zr/REE minerals and calcite. The alkali feldspars, 6 to 10 mm in length are randomly oriented and subhedral-granular in habit. Most sections examined have mesoperthite feldspar, and this (Ab=Or) bulk composition is reflected by the majority of the normative feldspar values (Table A3.2). The nepheline is pink in hand specimen. In section this colour can be seen to be caused by red, powdery material which is finely disseminated around the margins of the crystals. The nepheline occurs as equant subhedra, 4 to 6 mm in diameter and evenly distributed throughout the rock. For the most part, the crystals are fresh with only marginal replacement by micaceous material (gieseckite). Amphibole is the chief mafic mineral occuring as subhedral grains 2 to 4 mm in size and comprising 10 to 15% of the rock. Synneusis texture is again prevelant with the amphibole normally being associated with pyroxene, iron ore and apatite. Both

amphibole and pyroxene show strong zonation and a wide range of compositions. Amphibole compositions range from ferro-edenitic hornblende through to katophorite. The stage of evolution of the syenite largely determines predominant amphibole composition. For instance, specimen 304003 has a FI of 91.4 and the dominant amphibole is green to brown (pleochroic) katophorite. The larger katophorite crystals have discrete cores of golden-brown to pale brown ferro-edenitic hornblende. This zonation is discontinuous with the core being rimmed by small individual orange biotite and Fe-Ti oxides, all enclosed by the katophorite. Less evolved specimens ie, 326092 (FI = 85.5) have ferro-edenitic hornblende/ferro-edenite (green-brown - pale green-brown) as the main phase with only narrow deep green rims of katophorite. Similarly the pyroxene crystals (0.5 to 2 mm) range in composition from cores of pale salite-ferrosalite to deep green pleochroic rims of aegirine-augite or aegirine-hedenbergite. Aegirine develops individual crystals in the more evolved or pegmatitic varieties. Very small apatite crystals are confined to the mafic clusters and enclosed by all phases of mafic minerals. The thermal effect of the intrusion of the Flinks Dal Formation, where in evidence, is particularly strongly shown by the mafic minerals. Most commonly a granular aggregate of orange-brown biotite, aegirine, katophorite, iron ore, +/- sphene has developed. In addition, small (< 1 mm) pale brown crystals of high relief and grey 1st order birefringence may be developed eg, 326049. This mineral, probably of rinkite/lavenite composition, may be locally abundant (up to 2%) and is often associated with small (< 1 mm) skeletal/fibrous brown-opaque minerals and purple fluorite. This skeletal material is similarly found in the MSF-Altered syenite and is almost certainly a complex mineral containing incompatible elements (Th, Ce, Ta, Nb, Zr).

a.



MSF-Marginal syenite (SM1). NE Motzfeldt. Typical red euhedral, 'blocky' feldspars with arfvedsonite matrix. (CB.82.C.05.27).

b.



MSF-Marginal syenite (SM1). NE Motzfeldt. Example showing mafic/felsic phase layering. (CB.82.C.05.26).

a.



MSF-Marginal syenite (SM1). NE Motzfeldt. Example showing mafic rich clot-like segregations. (CB.83.C.10.14).

b.



MSF-Altered syenite (SM1). C Motzfeldt (north). Variety showing altered nepheline and fluorite vein. (CB.83.C.01.21).

a.



MSF-Altered syenite (SM1). NE Motzfeldt. Very altered variety from the 'hot' zone of the unit. Yellow-ochre staining and metallic (Fe-Mn?) coatings are characteristic. (CB.83.C.02.16).

b.



MSF-Altered syenite (SM1). NW Motzfeldt. Typical example of the red feldspathic syenite with very coarse pegmatitic patches. (CB.84.C.12.17).

a.



MSF-Altered syenite (SM1). E Motzfeldt. Massive pegmatite with giant alkali-amphibole crystals. The geologist (T.Tukiainen) is over 1.9 m in height. This location is over 1 km below the roof of the unit. (TT.84.C.01.10).

b.



MSF-Altered syenite (SM1). SE Motzfeldt. Sinuously banded pegmatite/microsyenite found at low-elevation exposures in the unit beside Sermia qiterdleq (CB.82.C.09.30).

Plate 5.5

a.



GF-Geologfjeld syenite/MSF-Altered syenite contact where viewed ENE with Qôrqup sermia in the background. (CB.84.C.12.15).

b.



MSF-Altered syenite/MSF-Nepheline syenite contact. View ESE of the northern tip of C Motzfeldt. (T.T).



Peralkaline Microsyenite Suite. NE Motzfeldt. (Storeelv). The whole cliff side is cut by thin microsyenite sheets. Camp 9 (alt. 190 m) in lower left of photograph. (CHE.82.)

b.



Peralkaline Microsyenite Suite. NE Motzfeldt. Closer view of Camp 9 with the dark sheets of microsyenite beyond. (CB.84.C.03.17).

a.



Peralkaline microsyenite. NE Motzfeldt (Storeelv). Poikilocrysts of blue-black amphibole, red nepheline and acmite in a fine trachytic matrix of alkali feldspar. (CB.83.C.01.08).

b.



Peralkaline microsyenite. NE Motzfeldt (Storeelv). As above showing variation in texture. Red mineral may be eudyalite. (CB.84.C.03.20).

a.



Peralkaline microsyenite. NE Motzfeldt (Storeelv). Typical porphyritic, banded, mesotypic microsyenite. (CB.82.C.10.32).

b.



Peralkaline microsyenite. NE Motzfeldt (Storeelv). Showing the common association of blue equigranular microsyenite net veined by porphyritic microsyenite similar to above.

a.



MSF-Nepheline syenite (SM1). SE Motzfeldt. Characteristically pale coloured, subhedral granular and containing grey or red nepheline. (CB.82.C.03.17).

b.



MSF-Nepheline syenite (SM1). SE Motzfeldt. Example showing the characteristic weathering by granular disintegration, leaving 'blocky' crystal aggregates. (CB.82.C.03.18).

Plate 5.10

a.

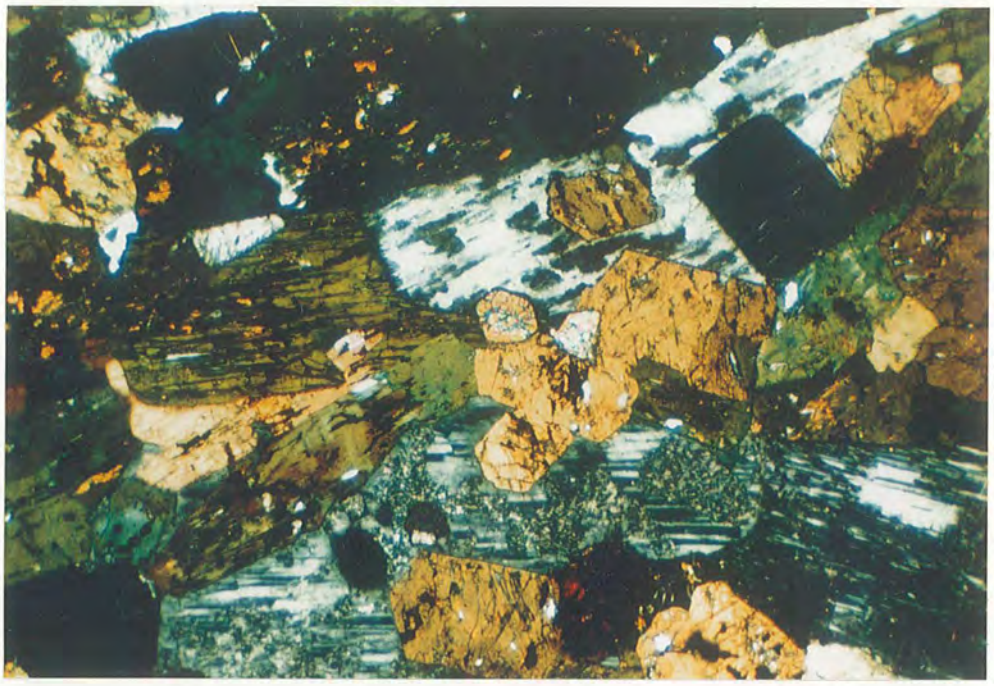


MSF-Nepheline syenite (SM1). SE Motzfeldt. Very coarse pegmatite. A common feature in the high ground of SE Motzfeldt. (CB.82.C.01.18).

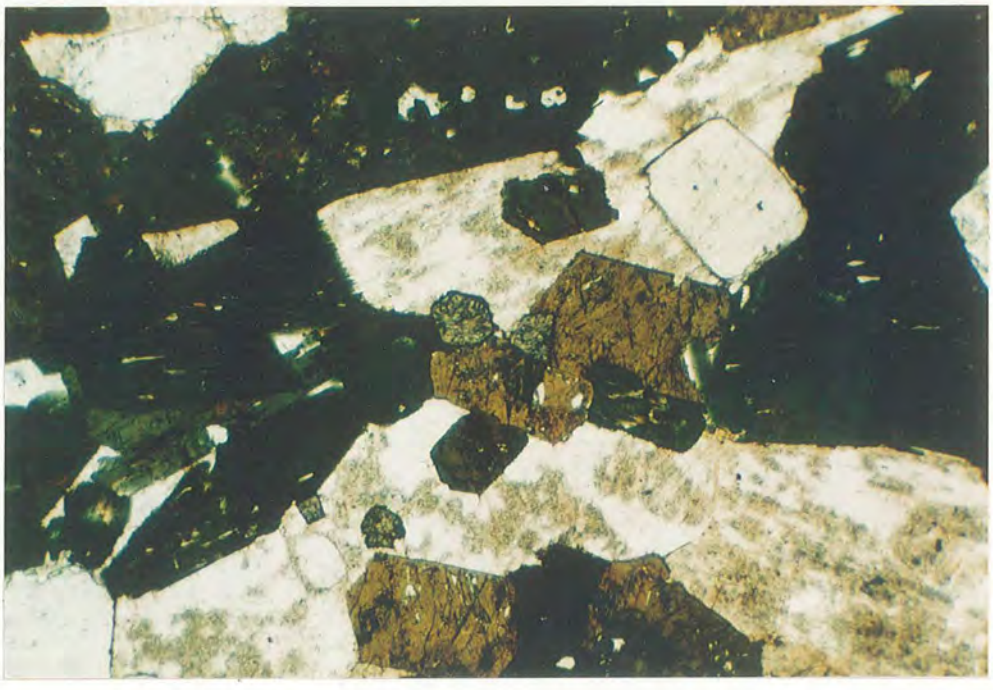
b.



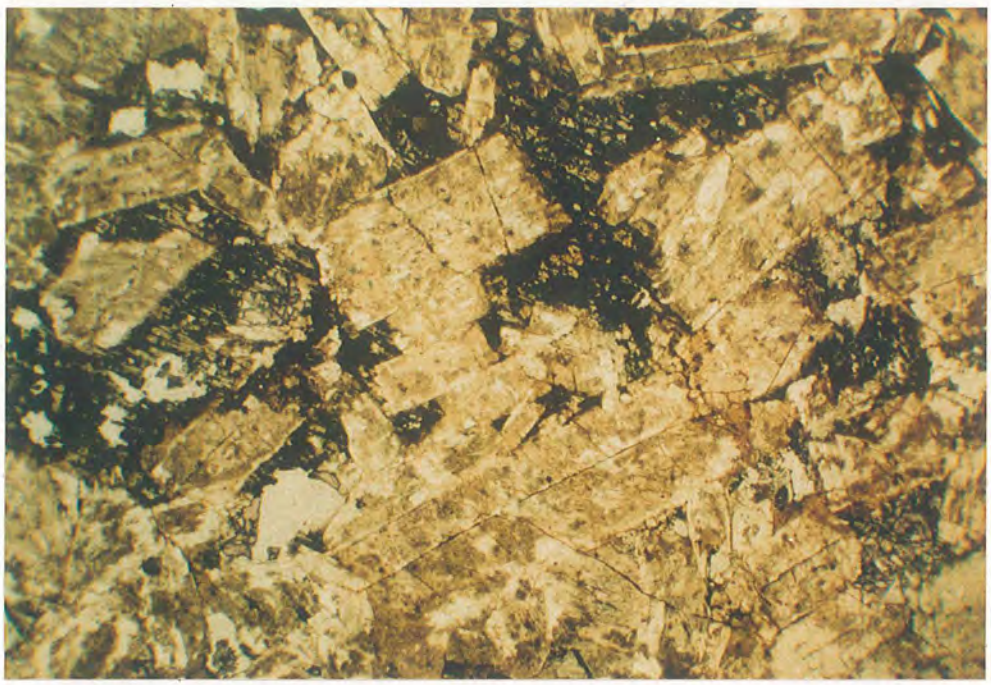
MSF-Nepheline syenite (SM1). SE Motzfeldt. Massive pegmatite vein (running diagonally across picture). Inward growing giant feldspars with interstitial nepheline terminate at a central tinguaitic core rich in aegirine prisms. (CB.84.C.06.23).



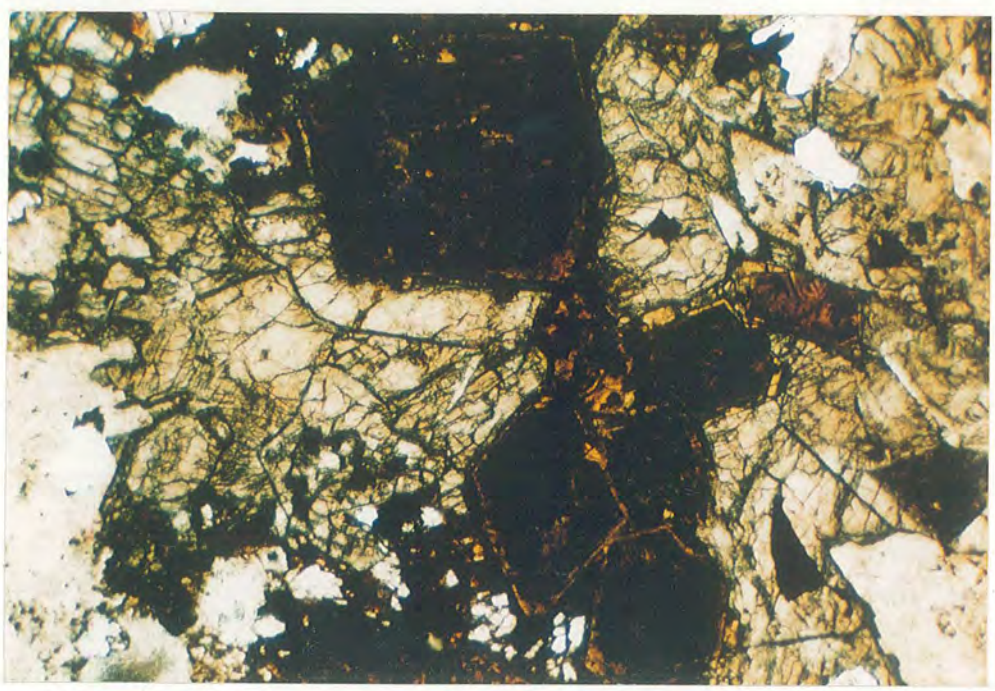
MSF-Marginal arfvedsonite syenite. NE Motzfeldt. (304052). Arfvedsonite and alkali feldspar with the latter showing striking albite twinning and coarse patches of altered k-feldspar. Brightly coloured zircons (centre) Isotropic fluorite and red aenigmatite (low-middle). X.P. 5mm.



As above P.L. The abundant green arfvedsonite subhedra and euhedra display a moderately well developed lamination. Fluorite occurs as clear equant crystals (bottom & top left and upper right).

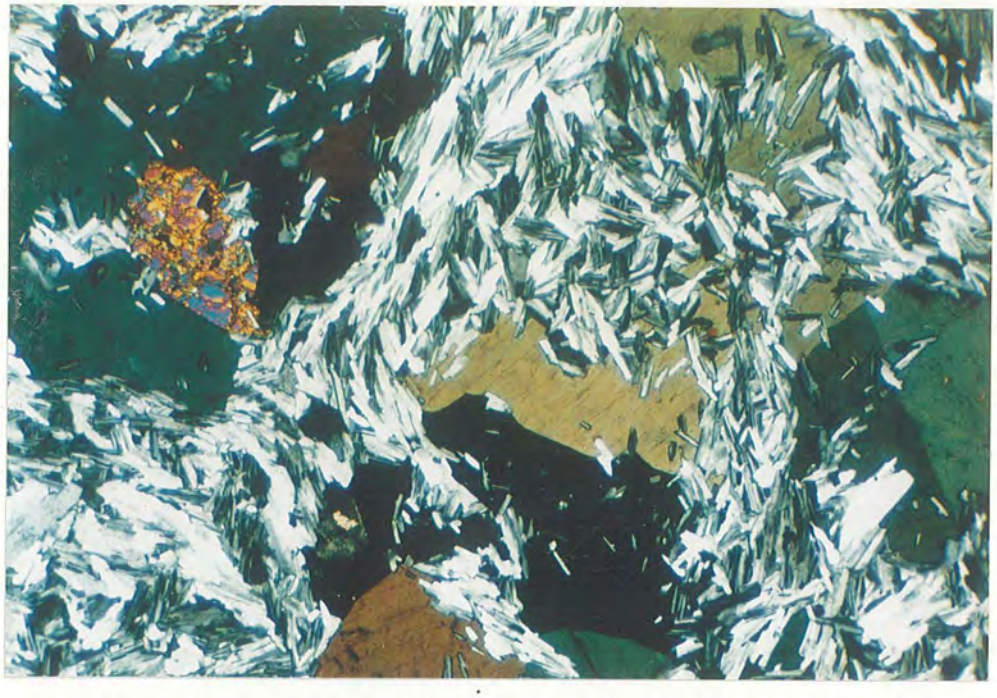


MSF-Altered syenite. NE Motzfeldt. (304053). Coarsely perthitic feldspar with leached and broken down mafic minerals are characteristic, particularly from highly mineralised zones. In addition fluorite (bottom left), zircon and pyrochlore (not shown) are common. P.L. 9mm.

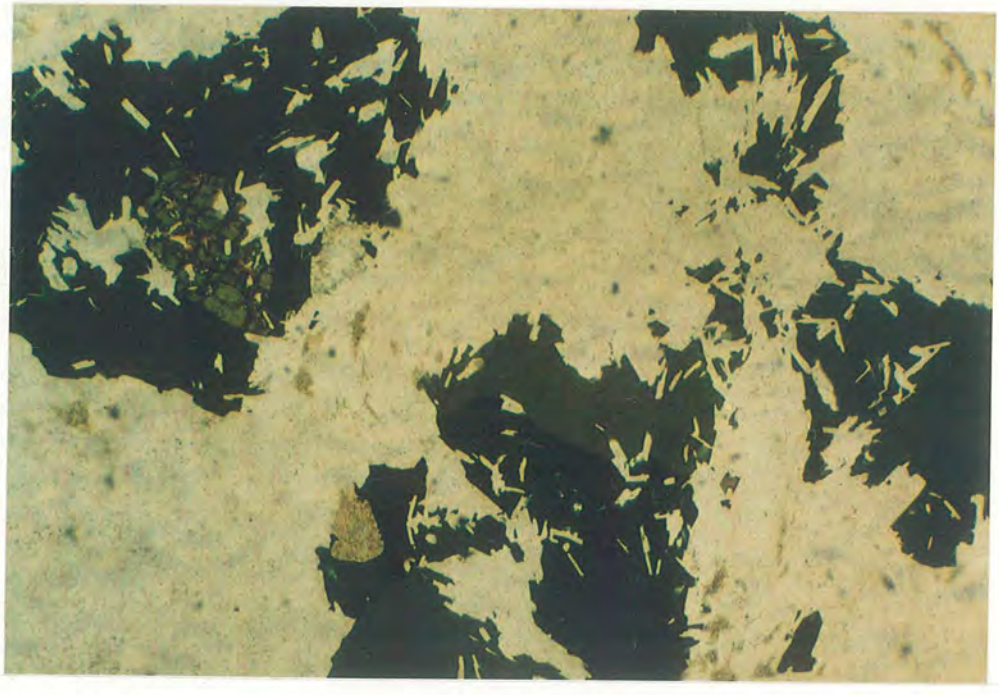


MSF-Altered syenite. NE Motzfeldt. (297652). Mineralised sample showing partly isotropic pyrochlore euhedra enclosed in an aggregate of zircon crystals. P.L. 5mm.

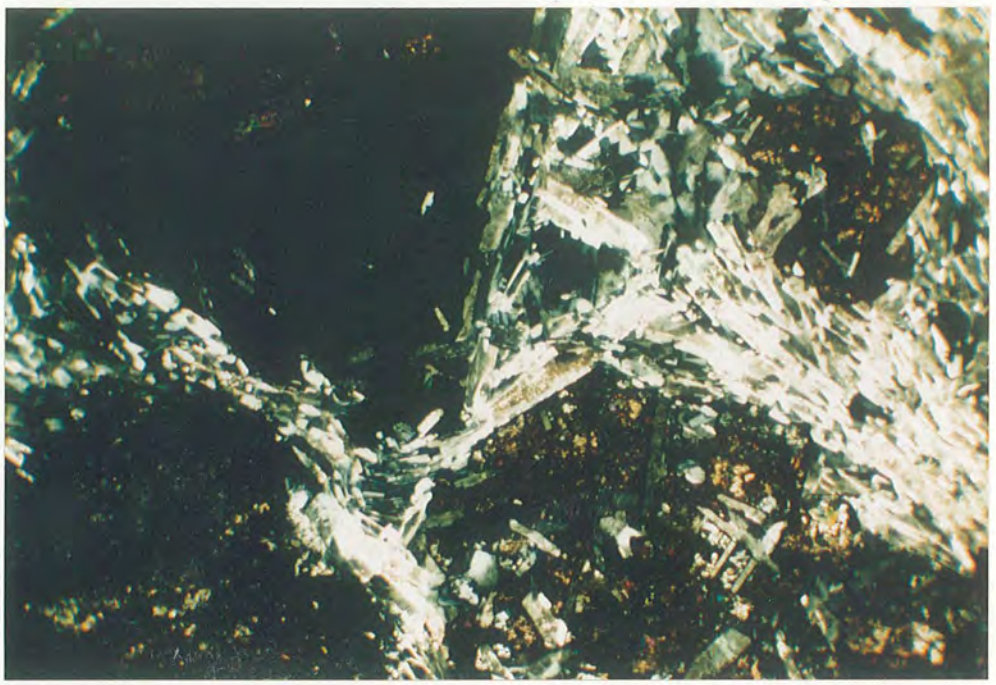
Plate 5.13



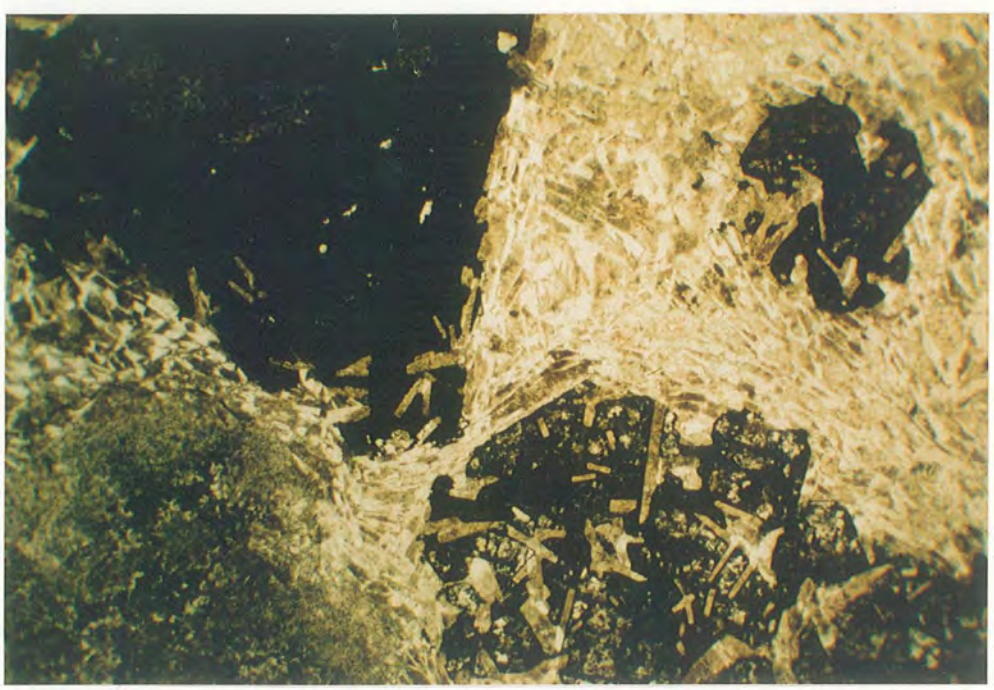
PMS-Peralkaline microsyenite. NE Motzfeldt. (304120). Showing commonly developed trachytic texture of albite laths. Blue-green arfvedsonite (poikilitic or corroded?) and aegirine-hedenbergite (upper left). X.P. 5mm.



As above. P.L.

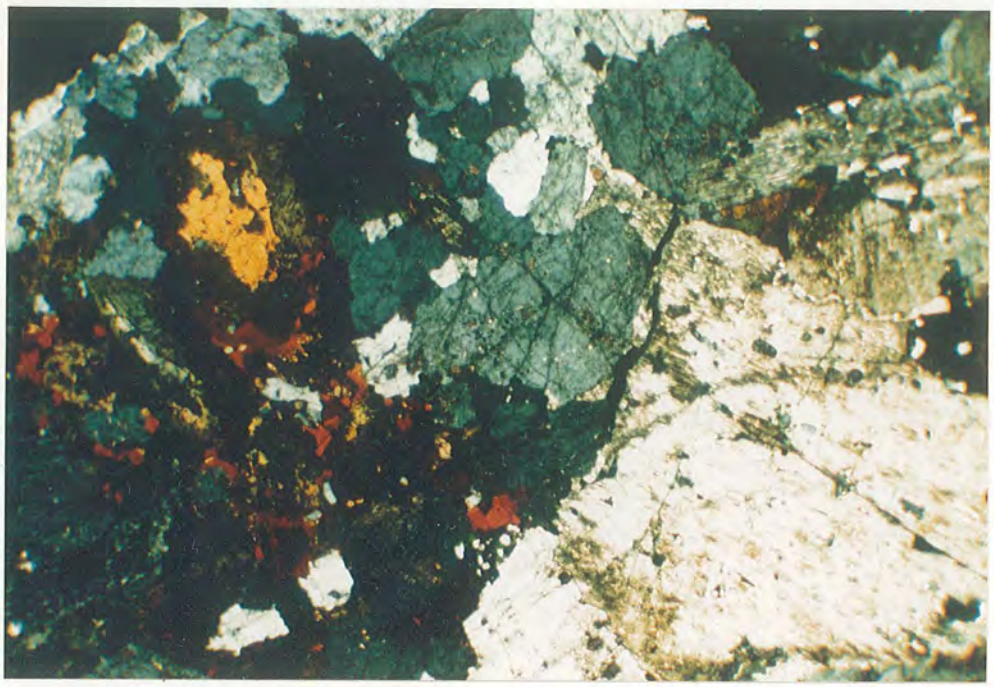


PMS-Peralkaline microsyenite. NE Motzfeldt. (304185). Alkali feldspar showing trachytic texture around blue arfvedsonite (upper left), highly altered and corroded pseudomorphs (after eudialyte?) and rounded isotropic analcite (lower left). X.P. 5mm.



As above. P.L.

Plate 5.15



MSF-Nepheline syenite. SE Motzfeldt. (304003). Showing granular aggregate of coarse nepheline (deep grey) and mesoperthite (lighter) crystals. Clot-like aggregates of strongly zoned mafic minerals are characteristic. X.P. 9mm.



As above P.L. The pyroxene seen is pale-green ferrosalite mantled by bright green aegirine-hedenbergite. Green-brown katophorite, orange-brown biotite, Fe-Ti oxide and apatite crystals make up the rest of the mafic cluster.

Chapter 6 - The Flinks Dal Formation

6.1 Introduction

Foyaites and Nepheline syenites of the Flinks Dal Formation outcrop over an area of about 75 km^2 and form the central core of the Motzfeldt Ring Series. The Formation includes the units SM2, SM3, SM4 and SM5 of Emeleus and Harry (1970).

The Formation comprises a number of intrusive members which were emplaced, younging inwards in a roughly concentric 'nested' plutonic form. The members, namely; **FDF-Porphyritic nepheline syenite** (SM2 & SM4), **FDF-Foyaite** (SM2,SM3 & SM4) and **FDF-Nepheline syenite** (SM5) are all phonolitic in composition (Fig 3.3.2c) and share similar chemical characteristics. They are all pale in colour, nepheline bearing, and typically, fresh and relatively free from mineralisation (Bradshaw & Tukiainen, 1983). Internal structures such as mineral layering, lamination and benching are often well developed. Pegmatite is rare,[1] whilst, conspicuous chilled margins are commonly developed around external and internal contacts. These features are indicative of relatively 'dry' and mobile magmas and are clearly quite different to those which formed the Motzfeldt Sø Formation. The Formation is cut by many Gardar Dykes but very few microsyenite sheets.

6.2 FDF-Porphyritic nepheline syenite/microsyenite (SM2 & SM4)

6.2.1 Rock character and structure (Plates 6.1 to 6.3)

The 'type' rock is a leucocratic porphyritic nepheline syenite or microsyenite which is fresh, blue-grey in colour and massive. Characteristically the rock contains an abundance of fist sized, dark grey porphyry xenoliths which often show preferred orientation (Plate 6.3). Although, cumulate layering is uncommon, the rock may display conspicuous

[1] although local development occurs adjacent to enclosed rafts of country rock, (Jones, 1980)

feldspar lamination. Both feldspar and nepheline occur as phenocryst euhedra. The grey and commonly transluscent feldspars are generally tabular and up to 10 mm in length, whereas the red or white (altered) nephelines occur as equant crystals about 4 mm in size. The phenocryst population is divided approximately 65% feldspar, 30% nepheline and 5% dark minerals. Mafic minerals (10-15%) occur mainly in the groundmass as 0.5 mm to 2 mm subhedra, although sporadic crystals up to 10 mm in size may be found. The phenocryst/groundmass ratio varies considerably, ranging from 0.66 to 9.

6.2.2 Field Observations

i. SE Motzfeldt

500 m W of Camp 2 the FDF-Porphyritic nepheline microsyenite forms a prominent ridge and peak rising to 1457 m (Plate 3.6). Westward the ridge precipitously drops 1300 m to Motzfeldt Sø (Plate 3.7). The unit is easily distinguished from the adjacent FDF-Foyaite and MSF-Nepheline syenite, being massive, very fresh and considerably more resistant to weathering. Hard and sharp, frost shattered blocks litter the outcrop and contrast strongly with the 'rotted' aspect of the neighbouring syenites. The curved (concave inward) FDF-Porphyritic nepheline syenite/MSF-Nepheline syenite contact is clearly marked by a snow-lined break in slope 200 m W of Camp 2. However, later dykes of FDF-Foyaite have pervaded this line of weakness and greatly obscured the original junction. Where the original contact is exposed it is very sharp and the FDF- Porphyritic syenite has clearly chilled against the MSF-Nepheline syenite. Sub-angular to rounded xenoliths of the older syenite, 10 to 40 cm in size, are common along the whole length of the contact (Plates, 6.1 & 6.2). In general the grain size of the unit increases inward, although the rock remains porphyritic throughout its whole outcrop. Coarser examples (eg, 304024) contain a lower proportion of groundmass than the finer varieties (eg, 304758). 200 m SW of Camp 2 weak feldspar lamination may be observed, dipping 70 degrees W and striking NNE approximately parallel with the contact. All varieties contain an abundance of the fist-sized dark grey porphyry xenoliths that are so characteristic of the unit. The porphyry xenoliths are often oriented parallel to a strong feldspar

lamination and appear to be 'drawn out' along the line of flow(?), (Plate 6.3a). The dark xenoliths are always rounded and often thoroughly corroded. Feldspar phenocrysts, infact, frequently penetrate the syenite-xenolith boundary without an apparent change in composition, reminiscent of the well known Shap Granite occurrence.

The contact relations around Camp 2 in SE Motzfeldt are very well exposed providing an excellent type-area for examining the Motzfelt Sø Formation/Flinks Dal Formation boundary.

ii. S Motzfeldt

The FDF-Porphyritic nepheline syenite is restricted to the eastern cliffs of Harry's Dal and is well exposed along much of the SSW-NNE ridge, overlooking Motzfeldt Sø, 1 km E of Camp 14. The rock is identical in varieties of grain size and texture to those described in SE Motzfeldt despite being a considerable distance from a vertical Motzfeldt Sø Formation contact. Similarly, many MSF- Nepheline syenite xenoliths occur in the area. These features indicate that the FDF-Porphyritic nepheline syenite is near its roof zone and has displaced the MSF-Nepheline syenite previously located in the area. Along the southern flank of the c. 1200 m SSW-NNE ridge the FDF- Porphyritic nepheline syenite is in sharp contact with the JF- Julianehåb granite. Westward the unit appears to be truncated by FDF- Foyaite (see section 6.3).

Camp 15, situated on the SW shore of Motzfeldt Sø, gave good access to low elevations within the FDF-Foyaite and FDF- Porphyritic nepheline syenite units. Unfortunately, most of the SW shore of Motzfeldt Sø is blanketed by coarse scree derived from the crags above. Sporadic stream gullys, however expose rock *in situ* . The scree becomes dominantly blue-grey FDF-Porphyritic nepheline syenite approximately 1.1 km NNE of Camp 15. Most of the scree has been derived from high levels, and is medium grained, porphyritic and contains dark porphyry xenoliths. *In situ,* the fresh FDF- Porphyritic nepheline syenite is coarse, blue, non-porphyritic, well laminated and devoid of xenoliths. 5 km NNE of Camp 15, and near the lake the rock exposed is a coarse syenite in which the blocky feldspars (3 x 1 cm) show a preferred orientation (220/70° W) and are surrounded

by clusters of squat (0.5 m) mafics (eg, 326182 or 537797). The rock contains dark, ghost like, oriented inclusions, and has a larvikitic pale blue appearance not unlike some marginal varieties of the FDF-Nepheline syenite. However, Emeleus (1963:field notes) found this rock in contact with the FDF-Foyaite outcrops to the N. The foyaite was seen to contain xenoliths of the larvikitic syenite and therefore it seems likely that the latter is a variety of the FDF-Porphyritic nepheline syenite. From Camp 15 the Julianehåb Formation/Flinks Dal Formation contact can be seen clearly in the SE facing cliffs of S Motzfeldt (Plate 3.4). The contact curves toward the centre of Motzfeldt, dipping outwards steeply at low elevations but shallowing upwards typical of a bell-jar shaped intrusion.

iii. C Motzfeldt

a. North

During the 1982 survey the author mapped this ground from Camp 7. Situated beside the 1133 m lake, and on the high, undulating plateau level, this Camp gave easy access to the well exposed FDF-Porphyritic nepheline syenite/MSF-Nepheline syenite and FDF-Porphyritic nepheline syenite/FDF-Nepheline syenite contacts. The FDF-Porphyritic nepheline syenite of this region (assigned to SM4 by Emeleus & Harry, 1970) shows identical field relationships with the adjacent the MSF-Nepheline syenite as those exibited by the FDF-Porphyritic nepheline syenite (assigned to SM2) in SE Motzfeldt. The Flinks Dal Formation/Motzfeldt Sø Formation contact is first reached 300 m E of Camp 7 and from there it follows an arcuate course, trending NW. The fine-medium grained (chilled) FDF-Porphyritic nepheline microsyenite of the contact zone contains abundant angular xenoliths of the older syenite as well as the dark-porphyry xenoliths that are so characteristic of the unit. The Motzfeldt Sø Formation/Flinks Dal Formation contact is exposed at progressively lower elevations northward. Significantly, at deeper levels and well below the roof zone, the syenite coarsens rapidly away from the contact (cf: S & SE Motzfeldt). Coarse varieties contain only very sporadic, much digested porphyry xenoliths and often show well developed feldspar lamination, parallel to the outer contact. (eg, 304750;

310/80° E). The FDF-Porphyritic nepheline syenite of C Motzfeldt encloses a large quantity of country rock material. Microsyenites, porphyritic trachytes and phonolitic rafts form an extensive, though discontinuous cap to much of the high ground of this area. The principal outcrops comprise an arcuate belt, concave to the SW and approximately 4 km in length. The rafts have an overall dip toward the NW, progressively descending from 1300 m in the SE to 800 m in the NW. Few rafts are enclosed below the 800 m contour. Supracrustal material outcrops over an area in excess of 6 km^2 and in places individual rafts reach c.200 m in thickness. Throughout the area the FDF-Porphyritic nepheline syenite has conspicuously chilled against these inclusions. The author has studied only isolated rafts in the vicinity of Camp 7. The main belt however, has previously been described (Emeleus & Harry, 1970, pp. 30-32: Jones, 1980, pp. 46- 54).

b. West

In western C Motzfeldt the FDF-Porphyritic nepheline syenite forms a prominent, arcuate ridge running NNE and rising to 956 m and overlooking Qôroq to Mellemlandet beyond. The rock is very variable in character, ranging from tightly laminated varieties (eg, 326012) to coarse, poorly laminated types (eg, 326020). The feldspar lamination is generally NNW in strike and steeply inclined (70 to 80 degrees WSW). Eastward the FDF-Porphyritic nepheline syenite ridge changes, with a marked break in slope to an undulating plateau-like area consisting of very pale, coarse, cumulate, FDF-Foyaite.

c. East (Upper Flinks Dal)

This area has been surveyed in detail by Emeleus and Harry (field season, 1963) and by Jones (field season, 1979). Additionally, the author established a camp (Camp 12, 1984) situated beside the 700 m lake in the centre of the large 'U' shaped valley of 'Flink's Dal' (Fig 2.3.1). In this area, the relation between the members of the Flinks Dal Formation are problematical and further complicated by the major fault displacement across the valley.

The most interesting find of the 1984 season was the discovery N of the Flinks Dal Fault, of a well exposed FDF-Porphyritic nepheline syenite/MSF-nepheline syenite contact. This contact is situated on the E facing slabs (alt. 400 m), 2.3 km ENE of Camp 12. The contact is definitely the same as that found in SE Motzfeldt and northern C Motzfeldt (cf: Plates 6.1b, 6.2a & 6.2b) and confirms the 6 km sinistral offset along the Flinks Dal Fault. The FDF-Porphyritic nepheline syenite here is a blue-grey porphyritic microsyenite. Fist-sized dark porphyry xenoliths are abundant and again appear to be 'drawn out' parallel to the feldspar lamination. Angular xenoliths of MSF-Nepheline syenite are common along the contact zone (Plate 6.2a). 750 m W of this contact, the FDF-Porphyritic nepheline syenite is truncated by the younger FDF-Nepheline syenite. W of the main mass of FDF-Nepheline syenite and 1.2 km W of Camp 12, the FDF-Porphyritic nepheline syenite is coarse grained, with tabular feldspars and conspicuous altered nepheline, and shows vague mafic layering (dip 40°W/380° strike). Above in the S facing valley sides, the rock changes character at an elevation of about 1000 m. The syenite becomes medium grained, porphyritic and contains porphyry xenoliths. This rock has chilled against the overlying roof rafts, which cap the ridge. It is unclear whether the coarser syenite fines gradually upwards or is a separate intrusive phase which is roofed by the finer rock.

S of the Flinks Dal Fault, the area is dissected by three large, N-S glaciers. Their steep craggy sides provide good exposure but are difficult of access. Geological relations are complex, poorly understood, and demand more detailed attention. Nowhere on the S side of the valley is the 'typical' FDF-Porphyritic nepheline syenite preserved. However, there is strong evidence that there is been a vertical movement of at least 400 m across the Flinks Dal Fault (downthrow to the N) and therefore the rocks exposed in this region are from deeper levels in the Flinks Dal Formation. 1.2 km SE of Camp 7 a FDF/MSF(?), N-S contact zone is located. The Flinks Dal Formation rock is a fresh medium grained nepheline syenite with pegmatite segregations. Juxtaposed to the W the rock is a coarse pinkish nepheline syenite with blocky texture and 'fuzzy' mafics. This rock is the 'HY' syenite of Jones (1980). 500 m ENE from the contact, the crags opposite consist of fresh

coarse foyaite (eg, 306052) which shows clear feldspar lamination (dip 70°E/160° strike). Nepheline is mainly restricted to small 1-2 mm euhedra poikilitically enclosed by the interstital black amphibole. There is no exposure between these localities, so again it is difficult to determine the true relations. The Foyaitic rock may well belong the the FDF-Foyaite. Restoring the c.6 km offset along Flinks Dal this section would be adjacent to the rocks of western C Motzfeldt and indeed there is definite hand specimen similarity between specimens 326054 and 326026 (medium grained and pinkish) and 326051 and 326021 (laminated foyaite). All the rocks are laminated striking 160° and each pair is on strike, after restoration.

6.2.3 Petrographic Features (Plate 6.9)

This unit includes SM2 and the marginal facies of SM4 of Emeleus and Harry (1970). The rock varies texturally in the phenocryst/groundmass ratio and generally becomes coarser grained inwards. The phenocryst assemblage is dominated by alkali feldspar 3 to 5 mm in length, accompanied by equant nepheline, early formed euhedral to rounded clinopyroxene and locally important neutral yellow-brown rounded olivine. Red-brown or green- brown amphibole is always present, often mantling the earlier mafic minerals. The groundmass comprises alkali feldspar and nepheline with additional green-blue amphibole, Na-pyroxene and often aenigmatite. Accessory minerals include sodalite, analcite some apatite, iron ore (where no aenigmatite), biotite and rinkite/lavenite minerals. The usual secondary breakdown products may be present.

The alkali feldspar phenocrysts (c.6 x 3 x 1 mm) are characteristically cryptoperthites which show moderate (40-60°), negative 2V's. Carlsbad twinning is normally the only type developed, however some coarser (and more altered) specimens (eg, 326077) show clear lamellar twinned albite rims. Exsolution is ordinarily confined to distinct parallel streaks and/or tiny blebs both showing turbid alteration. These streaks in otherwise fresh, transluscent feldspar are a common and almost characteristic feature of the unit in both hand specimen and thin section. Optical zoning is depicted by variation in extinction and represents an increased K/Na ratio outward (Jones, 1980). The feldspar

in the groundmass is of variable habit which is dependent upon its grain size and modal % in the rock. Granular crystals (eg, 326157) or distinct laths up to 0.5 mm in length (eg, 304752) may be present with the latter often showing mineral lineation. In both, albite twinning is commonly visible and is certainly more important than in the phenocryst assemblage. The small crystal size however, makes it difficult to distinguish perthitic forms. Texturally, mineral alignment may be displayed both by phenocryst and groundmass assemblages, the former being the most often strikingly apparent. Nepheline makes up between 20 and 40% of the phenocryst population and occurs as euhedra 2 to 4 mm in diameter. The crystals are normally fresh and clear in section and are evenly distributed throughout the rock. Many crystals show optically continuous, late rims, defined by numerous tiny inclusions of Na mafic minerals which outline the original crystal shape. The groundmass nepheline is often difficult to distinguish, occuring both as small squat individual crystals and as a matrix to the feldspar laths.

Neutral yellow-brown fayalitic olivine occurs as small (< 1 mm) rounded, early formed grains, comprising 0 to 5% of the mode. Interestingly olivine is most commonly found in the finer grained 'chill' specimens (eg, 304106). In coarser varieties olivine is mostly absent or heavily corroded and mantled by amphibole.

Pale green clinopyroxene phenocrysts are present in most varieties, occurring as stout, well formed crystals with 8 sided cross-sections usually less than 1 mm in diameter. The individual grains are evenly distributed throughout the rock, tending not to be glomeroporphyritic. Most crystals are neutral to pale apple-green and ferrosalite in composition. Optical zoning is confined to the outer margins, where pleochroism increases with shades of pale green to yellowish green (aegirine augite). Thin mantles of bright grass-green aegirine-hedenbergite are usual and elongated sections commonly display clear sector zoning (eg, 326079; 304752). Late stage aegirine is commonly developed in the groundmass. Amphibole is present in all specimens examined, commonly comprising up to 10 modal %. Crystals occur in both phenocryst and groundmass assemblages, very often showing a continuous range of sizes. For example, 304752 has a clear seriate-

porphyritic texture, where the amphibole occurs as large, stout deep green to yellowish brown, subhedral phenocrysts (c. 4 mm), deep green to greenish brown subhedral to poikilitic microphenocrysts (c. 0.5 mm) and small (< 0.3 mm) blue-green to yellowish green groundmass crystals. Microprobe analysis of these phases (Table A4.3; Fig 3.4.6) shows the chemical substitution $Ca^2 + Al^3 = Na^1 + Si^4$ takes place progressively, giving the compositions ferro-edenitic hornblende, katophorite and arfvedsonite respectively, there being little change in the relative proportions of $\sum$ Fe, Mn, Mg and K. Within the unit as a whole, however the dominant amphibole is reddish brown to lilac brown ferro-edenite, which occurs as sub to anhedral equant micro- phenocrysts approximately 0.5 mm in size. Very small feldspar inclusions are common and especially numerous around distinctly poikilitic margins. These margins normally tend toward katophorite composition and are reflected by an increased greenish colouration. Deep red brown to black aenigmatite is a locally common phase forming up to 5% of the mode (eg, 54139). Interstitial anhedral poikilocrysts 0.3 to 0.5 mm in size are usual and are similar in size and habit to most of the amphibole. Large isolated but heavily corroded plates of orange-brown biotite (up to 5 mm in length) are present in some specimens but are considered here to be xenocrysts derived from the breakdown of MSF-Nepheline syenite xenoliths. The accessories which frequently occur include minerals of rinkite/lavenite composition. In section, these normally form small prismatic crystals, less than 1 mm in length. They are colourless to pale yellow, of high relief and no visible cleavage. In crossed polars the crystals show 1st order greys/yellows up to low 2nd order (upper 1st) oranges and reds with occasional lamellar twinning. In fact without twinning they closely resemble members of the zoisite/epidote group. One pale yellow crystal from C Motzfeldt (west) proved on XRD investigation to be Hiortdahlite, (R. Hardy, pers. comm.). The occurrence of sodalite and/or analcite in the unit is not unusual, although these are always subordinate to nepheline.

6.3 FDF-Foyaite

6.3.1 Rock character and structure (Plate 6.3b to 6.7)

The foyaitic texture of this nepheline syenite is characteristically well developed. The rocks comprising the unit are pale, grey to pink-grey in colour and commonly display cumulate stuctures. The distinctly tabular feldspars may be as large as 30 x 15 x 3 mm and form an interconnecting framework enclosing pink euhedral (4-10 mm) nepheline and interstitial-subophitic mafic minerals. Although the grain size and modal percentages of minerals vary considerably the foyaite texture of the unit is a constant feature. On the basis of the field relationships (described here) the FDF-Foyaite is further divided into the Central and Transgressive types.

The Central FDF-Foyaite outcrops over an area of approximately 25 km^2 and comprises much of the low ground in C Motzfeldt and the high ground of S Motzfeldt. Despite this, it is the least studied of all the Motzfeldt major intrusions. The unit, now bisected and offset by 6 km along the Flinks Dal Fault, originally comprised an intrusion roughly circular in plan and almost central to the Motzfeldt Ring Series (Fig 10.5.3a). The intrusion was emplaced to a very high level but is almost entirely enclosed by the FDF-Porphyritic nepheline syenite. Although little is known of its structure at depth, at least the top 600 m consist of a saucer shaped (concave upwards), cumulate pile of foyaites, approximately 3 km in diameter, similar to those described from SI7 in the neighbouring Igdlerfigssalik Centre (Emeleus & Harry, 1970, fig 28). The unit displays well developed cyclic, asymmetric phase layering. The individual cyclic units are on a 1 to 3 m scale but subhorizontal benching depicted by the mineral layering may be traced over several kms (Plate 6.7). Although the central FDF-Foyaite is largely confined within the FDF-Porphyritic nepheline syenite, in southern Motzfeldt an arcuate ring-dyke of foyaite (SM3 of Emeleus & Harry, 1970) some 500 m broad shows clear intrusive relationships with the FDF-Porphyritic nepheline syenite and the MSF-Nepheline syenite. This, the Transgressive FDF-Foyaite is very well exposed in SE Motzfeldt where it has intruded

along the zone of weakness provided by the Flinks Dal Formation/ Motzfeldt Sø Formation contact. In SW Motzfeldt it is also well developed but less well exposed and the intrusive relations are conjectural.

6.3.2 Field Observations

i. SE Motzfeldt (transgressive type)

The transgressive FDF-Foyaite is very well exposed in the plateau area around Camp 2. The FDF-Foyaite occurs not in one solid arcuate band (cf. Emeleus & Harry, 1970, plate iv), but as a number of narrow, individual, near vertical intrusions ranging in widths from 1 to 20 m (Armour-Brown et al., 1983). The FDF-Foyaite cuts the MSF-Nepheline syenite and the FDF-Porphyritic nepheline syenite along a belt which roughly follows the contact between the two (Plate 3.6b). The belt which follows a curved course is approximately 500 m wide in the S, but tapers within 3 km northward (at the same altitude), to less than 100 m in width. The Plates 6.3 and 6.6a show the remarkable relationships readily exposed in this area, and indeed precise locations are unnecessary due to the abundance of examples. Plate 6.3a shows a classical feature where the FDF-Foyaite has sent a small vein into the FDF-Porphyritic nepheline syenite while carrying within it xenoliths of the neighbouring MSF-Nepheline syenite. Notably, the vein is oriented parallel to the lamination of the host rock. Plate 6.3b shows an example of the FDF-Foyaite veining MSF-Nepheline syenite. Textural distinctions between the two rock types are striking in this Plate. The feldspar tablets show well developed within-vein flow structure whereas those in Plate 6.5 flow around an enclosed MSF-Nepheline syenite xenolith. Most of the FDF-Foyaite in the area however occurs as larger intrusions of over 2 m wide, which show well developed cumulate structures (Plate 6.6a). Asymmetric phase layering on a 10 cm scale is common, with mineral lamination concordant with the outer contacts of the intrusion. Individual members of the FDF-Foyaite are petrographically very similar and probably emerge from a common source at some shallow depth (Armour-Brown, et. al. 1983).

ii. S Motzfeldt (transgressive type)

As shown on the original map of Emeleus and Harry (1970) the belt of FDF- Foyaite (SM3) can be traced from SE Motzfeldt, across Motzfeldt Sø into the E facing cliffs of S Motzfeldt. The FDF-Foyaite in this area is best investigated from Camp 15. At these low elevations and near the outer contact with JF-Julianehåb granite (Plate 3.4a) the rock is more densely packed in character than the FDF-foyaite of SE Motzfeldt. The feldspar tablets are of similar size but show stronger preferred orientation. Nepheline is less well developed and smaller in size (1-2 mm). The foyaite occurs as one solid band in this area and contains large rafts of MSF-Nepheline syenite up to 50 m in width (eg, 400 m N of Camp 15, alt. 200 m). In the region below the JF-Julianehåb granite roof, W and SW of Camp 15, rafts of gneissose material (20 to 30 m in width) abound. Feldspars in the foyaite are laminated around the blocks and biotite becomes conspicuous. To the N the contact with the FDF-Porphyritic nepheline syenite was not located due to the extensive and highly mobile scree cover. However, the lithology change in the scree itself gives a fairly good indication of the approximate position.

iii. SW Motzfeldt (transgressive type)

At high elevations near Camp 13, FDF-Foyaite with similar cumulate structures to those found in SE Motzfeldt are commonly encountered (Plate 6.6b). However, only loose blocks were found and therefore the true intrusive relationships in this area are conjectural. Intermingled with the foyaite are loose blocks of subhedral equigranular nepheline syenite (eg, 326121) which are considered here to belong to the MSF-Nepheline syenite member. At lower elevations, in Lower Flinks Dal the W facing cliffs overlooking Camp 11 have been shown by Jones (1980) to contain foyaites which intrude 'blocky-feldspar syenite'. It is suggested here that the foyaite belongs to the transgressive FDF-Foyaite and that it intrudes the MSF-Nepheline syenite of this region in a similar dyke and vein network to that described in SE Motzfeldt.

iv. C. Motzfeldt (central type)

In this region the FDF-Foyaite forms a low lying undulating plateau, roughly semi-circular in shape, and approximately 3 km in diameter, of pale grey, strongly weathered rock (Plate 3.10 & Plate 6.7b). More resistant dykes stand out strikingly from the pale regolith. The FDF-Foyaite outer contact with the FDF-Porphyritic nepheline syenite in the W and N is sharp and marked by an abrubt change of slope (the latter being more resistant). The contact is curved in a typical ring intrusion form and its weakness has been utilised by a later ring-dyke intrusion of larvikite (SM5* of Jones 1980). The eastern outer contact has been truncated by the emplacement of the younger FDF-Nepheline syenite. To the NE, although not investigated by the author, the foyaites appear to be capped by the FDF-Porphyritic nepheline syenite which itself contains massive sub-horizontal rafts of supracrustal country rock. The FDF-Porphyritic nepheline syenite may form a chilled crust to the FDF-Foyaite pile or be a separate earlier intrusive event, however, this question remains to be fully resolved. 3.5 km NNE of Camp 11 (alt. 690 m) the FDF-Foyaite is exposed *in situ* along the NW side of a dyke. The cumulate layering of the very pale coarse foyaite is clear. Graded asymmetric layering occurs, with each 'cell' approximately 0.7 m in depth. The bases of layers are iron stained and mafic rich but grade quickly into leucocratic foyaite over 5 to 10 cms. The layers are undulating and display vague channel structures with an overall trend dipping approximately 40° SE.

v. S Motzfeldt (central type)

S of the Flinks Dal Fault the FDF-Foyaite forms very high ground (alt. 1700 m) of the "Harry's Dal" area. The foyaite is best observed in the 500 m high E facing cliffs, overlooking Camp 14. The large scale benching in the cliffs is a striking feature and trends approximately NNW at a dip of between 20 and 40° (Plate 6.7a). This area almost certainly links up with the central FDF-Foyaite of C Motzfeldt. This agrees well with the 6 km sinistral offset along the Flinks Dal Fault and indicates a major downthrow of at least 600 m to the N.

6.3.3 Petrographic Features

i. Central FDF-Foyaite

No systematic vertical sampling of the foyaite crystal 'pile' has been undertaken and consequently little is known about mineralogical variation with depth. Petrographic description presented here outlines only the main characters.

The foyaites are coarse to very coarse grained, trachytoid nepheline syenites. Tablets of alkali feldspar often longer than 10 mm form a 'grain supported' framework to euhedral (2-4 mm) nepheline and interstitial-subophitic mafic minerals (dominantly ferro-edenitic amphibole). Intercumulus minerals include aegirine-hedenbergite/aegirine, arfvedsonite, sodalite and analcite.

Of the secondary replacement minerals the most frequent are aegirine, cancrinite (locally very abundant) and natrolite. Accessory minerals, are uncommon in the specimens examined, but include fluorite, apatite and Fe-Ti oxides. Exsolution and replacement textures are present in a whole range of varieties particularly within the felsic minerals, thus reflecting different magmatic environments and/or subsolidus permeabilities existing within the cumulate 'pile' (see Parsons & Becker, 1986).

ii. Transgressive FDF-Foyaite (Plate 6.10)

The cumulate assemblage includes large tabular alkali feldspar 10 to 15 mm in length, euhedral to subhedral equant nepheline (2-4 mm) and deep green-brown to red-brown ferro-edenitic hornblende (5-10 mm). The interstitial amphibole, characteristically is sub-ophitic to the feldspar tablets and often poikilitically encloses numerous chadocrysts of small nepheline euhedra (eg, 326114, 304005). The amphibole ranges from green-brown to red-brown ferro- edenite (eg, 326103) to green pale green-brown kataphorite (eg, 304005). Intercumulus (?) aegirine commonly forms radiating swathes up to 3 mm in length, examples of which Jones (1980) showed to contain up to 6.96 wt% Zr. Sodalite, analcite and fluorite are also locally important interstitial phases. Of the secondary replacement minerals the most frequent are aegirine, arfvedsonite, cancrinite (locally

very abundant) and natrolite. The samples studied from both SW and SE Motzfeldt show the felsic minerals to be badly affected by subsolidus alteration. Nepheline is usually turbid and the feldspars coarsely perthitic. The latter often show the internal development of randomly oriented feldspar micro-crystals. Although simple twinning is normally preserved only rarely do specimens contain feldspars with relict anorthoclase cores (2V: 45-60 degrees, eg, 326196). Accessory minerals are rare.

Samples of FDF-Foyaite of SW and SE Motzfeldt are from a similar elevation, however foyaite from low elevations, near camp 15, and near the outer contact with Julianehåb 'granite' , has a much more densely packed character. The feldspar tablets are of similar size but show stronger preferred orientation. Nepheline is less well developed and smaller in size (1-2mm). In section interstitial cancrinite after nepheline abounds (upto 10%) eg, 326175. Poikilitic Na-Ca amphibole is largely broken down to aggregates of biotite and Fe-Ti oxide. Feldspars are predominantly coarse patch microperthites with frequent albite rims and relict cores of braid-perthite (eg, 326175). This coarsening-replacement (Parsons, 1978) together with cancrinite and biotite development, is probably associated with interactive fluids derived from the adjacent country rock. Large rafts (10-15 m) of Julianehåb 'granite' abound in the FDF-Foyaite of this area (see field relations).

6.4 FDF-Nepheline syenite

6.4.1 Rock character and structure (Plate 6.8)

This very coarse nepheline syenite occurs as a stock like body occupying the core of the Motzfeldt Ring Series and is the youngest major intrusion of the Centre. The rock is subhedral, equigranular and homogeneous. "Typically the rock contains large rectangular feldspars (2-5 cm) prominent white weathering nepheline euhedra (1-3 cm) and smaller euhedral areas of mafic minerals...." Jones (1980). The modal percentages are approximately 60, 30 and 10 % respectively.

The unit as a whole has been well described previously (Emeleus & Harry, 1970; Jones, 1980) and for further details the reader is referred to these sources.

6.4.2 Field observations

i. C Motzfeldt

The unit occupies about 13 km^2 of C Motzfeldt and has chilled against the FDF-Porphyritic nepheline syenite. Contact zones between the two are generally well exposed and accessible. The northern contact, is easliy traced SW of Camp 7 across the 1133 m lake and over the 1278 m hill. The FDF-Nepheline syenite near the contact becomes nepheline free and porphyritic (eg, 304112). The mafic minerals occur as small rounded isolated crystals (< 5 mm), often surrounding the larger prominent, rectangular feldspars (c.10 mm). No xenolith material material was found at these localities. However, sample 304127, taken 500 m ENE of Camp 7 and within the FDF-Nepheline syenite, appears to be flinty, recrystallised FDF-Porphyritic nepheline syenite. Jones (1980) also mapped a very large raft (c.200 m long) of the latter enclosed by the FDF-Nepheline syenite, 300 m S of Camp 7 on the 1343 m hill. A notable feature of the FDF-Nepheline syenite is the large number of sub-horizontal, trachytic, xenolith rafts, 5 to 100 m in size, which are particularly concentrated in the vicinity of the 1133 m lake near Camp 7. The characteristic lithology is a blue, flinty, microsyenite often bearing small (2-4 mm) isolated coppery mica flakes. The rafts have been considerably recrystallised and are often net veined and brecciated by the nepheline syenite material (Plate 3.3b).

The FDF-Nepheline syenite/FDF-Porphyritic nepheline microsyenite contact was also examined in the Upper Flinks Dal region. Again the FDF-Nepheline syenite decreases in grain size and develops a nepheline free porphyritic texture (eg, 200 m NW of Camp 12, alt. 1200 m and 300 m E of Camp 12, alt 580 m). Other features of note in this area, include the occurrence of pegmatite sheets in the coarse nepheline syenite (a rare example in the Flinks Dal Formation), located in the waterfall exposures, 170 m E of Camp 12 and the occurrence of moderately well developed mineral lamination found in loose blocks of FDF-Nepheline syenite on the NE side of the 696 m lake (Plate 6.8b).

Because of the extremely coarse and relatively homogeneous character of the FDF-Nepheline syenite it is one of the most readily distinguished units of the Motzfeldt Centre.

6.5.3 Petrographic features (Plate 6.11)

This very coarse granular nepheline syenite principally consists of rectangular alkali feldspar (commonly up to c. 30 x 20 x 15 mm), large equant nepheline euhedra to subhedra (c. 20 mm) with interstitial clot-like areas of pyroxene, amphibole and accessory Fe-Ti oxide and apatite. Secondary biotite, aegirine-augite and Fe-Ti oxide are frequently associated with the mafic areas whereas sodalite, analcite, albite and gieseckite usually accompany the felsic minerals. The mafic mineral clots characteristically comprise early formed ferrosalite with rims of aegirine-augite (2-5 mm), mantled by subhedral red-brown to pale green-brown ferro-edenite (eg, 272490; Plate 6.11) or less commonly green katophorite (up to 10 mm). The alkali feldspar displays predominantly, coarse mesoperthitic texture and commonly includes small irregular blebs of nepheline (eg, 304113). Baveno 'herring bone' twinning is very common. In addition, several specimens examined have two generations of feldspar (eg, 272490). The second feldspar phase is seen to mantle the large feldspar crystals as well as forming separate bladed crystals (c.20 x 5 mm). This phase is distinguished in hand specimen by its whiter colour, and in thin section, usually by a finer mesoperthitic texture.

a.



FDF-Porphyritic nepheline syenite (SM2). SE Motzfeldt (SM2). Typical example containing distinctive dark grey porphyry xenoliths. The rock is fresh, hard and often shows feldspar lamination. (CB.82.C.03.21).

b.



FDF-Porphyritic nepheline microsyenite (SM2). SE Motzfeldt. Example close to the MSF contact and containing angular MSF-Nepheline syenite xenoliths. (CB.82.C.15.33).

a.



FDF-Porphyritic nepheline microsyenite (SM4). C. Motzfeldt, Flinks Dal (east). Example from contact zone containing MSF-Nepheline syenite and dark grey porphyry. (CB.84.C.05.27).

b.



FDF-Porphyritic nepheline syenite (SM4). C. Motzfeldt (north). Example from the contact zone showing similar features as above. (CB.82.C.09.07).

a.



FDF-Porphyritic nepheline microsyenite (SM2). SE Motzfeldt. Intruded by FDF-Foyaite containing xenoliths of coarse MSF-Nepheline syenite. Notice porphyry xenoliths 'drawn out' parallel to the feldspar lamination. (CB.82.C.02.16).

b.



FDF-Foyaite (SM3). SE Motzfeldt. The foyaite clearly intruding MSF-Nepheline syenite. Notice orientation of feldspar tablets. (CB.82.C.02.19).

a.



FDF-Foyaite (SM3). SE Motzfeldt. Coarse grained foyaite with tabular feldspars, poikilitic amphibole, grey sodalite and red nepheline. (CB.82.C.03.20).

b.



FDF-Foyaite (SM4). S Motzfeldt. Showing the characteristic 'framework' of feldspars, interstitial mafic minerals and nepheline. Small nepheline euhedra can be seen enclosed by poikilitic black amphibole. (CB.84.C.08.28).

a.



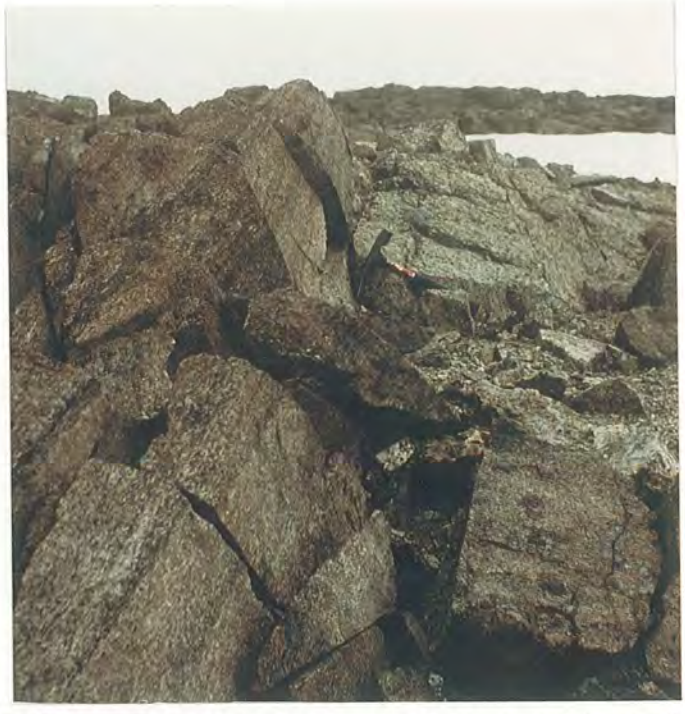
FDF-Foyaite (SM4). S Motzfeldt ("Harry's Dal"). Enclosed is a xenolith of coarse and blocky MSF-Nepheline syenite. (CB.84.C.11.07).

b.



FDF-Foyaite (SM3). SE Motzfeldt. Foyaite showing flow lineation around a MSF-Nepheline syenite xenolith. (CB.84.C.06.10).

a.



FDF-Foyaite (SM3). SE Motzfeldt. Showing cyclic mafic layering very well developed within a dyke of foyaite cutting MSF-Nepheline syenite (right of hammer). (CB.82.C.01.05).

b.



FDF- Foyaite (SM4). S Motzfeldt. (The Wall). Similar development of asymmetric, cyclic phase layering as above. Mafic phases decrease while nepheline in particular, increases. (CB.84.C.08.26).

a.



FDF-Foyaite (SM4). S. Motzfeldt. Large scale benching in the Foyaite, seen in the east facing cliffs of Harry's Dal. (CB.84.C.10.32).



FDF-Foyaite (SM4). C Motzfeldt (west). The central Foyaite N of the Flinks Dal Fault corresponding to above, ie. offset sinistrally by 6 km and downthrown c.400 m. Large scale benching is also developed.

a.



FDF-Nepheline syenite (SM5). C Motzfeldt (Flinks Dal). Typical example of very coarse rock with conspicuous nepheline and two generations of feldspar. The large feldspars have-digested cores. (CB.84.C.05.10).

b.



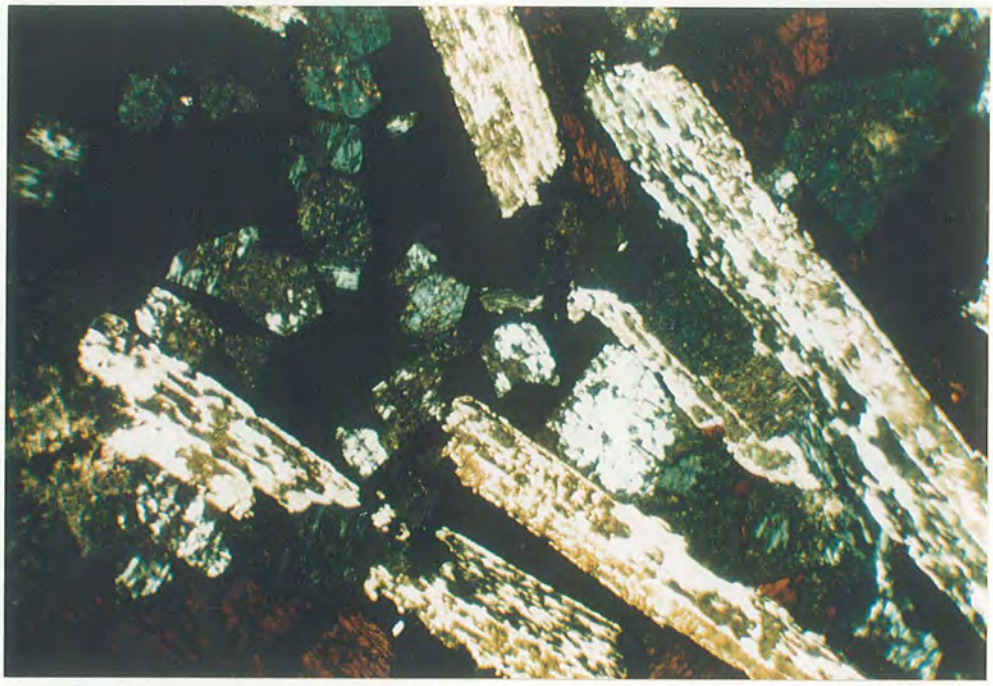
FDF-Nepheline syenite (SM5). C Motzfeldt. (Flinks Dal). Shows partially developed feldspar lamination.



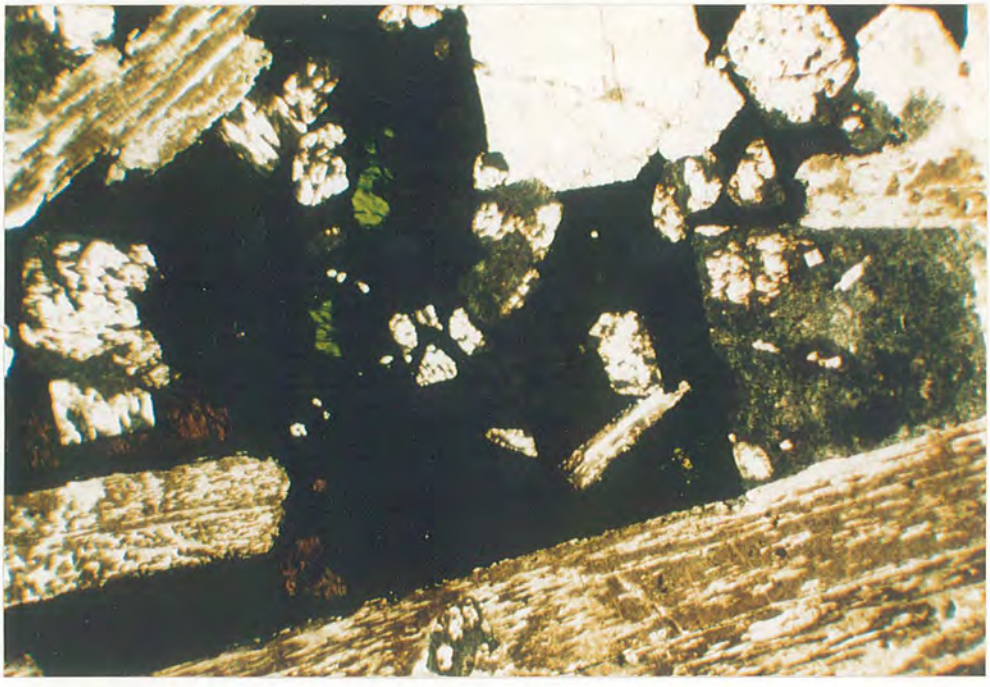
FDF-Porphyritic nepheline microsyenite. C Motzfeldt. (304101). Phenocrysts include elongated cryptoperthite, nepheline, ferrosalite and fayalite (note strong optical zonation - top right). X.P. 9mm.



As above. P.L. The groundmass consists of granular crystals of alkali feldspar, nepheline, blue-green amphibole and rare aenigmatite.



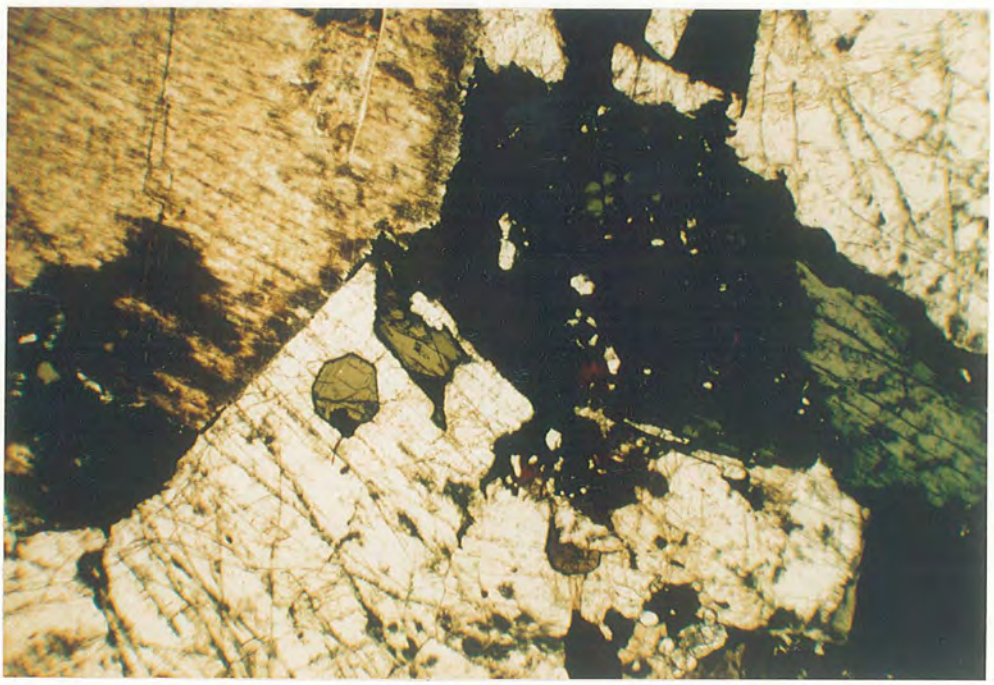
FDF-Foyaite. SW Motzfeldt. (326113). Interlocking framework of perthite laths with poikilitic brown-green ferro-edenite/katophorite amphibole which completely enclose grey nepheline euhedra. X.P. 9mm.



As above. SW Motzfeldt. (326114). P.L. 9mm.



FDF-Nepheline syenite. C Motzfeldt. (272490). Very coarse subhedral granular rock, comprising mesoperthite, nepheline and mafic aggregates. X.P. 9 mm.



As above P.L.

a.



FDF-Porphyritic nepheline syenite (SM2). SE Motzfeldt (SM2). Typical example containing distinctive dark grey porphyry xenoliths. The rock is fresh, hard and often shows feldspar lamination. (CB.82.C.03.21).

b.



FDF-Porphyritic nepheline microsyenite (SM2). SE Motzfeldt. Example close to the MSF contact and containing angular MSF-Nepheline syenite xenoliths. (CB.82.C.15.33).

Chapter 7 - The Ring-dykes and minor intrusions

7.1 Introduction

Minor intrusions are abundant throughout Motzfeldt and occur in various sizes (c.1 to c.300 m) as sub-horizontal sheets, dykes or ring-dykes. The minor intrusions which are demonstrably related to the major plutonic formations of Motzfeldt have been discussed earlier in this work. This section includes the units **Laminated alkali syenite, Laminated porphyritic syenite** and the Poikilitic arfvedsonite microsyenite which comprise the **Motzfeldt Hypabyssal Series**. In addition, briefly discussed are those units (more fully described by Jones, 1980) which are probably related to the Flinks Dal Formation, the **Larvikite ring-dyke** and the **Lujavrite** sheets of SW Motzfeldt.

The ubiquitous Gardar dykes which swarm roughly NE through the Centre are not discussed in this work (for details see Pearce, 1988).

7.2 Laminated alkali syenite

7.2.1 Rock character and structure (Plate 7.1)

This unit forms at least two major, closely associated sheet-like bodies restricted to NE Motzfeldt. These sheets outcrop low in the massive W facing cliffs that overlook Motzfeldt Sø between Ljer elv and Qiterdleq (Plate 7.1b). Together they comprise a thickness of about 300 m and dip approximately 45 degrees NE. This unit was previously described and mapped as belonging to the partial ring dyke SM3, by Emeleus and Harry (1970) and Jones (1980), the absence of nepheline being attributed to the lower elevation of exposure. Subsequent surveys have shown these units to be unrelated. The Laminated syenite, intruding MSF-Altered syenites, is cut by the Laminated porphyritic syenite ring dyke, and the Alkali-gabbro giant dyke.

The texture of the syenite is distinctive, though variable. Feldspar lamination is characteristic, however the direction of orientation is often laterally inconsistent. Typically

the pale grey to cream coloured, massive rock comprises well oriented bladed feldspars (> 65%), 5 to 10 mm in length and poikilitic rounded to subhedral crystals of black amphibole (< 25%), 5 to 15 mm in size. In fine grained varieties the mafic phase becomes interstitial and anhedral. Although igneous lamination is conspicuous, igneous layering is uncommon. One example was found in a loose block, where asymmetric cyclic phase layering (on a 10 cm scale) was well developed. A remarkable characteristic of the unit is the great variation of feldspar grain size within a single exposure. This texture can give the rock a streaky appearance often with a fine- grained facies enclosing mineralogically identical 'stringers' of coarser type.

Unfortunately most of the unit in the cliff face is inaccessible and exposure in the valleys is restricted due to extensive scree and vegetation cover.

S of the Flinks Dal Fault, no trace of Laminated alkali syenite has yet been found, and this remains a puzzle. On a large scale, all feldspar laminations measured in and around Ljer elv are oriented roughly parallel to the dip (NE) and strike (NW) of the visible structure of the unit. However in the area W of Camp 10 (viz, at the S end of the syenite body) the measured laminations have a similar strike (NW) but a prominent steep dip to the SW. Moreover, the sheet-like structure is not visible in the cliffs above this area. It is possible that the sheets change dip direction downwards, where they assume an inward dipping ring dyke form.

On the northern flanks of Ljer elv the Laminated alkali syenite forms much of the SW facing slopes. Northward, however the topography hindered mapping progress and this area needs further study.

7.2.2 Petrographic Features (Plate 7.7)

The rock has a distinctive texture consisting predominantly of trachytoid alkali feldspar and subophitic poikilitic green-brown katophorite amphibole. This texture is consistent throughout the unit although the grain size varies from fine-medium to

medium-coarse. The other main minerals include pyroxene and corroded fayalitic olivine. Zircon, iron ore and apatite are common accessories, as is secondary orange biotite.

Lamellar alkali feldspar (av 4 mm in length) showing moderate to strong trachytoid texture makes up the bulk of the rock (60-80%). The normative mineralogy indicates consistently Ab > Or in feldspar bulk composition (mean of 7. Or 39.2, Ab 59.6, An 1.2). In section both unexsolved cryptoperthite (anorthoclase) and mesoperthite or antiperthite often occur together. The anorthoclase may form central cores to coarse patch (anti)perthites as noted by Jones 1982 (eg, 304718) or, interestingly, be confined to the crystals enclosed by the amphibole poikilocrysts (eg, 304078). The high temperature form, therefore has been essentially isolated from the further actions of fluid interaction (see Parsons, 1978). In addition, the enclosed feldspar is persistently smaller and generally less well laminated than that of the 'matrix'. The amphibole poikilocrysts range in size from 3 to 10 mm and enclose not only feldspar but early formed olivine and pyroxene. Fluorite inclusions are also occasionally present. All amphiboles are iron rich (FeOT > 28% Wt), show strong absorption colours and are pleochroic in shades from deep green to deep brown. Compositionally the crystals usually straddle the ferro-edenite/katophorite border with the chemical substitution $Ca^2+Al^3 \Rightarrow Na^1+Si^4$ taking place outwards. This is marked optically by a change in dominant colouration from brown to green. One crystal analysed was zoned from a core of ferro-edenitic hornblende (brown) through ferro-edenite (green brown) to katophorite (green). Pyroxene ranges from 0 to 15% of the mode, usually occuring as small crystals (< 2 mm) with cores of pale-green ferrosalite and rims of bright green pleochroic aegirine-hedenbergite. Pyroxene is most abundant in the mafic rich layers where the pyroxene/amphibole ratio may be as high as 0.5. The crystals are invariably enclosed by the amphibole in all but the finest grained varieties (see below). Of similar occurence are rounded and corroded anhedra of fayalite (0.5 to 1 mm). The crystals may be locally abundant in mafic rich layers (up to 10% eg, 304095a) and frequently wholly or partially altered to orange- red iddingsite. In several specimens examined zircon is an important accessory (eg, 304078) and occurs as small isolated euhedra 0.5 to 1 mm in size. Fluorite is nearly always present, as small

(< 0.5 mm) rounded crystals within the amphibole and increases in importance with the appearance of zircon. Specimen 304078 is a partially mineralised variety with zircon, fluorite and pyrochlore all in evidence. Significantly biotite is present and the alkali feldspar is coarsely patch (anti)perthitic. Interstitial sodalite/analcite partially altered to white mica is also present (3-4%) and shows up in the normative mineralogy as 4.2% wt nepheline.

7.3 The Laminated porphyritic syenite

7.3.1 Rock character and structure (Plate 7.2)

Syenites belonging to this unit comprise a belt/suite of ring dykes and sheets that follow a curved course (concave inward) through NE and SE Motzfeldt. The belt is sinistrally offset by approximately 6 km along the Flinks Dal Fault. This 'unit' is much more extensive than previously described. During the 1982 survey the author noted the presence of the rock in NE Motzfeldt: "In this area coarse laminated syenites have been found cutting syenites of the Motzfeldt Sø Formation. However they are nepheline poor.....Correlation of the syenites is difficult and they can only tentatively be classified as belonging to the Foyaite member " (Bradshaw & Tukiainen, 1983). Further work in 1984 located the syenite in SE Motzfeldt and proved it to be unrelated to the FDF-Foyaite (SM3). In the accompanying geological map (Enc.1) the 'unit' is portrayed only diagramatically, as the syenite comprises many irregular/sinuous dykes and sheets of varying sizes (1 to 50 m in width) which intrude the older rocks (Plate 7.3 & 7.4). Very detailed mapping is necessary to accurately place the individual members of this unit. The recent surveys have shown however that the unit as a whole is laterally consistent and individual intrusions within the belt dip vertically or steeply to the W. The Laminated porphyritic syenite is a very distinctive rock and is easily distinguished from most other syenite bodies in the Centre. Typically the individual Laminated porphyritic syenite dykes or sheets are internally 'zoned' parallel to the outer contacts and comprise three gradational types. These variations in lithology are in part due to strong chilling and well-developed flow differentiation which are characteristic of the unit. Almost every

contact zone found is marked by a distinctive chilled margin. This margin is steel-grey in colour, 10 to 50 cm wide, fine grained and almost invariably aphyric. Often glassy flow banding may be seen as thin bands which parallel the contact, or, where the contact is irregular, as swirling eddy currents along the margins. This outer zone grades abruptly into a distinctly porphyritic rock (Plate 7.4a). This syenite is characterised by a predominance of tabular feldspar phenocrysts (c.12 x 8 x 2.5 mm) in a fine-medium grained matrix. Mafic minerals also occur in the phenocryst assemblage. Rounded sub- to anhedral crystals of dark-green alkali amphibole containing grass green pyroxene cores are common (15%) and range in size from 0.5 to 6 mm. Feldspars, unlike the mafic minerals, often display a well developed preferred orientation and remain of remarkably consistent size throughout the unit. Conversely the mafic minerals show a range of sizes in hand specimen giving the rock a seriate texture. The modal proportion of the phenocryst assemblage gradually increases inwards from the contact until the groundmass disappears altogether. The rock of this 'central zone' is a laminated syenite with tightly packed mafic minerals (Plate 7.2b). This densely phyric rock is grey in colour, massive and noticeably heavy. Mafic minerals are interstitial, less than 5 mm in size and commonly poikilitic. Poikilitic, dark-grey aenigmatite is often conspicuous in hand specimen and may comprise up to 10% of the rock. This variety does not develop in the smaller intrusions of Laminated poikilitic syenite (ie. < 10 m wide) but is important in the larger bodies, particularly near Storeelv and in the very high ground of SE Motzfeldt, where slightly red stained varieties can look very like MSF-Marginal syenite. Unlike the latter the Laminated porphyritic syenite commonly contains accidental inclusions. Xenoliths of neighbouring syenites are common, but also frequent and more widespread are 'giant' feldspar xenocrysts 5 to 15 cm in length.

7.3.2 Field Observations

i. SE Motzfeldt

The belt of Laminated porphyritic syenite roughly follows the line of a high ridge (> 1600 m alt.) and its W facing cliffs, situated 1.5 km E of Camp 2. The geological relations are well displayed in the steep W facing cliffs (1548 m summit), 1.5 km NE of Camp 2 (Plate 7.5a). The cliff face contains a number of dyke like bodies (< 10 m in width) of Laminated porphyritic syenite which intrude red-stained MSF-Altered syenite. The 'dykes' trend roughly parallel to the cliff face and make it appear that they comprise the whole face. Field work undertaken by GGU-Pyrochlore geologists located many contact zones between the MSF-Altered syenite and the Laminated porphyritic syenite (see Bliksted, 1984; field notes). Field evidence shows the Laminated porphyritic syenite has clearly chilled against the Motzfeldt Sø Formation and the characteristic features of flow differentiation and flow banding are commonly encountered. The Laminated porphyritic syenite contains numerous rounded xenoliths of very coarse nepheline syenite and also large feldspar xenocrysts, 5 to 10 cm in length. In the very high ground of SE Motzfeldt around Camp 5 the Laminated porphyritic syenite was previously mistaken for the MSF-Marginal syenite (Bradshaw & Tukiainen, 1983). Most of the outcrop in this region is plateau-talus and although this has not moved far, the complex intrusive relations of the Laminated porphyritic syenite are difficult to follow.

ii. NE Motzfeldt

Storeelv

Much of the low ground adjacent to, and S of Camp 9 is Laminated porphyritic syenite. The dense grey rocks stand out from the pink Geologfjeld Formation syenites which they intrude. The Laminated porphyritic syenite forms a belt of intrusions at least 50 m wide, which follow a curving SE course. The sharp outward contact is very well exposed beside Camp 9 and can be traced SE for about 400 m. The contact is then 'lost' in the steep cliff faces that overlook Sermia Avanardleq and Motzfeldt Sø. The inner (westerly)

contact is hidden by scree and glacial moraine. The marginal facies of the Laminated porphyritic syenite near Camp 9 is extremely porphyritic and contains numerous angular inclusions of the adjacent pink laminated syenite of the Geologfjeld Formation. Within 2 m from the outer contact the phenocryst/groundmass ratio increases from 0.25 to 9, with the densely phyric variety predominating. Accidental inclusions are particularly common in the Laminated porphyritic syenite of this area. In addition to the characteristic grey feldspar xenocrysts, massive, rounded feldspar pegmatite xenoliths occur that may be up to 50 cm. in size. This rock may represent the source of the frequent xenocrysts. The Laminated porphyritic syenite is clearly cut by rusty mineralised PMS-microsyenite sheets although the xenolith varieties include angular blocks of felsic porphyritic MSF-microsyenite up to 30 cm in size.

Ljer elv

300 m N of Camp 6 the Laminated porphyritic syenite truncates two dykes that follow the normal Gardar trend for the area whereas the Gardar dykes at Storeelv unequivocally cut the Laminated porphyritic syenite (Pearce & Emeleus, 1985). The Laminated porphyritic syenite intrudes the MSF- syenites and the laminated alkali syenite intrusions 500 m NNW of Camp 6 in the foot slopes of the cliffs these relationships are clearly exposed. Here porphyritic and aphyric Laminated porphyritic syenite intrudes in a highly irregular manner leaving screens of Laminated alkali syenite which contains xenoliths of MSF-Altered syenite (Plate 7.3b). Good exposure is also found in the stream gorge 200 m SE from Camp 6 where several roughly N-S. Laminated porphyritic syenite dykes intrude the Laminated alkali syenite and Motzfeldt Sø Formation. The intrusions in the gully are generally narrow and well spaced apart (ie, > 20 m). On the south side of the stream a Laminated porphyritic syenite/Laminated alkali syenite contact is well exposed. The Laminated porphyritic syenite dyke is 15 m wide, strikes N-S and dips 55 degrees E, truncating the feldspar lamination of the Laminated alkali syenite clearly (Plate 7.3a). The 15 cm wide aphyric chilled margin of the Laminated porphyritic syenite

grades quickly into the porphyritic variety, where the feldspar phenocrysts show strong orientation parallel to the contact.

The Laminated porphyritic syenite in the Lejr elv area also contains the characteristic pegmatite xenoliths and 'giant' feldspar xenocrysts.

7.3.3 Petrographic features (Plate 7.8)

This rock occurs in a suite of arcuate dyke-like units in NE and SE Motzfeldt. Texturally the rock may vary considerably (see 5.3.2) particularly in the phenocryst/groundmass ratio. The dominant feature, however is its inequigranular, laminated feldspar-phyric nature. Chemically, the rock is generally peralkaline with an average (Na+K)/Al ratio of 1.12 (mean of 14); and this is reflected in the mineralogy throughout. Characteristically, lamellar alkali- feldspar euhedra predominate and when densely packed, form a trachytoid framework to the groundmass. The feldspar is very similar to that of the laminated alkali syenite. Mesoperthite predominates, with coarse patches and rims showing albite twinning with cores and isolated patches of anorthoclase (cryptoperthite). Simple twinning is usual and relatively unexsolved varieties also show 'herring-bone' manebach textures. In the groundmass, the subhedral lath-like feldspars generally form an equigranular, randomly oriented matrix. Most are coarse patch perthites (Parsons, 1978) with the Or portion being most common in the centre of the crystals. Separate interstitial anhedral microcline however, does occur in some specimens examined.

In the field the unit shows very well developed flow differentiation (Plate 7.4a) where the early formed minerals are crowded toward the centre of the intrusion. Accordingly, the most 'primitive' mafic minerals are found in the densely phyric varieties (eg, 304032). Typically rounded anhedra of zoned pyroxene (ferrosalite-aegirine hedenbergite) 1 to 3 mm in size are mantled by the amphibole. Corroded olivine or olivine pseudomorphs may be similarly disposed. Amphibole shows a wide range of composition and habit even on thin section scale. The early formed amphibole is usually red-brown to brown ferro-edenite or even ferro-edenitic hornblende. These crystals are clearly zoned (although the change is abrupt) to green-brown kataphorite margins. This compositional change

is coupled with a change in habit. The direction of further growth has been noticeably governed by the large feldspar phenocrysts and the amphibole has become distinctly poikilitic to the small feldspar laths of the groundmass (eg, 304032). Further zoning and poikilitic growth continued with the development of blue-green to green ferro-richterite. Greenish blue to yellow green arfvedsonite is the normal amphibole of the groundmass. Aenigmatite, (5-10%) forms interstitial deep red-brown poikilocrysts 1 to 2 mm in diameter. The groundmass feldspar laths (< 0.3 mm) enclosed are generally larger than those enclosed by the similarly poikilitic green-blue amphibole.

7.4 Poikilitic arfvedsonite microsyenite

7.4.1 Rock character and structure (Plate 7.5)

This rock has been previously described petrographically and analysed by Jones (1980) under the heading East Motzfeldt Satellite (EM.b). It occurs as a sheet > 60 m thick, dipping E at approximately 20-30°, and capping the central high ground of SE Motzfeldt (alt. 1739 m). In hand specimen the grey-green 'glassy' rock has a mossy appearance due to irregular rounded patches of poikilitic black amphibole and poikilitic aenigmatite both about 10 mm in size. Together they comprise approximately 30% of the rock. The fine grained to glassy felsic matrix also contains sporadic bladed feldspar crystals 5 to 8 mm in length. Xenoliths of both MSF-Altered syenite and laminated porphyritic syenite are common. The feldspar 'phenocrysts' are in fact xenocrysts derived from the latter rock and examples are common showing how the Laminated porphyritic syenite xenoliths are broken down and 'stripped' of their feldspar phenocrysts.

The sheet is clearly exposed (although inaccessible) high in the west facing cliffs (1548 m peak) 1.5 km NE of Camp 2 (Plate 7.4a). The sheet dips approximately 30° ESE. S from this cliff face, due to displacement along the SE Motzfeldt Fault (Tukiainen, 1986b; Fig 9.1.2c, this work) the sheet outcrops on the central high ground of SE Motzfeldt and is extensive as loose block material. *In situ* exposure is restricted and indeed has not been found by the author (slide CB.82.C.05.34).

7.4.2 Petrographic Features (Plate 7.9a)

The rock is very distinctive due to 'moss-like' rounded 3 to 6 mm poikilocrysts of arfvedsonite and aenigmatite. These occur in roughly equal proportions and comprise between 20 and 35% of the mode. The remainder is taken up mainly by a fine grained groundmass of alkali feldspar showing trachytic texture, together with very small crystals or needles of Na mafic minerals. The arfvedsonite poikilocrysts are pleochroic in shades of deep green-blue to yellowish-green, They enclose c.60% by volume of small (< 0.2 mm), but distinct feldspar laths which often show preferred orientation although now 'closed' from the groundmass. The feldspar in the latter differ little in size but are more difficult to distinguish individually. Flow alignment around the poikilocrysts is normally developed. The deep red-brown to opaque aenigmatite poikilocrysts are on the whole, more 'open' to the groundmass and the feldspars enclosed show less alignment. Commonly the crystals become partially skeletal with a ghost-like cleavage being apparent. Xenocrysts of cryptoperthite (1 to 6 mm) may be abundant (up to 5%); they invariably have resorbed and corroded margins having been stripped from the Laminated porphyritic syenite through which the unit intrudes. The alkali feldspar of the groundmass, because of its small size is difficult to establish optically. Lamellar twinning however can be distinguished clearly and is probably confirmation of the albite dominated bulk feldspar composition as given in the normative analysis (Table A3.2), that is (mean of 7) Or 37, Ab 63, An 0.

7.5 Other Minor Intrusions

7.5.1 Introduction

Included in this section are the minor intrusions; (FDF?)-Larvikite ring-dyke (SM5*) of Jones (1980) and (FDF?)-Lujavrite sheet intrusions (SM6) of Jones (op. cit.). They are summarised here to give an overall coverage of the intrusive members of the Motzfeldt Centre. Both rocks are considered to be members of the Flinks Dal Formation. The Larvikite has been related genetically, by Jones, (1980), to the marginal facies of the FDF-Nepheline syenite (SM5), whereas the (FDF)-Lujavrite was considered to have evolved

from the highly alkaline residuum (probably) of the FDF-Porphyritic nepheline syenite (SM4). Remarkably, these rock types represent the two end-member lithological and geochemical compositions found in the fresh intrusive units of Motzfeldt.

7.5.2 (FDF)-Larvikite (SM5*) (Plate 7.6 & Plate 7.10)

This rock occurs in C Motzfeldt (west) as an arcuate ring-dyke, approximately 8 km long and up to c.60 m wide. The dyke appears to have intruded along the weakness provided by the FDF-Porphyritic nepheline syenite / FDF-Foyaite contact, and now partially circumscribes the latter. The unit is probably the last intrusive phase of the Motzfeldt Ring Series, and indeed possibly the Motzfeldt Centre. This 'last gasp' intrusion of more basic magma is a common occurrence in many of the central complexes of the Gardar Province (eg. Upton, 1960), and has been used to imply the existence of fractionating basic magmas at depth (Upton, 1976). The rock itself was described originally as a syeno-gabbro (Emeleus & Harry, 1970), however the petrographic studies of Jones noted the similarity with the larvikites of the Oslo district of Norway. In hand specimen the characteristic schillerisation of the feldspars is often visible, despite the often well developed chocolate brown weathered staining. Thin sections (Plate 7.10), show the subhedral- equigranular rock comprises cryptoperthite, deep-brown amphibole (Ferro- edenitic hornblende), salite and rounded fayalitic olivine. Nepheline is frequently present in small amounts (<5%) occurring mainly as irregular blebs within the feldspar crystals. Apatite and Fe-Ti oxide are common accessory minerals.

7.5.3 (FDF?)-Lujavrite (SM6)

Subhorizontal microsyenite sheets, many of which are of peralkaline Lujavrite composition (Jones, 1980), are numerous in the N and W facing cliffs of the Flinks Dal Valley (Plate 3.10). This complex but largely inaccessible array of intrusions can be traced from the 'HY' syenite of Jones (1980) for over 5 km westward to Lower Flinks Dal. If the host rocks of this area do prove to be members of the Motzfeldt Sø Formation as conjectured by Tukiainen, Bradshaw and Emeleus, (1984); Bradshaw (1985), then the Lujavrites are probably intrusive bodies derived and extended from the adjacent Flinks Dal Formation.

This relationship would be analagous to that seen in NE Motzfeldt, where the MSF-Peralkaline microsyenite sheets intrude the older and previously consolidated Geologfjeld Formation.

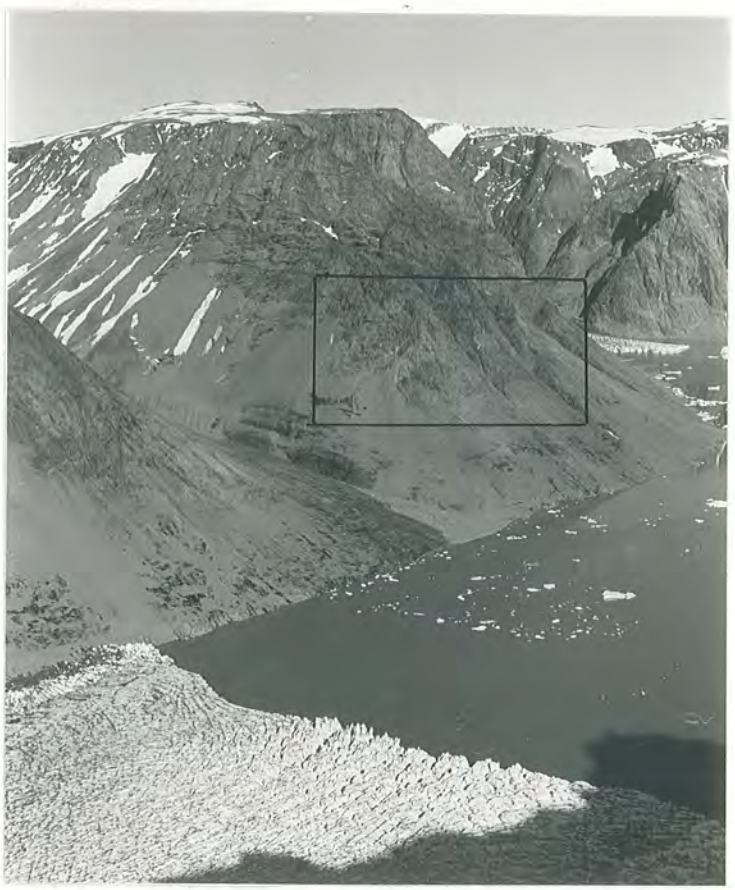
Lithologically, the sheets consist of white and dark lujavrite in roughly equal proportions with very subordinate green lujavrite (Jones, 1980). Phase 'banding' and flow structures are very common and similar to those described in the Peralkaline microsyenite of NE Motzfeldt. As in those rocks, eudialyte appears to be sparse in many lujavrites. In addition, the feldspars display strikingly similar forms and compositions with trachytic texture prominent among the small laths (1-3 mm). They are predominantly albite dominant patch perthites with the microcline component commonly restricted to the central cores of their crystals. Jones (1980), however, notes the paucity of amphibole in the lujavrites which is in contrast to the Peralkaline microsyenites of NE Motzfeldt. This possibly reflects the 'drier' character of the Flinks Dal Formation magmas compared to those of the Motzfeldt Sø Formation as displayed by their lack of pegmatite and well developed cumulate layering. Rare minerals include; eudialyte, pectolite, manganoan pectolite and pyrochlore. Jones (1985), concluded that the lujavrites are "Late stage products derived by extensive fractionation of nepheline syenites, either of unit SM1 or SM4."

In summary, lujavrites form a swarm of sub-horizontal sheets, intruded (as magma) at high levels into the older syenites (probably MSF) of SW Motzfeldt.

a.



Laminated alkali syenite. NE Motzfeldt ('Lejr elv'). Example showing poikilitic amphibole and weakly laminated feldspar tablets. (CB.82.C.07.25).



Three separate 'sheets' of Laminated alkali syenite visible (as indicated) in the W facing cliffs of NE Motzfeldt (Lejr elv).

a.



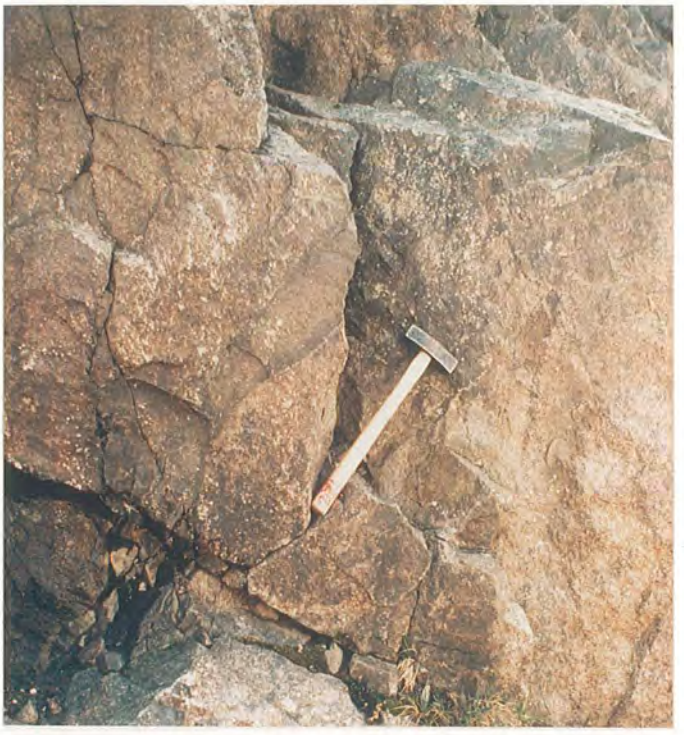
Porphyritic laminated syenite. NE Motzfeldt (Storeelv). Strongly porphyritic-seriate variety enclosing xenolith of altered GF-Geologfjeld syenite. (CB.84.C.03.35).

b.



Laminated porphyritic syenite. NE Motzfeldt (Storeelv). Densly phyric variety enclosing xenocryst of feldspar (a common feature of the unit). (CB.84.C.03.24).

a.



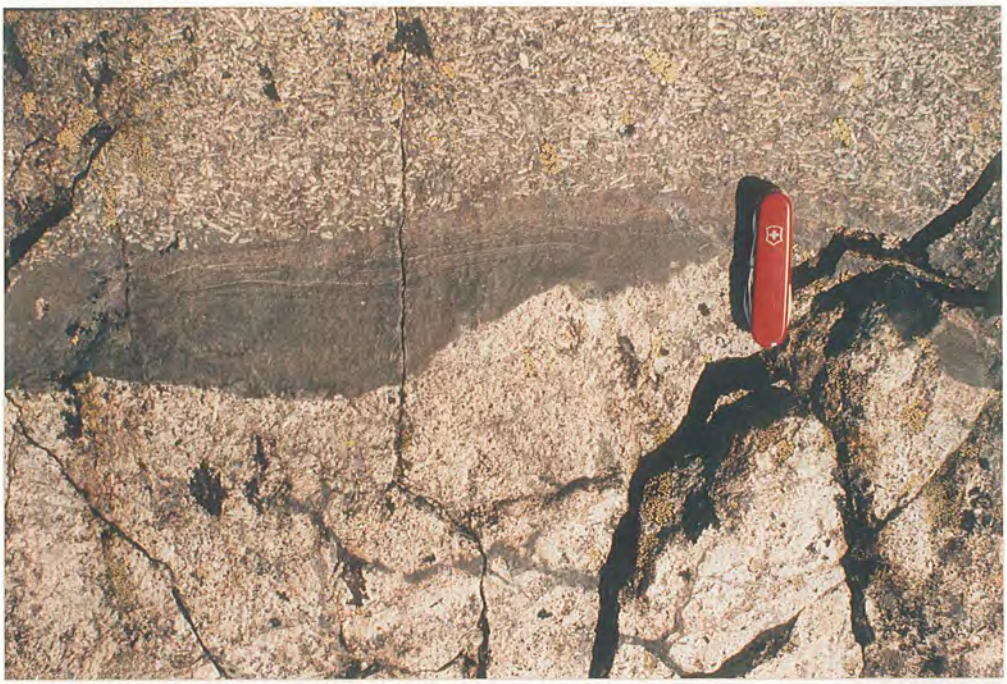
Porphyritic laminated syenite cutting Laminated alkali syenite. Note aphyric margin to the former. NE Motzfeldt ('Lejr elv'). (CB.84.C.10.03).

b.



Laminated alkali syenite enclosing blocks of MSF syenite, both being cut by the aphyric margin of the Porphyritic laminated syenite. NE Motzfeldt ('Lejr elv'). (CB.82.C.07.34).

a.



A dyke of Laminated porphyritic syenite showing flow differentiation and an aphyric margin. NE Motzfeldt ('Lejr elv'). (CB.82.C.08.22).

b.



Dykes of Porphyritic laminated syenite cutting pink syenite of the Geologfjeld Formation. NE Motzfeldt (Storeelv). (CB.84.C.03.08).



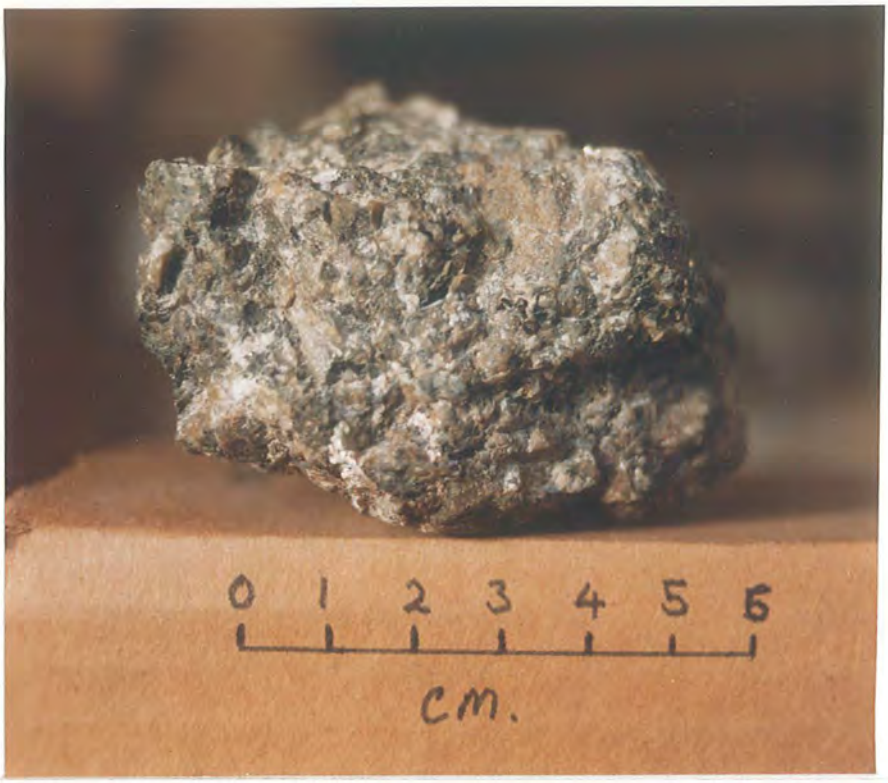
b.

Poikilitic arfvedsonite microsyenite. SE Motzfeldt. Sheet cutting red MSF-altered syenite and grey Laminated porphyritic syenite. View W-E (CHE.82.).



a.

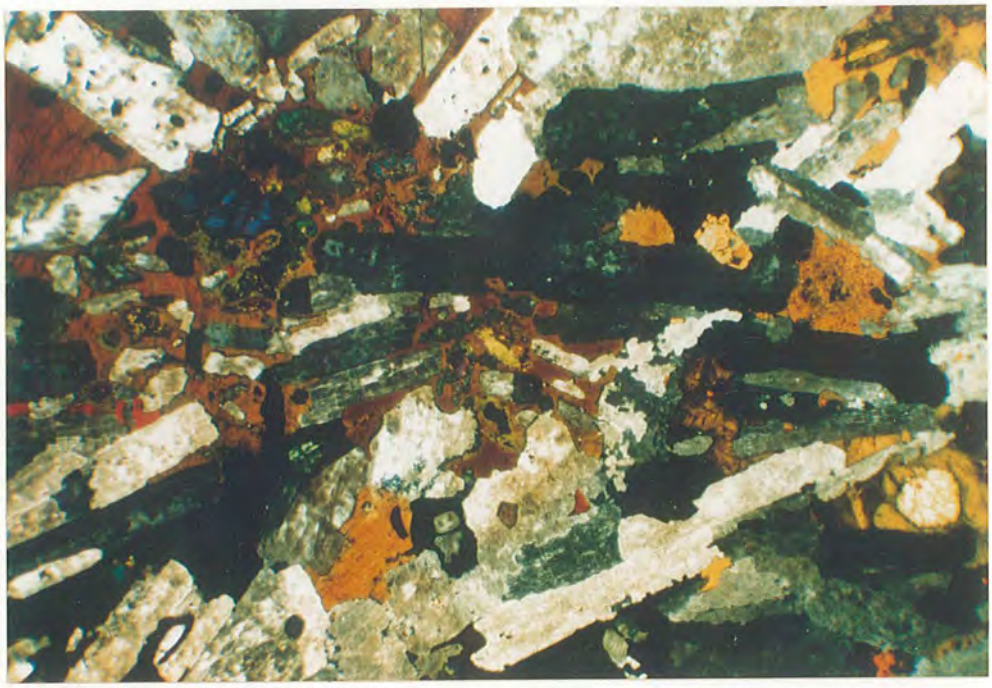
Poikilitic arfvedsonite microsyenite. SE Motzfeldt. Typical example with characteristic mossy aggregates of arfvedsonite and aenigmatite in a grey-green trachytic matrix. (CB.83.C.01.15).



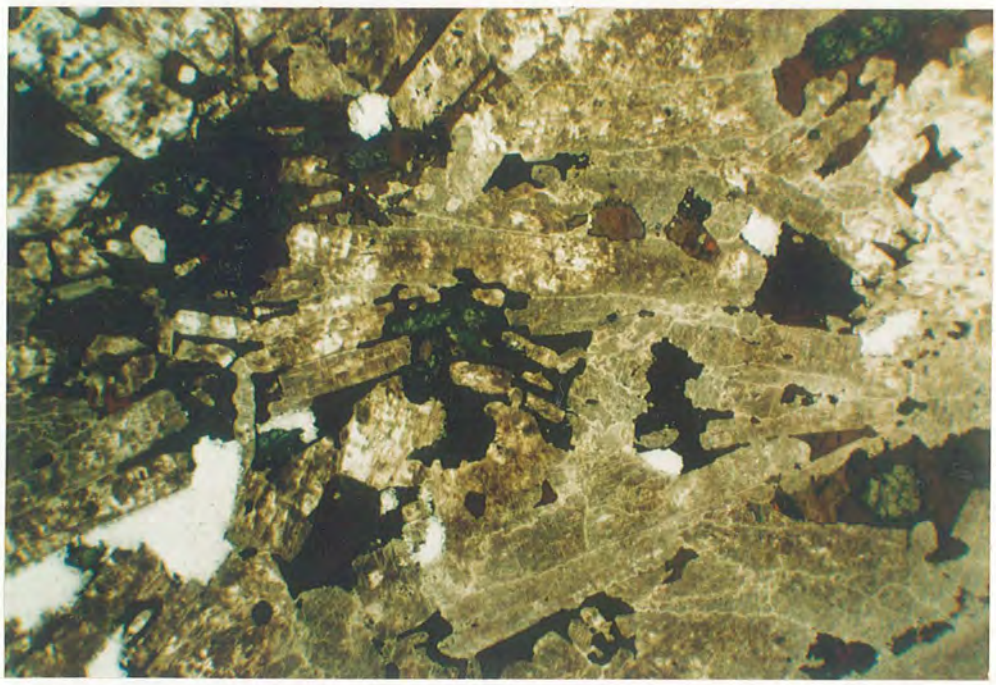
Larvikite (SM5*). From the ring-dyke in C Motzfeldt (west). A coarse, blocky, mesotypic rock with iridescent feldspar.



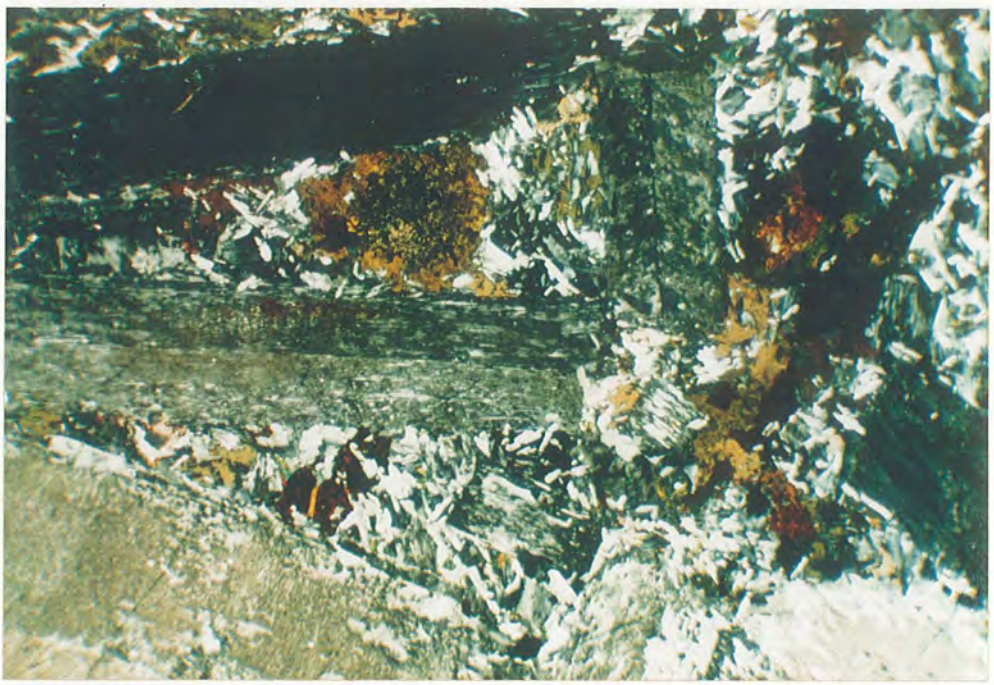
Alkali gabbro. C Motzfeldt. From the composite giant dyke. Typical aphyric microgabbro from the chilled margin and a medium-coarse variety.



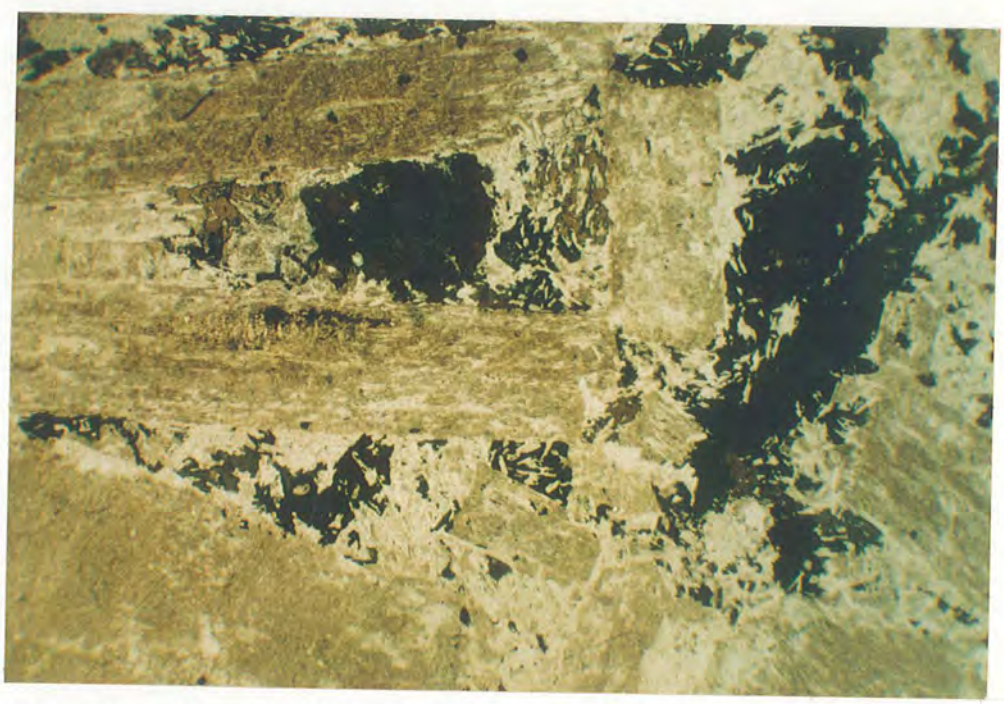
Laminated alkali syenite. NE Motzfeldt. (304097). Laminated alkali feldspar (Simple twins) with subophitic amphibole is the characteristic texture of the unit. X.P. 9mm.



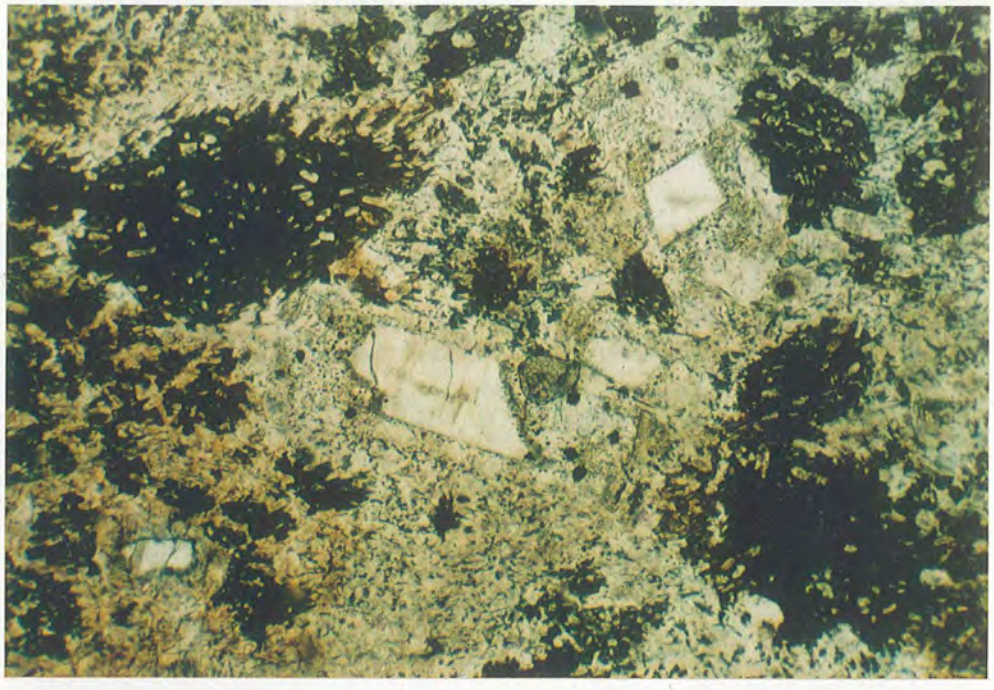
As above P.L. The amphibole is green-brown katophorite with occasional cores of brown ferro edenitic hornblende. Sporadic, corroded crystals of olivine (upper left), ferrosalite (lower right) and aegirine-hedenbergite (central) are commonly enclosed by the amphibole. Common accessories include zircon, orange-red biotite (middle left) and Fe-Ti oxides.



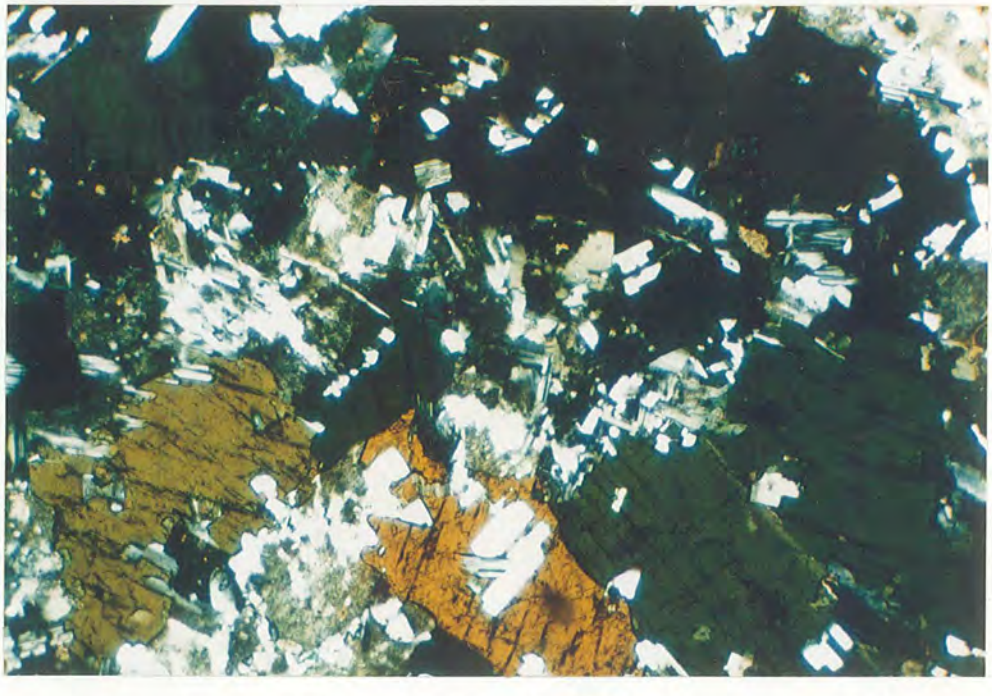
Laminated porphyritic syenite. NE Motzfeldt. (304090). Bladed alkali feldspar (invariably laminated) forms a framework to the groundmass, which comprises, small feldspar laths, Na-pyroxene and blue-green amphibole. The poikilitic mafic minerals include amphibole and red aenigmatite. X.P. 9mm.



As above. P.L. Corroded crystals of olivine (not seen) and ferrosalite (left centre) are common and usually enclosed by the amphibole (dominantly katophorite).



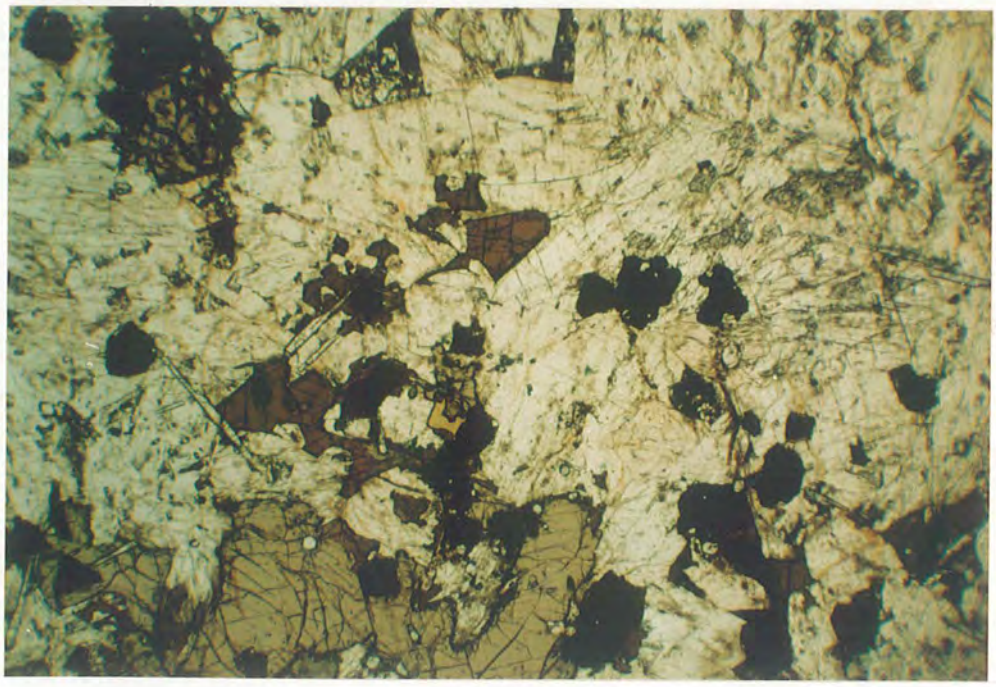
Poikilitic arfvedsonite microsyenite. SE Motzfeldt. (304033). Typical texture shown. Rounded poikilocrysts of blue-green amphibole and red-black aenigmatite (as indicate). Corroded clear feldspar xenocrysts (central) are a common feature and are derived from the adjacent laminated porphyritic syenite unit. P.L. 5mm.



MSF-Marginal syenite. NE Motzfeldt. (304710). From pegmatitic apophyses cutting basement country rock. Blue-green arfvedsonite and albite rich feldspar. P.L. 5mm.



Larvikite. Ring-dyke. C Motzfeldt (west). (272454). Subhedral granular rock with corroded olivine, (top left), zoned pyroxene (lower left), amphibole (central), biotite, Fe-Ti oxides and apatite needles. Alkali feldspar (anorthoclase/cryptoperthite) makes up the bulk of the rock although nepheline occurs sporadically as distinct crystals (top-middle) and as exsolved blebs (top right). X.P. 9mm.



As above P.L. The pyroxene, mauve coloured Ti-salite is partially mantled by brown ferro edenitic hornblende.

PART THREE

GEOCHEMISTRY AND EVOLUTION

Chapter 8
Geochemistry and Mineralisation

8.1 Geochemical Features

8.1.1 Introduction

170 samples[1] from different units of the Motzfeldt Centre were analysed by X-ray fluorescence[2] for 10 major elements (Si, Al, Fe, Mg, Ca, Na, K, Ti, Mn, P) and 13 minor elements (Ba, Nb, Zr, Y, Sr, Rb, Zn, Pb, U, Th, Ga, La, Ce). The results of these investigations are listed in Formation/ Member order in Table A3.2, Appendix Three. Additionally, Table A3.2 gives each sample its CIPW norm values; lithological code (see Table A2.6); Colour Index (CI); Fractionation Index (FI); Differentiation Index (DI); Na/(Na+K); Peralkalinity Index (PI) - (Na+K)/Al; and the Fe_2O_3/FeO ratio as used in the norm calculation[3]

Rare-earth element (REE) (La, Ce, Nd, Sm, Eu, Tb, Yb, Lu, Ta) analyses of 68 rock and mineral specimens are presented in Table A3.3, Appendix Three. These were produced by INAA[4] at the University of Berlin by Dr P. Möller and kindly made available to the PYROCHLORE team.

Like the rest of this thesis emphasis in this section is placed on the discrimitive value of the geochemical data, particularly where it provides evidence which clarifies ambiguous field observations. Due to the small sample sets used here and because trace element concentrations are not generally normally distributed (Hall, 1983), (see also Fig 8.1.17), non-parametric statistical methods are used throughout this work and include the Mann-Whitney U, Kruskal-Wallis H tests and Spearman Rank Correlation Coefficients (Ebdon, 1985). Where any geochemical differences between the groups become statistically valid they are described here as 'significant'.

[1] see Appendix Two for sampling details
[2] see Appendix Three for preparation and operating conditions
[3] derived from data supplied by L.M. Larsen (GGU)
[4] Instrumental Neutron Activation Analysis

Geochemical features of the 'fresh' rocks comprising the Centre are described here under the two lithological headings: Nepheline syenites and Syenites. The economically important geochemistry of the mineralised units has been investigated by members of the PYROCHLORE team to whom reference should be made (Tukiainen, 1986c; Morteani et. al. 1986).

The following section introduces the general geochemical behaviour of the elements and their general distribution in the Motzfeldt units. Comparison is also made with some other members of the Igaliko Nepheline Syenite Complex (Emeleus & Harry, 1970).

8.1.2 Geochemical range and overall characteristics

Most Motzfeldt units show a range of major and minor element values similar to other Igaliko Complex Centres (Stephenson, 1971; Chambers, 1976). Motzfeldt differs however, in that localised extreme enrichment of incompatible elements has occurred both as a result of extreme fractionation (ie, lujavrites of SW Motzfeldt; Jones, 1980) and by wholesale infiltration of incompatible-rich metasomatic 'fluids' (ie, MSF-Altered syenite & MSF-Peralkaline Microsyenite Suite). The fresh rocks of Motzfeldt range from larvikite to lujavrite. This wide range of composition is reflected by the wide range of elemental concentrations shown on Table 8.1.1 ie, Ba decreases from 4,596 ppm to 0 ppm with increasing fractionation while Zr increases from a minimum of 216 ppm to 5,022 ppm. The Peralkalinity Index of the rock type, as previously mentioned (section 3.3) is probably the best *Index of fractionation* for the rock types of Motzfeldt and as such is used here to describe the general behaviour of the elements during this process.[6] Previous workers in the Igaliko Complex have used Fractionation Index (FI) (normative Or + Ab + Ne + Ac + Q), to display elemental behaviour (Stephenson, 1973; Chambers, 1976; Jones, 1980). However, whilst the FI does actually vary between approximately 50 to 100 in Motzfeldt, over 85% of the fresh rocks analysed have FI's in the narrow range of 80 and 92. This is a reflection of the small variation in major element geochemistry between the rock units. The trace element values on the other hand show a much wider

[6] when the PI range is narrow (ie, Nepheline Syenites) K/Rb is better

Motzfeldt geochemical range Table 8.1.1

Motzfeldt –	Fresh rocks (N=113)				Altered rocks (N=50)			
	Min	Max	Mean	S.D.	Min	Max	Mean	S.D.
Majors (wt%)								
SiO2	51.10	63.30	57.69	2.69	43.96	69.81	58.16	4.70
Al2O3	13.39	22.24	18.76	2.46	5.52	22.42	14.18	3.48
Fe2O3T	2.59	12.07	6.53	2.10	0.61	27.37	10.26	5.59
MgO	0.01	2.72	0.48	0.36	0.00	2.68	0.74	0.68
CaO	0.35	5.65	1.58	0.78	0.21	8.28	1.75	1.47
Na2O	4.38	11.02	7.24	1.35	2.53	9.70	6.10	1.62
K2O	3.61	6.94	5.53	0.65	0.02	7.47	4.30	1.67
TiO2	0.02	2.47	0.55	0.33	0.01	3.81	0.62	0.70
MnO	0.10	0.46	0.24	0.06	0.01	0.89	0.36	0.21
P2O5	0.00	1.89	0.17	0.25	0.00	1.49	0.08	0.22
Traces (p.p.m)								
Ba	0	4596	547	690	0	2588	302	496
Nb	49	789	250	144	0	5503	974	1210
Zr	216	5022	1046	811	42	22437	4203	4738
Y	28	223	87	44	33	1247	280	252
Sr	15	1841	267	286	19	1390	148	230
Rb	43	548	213	84	0	738	309	154
Zn	67	1055	201	137	14	5434	556	831
Pb	0	164	23	24	2	1367	145	265
U	0	65	8	8	0	471	55	100
Th	0	254	18	28	0	10975	277	1547
Ga	20	107	39	13	29	122	49	16
La	43	636	184	138	6	4865	755	954
Ce	73	1234	340	239	10	8330	1288	1629
FI	58.35	97.40	86.20	5.35	51.00	96.10	81.97	8.55
PI	0.71	1.30	0.99	0.12	0.62	2.29	1.09	0.28
Zr/Nb	0.38	9.52	4.21	1.28	0.67	17.50	4.86	2.64
K/Rb	37.10	378.40	124.62	55.40	21.20	186.13	67.80	39.34

The geochemical range shown by the fresh and altered intrusive rocks of Motzfeldt computed from the data derived by this study. The altered rocks were sampled at random and consequently extremely incompatible-element enriched, ore-grade material is not represented by these figures (see Tukiainen, 1986c).

The mean values do not reflect the 'bulk' rock of Motzfeldt because the percentage volume of each unit has not been used in the computation.

range of concentrations and are consequently of much greater value in characterising and discriminating between the rock units (Table 8.1.1). Table 8.1.4 clearly shows the poor correlation between trace element concentrations and FI. The Peralkalinity Index (PI) however displays strong, significant correlation with the trace element values. FI does show good correlation with many of the major elements but as indicated by Jones (1980) this is partly because they are inherent in the initial FI calculation. In Chapter 3 the rocks of Motzfeldt were said to be characterised by their PI and on this basis divisible into the groups: hypoalkaline, alkaline and peralkaline. This grouping is well displayed by the geochemical data and although there is overlap between the elemental ranges the mean values given here (Table 8.1.2) give a good approximation of the overall geochemical properties. Figs 8.1.3a & 8.1.3b show the relative concentration levels of several elements from hypoalkaline and peralkaline rock types normalised against alkaline types.[7] Table 8.1.2 gives more quantitative data on the geochemical variation between these groupings. These figures, used in conjunction with the Spearman Rank Correlation charts (Tables 8.1.4 & 8.1.5) and the sequence of element/PI plots (Figures 8.1.6 to 8.1.12) clearly display the range of values found in Motzfeldt and, with the PI plots and their captions, describe the general elemental behaviour during the evolution of the rock types. The linearity of the elemental changes has prompted some to stress the importance of fractional crystalisation as a mechanism for the evolution of the Motzfeldt Centre and other Igaliko Centres (Stephenson, 1976b; Jones, 1980). Others however, stress that the consistency between the peralkaline rocks and large amounts of incompatible elements does not "vouchsafe to crystal fractionation" but is merely an association of that chemical condition (Nicholds & Carmichael, 1969).

Interestingly, the indices of fractionation used for the fresh rocks of Motzfeldt (ie, PI or K/Rb) show very poor correlation with trace elements from the altered and mineralised units (Table 8.1.5). This is probably a reflection of the highly localised areas of extreme incompatible element enrichment found within these rocks due to late-stage 'metasomatic' processes (see section 8.2). The uneven distribution being caused by mechanisms such as selective leaching, complexing, migration and deposition.

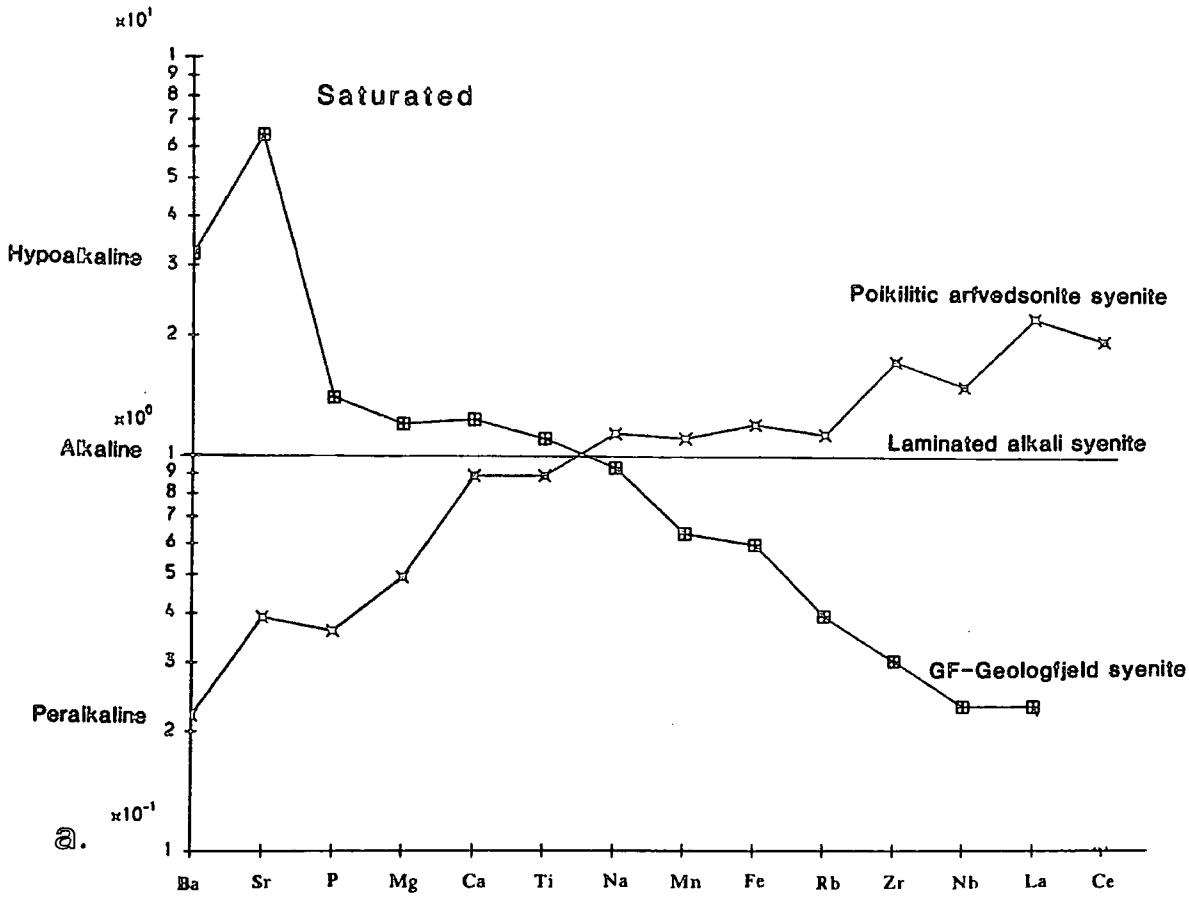
[7] mean values from selected rock units are used

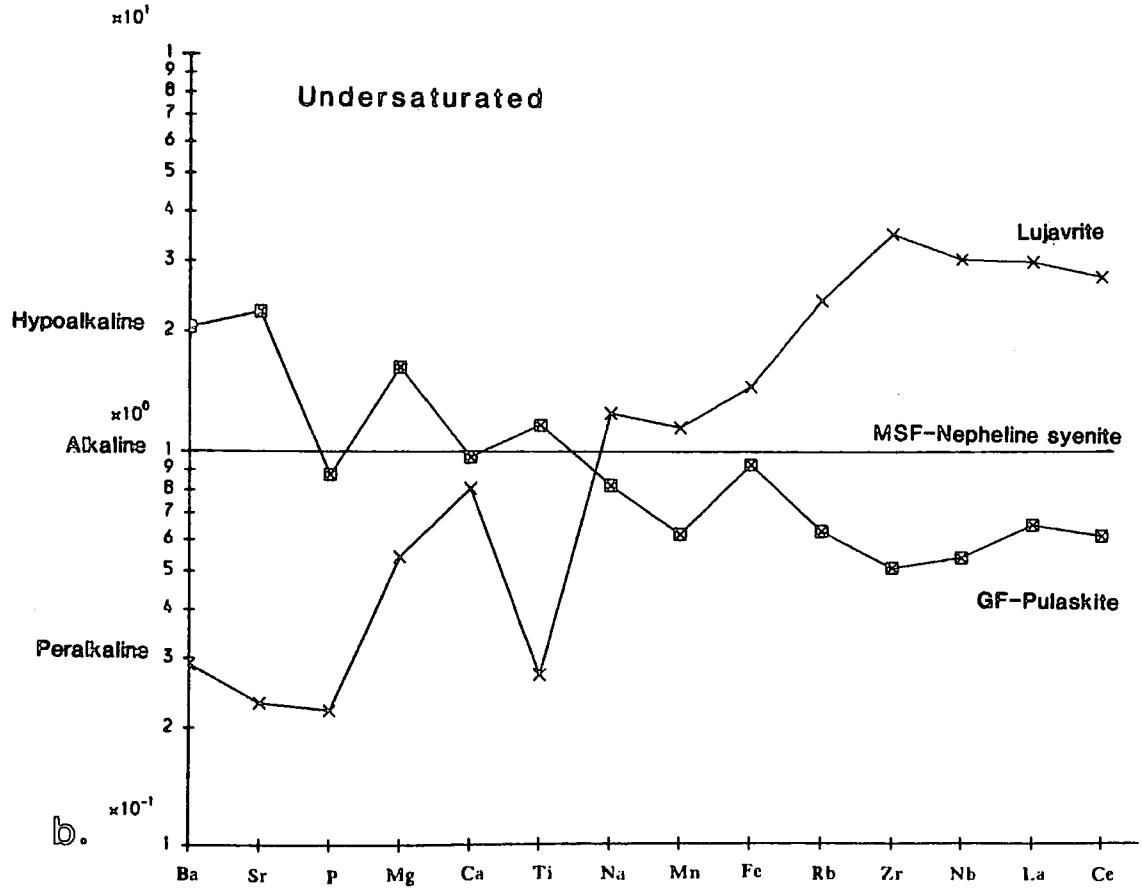
	HYPOALKALINE (N=16)				ALKALINE (N=27)					PERALKALINE (N=19)					
	Min	Max	Mean	STD	Min	Max	Mean	STD	%Diff1	Min	Max	Mean	STD	%Diff2	%Diff3
Ba	361	1250	894	279.32	47	966	419	296.05	-53.13	0	1010	172	279.91	-58.95	-80.76
Sr	197	809	464	213.66	19	452	212	159.06	-54.31	15	493	85	142.43	-59.91	-81.68
P2O5	.07	.90	.23	.20	.01	.51	.13	.10	-43.48	0	.34	.01	.01	-92.31	-95.65
MgO	.317	.96	.62	.19	.11	.93	.43	.21	-30.65	.01	.71	.25	.17	-41.86	-59.68
CaO	.91	2.58	1.83	.45	.68	2.14	1.41	.41	-22.95	.50	2.32	1.28	.42	-9.22	-30.05
TiO2	.24	.79	.58	.14	.17	1.07	.52	.21	-10.34	.02	.68	.51	.17	-1.92	-12.07
Na2O	5.71	7.51	6.61	.56	5.76	9.58	7.85	1.17	+18.76	6.41	11.02	7.64	1.45	-2.68	+15.58
K2O	5.31	6.94	6.02	.44	4.48	6.69	5.61	.54	-6.81	3.61	5.10	4.77	.42	-14.97	-20.76
MnO	.13	.29	.18	.04	.14	.33	.23	.05	+27.78	.17	.37	.28	.05	+21.74	+55.56
Rb	86	228	141	40.90	136	433	212	56.59	+50.35	171	486	257	73.91	+21.23	+82.27
Fe2O3	4.18	6.61	4.87	.63	3.67	9.98	6.17	1.84	+26.69	6.55	12.01	8.74	1.33	+41.65	+79.47
Nb	51	251	142	62.90	79	537	238	94.75	+67.61	218	675	388	129.91	+63.03	+173.24
Y	28	74	48	14.27	39	163	84	32.27	+75.00	74	223	139	44.02	+65.48	+189.58
Zr	224	1055	591	240.66	305	1824	976	400.24	+65.14	216	4655	1674	923.29	+71.52	+183.25
Zn	67	174	109	30.91	93	288	174	57.71	+59.63	110	675	324	126.61	+86.21	+197.25
Ce	73	269	151	54.80	109	586	295	148.79	+95.36	176	1234	651	257.48	+120.68	+331.13
La	43	134	78	26.83	53	376	158	89.57	+102.56	85	636	362	152.59	+129.11	+364.10
Pb	6	13	9	2.07	0	42	18	11.17	+100.00	9	164	49	35.70	+172.22	+444.44
U	1	8	5	2.51	0	11	6	2.23	+20.00	4	36	19	7.24	+216.67	+280.00
Th	0	11	6	3.27	0	46	13	10.81	+116.67	0	96	35	25.01	+169.23	+483.33
Zr/Nb	2.27	4.83	4.00	0.66	2.07	9.52	4.23	1.40	+5.75	0.38	8.59	4.28	1.72	+1.18	+7.00
Ba/Sr	1.03	8.42	2.71	1.86	0.53	6.58	2.46	1.36	-9.23	0.00	6.81	2.25	1.82	-8.54	-16.97
K/Rb	99.91	314.97	182.76	65.28	48.64	171.83	116.56	29.04	-36.22	43.56	115.30	79.02	22.81	-32.21	-56.76

%Diff1 = % change from mean hypoalkaline value to mean alkaline value
%Diff2 = % change from mean alkaline value to mean peralkaline value
%Diff3 = % change from mean hypoalkaline value to mean peralkaline value

Table to show the geochemical range and mean for the three-way classification proposed in this work; Hypoalkaline (PI > 0.85 < 0.96), Alkaline (PI > 0.95 < 1.12) and Peralkaline (PI > 1.11). The percentage increases and decreases of the elements between the groups are indicated.

Hypoalkaline v Alkaline v Peralkaline Fig 8.1.3





Geochemical correlation - fresh rocks

Table 8.1.4

	BA	SR	P2O5	MGO	CAO	K2O	TIO2	NA2O	MNO	FE2O3T
SR	.8656**									
P2O5	.6918**	.5647**								
MGO	.6466**	.6102**	.6979**							
CAO	.3814**	.3298**	.4406**	.5460**						
K2O	.4976**	.4707**	.3585**	.4358**	.1232					
TIO2	.2095	.0667	.4282**	.2728*	.5493**	-.1896				
NA2O	-.1963	-.0957	-.1740	-.0572	-.3857**	.0191	-.5741**			
MNO	-.4263**	-.3531**	-.2666*	-.2231*	-.1353	-.6173**	.2168	.0544		
FE2O3T	-.5040**	-.4589**	-.2974**	-.3020**	.1159	-.7826**	.3884**	-.2071	.6950**	
RB	-.5973**	-.5317**	-.5357**	-.4279**	-.3838**	-.3190**	-.3416**	.3704**	.3708**	.3268**
ZR	-.4652**	-.3560**	-.4638**	-.4277**	-.4410**	-.4133**	-.2666*	.3552**	.4257**	.3392**
NB	-.5628**	-.4637**	-.4545**	-.4522**	-.4138**	-.5509**	-.1528	.3517**	.5843**	.4857**
LA	-.6737**	-.6325**	-.4058**	-.5328**	-.3380**	-.6119**	-.0429	.1240	.5965**	.5439**
CE	-.6766**	-.6433**	-.4178**	-.5220**	-.3229**	-.6180**	-.0330	.1425	.6042**	.5413**
PB	-.5449**	-.5375**	-.3638**	-.4621**	-.2743*	-.4664**	.0720	.0233	.5014**	.4545**
U	-.1372	-.1068	-.1131	-.1800	-.2144	-.4335**	.0863	.1176	.3332**	.2378*
TH	-.4343**	-.4346**	-.3064**	-.3876**	-.2308*	-.3300**	.0042	.1186	.3903**	.2822*
ZN	-.5938**	-.5615**	-.4035**	-.4302**	-.3032**	-.6796**	.0884	.0837	.8057**	.6634**
GA	-.7151**	-.5638**	-.6765**	-.6016**	-.5073**	-.5399**	-.3271**	.3602**	.5066**	.5231**
FI	-.1558	-.1899	-.2022	-.2323*	-.6151**	.1360	-.5964**	.7487**	-.0904	-.3947**
PI	-.4894**	-.5746**	-.3159**	-.3700**	-.2368*	-.4063**	-.0503	.4555**	.4249**	.3377**
KRB	.6974**	.6412**	.5744**	.5174**	.3732**	.5455**	.2189*	-.2988**	-.5214**	-.5051**

	RB	ZR	NB	LA	CE	PB	U	TH	ZN	GA
ZR	.6581**									
NB	.7088**	.8406**								
LA	.6114**	.6206**	.7643**							
CE	.6257**	.6051**	.7690**	.9876**						
PB	.5531**	.6255**	.7081**	.7783**	.7636**					
U	.3703**	.5514**	.5812**	.4815**	.4809**	.5645**				
TH	.5325**	.5381**	.6232**	.7127**	.6953**	.8226**	.5539**			
ZN	.6000**	.6505**	.7646**	.8159**	.8094**	.7859**	.5795**	.6541**		
GA	.7852**	.6991**	.7501**	.6266**	.6222**	.5692**	.3281**	.4545**	.6931**	
FI	.2602*	.2862*	.1944	.1220	.1254	.0973	.1688	.1981	.0439	.2063
PI	.5034**	.4896**	.5563**	.5814**	.6006**	.5311**	.4190**	.5655**	.5589**	.4734**
KRB	-.9526**	-.7008**	-.7883**	-.7438**	-.7581**	-.6539**	-.4481**	-.5879**	-.7502**	-.8372**

	FI	PI
PI	.5428**	
KRB	-.1976	-.5899**

* - SIGNIF. LE .01 ** - SIGNIF. LE .001 " . " IS PRINTED IF A COEFFICIENT CANNOT BE COMPUTED.

Spearman Rank – Correlation ceofficients (N = 112)

	BA	SR	P2O5	MGO	CAO	K2O	TIO2	NA2O	MNO	FE2O3T
SR	.3517*									
P2O5	.4159*	.3960*								
MGO	.2205	.3648*	.4677**							
CAO	.1360	.3488*	.5094**	.5088**						
K2O	.4015*	-.1421	.3111	.2669	.0019					
TIO2	.3893*	.4470**	.7970**	.4972**	.5287**	.0658				
NA2O	-.0304	-.1535	-.2687	-.4801**	-.0208	-.3971*	-.1982			
MNO	-.2681	.2551	-.2480	.0080	.1829	-.5640**	.0432	.1047		
FE2O3T	-.2274	.0596	-.2499	.1533	.2099	-.5842**	.1184	.0039	.7768**	
RB	-.0445	-.3634*	-.3191	-.1084	-.2073	.3452*	-.3965*	-.0650	-.2381	-.1513
ZR	-.4547**	.0433	-.5027**	-.1159	-.2228	-.3811*	-.3606*	.0518	.4277**	.3498*
NB	-.4918**	-.1062	-.5372**	-.0982	-.1940	-.4090*	-.3440*	.0261	.4751**	.4895**
LA	-.6552**	-.0495	-.2805	-.1437	-.0982	-.4710**	-.1815	-.0922	.3623*	.3561*
CE	-.6400**	-.0407	-.3300*	-.1500	-.0801	-.4920**	-.2108	-.0718	.4205*	.4142*
PB	-.4861**	.0450	-.3350*	-.0854	-.0975	-.4547**	-.1999	-.0547	.3791*	.3043
U	-.3511*	.1317	-.1048	-.0057	.1446	-.4824**	-.0095	-.0121	.4460**	.3712*
TH	-.2664	.0456	.1029	.0568	.0821	-.2819	.0915	-.2374	.1961	.1494
ZN	-.4761**	.0846	-.1835	.0718	.1529	-.5096**	.0630	.0518	.5519**	.5209**
GA	-.3961*	-.2222	-.4528**	-.2814	-.3268	-.3063	-.4593**	.1993	-.0314	-.0558
FI	-.0459	-.4227*	-.3922*	-.7515**	-.5755**	.0629	-.5180**	.4783**	-.3978*	-.5668**
PI	-.1059	-.0495	-.3481*	-.2412	.2229	-.6054**	.0231	.6605**	.5414**	.5820**
KRB	.2404	.1074	.5508**	.2359	.2124	.4717**	.3465*	-.1958	-.2861	-.3119

	RB	ZR	NB	LA	CE	PB	U	TH	ZN	GA
ZR	.3307*									
NB	.3204	.8819**								
LA	.1056	.7376**	.7727**							
CE	.0996	.7571**	.7917**	.9825**						
PB	.0515	.7055**	.6772**	.7684**	.7869**					
U	.0421	.6026**	.6958**	.7373**	.7522**	.7455**				
TH	-.0670	.3299*	.4200*	.6593**	.6406**	.6512**	.7847**			
ZN	.0468	.5345**	.5850**	.6548**	.6576**	.6501**	.6077**	.4678**		
GA	.3146	.3937*	.3991*	.3014	.3051	.3585*	.3186	.0900	.2885	
FI	.1248	-.1277	-.1698	-.1348	-.1498	-.1099	-.2441	-.1899	-.3429*	.3184
PI	-.1025	.2025	.2616	.1325	.1908	.1454	.2384	-.0862	.4145*	.1312
KRB	-.5458**	-.5626**	-.6358**	-.3967*	-.3948*	-.3871*	-.4454**	-.1695	-.4673**	-.5940**

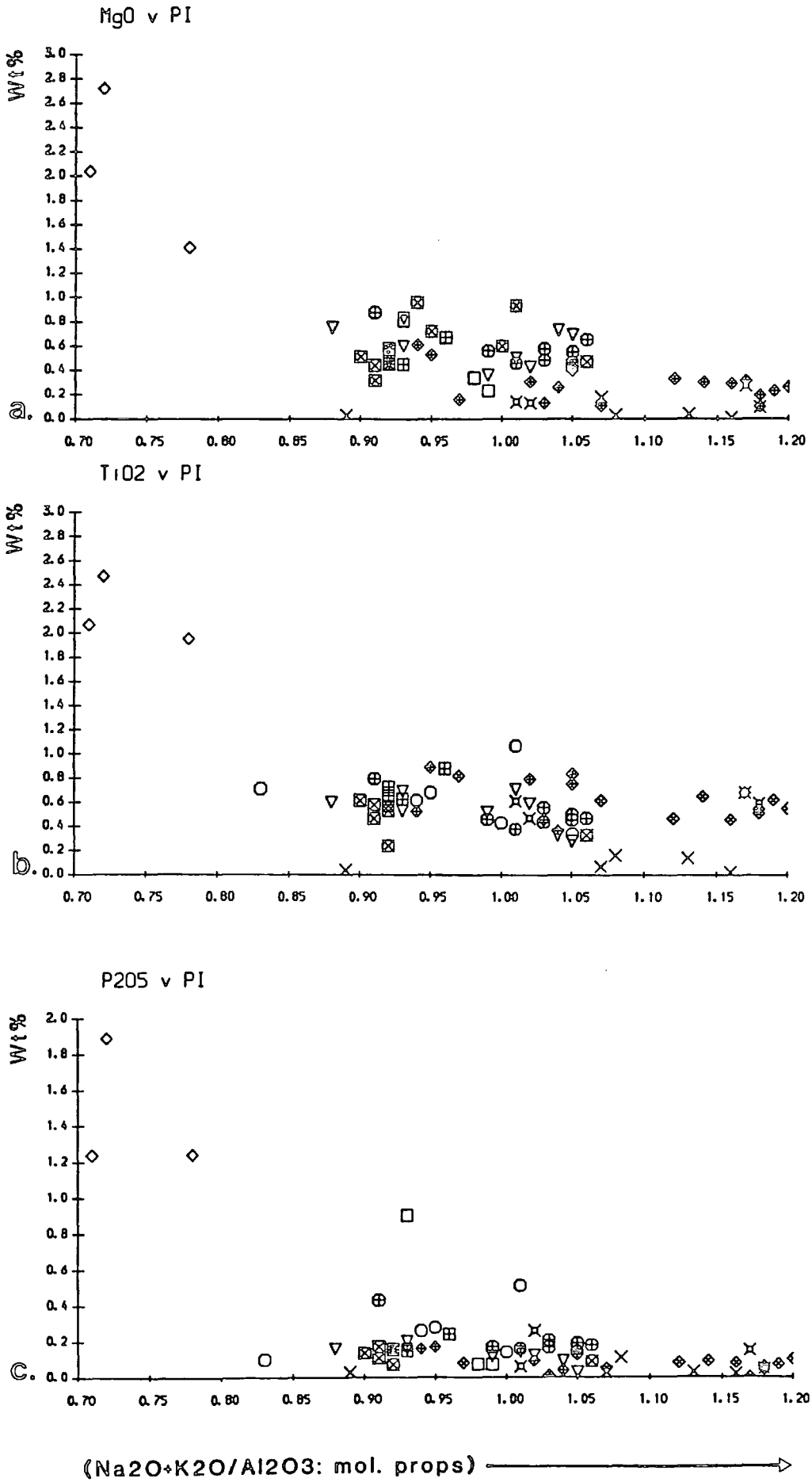
	FI	PI
PI	.0012	
KRB	-.0590	-.3654*

* - SIGNIF. LE .01 ** - SIGNIF. LE .001 " . " IS PRINTED IF A COEFFICIENT CANNOT BE COMPUTED.

Spearman Rank - Correlation ceofficients (N = 52)

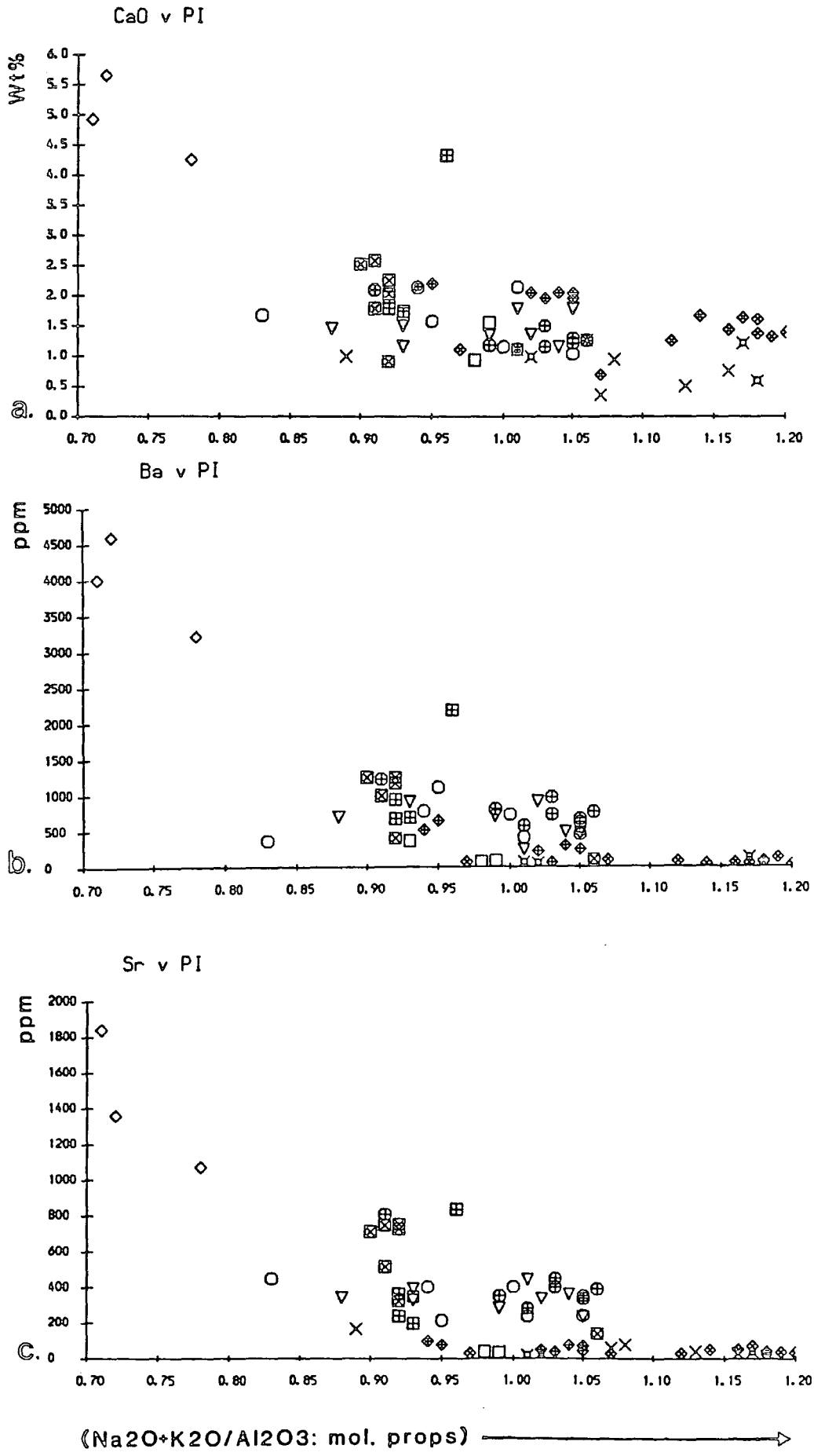
Element v Peralkalinity Index (PI)

Fig 8.1.6



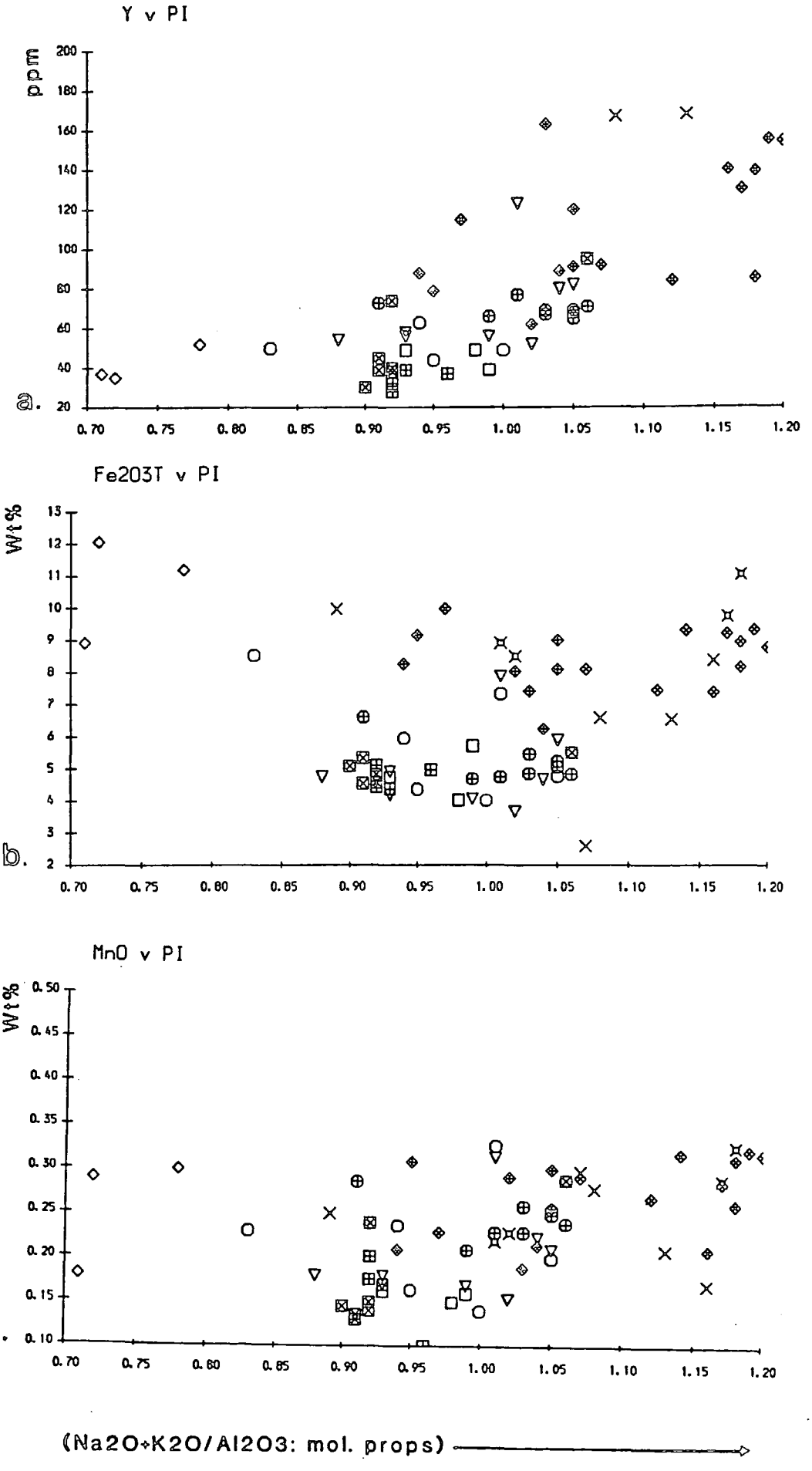
Element v Peralkalinity Index (PI)

Fig 8.1.7



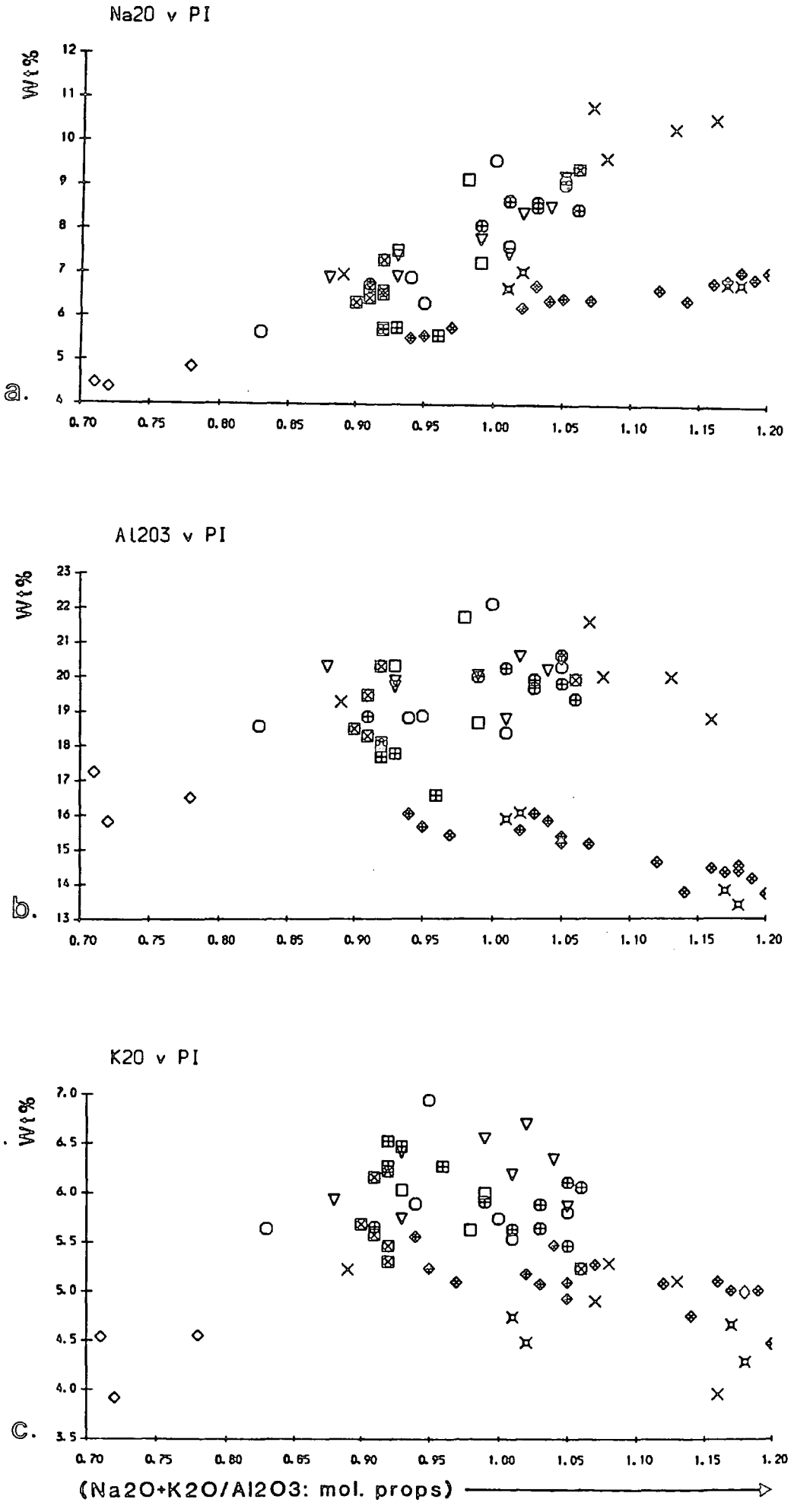
Element v Peralkalinity Index (PI)

Fig 8.1.8



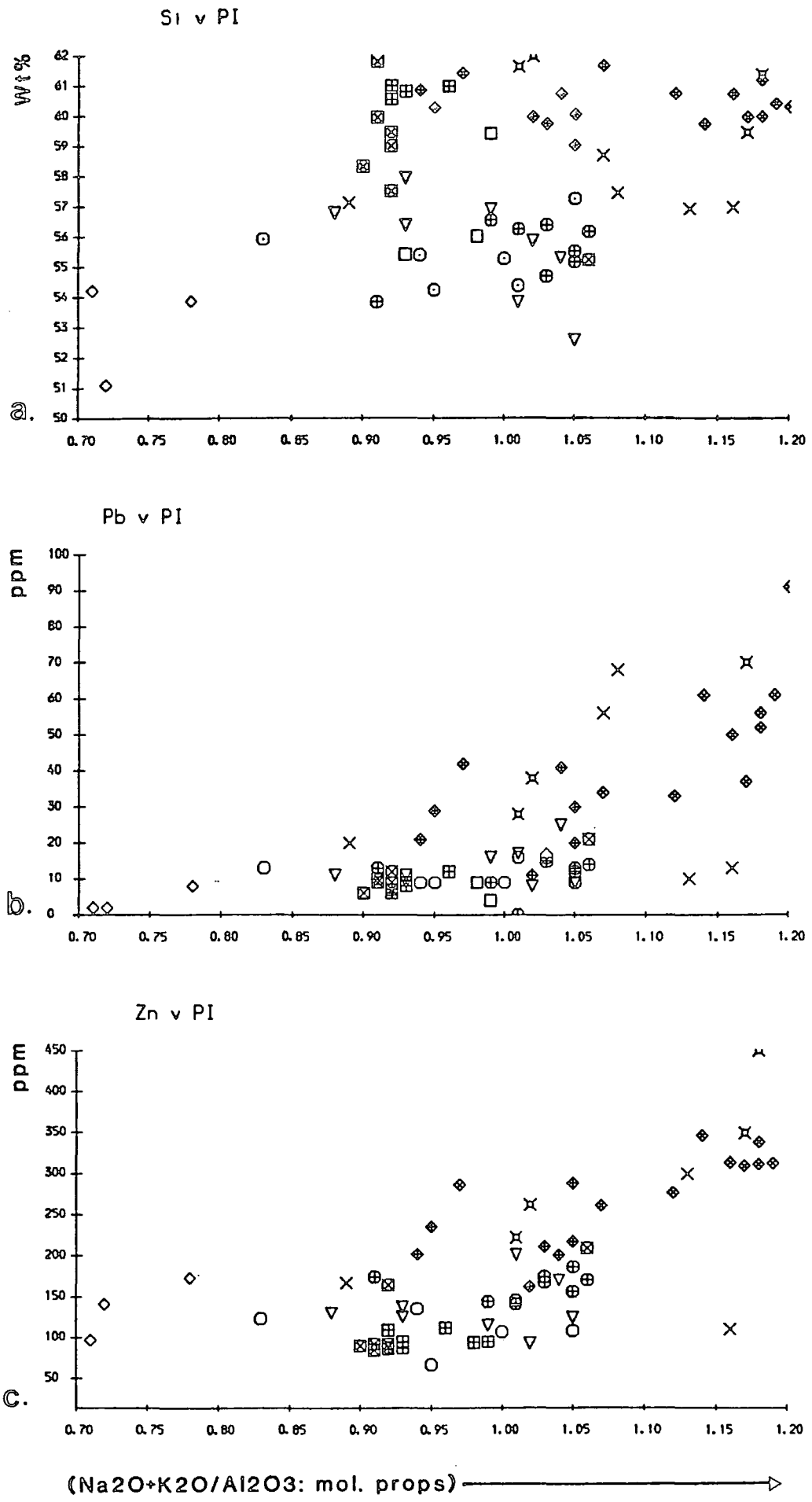
Element v Peralkalinity Index (PI)

Fig 8.1.9

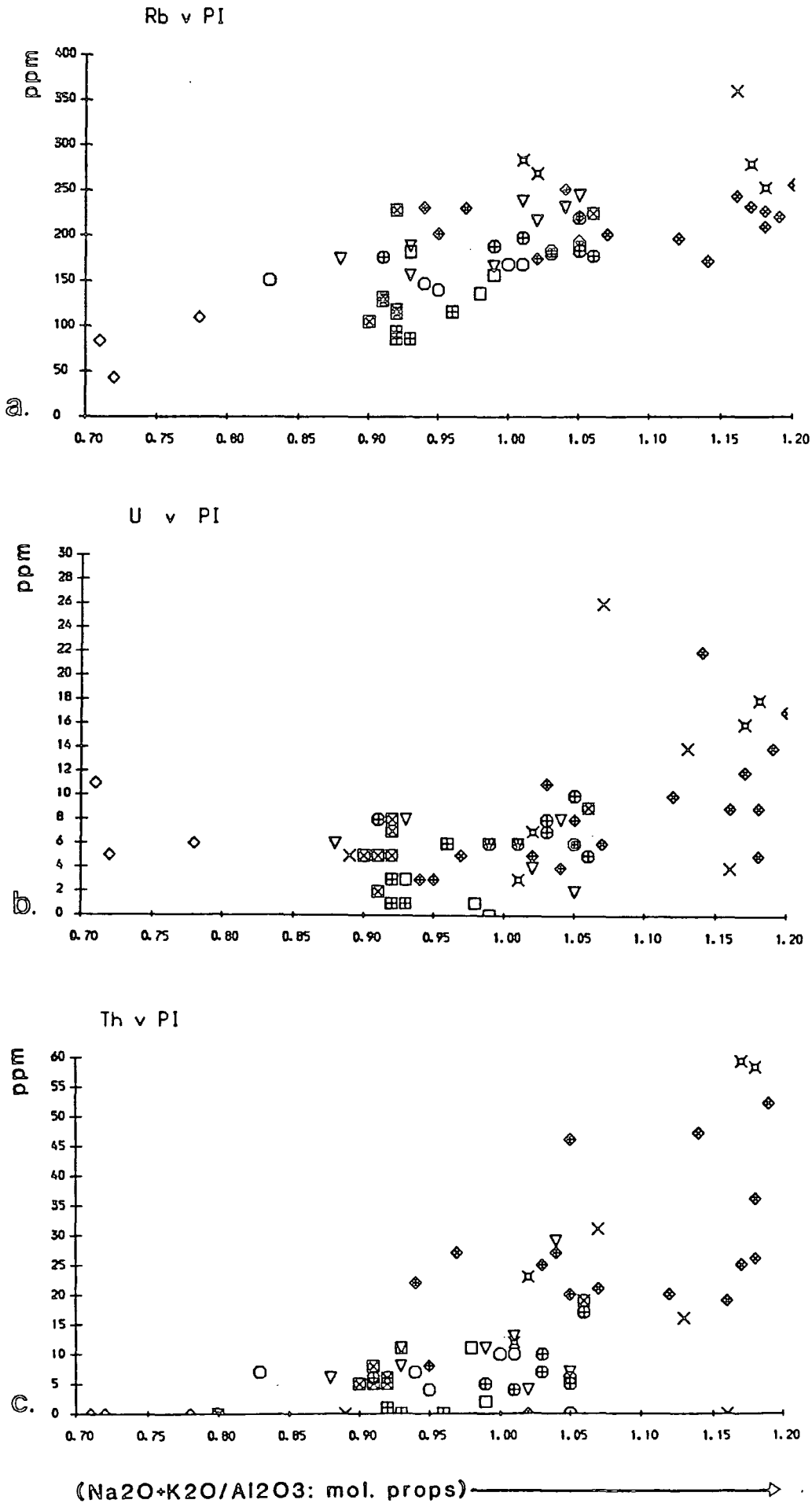


Element v Peralkalinity Index (PI)

Fig 8.1.10



Element v Peralkalinity Index (PI) Fig 8.1.11



Element v Peralkalinity Index (PI) Fig 8.1.12

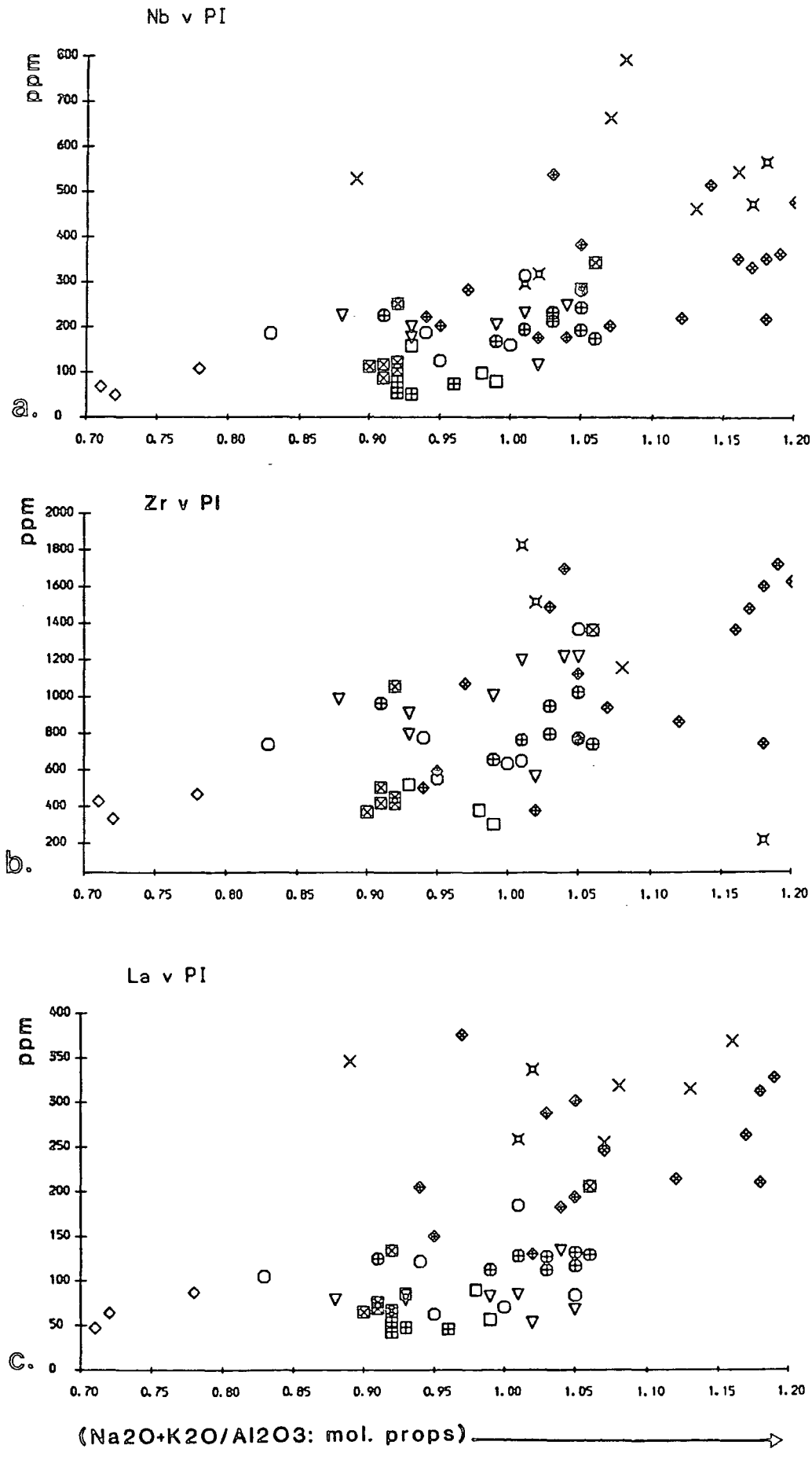


Table 8.1.13 lists selected geochemical data from Motzfeldt and a number of nepheline syenite units from other Igaliko Centres as well as data from the well known alkaline intrusions of Ilimaussaq, Lovozero and Khibina. Very clear geochemical similarities between the Igaliko Centres are diagramatically displayed on the rock/chondrite spidergrams (Figures 8.1.14 & 8.1.15; after Thompson, 1982; Thompson et. al. 1983). These plots are designed to give a smooth spidergram for average MORB chemical concentrations (Sun, 1980). The elements are ordered from left to right to show generally increasing compatibility (Ba to Yb) when melting a lherzolite source (Sun, op. cit). The plots Fig 8.1.14a to 8.1.15b all show marked troughs[8] for the elements Ba, Sr, P and Ti, and lesser depletion for Th and K. These relative depletions indicate the importance of feldspar, apatite and Fe-Ti oxide / mafic-mineral fractionation during the evolution of these rock types. The patterns for the rocks of the Motzfeldt Sø Formation and Flinks Dal Formation are extremely similar to those of S and N Qôroq. Both absolute abundances and the ratios of the elements are similar (except higher La and Rb in the FDF). The Geologfjeld Formation rock however contains lower absolute values across the whole range of elements (for additional comments see next section). The peralkaline samples (Fig 8.1.15a) show extreme enrichment in the incompatible elements La, Ce, Zr, Y, Nb and greater depletion of the previously mentioned residual elements.

Plot 8.1.15b shows similarly the mean values of the groups hypoalkaline, alkaline and peralkaline in Motzfeldt (fresh rocks)[9]. There is a remarkable consistency of behaviour, with the progressive depletion of Ba, Sr, P, Ti continuing as predicted from extended feldspar, apatite and oxide / mafic-mineral fractionation while concomitantly the incompatible elements increase. All the peralkaline rocks,[10] however, show a marked relative depletion of K and slight depletion of Rb. This presumably indicates the increasing importance of fractionating K rich alkali-feldspar. Thus driving the residuum melt toward Na oversaturated peralkaline compositions. The preferential partitioning of K into alkali-feldspar (or other phases) relative to the liquid in peralkaline magma has been called the

[8] relative to neigbouring elements
[9] data from Table 8.1.2
[10] ie, Motzfeldt, Lovozero and Ilimaussaq

Element		Motzfeldt			S Qôroq		N Qôroq	Khibina	Ilímaussaq	Lovozero
ppm	334	434	514	SS2	SS3		SN1b			
	58352	54132	304024	58231	52297		155135	(Average nepheline syenites)		
Ba	87	899	966	191	136		844	1190	90	700
Rb	156	188	452	233	279		234	215	590	230
Th	2	11	7	13	15		12	14	38	35
K	49828	53233	48831	48915	50327		51240	54000	33500	48640
Nb	79	176	213	228	443		262	152	525	696
Ta	4.71	14.2	11.3	-1	-1		-1	14	32	60
La	54	82	124	97	77		93	-1	850	481
Ce	116	151	266	-1	-1		-1	-1	1395	860
Sr	35	328	452	138	237		208	1070	47	610
Nd	56	52	93	-1	-1		-1	-1	495	298
P	305	698	916	610	524		524	1250	214	880
Sm	8.5	10.8	17	-1	-1		-1	-1	95	45
Zr	305	794	795	954	1297		947	625	4735	3480
Hf	-1	-1	-1	-1	-1		-1	-1	-1	-1
Ti	1618	3177	3357	3057	3357		4017	6300	2070	6700
Tb	1.04	1.25	1.89	-1	-1		-1	-1	15	6
Y	39	58	66	50	37		57	-1	390	135
Tm	-1	-1	-1	-1	-1		-1	-1	-1	-1
Yb	-1	-1	-1	-1	-1		-1	-1	-1	-1

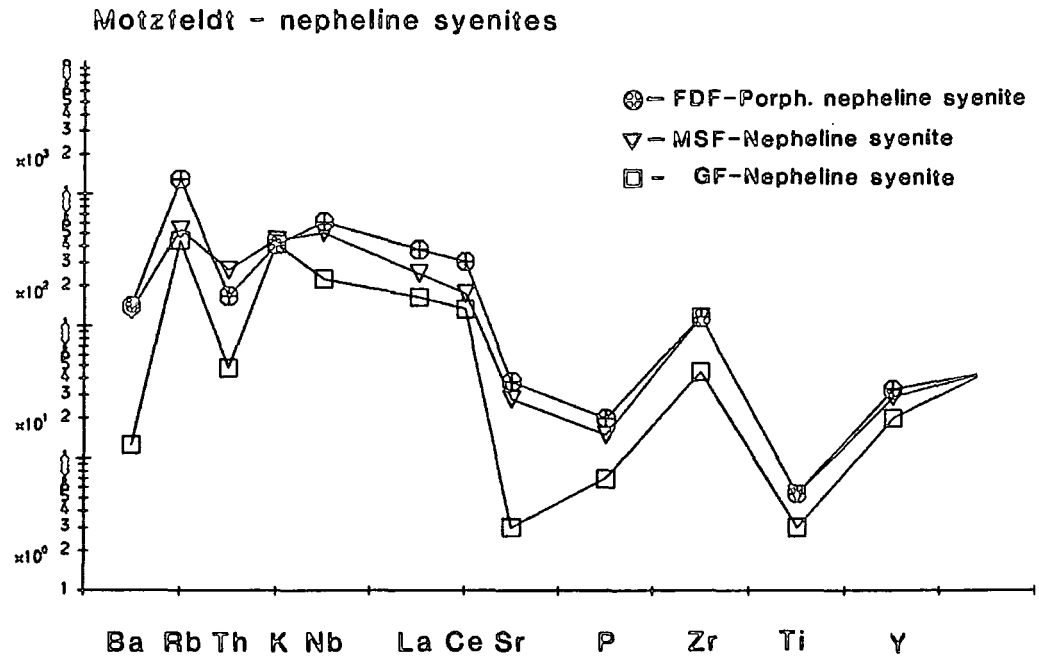
Table 8.1.13 Comparison table of nepheline syenites from the Igaliko Complex (data from: this work; Stephenson, 1973; Chambers, 1976), Lovozero, Khibina and Ilimaussaq (data from Gerasimovsky, 1974). -1 indicates element not analysed.

Figs 8.1.14 and 8.1.15 (following)

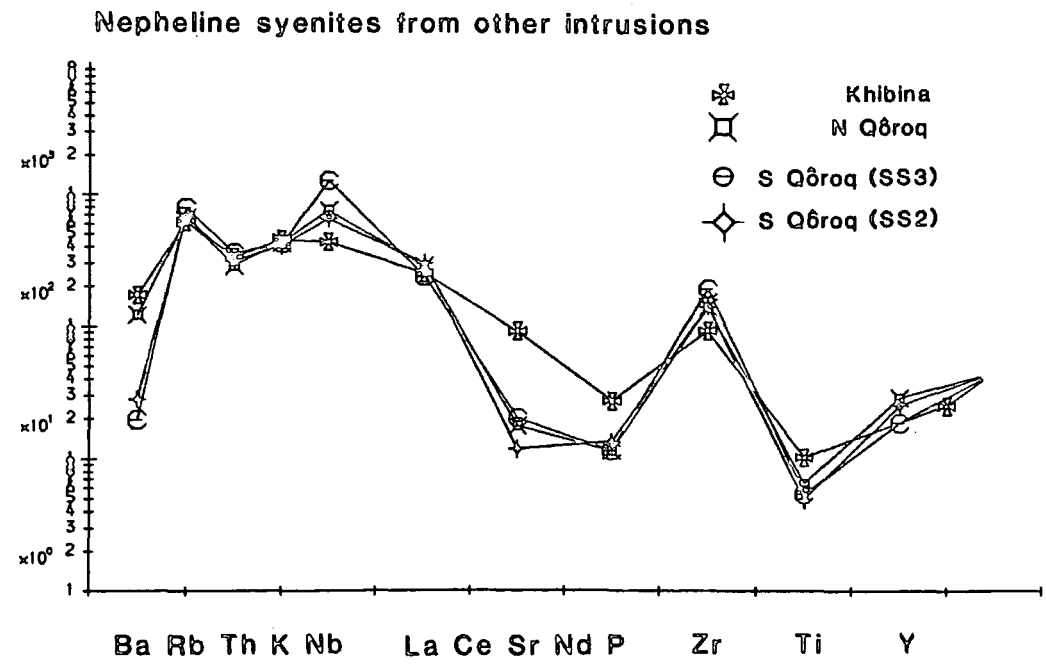
Diagramatic representations of the above data (incompatible element spidergrams: after Thompson et al, 1983; modified from Sun, 1980) normalised against chondrite values (except Rb, K, P; data from Thompson op. cit.)

Incompatible element spidergrams Fig 8.1.14

a.

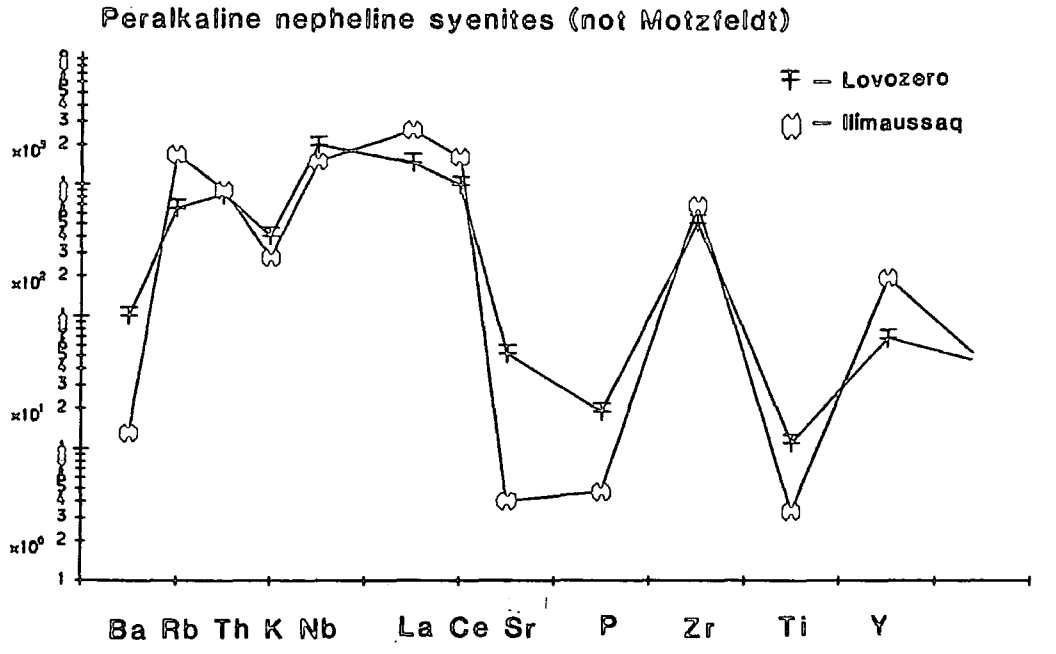


b.

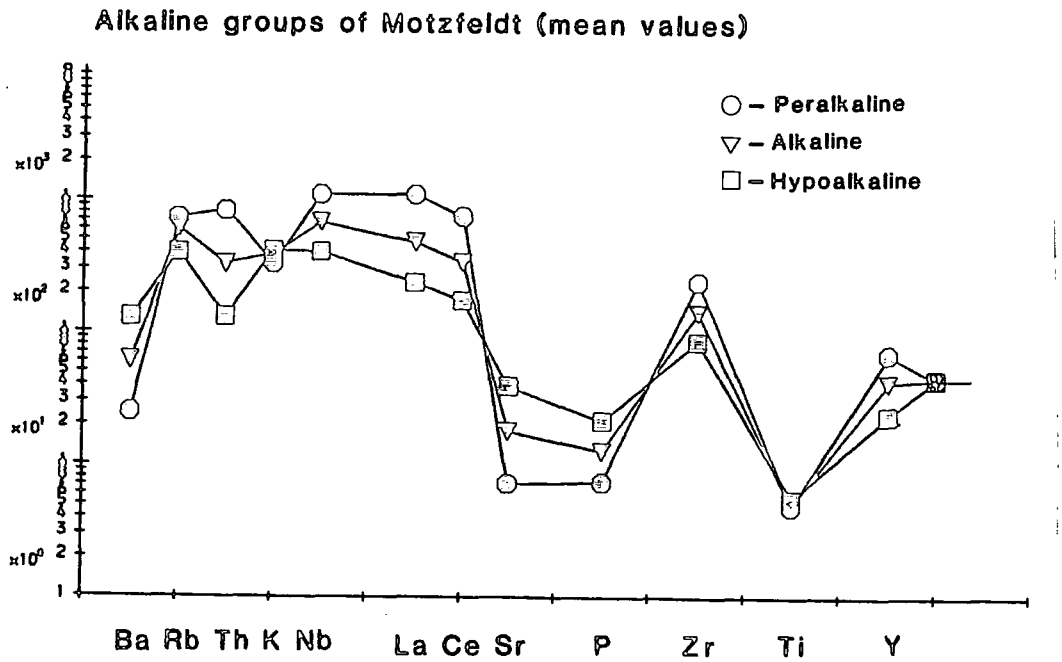


Incompatible element spidergrams Fig 8.1.15

a.



b.



'orthoclase' effect by Bailey and Schairer (1964). The felsic minerals constitute over 80% of the rocks of Motzfeldt and, as stressed by MacDonald (1974), it is of little surprise that their crystallisation has such a strong influence upon the nature of the residual liquid. The surprisingly large trough shown by Th in Motzfeldt and to a lesser extent by the other Centres is probably due to Th incorporation in cumulate sphene/apatite and possibly Fe-Ti oxides. However, this small Th trough is not unusual in oceanic or continental alkali basaltic magmas (Norry & Fitton, 1983) and may therefore, be an 'inherited' effect. A third explanation could be analytical error because of the low values involved.

8.1.3 The Nepheline syenites

i. Introduction

Approximately 50 to 60 % of the surface outcrop of the Motzfeldt centre comprises rock units of nepheline syenite lithology. Much of the remaining area being comprised of the saturated syenites of the MSF-Altered syenite and Si - saturated rocks of the Hypabyssal Series. On the basis of the percentage surface area of the individual nepheline syenite units and their respective geochemical data the following 'typical' nepheline syenite was calculated (Table 8.1.16a & b) hereafter referred to as the **Motzfeldt-Nepheline syenite.**

Table 8.1.16a shows that the Motzfeldt-Nepheline syenite is of classical phonolite composition with SiO_2 of 55%, Al_2O_3 of 20% and $Na_2O + K_2O$ of 13.85%. Indeed the rock plots virtually in the Centre of the phonolite field in the $(Na_2O+K_2O)/SiO_2$ plot of Cox et. al. (1979). This scheme was used in preference to the TAS classification of LeBas et. al., (1986) in order to remain compatible with previous workers in the Gardar (eg, Upton, 1974; Upton & Fitton, 1985; Upton & Emeleus, 1987).

When compared to the world-wide average nepheline syenite of Le Maitre (1976a), the Motzfeldt-Nepheline syenite major element concentrations are essentially similar but with slightly less MgO, CaO, TiO_2 and correspondingly more $\sum Fe_2O_3$ and MnO. The

a. 'Typical' geochemical characteristics of a nepheline syenite from Motzfeldt. The figures are derived from the mean values of each nepheline syenite unit with their percentage volume within Motzfeldt taken into considersation. The figures are a working approximation of the 'bulk' nepheline syenite of Motzfeldt and at least can be used for comparative purposes.

b. The rare-earth data are similarly treated but from a much smaller data-set (Berlin).

a.

Motzfeldt-Nepheline syenite	
Major elements	(wt%)
SiO2	55.67
Al2O3	20.00
Fe2O3T	5.35
MgO	0.54
CaO	1.38
Na2O	8.00
K2O	5.85
TiO2	0.48
MnO	0.23
P2O5	0.17
Total	97.67
Trace elements	(ppm)
Ba	550
Nb	206
Zr	860
Y	70
Sr	309
Rb	194
Zn	151
Pb	12
U	5
Th	9
Ga	33
La	108
Ce	214
C.I.P.W norms	
Orthoclase	35.5
Albite	33.3
Anorthite	1.4
Nepheline	19.6
Diopside	3.8
Olivine	1.3
Magnetite	3.8
Ilmenite	0.9
Apatite	0.4
Colour Index	10.18
FI	88.40
PI	0.98
Fe2O3/FeO	1.00
Zr/Nb	4.18
Rb/Sr	0.63
K/Rb	123

b.

Rare Earth Elements	
	(ppm)
La	91.45
Ce	192.00
Nd	70.20
Sm	12.40
Eu	2.35
Tb	1.44
Yb	3.50
Lu	0.53
Ta	11.8

c.

Total trace element contents	
Nepheline syenites	(p.p.m) (means)
GF-Nepheline syenite	1399
MSF-Nepheline syenite	2916
FDF-Porph. Neph. Sy.	3098
FDF-Foyaite (T)	2857
FDF-Foyaite (C)	2297
FDF-Nepheline syenite	2668
Syenites	
GF-Geologfjeld syenite	2275
GF-Pulaskite	2853
Lam. alkali syenite	2887
Lam. porph. syenite	3628
Polk. Arf. syenite	4220
Larvikite	6325
Lujavrite	5913
Mineralised units	
MSF-Marginal syenite	5321
MSF-Altered syenite	6953
MSF-Per. microsyenites	18361

c. Table of the mean $\sum$trace-element (13 analysed) values from the different intrusive units of Motzfeldt.

Peralkalinity Index of 0.98 gives the rock an intermediate or alkaline[11] character. Figure 8.1.17 shows the range of trace element values (this study) contained within the nepheline syenites (all units) of Motzfeldt. The solid line superimposed on this range represents the elemental concentrations of the Motzfeldt-Nepheline syenite. These 'typical' values clearly show how the overall range of each element (except Rb) has a positively skewed distribution and therefore the necessity to use non-parametric statistical methods in accordance with Hall (1983), Dr D. Hirst (pers. comm.).

The units of nepheline syenite lithology encountered in Motzfeldt include;

GF-Nepheline syenite (NM2)

MSF-Nepheline syenite (SM1)

FDF-Porphyritic nepheline syenite (SM2 & SM4)

FDF-Foyaite (transgressive type) (SM3)

FDF-Foyaite (central type) (SM4)

FDF-Nepheline syenite (SM5)

In this study the criteria used to distinguish between these units have included;

1/ Field relationships

2/ Colour and texture

3/ Mineralogy

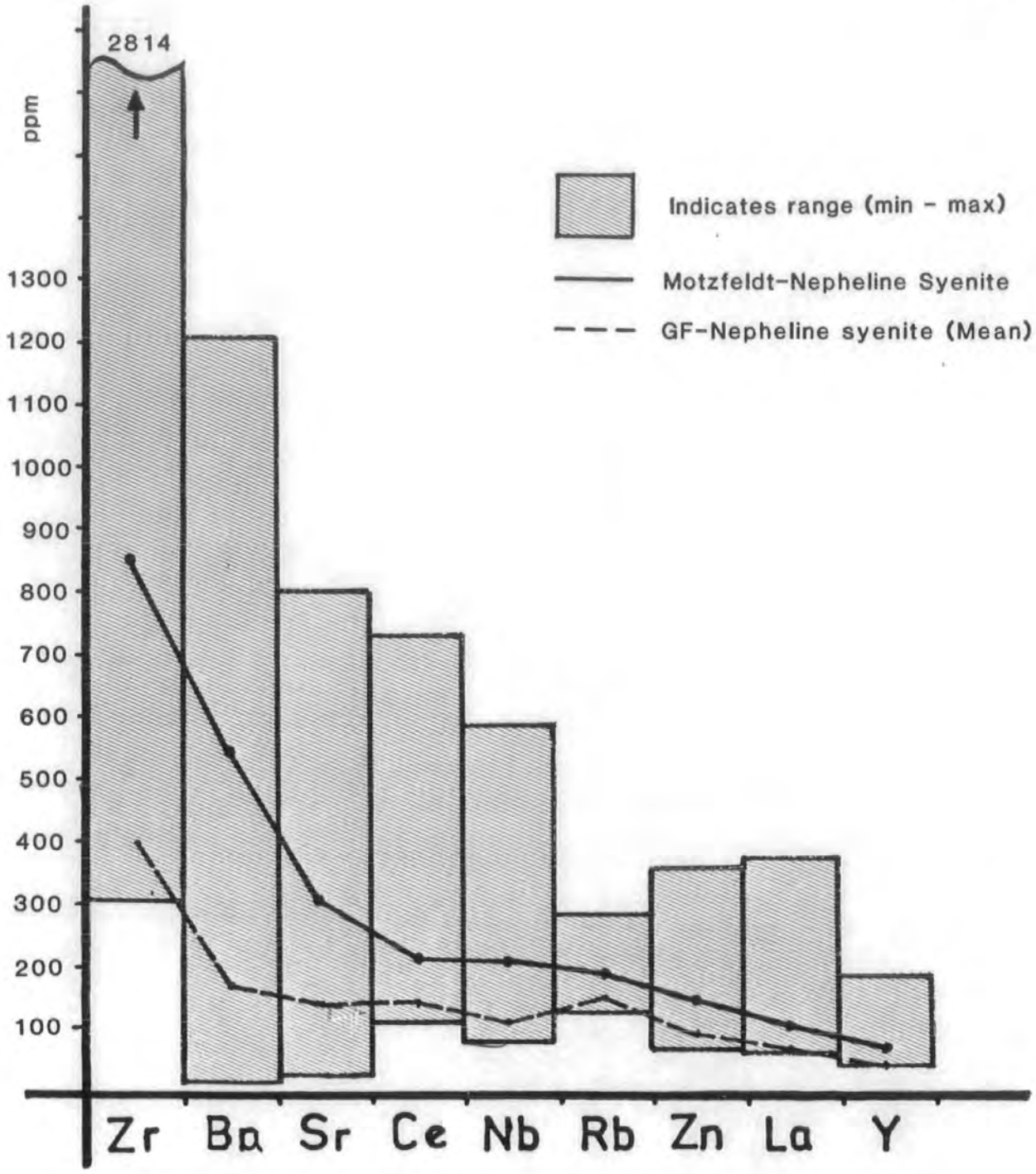
4/ Geochemistry

Often a combination of the above is necessary for confident classification. Indeed, the geochemistry is probably of least value in this respect because of the narrow compositional range and often well developed cumulate tendencies. Geochemical data from the different units are listed in Table A3.2, Appendix Three and displayed on the PI plots Figures 8.1.6 to 8.1.12. and therefore are not described in detail here. However, significant differences do occur between some units and these are outlined below.

[11] this work, see section 3.3

Geochemical range - nepheline syenites

Fig 8.1.17



Graph showing the range of selected trace element concentrations in the nepheline syenites of Motzfeldt. The Motzfeldt-Nepheline syenite is indicated (solid line) and shows how the geochemical range has a positive (or right) skewed distribution. The mean values of the GF-Nepheline syenite are shown (dashed-line) and clearly indicate the lower abundances of the elements compared to the 'typical' nepheline syenite.

ii. Geochemical variation between the Formations (GF vs MSF vs FDF)

The most striking dissimilarity between the nepheline syenite units is the difference in the trace element values of the GF-Nepheline syenite and the nepheline syenite members of the Motzfeldt Ring Series (MSF and FDF). Table 8.1.16c shows how the GF-Nepheline syenite (mean of 4)[12] values are roughly half those of the other nepheline syenite units. This difference is 'across the board',[13] where both compatible and incompatible elements are significantly lower, as shown by Fig 8.1.17. The major element values on the other hand are similar between the Formations. These low trace element values suggest a completely separate evolution from the Ring Series of Motzfeldt and confirm the 'satellitic' nature of the Geologfjeld Formation.

Within the Motzfeldt Ring Series itself, the rock units which show strong cumulate textures show a greater 'spread' of major and minor element concentrations than those of subhedral-equigranular or 'granitic' texture. For instance, the members of the latter group which include the GF-Nepheline syenite, MSF-Nepheline syenite, FDF-Nepheline syenite and FDF-Porphyritic nepheline syenite (included here despite textural variations) show no significant differences in any of their major element concentrations. Therefore from such data alone, it would be difficult to discriminate between these units.

The FDF-Foyaites in contrast have undergone demonstrable *in situ* mineral accumulation, layering and fractionation. This is reflected in the sample range of this work (from high up in the cumulate pile) by generally lower MgO, CaO, P_2O_5, Ba and Sr values. However, a large range of values is shown and because much depends on the vertical position of the sample-site both on a large and small scale, the discriminatory value of the data is of little value.

Pie Diagrams (Fig 8.1.18) display the mean relative abundances of the elements Zr, Nb, Ba, Sr, Rb (and the mean ppm values) of the various nepheline syenite lithologies of Motzfeldt. It is clear from these diagrams that in the rocks which have not undergone

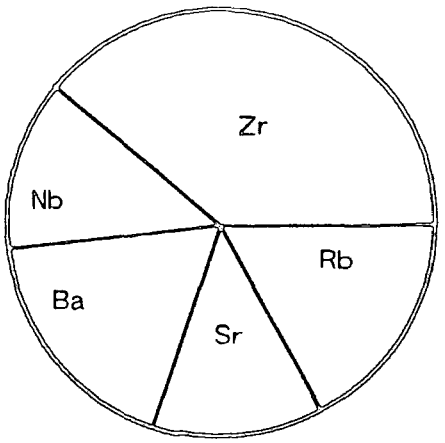
[12] unfortunately small sample population
[13] only Rb is not significantly lower

Nepheline syenite - Pie diagrams

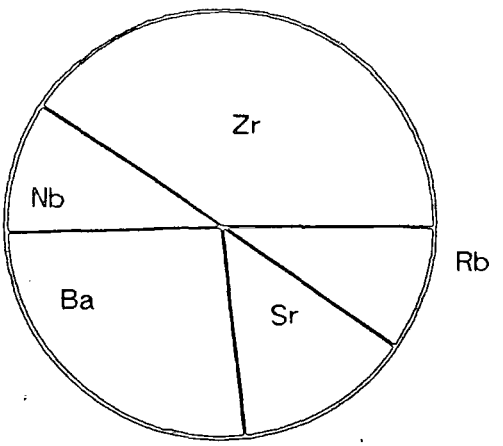
Fig 8.1.18

Mean values from the six nepheline syenite units of Motzfeldt of Zr, Nb, Ba, Sr and Rb plotted as Pie-diagrams to show their relative abundances.

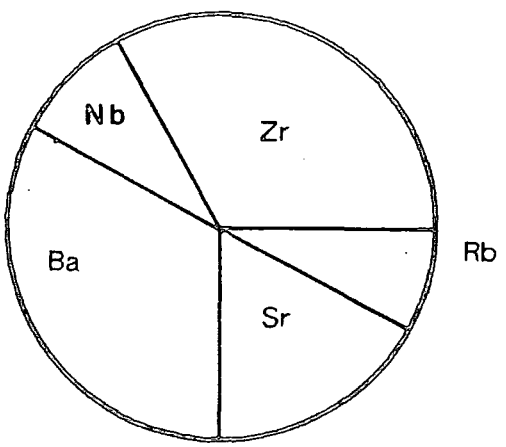
a. GF-Nepheline syenite



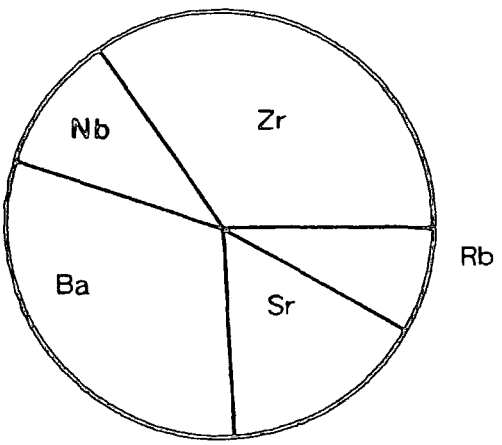
b. MSF-Nepheline syenite



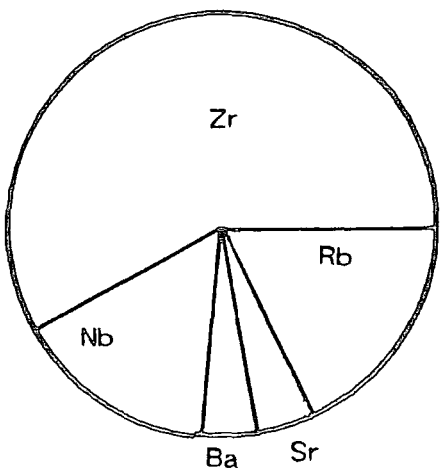
c. FDF-Porphyritic neph. syenite



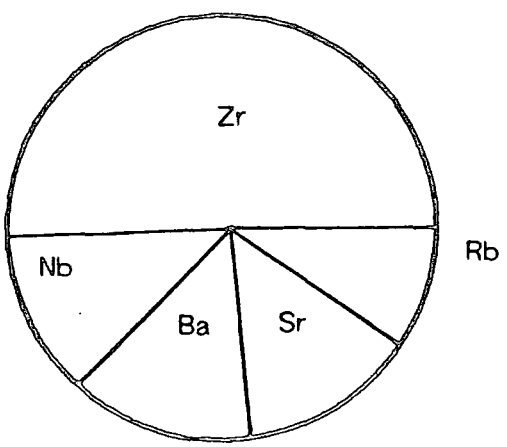
d. FDF-Nepheline syenite



e. FDF-Foyaite (central)

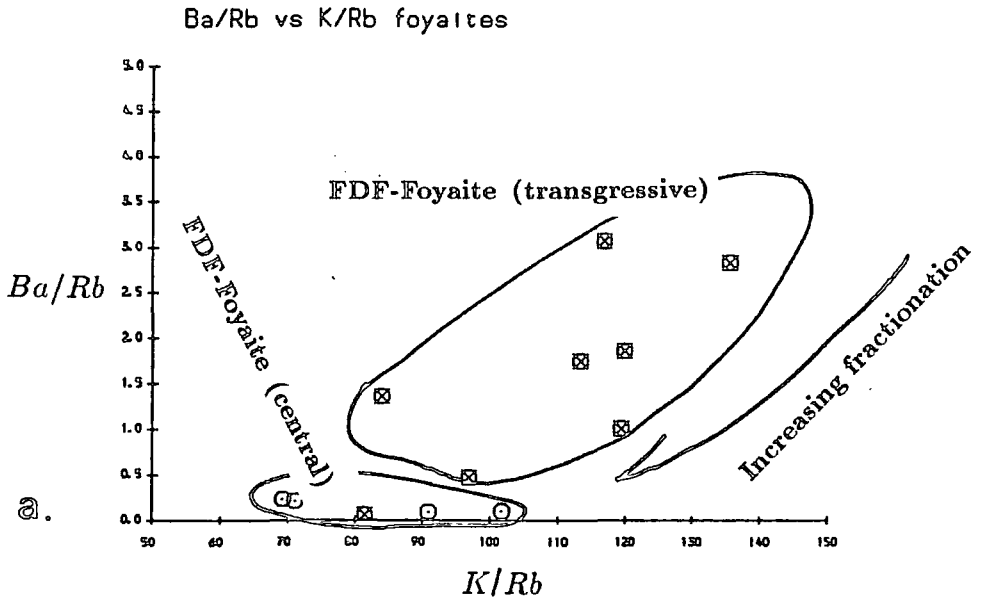


f. FDF-Foyaite (transgressive)

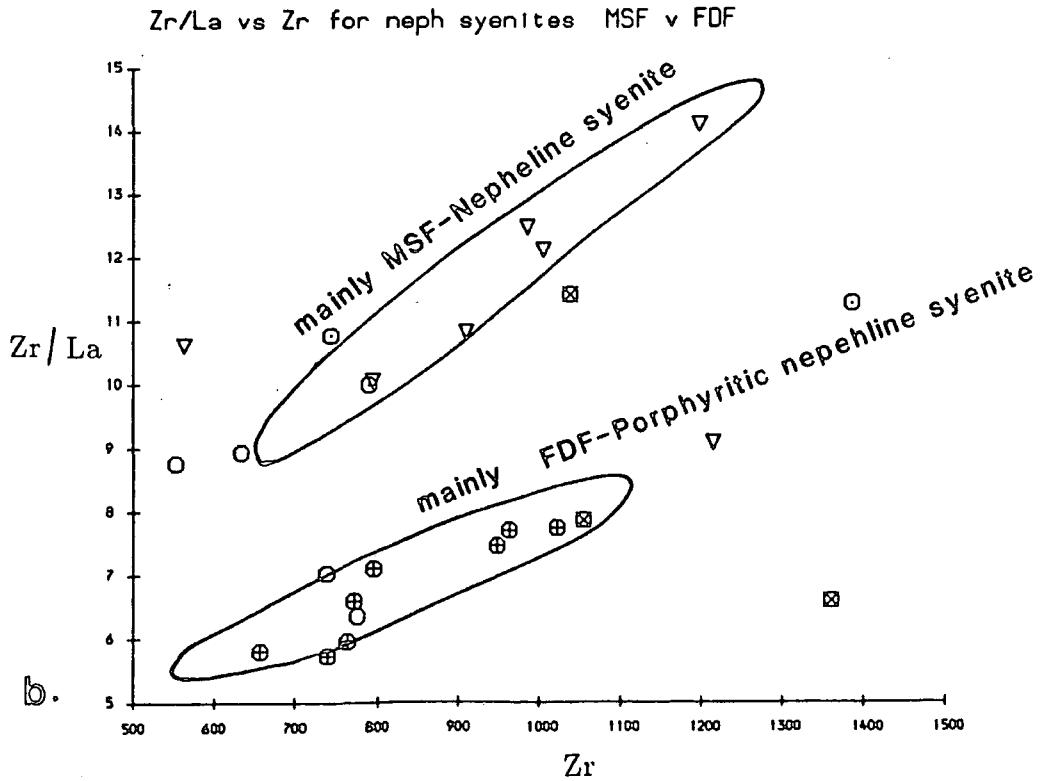


in situ cumulate fractionation, the ratios of the antithetic elements ie, (Zr + Nb) / (Ba + Sr) remain largely similar. Therefore fractionation of these rock types at this level has probably not played an important role. It must be stressed however, that most of the samples analysed in this work have been taken from high levels in the Centre and therefore little is known of lithological and geochemical variation with depth.

Of the trace elements compared between the Motzfeldt Sø Formation and Flinks Dal Formations (not including the FDF-Foyaites) only La, Ce and Zn showed significant differences. The La and Ce concentrations of the FDF-Porphyritic nepheline syenite are consistently higher by about one third than those of the neighbouring MSF-Nepheline syenite of SE Motzfeldt (Fig 8.1.19b). Whilst this is possibly valid for discrimination purposes in SE Motzfeldt, the MSF-Nepheline syenite shows a wider distribution of La values elsewhere in the Centre. For instance, the samples of MSF-Nepheline syenite from xenolithic rafts within the FDF-Porphyritic nepheline syenite near Camp 12 (eg. 326059 and 326049) and Camp 14 (326121 and 326124) have unusually high La and Ce contents. This may be due to contamination from the younger rock or merely a reflection of greater fractionation. For example, pegmatitic segregations from the MSF-Nepheline syenite show large increases in La and Ce content. However, these are normally accompanied by the concomitant increase in other incompatible elements such as Zr and Nb (eg, 304019). The FDF-Foyaites have significantly lower Ba and Sr concentrations than the other nepheline syenite members of the Ring Series (Fig 8.1.18). This gives a good indication of the importance of feldspar fractionation prior to or during their formation. In addition, the transgressive FDF-Foyaite contains significantly higher levels of Ba and Sr than the central type. When plotted against the fractionation index K/Rb these levels appear to reflect their relative stages of evolution (Fig 8.1.19a).



Plot to show differences in Ba between the FDF-Foyaite (transgressive) and FDF-Foyaite (central) and its behaviour during fractionation.



Plot showing the consistently higher Zr/La ratio in the MSF-Nepheline syenite compared to the FDF-Porphyritic nepheline syenite (SE Motzfeldt).

8.1.4 The Syenites (*sensu stricto*)

i. Introduction

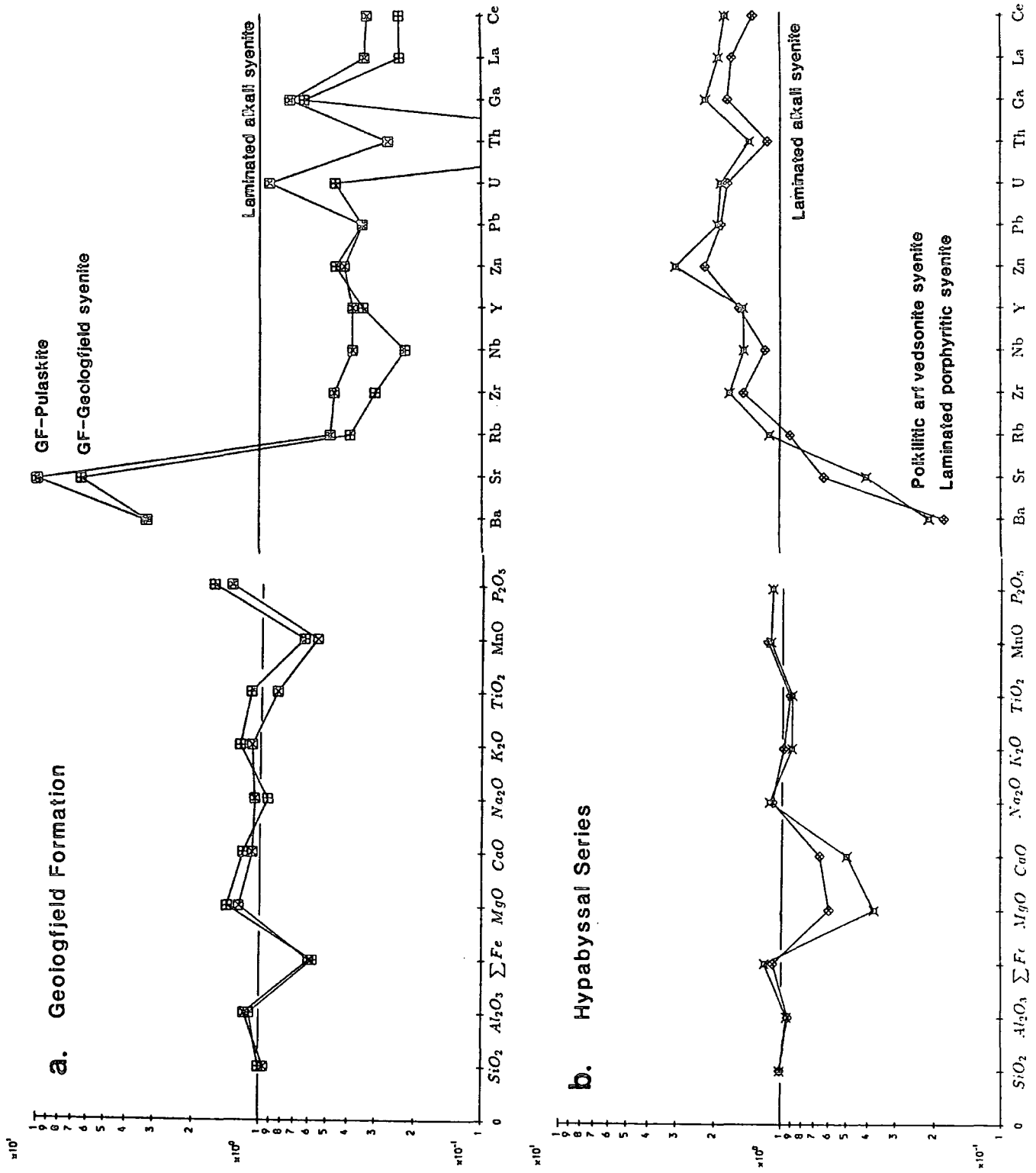
A remarkable variety of syenites (*sensu stricto*) are found in Motzfeldt and include:[14] GF-Geologfjeld Syenite, GF-Pulaskite[15] and the units belonging to the Hypabyssal Series; Laminated alkali syenite, Laminated porphyritic syenite and the Poikilitic arfvedsonite microsyenite.

A broad range of elemental concentrations is shown by these lithologies which range from hypoalkaline to peralkaline in character (Table 8.1.1; Table 8.1.2 & Fig 8.1.3). Consequently, discrimination between the units is generally clear both petrographically and geochemically. The geochemical data for the various units are listed in Table A3.2, Appendix Three and displayed on Figures 8.1.6 to 8.1.12. In this section the data are discussed with particular reference to their discriminative value. The alkaline and peralkaline syenites in Motzfeldt show tendencies toward silica-oversaturation (Fig 3.3.4). This trend can often be shown to be due to incorporation of siliceous country rock. Significantly, the slightly oversaturated rocks show typically higher incompatible element values than the undersaturated equivalents of the same PI (Figs 8.1.6 to 8.1.12) which has led some workers to conclude that significant levels of incompatible elements (and mineralising fluids) have been incorporated from the country rock (Morteani et. al. 1986). The detailed geochemistry of the MSF-Altered syenite, which has been profoundly altered due to interaction with the country rock is not discussed in this study. However, some aspects of its possible origin are summarised in section 8.2 of this work.

ii. GF-Geologfjeld syenite vs. GF-Pulaskite

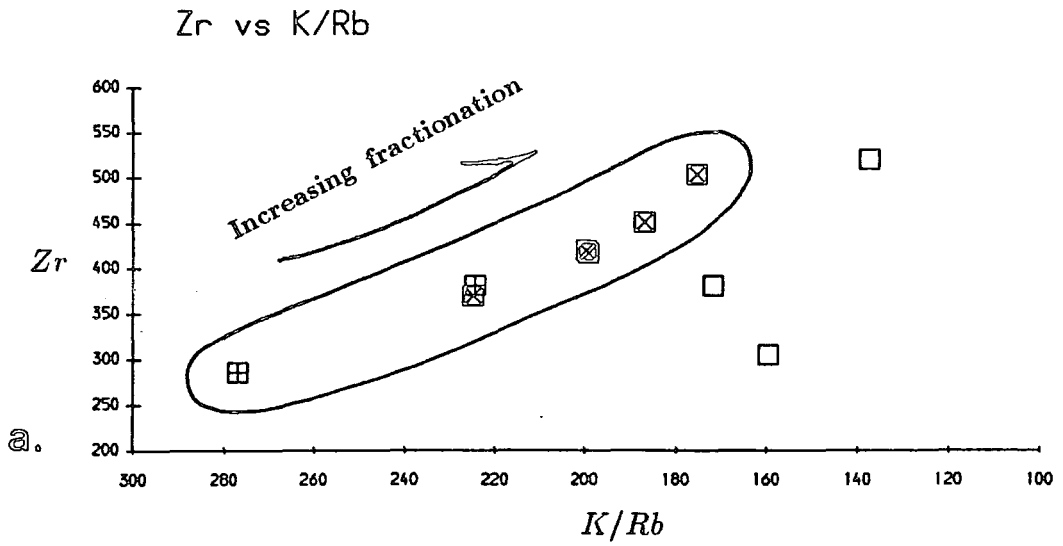
It is the contention of this work that these units are either different facies of the same unit, or closely related separate intrusions. Both are hypoalkaline and typically characterised by high Ba, Sr and relatively low Zr, Nb, Rb (see Fig 8.1.20a; PI plots). The

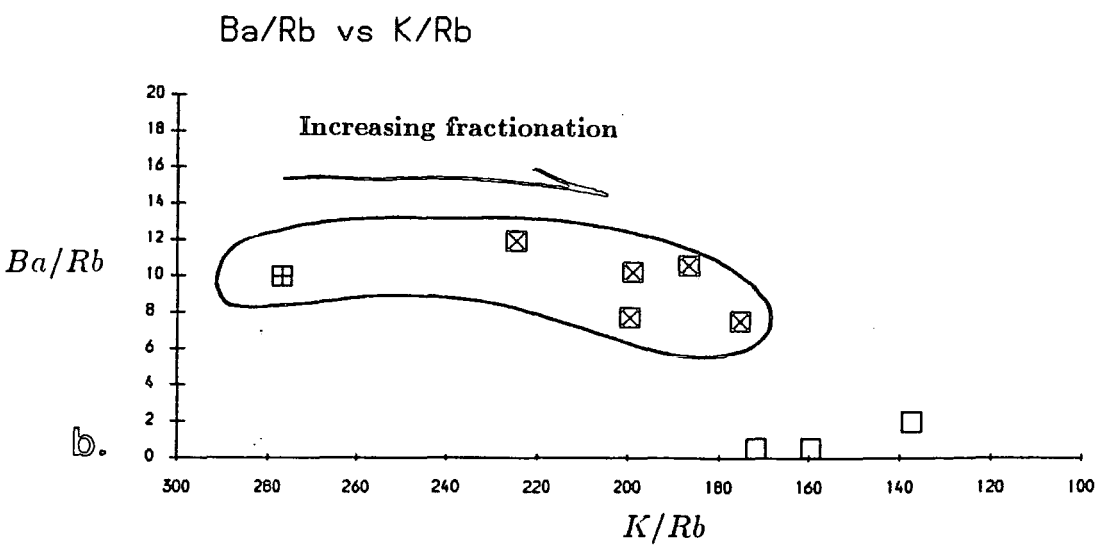
[14] not included are feldspathoid poor varieties of the main units
[15] included here because of its similarity to GF-Geologfjeld syenite



a. Mean geochemical values of the GF-Geologfjeld syenite and GF-Pulaskite normalised against the mean values of the Laminated alkali syenite.

a. Mean geochemical values of the Laminated porphyritic syenite and Poikilitic arfvedsonite microsyenite normalised against the mean values of the Laminated alkali syenite.





a & b. Plots showing behaviour of Zr and Ba/Rb in the units , (decreasing K/Rb), in the units of the Geologfjeld Formation.

higher levels of Al_2O_3 and Na_2O in the GF-Pulaskite compared to the GF-Geologfjeld syenite (Fig 8.1.20a) are reflected by modal nepheline and/or analcite (c.5%). Additionally, the GF-Geologfjeld syenite is the only unit in Motzfeldt to have Na/K ratios consistently less than 1. Fig 8.1.20a shows their respective major and trace-element concentrations normalised against those of the Laminated alkali syenite. Marked similarities are clearly exhibited by these patterns and indicate the greater abundance of the elements MgO, CaO, Ba, Sr and P_2O_5 and considerably lower values of the incompatible elements in these hypoalkaline rocks.

Petrographically, the GF-Pulaskite contains a higher modal proportion of intercumulus low temperature minerals than the GF-Geologfjeld syenite and this is reflected by the slightly increased levels of incompatible elements. Although the PI and FI values show similar narrow ranges for both rocks, (around 0.92 and 84.5 respectively) the K/Rb ratio decreases significantly in the GF-Pulaskite and is accompanied by a concomitant rise in Zr, Nb, La and Ce (ie, Fig 8.1.21a). This steady rise of incompatible elements levels off and does not significantly change in the next more evolved stage of the Formation, the GF-Nepheline syenite. Furthermore this rise in incompatible elements is not accompanied by a corresponding steady decrease in Ba, Sr, Ba/Rb. However the next intrusive unit of GF-Nepheline syenite shows a dramatic depletion of these elements while having insignificant increases in incompatible elements (Fig 8.1.21b). It is concluded that the GF-Nepheline syenite is related through feldspar-dominated fractional crystallisation (MacDonald, 1974), to the GF-Gelogfjeld syenite and GF-Pulaskite units. This example provides evidence to support the importance of feldspar fractionation in the development of phonolite magmas from (augite-)trachyte compositions.

iii. Laminated porphyritic syenite vs. Poikilitic arfvedsonite microsyenite

These units are separate (possibly multiple) intrusions, intimately associated in SE Motzfeldt (see Chapter 7). They are easily distinguished in hand specimen but probably emanate from the same magma source, separated only by time. The hyalocrystalline microsyenite has clearly cooled considerably more quickly than the Laminated porphyritic syenite, but geochemically the rocks are very similar, (Fig 8.1.20b). The generally lower

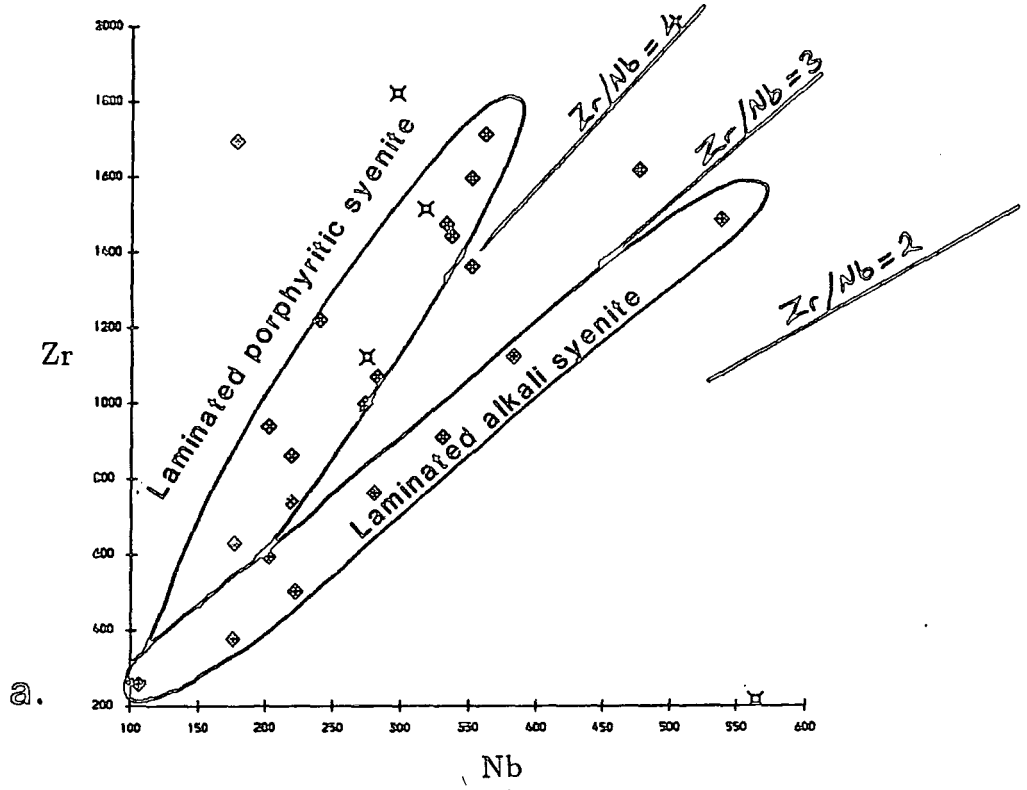
K/Rb and higher PI values of the Poikilitic arfvedsonite microsyenite indicate a higher degree of fractionation which is reflected in the slightly increased values of the incompatible trace elements and decreased compatible elements, (eg, Mg, Ca, Ba) (Fig 8.1.20b).

iv. Laminated alkali syenite vs. Laminated porphyritic syenite

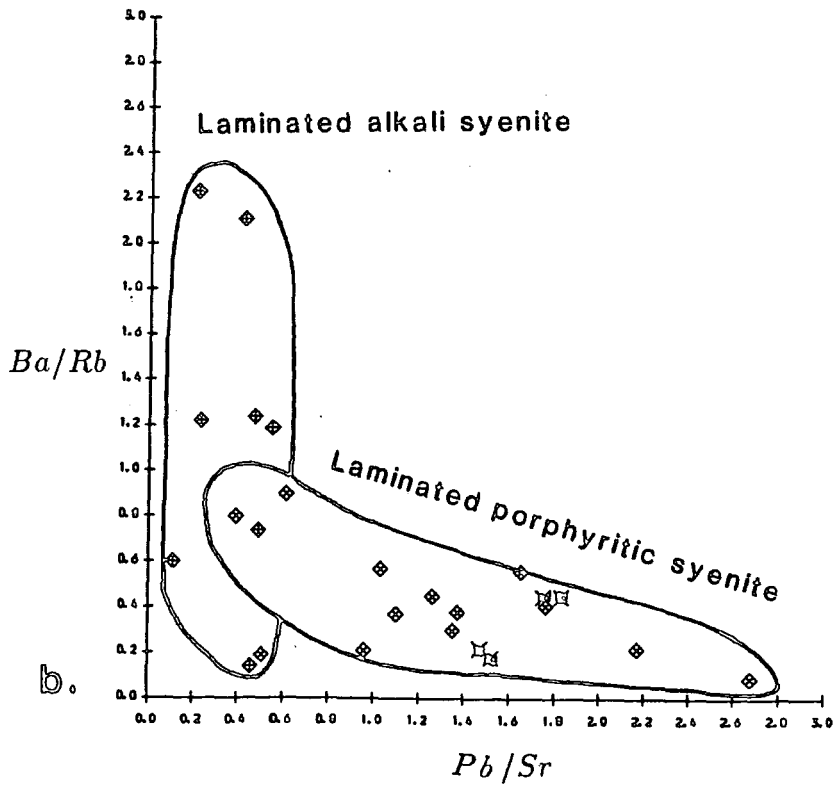
As noted in the field observations these units occur intricately associated, and although the Laminated porphyritic syenite clearly intrudes the Laminated alkali syenite, coarse feldspathic varieties of both can look very much alike. Both are dominated texturally by laminated bladed feldspars, plot in the same general compositional field of trachyte on the $(Na_2O + K_2O)/SiO_2$ diagram (Fig 3.3.2d) and have generally similar ranges of major element concentrations (Fig 8.1.20b). Mg and Ca, however are significantly higher in the older, laminated alkali syenite with levels of around 0.4 and 2%, whereas those of the younger unit are around 0.23 and 1.3% respectively. The Laminated porphyritic syenite and Poikilitic arfvedsonite microsyenite are more fractionated than the Laminated alkali syenite. They are both generally peralkaline and have consequently greater contents of incompatible elements (Gerasimovsky, 1966; Hamilton, 1964; Siedner, 1965; Fergusen, 1969; Taylor et. al., 1981). Furthermore, they show a striking depletion of the elements Ba and Sr compared to the Laminated alkali syenite (Fig 8.1.20b & Fig 8.1.21a).

The Laminated porphyritic syenite often shows very well-developed flow differentiation (see Chapter 7) with the phenocrysts of feldspar congregating along the central axes of dyke-like bodies. The geochemical results however, show very little change in the whole-rock values of Ba or Sr[16] between the aphyric margins and the feldspar rich core. (eg, 304093 cf. 304032 respectively). In contrast, fine grained varieties of the Laminated alkali syenite show significant Ba and Sr depletion eg, 304085, which has a Ba content of 102 ppm, approximately one third of the mean value for the unit. Fig 8.1.22b shows how the plot Ba/Rb v Pb/Sr usefully discriminates between the units, but does not rule out a generic link through feldspar fractionation. Fig 8.1.22a, on the other hand displays a significant and an unusual (for Motzfeldt) variance in the Zr/Nb ratio between the units.

[16] these values are already low



a. Plot showing the differences in the Zr/Nb ratios between the units Laminated porphyritic syenite and Laminated alkali syenite.



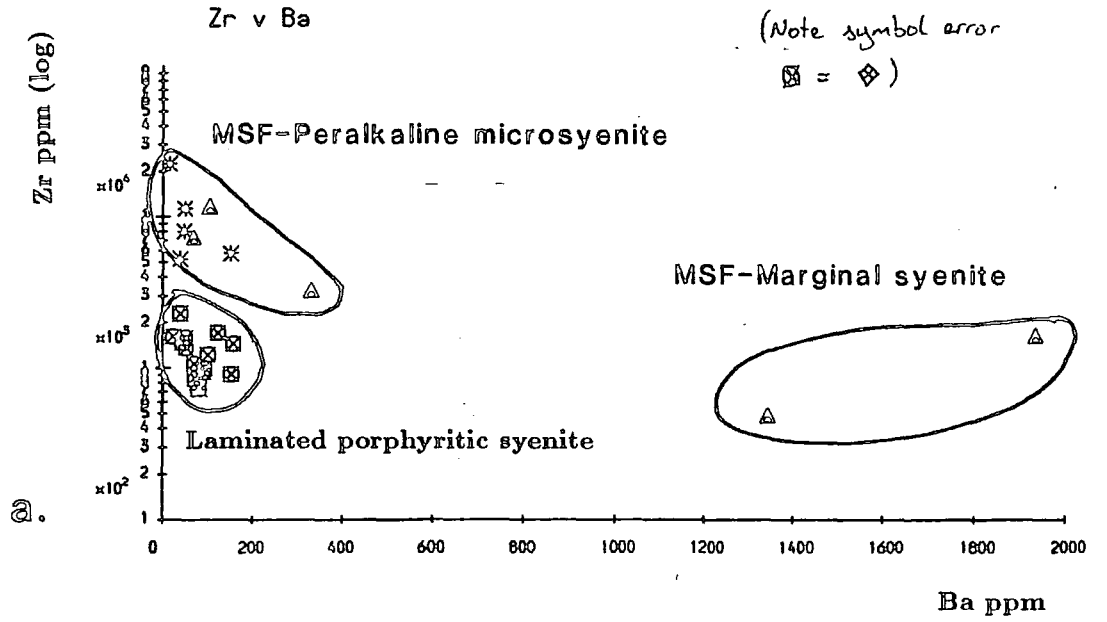
b. Plot discriminating between the units Laminated porphyritic syenite (with Poikilitic arfvedsonite microsyenite) and laminated alkali syenite using Ba/Rb vs Pb/Sr.

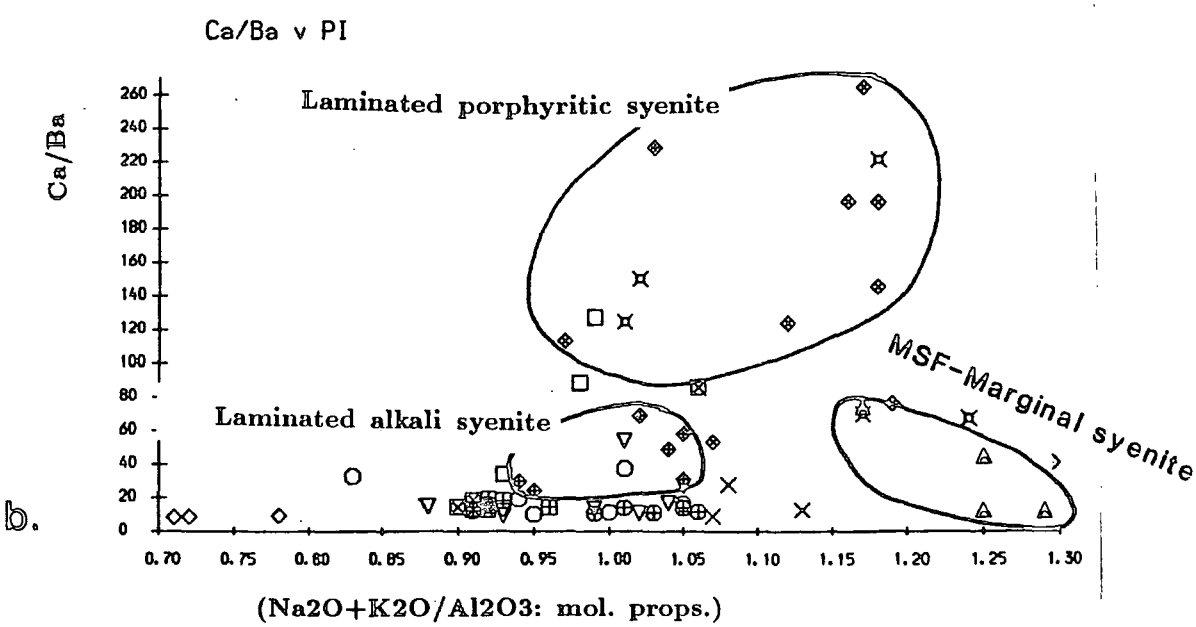
The Zr/Nb ratio in most rock types of trachytic or phonolitic composition in Motzfeldt is usually around 4.00 (altered rocks excluded). The Laminated alkali syenite unit however, has a significantly lower ratio, usually of just under 3.00 (Fig 8.1.22a). Strangely, the most conspicuous accessory mineral in the Laminated alkali syenite is zircon. However, Nb does not readily substitute Zr in zircon, usually comprising less than 2% (Vlasov, 1966; Wedephol, 1978). Pyrochlore is occasionally evident in these rocks however, and is possibly more abundant than observed (see petrographic details Chapter 7).

v. Laminated porphyritic syenite v MSF-Marginal syenite

Discrimination between these two units in the field, particularly in SE Motzfeldt has proved very difficult. They are texturally very similar, peralkaline and trachytic in composition, comprising essentially brick-shaped alkali feldspars and arfvedsonite with aenigmatite a common accessory. In NE Motzfeldt the units are geographically separate, and therefore discrimination is not a problem. Even if it were, the distinct and consistent colour contrast between the units would be sufficient for easy classification. In SE Motzfeldt however, the usual steel grey colour of the Laminated porphyritic syenite is lost in large areas due to pervasive red staining which so characterises the altered rocks of the Motzfeldt Sø Formation. This discolouration, coupled with interspersing of the units in this area, has prevented satisfactory discrimination in the field. Unfortunately, the sample range for MSF-Marginal syenite of this work is too small for accurate statistical comparison, nevertheless, it is clear that significant geochemical differences do exist and it should be relatively easy to discriminate between the units. Despite having a mean PI of 1.36, MgO and CaO levels are significantly higher in the MSF-Marginal syenite (even when colour Index is taken into consideration). Na_2O, K_2O, P_2O_5, TiO_2 and MnO are similar in both units. The most significant differences occur however in the concentrations of Ba and Sr. The highest Sr value in the Laminated porphyritic syenite is 72 ppm but most samples contain around the mean value of 40 ppm. Ba similarly is characteristically low, usually between 50 and 80 ppm and rarely up to 130 ppm (Fig 8.1.23a). This contrasts strongly with the Ba and Sr concentrations of the MSF-Marginal syenite. The latter shows a Ba range from 331 to 1933 and a Sr range from 331 to 1390. Where the

Peralkaline syenite - discrimination plots Fig 8.1.23





a & b. Discrimination plots between the peralkaline arvedsonite syenites; MSF-Marginal syenite and the Laminated porphyritic syenite.

MSF-Marginal syenite shows extreme fractionation as in the pegmatitic apophyses near Camp 10 (eg, 304711), the Ba and Sr levels are however similar to those of the Laminated porphyritic syenite. This fractionated facies however, is characterised by increases in the Zr, Nb, La and Ce levels (of 11,778, 1,532, 1,277 & 2,360 ppm respectively) well beyond those measured in the Laminated porphyritic syenite (Fig 8.1.23a).

One of the most distinctive features of the Laminated porphyritic syenite and the Poikilitic arfvedsonite microsyenite is the unusually high Ca/Ba ratio compared to all the other (fresh) units of Motzfeldt (Fig 8.1.23b).

Sr and to a lesser extent Ba are admitted as isomorphous substitutes for Ca due to their similar ionic radii and charge. However both elements are preferentially incorporated into the 8-fold coordination sites of feldspars compared to other Ca - phases (particularly the 6 fold sites of pyroxene and amphibole) (Taylor, 1965). Therefore the Ca/Ba ratio increases as the ratio of the fractionating phases (feldspar(+apatite) / Ca-mafic minerals) increases. Moreover, Ba and Sr are captured readily in place of K at the onset of anorthoclase crystallisation (and subsequently fractionated). In Gardar this has been shown to be particularly important in rocks of benmoreite composition (Pearce, 1988). Feldspar-dominated fractionation (at least just prior to intrusion) in the Laminated porphyritic syenite is upheld by the field evidence where ubiquitous anorthoclase megacrysts (commonly 5 cm, but up to 20 cm in length) and rare anorthite xenoliths, are contained within the rock (Plate 7.2b).

The MSF-Marginal syenite characteristically displays a strange combination of high-levels of elements ie, Ba, Sr Mg and Ca in combination with enrichment of incompatible elements and alkalis. This confirms the field evidence, that the unit developed as a congelation cumulate of high temperature phases which has been metasomatically overprinted by secondary (auto?)metasomatic processes.

8.1.5 Rare-earth elements

The paper of Jones and Larsen (1985) gives a good account of the REE concentrations, behaviour and mineralogy in Motzfeldt. Here additional data provided by the PYROCHLORE team (Berlin-Munich group) are presented and their significance reviewed.

REE whole rock and selected mineral data are given in Table A3.3, Appendix Three. Chondrite[17] normalised plots are used to display the data for the different formations and their members (Figs 8.1.24 & 8.1.25). The charge (3^+) and comparatively large ionic radius (La 1.06 Åto Lu 0.85 Å) of the REE's together with their low abundances suggests that they don't readily enter into the structures of the main rock- forming minerals (Taylor, 1965). They all show similar electronegativity and ionization potential but show decreasing ionic radius (and therefore increasing compatability) with atomic number (Goldschmidt, 1954). Thus with fractionation both the absolute REE abundances increase as well as the LREE/HREE ratio. These properties are reflected in the highly evolved rocks of Motzfeldt where the units are all LREE enriched and have high $(La/Lu)_n$[18] ratios.

The samples analysed include a compositional range from hypoalkaline syenites to Peralkaline microsyenites. The $\sum$REE contents correspondingly increase from around 200 - 300 ppm in the hypoalkaline rocks to 400 - 500 ppm in the alkaline rocks and to 800 - 1500 ppm in the peralkaline varieties (Fig 8.1.27).

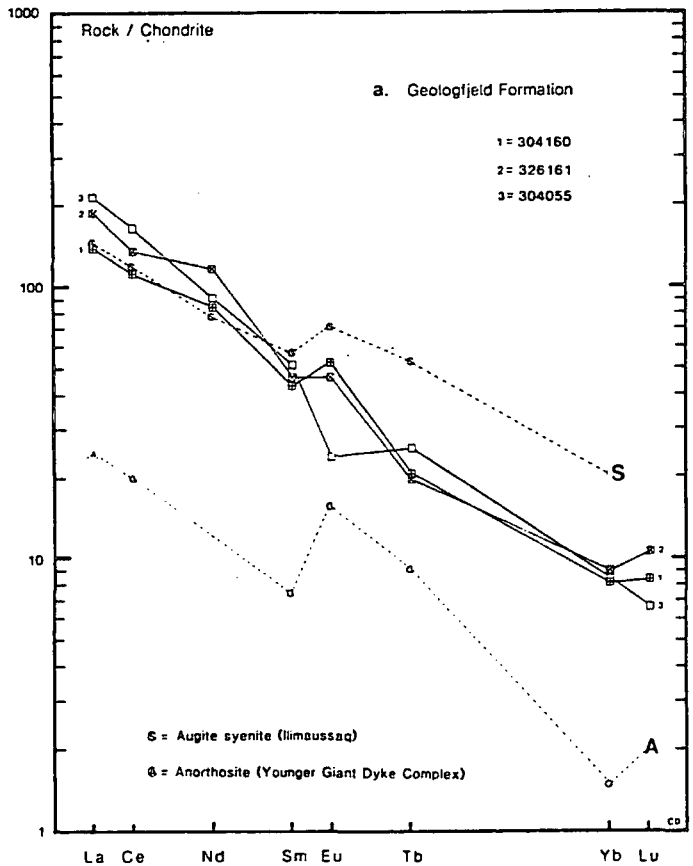
With this increase of $\sum$REE values there is a general decrease in the relative abundance of Eu. This trend is due to the occurrence under moderately reducing conditions of the divalent Eu^{2+} (1.24Å) (Goldschmidt, 1954) which can be preferentially incorporated in place of Ca^{2+} (1.06Å) and/or K^+ (1.33Å) in feldspar (Chase et. al. 1962) in much the same fashion as Sr^{2+} (1.27Å) (Philpotts, 1970). Jones and Larsen (1985) indeed pointed out the strong positive correlation between Eu/Eu*[19] and Sr content. The hypoalkaline

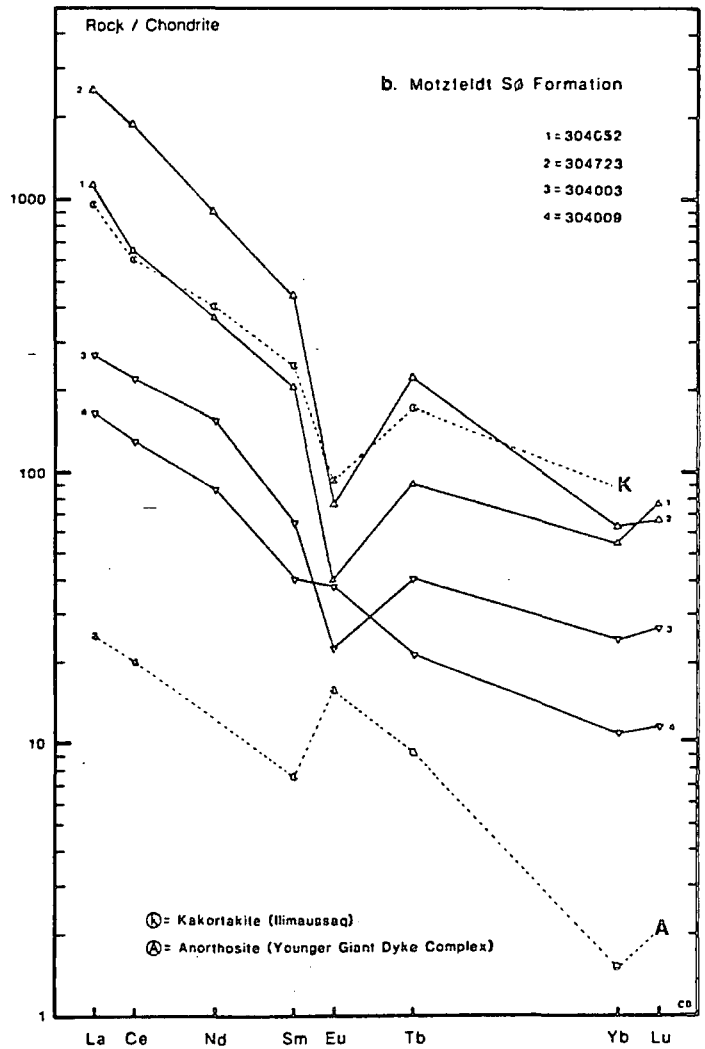
[17] Nakamura (1974) - chosen to be compatible with Jones and Larsen, 1985.
[18] $_n$ = normalised
[19] Eu* interpolated from line drawn between adjacent rare-earths

rocks generally have a small positive Eu (Fig 8.1.24a) whereas in the alkaline units the anomaly is usually small but negative (Figs 8.1.24 & 8.1.25) and the peralkaline rocks display deep negative anomalies (Fig 8.1.24b & 8.1.25b). The increase in $\sum$REE shows a strong correlation with PI and Rb/K in the rock units[20], of +0.664 and +0.883 respectively and thus emphasises their value as indic es of fractionation. Clearly Eu has been incorporated, as would be expected in the feldspars of the least evolved hypoalkaline syenites. The progressive Eu depletion with differentiation, stresses the importance of feldspar fractionation in these later stages of the evolution of the Motzfeldt magmas. It would appear that rocks of 'benmoreite' composition commonly contain small positive Eu anomalies ie, SM5* of Motzfeldt (Jones & Larsen, 1985), the Augite syenite of Ilimaussaq (Larsen, 1979), the GF-Geologfjeld syenite of Motzfeldt[21] and in Larvikites from Oslo (Neumann, et. al. 1977; Neuman, 1980). The Eu is probably largely contained within plagi- anorthoclase feldspars which are prevalent in these rocks. In fact, relict cores of plagioclase (oligoclase) are commonly detected in the Motzfeldt Larvikite, FDF-Nepheline syenite and GF-Geologfjeld syenite units. These may or may not be cognate inclusions. Jones and Larsen 1985, for instance, speculate that the positive anomalies result from the large scale incorporation of pre-existing feldspar rich cumulates. The relative depletion of Eu is dependent both on the fo_2 of the magma and the crystallising phases present (Möller & Mueke, 1984). Weill and McKay (1975) showed how, as the fo_2 decreased the distribution coefficient of Eu increased due to increasing Eu^{2+}/Eu^{3+}. Morris and Haskins (1974) also pointed out that this effect could be caused by increasing the polymerisation of the melt. Larsen (1979) also confirmed that lowering the polymerisation of the melt decreases the partition coefficients for the elements generally. In addition, Schnetzler and Philpotts (1970) convincingly showed how the size of the Eu anomaly was also a function of the composition of the feldspar, showing how Eu was preferentially incorporated into alkali feldspar compared to plagioclase. It is possible therefore, that in the magmas of the Gardar (Upton & Emeleus, 1987) and more particularly those of the Tugtutoq - Ilimaussaq zone (to

[20] except in the altered samples
[21] strictly trachyte in composition

Chondrite normalised REE plots of representative samples from the Geologfjeld Formation and Motzfeldt Sø Formation

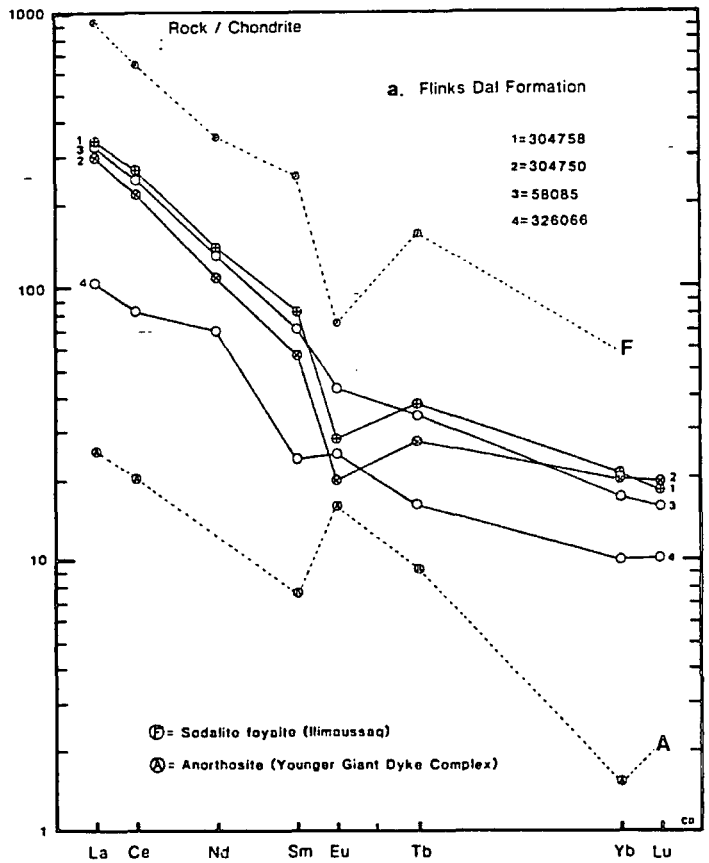


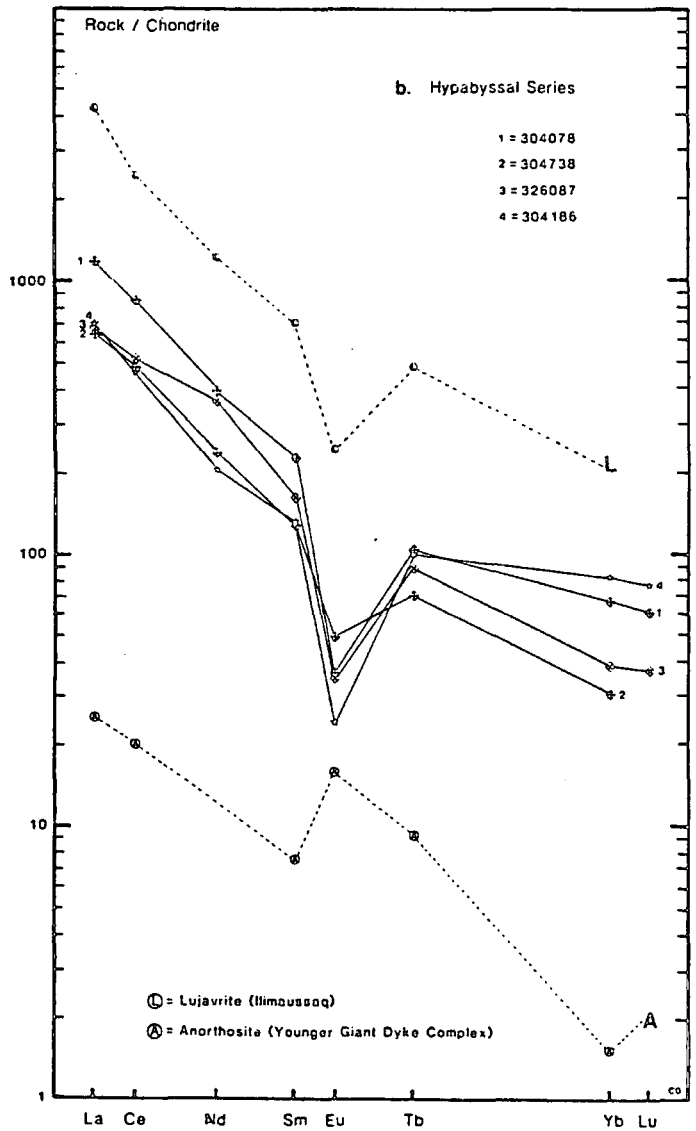


REE spidergrams

Fig 8.1.24

Chondrite normalised REE plots of representative samples from the Flinks Dal Formation and Hypabyssal Series



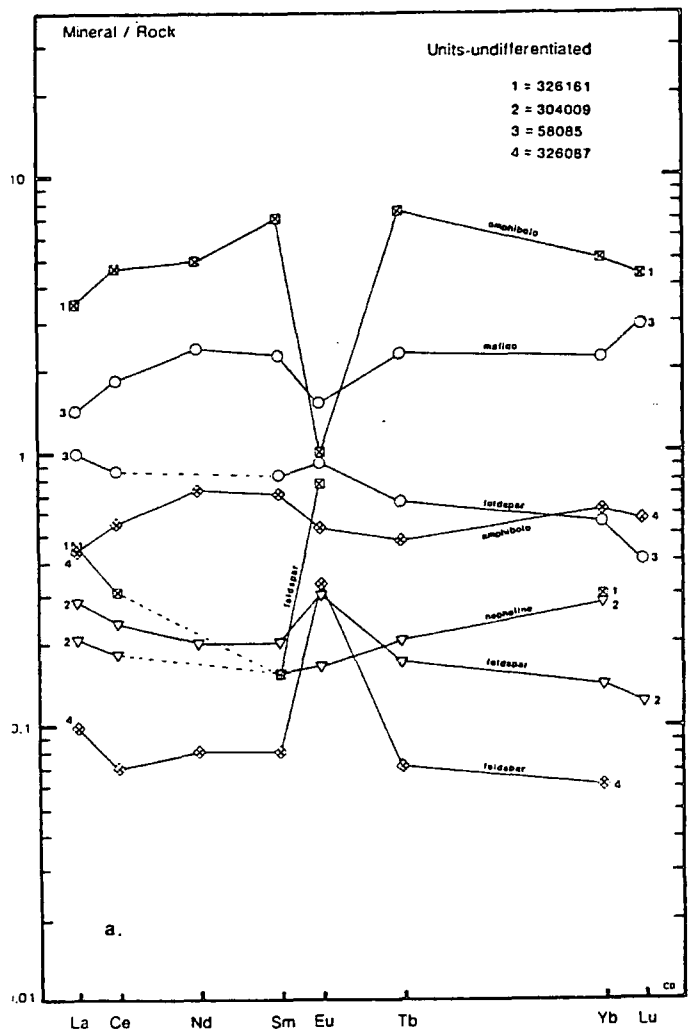


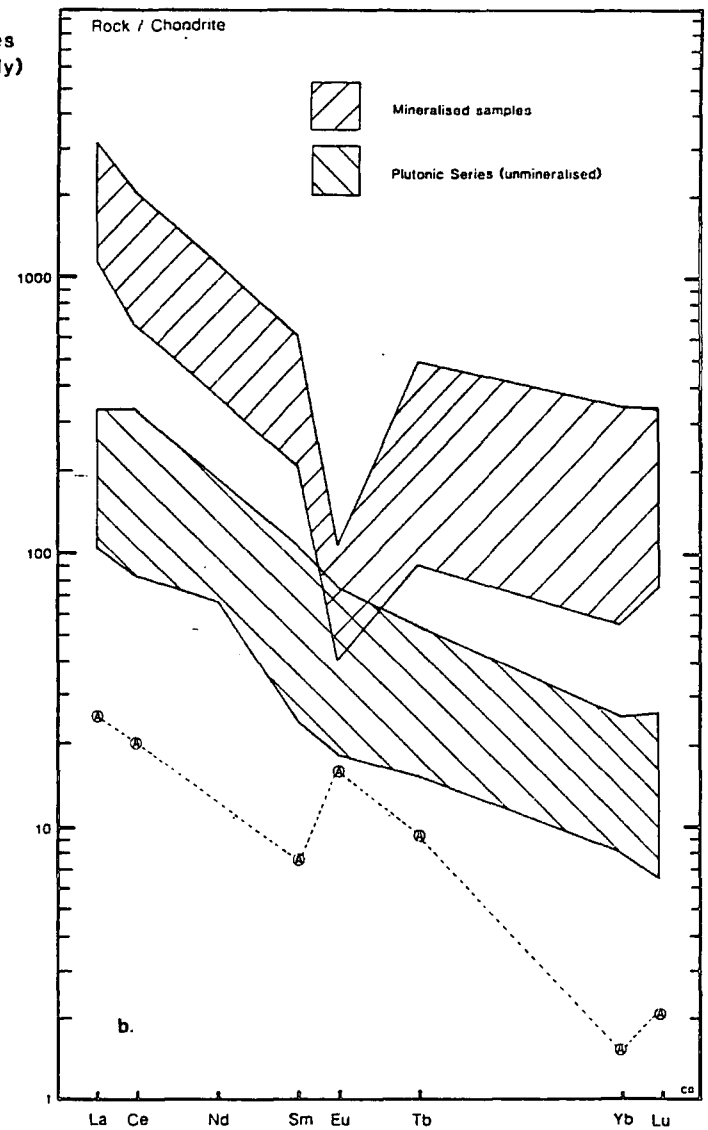
REE spidergrams

Fig 8.1.25

a. Mineral / rock REE plot showing REE distibution within primary (Derived from Mineral seperates) minerals (four units of the Motzfeldt Centre)

b. Chondrite normalised REE plot showing Maximum and minimum values for mineralised and unmineralised units analysed (Plutonic Series only)

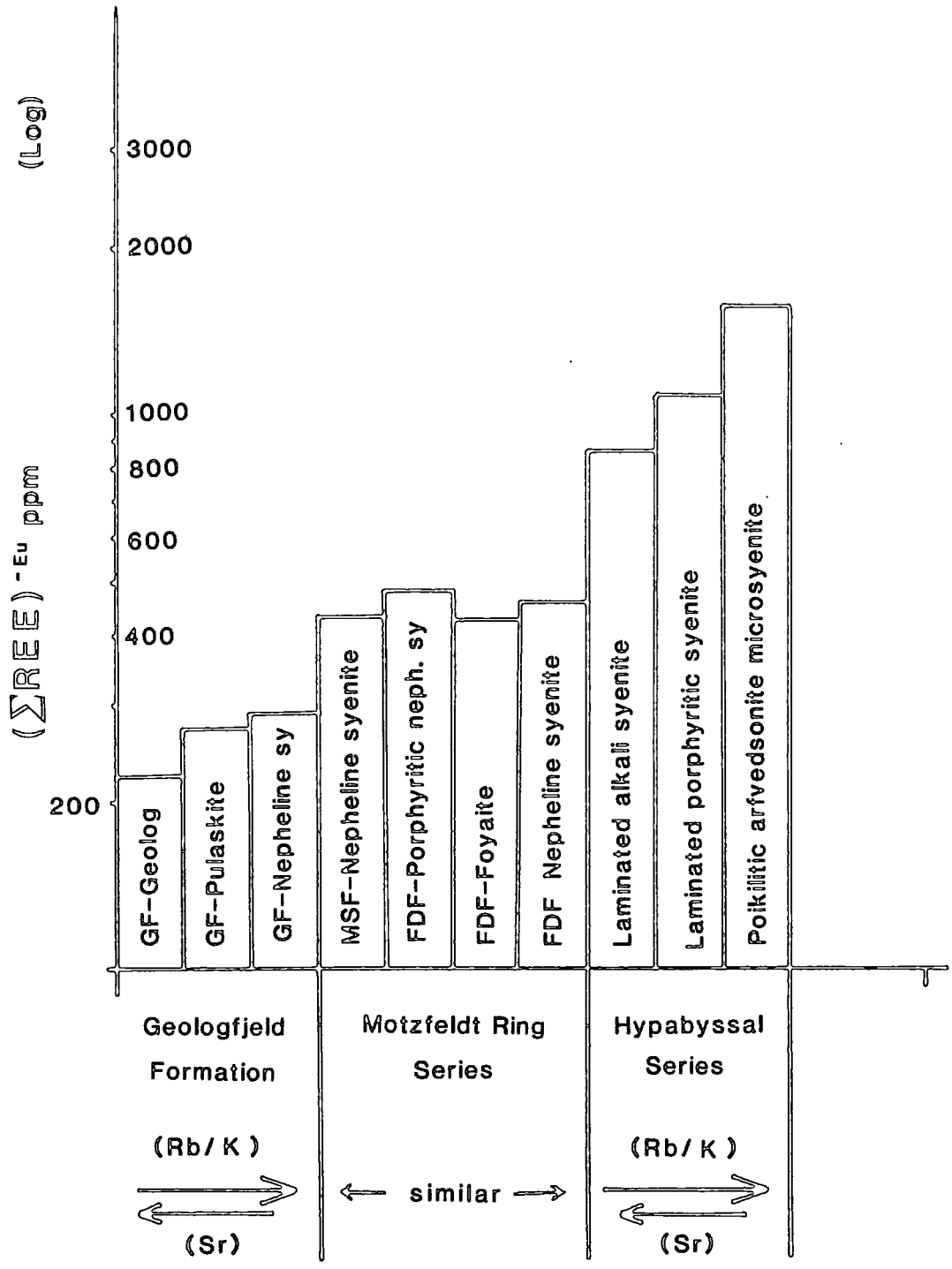




REE spidergrams

Fig 8.1.26

Total REE - Motzfeldt range Fig 8.1.27



which Motzfeldt is most similar) incorporation of Eu into feldspar was 'buffered' by the generally high polymerisation of the magmas (high content of network modifiers such as fluorine, low activity of silica) and their relatively high fo_2 (Larsen, 1979; Sørenson & Larsen, 1978) and 'delayed' until (K bearing) anorthoclase began to crystallise at benmoreitic (ie, larvikitic) compositions. Blaxland and Upton (1977) and Pearce (1988) have shown how Eu rich megacrysts could not have been derived from the rock in which they were contained. Pearce (1988) concluded that while the incorporation of megacrysts may explain the lack (or small size) of the Eu anomaly in some of the undersaturated evolved rocks, the most likely cause was the low activity of silica and relatively high fo_2. As evidence of this, he showed how a suite of silica oversaturated dyke rocks, at the same evolutionary stage (benmoreite - trachyte - phonolite) in comparison, displayed considerable negative Eu anomolies.

Thus the nepheline syenites of Motzfeldt display only small negative Eu anomalies despite protracted feldspar fractionation having taken place in their parental magmas.

The peralkaline rocks of Motzfeldt however show deep negative Eu anomalies and greater absolute abundances of the other REE's (Figs 8.1.24b & 8.1.25b; 8.1.26b). The peralkaline rocks shown in these figures are all silica saturated which (as discussed) will enhance Eu depletion. In addition they have undergone considerable alkali-feldspar fractionation and therefore the large negative Eu anomalies are as expected. The extreme enrichment in $\sum$REE's of the mineralised units (Fig 8.1.26b) is almost certainly a product of the complex combination of extreme fractionation and late-stage metasomatism (Larsen & Jones, 1980). For the detailed analysis of which see Tukiainen (1986c) and Morteani, et. al. (1986).

Fig 8.1.26a shows some mineral/rock REE distributions from selected minerals in Motzfeldt. Predictably the feldspars show very large positive Eu anomalies. The amphibole analysis (326161) belonging to the GF-Pulaskite shows remarkable enrichment in all the REE but particulary the MREE (other than a depletion in Eu). The calcic amphiboles (hastingsites) of this rock invariably contain inclusions of apatite (Plate 4.4b) which is considered here to be the cause of the elevated values (Henderson, 1982;

Nagasawa, 1970). Jones & Larsen (1985) have shown that the main REE bearing minerals in Motzfeldt include feldspar (Eu), apatite, zircon, sphene and members of the lavenite/rinkite family. In the mineralised units the REE can occur in a whole suite of minerals such as pyrochlore, zircon, thorite, eudialyte, bastnastite, monazite, and a host of unidentified Zr-REE silicates and REE carbonates (Tukiainen, 1986b).

Discrimination between the units

The $\sum$REE concentrations of the members of the Geologfjeld Formation are significantly lower than those of the members of the Motzfeldt Ring Series. This accords well with the other trace element findings. In addition the La to Yb gradient is steeper (ie, higher $(La/Yb)_n$ ratio) in the Geologfjeld Formation units.

The nepheline syenite units of the Motzfeldt Sø and Flinks Dal Formations have very similar ranges of $\sum$REE values and describe similar La to Yb gradients. However, it would appear that the MSF-Nepheline syenite[22] has lower $(La/Nd)_n$ and $(Yb/Lu)_n$ ratios compared to the members of the Flinks Dal Formation and the various ring-dyke units (Figs 8.1.24 & 8.1.25). The small sample range however means these observations can only be used tentatively for any discriminative purposes.

The slightly concave upwards profile of the spidergrams shown in the nepheline syenite units proably reflects the early separation of apatite which has a preferential affinity for the intermediate rare-earths (Haskin, 1979; Henderson, 1982).

[22] also the GF-Geologfjeld syenite & GF-Pulaskite



8.2 Economic mineralisation

8.2.1 Introduction

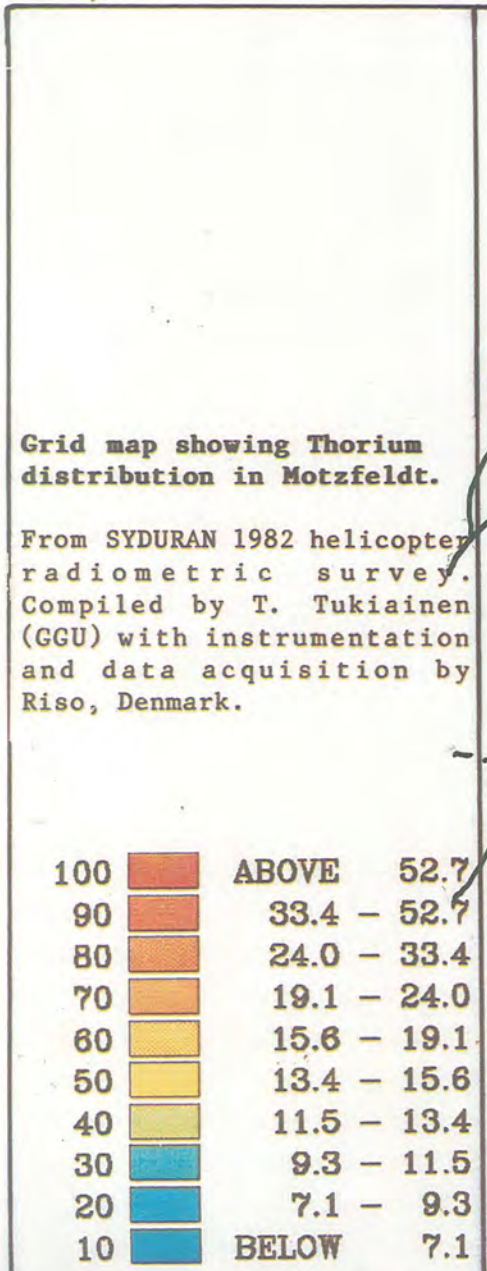
The MSF-Altered syenite and the associated MSF-Peralkaline Microsyenite Suite host complex ore reserves of Nb, Ta and Zr (with by- product LREE, U and Th) in the order of at least 130 million tons (Tukiainen, 1986b). This section gives a brief outline of the mineralisation in the Motzfeldt Centre with regard to distribution and possible evolution. For a detailed geochemical, mineralogical and economic assessment the reader is referred to Tukiainen (1986b; 1986c).

8.2.2 Distribution of the mineralisation

The results of the SYDURAN airborne-radiometric survey in Motzfeldt showed the uneven distribution of radioactive mineralisation (Tukiainen, Bradshaw & Emeleus, 1984; fig 35). Figures 8.2.1 and 8.2.2 (derived from the SYDURAN survey) show the regional Th and U distribution in Motzfeldt. The data discriminate between the Formations remarkably well and indicate the value of this kind of survey in highly evolved alkaline Centres. Clearly the Motzfeldt Sø Formation hosts consistently higher values than the Juliainehåb, Eriksfjord, Geologfjeld and Flinks Dal Formations. The economic concentrations of Nb, Ta, Zr, U, Th and LREE are restricted to the MSF-Altered syenite and MSF-Peralkaline microsyenite suite (see sections 5.3 & 5.4 for mineralogical details). These mineralised rocks have developed within a shell-like zone, 2 to 4 km wide which is easily recognisable in the field because of pervasive brick-red staining of the rocks. While the mineralisation of the MSF-Altered syenite is largely confined within the intrusion, mineralised MSF-Peralkaline sheets in places extend for up to 5 km into the surrounding country rock. These are associated with the ubiquitous development of microsyenite/pegmatite segregations which occur within the MSF-Altered syenite, ranging from miarolitic cavities to very extensive subhorizontal sheets. The highest concentrations of economic minerals (and pegmatite sheets) occur high in the roof zones of the Motzfeldt Sø Formation , particularly in NE and SE Motzfeldt, where extensive

Grid map showing Thorium distribution in Motzfeldt.

From SYDURAN 1982 helicopter radiometric survey. Compiled by T. Tukiainen (GGU) with instrumentation and data acquisition by Riso, Denmark.



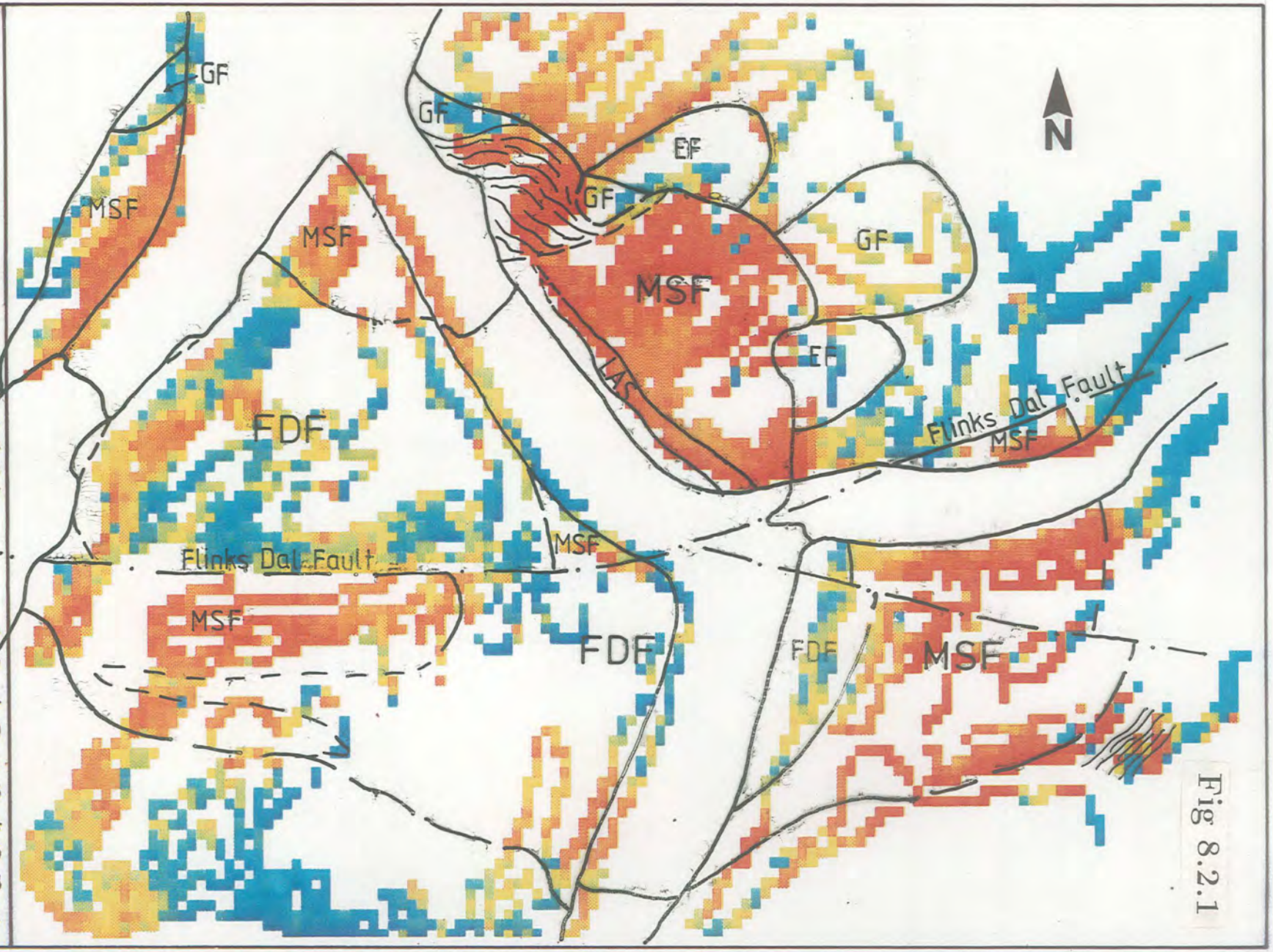
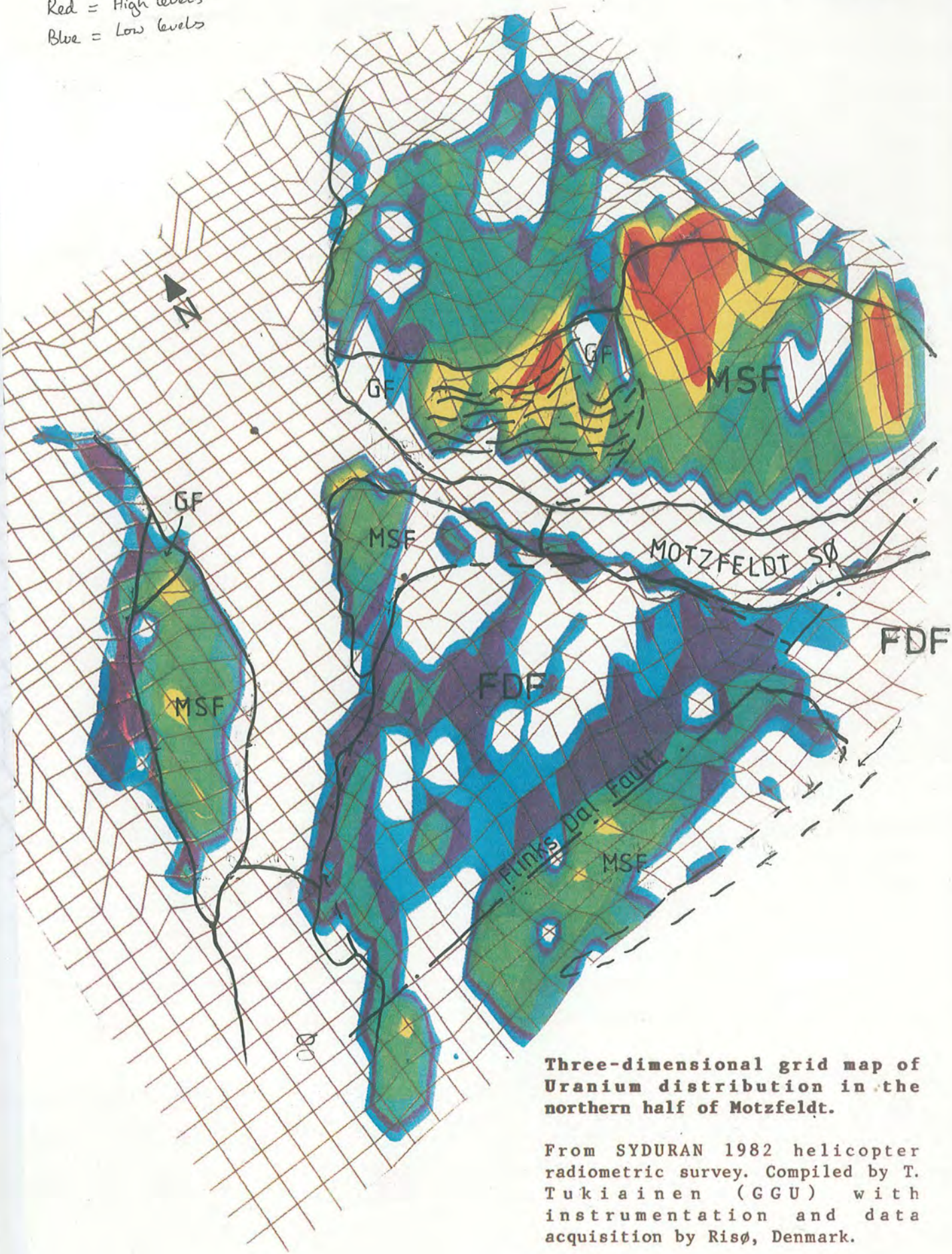


Fig 8.2.1

Fig 8.2.2



Three-dimensional grid map of Uranium distribution in the northern half of Motzfeldt.

From SYDURAN 1982 helicopter radiometric survey. Compiled by T. Tukiainen (GGU) with instrumentation and data acquisition by Risø, Denmark.

fracturing, induration and part- assimilation of the EF-basalts, tuffs and quarzites has taken place.

8.2.3 Evolution of the mineralised zones

Petrographic studies have shown that the main difference between the mineralised members of the Motzfeldt Sø Formation and the Flinks Dal Formation units (other than the mineralisation) is the evidence in the former of extremely high levels of volatiles (including H_2O), alkalis and considerable silica enrichment. Certainly the evidence for large scale assimilation of EF-Quartzite by the Motzfeldt Sø Formation is very strong, cause and effect being readily visible in the high ground of NE, E and SE Motzfeldt. Stable isotope methods could help determine these effects quantitively (eg, Taylor, 1980).

The extreme enrichment in the mineralising fluids in the Motzfeldt Sø Formation may be due to one or more of the following three origins:

a. 'Primary' high-levels of volatiles and incompatible elements caused initially by decompressional melting and the subsequent influx of volatiles at mantle source (Bailey, 1976: Thompson et. al. 1984) or similarly, partial melting at source due to volatile influx (ie, Blaxland et. al. 1978). The Motzfeldt Sø Formation being the first major phase of the Motzfeldt Ring Series could reflect this initial high volatile component.

b. Tapping of a volatile saturated (and incompatible element rich) 'juvenile' residuum melt from the upper-layer of a stratified, fractionating magma chamber which had developed at depth, following fractionation by crystal accumulation of anhydrous phases such as olivine, plagioclase and pyroxene (as seen elsewhere in the Gardar). On rising, the decreasing confining pressure caused the low density fluid phase to separate, gravitate and accumulate naturally toward the top and sides of the high-level (subvolcanic) chamber.

c. The Motzfelt Sø Formation magma[1] incorporating large quantities of formation and/or meteoric water from the surrounding country rock, particularly the EF-

[1] of similar characteristics to the FDF magma

supracrustal succession (cf. Taylor, 1977) and the mineralisation developing through a combination of *in situ* fractionation, diffusion, gas-transfer, leaching/migration and accumulation.

In fact, all of these processes may have been involved to some extent and it would be interesting to determine the relative roles between juvenile magmatically derived fluids, formation and circulating ground water, using fluid inclusion studies and stable isotope methods (eg, Taylor, 1974). McMillan and Panteleyev (1980) described the two end-members of such a hydrothermal system, namely orthomagmatic if dominated by fluids of magmatic origin and convective if dominantly meteoric. In both cases they showed how a roof-zone of alteration and mineralisation occurred and confirmed Taylors (1974) earlier view that if the magmatic fluids were dominant the alteration was more confined to the intrusive body than in a convective hydrothermal system.

What is certain is that the Motzfeldt Sø Formation was extremely enriched in volatiles (a study of fluid inclusions is needed). The majority of Gardar alkaline magmas were rich in F, Cl and C compounds (Konnerup- Madsen & Rose-Hansen, 1982), but on the other hand relatively anhydrous (Upton & Emeleus, 1987). Alkaline melts have a high capacity for dissolving and retaining volatile compounds (therefore decreasing their concentrations in a coexisting gas phase) (Kogarko, 1974) which not only act as depolymerising agents but also increase the solubility of some incompatible elements (eg, Watson, 1979), and significantly increase the crystallisation interval of the magma (Sood & Edgar, 1970). The members of the Flinks Dal Formation exemplify these properties. They all contain relatively high concentrations of, for example Zr and Nb (see section 8.1), evenly distributed throughout, and cumulate layering is normal. Pegmatite is rare and local accumulations of highly mineralised zones absent. This work has shown that the various units of nepheline syenite belonging to the Motzfeldt Ring Series have few significant[2] differences in their incompatible element concentrations (see section 8.1). This geochemical consistency possibly represents the **primary magmatic concentration** of

[2] Mann-Whitney U test

incompatible elements for all members of the Motzfeldt Ring Series. It is considered probable from this and the field observations that the high concentrations in the altered units have been largely controlled by the chemical changes, caused by *in situ* interaction of magma, water and the surrounding country rock. It is considered here that H_2O derived largely from the country rock interacted and combined with the F, Cl rich magmatic fluid to form an enveloping volatile-(over)saturated carapace such as envisaged in the formation of porphyry copper deposits (Burnham, 1979). The most obvious chemical change that this must have caused was to increase the fugacity of oxygen. Red hematite staining is extensive and pervasive throughout the altered rocks. An influx of water may have caused this, where H_2 could have diffused out of the system (Tukiainen, 1986c). Breakdown of amphiboles (commonly seen) would also release OH and F into the system giving rise to the reaction (amongst others) $OH^- + Fe^2 = Fe^3 + O^2 + \frac{1}{2} H_2$. In addition H_2 may have combined with F and/or Cl to form the acid volatiles H_2S , HCl and HF. Fluorite is a very common accessory in the altered rocks of Motzfeldt and, while F complexing is still unproven, and some say unlikely (eg, Taylor et. al. 1981) the reactivity of Cl is well established (Helgeson, 1964). Halogen complexing may have provided the transporting mechanism needed for the migration of the incompatible elements (Bailey & MacDonald, 1975; Collerson, 1982; Currie, 1986). The magmas of the altered rocks became silica-saturated and in extreme cases over-saturated as a consequence of assimilation of EF-Quartzite.

The ubiquitous albitisation characteristic of these rocks possibly occurred at this stage or much later as a result of Na-rich fluids permeating through the rock. Research using Cathodoluminescence studies may help ascertain the timing of this albitisation event.

Because of water oversaturation, particularly near the roof of the intrusion, boiling probably occurred. The extreme breakdown of mafic phases in the rocks examined from the high ground in NE Motzfeldt also suggests this, and it is in these rocks that the highest concentration of radioactive minerals are found. In addition, boiling would remove volatile constituents from solution and therefore leave a residue less capable of metal transport. Deposition would be the consequence. Moreover, Drummond and Ohomto

(1985) have shown that "Metals that are compexed by chloride are deposited largely as a result of decreasing proton concentration associated with CO_2 exsolution during boiling."

Peralkaline magmas have the ability to carry incompatible elements in solution (eg, Watson, 1979: Gableman, 1984). This is aided by their increased capability of dissolving volatile components so that they do not enter a gas phase, even at high concentrations (Kogarko, 1974). This capability decreases with increasing silica content of the magma (Sørenson & Larsen, 1978). Therefore the wholesale influx of water and silica into the Motzfeldt Sø Formation would not only have caused complex chemical changes (see Tukiainen, 1986c) but would also have ultimately led to the expulsion of volatiles in a gas phase (boiling) and formation of a zone enriched in incompatible element precipitation.

Water circulation as envisaged in Fig 8.2.3 combined with magmatic boiling at high levels in the intrusion could have acted as the driving force for the continued migration of the incompatible element and halogen rich, peralkaline, juvenile fluids from lower in the magma body.

The detailed investigations of Tukiainen (1986b; 1986c) have proved that the ore minerals have undergone several generations of nucleation and show continuous readjustment (precipitation/leaching) in response to the hydrothermal activity. This model of 'leaching', migration and accumulation necessitates the existence of a depleted source zone at depth, which remains to be investigated.

Why is the mineralisation and red-staining largely restricted to the Motzfeldt Sø Formation if it is mainly due to interaction with the country rock? The question arises because both the Geologfjeld and Flinks Dal Formation rocks penetrate into the supracrustal succession.

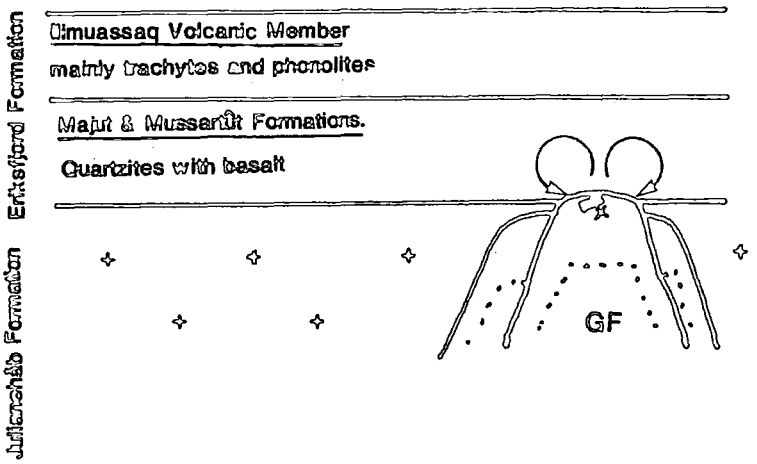
The Geologfjeld Formation, in fact is largely roofed by EF-Julianehåb Granite (Plate 3.4b) which presumably was generally impermeable to ground water migration. In addition, the Geologfjeld magmas were demonstrably lower in absolute trace element and REE concentrations (section 8.1) and almost certainly in fugitive components as well. Despite this, where the GF-Nepheline syenite does contain large rafts of EF-Basaltic material for example, 2 km west of Camp 4, the syenite is extremely discoloured (chocolate-brown) and shows elevated radioactivity counts.

The Flinks Dal Formation contains huge raft xenoliths of EF-trachytic and phonolitic material (for details see Jones, 1980) up to 300 m thick and covering areas of several km^2. Development of highly mineralised zones is limited however and largely confined to lujavrite development below the rafts, probably due to entrapment of volatiles in these local 'roofed' areas (Jones, 1980). Earlier in this work (section 3.6), it was noted that the raft material contained within the Flinks Dal Formation belonged to the Ilimaussaq Volcanic Member (Jones, 1980) whereas the Motzfeldt Sø Formation contained rock from the Majut Sandstone Member and Mussartût Volcanic Member (Larsen & Tukiainen, 1985) from lower in the Eriksfjord Succession. The latter contain considerably more sedimentary rock, particularly quartzite and a higher proportion of basalt (often vesicular). It is considered likely that these strata would have contained a much higher proportion of formation water than the more evolved trachytes and phonolites above and were probably more permeable to water circulation. Moreover, because the Flinks Dal Formation is completely enclosed by the earlier Motzfeldt Sø Formation (Bradshaw, 1985) this would have considerably reduced the circulation of water in and around the Flinks Dal intrusions (Fig 8.2.3). Taylor (1974) for instance envisaged that igneous intrusions emplaced into permeable country rocks (particularly in highly fractured volcanic areas) would act as "gigantic 'heat engines' that set up long-lived hydrothermal convection systems that persist throughout the crystallisation and cooling of the intrusion."

In summary, it is likely that the mineralisation which is largely concordant with the outer members of the Motzfeldt Sø Formation was deposited in a zone caused by the

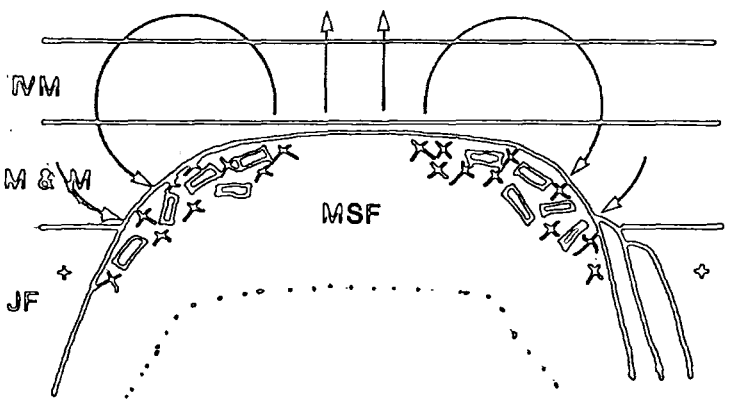
Evolution of Mineralisation

Fig 8.2.3



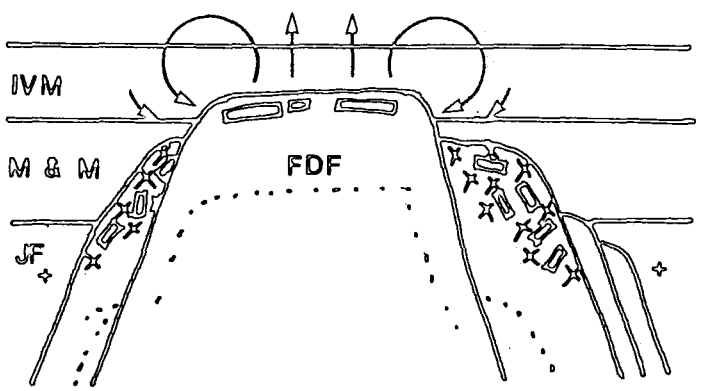
Geologfjeld Formation

Largely enclosed by granite–gneiss.
Localised water intake.



Motzfeldt Sø Formation

Large scale circulation of water & incorporation of country rock.
Development of volatile saturated carapace. Influx of siliceous rock.



Flinks Dal Formation

Reduced circulation, low water intake.
Little influx of siliceous material.

complex interaction between the volatile and incompatible-rich peralkaline Motzfeldt Sø Formation magma and the country rocks, coupled with a wholesale influx of water. Mantle metasomatism, extensive fractionation, leaching and migration may all have played a part in the development of the highly mineralised roof zones, migration and deposition of the highly charged fluids being driven and facilitated by the water/halogen rich outer carapace provided by the country rock interaction.

Whatever the balance between these several factors, what is unquestionable is the contemporaneity between the mineralising fluids and magmatic intrusion.

Chapter 9 - Tectonic and Magmatic evolution

9.1 Tectonic control

9.1.1 Introduction

The Gardar represents a cyclic period of intracontinental fault controlled red-bed deposition and alkaline igneous activity. The Gardar structures are superimposed on the older peneplained orogenic Ketilidian basement (see Chapter 1) and have not been affected by younger orogenic activity. In this chapter the tectonic evolution of the Gardar Province is discussed firstly in isolation and then in a continental setting.

9.1.2 Lineaments

The two main directions of lineaments are WNW-ESE and WSW-ENE (Berthelsen, A. & Noe-Nygaard, A. 1965; Stephenson 1976a; Thyrsted et. al. 1986). The former are major strike-slip faults with large sinistral movements, commonly in the range of 6 to 8 km (Henriksen 1960; Emeleus and Stephenson, 1970; Tukiainen et al., 1984), (Fig 9.1.1). Moreover, field mapping has shown that crustal movement occurred intermittently along these faults throughout the Gardar Period (Henriksen, 1960). The WSW-ENE lineaments are associated with faults which show small (10-100 m), if any dextral displacements. Most of the Gardar dykes and metamorphic grain in the basement gneiss also trend ENE. Vertical movements although difficult to assess, have been recorded throughout the Province along both lineament directions (Emeleus 1964; Emeleus & Stephenson 1976a; Boshe et. al. 1971). The thick Eriksfjord Formation succession preserved on the Ilimaussaq peninsula for instance, represents a downthrown block of some 2-3 km (Emeleus & Upton, 1976). In Motzfeldt, vertical movements in the range 100 to 800 m, are clearly defined using the base of the Eriksfjord Formation as a guide (Tukiainen, 1985b). The Flinks Dal Fault (6 km sinistral movement) for example has a downthrow of at least 500 m to the N (cf: Jones 1980).

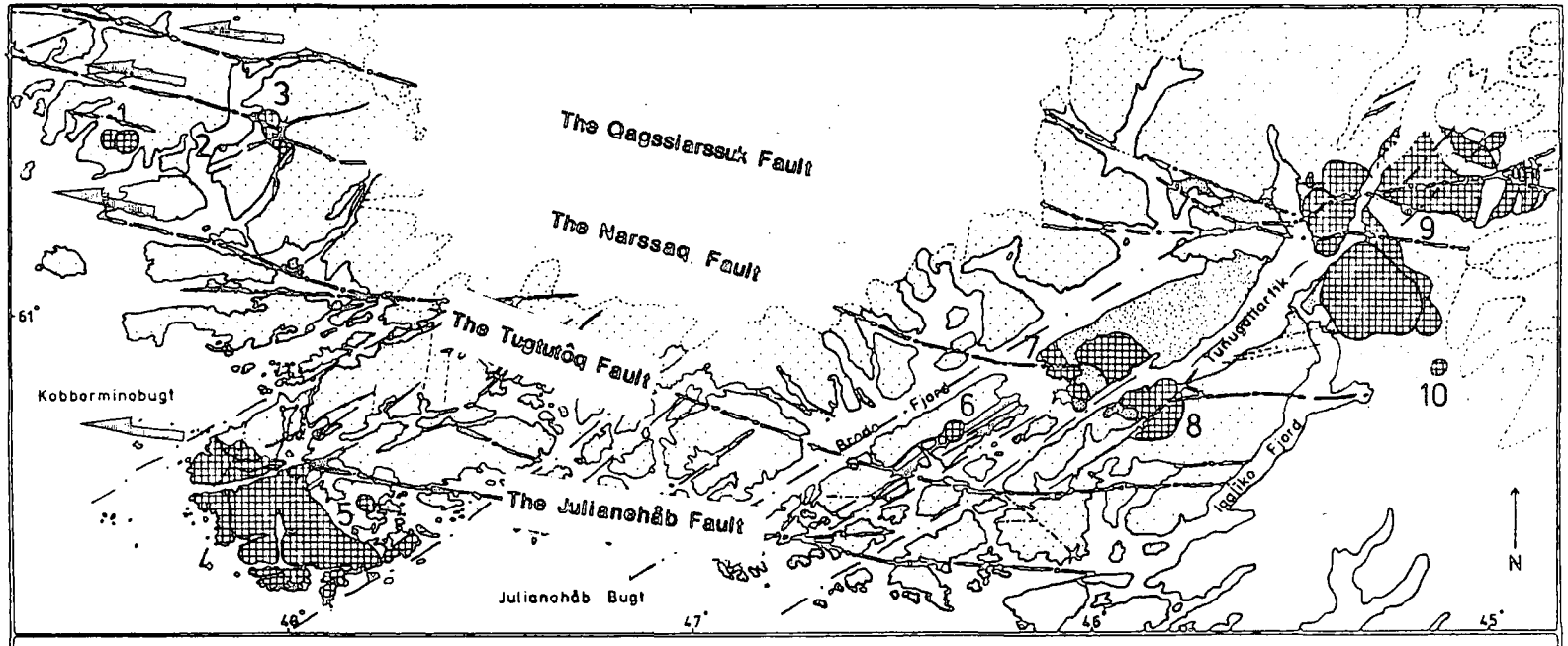


FIG. 1. General geological map of the Gardar Province showing major faults, positions of main dyke swarms and major intrusive complexes: 1 Kûngnât, 2 Ivigtut, 3 Grønnedal-Îka, 4 Nunarsuit, 5 Puklen, 6 Central Tugtutôq, 7 Dyrnaes-Narssaq, 8 Ilîmaussaq, 9 Igaliko, 10 Klokken.

After Stephenson (1976a). Showing the relationship of the major strike-slip faults (here named) and the Gardar igneous intrusives and ENE lineaments.

The major strike-slip faults of the Gardar Province Fig 9.1.1

It is well established that the major Gardar central complexes are situated at and controlled by the major lineament intersections (Berthelsen & Noe-Nygaard 1965; Stephenson, 1976a). In the following section the role of the major strike-slip fault system is emphasised.

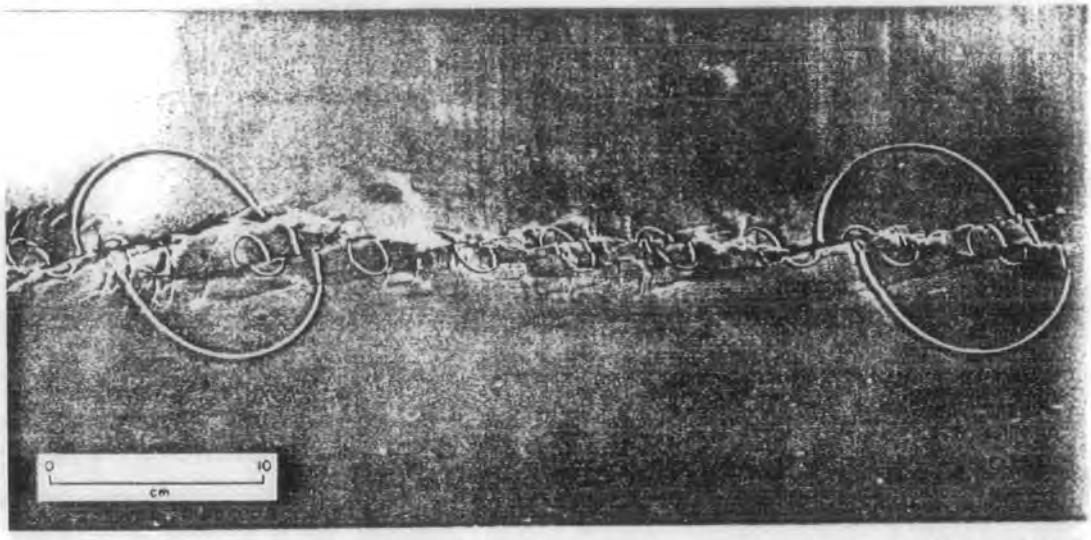
9.1.3 Gardar rifting

The Gardar Province has well established affinities with a continental rift system including; i) distinct parellelism of regular and intersecting lineaments with a long history of regular movement; ii) fault bounded red bed/volcanic succession; iii) dyke swarms and subvolcanic central complexes; iv) mantle derived igneous rocks with alkaline affinites; v) axial gravity anomaly (+ve). (Stewart, 1970; Sørensen, 1970; Upton, 1974; Upton & Blundell, 1978)

From the spatial distribution of the intrusive igneous rocks in the Gardar Province (Fig 9.1.1) and associated ENE trending axial gravity high (Blundell, 1978) it is clear that 'rifting' is not confined to a linear belt analogous to the East African Rift System. The igneous 'zones' (Upton & Blundell, 1978) are ENE trending and parallel but offset in a roughly en echelon system covering a broad area over 120 km across (E-W). The structure of the Province comprises a network of ENE horst/grabens controlled by WNW-ESE sinistral simple shear (wrench tectonics). Four major WNW-ESE strike-slip fault zones extend across the Gardar Province, (here named for reference purposes from N to S); The Qagssiarssuq Fault; The Narssaq Fault; The Tugtutôq Fault; and The Julianehåb Fault (Fig 9.1.1). They have acted as sinistral left stepping transcurrent faults, giving a framework of ENE trending pull-apart basins (see Fig 9.1.3). A simple, sinistral, coupling stress regime satisfactorily explains the orientation of the Gardar dyke swarms on both the large and small scale. The Motzfeldt Centre for instance is dissected by the Flinks Dal Fault representing 6 km of E-W sinistral movement. Dyke emplacement has been shown to be contemporaneous with at least some of this movement (Pearce, 1988), and in Motzfeldt the magnificently exposed en echelon SW-NE dyke swarms clearly are products of tensional stresses induced by sinistral shear coupling. Graphic corroborative evidence

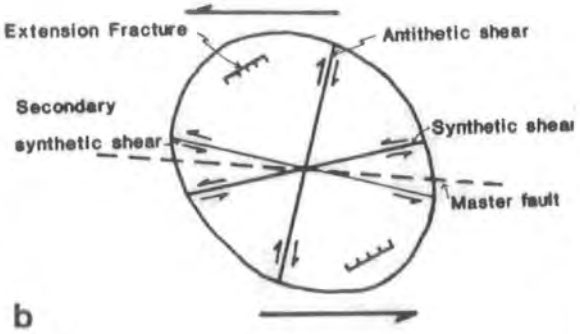
of this is readily provided by experimental work with clay models (Cloos, 1955; Badgley, 1965; Wilcox, et al. 1973). Fig 9.1.2a is taken from Wilcox et al. (op. cit.) and shows a striking similarity to the major tectonic structure of the Motzfeldt Centre (Fig 9.1.2c). The model shows an example of failure under parallel sinistral shear. Major sinistral strike-slip failure is accompanied by sigmoidal tension gashes and conjugate NW and NE faulting (normal & reverse, often with a small dextral component). If the shear is divergent, tensional and compressional stresses are enhanced (Badgley, 1965). On the larger scale it is probable that this similar stress pattern extended over the whole of the Gardar Province (Stephenson, 1976a). A similar strike-slip controlled graben system has recently been proposed for the evolution of the Benue trough in West Africa (Benkhelil & Robineau, 1983; Maurin et al., 1986; see also Marsh, 1973). Fig 9.1.3a shows a plan view of their interpretation of the controlling structure of the Benue trough (after Blenkhelil and Robinseau, op. cit.). Fig 9.1.3c shows three stages in the development of divergent plate boundaries in extensional continental settings (after Harding et. al., 1986) each of which is controlled by strike-slip motion and represent progressive degrees of extension. It is proposed here that the Gardar Province represents relatively limited crustal extension and comprises a series of extensional fault blocks. Major graben formation has been arrested except perhaps in the Tugtutôq-Narssaq zone (Upton & Blundell, 1978) where the gravity high indicates a zone of axial dyking (Blundell, 1978).

Stephenson (1976a) proposed a simple shear model to explain the ductile deformation and elliptical plan of many of the Gardar Central complexes. He noted that they define simple strain ellipsoids about a shear direction of 105° and occur at the intersection of the major lineaments. These features correspond to pull-apart graben structures formed in response to E-W simple shear wrench tectonics. Dyke emplacement is controlled by tension parallel to the graben direction which is ENE, as predicted by a theoretical strain ellipse model (Fig 9.1.2b). The central complexes occur where the sinistral decoupling intersects the ENE lineaments. The movement is transferred in the ENE direction producing a 'Rhombochasm' (Fig 9.1.3b; Biddle and Christie- Blick, 1986). This produces block faulting and rapid subsidence, facilitating the migration and accumulation of salic



a

Clay model of parallel left-lateral wrench fault (from Wilcox et al 1973)



b

Structures which form in left-lateral simple shear conditions.

Terminology from Wilcox et el (op cit) on a strain ellipse.



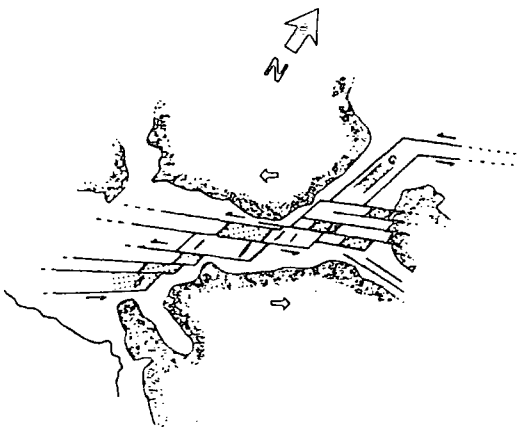
c

Major faulting in the Motzfeldt Centre.

(Dotted outer circle sea level extension of the Centre)

Extensional tectonic settings

Fig 9.1.3



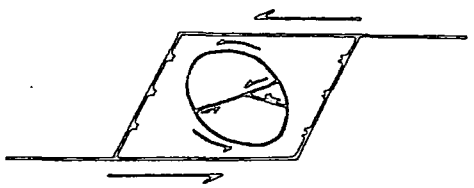
Strike-slip controlled graben and basin formation in the Benue Trough (from Blenkhelil & Robineau (1983).

G = Graben

/ = Megashear

= Transtensional Basin

a

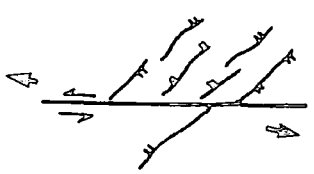


Releasing overstep forming pull-apart basin (Rhombochasm) showing theoretical block rotation and failure.

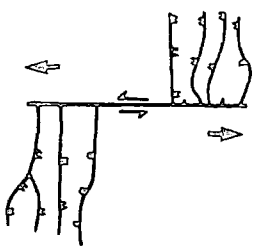
Harding et. al., (1986)

b

Divergent plate boundaries in extensional continental settings.

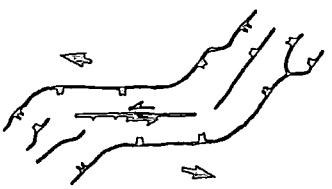


Basement extensional tear fault accomodating differential extention giving exten[sional] fault blocks eg, Benue Trough



Graben overstep, offset.

eg, Rhine graben, Baikal rift, Keweenawan.



Graben dogleg.

eg, East African Rift system.

c

(from Biddle and Christie-Blick, 1986)

magmas and the formation of the ring complexes. Rotation of the central block in the Rhombochasm (Fig 9.1.3b) combined with stresses imparted by the rising and accumulating magma produce circular fractures and cauldron subsidence (Anderson, 1951). This environment produces ring-dykes and nested plutons, vented to the surface through circular fractures leading to caldera formation.

9.1.4 Continental tectonic setting

Rifting has been divided into two main groups 'passive' and 'active' (Sengor & Burke, 1978). This terminology refers to the rift formation. Passive rifts are formed in passive response to a regional stress field (Morgan & Baker, 1983) whereas 'active' rifting is a result of a thermal upwelling of the asthenosphere (Bailey, 1964; Burke & Dewey, 1973; Bott, 1981). This is a somewhat generic classification and open to a chicken and egg argument as to the role of the mantle. In real terms there are four main continental rift settings (Illes, 1985):

1. Rifting at continental margins forming parallel or penetrative aulacogens from triple junctions (Burke & Dewey, 1973, Burke, 1980) (active?)
2. Domal uplift and hot spot rifting (Rhodes, 1971, Bott, 1981) (active)
3. Intracratonic rifting formed by intraplate strain (passive)
4. Collision of continents giving rise to localised extensional grabens and strike slip structures (ie, the impactogens of Burke 1980) (passive)

South Greenland up to the Mesozoic was contiguous with North America and probably Northern Europe (Piper 1982). Sawkins (1976) proposed a worldwide continental rifting episode (1.2 MY BP) representing the break up of a 'protopangea') Stewart (1976) on the other hand suggested that Proterozoic (1700-1200 MY) deposition was dominated by scattered, locally deep epicratonic troughs and only after 800 MY BP did continental scale extension occur. Baragar, (1977) suggested that the continental sequences of red bed/volcanic strata of the Keweenawan supergroup, Seal Lake group, Labrador and the

Gardar where synchronous and representative of a major continental rifting event. The Keweenawan rift of central N America has received a great deal of study. Keweenawan (1.2-1.0 MY BP) mafic rocks (mainly tholeiitic) and associated red clastic sediments occupy an arcuate belt over 2000 km long with an average width of 60 km (Halls, 1978). The axial gravity high (+ 60 mgals) associated with the rift has been associated with a major crustal suture with the limited formation of oceanic crust (Chase & Gilmar, 1973) analogous to the Red Sea area of Africa. This has been convincingly disputed by Green (1983) who states that the rift was aborted before the birth of new ocean. The rift comprises several lava plateaux 2.5 to 7 km in depth and 100 x 250 km across. Most are tholeiitic in composition although notably the early volcanics were rich in incompatible elements (Green, 1983). Intrusions include basaltic dyke swarms, sills and small plutons. If the Gardar Province is, as seems likely, associated with this mid-continental rift of N. America (Baragar, 1977) it represents considerably less crustal extension (Upton, 1974; Upton & Emeleus, 1987) as exemplified by its network graben structure, smaller gravity high and more alkaline petrology (Gass, 1968; Harris, 1969; McKenzie, 1985). There is no general agreement as to the origin of the central N American Proterozoic rifting episode. Although the role of the Grenville event (1.0 my BP) has been stressed.

The Keweenawan, Seal Lake and Gardar may represent penetrative aulacogen systems related to the opening of the Grenville ocean (subsequently closed) (Burke, 1980). The mechanism of rifting and alkaline magmatism may follow the proposals of Marsh (1973) and Sykes (1978) and be related to the continental extension of transform faults or reactivated preexisting zones of weakness controlled by transform stress systems. Sykes (1978) has shown that unlike oceanic transforms, reactivated zones of weakness in continents usually involve only relatively small horizontal displacement. The seismic activity and alkaline magmatism however, is controlled by deep fractures that penetrate the whole thickness of the lithosphere. Moreover, Sykes (op cit) points out "During the fragmentation of a supercontinent, multibranched rifting usually follows the youngest zone of previous orogenesis and as much as possible avoids passing through old cratonic areas where the lithosphere is thick, cold and strong ..... During the early development of

an ocean the preexisting mosaic of structural elements within the thick craton produce normal forces across some plate margins, leaky transform faulting, and localised stress concentrations" .

Sykes (op cit.) also points out that 'hot spots' appear to be related to nodes or junctions in this mosaic pattern and therefore are passive features and not the surficial expression of mantle plumes (cf: Burke & Dewey, 1973; Rhodes, 1971; Fletcher & Litherland, 1981). Donaldson and Irving (1972) suggest the Keweenawan to be the product of tensional phases related to the waning stages of the strike-slip (dextral) collision of the Grenville Plate from the ESE. This is endorsed by Gordon and Hempton (1986) who show the Keweenawan rift to have formed from right-lateral NW-SE strike-slip faults propagating into the N American interior from the NNE-SSW Grenville plate collision zone. Left stepping offsets along the strike-slip faults produced NE-SW pull-apart basins and tension gashes. These focused magmatic activity giving rise to axial dyking and fissure eruption. Gordon and Hempton (op cit) further consider this impactogen origin (Burke, 1980) to be responsible for the Baikal extensional system; the Rhine Graben; and the Oslo Graben, all being strike-slip controlled. Halls (1978) points out however that there is no evidence of any plate suture anywhere within the Grenville Province.

In conclusion, the Gardar represents a prolonged (c. 200 MY) and cyclic period of intracratonic rifting. The structures developed were in response to intraplate sinistral shear stresses controlled by continental scale tectonics. Crustal interaction between the N. American and the Grenvillian plates was responsible. This stress regime could be related to the continental extension of major transform faults concomitant with the break up of the N American supercontinent. A strong case however has been presented for an impactogen origin for the rifting. What ever the driving force, intraplate strain preferentially reactivated the younger Ketilidian mobile belt which was subjected to sinistral shear. Passive continental extension and crustal thinning induced a rise in the geothermal gradient (Mackenzie, 1978) and partial melting in the upper mantle. Deep fracture zones facilitated the rapid rise of magma which followed the ENE zones of tension

in the brittle upper crust. ENE extensional fault blocks developed and crustal decoupling occurred along several roughly parallel WNW-ESE strike-slip faults. Rhombochasms developed where these intersected giving rapid block subsidence and facilitating the high level rise and accumulation of salic magma to form subvolcanic ring complexes. These zones are analogous to 'leaky transform faults' in oceanic lithosphere.

The Gardar Province is bounded by an Archaean cratonic block to the N and it is probable that during continental scale tectonics a sinistral wrench developed between this craton and the opening or closing of the Grenville plate to the S.

9.2 Magmatic Development

The preceding section indicated the importance of continental scale tectonics in the development of the Gardar Province and showed how the Gardar structures represent considerably less crustal extension than the associated mid-continental rift of N America (Baragar, 1977). Because of this the province has produced less extensive but more alkaline igneous activity (Upton, 1974; Harris, 1969).

In the recent comprehensive review on the Gardar magmatism by Upton and Emeleus (1987) a number of important conclusions were drawn. Some of these are summarised below (with additional comments) in order to complete the overall generic picture of the Province, for this work.

1. The cause of repetitive alkaline magma generation may be related to partial melting of the lithospheric mantle triggered by deep mantle emanations of F, Cl and C rich fluids.

The rise of these fluids could possibly be in response to tectonic decompression caused by lithospheric thinning and corresponding rising geothermal gradients (McKenzie, 1978; Morgan & Baker, 1983) or the converse (Bailey, 1964; 1970; 1974a; 1977).

2. The mantle source rocks partially melted were probably clinopyroxene depleted, lightly metasomatised [1] (cf, Lloyd & Bailey, 1975) garnet lherzolites (ie, with low Cpx/Gnt ratios).

3. Early fractionation of Mg-olivine and Mg-clinopyroxene at subcrustal levels then gave rise to the typically mildly alkaline or transitional olivine basaltic magmas with characteristically high Al_2O_3/CaO and FeO/MgO ratios.

4. Low H_2O but high halogen and C compounds lowered viscosity and facilitated easy mobility and formation of fractionating layered intrusions.

5. More evolved magmas were produced from the basaltic[2] - hawaiitic parents largely by low pressure crystal fractionation of Fe-Ti oxide, olivine, pyroxene and plagioclase. The mugearitic/benmoreitic residues derived from these processes continued to evolve to benmoreitic/trachyte composition by continued removal of olivine and pyroxene with increased fractionation of feldspar (including anorthoclase) and apatite. At high crustal levels continued fractionation leads to the undersaturated sequence of syenite - pulaskite - nepheline syenite or an oversaturated trend toward syenite - qtz-syenite - granite.

6. The magmas parental to the N American anorthosites were tholeiitic and were produced from melting much more extensive than that which later formed the rocks characteristic of the Gardar igneous province.

The Gardar Province is underlain by Massif-type anorthosites of Mid-Proterozoic age (Bridgwater, 1967; Bridgewater & Harry, 1968). They are thought to be part of a continental scale event (1.7 to 1.2 MY; Morse, 1977) which predated the Gardar rifting episode (Emslie, 1978). Feldspar crystallisation, fractionation and cumulate layering has played a role in the Gardar magmatic evolution and particularly in the more evolved

[1] at least in the Tugtutôq - Ilimaussaq zone

[2] Basanite however, is apparently more widespread than previously considered (Pearce, 1988)

stages. However, from trace and rare earth element studies it is now considered that there is no direct genetic link between the massif-type anorthosites (as represented by many of the feldspar megacrysts in the Big feldspar dykes) and the Gardar magmatic evolution (Upton & Thomas, 1980; Blaxland & Upton, 1978; Pearce, 1988).

7. The Gardar Province magmatism was cyclic.

Upton and Emeleus, (1987) stress the importance of cycles of activity in the Gardar (see also Upton & Blundell, 1978), and state that during episodes of high tensional stresses, (begining of each cycle unit) large quantities of basalts reach the surface (ie, dykes and plateau lavas) whereas in later, (end of each cycle unit) quieter stress regimes, salic lavas develop in trapped, fractionating magma chambers. The mobile, low density salic magmas rise and are 'ponded' at high levels, forming sub-volcanic magma chambers. For example, Upton and Emeleus (op. cit.) consider the Eriksfjord Formation to represent the begining of the first (Early) Gardar cycle and the salic intrusions of Motzfeldt and N Qôroq to mark the end (see Chapter 1).

Weaver et. al. (1972), postulated a similar model for the development of trachytic lavas in the East African Rift System. They envisaged an axial dyke-like basaltic body of batholithic proportions (with similar positive gravity anomaly to that of the Tugtutôq - Ilimaussaq zone of Gardar) would form by crystal -liquid fractionation, a zoned profile with more salic fractions upward.

The spatial and temporal distribution of the Gardar ring-centres suggest that they represent high level salic magma chambers which developed above a regional scale, axial complex of dykes and magma chambers (cf: Chapman, 1967). The higher tensional stresses early in each cycle facilitated the rapid upward venting of basaltic/hawaiitic magmas in the form of dyke swarms and associated fissure volcanics. Lower to mid crustal magma chambers would also be repenished and formed particularly as the stress regime waned. With lower stresses, quiescence and entrapment caused fractionating chambers to develop toward benmoreitic compositions and salic cupolas to form (Chapman, 1966). As the high crustal levels continued to tectonically readjust, later in each cycle, tapping

and migration of the salic residuum was possible (Gill, 1973). Wolff (1987) suggests that each lithological discontinuity in a ring-complex may be the product of an event, in a single magma chamber, such as partial replenishment or partial eruption. Others stress the importance of chemical/mineralogical stratification (Upton, 1960; Stephenson, 1973; Jones, 1980; Stephenson & Upton, 1982). Whatever the case, subvolcanic ring-centres in the Gardar developed preferentially where the tectonic regime of intersecting faults / fault blocks interacted with the axial magmatic zones and allowed rapid block subsidence, accumulation and venting of magma.

PART FOUR

CONCLUSIONS

Chapter 10 - Concluding Remarks

10.1 Introduction

This study was instigated primarily to reassess the field relationships of the Motzfeldt Centre. The results of the early SYDURAN surveys (Armour-Brown, Tukiainen & Wallin, 1980; 1981; Tukiainen, 1981) indicated a need for this reappraisal with the discovery of large areas of previously unsuspected, highly mineralised and economically valuable rock units. The combination of field surveys and airborne-radiometric and geochemical analyses[1] has provided the data for the geological revision of Motzfeldt presented here. Throughout the SYDURAN 1982 and PYROCHLORE 1984 projects, the geological progress has been documented and the author has been directly involved in a number of reports (see Appendix One). This thesis is the culmination of this progress [2] and whilst still only a 'progress' report the work is aimed at giving a comprehensive documentation of the general characteristics of the rock units. Further progress in the 'understanding' of Motzfeldt will necessitate; continued field surveys and geochemical analysis with the 'pooling' of geochemical results to form a single data-base[3]; and the instigation of stable isotope and fluid inclusion studies.

10.2 Field interpretation

The following observations describe the major changes in the geological interpretation since the begining of the SYDURAN (1982) survey. The main conclusions drawn from this study are indicated together with possible areas of further research which would be particularly beneficial to the overall synthesis.

---

[1] greatly enhanced by superb 1:10000 contoured orthophoto maps
[2] at least for the author's geological interpretations
[3] apparently well under way (Tukiainen. pers. comm.)

10.2.1 New nomenclature

The main intrusive units of Motzfeldt can be grouped into three generically related intrusive sequences or Formations.

This division was based primarily on field observations (Bradshaw & Tukiainen, 1983) but has subsequently been endorsed by petrographic and geochemical study (Tukiainen, Bradshaw & Emeleus, 1984; this work). The Motzfeldt Sø and Flinks Dal Formations comprise the main centralised ring intrusion of Motzfeldt (SM1 to SM5 of Emeleus & Harry, 1970 ; SM5* & SM6 of Jones, 1980) now called the Motzfeldt Ring Series (Bradshaw & Tukiainen, 1983).

The following previously undiscovered or undescribed units (or unit variations) have been documented:
GF-Geologfjeld syenite
MSF-Marginal arfvedsonite syenite
MSF-Altered syenite
MSF-Peralkaline microsyenite suite
Laminated alkali syenite (partly described by Jones (1980) as SM3)

The following units have been described in the areas indicated in brackets for the first time:
Laminated porphyritic syenite (in NE Motzfeldt)
MSF-Nepheline syenite (C Motzfeldt (east and west))
MSF-Nepheline syenite (SW Motzfeldt)
FDF-Foyaite (central type) (S Motzfeldt)

10.2.2 The Geologfjeld Formation

The intimate field and generic relationship is confirmed between the N Motzfeldt Satellite syenites GF-Pulaskite and GF-Nepheline syenite (NM1 & NM2). The discovery of GF-Geologfjeld syenite in NE and NW Motzfeldt (Bradshaw & Tukiainen, 1983), which

is very similar petrographically and geochemically to the GF-Pulaskite (NM1), indicates the greater importance and much larger extent of these early satellitic intrusions. The sodalite-nepheline syenite of SE Motzfeldt assigned to this Formation by Bradshaw and Tukiainen (1983) is considered by Bliksted (1984 - GGU field notes) to be a 'fresh' variety of the MSF-Altered syenite. If this is so then detailed study may place some constraints on the timing of the mineralising hydrothermal event. The field evidence in NW Motzfeldt showed that the consolidated GF-Geologfjeld syenite was essentially impervious to this mineralising and staining process which so effected the Motzfeld Sø Formation (Bradshaw, 1985).

The Geologfjeld Formation / Motzfeldt Sø Formation contact whilst discovered in the NW has not been located conclusively in NE Motzfeldt and the pink nepheline bearing syenites discovered at low elevations (presumably near this contact) in Storeelv need further investigation.

10.2.3 The Motzfeldt Sø Formation

This unit originally SM1 of Emeleus and Harry, 1970 has been divided into three distinct concentrically zoned variants: the MSF-Marginal arfvedsonite syenite, MSF-altered syenite (with sheet segregations) and the MSF-Nepheline syenite (Bradshaw & Tukiainen, 1983). The Formation was shown to extend vast swarms of microsyenite sheets (Peralkaline Microsyenite Suite) into the country rock (Tukiainen, 1981) and older syenite units (Bradshaw & Tukiainen, 1983).

Previous studies indicated the possible role played by assimilation of the siliceous country rock (mainly quartzites) in forming the saturated and sometimes oversaturated outer members of SM1 (Emeleus & Harry, 1970; Jones, 1980). The SYDURAN and PYROCHLORE surveys have confirmed this relationship and stressed the importance of crustal interaction in the development of this outer zone of mineralisation in the MSF-Altered syenite (Tukiainen, Bradshaw & Emeleus, 1983; Tukiainen, 1986c).

In addition, these works have shown how the Peralkaline Microsyenite Suite of intrusions is related generically spatially and temporally to this altered zone.

The preliminary results of the airborne-radiometric survey indicated that contrary to earlier interpretations, the Motzfeldt Sø Formation probably completely enveloped the Flinks Dal Formation units. Subsequent PYROCHLORE field investigations confirmed this, with the discovery of an outer band of Motzfeldt Sø Formation rocks in SW and C Motzfeldt (west) (Bradshaw, 1985).

Large raft xenoliths of MSF-Nepheline syenite discovered in the Flinks Dal Formation in the high-ground of S Motzfeldt (Bradshaw, 1985) indicate that the Motzfeldt Sø Formation possibly extended over (roofed) the whole area it now circumscribes.

10.2.4 The Flinks Dal Formation

A major revision of units comprising the Flinks Dal Formation has taken place since the early surveys. Bradshaw and Tukiainen (1983), noted the striking similarity between the outer porphyritic margins of SM4 in C Motzfeldt (north) and the rock described as SM2 in SE Motzfeldt; and suggested that they may be in fact the same unit. This relationship was endorsed by the discovery of the MSF-Nepheline syenite/FDF-Porphyritic nepheline syenite (SM2) contact in C Motzfeldt (east), (Bradshaw, 1985). This proved both the existence for the first time of SM2 N of the Flinks Dal Fault and that the SM3 ring-dyke in SE Motzfeldt could not extend into NE Motzfeldt (as suggested by the earlier surveys). This gave further confirmation of the 6 km offset along the Flinks Dal Fault. With the recognition of the Motzfeldt Sø Formation in W Motzfeldt it is considered here that the porphyritic nepheline microsyenites comprising SM2 and the outer members of SM4 in C Motzfeldt (north and west) represent the initial intrusion and outer 'chilled' facies of the Flinks Dal Formation.

Jones (1980) noted the complexity of the unit SM4 ..."Within SM4 there are several distinct facies, possibly representing separate intrusive or cooling events" and described

SM4 in two sections: Foyaite and Porphyritic nepheline microsyenite/phonolite. The foyaite he noted, displayed complex intrusive 'dyke-like' affinities in SW Motzfeldt, whereas similar rocks occurred in sub-horizontal cumulus horizons just E of the larvikite ring dyke (C Motzfeldt, west).

The current survey groups these foyaite types into FDF-Foyaite (transgressive) and FDF-Foyaite (central) facies respectively.

The large, saucer shaped cumulate 'pile' (>300 m thickness and c. 3 km diameter) of central type FDF-Foyaite discovered in the high ground of S Motzfeldt (Bradshaw, 1985) petrographically matches that described by Jones (1980), just E of the larvikite ring dyke, N of the Flinks Dal Fault. When the movement along this fault is reversed, these foyaites clearly belong to a single unit analogous to the central SI7 of the Igdlerfigssalik intrusion (Emeleus & Harry, 1970).

This foyaite cumulate succession has either developed within the contemporaneous FDF-Porphyritic nepheline syenite envelope or has intruded and 'cored out' the latter at some later stage. There is conclusive evidence that the foyaite is younger, with brittle intrusive relations seen in S Motzfeldt (see Chapter 6). The contact between the two units in C Motzfeldt (west) is very sharp (but masked by the larvikite). These features, however could also be developed if the outer zone chilled and acted as an independent brittle crust to the very mobile magmas within, with little or no exchange of material. The thermal or physical dynamics of this occurrence on such a large scale however, have not been investigated.

It also remains to be clarified whether or not the transgressive FDF-Foyaite, which demonstrably invades the FDF-Porphyritic nepheline syenite and/or MSF-Nepheline syenite in SW, S and SE Motzfeldt, with a series of partial ring dykes is contemporaneous with the central FDF-Foyaite or entirely separate (at least at these intrusive levels).

The FDF-Nepheline syenite is demonstrably the youngest major intrusive unit of the Motzfeldt Ring Series and the Motzfeldt Centre. The view that the larvikite ring dyke is closely related to this unit and is probably the last intrusive phase of the Motzfeldt Centre (Jones, 1980) is upheld here.

10.2.5 The Hypabyssal Series

The minor intrusive units of partial ring-dyke or sheet form which are not demonstrably connected with any Formation have been reappraised. They are collectively referred to for descriptive purposes as the Hypabyssal Series (this work) and correspond to the following units of Emeleus and Harry, 1970;

Laminated alkali syenite[2] = SM3

Laminated porphyritic syenite = EMa

Poikilitic arfvedsonite microsyenite = EMb

The arcuate band of SM3 curving throughout NE Motzfeldt mapped and described by Emeleus and Harry (1970), was shown to comprise a multi-intrusive network of partial ring-dykes/sheets belonging to two separate units (Bradshaw & Tukiainen, 1983). The Laminated alkali syenite consisting of at least 3 parallel intrusions, is clearly invaded by the younger irregular and smaller dykes of the Laminated porphyritic syenite.

The Laminated alkali syenite was briefly described petrographically by Jones, 1980 as SM3: N of the Flinks Dal Fault. In the light of the discovery of the 6 km lateral offset along this fault it became clear that the SM3 of SE Motzfeldt could not extend into the NE area. This therefore ruled out the possibility that the Laminated alkali syenite was a nepheline-free variety of the same unit. Indeed the Laminated alkali syenite has yet to be discovered at all in SE Motzfeldt. Certainly it should be located in the N facing cliffs of SE Motzfeldt and the S facing cliffs of E Motzfeldt. However, access is severely restricted in these areas by steep cliffs, scree and glacial moraine. Dykes of Laminated porphyritic syenite on the other hand have been traced throughout the length of the SE

[2] named Fayalite alkali syenite by Bradshaw and Tukiainen, 1983

and NE Motzfeldt. Mapping difficulties occur in SE Motzfeldt where the lithologically similar MSF-Marginal syenite exists in close proximity.

The younger Poikilitic arfvedsonite microsyenite is generically related to the Laminated Porphyritic syenite. The unit is younger (although possibly overlapping) and occurs as hyalocrystalline sub-horizontal sheets (or sheet) only in SE Motzfeldt.

The units comprising the Hypabyssal Series are definitely younger than the Geologfjeld and Motzfeldt Sø Formations but because they are nowhere in contact with any units of the Flinks Dal Formation the age relations between these two groups are uncertain. On the basis of geochemical considerations it is conjectured here that the Flinks Dal Formation is the younger.

10.3 Mineralogical and Geochemical Conclusions

10.3.1 Mineralogy

The majority of rock types comprising the Motzfeldt Centre occur within a narrow range of compositions, over 90% being syenite or nepheline syenite in lithology. They represent the end member compositions of protracted fractionation in the alkaline olivine basalt (sodic) series (of; Irvine and Baragar, 1976). Although most follow an undersaturated course, a number of units display saturated or oversaturated characteristics particularly where they have been contaminated by siliceous country rock.

This thesis has emphasised the importance of peralkalinity in typifying the geochemical and mineralogical features found in the rock units. A broad three-fold classification is used. Hypoalkaline (PI < 0.95) syenites and nepheline syenites (miaskitic) are characterised by relatively[1] low concentrations of the incompatible elements whilst containing high Ca, Ba, Sr, Mg, and Ti. Typically the mineralogy comprises; calcic mafic minerals - hasting sitic hornblende and salite or ferrosalite, (Ca) alkali-feldspar often with

[1] in comparison to alkaline and peralkaline types

plagioclase cores, Fe-Ti oxides and apatite, and/or nepheline. The dominant substitution in the mafic minerals is $Mg^{2+} \Rightarrow Fe^{2+}$. Zoning however is not strongly developed and the crystallisation interval was probably short (Sood & Edgar, 1970). The term hypoalkaline is used here strictly for rocks of trachytic and phonolitic compositions and not benmoreitic types (ie, larvikites). From the review of previous Gardar geochemical data it appears that the terms 'augite syenite' and 'larvikite' are commonly used synonymously to describe coarse grained rocks of both benmoreitic and trachytic (hypoalkaline) compositions. There are many syenites (*sensu stricto*) in the Gardar, from both the giant dykes and the ring complexes, which appear very similar to the GF-Geologfjeld syenite described here.

The alkaline rocks ($0.95 < PI < 1.1$) incorporate the alkali syenites and most nepheline syenites (khibinitic) of Motzfeldt. The rocks show a wide range of mineralogical and geochemical characteristics. They show moderate to strong zoning and an increased interval of crystallisation. Early cumulus minerals often have hypoalkaline affinities whereas the intercumulus mineralogy is often peralkaline. Typically the mafic minerals include (zoned) ferro-edenites - kataphorites and ferrosalites - aegirine hedenbergites. Coarsely unmixed mesoperthite enclosing cores of cryptoperthite (anorthoclase?) are usual. If present, nepheline, like the feldspar, behaves as an important cumulus phase. Zircon and other incompatible element accessory minerals become more common and apatite less so. Very few rock types in Motzfeldt have evolved beyond this stage.

The 'fresh' peralkaline rocks in Motzfeldt are restricted to minor intrusions. These include the laminated porphyritic syenite and peralkaline arfvedsonite microsyenite belonging to the Hypabyssal Series; certain members of the the MSF-Peralkaline Microsyenite Suite and the Lujavrites of SW Motzfeldt. In addition, the extensive, metasomatised,

outer areas of the Motzfeldt Sø Formation comprise rocks of peralkaline chemistry.[3] The 'fresh' undersaturated examples in Motzfeldt (ie, low sequences in the Peralkaline Microsyenite Suite, near Camp 9) exhibit remarkable rock textures which indicate a very high degree of fluidity. They are characteristically very rich in Na minerals such as arfvedsonite, aenigmatite and albite. Late stage aegirine is also common. Very high levels of incompatible elements are in evidence and contained in complex silicates such as eudialyte, rinkite/lavenite and many unidentified accessory minerals. Complex (incompatible element rich) oxides are most common in the altered peralkaline rocks where this condition has been overprinted through metasomatic effects.

10.3.2 Geochemistry

The mineralogical changes between these groupings are obviously also reflected by similar changes in their major element geochemical characteristics. The trace element and REE data given here, however, also indicate the relevance of these divisions. There is a gradual, systematic change through the groups with increasing peralkalinity. The elements Na, Zr, Nb, La, Ce, Th, U, Rb, and Pb, increase in concentration, whereas the residual elements Ba, Sr, P, Mg and Ca significantly decrease. This process is driven by crystal-liquid fractionation and possibly aided by volatile (gaseous) transfer, certainly in the later stages.

As an aid to the field investigations non-parametric statistical tests of the geochemical data were undertaken and evaluated as a method of discriminating between the units.

The nepheline syenites of Motzfeldt are all very similar in mineralogy and chemistry. They have undergone slow cooling and evolution *in situ*, and are therefore not homogeneous. Discrimination between these units, by geochemical means (at least from the major and trace element abundance and ratios) is probably less reliable than petrographic studies. The foyaitic rocks which have clearly been involved in large scale *in*

[3] coarse-grained agpaitic nepheline syenites are not developed in Motzfeldt)

situ mineral accumulation and fractionation show significantly lower absolute levels of Ba and Sr than those which have not. The MSF-Nepheline syenites have also been shown to have significantly higher Zr/La ratios than the adjacent FDF-Porphyritic nepheline syenite in SE Motzfeldt. The most important difference observed between the nepheline syenites is the considerably lower (c.$\frac{1}{2}$) absolute trace element abundances between the GF-Nepheline syenite and those which belong to the Motzfeldt Ring Series. This suggests a completely separate evolution for the Geologfjeld Formation and confirms its 'satellitic' origin.

The syenites (*sensu stricto*) of Motzfeldt show a much wider range of petrography and geochemistry than the nepheline syenites. Discrimination between the units is generally clear in both of these terms. The geochemical data confirm the suspicions of Bradshaw and Tukiainen, (1983) that the GF-Geologfjeld syenite and the GF-Pulaskite are in fact slightly different facies of the same rock unit or at least are generically related (probably from the same magma source). Similarly the Laminated porphyritic syenite and the Poikilitic arfvedsonite microsyenite are shown to be extremely similar geochemically and probably share a common magma source (of quite different composition to the Geologfjeld Formation magmas). In SE Motzfeldt, the Laminated porphyritic syenite has been confused with the petrographically similar MSF-Marginal arfvedsonite syenite. This is not totally resolved because of the limited geochemical data set for the latter, but the provisional results, however indicate significant differences between the units, particularly in the Ca/Ba and Ba/Zr ratios.

The REEs show that in general the hypoalkaline rocks display small positive Eu anomalies, the alkaline rocks small negative Eu anomalies and the peralkaline rocks strong negative Eu anomalies. At the same time, absolute abundances of the remaining REEs increase. They are all (REE enriched with high $(La/Lu)_n \sim 15$). The generally small Eu anomalies displayed by the nepheline syenites despite their highly evolved chemistry are best explained by the combination of relatively high fO_2, low polymerisation (low SiO_2 and high F, Cl) and limited anorthosite development during their magmatic evolution.

Incorporation of plagioclase megacrysts may also produce a similar, more localised effect (Jones, 1980).

The incompatible element spidergrams show that the progressive removal of feldspar, apatite, Fe-Ti oxides and mafic minerals have determined the geochemistry of the evolved rocks of the Motzfeldt Centre.

10.3.3 Economic mineralisation

This very complex topic continues to be investigated by the economic geologists of the Greenland Geological Survey. Airborne radiometric surveys and comprehensive field work have shown the oldest, outermost unit of the Motzfeldt Ring Series (the Motzfeldt Sø Formation) to host extensive Th, U, Nb, Ta, Zr and REE mineralisation. Pyrochlore is the most important economic phase. It is associated with zircon, and rare-metal silicates and carbonates. Reserves are put at an estimated 130 million tons of ore grade rock and the centre is potentially a very large source of tantalum. The mineralisation is not evenly distributed throughout the Formation, but occurs in a 2 to 4 km wide, side-wall and roof zone of brick-red hydrothermally altered syenite. Unlike any other major unit in the Centre, the altered syenite contains ubiquitous pegmatitic segregations ranging from miarolitic cavities to very extensive subhorizontal sheets; furthermore, large numbers of similarly mineralised microsyenite/pegmatite sheets extend from the altered zone for up to 5 km into the surrounding country rocks. Large quantities of the roofing quartzites and basalts (belonging to the EF-Majut and Mussartût Members) have been incorporated into the outer zone, where the basalts in particular are preserved as huge, spectacular raft xenoliths. The quartzites have, however been largely assimilated and have given the altered syenite its unusual (for the Centre) quartz normative character. The mineralisation is probably the result of the interaction of an incompatible element/volatile enriched magmatic residuum and the influx of silica and meteoric water, which resulted in a dramatic increase in fO_2, acidity and hydrothermal activity. A volatile-saturated outer shell developed which facilitated the migration, accumulation and precipitation of the incompatible elements. In contrast, the younger intrusions of the Flinks Dal Formation,

although geochemically similar to the fresh members of the Motzfeldt Sø Formation, are poor in pegmatite and commonly display chilled margins and cumulate layering. They intrude into higher levels of the country rock succession where intermediate rocks of the EF-Ilimaussaq Volcanic Member (Jones, 1980) dominate. Consequently they have not been significantly modified by their incorporation whilst also being shielded from large scale ground water circulation by the surrounding, largely impermeable Motzfeldt Sø Formation.

Fluid inclusion and stable isotope studies are necessary to narrow down the possible number of processes which may have helped to form these economic reserves.

10.4 Structure and Faulting

The Gardar Province has the following combination of features typical of intracontinental rifting:

1, A network of parallel and intersecting lineament sets

2, Fault bounded volcano-sedimentary red-bed succession

3, Dyke swarms and subvolcanic ring centres

4, Positive, axial gravity anomaly.

The rifting was prolonged (200 MY), repetitive and cyclic. The events were probably in response to intraplate, sinistral shear stresses controlled by the crustal interaction of the American and Grenvillian plates. The intraplate strain preferentially reactivated the younger (and weaker) Ketilidian mobile belt (bounded by the rigid Archean craton to the N) which was subjected to sinistral shear. The combination of crustal thinning, brittle fracturing and the subsequent rise in geothermal gradient facilitated the rise of magma. The location of dyke swarms and central complexes are controlled by the dominant lineament direction and the latter are particularly governed by the loci of intersecting lineaments. The 'space problem' is for the central complexes solved by high-level crustal decoupling, forming 'rhombochasms' analogous to the 'leaky transform' faults of the oceanic lithosphere. It is proposed here that the Gardar is the product of passive rifting

of relatively limited crustal extent which has been arrested before major lithospheric decoupling has taken place (cf. East African Rift Valley).

The predominantly sinistral crustal stresses which have affected the whole province are represented by the fault structures of Motzfeldt. The area is bisected along the sinistral strike-slip lineament known as the Flinks Dal Fault. This represents a sinistral throw of 6 km and has up to 700 m of downthrow to the N. Tensional dyke swarms and numerous dextral faults (of limited movement) are oriented ENE across the Centre and thus replicate on a small scale the overall Gardar pattern. The brittle faulting apparent in Motzfeldt is remarkably similar to that predicted by experimental studies in clay (Cloos, 1955; Badgley, 1965; Wilcox et. al., 1973). The lineaments seen can be shown to be in response to simple parallel sinistral shear (Stephenson, 1976a).

10.5 Geological summary and chronology

The evolutionary sequence of the Motzfeldt Centre proposed here is listed on Table 10.5.1 and schematically shown in Figs 10.5.2 and 10.5.3. In this simplified reconstruction, topographic effects on the plan view unit outlines have been ignored. Many questions obviously remain however, particularly in the complex and poorly understood SW regions.

The Motzfeldt Centre commenced with the emplacement of the Geologfjeld Formation. This first, satellitic igneous phase comprises three poorly centralised, overlapping intrusions of syenite (*sensu stricto*) pulaskite and nepheline syenite (Fig 10.5.2a)

The GF-Pulaskite (Fig 10.5.2a; **2**) and GF-Nepheline syenite (Fig 10.5.2a; **3**) are the NE-Motzfeldt Satellite syenites NM1 and NM2 of Emeleus and Harry (1970). From these, the previously undescribed GF-Geologfjeld syenite (Bradshaw & Tukiainen, 1983) has been geographically separated by the later intrusion of the 'centralised' main igneous phase known as the Motzfeldt Ring Series (Fig 10.5.2b).

Motzfeldt Chronology

Table 10.5.1

Proposed intrusive evolutionary sequence of the Motzfeldt Centre.

		Classification
9b	Larvikite ring-dyke	–
9a	FDF-Nepheline syenite	Alkaline
8b	FDF-Foyaite (central)	Alkaline
8a	FDF-Foyaite (transgressive)	Alkaline
7b	FDF?- Lujavrite Suite	Peralkaline
7a	FDF-Porphyritic nepheline syenite	Alkaline
6b	Poikilitic arfvedsonite microsyenite	Peralkaline
6a	Laminated porphyritic syenite	Alk/Peralk
5	Laminated alkali syenite	Alkaline
4b	MSF-Peralkaline microsyenite Suite	Peralkaline
4a	Motzfeldt Sø Formation	Alk/Peralk
3	GF-Nepheline syenite	Alkaline
2	GF-Pulaskite	Hypoalkaline
1	GF-Geologfjeld syenite	Hypoalkaline

Shared numbers ie, a & b indicate close genetic links and semi-contemporaneous intrusion.

Nos 5 and 6 could possibly be younger than the Flinks Dal Formation.

The GF-Geologfjeld syenite (Fig 10.5.2a; 1) and GF-Pulaskite are very similar both chemically and petrographically. They are either, separate intrusions from the same magma source or different facies of the same intrusive episode (Bradshaw & Tukiainen, 1983). The GF-Nepheline syenite intrudes and 'cores' out the GF-Pulaskite to which it is probably related through protracted, feldspar-dominated fractionation. In the Geologfjeld Formation therefore, the evolutionary trend is for increasing undersaturation and peralkalinity with time.

The main igneous phase, the Motzfeldt Ring Series (SM1 to SM5 of Emeleus & Harry, 1970), which followed the Geologfjeld Formation, is further divided into two distinct episodes of the magmatic activity known as the Motzfeldt Sø (Fig 10.5.2b; **4a** & **4b**) and Flinks Dal Formations (Fig 10.5.3a). Together these comprise at least four separate overlapping intrusions which roughly follow a common focus, younging inwards in the typical nested-pluton form. The Motzfeldt Sø Formation is divided into three roughly concentric petrographically distinct members, namely; MSF-Marginal arfvedsonite syenite; MSF-Altered syenite; and the innermost MSF-Nepheline syenite. The Formation is some 18 km in diameter and is the largest and outermost intrusion of the Motzfeldt Ring Series. The outer members of the unit host extensive Nb-Ta-Zr-U-Th-LREE mineralisation with pyrochlore the most important economic phase. Although the Formation is divided, the members appear to belong to a single major intrusion and are the products of both *in situ* magmatic differentiation and country rock interaction. The Formation was rich in volatiles and hosts many pegmatite segregations and sheets many of which extend into the country rock (SE Motzfeldt) and the older, adjacent GF-Geologfjeld syenite (NE Motzfeldt). These sheets are known collectively as the Peralkaline Microsyenite Suite (Fig 10.5.2b; **4b**).

It is still unclear whether the Motzfeldt Sø Formation was either primarily extremely enriched in incompatible elements (see section 8.2) ; or has hidden incompatible element depleted zones at depth; or has derived the 'extra' concentrations from the assimilation of the country rock? Whatever the cause, the syenites of the Motzfeldt Sø Formation

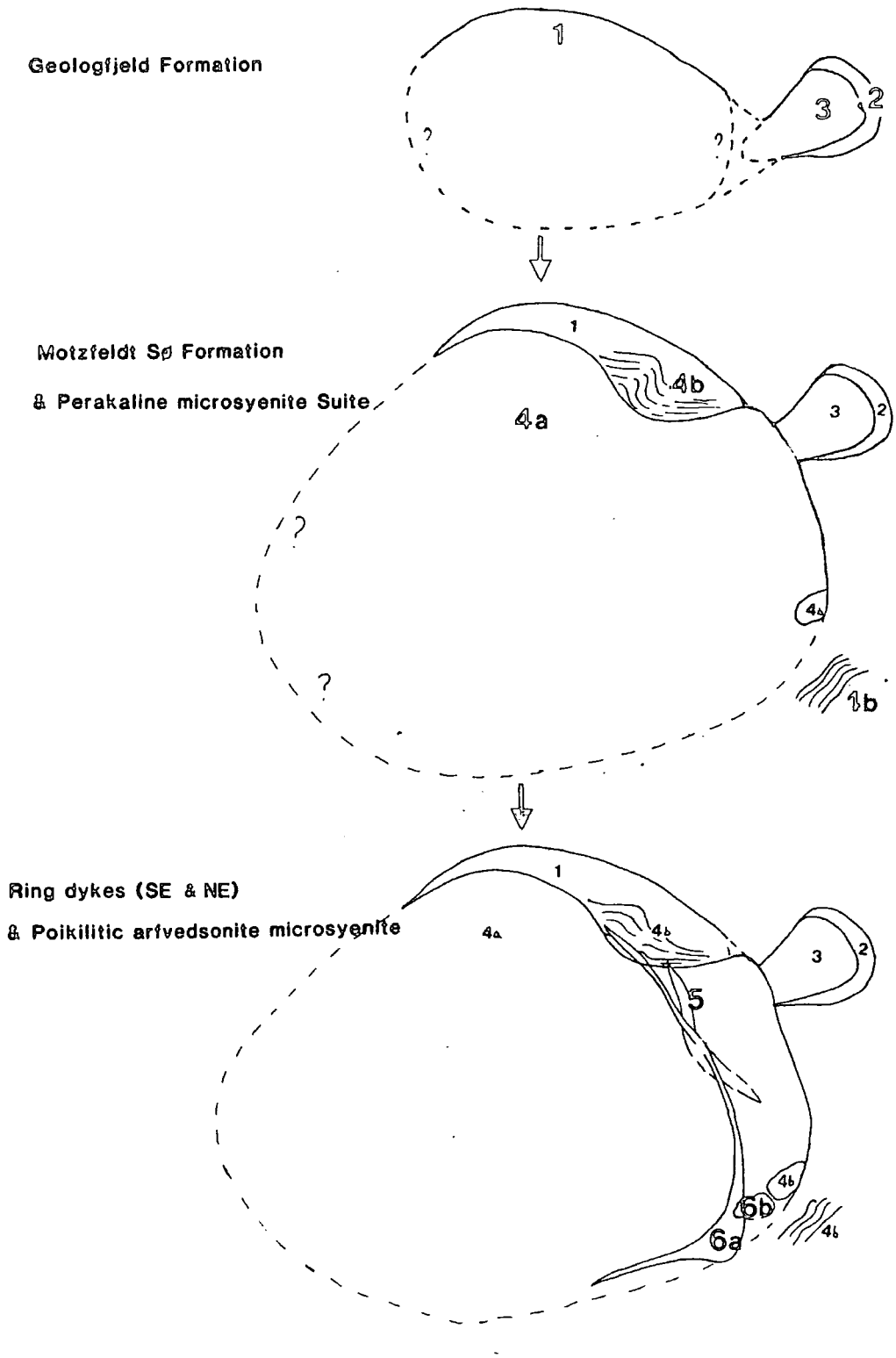
provide a resource of economic potential in rare elements, particularly Nb & Ta, and have clearly been largely modified in geochemistry and composition by the interaction with country rock.

The Flinks Dal Formation occupies the central core of the Ring Series with an outer diameter of approximately 9 km. The three members; FDF-Porphyritic nepheline syenite, (Fig 10.5.3a; 7a) FDF-Foyaite (Central type and Transgressive type) (Fig 10.5.3a; 8a & 8b); and FDF-Nepheline syenite (Fig 10.5.3a; 9a) are all predominantly phonolitic in composition and contain mineralogical and chemical features typical of khibinitic (intermediate) or alkaline nepheline syenites (see Table 3.3.3). They clearly differ from the members of the Motzfeldt Sø Formation however, being fresh, having often, well developed cumulate structures, chilled margins and poorly developed pegmatite segragations and little or no mineralisation.

It is feasible that the FDF-Porphyritic nepheline syenite represents the 'chilled' outershell or crust of a single major intrusion within which the cumulate pile of FDF-Foyaite (central type) developed. The FDF-Foyaite (transgressive type) could be a discordant extension from this magma which pierced the crust and intruded into the older MSF-Nepheline syenite. The last major intrusive unit of the Flinks Dal Formation (and Motzfeldt) the FDF-Nepheline syenite is slightly less evolved and commonly contains relict Ca-rich (relatively) feldspar (xeno?)crystals. In addition, probably the last actual intrusive unit of the Motzfeldt Centre, the larvikite (SM5*) is considered to be closely related to this intrusion (Jones, 1980). It would appear therefore that while the members of the Flinks Dal Formation are all essentially phonolitic in composition, the last intrusive units display a link between less evolved and possibly parental lithologies during the waning stages of the Motzfeldt igneous episode.

The complex roof-zone of SW Motzfeldt contains peralkaline lujavrites (Jones, 1980) and microsyenites which are thought to be projections from the Flinks Dal Formation. Therefore the two major sheet intrusive sequences; The Peralkaline microsyenite suite (NE & SE Motzfeldt); and the Lujavrite Suite (SW Motzfeldt) are contemporaneous

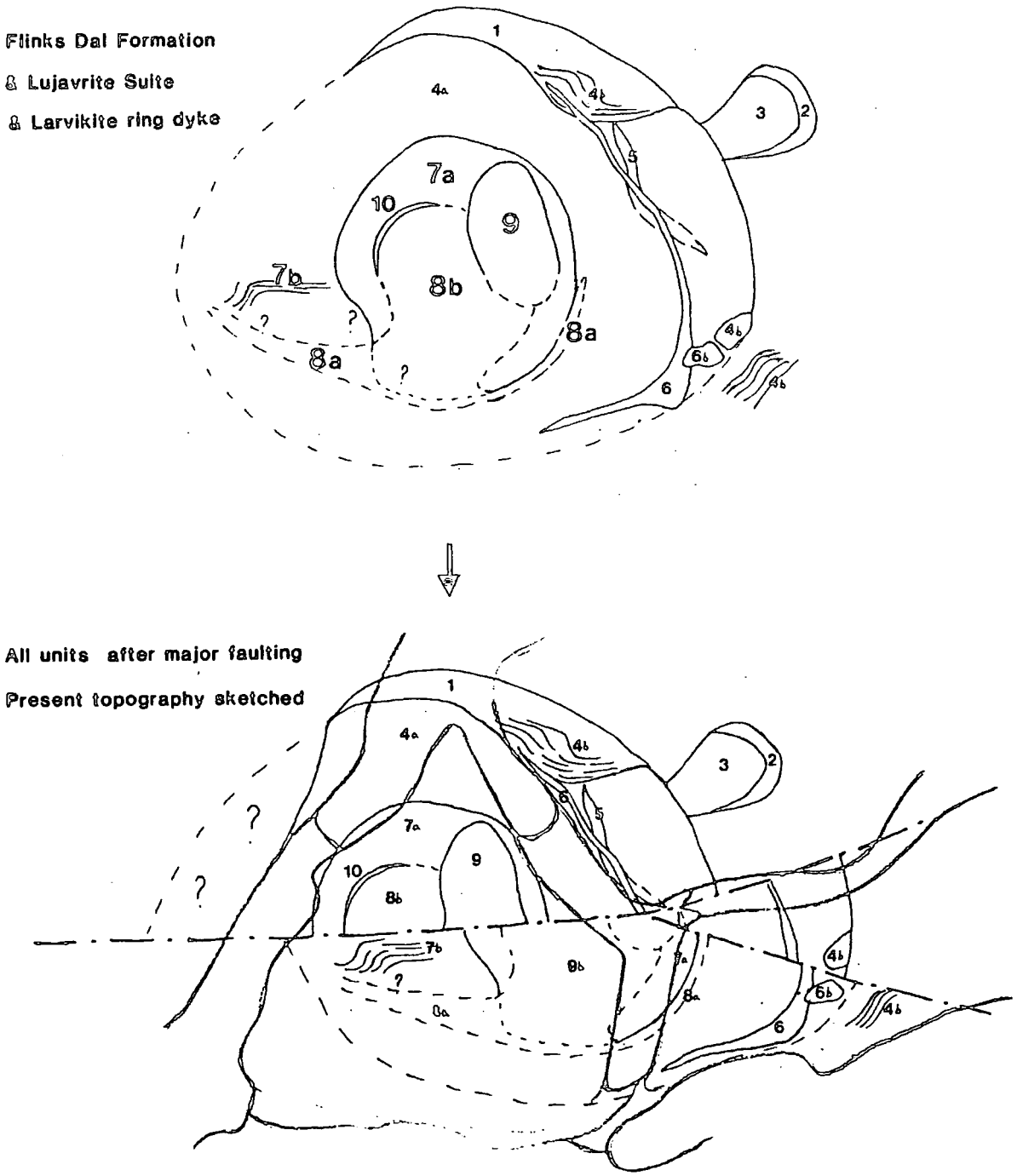
Motzfeldt intrusive sequence Fig 10.5.2



Sketched - plan views of the intrusive sequence of Motzfeldt.

Scale: approximately 2cm - 6km.

Topographic effects are removed to give the general unit outlines.



Sketched – plan views of the intrusive sequence of Motzfeldt. continued.

Scale: approximately 2cm – 6km.

with the intrusions of the Motzfeldt Sø and Flinks Dal Formations respectively. Three important minor intrusions representing the Hypabyssal Series (this work), cut the Centre and include; the Laminated alkali syenite (Fig 10.5.2c 5); the Laminated porphyritic syenite (Fig 10.5.2c; 6a) and the Poikilitic arfvedsonite microsyenite (Fig 10.5.2c; 6b) The first is restricted to NE Motzfeldt the second to NE & SE Motzfeldt and the third to SE Motzfeldt. They were intruded in that order and are all at least younger than the Geologfjeld and Motzfeldt Sø Formations. They are geographically separate from the units of the Flinks Dal Formation and therefore the age relationship between the two groups is unknown. However, because the Hypabyssal units tend toward oversaturation, peralkalinity and occasionally show evidence of country rock interaction they are considered here to precede the undersaturated magmas of the Flinks Dal Formation.

APPENDIX ONE

PUBLISHED WORK

APPENDIX ONE - PUBLISHED WORK AND OTHER PROJECTS.

1.1 Publications.

1.1.1 Armour-Brown, A., Tukiainen, T., Wallin, B., Bradshaw, C., & Emeleus, C.H., 1983. Uranium exploration in South Greenland. Rapp. Grønlands. Geol. Unders. 115, 68-75.

Uranium exploration in South Greenland

Ashlyn Armour-Brown, Tapani Tukiainen, Bjarne Wallin, Colin Bradshaw and C. Henry Emeleus

Following the promising reconnaissance results in 1979 and the finding of uranium and niobium mineralisation in 1980 (Armour-Brown *et al.*, 1981), the Syduran project was extended under the Ministry of Energy's Research Programmes of 1981 and 1982 which has allowed one further field season for following up some of the more promising anomalies and uranium mineral occurrences.

The main objectives of this season's work was firstly to initiate the detailed mapping of the U-Nb mineralised zones and the geology of the Motzfeldt Centre and secondly to locate the source of as many geochemical and gamma-spectrometer anomalies as possible which occur in the Granite Zone and Migmatite Complex of South Greenland (fig. 21), at the same time as evaluating the appropriate exploration techniques in the different environments.

Motzfeldt Centre

The geological mapping of the Motzfeldt Centre is being carried out in collaboration with Colin Bradshaw who is preparing a Ph.D. thesis on the petrology of the centre under the

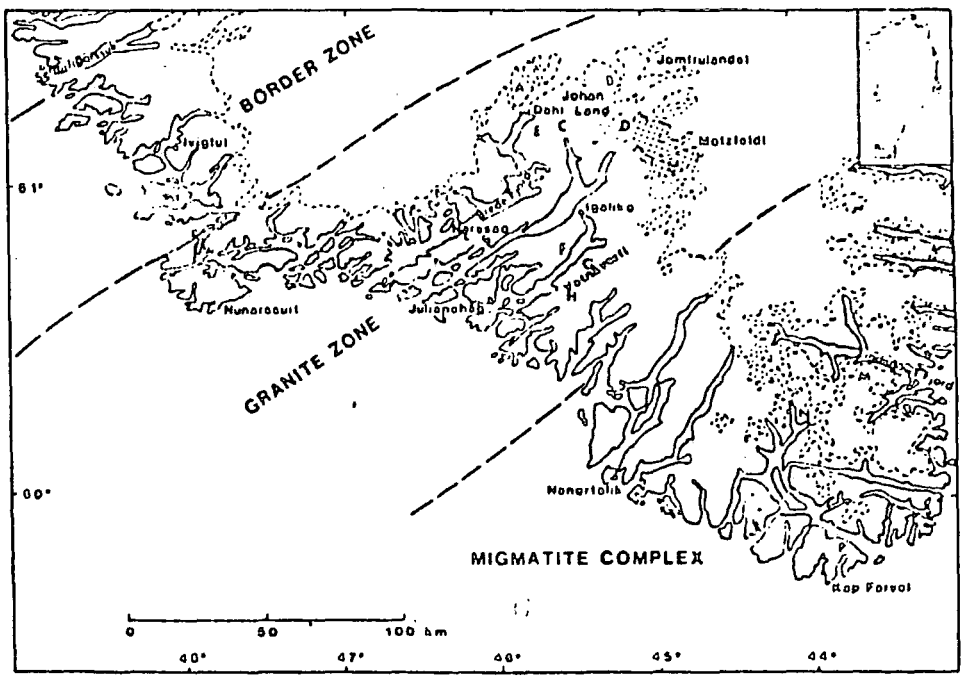


Fig. 21. Map of South Greenland showing the desribed locations.

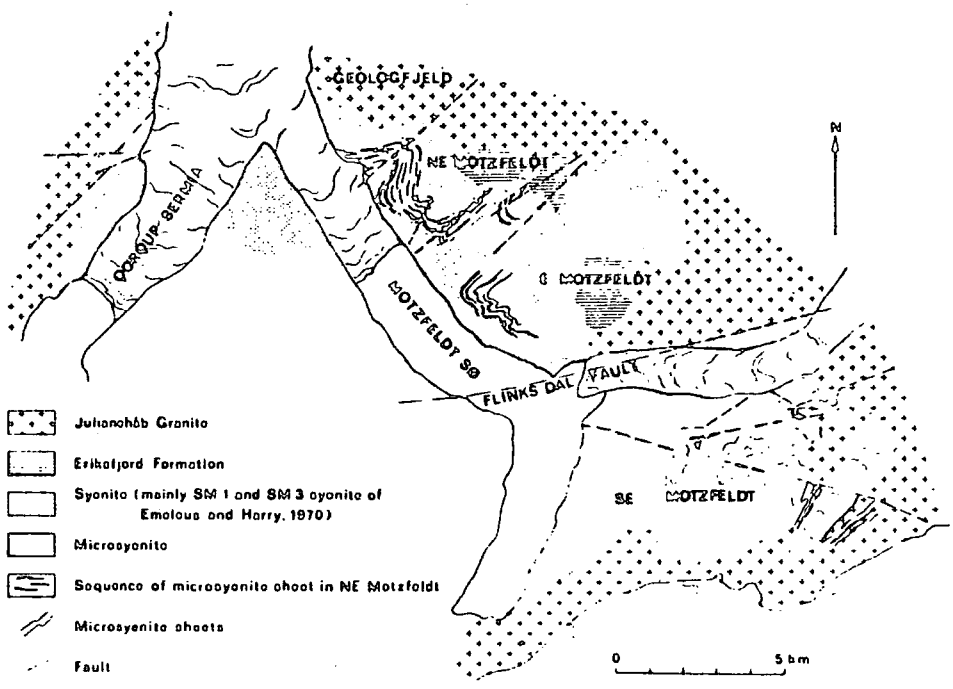


Fig. 22. Geological sketch map and locations in the Motzfeldt Centre.

supervision of Henry Emeleus at the University of Durham. The U-Nb mineralisation was mapped by Tapani Tukiainen using the helicopter-borne gamma-spectrometer equipment developed at Risø National Laboratory supplemented by ground sampling and observations. New, excellent 1:50000 aerial photographs and 1:10000 contoured orthophoto maps provided a good basis for collating this data.

The Motzfeldt Centre is one of four alkaline igneous centres belonging to the Igaliko nepheline syenite complex (Emeleus & Harry, 1970). The intrusions within the centre show a range of compositions from syenogabbro to lujavrite (Jones, 1981) and host considerable radioactive occurrences (Tukiainen, 1981).

Most of the previously established syenite units and their age relationships have been confirmed and the original syenite terminology of Emeleus & Harry (1970) and Jones (1981) is retained. Some important observations are outlined below.

South-east Motzfeldt. In south-east Motzfeldt (fig. 22) the syenite SM 3 occurs not in one solid arcuate band (Emeleus & Harry, 1970, plate IV), but as a number of narrow, individual, near vertical intrusions with a range of widths of approximately 4 to 20 m which cuts the syenite units SM 1 and SM 2. This belt of the SM 3 syenite follows approximately the SM 1-SM 2 contact. The individual members of this unit are petrographically very similar and probably emerge from a common source at some shallow depth. Most of the exposed ground in the eastern part of south-east Motzfeldt is composed of a suite of peralkaline microsyenite sheets sandwiched between medium grained syenite which resembles SM 1. These sheets,

which are up to at least 200 m thick, also extend far into the basement granite where they thin out. Evidence of roof collapse was obtained near the eastern margin of the centre where large rafts (from 5 to 20 m thick) of Gardar supracrustal rock composed of agglomerate, tuff and sandstone are seen enclosed by the microsyenite. The microsyenite probably welled up and filled the cavity left by the foundered crust. The presence of rafts confirms the previous existence of Gardar supracrustal rocks over this part of the centre.

East and north-east Motzfeldt. The broad belt of SM 3 syenite in east and north-east Motzfeldt (Emeleus & Harry, 1970, Plate IV) is composed of a complex suite of syenites. Although characterised by a well developed feldspar lamination the rocks vary in grain size and texture. The SM 1 syenite, similarly, is remarkably variable in texture and composition containing some mappable units in east Motzfeldt. The SM 3 and SM 1 syenite units are truncated by a suite of peralkaline microsyenite sheets which are most abundant in north-east Motzfeldt ranging from 1 to 10 m in thickness. Within the unit as a whole the frequency of the sheets increases upwards until they make up over 80% of the bulk and comprise a thickness of greater than 400 m. In east Motzfeldt they are subhorizontal but in north-east Motzfeldt they strike approximately E–W and dip 25 to 45° north. The roof zone of the intrusion is exposed in north-east Motzfeldt where the Julianehåb Granite overlies a homogeneous leucocratic syenite (SM 1?). The planar syenite-granite contact dips approximately 30° to the north.

Faulting and its effect on the distribution of lithology. The Motzfeldt Centre is dissected by two sets of vertical or steeply dipping faults, one striking NE–SW and another one approximately E–W. The most dramatic dislocations, both vertically and laterally, took place along the E–W striking sinistral faults. The lateral displacement along the Flinks Dal fault is estimated to be 6 km. The magnitude of the vertical movements is not known but on the basis of the lithological characteristics, lack of roof rocks and steep external contacts, east Motzfeldt is probably an upthrown block.

Airborne gamma-spectrometric survey and radioactive mineralisation. The helicopter-borne gamma-spectrometer survey comprised some 900 km of contour flying with an average speed of 30 knots and a terrain clearance of 30 m. The radiometrically and geologically complex eastern and northern part of the centre were flown with 100 m contour intervals whereas the rest of the centre, including the adjacent basement, were flown with 200 m contour intervals.

The radiometric survey outlined several extensive zones of highly radioactive alkaline rocks with maximum values of 150 ppm eU and 400 ppm eTh. These radioactive anomalous zones are underlain by the microsyenite-suite and the texturally and mineralogically heterogeneous medium-grained syenite, most of which is tentatively classified as belonging to the SM 1 syenite unit. The reddish brown colour due to hematite is a diagnostic feature of all the radioactive rocks.

A preliminary evaluation of the airborne radiometric results indicates that the enrichment of the radioactive elements increases upwards because the radioactivity is highest in south-east and north-east Motzfeldt. This suggests that the radioactive elements migrated upwards and were trapped by the roof zone of the intrusion. This is well demonstrated by the follow-up on a minor anomalous zone with a maximum of 65 ppm eU and 60 ppm eTh south

of Geologfjeld in north-east Motzfeldt. The anomaly here is caused by uranium enrichment at the very top of the microsyenite sequence. The gamma-spectrometer assays of the samples from this 10 to 15 m wide, 2 km long zone, range from 250 to 1200 ppm eU and 70 to 400 ppm Th.

The size of these areas of high radioactivity indicates that the possibility of finding zones of uranium enrichment with economic potential is good. In addition, niobium, tantalum and rare earth elements are known to be associated with this uranium in quantities sufficient to warrant further exploration (Tukiainen, 1981).

Molybdenite was also found associated with microsyenite veins, in a loose block of lamprophyre (*c.* 100 × 150 × 80 cm in size) in south-east Motzfeldt. Whether this molybdenum enrichment has any economic interest remains to be investigated.

Uranium occurrences in the Migmatite Complex

Uranium occurrences in the Kap Farvel – Lindenows Fjord region. The most interesting find of the summer was at locality N (figs 21, 23) in the Kap Farvel – Lindenows Fjord region where there are some particularly high gamma-spectrometer anomalies in the reconnaissance work from 1979. A sizeable uranium mineral occurrence of over 125 m in length and width from 1 to 5 m was discovered in meta-arkose rafts and xenoliths in rapakivi granite. The radioactivity does not extend beyond the xenoliths and there does not seem to

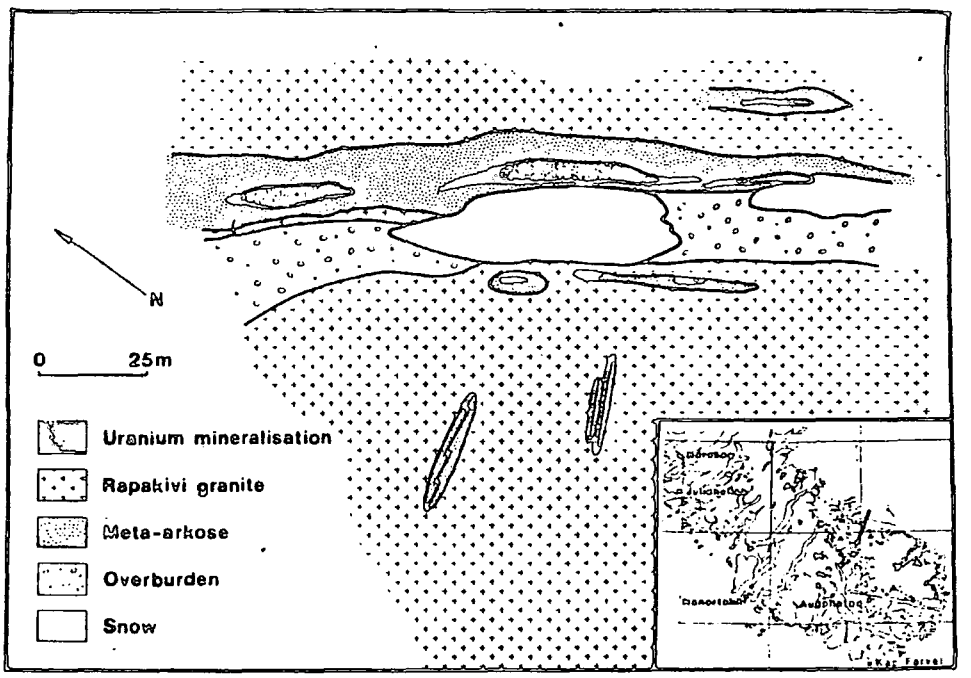


Fig. 23. Sketch map illustrating the geology and extent of the radioactivity of the uranium occurrence (loc. N, fig. 21) in the Migmatite Complex.

be any relation between the uranium and the surrounding granite (fig. 23). Grab samples vary from 2.8% to 1.0% U and, judging from the radioactivity, mineable thicknesses of over 1 m may grade from 0.3% to 1.0%. The thorium content of these mineral occurrences is very low and is comparable with that of the uraniferous neosome discovered in the Tasermiut area (Nielsen & Tukiainen, 1981), and similar conclusions can be drawn that the uranium is syn-sedimentary on the premise that U-Th partitioning only takes place below the temperature of 300°C.

The implications of this finding are that the supracrustal units throughout the Migmatite Complex, especially where there are radiometric or geochemical anomalies, are favourable for uranium mineralisation and should be prospected in detail. The area is large and the chances of finding other equally promising showings, are good. Very high radioactivity readings have already been recorded from a cliff face at locality M (fig. 21) but it was impossible to land with a helicopter to take samples.

This uranium was discovered using helicopter-borne scintillometric equipment. The good exposure in the mountainous terrain and the fact that the supracrustal units tend to overly the granite and therefore occur at high altitudes, favour this method of exploration.

Uranium occurrences in the Granite Zone

Prospecting for veins and other uranium mineral occurrences was concentrated in areas not already followed up in 1980, in particular the nunataks north of Bredefjord, Johan Dahl Land, and the Vatnaverfi peninsula by ground scintillometry, stream-water and stream-sediment sampling. In addition detailed prospecting at Puissataq on the Igaliko peninsula (figs. 21, 24, loc. F) revealed three small pitchblende veins. Detailed mapping was carried out there to evaluate these showings and to determine the usefulness of electromagnetic geophysical methods for locating buried uraniferous structures (Nyegaard & Thorning, this report).

Uranium occurrences in the nunataks north of Bredefjord and in Johan Dahl Land. There were a number of extremely interesting high uranium values from the gamma-spectrometer results, as well as the geochemical data over the nunataks north of Bredefjord and in Johan Dahl Land. At one of these anomalies (figs. 21, 24, loc. A) numerous uraniferous gneiss boulders and blocks associated with meta-rhyolite and meta-arenite were found. The grade of samples of these uraniferous boulders, some of which contained visible pitchblende and secondary uranium minerals, range from 1–10% U. Unfortunately early snow made it impossible to map their exact source but, since they were widely distributed below a steep cliff face of the same rock types, they presumably are derived from there. In Johan Dahl Land (figs. 21, 24, loc. B) uraniferous meta-arenite was found associated with meta-rhyolite. The uranium is relatively low grade (100 ppm) but was in a disseminated mineral in the host rock associated with iron oxide, and not in a vein. Both these showings, like those in the Migmatite Complex, lack associated thorium which would be expected if they were derived from granitic or metamorphic processes.

There seems every reason, therefore, to believe that these uranium occurrences are of syn-sedimentary origin, and that they were already present in the overlying supracrustal units before their metamorphism and intrusion by the granite. These findings are the first indications that uranium occurred in the rocks of the Granite Zone prior to the Gardar and

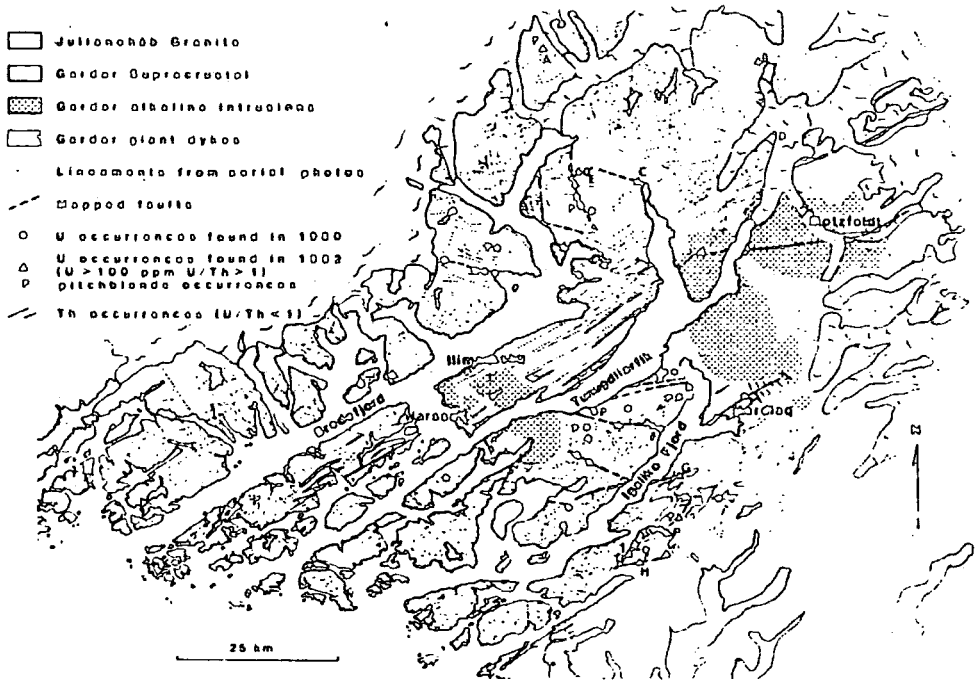


Fig. 24. Uranium occurrences in the Granite Zone.

gives support to the hypothesis that uranium may have been redistributed by the hydrothermal activity related to Gardar magmatic events and deposited in the veins.

Uranium occurrences on the Vatnaverfi peninsula. Considerable efforts were spent on exploring the Vatnaverfi peninsula this season (fig. 21). This was based firstly on the hypothesis that the high mobility of uranium would favour its deposition further from the heat sources (i.e. the Gardar alkaline intrusions) for the hydrothermal activity, secondly because of the high geochemical anomalies in both the stream waters and the stream sediments and the structural conditioning which is similar to the rest of the Granite Zone. However, exploration is hampered in this area by the lack of outcrop due to vegetation covered overburden which is particularly thick along the lineaments which would be expected to host mineral occurrences.

The results of prospecting with scintillometers show that there are numerous radioactive mineral occurrences in this area most of which are uranium dominated and associated with the faults and fractures. Some 45 localities were found which had over 100 ppm U in anomalous radioactive rock samples. Some of these have been shown on the accompanying map (fig. 24). The three most interesting showings (fig. 24, loc. G, H, I) contain minor amounts of pitchblende. Radioactivity along the ENE-trending structure (G) can be traced for almost 3 km with values up to 800 ppm U at some localities and must be considered a very good prospect. The radioactive showings (H) trend in an E–W direction and tend to be

associated with small fractures rather than in the main lineament. The radioactive showings (I) also occur in the minor fractures along the main lineament rather than the lineament itself. Another interesting feature of the radioactive showings along this structure is that the U/Th ratios are very erratic and some samples are dominated completely by Th. This suggests that the assumption that the mineralising fluids were relatively cool in this area may be a little simple. These mineral showings are dominated by siliceous and hematitic material along with quartz and carbonate veining with minor amounts of fluorite and disseminated sulphides similar to those found elsewhere in the Granite Zone.

Conclusions

The main conclusions that can be drawn from these results are that South Greenland is definitely a part of a uranium geochemical province and that the potential for locating economically mineable uranium deposits is very high.

The increase in both the number and size of the anomalies in the Motzfeldt Centre confirms the already stated mineral potential there. The detailed geological mapping and gamma-spectrometer survey will also prove to be very interesting from the purely geological point of view.

The syn-sedimentary uranium occurrences found in the Migmatite Complex demonstrates that all the supracrustal units in the area could be prospected for uranium particularly those zones containing anomalies from the reconnaissance data. The size and grade of the first occurrence to have been found certainly indicate that this area deserves to be on a higher priority than it has been given so far. They are possibly more important than the uranium veins found in the Granite Zone.

Uranium showings in the Granite Zone continue to be found although the surface expression of the veins still tends to be limited in size. The finding of probable syn-sedimentary uranium showings in the pre-Julianehab Granite supracrustal units not only suggests new targets for mineral exploration in the zone, but also supports the hypothesis that there was uranium in the area prior to Gardar magmatic activity. At least some, if not all, of the uranium which is found in the veins, therefore, may have been derived from this source and simply been redistributed by the hydrothermal activity related to the Gardar events.

The exploration methods to be used should depend on the environment and target.

The exposure in the Motzfeldt Centre is for the most part so good that mapping, sampling and ground gamma-spectrometric surveys are still the most effective means of evaluation. These could probably be usefully supplemented by geophysical (VLF and magnetometer) surveys in order to elucidate the structure and locate possible sulphide occurrences prior to any drilling.

In the Migmatite Complex where the outcrop is good, relief is extreme, access is poor and the showings are in the supracrustals which tend to outcrop at high altitudes. Detailed gamma-spectrometer flying with a helicopter would be the most effective way of locating the occurrences. The same method could be used in the well exposed nunataks and at high altitudes in the Granite Zone where the syn-sedimentary showings appear to be preferentially located.

The uranium veins in the faults and fractures, which cannot be detected by gamma-spectrometer from the air because they are usually covered by overburden, should be explored in the first place by a structural analysis using all available imagery. This should be followed up

by a detailed water sampling programme to locate the uraniferous structures prior to ground geophysical methods and prospecting with ground scintillometers.

References

Armour-Brown, A., Tukiainen, T. & Wallin, B. 1981: Uranium districts in South Greenland. *Rapp. Grønlands geol. Unders.* **105**, 51–55.

Emeleus, C. H. & Harry, W. T. 1970: The Igaliko nepheline syenite complex. General description. *Bull. Grønlands geol. Unders.* **85** (also *Meddr Grønland* **186**,3) 116 pp.

Jones, A. P. 1980: The petrology and structure of the Motzfeldt Centre, South Greenland. Unpubl. PhD. thesis, University of Durham.

Nielsen, B. L. & Tukiainen, T. 1981: Uranium-bearing metasediment and granite in the Tasermiut area, South Greenland. *Rapp. Grønlands geol. Unders.* **105**, 47–51.

Tukiainen, T. 1981: Preliminary results of the geological and radiometric reconnaissance in the Motzfeldt Centre of the Igaliko Complex. Unpubl. intern. GGU rep., 27 pp.

Geophysical and geological field work on fault structures at the Igaliko peninsula, South Greenland

Per Nyegaard and Leif Thorning

Uranium exploration carried out in South Greenland by the Syduran project in the last few years (Armour-Brown *et al.*, 1981) has indicated that certain major E–W fault structures are features worthy of attention in this connection. During August 1982 geological and geophysical field work was carried out 10 km south-south-east of Igaliko (fig. 25) around a fault zone which had earlier given indications of the presence of uranium mineral occurrences.

The object of the geological work was to map the surface within the geophysical grid and to make a gamma-radiation survey of the area. Pitchblende veins, found in connection with geochemical prospecting, were traced by trenching and were sampled.

The object of the geophysical work was firstly to evaluate the usefulness of various electromagnetic methods for locating and mapping the structures in the Julianehåb granite which contain uranium minerals and secondly to evaluate the extent of the known uranium mineral occurrences. Logistic support was supplied by the Syduran project base camp at Dyrnes.

Geology

The area investigated is underlain by the Ketilidian Julianehåb granite (1810–1770 m.y.; Van Breemen *et al.*, 1974). During the Gardar period (1330–1150 m.y.; Emeleus & Upton,

1.1.2 Bradshaw, C., & Tukiainen, T., 1983. Geological and radiometric mapping of the Motzfeldt Centre of the Igaliko Complex, South Greenland. Unpubl. intern. GGU rep., 35 pp.

(Front cover only)

GEOLOGICAL AND RADIOMETRIC MAPPING OF THE MOTZFELDT CENTRE OF THE IGALIKO COMPLEX, SOUTH GREENLAND

Colin Bradshaw [1] and Tapani Tukiainen

(with additional comments by Henry Emeleus [1])

PROGRESS REPORT.

GRØNLANDS GEOLOGISKE UNDERSØGELSE
Copenhagen October 1983

[1] University of Durham
Department of Geological Sciences
United Kingdom

1.1.3 Tukiainen, T., Bradshaw, C., Carle, C., & Olesen, L.B., 1984. New extensive Th-Zr-Nb-REE mineralisation in the Motzfeldt Centre, S. Greenland, as outlined by an airborne gamma-spectrometric survey. 16th Nordiska Geologiska Vintermotet, Stockholm.

New extensive Th-U-Zr-Nb-REE mineralisation in the Motzfeldt Centre of the Igaliko Complex, South Greenland, as outlined by an airborne gamma-spectrometric survey

Tapani Tukiainen, Colin Bradshaw, Christen Carle and Bjarne Lund Olesen

A B S T R A C T

The Motzfeldt Centre (1310 +/- 31 m.y.) is one of the major alkaline intrusive complexes in the Gardar province of alkaline igneous activity. The Motzfeldt Centre is made up of at least 6 intrusions of syenite with a wide range of textural and compositional characteristics grouped as two main igneous phases. The syenites were emplaced in the Proterozoic Julianehåb Granite and the unconformably overlying Gardar supracrustal rocks.

Nepheline and sodalite syenites of the early igneous phase occur as isolated bodies which are highly truncated by the syenite units of the main igneous phase - the Motzfeldt Ring Series. The Ring Series constitutes at least three steep sided, outward dipping ring dyke intrusions of syenite and nepheline syenite younging inwards. The outermost syenite unit contains a suite of peralkaline microsyenite sheets, which are most abundant at the highest levels of the Ring Series. The apparent intrusion mechanism was a combination of ring fracture and block subsidence.

The systematic helicopterborne gamma-spectrometric survey outlined an extensive Th-U-Zr-Nb-REE mineralisation in the outermost syenite unit of the Motzfeldt Ring Series where both the mineralisation and associated hydrothermal alteration increase in intensity towards the apical part of the syenite unit being strongest where the roof zone of the Motzfeldt Ring Series is preserved. The mineralisation is essentially due to the formation of zircon minerals and pyrochlore. The present evidence suggests that the mineralisation and the alteration was effected by an upwards migrating volatile fluid phase rich in alkalis, fluorine and incompatible elements.

The data from the airborne gamma-spectrometric survey are interpolated to a regular grid and presented in a 3-dimensional digital terrain model in order to enhance and differentiate the radiometric response from the syenite units.

Tapani Tukiainen
Geological Survey of Greenland
Copenhagen, Denmark

Colin Bradshaw
University of Durham
Department of Geological Sciences
Durham, United Kingdom

Christen Carle
Regional Computer Centre for
Research and Education of the
University of Copenhagen (RECKU)
Copenhagen, Denmark

Bjarne Lund Olesen
Technical University of Denmark
Copenhagen, Denmark

1.1.4 Tukiainen, T., Bradshaw, C., & Emeleus, C.H. 1983. Geological and radiometric mapping of the Motzfeldt Centre of the Igaliko Complex, South Greenland. Rapp. Grønlands geol. Unders., 120, 78-83.

References

Appel, P. W. U. 1974: On an unmetamorphosed iron-formation in the early Precambrian of South-West Greenland. *Miner. Deposita* 9, 75–82.

Appel, P. W. U. & Secher, K. 1984: On a gold mineralization in the Precambrian Tartoq Group, South-West Greenland. *J. geol. Soc. Lond.* 141, 273–278.

Berthelsen, A. & Henriksen, N. 1975: Geological map of Greenland 1:100 000 Ivigtut 61 V. 1 Syd. Copenhagen: *Grønlands geol. Unders.* (also *Meddr Grønland* 186, 1) 169 pp.

Fripp, R. E. P. 1976: Stratabound gold deposits in Archean banded iron-formation, Rhodesia. *Econ. Geol.* 71, 58–75.

Higgins, A. K. 1968: The Tartoq Group on Nuna qaqertoq and in the Iterdlak area, South-West Greenland. *Rapp. Grønlands geol. Unders.* 17, 17 pp.

Higgins, A. K. 1970: The stratigraphy and structure of the Ketilidian rocks of Midternæs, South-West Greenland. Bull. *Grønlands geol. Unders.* 87 (also *Meddr Grønland* 189, 2) 96 pp.

Higgins, A. K. & Bondesen, E. 1966: Supracrustals of pre-Ketilidian age (the Tartoq Group) and their relationships with Ketilidian supracrustals in the Ivigtut region, South-West Greenland. *Rapp. Grønlands geol. Unders.* 8, 21 pp.

Kanasevich, E. R. & Slawson, W. F. 1964: Precision intercomparisons of lead isotope ratios: Ivigtut, Greenland. *Geochim. cosmochim. Acta* 28, 541–549.

Larsen, O. 1971: Preliminary report on K/Ar dating in the southeastern part of the Ivigtut region. *Rapp. Grønlands geol. Unders.* 35, 49–52.

Michaelsen, H. 1955: Rapport over det geologiske feltarbejde i Sermiligârssuk i sommeren 1955. Unpubl. intern. GGU rep., 14 pp.

Ulrych, T. J. 1964: The anomalous nature of Ivigtut lead. *Geochim. cosmochim. Acta* 28, 1389–1396.

Weidmann, M. 1964: Géologie de la région située entre Tigssaluk fjord et Sermiligârssuk fjord (partie médiane), SW-Groenland. Bull. *Grønlands geol. Unders.* 40 (also *Meddr Grønland* 169, 1), 146 pp.

Windley, B. F., Henriksen, N., Higgins, A. K., Bondesen, E. & Jensen, S. B. 1966: Some border relations between supracrustal and infracrustal rocks in South-West Greenland. *Rapp. Grønlands geol. Unders.* 9, 43 pp.

Geological and radiometric mapping of the Motzfeldt Centre of the Igaliko Complex, South Greenland

Tapani Tukiainen, Colin Bradshaw and C. Henry Emeleus

The geological and radiometric mapping of the Motzfeldt Centre was commenced in 1982 as part of the extended Syduran project under the Ministry of Energy's Research Programmes of 1981 and 1982 (Armour-Brown *et al.*, 1983). The purpose of the study was to make a detailed geological and radiometric map of the centre with a view to provide a reliable reference framework for the evaluation of the economic mineral potential of the centre where an extensive Th–U–Zr–Nb–REE mineralisation was discovered by the reconnaissance surveys of the Syduran project, which was partly financed by the European

Economic Communities during the period 1st Dec. 1979 – 1st Dec. 1980 under article 70 (Armour-Brown *et al.*, 1982, 1983). Apart from a short visit by Agnete Steenfelt, who carried out a detailed rock-sampling programme of a section in the north-east part of the centre, no field work was done during the 1983 season. The geological mapping of the centre is planned to be finished during the 1984 season. The airborne gamma-spectrometric and field mapping data of the 1982 season have been processed and compiled, so we are able to summarise the most important results.

Geology

The Motzfeldt area with steep-sided glacially dissected valleys provides a virtually three-dimensional, *c.* 1500 m high vertical exposure across a major multiphase, high-level alkaline intrusion where an extensive hydrothermal alteration and mineralisation took place in the roof zone as a result of the upward migration of a highly mobile volatile phase, rich in incompatible elements.

The revised geology of the Motzfeldt Centre is shown in fig.34 which also gives a new rock-unit nomenclature. The new nomenclature was developed because of its flexibility in allowing previously undescribed syenite units, found during Syduran mapping and in the future mapping studies, to be included without confusing changes in the 'SM' notation of Emeleus & Harry (1970). The new nomenclature has been established on the basis of the present mapping. The extension of the syenite formations to the southern and western parts of the centre are still tentative as they are based on the available fragmentary field evidence and results of the gamma-spectrometric survey.

The Motzfeldt Centre developed through two major phases of igneous activity. The syenite units of the early igneous phase, the Geologfjeld Formation, originally comprised a number of separate syenite stocks which are now truncated by the syenite units of the main igneous phase, the Motzfeldt Ring Series. The wide extent of the Geologfjeld Formation Syenite in the north-east part of the centre indicates that at least some of these early syenite bodies may have been considerable.

The Motzfeldt Ring Series is made up of concentric steep-sided intrusions whose marginal contacts dip outwards. The syenite intrusions young inwards. The obvious intrusion mechanism, as already proposed by Emeleus & Harry (1970), was the successive emplacement of syenite guided by a combination of ring fractures and block subsidence.

The main igneous phase commenced with the emplacement of the Motzfeldt Sø Formation which now occupies the outer zone of the Motzfeldt Ring Series. This formation is divided into three concentric units, namely: the outermost marginal arfvedsonite syenite, heterogeneous altered nepheline syenite and the innermost fresh nepheline syenite. The Motzfeldt Sø Formation hosts extensive radioactive mineralisation and the metasomatic alteration described below. The boundary of the alteration is in places conspicuously sharp, but no evidence of the syenite units as separate intrusions was found. It appears more probable, therefore, that the Motzfeldt Sø Formation is a single major intrusion whose margins were extensively modified by late magmatic processes resulting in the altered nepheline syenite unit.

The Flinks Dal Formation is made up of at least three separate intrusions, emplaced in the following order: porphyritic nepheline microsyenite, foyaite and a coarse-grained nepheline syenite. The foyaite occurs as a number of narrow, near vertical sheet-like intrusions with a

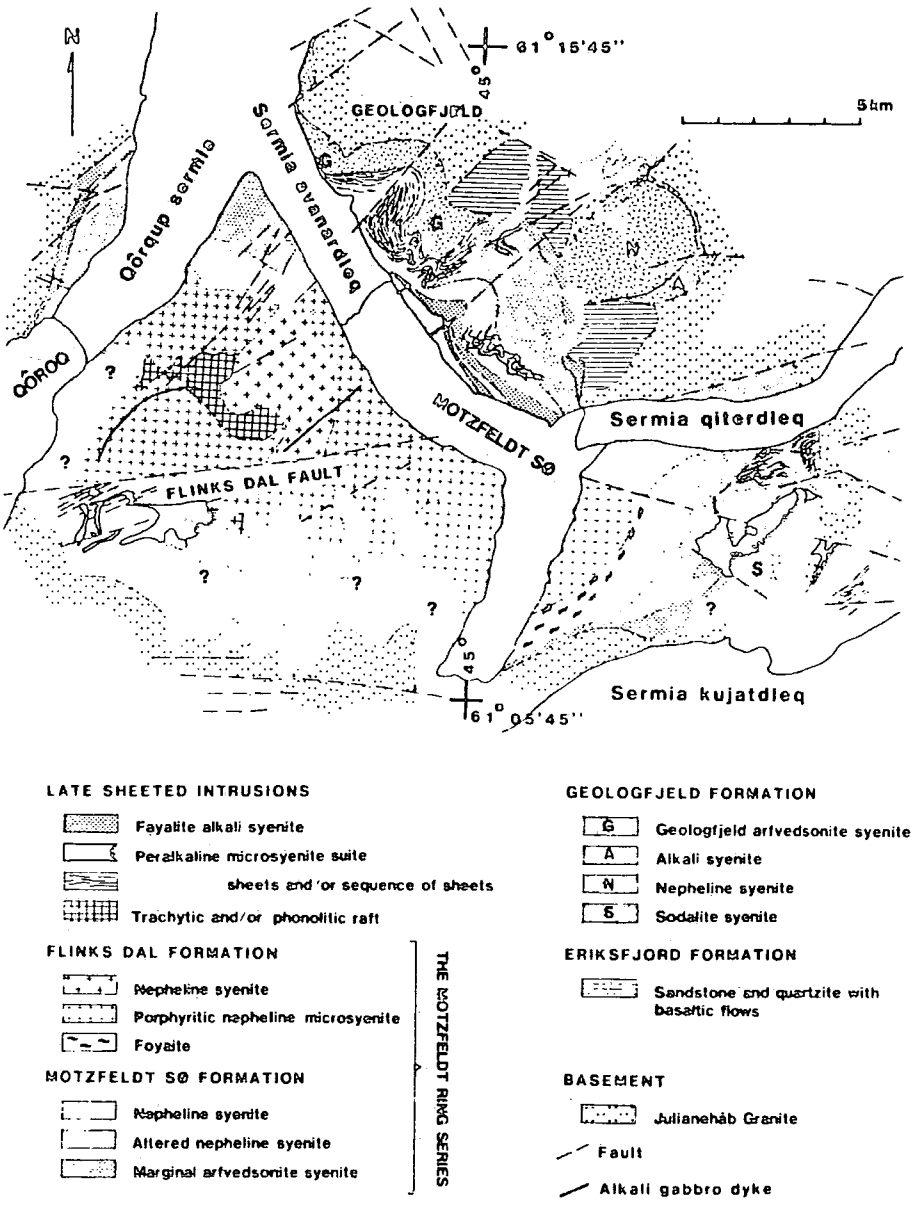


Fig. 34. Revised geology of the Motzfeldt Centre.

range of widths from about 1 to 20 m, cutting both the Motzfeldt Sø Formation nepheline syenite and the Flinks Dal Formation porphyritic nepheline microsyenite. The relative age of the coarse-grained nepheline syenite and foyaite remains uncertain because of the lack of definite field evidence.

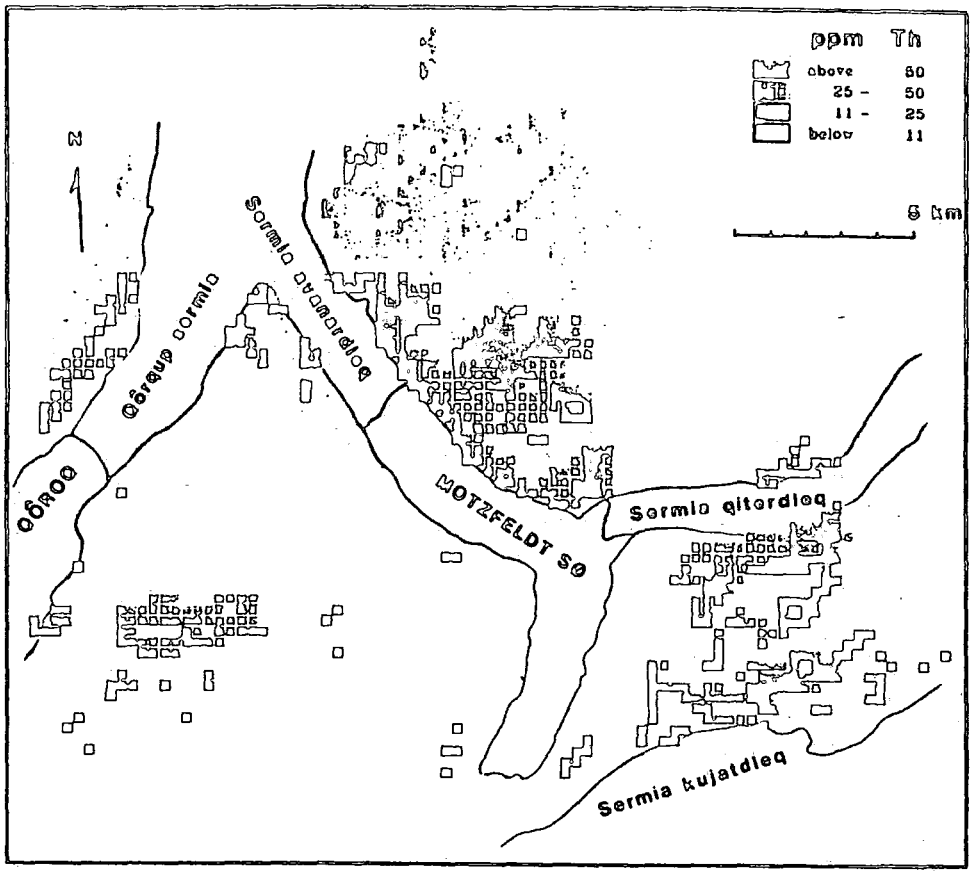


Fig. 35. Thorium airborne radiometric map of the Motzfeldt Centre. The grid size is 300×300 m, the average of the measurements in each grid is shown.

The syenite units of the late sheeted intrusions are both mineralogically and texturally highly variable, and their relations with each other and the syenite formations of the Motzfeldt Ring Series are not understood. They are, however, definitely younger than the Motzfeldt Sø Formation. There is some field evidence to suggest that at least the peralkaline microsyenite suite could be genetically related to the Motzfeldt Sø Formation because (a) the peralkaline microsyenite sheets were not found to intrude the Flinks Dal Formation, (b) the microsyenite sheets are almost exclusively found within the Motzfeldt Sø Formation increasing in width and number upwards in this formation, and (c) both the Motzfeldt Sø Formation and peralkaline microsyenite are enriched in the incompatible elements.

The syenite units of the centre were affected by two major sets of vertical or nearly vertical faults, one striking NE–SW (older), and another E–W (younger). The most dramatic dislocations in the centre took place along the E–W striking faults. The most spectacular of these faults, the Flinks Dal Fault, traverses the whole Motzfeldt Centre with a horizontal sinistral component of about 6 km. The E–W striking faults also have a distinct

148

vertical component; the biggest observed vertical displacement along one of these faults is 180 m.

Distribution of uranium and thorium

The airborne gamma-spectrometric survey has outlined the extent of the radioactive mineralisation, showing that it is intimately associated with the rock units of the Motzfeldt Sø Formation and the late sheeted intrusions within it (fig. 35). The overall picture of K, eU and Th distribution on the airborne radiometric maps of the centre is essentially similar.

The Motzfeldt Sø Formation together with the peralkaline microsyenite suite has the highest content of eU and Th in the Motzfeldt Centre (fig. 35). It contains numerous zones of very high eU and Th. The areas with 9 ppm eU and 15 ppm Th coincide well with the mapped outlines of the Motzfeldt Sø Formation.

The ground underlain by the Flinks Dal and Geologfjeld Formations has a relatively low level of eU and Th without prominent anomalies. Distinct aerial variations do occur but whether these reflect lithological variations is not known.

The Eriksfjord Formation is characterised by a low and relatively uniform content of eU and Th. Even in the areas where this formation caps the radioactive Motzfeldt Sø Formation it appears to have remained virtually unaffected by the radioactive mineralisation.

The patterns of distribution of the radioactive element in the basement granite have no obvious correlation with the distribution of the various rock types as indicated on the 1:100 000 scale geological map (Allaart, 1970). There are two areas, one south-west of the centre and another at Geologfjeld, which have a strikingly high background content of radioactive elements.

Th–U–Zr–Nb–REE mineralisation

The metasomatic alteration and mineralisation are spatially related and increase in intensity towards the uppermost parts of the Motzfeldt Sø Formation, being most intense where the roof zone of the intrusion is preserved. The alteration is essentially due to the breakdown of mafic minerals and the formation of iron oxides and micas and to albitisation. The altered rocks are also notably enriched in fluorine as manifested by the abundance of fluorite. The bulk of the radioactive elements are contained in two groups of minerals, namely zirconium-bearing minerals and pyrochlore.

The predominance of thorium over uranium in the Motzfeldt Sø Formation is due to the high content of the zirconium minerals with a high thorium content. The study of thin sections and preliminary microprobe assays suggest that the zirconium minerals in the altered rocks belong to the zircon group, ranging from a typical fresh zircon to probably hydrous metamict phases rich in thorium. The fresh rocks of the peralkaline microsyenite suite are also rich in zirconium due to the abundance of eudialyte.

Pyrochlore is a common accessory in the altered rocks, but locally it is found in considerable amounts occuring as disseminated grains and small veinlets. It is characteristic of the pyrochlore in the Motzfeldt Centre that it has a high content of uranium and LREE (Table 3). The analyses of pyrochlore-bearing rocks, especially those from the altered nepheline syenite, indicate an interestingly high tantalum content of up to 0.6% Ta (analysed by the neutron activation method).

Table 3. Microprobe analysis (90 points analysed) of pyrochlore grains from the altered microsyenite south of Geologfjeld

Element	Mean %	Max %	Min %	Std. dev.
Na_2O	1.56	7.08	0.00	2.13
SiO_2	2.58	9.41	0.13	2.77
CaO	4.71	9.54	0.11	2.37
TiO_2	3.97	5.37	1.49	0.87
ZrO_2	0.66	8.48	0.00	0.93
Nb_2O_5	48.43	63.00	32.01	5.92
Ta_2O_5	1.79	3.69	0.00	0.52
Ce_2O_3	6.17	8.56	1.88	1.60
La_2O_3	3.96	6.13	0.62	1.21
Y_2O_3	0.22	0.32	0.00	0.20
ThO_2	0.24	1.02	0.00	0.19
UO_2	6.46	8.91	2.95	0.97

Conclusions

The Motzfeldt Centre appears to be a classic example of a large multiphase alkaline intrusion where an extensive hydrothermal alteration and associated mineralisation, due to the upward migration of a highly mobile alkaline volatile phase rich in incompatible elements, occurred in the roof zone of the intrusion.

The extent and intensity of the enrichment of Th, U, Zr, Nb and REE makes the Motzfeldt Centre an interesting counterpart to the celebrated Ilímaussaq Intrusion in the Gardar province of South Greenland. The excellent exposure makes the centre a rewarding target for both economic, geological, and other scientific studies.

References

Allaart, J. H. 1970: Geological map of Greenland 1:100 000, Narssarssuaq, 61 V.3 Syd. Copenhagen: Geol. Surv. Greenland.

Armour-Brown, A., Tukiainen, T. & Wallin, B. 1982: The South Greenland Uranium Exploration Programme. Final Report. Unpubl. intern GGU rep., 92 pp.

Armour-Brown, A., Tukiainen, T., Wallin, B., Bradshaw, C. & Emeleus, C. H. 1983: Uranium exploration in South Greenland. *Rapp. Grønlands geol. Unders.* 115, 68–75.

Emeleus, C. H. & Harry, W. T. 1970: The Igaliko nepheline syenite complex. General description. *Bull. Grønlands geol. Unders.* 85 (also *Meddr Grønland* 186,3) 116 pp.

C.B. & C.H.E.,
Department of Geological Sciences,
Sciences Laboratories,
University of Durham,
U.K.

1.1.5 Bradshaw, C., 1985. The alkaline rocks of the Motzfeldt Centre; progress report on the 1984 field season. Rapp. Grønlands geol. Unders., 125, 62-64.

The alkaline rocks of the Motzfeldt Centre; progress report on the 1984 field season

Colin Bradshaw

The detailed mapping programme in the Motzfeldt Centre that commenced in 1982 with the Syduran project (Armour-Brown *et al.*, 1983) continued in collaboration with the GGU Pyrochlore project in 1984 (Tukiainen, this report). The results obtained during the 1982 field season enabled the various syenite units of the centre to be grouped (from older to younger) into Geologfjeld (GF), Motzfeldt Sø (MSF) and Flinks Dal (FDF) Formations (Tukiainen *et al.*, 1984). The purpose of the work in 1984 was to study the structure and spatial distribution of the rock formations in the lesser known western and southern parts of the Motzfeldt Centre. The revised map is shown in Tukiainen (this report) and some of the more important observations are outlined below.

The boundary between the Geologfjeld and Motzfeldt Sø Formations

Tukiainen *et al.* (1984) proposed that the Geologfjeld syenite is truncated downwards by the syenites of the Motzfeldt Sø Formation. In north-east Motzfeldt the boundary relations remain problematical. No clear cross-cutting relations were found, but the Geologfjeld Formation grades rapidly downwards from a white, coarse, homogeneous nepheline-free syenite into pink-brown feldspar-laminated syenite with conspicuous nepheline.

In north-west Motzfeldt the Geologfjeld syenite is of restricted occurrence. A narrow wedge (<400 m wide) is roofed by Julianehåb granite to the north and is clearly truncated by syenites of the Motzfeldt Sø Formation to the south. The MSF/GF contact is well exposed in places and is found to be sharp with several pegmatitic apophyses extending into the Geologfjeld syenite. Though the older syenite is stained over a 10 m zone, the characteristic white colour of the Geologfjeld syenite is rapidly encountered away from the contact. This suggests that the rock was consolidated and therefore essentially impervious to the volatile phase that altered and mineralised the syenite of the Motzfeldt Sø Formation (Tukiainen *et al.* 1984).

Motzfeldt Sø Formation

The revised distribution of syenites of this formation in western and south-western Motzfeldt Centre (fig. 19) accords well with that indicated by radiometric data (Tukiainen *et al.*, 1984). Of particular note is the position of the MSF/FDF boundary on the north side of the Flinks Dal fault, east-central Motzfeldt, located for the first time this summer. This confirms the *c.* 6 km sinistral offset along the Flinks Dal Fault (Tukiainen, this report).

A new find was a large screen (more than 300 m wide) of MSF nepheline syenite contained within the Flinks Dal Formation syenite which is chilled against the Motzfeldt Sø Formation syenite. The screen is located in the high ground 3 km NNE from the south-east corner of Motzfeldt Sø.

Most of the ground in south-central Motzfeldt Centre, adjacent to and south of the Flinks Dal fault, is provisionally ascribed to the Motzfeldt Sø Formation, because the field evidence

demonstrates that it is made up of a variety of syenites which are older than the Flinks Dal Formation. It is possible that the syenites here represent the inner facies of the Motzfeldt Sø Formation, or that they contain partially assimilated material from the Geologfjeld Formation. The classification of the syenite types remains to be solved by geochemical studies.

Flinks Dal Formation

Recent evidence suggests that the foyaite of south-east Motzfeldt Centre is considerably more extensive than previously determined (Tukiainen *et al.*, 1984). The unit comprises a wide (100–700 m) arcuate sheet, concave toward the centre of the intrusion and restricted to the area south of the Flinks Dal fault (Tukiainen, this report, fig. 19). The foyaite tapers and appears to terminate in south-east Motzfeldt. The relationship between this foyaite and the foyaitic rock types found in the inner part of the Flinks Dal Formation porphyritic nepheline syenite requires further study.

The late sheeted intrusions

Particular interest was attached to a partial ring dyke of laminated porphyritic syenite (Tukiainen, this report, fig. 19) discovered in south-east Motzfeldt this season. This unit had previously been found only in north-east Motzfeldt and had been tentatively classified as a nepheline-free variety of the Flinks Dal Formation foyaite of south-east Motzfeldt. The absence of nepheline and the abundance of mafic phases were explained by the deeper exposure levels in north-east Motzfeldt. This summer the nepheline-free unit was discovered at high elevations in south-east Motzfeldt. This and the field relations as now known clearly indicate that the unit is unrelated to the Flinks Dal Formation foyaite.

Conclusions

The 1984 field season was of particular value in furthering understanding of the complex geology of the Motzfeldt Centre. Definite correlations have been established between the syenites of the southern part of the centre and those of the north-east and south-east which were mapped earlier. The revised, more symmetrical geology of the centre (cf. Tukiainen, this report, fig. 19, and Bradshaw & Tukiainen, 1984, fig. 34) correlated well with radiometric mapping of the area, proving the value of this technique in alkaline igneous terrains. Detailed mapping of the syenite boundaries has confirmed the approximately 6 km sinistral horisontal movement across the Flinks Dal fault.

It had been hoped to complete the survey of the centre during this season but bad weather hindered progress. Overall coverage was consequently restricted and further field studies are needed.

Acknowledgements. The author thanks NERC, United Kingdom, for financial support and also the members of the GGU Pyrochlore project, 1984, for their kind co-operation and invaluable field assistance.

References

Armour-Brown, A., Tukiainen, T., Wallin, B., Bradshaw, C. & Emeleus, C. H. 1983: Uranium exploration in South Greenland. *Rapp. Grønlands geol. Unders.* **115**, 68–75.

Tukiainen, T., Bradshaw, C. & Emeleus, C. H. 1984: Geological and radiometric mapping of the Motzfeldt Centre of the Igaliko Complex, South Greenland. *Rapp. Grønlands geol. Unders.* **120**, 78–83.

Department of Geological Sciences,
University of Durham,
Science Laboratories,
South Road,
Durham,
U.K.

1.2 Additional Projects

1.2.1 Project to be undertaken at the Faculty of Art and Design, Sunderland Polytechnic

April, 1985

Student - Paul Nicholson,
Model Making Department 2nd year.

Client - Colin Bradshaw,
Department of Geological Sciences,
Science Laboratories,
University of Durham. Tel. 64971 ext. 382.

The Project

The project aim is to construct a full colour three dimensional model on a 1:50,000 scale, showing the geological structure and topography of the Motzfeldt Centre, S. Greenland.

Introduction

The Motzfeldt Centre is a plutonic alkaline igneous ring complex which covers an area of approximately 260 sq. km. The area is bleak and mountainous and deeply dissected by major glaciers. The rock types that comprise the Centre are generally coarse grained, light coloured syenites and nepheline syenites. They have a 'granitic' appearance but are deficient in quartz. The Centre is approximatley 1300 million years old and represents the deep magma chambers (now consolidated) that underlay an area of active volcanism and rifting.

Brief

The results of this work will be displayed in the University of Durham, Geology Department, and also loaned for display to the Greenland Geological Survey (Copenhagen). In addition the model will be shown at geological conferences, meetings and in particular at the EEC scientific meeting in West Germany this autumn. With this coverage we hope the model will help promote further scientific interest in the area.

Method

- The student's task is to construct a 3D topographic and geologic

-The student has complete control on material and methodology of model construction.

- Collaboration with the client will be essential with regard to geological interpretation and final topographic detail.

Supplied Material

- The student will be supplied with the following.

  a) 1:50,000 Scale Geological map with 100 m contours.

  b) 1:50,000 Scale paired steroscopic aerial photographs.

  c) 35mm photographs on more local scale.

Conclusion

The completed work will be of great scientific value to the University of Durham. The construction should also prove to be a valuable exercise for the student as it is an artistically challenging project which encompasses both individual creativity and solid scientific judgement.

1.2.2 Project to be undertaken at the Faculty of Art and Design,

Sunderland Polytechnic

April 1985

Student - Joan Nichols,
Art and Design Department 2nd year

Client - Colin Bradshaw
Department of Geological Sciences,
Science Laboratories,
University of Durham. Tel. 64971 ext. 382.

The Project

The aim of the client is to produce an illustrative guide to the geology and field relations of an alkaline igneous ring centre in S. Greenland; The Motzfeldt Centre.

The students project will encompass all the illustration work to be subsequently used in the guide.

Introduction

The Motzfeldt Centre is a plutonic alkaline igneous ring complex which covers an area of approximately 260 sq. km. The area is bleak, mountainous and deeply dissected by major glaciers. The rock types that comprise the Centre are generally coarse grained, light coloured syenites and nepheline syenites. They have a 'granitic' appearance but are deficient in quartz. The Centre is approximately 1300 million years old and represents the deep magma chambers (now consolidated) that underlay an area of active volcanism and rifting.

Brief

Currently active research is being undertaken in the Motzfeldt Centre, with particular regard to its Geological structure (Colin Bradshaw) and mineralisation (Greenland Geological Survey).

The recent exciting discoveries in the area are such that continued active research is likely. The completed maps and guide will be used to advertise the importance and potential of the Motzfeldt Centre at geological meetings and EEC financial conferences.

Student Work Plan

Section A

Front Cover

- Student is to design a bold and eye catching - though scientifically meaningful - front cover which contains the following text:

The Motzfeldt Centre, S. Greenland

An illustrated geology guide.

by,

Colin Bradshaw and Joan Nichols

- To be on front cover (the underlined in bold type)

Section B

Diagram 1 - View ENE of the cliffs of SE Motzfeldt showing with the use of careful stipple the various Geological features.

- 35mm slide provided.

Diagram 2 - View North of the cliffs overlooking Camp 'Osterport'in NE. Note as 2. - photo provided.

Diagram 3 - View SE of Camp 6 and surrounding mountains. As 2. - photo provided.

Diagram 4 - View west showing east facing cliffs of "Harry's Dal." - 35 mm slide provided.

Diagram 5 - Panoramic view of NE Motzfeldt as Diagram 2 - photo provided.

Section C

From 8 rock thin-sections the student is to draw the microscopic view (plain light) of a $1.5m^2$ area on a 10:1 scale. At least 4 thin-section drawings should be undertaken (more if time permits).

The drawings should be in black ink and show the various mineral types and their textural relations.

Section D

- Colour geological map.

From the rough 1:50,000 geological map of the Motzfeldt Centre (provided) the student is to produce a colour map of quality for public display. The use of colour and symbols are left to the students judgement but must follow scientific guidelines.

Conclusion

With the text (client) and illustrations (student) it is hoped that subsequently a brochure style guide will be constructed. This project requires much collaboration between student and client to achieve the best results.

The topic will involve much interplay between creativity, graphic skills and a selling 'marketing' style. Because these disciplines are controlled by the scientific constraints the student should find the project challenging and rewarding.

The finished guide will be of much value to the University of Durham, Geology Department and to the Greenland Geological Survey (of Denmark).

Signed

APPENDIX TWO

FIELD INFORMATION

2.1 The members of the SYDURAN expedition 1982.

		To Narssaq:	To Copenhagen:
- Jørgen Lau	Base manager	June 16th.	*
- Tapani Tukiainen	geologist	June 22nd.	*
- Allan Pratt	assistant	do.	*
- Kim Hansen	assistant	do.	*
- A.Armour-Brown	expedition leader	June 25th.	*
- Bjarne Lund Olesen	analyst	do.	*
- Henry Emeleus	geologist	June 29th.	August 27th.
- Colin Bradshaw	geologist	do.	*
- Bjarne Wallin	geologist	do.	*
- Per Nyegaard	geologist	do.	*
- Poul E.Holm	geologist	do.	*
- Jari Øhberg	assistant	do.	*
- Arent Heilmann	assistant	do.	*
- Eva Nørringgaard	lab technician	do.	*
- Jann Larsen	cook	do.	*
- Ole Vejbæk	assistant	do.	*
- Erik M.Christiansen	gamma-spec expert	July 5th.	July 19th.
- Stig Thinghus	technician	do.	do.
- Ove Plesner	handyman	Resident of Narssaq.	
- Lief Thorning	geophyscist	c. July 30th.	*
- Egon Hansen	technician	do.	*
- Ingrid Salinas	assistant	do.	*

* Departure from Greenland approx mid Sept.

2.2 The members and associates of the PYROCHLORE expedition 1984.

Institution	Name	Function
GGU	Jørgen Lau	base leader/radio operator
GGU/geophysics	Leif Thorning	geophysicist, leader of geophysics and the helicopter programme
	Egon Hansen	technician
	Maja Boserup	geophysicist
	Jette Halskov	field assistant
GGU/Geochemistry	Lotte Melchior Larsen	geologist
	Gitte Schwartz	field assistant
GGU/Sydex[1] uranium exploration	Ashlyn Armour-Brown	geochemist, leader of Sydex
	Per Nyegaard	geologist
	Jens P. Nielsen	field assistant
	Ole Christiansen	field assistant
	Hans Chr. Olsen	field assistant
GGU/pyrochlore project	Tapani Tukiainen	geologist, leader of pyrochlore project
	Torsten F. Bliksted	geologist
	Tobias Winther	field assistant
	Michael Hjort	field assistant
RISØ/Sydex[1]	Bjarne Wallin	geologist
	Poul T. Sørensen	technician
Munchen/ pyrochlore project	Giulio Morteani	geologist, project leader
	Berndt Kronimus	geologist
	Peter Moller	chemist
	Dietrich Ackermand	geologist
University of Durham	Henry C. Emeleus	Leader of Durham group
	Colin Bradshaw	geologist
	Nicholas Pearce	geologist

1 - Not involved in Motzfeldt 1984

2.3 Field Statistics

2.3.1 Field work accomplished.

Table
a. SYDURAN 1982 81 days in Greenland < 20 nights at Base Camp (Dyrnes) 60 nights in Motzfeldt (10 camp sites) 31 days (total[1]), lost due to bad weather and camp movements 28 days (total[2]), field work completed in Motzfeldt +2 days helicopter reco., based from Dyrnes Average 2.8 days (total[1]) field work per camp site.
b. PYROCHLORE 1984 64 days in Greenland < 9 nights in Narssarssuaq 54 nights in Motzfeldt (9 camp sites) 26.5 days (total[1]), lost due to bad weather and camp movements 27.5 days (total[3]), field work completed in Motzfeldt Average 3 days (total[1]) field work per camp site.

1 - includes all 1/2 or part days
2 - includes 23 x full days and 10 x 1/2 days
3 - includes 23 x full days and 9 x 1/2 days.

2.3.2 Camp site information (see also Fig. 5.b)

SYDURAN 1982

Date	Camp	Region	Altitude	Grid Reference	Base map	Samples	Photographs
1 July - 3 July	C.1	SE	665m	W 44° 51′ 30″ N 61° 08′ 45″	B17sø	-	-
6 July - 22 July	C.2	SE	1175m	W 44° 54′ 50″ N 61° 08′ 37″	B17sv	304001-304038	CB.82.C.01.01 CB.82.C.03.30
22 July - 27 July	C.3	E	1150m	W 45° 51′ 00″ N 61° 11′ 20″	B17nø	304039-304047	CB.82.C.03.31 CB.82.C.04.04
27 July - 3 Aug	C.4	NE	1192m	W 44° 54′ 50″ N 61° 12′ 50″	B17nv	304048-304058	CB.82.C.04.05 CB.82.C.06.18
3 Aug - 7 Aug	C.5	SE	1520m	W 44° 51′ 40″ N 61° 08′ 20″	B17sø	304059-304075	CB.82.C.06.24 CB.82.C.07.14
7 Aug - 13 Aug	C.6	NE	200m	W 45° 01′ 30″ N 61° 11′ 45″	B16nø	304076-304100	CB.82.C.07.15 CB.82.C.08.31
13 Aug - 18 Aug	C.7	C	1140m	W 45° 06′ 50″ N 61° 11′ 36″	B16nø	304101-304121 (inc.heli.reco)	CB.82.C.08.32 CB.82.C.10.05
21 Aug - 25 Aug	C.8	NE	1058m	W 44° 57′ 20″ N 61° 12′ 37″	B17nv	304122-304145	CB.82.C.10.09 CB.82.C.10.15
25 Aug - 31 Aug	C.9	NE	175m	W 45° 03′ 40″ N 61° 13′ 20″	B16nø	304146-304196	CB.82.C.10.16 CB.82.C.11.17
31 Aug - 10 Sept	C.10	NE	190m	W 44° 57′ 02″ N 61° 10′ 25″	B17sv	304197-304200 304708-304779 (inc.heli.reco)	CB.82.C.11.18 CB.82.C.13.36

2.3.2 Camp site information continued.,

PYROCHLORE 1984

Date	Camp	Region	Altitude	Grid Reference	Base map	Samples	Photographs
28 June - 4 July	C.9	NE	175m	W 44° 57′ 02″ N 61° 10′ 25″	B17sv	326001-326016	CB.84.C.02.18 CB.84.C.04.01
4 July - 10 July	C.11	S	255m	W 45° 12′ 40″ N 61° 08′ 50″	B16sv	326017-326038	CB.84.C.04.02 CB.84.C.05.06
10 July - 17 July	C.12	C	700m	W 45° 05′ 15″ N 61° 09′ 37″	B16sø	326039-326070	CB.84.C.05.07 CB.84.C.05.29
17 July - 22 July	C.2	SE	1175m	W 44° 54′ 45″ N 61° 08′ 45″	B17sv	326071-326106	CB.84.C.05.30 CB.84.C.07.22
28 July - 3 Aug	C.13	S	1200m	W 45° 09′ 30″ N 61° 07′ 45″	B16sv	326107-326139	CB.84.C.08.02 CB.84.C.09.25
3 Aug - 8 Aug	C.6	NE	200m	W 45° 01′ 30″ N 61° 11′ 45″	B16nø	326140-326145	CB.84.C.09.33 CB.84.C.10.05
8 Aug - 16 Aug	C.14	S	1200m	W 45° 02′ 40″ N 61° 07′ 15″	A15nø	326146-326160	CB.84.C.10.06 CB.84.C.11.20
16 Aug - 22 Aug	C.15	S	170m	W 45° 01′ 00″ N 61° 06′ 20″	A15nv	326160-326197 (inc.hel,Reco)	CB.C4.C.11.21 CB.C4.C.12.08
22 Aug - 27 Aug	C.16	NW	480m	W 45° 14′ 00″ N 61° 12′ 50″	B16nv	326198-326200 325651-325654	CB.84.C.12.09 CB.84.C.13.25

Table A2.5

Table

Rock code for the Motzfeldt Centre

This is the rock nomenclature code for the Motzfeldt Centre, S. Greenland. The format was decided at the Motzfeldt meeting in Munich, January 1985.
The code consists of a three digit number. The first digit represents the code for the ROCK GROUP, the second for the ROCK UNIT and the third for the ROCK APPEARANCE.

		2	ANYOTHER
9	UNDIFFERENTIATED	1	HY SYENITE
		5	LAMPROPHYRIC
		4	ACID
8	GARDAR DYKES	3	INTERMEDIATE
		2	BASIC
		1	CARBONATITE
		3	PERALKALINE MICROSYENITE SUITE
7	SHEET INTRUSIONS	2	POIKILITIC ARFVEDSONITE MICROSYENITE
		1	LUJAVRITE
		4	LAMINATED PORPHYRITIC SYENITE
6	'RING DYKE'	3	LAMINATED ALKALI SYENITE
	INTRUSIONS	2	SYENOGABBRO/LARVIKITE DYKE
		1	ALKALI GABBRO DYKE
		3	NEPHELINE SYENITE
5	FLINKS DAL	2	FOYAITE
	FORMATION	1	PORPHYRITIC NEPHELINE SYENITE
		3	NEPHELINE SYENITE
4	MOTZFELDT SØ	2	ALTERED SYENITE
	FORMATION	1	MARGINAL ARFVEDSONITE SYENITE
		3	NEPHELINE SYENITE
3	GEOLOCFJELD	2	PULASKITE
	FORMATION	1	GEOLOCFJELD SYENITE
		4	METASOMATISED IGNEOUS ROCKS
2	ERIKSFJORD	3	SEDIMENTARY ROCKS
	FORMATION	2	INTERMEDIATE IGNEOUS ROCKS
		1	BASIC IGNEOUS ROCKS
1	JULIANEHÅB	1	GNEISS, GRANITE,DIORITE, ETC
	FORMATION		

ROCK APPEARANCE

5	PEGMATITE
4	TYPE 'REPRESENTATIVE' SAMPLE
3	ALTERED / MINERALISED
2	WEATHERED
1	FRESH

EXAMPLE,

434 = Motzfeldt Sø Formation, Nepheline syenite, Type sample.
If any part of the code is unknown then a nine should be used! eg. 492 = Motzfeldt Sø Formation, unit unknown, weathered sample.

999 = missing sample

2.4 The Motzfeldt samples; the facts and figures

2.4.1 Sample quantity, variation and usage

To date, over 2000 samples have been collected from the Motzfeldt Centre. These include samples collected by, C.H. Emeleus & W.T. Harry (field seasons 1961-1963), A.P. Jones (field seasons 1977 & 1979) and members (including the author) of the GGU-SYDURAN (field seasons 1979-1983) and PYROCHLORE (field seasons 1984 & 1985) teams. Of these, 1048 are housed at Durham and have been available for study. The author has collected 480 samples in two field seasons. Approximately 200 of these have been processed in XRF investigations with 160 complete major trace analyses tabled here (Table A3.2). Because of the coarse nature of many of the syenites and because geochemical studies were to be undertaken large samples were collected, usually around 1 to 2 kg in weight. The freshest available material was collected and most weathered surfaces removed in the field.

The many syenite and nepheline syenite units show a remarkable variation in texture and mineralogy both between and within individual units. There are however distinct recognisable characters to most of the units, making identification, although often uncertain, possible. Sampling was not restricted to 'representative' specimens therefore most lithological varieties encountered in Motzfeldt are represented in the collection. Many, very 'peculiar' rock types have not been studied in detail, purely because they are unusual and consequently beyond the scope of this work. 'Representative' samples are really those that clearly show the definitive features which most frequently are found in a particular unit. These features were provisionally described in the GGU internal report; Bradshaw & Tukiainen, 1983 and are expanded in Part Two and Part Three of this thesis.

Difficulties have remained however, with certain individual units being almost indistinguishable from one another, except perhaps by their field relations. In addition to the identification problem, weathering and alteration are a great hinderance to sampling

in Motzfeldt. The coarse and very coarse rock types are invariably friable and weathered to some degree and tend to outcrop in rounded crumbling mounds whereas the fine and medium-grained rocks are easily sampled and often fresh. This may lead to sampling bias. For instance, the paucity of FDF-Nepheline syenite in the sample range and geochemical investigations is simply due to its very coarse grain and consequently its weathered character.

2.4.2 Lithological coding

Because of the large numbers of specimens, collected by several different teams during the PYROCHLORE survey, a lithological code system was developed (Table A2.6). This was devised by the author at a meeting of the PYROCHLORE group in Munich. The code is flexible in allowing any identification uncertainty as well as the physical state of the specimen to be included.

2.4.3 Sample Locations and distribution.

Enc.2 shows the sample location distribution for all specimens housed at Durham. If Enc.2 is used as an overlay to the contoured geological map (Enc.1) it becomes clear that the topography has greatly determined the sampling distribution. Grid-type sampling proved virtually impossible, with many of the suitable sampling exposures being restricted to cliff faces often above the scree fans. Most samples have been taken while traversing valley sides or along ridge sections. Helicopter reconnaissance also proved invaluable for sampling especially in the very high ground of NE and S Motzfeldt. Nevertheless, a fairly good coverage of Motzfeldt has been possible and this has formed the basis of this study. Grid reference locations of all the samples taken in Motzfeldt are available from a computer data-base housed in the Greenland Geological Survey, Copenhagen.

APPENDIX THREE

WHOLE ROCK CHEMISTRY

APPENDIX THREE

ROCK CHEMISTRY

3.1 X-ray fluorescence spectroscopy

3.1.1 Sample preparation

Samples (>500 gms) were broken using a Cutrock Engineering hydraulic splitter and any weathered surfaces removed. The fragments were then crushed into a coarse gravel (1-2 cm) using a Stuĺevant 2" x 6" Roll Jaw crusher. This material was systematically quartered and reduced until approximately 60-80 gms remained and then powdered using a Tema Laboratory Disc Mill, with a tungsten carbide barrel. Grinding usually took three to four minutes until a very fine powder remained. Fitton & Gill (1970) showed that oxidation of FeO to Fe_2O_3 could occur during grinding. Therefore, for a number of representative samples a few gms were withdrawn after just 30 seconds of grinding and this coarser powder used in subsequent whole rock FeO determinations. All powdered samples were pressed into briquettes using a hydraulic press operating at 5 to 7 tons per square inch. Between 5 and 10 drops of MOWIOL were used as a binding agent. The briquettes were dried in an oven at 110° for one hour, before use in trace element determination.

There is little doubt that for major element analysis fused-beads are better than powder briquettes. In this study approximately 65% of the samples have been analysed for major elements by fusion disc techniques. These have been prepared both in Edinburgh and Durham with techniques described below.

i. Edinburgh

120 fused glass discs (45 mm diameter) were prepared in Edinburgh following a procedure comprehensively described in Fitton & James (1980) and summarised here.

1. The powder is dried at 110° for 1 hour.

2. 1 gm of sample is weighed into a Pt-Au crucible (four at a time).

3. 5x sample weight of Johnson Matthew SPECTROFLUX 105 is added, with an additional 0.03 grams to allow for volatile loss in the flux.

4. The crucibles are placed (with Pt-Au lids) in a furnace at 1100° for 20 minutes. If chromite or other refractory minerals are suspected then this is increased to 1200° for 2 hours.

5. The removed samples are swirled and cooled in the crucibles then re-weighed.

6. Any weight loss is accurately made up with additional flux.

7. The crucibles are then re-heated over Meker burners until the sample is completely fused. Swirling of the mixture ensures thorough mixing

8. The molten mixture is poured onto a graphite mould enclosed by a stainless steel ring and the disc formed by insertion of an aluminium plunger. All this moulding process is done on a hotplate at 220°C.

9. The plunger is removed after about 5 to 10 seconds and the disc covered with a silica dish then left for 30 minutes.

10. The disc should have a uniform 'orange peel' surface texture.

11. The crucibles are quenched in cold water then immersed in warm 50/50 HCL for 10 to 15 minutes.

12. The analytical surface of the disc is the one which was in contact with the aluminium plunger. The other side is labelled.

ii. Durham

Fused glass discs (35mm diameter) were made at Durham following a similar method to the Edinburgh preparation procedure except for the following departures:

Operating conditions of the PW1400 X-ray specrometer.

	ELEMENT	FLT	COL	DET	XTL	ORD	UPL	LWL	KV	MA	ANGLE	+OFFS	-OFFS
Mg	ZD	KA	NO	C	F	4	1	70	30	80	35	45.125	2.40	2.40
P	ZJ	KA	NO	C	F	5	1	75	25	80	35	141.025	4.00	3.50
Na	ZF	KA	NO	C	F	4	1	84	28	80	35	55.000	2.40	1.30
Al	ZB	KA	NO	C	F	3	1	75	30	80	35	145.190	1.80	4.00
Si	ZA	KA	NO	C	F	3	1	75	25	80	35	109.235	3.80	2.00
S	ZK	KA	NO	C	F	3	1	75	25	80	35	75.865	1.20	.00
Ca	ZG	KA	NO	F	F	2	1	70	30	80	35	136.885	3.00	1.80
Ti	ZE	KA	NO	F	F	2	1	75	25	80	35	113.285	4.30	2.00
V	ZH	KA	NO	C	F	2	1	75	25	80	35	86.280	5.00	2.00
Cr	ZQ1	KA	NO	F	F	1	1	62	35	80	35	123.420	2.00	2.00
Mn	ZQ2	KA	NO	C	F	1	1	60	34	80	35	107.355	2.00	2.00
Fe	ZI	KA	NO	C	F	1	1	70	40	80	35	95.415	4.60	2.00
Nd	ZC	KA	NO	F	FS	2	1	75	25	80	35	57.635	2.30	2.00
Ni	ZQ3	LA	NO	C	F	1	1	75	35	80	35	112.875	1.40	2.00
Cu	ZQ3	KA	NO	C	S	1	1	65	30	80	35	71.325	2.00	1.30
Zn	ZQ2	KA	NO	F	FS	1	1	70	30	80	35	65.610	1.10	.50
Ga	ZQ1	KA	NO	C	S	1	1	65	30	80	35	60.640	1.00	1.00
Ge	ZR1	KA	NO	C	S	1	1	65	30	80	35	56.245	.90	.40
Rb	ZR2	KA	NO	C	F	1	1	75	25	80	35	52.300	1.00	1.00
Sr	ZN3	KA	NO	C	S	1	1	60	30	80	35	38.020	.70	.00
Y	ZN2	KA	NO	C	S	1	1	60	30	80	35	35.900	1.10	1.00
Zr	ZN1	KA	NO	C	S	1	1	60	30	80	35	33.925	.00	.90
Nb	ZH3	KA	NO	C	S	1	1	60	30	80	35	32.100	.90	.90
Mo	ZH2	KA	NO	C	S	1	1	60	30	80	35	30.475	.60	.60
Hg	ZS1	KA	NO	C	S	1	1	65	35	80	35	28.840	1.20	.60
W	ZS2	LB	NO	C	FS	1	1	75	25	80	35	43.140	1.50	1.50
Cd	ZS3	LA	NO	C	S	1	1	75	25	80	35	53.445	1.00	.50
Sn	ZT1	KA	NO	C	S	1	1	75	25	80	35	21.685	1.20	.60
Sb	ZT2	KA	NO	C	S	1	1	75	25	80	35	19.900	.90	1.20
Ta	ZT3	KA	NO	C	S	1	1	75	25	80	35	19.005	1.72	.74
Ba	ZU1	LA	NO	C	F	1	1	75	25	80	35	64.680	.50	1.50
La	ZH1	KA	NO	F	S	1	1	62	32	80	35	15.625	1.38	.78
Ce	ZU2	KA	NO	C	F	1	1	62	30	80	35	139.155	2.00	2.00
Pb	ZU3	LB	NO	C	F	1	1	70	28	80	35	111.930	2.60	1.50
F	ZP1	KA	NO	C	S	1	1	60	40	80	35	40.440	1.20	1.60
Th	ZV1	KA	NO	C	F	4	1	80	20	80	35	90.615	2.40	2.50
U	ZP3	LA	NO	C	S	1	1	80	25	80	35	39.290	.60	.76
Co	ZP2	LA	NO	C	S	1	1	80	25	80	35	37.360	1.40	.60
	ZV2	KA	NO	C	S	1	1	70	30	80	35	77.965	1.00	.80
	CU	KA	NO	F	F	2	1	80	20	0	0	45.075	.00	.00

Crystal;
1=LIF220
2=LIF200
3=PE
4=THAP
5=GE

Detector;
F= Flow
S= Scint
FS= Flow & Scint

Collimator;
C= Coarse
F= Fine

1. A Leco Instruments induction furnace was used. The crucible is heated by induction coil for 10 minutes at approximately 1100°C.

2. Smaller (35mm diameter) discs were made so as to be compatible with the automatic sample loader at Durham.

3.1.2 Operating conditions and data processing

i. Edinburgh

The major element analyses were made using a Phillips PW1450 XRF system. Determinations were made on fused glass discs (Norrish & Hutton, 1969) with corrections applied for inter-element mass absorption effects, using the tables of Theisen & Vollach, (1967). The following International Standards were used; G2, GSP1, AGV1, BCR1, PCC1, DTS1, GA, GH, BR, BEN, ANG & MAN; with data from Abbey (1983). Full descriptions of the theory of the techniques and of the computer programs used in data processing at Edinburgh are given by Thirlwall (1979). No trace analyses were processed at Edinburgh.

ii. Durham

The analyses were performed using a Phillips PW1400 x-ray spectrometer incorporating a PW1500/10 automatic sample changer and using Rhodium K radiation. The operating conditions are listed in Table A3.1. The data were calibrated against a selection of International standards (data from Goviandaraju, 1984) together with a number of internal standards of syenitic composition.

a. Major elements

In fusion data processing, inter-element interference was corrected using coefficients derived from selected multiple regression analysis obtained from MIDAS (a statistical package on Durhams main- frame computer) . Major element determination was also carried out on powder-discs. This method was used because of its speed of preparation. The programme XRF.QD written by Mr.C. Watson (this department) was used

for data processing. The programme follows a procedure similar to that given in Brown et al.,(1973) and uses the mass absorption tables of Heinrich (1966). In summary, intensities of the standards are regressed against their known composition and the least squares quadratic equation derived, is applied to give first approximation values to the unknowns. Mass absorption values are then applied to the standard intensities and a new corrected quadratic regression line obtained. The approximate analyses of the unknowns are then used to calculate their mass absorption effects, which together with the corrected regression line from the standards are used on the unknown intensities to acquire improved analyses. This procedure is reiterated until a fixed convergence is obtained as in accordance with the method of Holland and Brindle (1966). The author obtained satisfactory results when a large number (10) of internal standards were added to the International batch. These internal standards were all from the Motzfeldt Centre and of syenite or nepheline syenite composition. The data being derived from the fusion analyses of Edinburgh.

b. Trace elements

17 trace elements were analysed for each sample, raw counts processed here with the programme TRATIO by R.C.O. Gill. The trace element data used and tabled in this work however, have been processed (from the raw-counts derived at Durham) exclusively, at GGU by Tapani Tukiainen. The procedure used, is a method, given in Bailey & Sørenson (1976) which follows the guidelines of Norrish & Chappell (1967).

The method is based on the formula:

(1) ppm = net c/s (net counts per sec) x u/p (mass absorption coefficient) x (K) constant.

The following three steps are taken to give the ppm;

1. Determination of net c/s free of spectral interferences and of the background value. Measurements of peak and background intensities from a number of blank standards

such as Specpure SiO_2, Al_2O_3, and MgO or even PCC-1, are used to accurately determine the background intensities of the different elements.

2. The constant (K) is calculated using International Standards of known ppm and u/p and whose net c/s were determined under the same analytical conditions as the unknowns.

   ie, K = ppm / (net c/s x u/p)

3. The u/p correction factor for each element analysed was determined by taking into account the total u/p effects of the major element data of the sample and in addition (by an iterative procedure) the total u/p effects of selected trace elements namely; Zr, Nb, Ba, Sr, Ce, Nd and La.

The improved u/p total is then used in the original formula (1) with the net c/s and the average K value (derived from the International Standards) to give the ppm.

3.1.3 Notes on tables of XRF data

Disc type:[1] (Major elements)

Fs.1 = Fusion Disc, Edinburgh.

Fs.2 = Fusion Disc, Durham.

Pd.1 = Powder Disc, Durham (Holland & Brindle, 1966 method)

Pd.2 = Powder Disc, Durham (Watson method)

Pd.3 = Powder Disc, Durham (data from Jones, 1980)

Missing data: = -1

[1] all trace element data from powder discs using Bailey & Sørenson, 1976 method

Whole-rock geochemical analyses – Geologfjeld Formation.

Sample no.	304166	304167	304172	63703	304159	304160	304740
Disc type	Fs.1	Fs.1	Pd.1	Pd.3	Fs.1	Fs.1	Fs.1
Major elements (wt%)							
SiO2	63.29	60.93	60.01	60.98	60.54	60.80	61.00
Al2O3	16.25	15.93	17.25	16.55	17.68	17.75	17.81
Fe2O3T	4.46	4.18	4.39	4.96	5.10	4.38	4.43
MgO	0.35	0.78	0.81	0.67	0.57	0.45	0.45
CaO	0.94	2.05	2.29	4.32	1.97	1.75	1.79
Na2O	5.73	5.66	5.20	5.58	5.74	5.75	5.71
K2O	5.72	6.20	6.36	6.27	6.27	6.47	6.53
TiO2	0.64	0.68	0.48	0.88	0.73	0.63	0.65
MnO	0.18	0.18	0.18	0.10	0.20	0.17	0.18
P2O5	0.11	0.46	0.15	0.24	0.15	0.15	0.15
Total	97.67	97.07	97.12	100.55	98.96	98.29	98.70
Trace elements (p.p.m)							
Ba	479	293	1055	2178	938	842	673
Nb	103	123	66	73	78	57	54
Zr	563	491	288	381	286	239	233
Y	70	158	50	37	32	37	28
Sr	128	168	252	838	366	241	240
Rb	214	422	183	116	94	92	86
Zn	120	164	92	112	109	83	86
Pb	31	20	11	12	6	9	7
U	10	14	5	6	3	4	3
Th	24	38	3	0	6	9	8
Ga	31	26	23	25	22	23	22
La	77	545	53	46	54	48	43
Ce	164	1011	111	88	101	97	73
C.I.P.W. norms							
Quartz	4.0	0.0	0.0	0.0	0.0	0.0	0.0
Zircon	0.1	0.1	0.1	0.1	0.1	0.1	0.0
Orthoclase	34.7	37.8	38.8	36.9	37.6	39.0	39.2
Albite	49.8	49.0	44.9	38.3	44.9	45.6	45.3
Anorthite	1.7	0.0	5.1	1.6	4.0	3.6	3.7
Nepheline	0.0	0.0	0.3	4.7	2.3	2.2	2.0
Acmite	0.0	0.4	0.0	0.0	0.0	0.0	0.0
Diopside	2.1	6.3	5.0	15.1	4.4	3.7	3.8
Wollastonite	0.0	0.0	0.0	0.5	0.0	0.0	0.0
Hypersthene	5.0	1.2	0.0	0.0	0.0	0.0	0.0
Olivine	0.0	2.1	3.3	0.0	3.8	3.3	3.3
Magnetite	1.9	1.6	1.9	2.1	2.2	1.9	1.9
Hematite	0.0	0.0	0.0	0.0	0.0	0.0	0.0
Ilmenite	0.3	0.4	0.4	0.2	0.4	0.3	0.3
Apatite	0.3	1.1	0.4	0.6	0.4	0.4	0.4
Lith. code	312	312	313	314	314	314	314
Camp site	Cmp.09	Cmp.09	Cmp.09	Cmp.04	Cmp.09	Cmp.09	Cmp.09
Colour index	9.63	9.63	10.89	17.88	11.55	9.52	9.68
Frac. index	88.50	87.20	83.94	79.97	84.78	86.79	86.53
Diff. index	88.50	86.80	83.90	80.00	84.80	86.80	86.50
Na/(Na+K)	0.60	0.58	0.55	0.57	0.58	0.57	0.57
(Na+K)/Al	0.96	1.01	0.89	0.96	0.92	0.93	0.92
Fe2O3/FeO	0.45	0.45	0.45	0.45	0.45	0.45	0.45

Whole-rock geochemical analyses – Geologfjeld Formation.

Sample no.	58352	58367	304051	326161	326189	58370	58373
Disc type	Fs.1	Pd.3	Fs.1	Pd.2	Pd.2	Pd.3	Pd.3
Major elements (wt%)							
SiO2	61.81	59.94	58.32	59.44	58.99	59.44	58.23
Al203	19.43	18.27	18.47	18.09	18.03	18.68	19.29
Fe203T	4.54	5.34	5.08	4.56	4.82	5.44	6.48
MgO	0.32	0.44	0.51	0.53	0.58	0.43	0.23
CaO	1.79	2.58	2.52	2.03	2.25	2.28	1.33
Na20	6.67	6.43	6.32	6.52	6.60	6.88	8.02
K20	6.16	5.58	5.69	5.47	5.31	5.79	5.65
TiO2	0.47	0.58	0.62	0.53	0.57	0.59	0.35
MnO	0.14	0.13	0.14	0.14	0.15	0.15	0.20
P205	0.11	0.17	0.13	0.16	0.15	0.16	0.10
Total	101.43	99.46	97.80	97.47	97.45	99.84	99.88
Trace elements (p.p.m)							
Ba	986	996	806	1166	1246	901	171
Nb	87	117	56	105	122	187	130
Zr	420	504	243	417	451	676	576
Y	39	45	30	38	40	54	70
Sr	517	746	236	729	755	481	54
Rb	128	132	87	114	118	150	163
Zn	92	85	79	88	92	102	140
Pb	9	10	6	9	7	15	9
U	2	5	2	7	8	5	2
Th	8	5	3	5	5	13	5
Ga	30	31	23	25	27	29	39
La	69	76	48	68	66	100	123
Ce	118	142	86	122	130	182	239
C.I.P.W. norms							
Quartz	0.0	0.0	0.0	0.0	0.0	0.0	0.0
Zircon	0.1	0.1	0.1	0.1	0.1	0.1	0.1
Orthoclase	36.0	33.2	34.5	33.2	32.3	34.3	33.5
Albite	44.6	44.2	40.8	46.8	45.8	41.4	39.2
Anorthite	4.9	4.5	5.4	4.1	4.0	3.0	0.0
Nepheline	6.0	5.8	7.6	5.4	6.3	9.2	15.6
Acmite	0.0	0.0	0.0	0.0	0.0	0.0	0.1
Diopside	3.0	6.5	5.8	4.7	5.8	6.5	5.3
Wollastonite	0.0	0.0	0.0	0.0	0.0	0.0	0.0
Hypersthene	0.0	0.0	0.0	0.0	0.0	0.0	0.0
Olivine	3.1	2.8	3.1	3.1	3.0	1.5	1.7
Magnetite	1.9	2.2	2.2	2.0	2.1	3.3	3.9
Hematite	0.0	0.0	0.0	0.0	0.0	0.0	0.0
Ilmenite	0.3	0.2	0.3	0.3	0.3	0.3	0.4
Apatite	0.2	0.4	0.3	0.4	0.4	0.4	0.2
Lith. code	324	324	324	324	324	331	331
Camp site	Cmp.04	Cmp.04	Cmp.04	Cmp.04	Cmp.04	Cmp.04	Cmp.04
Colour index	8.46	12.16	11.73	10.44	11.55	11.92	11.44
Frac. index	86.60	83.19	82.86	85.40	84.36	84.95	88.50
Diff. index	86.60	83.20	82.90	85.40	84.40	84.90	88.40
Na/(Na+K)	0.62	0.64	0.63	0.64	0.65	0.64	0.68
(Na+K)/Al	0.91	0.91	0.90	0.92	0.92	0.94	1.00
Fe203/FeO	0.45	0.45	0.45	0.45	0.45	0.80	0.80

Whole-rock geochemical analyses – Geologfjeld Formation.

Sample no.	58377	304048	304137	58368	304055	304135
Disc type	Pd.3	Pd.1	Pd.1	Pd.3	Pd.2	Pd.1
Major elements (wt%)						
SiO2	57.59	58.04	55.68	59.39	56.01	55.41
Al2O3	20.15	18.15	19.87	18.63	21.66	20.27
Fe2O3T	5.69	5.63	5.77	5.71	4.02	4.74
MgO	0.36	0.38	1.02	0.23	0.34	0.81
CaO	1.24	1.97	1.65	1.55	0.93	1.71
Na2O	8.26	6.13	7.90	7.24	9.14	7.51
K2O	5.53	6.06	6.42	6.00	5.63	6.03
TiO2	0.26	0.61	0.31	0.27	0.17	0.32
MnO	0.21	0.19	0.20	0.16	0.15	0.16
P2O5	0.08	0.14	0.08	0.07	0.07	0.90
Total	99.37	97.29	98.90	99.25	98.12	97.86
Trace elements (p.p.m)						
Ba	125	809	304	87	118	361
Nb	255	172	159	79	141	158
Zr	959	717	537	305	467	520
Y	80	60	53	39	49	49
Sr	182	371	291	35	43	349
Rb	242	158	225	156	148	182
Zn	142	124	108	95	91	95
Pb	8	19	10	4	9	11
U	9	7	4	0	1	3
Th	0	21	8	2	11	11
Ga	43	32	39	37	34	34
La	121	108	78	57	90	86
Ce	217	194	133	114	171	138
C.I.P.W. norms						
Quartz	0.0	0.0	0.0	0.0	0.0	0.0
Zircon	0.2	0.1	0.1	0.1	0.1	0.1
Orthoclase	33.0	36.9	37.3	35.8	34.0	36.5
Albite	37.9	41.1	28.7	41.7	32.0	34.0
Anorthite	1.6	4.3	2.5	0.6	1.5	2.7
Nepheline	17.6	6.7	20.1	10.9	25.4	16.8
Acmite	0.0	0.0	0.0	0.0	0.0	0.0
Diopside	3.6	4.3	4.3	5.9	2.4	0.0
Corundum	0.0	0.0	0.0	0.0	0.0	0.4
Hypersthene	0.0	0.0	0.0	0.0	0.0	0.0
Olivine	2.1	2.4	3.0	1.0	1.7	4.0
Magnetite	3.5	3.5	3.4	3.5	2.5	2.9
Hematite	0.0	0.0	0.0	0.0	0.0	0.0
Ilmenite	0.4	0.4	0.4	0.3	0.3	0.3
Apatite	0.2	0.3	0.2	0.2	0.2	2.2
Lith. code	331	331	331	334	334	334
Camp site	Cmp.04	Cmp.04	Cmp.08	Cmp.04	Cmp.04	Cmp.08
Colour index	9.70	10.95	11.33	10.83	7.03	9.45
Frac. index	88.52	84.65	86.08	88.49	91.40	87.29
Diff. index	88.50	84.60	86.10	88.50	91.40	87.30
Na/(Na+K)	0.69	0.61	0.65	0.65	0.71	0.65
(Na+K)/Al	0.97	0.92	0.96	0.99	0.98	0.93
Fe2O3/FeO	0.80	0.80	0.80	0.80	0.80	0.80

Whole-rock geochemical analyses – Motzfeldt So Formation.

Sample no.	304052	304165	325651	304710	304711	304040	304053
Disc type	Fs.1	Fs.1	Pd.2	Fs.1	Pd.1	Fs.1	Fs.1
Major elements (wt%)							
SiO2	48.12	59.01	58.89	56.47	57.20	63.48	61.20
Al2O3	6.39	13.15	13.52	9.21	10.03	15.86	16.02
Fe2O3T	26.25	10.42	8.29	17.37	15.63	5.77	6.27
MgO	0.95	0.51	0.64	0.22	0.17	0.13	0.06
CaO	3.33	2.35	3.43	1.26	0.65	0.39	0.42
Na2O	5.05	7.11	6.43	6.90	5.45	6.02	5.41
K2O	2.16	4.35	4.88	3.65	4.16	4.91	5.51
TiO2	2.25	0.43	0.42	0.38	0.29	0.41	0.39
MnO	0.75	0.32	0.25	0.65	0.51	0.06	0.11
P2O5	0.04	0.03	0.08	0.0	0.0	0.02	0.00
Total	95.28	97.69	96.83	96.10	94.10	97.05	95.40
Trace elements (p.p.m)							
Ba	1933	1344	331	69	105	146	134
Nb	389	137	333	1289	1532	665	1572
Zr	1651	487	3256	7337	11778	2303	6776
Y	127	46	142	520	701	236	505
Sr	1390	831	130	128	44	34	19
Rb	305	136	308	331	364	411	621
Zn	297	92	359	871	809	249	377
Pb	20	10	56	72	69	108	156
U	17	4	18	10	16	21	24
Th	8	6	34	2	18	137	102
Ga	59	32	39	44	43	49	48
La	123	69	375	1000	1277	772	1403
Ce	250	119	699	1768	2360	1262	1529
C.I.P.W. norms							
Quartz	2.3	0.0	0.0	1.9	7.8	8.7	7.4
Zircon	0.4	0.1	0.7	1.5	2.5	0.5	1.4
Orthoclase	13.6	26.4	29.8	22.4	25.9	29.9	33.9
Albite	22.1	41.8	39.3	28.1	30.0	52.4	47.6
Anorthite	0.0	0.0	0.0	0.0	0.0	1.8	2.2
Nepheline	0.0	1.6	2.4	0.0	0.0	0.0	0.0
Acmite	20.5	15.2	10.9	27.1	16.4	0.0	0.0
Diopside	15.5	10.6	14.8	5.7	3.1	0.1	0.0
Corundum	0.0	0.0	0.0	0.0	0.0	0.0	0.4
Hypersthene	13.6	0.0	0.0	11.5	9.2	0.6	0.3
Olivine	0.0	3.3	0.5	0.0	0.0	0.0	0.0
Magnetite	10.7	0.5	1.0	0.0	4.2	6.0	6.5
Sod. metasil.	0.0	0.0	0.0	0.4	0.0	0.0	0.0
Ilmenite	1.5	0.6	0.5	1.3	1.0	0.1	0.2
Apatite	0.1	0.1	0.2	0.0	0.0	0.1	0.0
Lith. code	414	414	414	415	415	423	423
Camp site	Cmp.04	Cmp.08	Cmp.16	Cmp.10	Cmp.10	Cmp.03	Cmp.03
Colour index	41.29	15.01	16.90	18.52	17.48	6.80	7.08
Frac. index	68.36	84.89	82.42	79.53	80.02	90.90	88.90
Diff. index	37.90	69.70	71.50	52.40	63.70	90.90	88.90
Na/(Na+K)	0.78	0.71	0.67	0.74	0.67	0.65	0.60
(Na+K)/Al	1.67	1.25	1.17	1.66	1.34	0.96	0.93
Fe2O3/FeO	1.20	1.20	1.20	1.20	1.20	2.50	2.50

Whole-rock geochemical analyses – Motzfeldt So Formation.

Sample no.	304140	304142	304144	304145	304712	304715	304719
Disc type	Pd.1	Pd.1	Pd.1	Pd.1	Pd.1	Pd.1	Pd.1
Major elements (wt%)							
SiO2	57.71	61.02	61.92	56.55	56.12	54.62	56.43
Al2O3	19.03	16.71	16.42	15.02	9.73	5.52	16.96
Fe2O3T	6.99	2.17	4.75	9.93	18.65	24.34	7.64
MgO	1.06	0.26	1.16	1.83	1.93	1.96	1.47
CaO	1.29	1.29	1.48	0.77	2.84	1.34	2.47
Na2O	5.74	6.09	5.67	4.45	6.82	6.05	5.55
K2O	4.51	5.50	5.65	5.41	1.76	2.50	5.40
TiO2	0.41	0.04	0.59	0.83	0.47	0.99	0.94
MnO	0.14	0.20	0.16	0.13	0.56	0.57	0.26
P2O5	0.12	0.01	0.08	0.11	0.01	0.0	0.18
Total	97.00	93.29	97.88	95.03	98.88	97.89	97.30
Trace elements (p.p.m)							
Ba	467	113	782	271	255	143	441
Nb	276	1085	81	335	3299	4239	262
Zr	945	4627	540	1214	6697	13534	1349
Y	94	552	46	138	390	647	103
Sr	265	48	111	68	134	168	216
Rb	369	519	126	402	175	300	311
Zn	150	79	117	426	1189	1748	203
Pb	19	53	18	45	116	395	51
U	7	89	3	15	255	342	7
Th	17	287	4	69	141	118	25
Ga	40	73	29	53	64	42	39
La	163	786	70	281	822	1075	128
Ce	226	1415	141	509	1492	2123	253
C.I.P.W. norms							
Quartz	3.0	2.2	3.3	5.8	6.0	9.2	0.0
Corundum	2.7	0.0	0.0	0.7	0.0	0.0	0.0
Zircon	0.2	1.0	0.1	0.3	1.4	2.7	0.3
Orthoclase	27.5	34.6	34.1	33.7	10.5	14.9	32.8
Albite	50.1	54.9	49.0	39.7	40.6	14.6	43.6
Anorthite	5.9	2.1	2.7	3.3	0.0	0.0	5.6
Nepheline	0.0	0.0	0.0	0.0	0.0	0.0	2.6
Acmite	0.0	0.0	0.0	0.0	15.5	32.7	0.0
Diopside	0.0	1.5	3.5	0.0	11.6	5.7	4.7
Wollastonite	0.0	1.1	0.0	0.0	0.0	0.0	0.0
Hypersthene	2.8	0.0	1.8	5.5	2.4	10.7	0.0
Olivine	0.0	0.0	0.0	0.0	0.0	0.0	1.7
Magnetite	7.2	1.6	4.9	10.5	11.1	8.3	7.9
Hematite	0.0	0.5	0.0	0.0	0.0	0.0	0.0
Ilmenite	0.3	0.4	0.3	0.3	1.1	1.1	0.5
Apatite	0.3	0.0	0.2	0.3	0.0	0.0	0.4
Lith. code	423	423	423	423	423	423	423
Camp site	Cmp.08	Cmp.08	Cmp.08	Cmp.08	Cmp.10	Cmp.10	Cmp.10
Colour index	10.62	3.51	10.70	16.60	26.14	25.83	15.20
Frac. index	80.60	91.72	86.50	79.10	72.50	71.43	78.90
Diff. index	80.60	91.70	86.50	79.10	57.00	38.70	78.90
Na/(Na+K)	0.66	0.63	0.60	0.56	0.85	0.79	0.61
(Na+K)/Al	0.75	0.96	0.94	0.88	1.35	2.29	0.88
Fe2O3/FeO	2.50	2.50	2.50	2.50	2.50	2.50	2.50

Whole-rock geochemical analyses – Motzfeldt So Formation.

Sample no.	304720	304722	304723	304725	304726	304727	304732
Disc type	Pd.1	Pd.1	Fs.1	Pd.1	Pd.1	Fs.1	Fs.1
Major elements (wt%)							
SiO2	43.96	55.99	55.55	59.99	59.61	58.07	58.52
Al2O3	11.07	13.40	15.27	18.49	19.33	16.40	14.21
Fe2O3T	20.81	10.32	10.78	6.02	5.36	8.36	8.25
MgO	1.63	0.96	0.01	1.65	1.10	0.59	0.24
CaO	8.28	3.34	2.73	0.89	1.04	1.95	2.02
Na2O	4.18	5.69	6.35	4.66	5.00	5.63	6.76
K2O	3.97	4.66	4.11	6.77	6.62	5.90	4.12
TiO2	3.81	0.34	0.50	0.90	0.60	0.86	0.50
MnO	0.46	0.27	0.44	0.19	0.16	0.36	0.37
P2O5	0.17	0.02	0.06	0.19	0.10	0.15	0.05
Total	98.34	94.99	95.81	99.75	98.92	98.27	95.04
Trace elements (p.p.m)							
Ba	0	23	149	164	194	71	233
Nb	588	389	358	154	189	204	553
Zr	393	1386	1303	695	1152	843	9677
Y	450	151	169	70	86	65	241
Sr	69	36	75	89	100	43	111
Rb	109	364	204	214	228	178	298
Zn	566	334	304	173	100	217	295
Pb	20	141	56	17	19	12	57
U	27	33	32	0	7	1	52
Th	649	63	108	9	19	9	91
Ga	32	46	35	38	38	38	36
La	3889	827	622	155	130	123	850
Ce	6969	1538	1096	0	248	213	1661
C.I.P.W. norms							
Quartz	0.0	0.8	0.0	2.6	1.3	0.0	1.3
Corundum	0.0	0.0	0.0	2.3	2.3	0.0	0.0
Zircon	0.1	0.3	0.3	0.1	0.2	0.2	2.0
Orthoclase	24.0	29.0	25.4	40.1	39.5	35.6	25.3
Albite	15.9	45.3	55.5	39.6	42.8	46.9	52.2
Anorthite	0.0	0.0	1.1	3.2	4.6	2.1	0.0
Nepheline	10.7	0.0	0.4	0.0	0.0	0.9	0.0
Acmite	0.5	4.8	0.0	0.0	0.0	0.0	6.5
Diopside	18.8	7.1	0.0	0.0	0.0	4.2	4.4
Wollastonite	7.6	3.6	5.3	0.0	0.0	0.7	2.1
Hypersthene	0.0	0.0	0.0	5.1	3.3	0.0	0.0
Olivine	0.0	0.0	0.0	0.0	0.0	0.0	0.0
Magnetite	21.1	8.5	10.4	6.1	5.4	8.6	5.4
Hematite	0.0	0.0	0.6	0.0	0.0	0.0	0.0
Ilmenite	0.9	0.5	0.9	0.4	0.3	0.7	0.7
Apatite	0.4	0.0	0.1	0.5	0.2	0.4	0.1
Lith. code	423	423	423	423	423	423	423
Camp site	Cmp.10	Cmp.10	Cmp.05	Cmp.05	Cmp.05	Cmp.05	Cmp.10
Colour index	41.25	16.18	11.50	11.90	9.30	13.80	10.60
Frac. index	51.03	80.00	81.30	82.30	83.60	83.30	85.30
Diff. index	50.60	75.20	81.30	82.30	83.60	83.30	78.80
Na/(Na+K)	0.62	0.65	0.70	0.51	0.53	0.59	0.71
(Na+K)/Al	1.01	1.07	0.98	0.81	0.80	0.95	1.10
Fe2O3/FeO	2.50	2.50	2.50	2.50	2.50	2.50	2.50

Whole-rock geochemical analyses – Motzfeldt So Formation.

Sample no.	304737	304748	304754	304756	304114	304115	304116
Disc type	Pd.1	Fs.1	Pd.1	Pd.1	Pd.1	Fs.1	Pd.1
Major elements (wt%)							
SiO2	60.47	58.99	55.88	60.87	56.05	59.73	65.51
Al203	15.54	16.01	22.42	15.66	17.35	15.31	15.19
Fe203T	7.95	7.52	6.96	8.09	8.00	9.84	9.04
MgO	0.99	0.57	1.14	0.82	2.18	0.0	0.84
CaO	1.68	2.21	0.47	1.59	1.74	0.66	1.63
Na20	5.84	5.85	4.39	6.20	3.34	7.45	7.79
K20	5.25	5.52	6.20	5.03	7.40	3.77	3.12
TiO2	0.56	0.95	0.38	0.54	1.15	0.20	0.14
MnO	0.26	0.27	0.24	0.22	0.19	0.24	0.22
P205	0.08	0.19	0.09	0.05	0.36	0.0	0.0
Total	98.62	98.10	98.17	99.07	97.76	97.20	103.48
Trace elements (p.p.m)							
Ba	751	1275	488	194	2588	35	34
Nb	191	152	276	449	112	713	125
Zr	669	671	1241	1489	595	3680	680
Y	83	−1	86	164	63	344	55
Sr	73	191	170	37	585	39	27
Rb	209	154	283	282	185	738	185
Zn	186	199	140	334	106	374	247
Pb	22	23	23	69	16	20	23
U	6	3	6	24	5	2	0
Th	15	0	13	70	7	2	0
Ga	37	32	43	47	31	49	69
La	138	150	97	472	95	373	27
Ce	264	254	250	812	170	660	83
C.I.P.W. norms							
Quartz	3.0	0.1	4.1	2.5	1.5	2.0	5.9
Zircon	0.1	0.1	0.3	0.3	0.1	0.8	0.1
Orthoclase	31.5	33.3	37.3	30.0	44.7	22.9	17.8
Albite	50.2	50.5	37.8	53.0	28.9	59.3	58.8
Anorthite	0.7	1.1	1.9	0.0	7.0	0.0	0.0
Nepheline	0.0	0.0	0.0	0.0	0.0	0.0	0.0
Acmite	0.0	0.0	0.0	0.0	0.0	4.8	4.4
Diopside	5.6	4.7	0.0	4.7	0.0	1.3	5.5
Wollastonite	0.1	1.4	0.0	0.7	0.0	0.8	0.4
Hypersthene	0.0	0.0	2.9	0.0	6.9	0.0	0.0
Corundum	0.0	0.0	8.0	0.0	1.4	0.0	0.0
Magnetite	8.1	7.7	6.9	8.2	8.2	7.7	6.6
Hematite	0.0	0.0	0.2	0.0	0.0	0.0	0.0
Ilmenite	0.5	0.5	0.5	0.4	0.4	0.5	0.4
Apatite	0.2	0.5	0.2	0.1	0.9	0.0	0.0
Lith. code	423	423	423	423	425	425	425
Camp site	Cmp.10	Cmp.07	Cmp.07	Cmp.07	Cmp.10	Cmp.10	Cmp.10
Colour index	14.40	13.40	10.46	13.40	16.40	9.53	12.48
Frac. index	84.70	83.95	79.30	85.54	75.17	88.90	86.99
Diff. index	84.70	84.00	79.30	85.50	75.20	84.10	82.60
Na/(Na+K)	0.63	0.62	0.52	0.65	0.41	0.75	0.79
(Na+K)/Al	0.98	0.97	0.62	1.00	0.78	1.07	1.07
Fe203/FeO	2.50	2.50	2.50	2.50	2.50	2.50	2.50

Whole-rock geochemical analyses – Motzfeldt So Formation.

Sample no.	304117	304731	243141	272404	287157	304753	304755
Disc type	Pd.1	Pd.1	Fs.2	Pd.3	Fs.2	Fs.1	Fs.1
Major elements (wt%)							
SiO2	61.71	59.04	56.50	56.51	56.83	55.16	56.63
Al2O3	11.92	14.40	19.88	20.51	19.70	20.55	21.76
Fe2O3T	12.77	10.02	4.12	5.62	4.61	5.12	4.26
MgO	1.04	0.89	0.44	0.60	0.49	0.35	0.22
CaO	1.22	2.29	1.21	1.45	1.15	1.52	0.94
Na2O	3.90	5.36	8.98	8.06	7.78	5.92	6.77
K2O	4.58	5.93	6.60	5.94	6.28	6.13	6.00
TiO2	0.23	0.32	0.26	0.36	0.53	0.34	0.24
MnO	0.05	0.29	0.20	0.18	0.18	0.22	0.19
P2O5	0.0	0.0	0.12	0.11	0.18	0.09	0.06
Total	97.42	98.54	98.31	99.34	97.73	95.41	97.07
Trace elements (p.p.m)							
Ba	62	184	810	587	645	791	305
Nb	1249	821	180	206	285	244	155
Zr	7355	915	981	881	1250	1001	617
Y	710	133	87	66	72	66	42
Sr	38	50	362	290	230	438	375
Rb	371	581	269	225	215	220	125
Zn	132	455	133	144	141	133	102
Pb	29	100	14	15	23	9	9
U	5	57	9	6	8	5	5
Th	5	48	26	5	24	12	7
Ga	43	48	38	43	36	35	34
La	1032	152	146	73	109	91	98
Ce	1815	267	274	157	210	174	179
C.I.P.W. norms							
Quartz	18.2	2.1	0.0	0.0	0.0	0.0	0.0
Corundum	0.0	0.0	0.6	0.0	0.0	1.6	2.6
Zircon	1.5	0.2	0.2	0.2	0.3	0.2	0.1
Orthoclase	27.6	35.6	39.7	35.4	38.0	38.0	36.6
Albite	33.7	41.7	21.1	32.7	34.2	37.6	40.9
Anorthite	1.5	0.0	0.0	2.3	0.3	7.5	4.5
Nepheline	0.0	0.0	24.7	19.5	18.0	8.1	9.8
Acmite	0.0	3.9	7.0	0.0	0.0	0.0	0.0
Diopside	3.6	5.9	4.7	3.6	3.7	0.0	0.0
Wollastonite	0.0	1.7	0.0	0.0	0.0	0.0	0.0
Hypersthene	1.0	0.0	0.0	0.0	0.0	0.0	0.0
Olivine	0.0	0.0	1.4	1.0	0.9	1.8	1.3
Magnetite	12.2	8.3	0.0	4.7	3.9	4.5	3.7
Hematite	0.6	0.0	0.0	0.0	0.0	0.0	0.0
Ilmenite	0.1	0.6	0.4	0.3	0.3	0.4	0.4
Apatite	0.0	0.0	0.3	0.3	0.4	0.2	0.1
Lith. code	425	425	431	431	431	431	431
Camp site	Cmp.10	Cmp.10	Cmp.02	Cmp.17	Cmp.02	Cmp.07	Cmp.07
Colour index	16.90	14.80	6.73	9.97	9.30	6.93	5.45
Frac. index	79.47	83.29	92.44	87.60	90.13	83.70	87.30
Diff. index	79.50	79.40	85.50	87.60	90.10	83.70	87.30
Na/(Na+K)	0.56	0.58	0.67	0.67	0.65	0.59	0.63
(Na+K)/Al	0.95	1.06	1.10	0.96	0.99	0.80	0.81
Fe2O3/FeO	2.50	2.50	1.50	1.50	1.50	1.50	1.50

Whole-rock geochemical analyses - Motzfeldt So Formation.

Sample no.	326059	326121	326124	326049	54132	54141	243189
Disc type	Pd.2	Pd.2	Pd.2	Pd.2	Fs.1	Fs.1	Fs.2
Major elements (wt%)							
SiO2	56.95	55.71	53.45	56.12	56.89	53.83	55.29
Al2O3	20.22	19.55	20.41	20.22	20.01	18.74	20.13
Fe2O3T	3.90	5.53	5.28	4.80	4.06	7.88	4.67
MgO	0.49	0.60	0.53	0.33	0.36	0.50	0.73
CaO	1.43	1.55	2.17	1.52	1.35	1.78	1.15
Na2O	8.01	8.11	9.40	7.98	7.77	7.46	8.52
K2O	6.09	5.69	5.67	6.17	6.55	6.19	6.34
TiO2	0.43	0.52	0.42	0.28	0.52	0.71	0.33
MnO	0.17	0.19	0.19	0.20	0.17	0.32	0.22
P2O5	0.14	0.14	0.12	0.12	0.12	0.14	0.09
Total	97.83	97.59	97.64	97.74	97.79	97.53	97.47
Trace elements (p.p.m)							
Ba	728	249	287	245	705	236	489
Nb	247	245	189	160	205	231	248
Zr	1109	951	724	551	1005	1198	1215
Y	69	78	188	86	56	123	80
Sr	339	132	152	108	285	446	362
Rb	160	215	233	200	166	238	231
Zn	133	158	123	129	115	201	170
Pb	18	15	13	12	16	17	25
U	7	7	2	3	6	6	8
Th	17	9	33	17	11	13	29
Ga	31	33	36	30	31	49	37
La	127	137	374	281	83	85	134
Ce	246	269	738	477	132	146	245
C.I.P.W. norms							
Quartz	0.0	0.0	0.0	0.0	0.0	0.0	0.0
Zircon	0.2	0.2	0.1	0.1	0.2	0.2	0.3
Orthoclase	36.8	34.5	34.4	37.3	39.6	37.5	38.4
Albite	33.8	33.6	17.2	31.7	31.3	26.3	24.2
Anorthite	1.3	0.1	0.0	1.2	0.4	0.0	0.0
Nepheline	19.2	19.9	31.5	20.3	19.5	20.2	24.8
Acmite	0.0	0.0	5.5	0.0	0.0	1.1	3.5
Diopside	4.3	5.7	8.8	4.3	4.9	7.0	4.5
Wollastonite	0.0	0.0	0.0	0.3	0.0	0.0	0.0
Hypersthene	0.0	0.0	0.0	0.0	0.0	0.0	0.0
Olivine	0.4	0.5	0.1	0.0	0.1	0.5	1.5
Magnetite	3.3	4.7	1.7	4.1	3.5	6.2	2.2
Hematite	0.0	0.0	0.0	0.0	0.0	0.0	0.0
Ilmenite	0.3	0.4	0.4	0.4	0.3	0.6	0.4
Apatite	0.3	0.3	0.3	0.3	0.3	0.3	0.2
Lith. code	431	431	431	432	434	434	434
Camp site	Cmp.12	Cmp.13	Cmp.13	Cmp.12	Cmp.02	Cmp.02	Cmp.02
Colour index	8.70	11.60	11.30	9.07	9.06	14.70	8.83
Frac. index	89.80	88.00	88.60	89.40	90.37	85.10	90.92
Diff. index	89.80	88.00	83.00	89.40	90.40	84.00	87.40
Na/(Na+K)	0.67	0.68	0.72	0.66	0.64	0.65	0.67
(Na+K)/Al	0.98	1.00	1.06	0.98	0.99	1.01	1.04
Fe2O3/FeO	1.50	1.50	1.50	1.50	1.50	1.50	1.50

Whole-rock geochemical analyses – Motzfeldt So Formation.

Sample no.	304003	304009	326089	326090	326092	326151	304019
Disc type	Fs.1	Fs.1	Pd.2	Pd.2	Pd.2	Pd.2	Fs.1
Major elements (wt%)							
SiO2	55.86	52.58	57.93	56.37	56.78	54.43	58.18
Al2O3	20.53	20.44	19.68	19.83	20.27	18.30	19.26
Fe2O3T	3.67	5.90	4.18	4.91	4.75	7.34	5.52
MgO	0.43	0.69	0.60	0.83	0.75	0.64	0.20
CaO	1.35	1.78	1.16	1.51	1.46	1.79	1.01
Na2O	8.37	9.21	6.92	7.40	6.88	7.69	5.61
K2O	6.69	5.86	6.41	5.74	5.93	6.19	5.61
TiO2	0.59	0.28	0.53	0.69	0.60	0.55	0.30
MnO	0.15	0.21	0.17	0.18	0.18	0.24	0.18
P2O5	0.12	0.03	0.16	0.20	0.16	0.15	0.03
Total	97.78	96.98	97.74	97.66	97.76	97.32	95.91
Trace elements (p.p.m)							
Ba	902	471	899	910	698	242	131
Nb	116	284	176	200	225	231	628
Zr	563	1215	794	909	985	649	5022
Y	52	82	58	56	54	73	196
Sr	338	236	328	392	344	86	81
Rb	216	244	188	156	174	271	282
Zn	93	124	125	137	130	136	277
Pb	8	9	11	9	11	1	133
U	4	2	8	8	6	2	21
Th	4	7	11	8	6	10	58
Ga	28	45	30	30	29	36	51
La	53	68	79	84	79	94	317
Ce	109	155	151	176	151	205	558
C.I.P.W. norms							
Quartz	0.0	0.0	0.0	0.0	0.0	0.0	0.7
Zircon	0.1	0.3	0.2	0.2	0.2	0.1	1.0
Orthoclase	40.5	35.7	38.8	34.7	35.9	37.7	34.4
Albite	23.6	15.7	38.2	36.7	37.8	24.0	49.3
Anorthite	0.0	0.0	3.8	4.0	6.5	0.0	5.0
Nepheline	25.1	32.0	11.8	14.9	11.8	20.3	0.0
Acmite	2.3	4.9	0.0	0.0	0.0	4.9	0.0
Diopside	5.3	7.6	1.0	2.1	0.0	7.0	0.0
Corundum	0.0	0.0	0.0	0.0	0.2	0.0	2.3
Hypersthene	0.0	0.0	0.0	0.0	0.0	0.0	2.1
Olivine	0.6	0.7	2.0	2.4	2.8	1.4	0.0
Magnetite	2.0	2.6	3.6	4.2	4.0	3.8	4.8
Hematite	0.0	0.0	0.0	0.0	0.0	0.0	0.0
Ilmenite	0.3	0.4	0.3	0.4	0.3	0.5	0.4
Apatite	0.3	0.1	0.4	0.5	0.4	0.4	0.1
Lith. code	434	434	434	434	434	434	435
Camp site	Cmp.02	Cmp.02	Cmp.02	Cmp.02	Cmp.02	Cmp.14	Cmp.02
Colour index	8.45	11.36	7.30	9.50	7.63	13.04	7.30
Frac. index	91.43	88.40	88.70	86.30	85.50	86.80	84.40
Diff. index	89.20	83.50	88.70	86.30	85.50	81.90	84.40
Na/(Na+K)	0.66	0.70	0.62	0.66	0.64	0.65	0.60
(Na+K)/Al	1.02	1.05	0.93	0.93	0.88	1.06	0.79
Fe2O3/FeO	1.50	1.50	1.50	1.50	1.50	1.50	1.50

Whole-rock geochemical analyses - Motzfeldt So Formation.

Sample no.	304020
Disc type	Fs.1
Major elements (wt%)	
SiO2	55.44
Al2O3	19.71
Fe2O3T	5.33
MgO	0.81
CaO	2.03
Na2O	7.13
K2O	6.32
TiO2	0.99
MnO	0.21
P2O5	0.26
Total	98.24
Trace elements (p.p.m)	
Ba	575
Nb	116
Zr	487
Y	44
Sr	193
Rb	159
Zn	113
Pb	7
U	2
Th	3
Ga	25
La	65
Ce	123
C.I.P.W. norms	
Quartz	0.0
Zircon	0.1
Orthoclase	38.0
Albite	29.1
Anorthite	3.2
Nepheline	17.5
Acmite	0.0
Diopside	4.6
Wollastonite	0.0
Hypersthene	0.0
Olivine	1.9
Magnetite	4.5
Hematite	0.0
Ilmenite	0.4
Apatite	0.6
Lith. code	435
Camp site	Cmp.02
Colour index	12.00
Frac. index	84.70
Diff. index	84.70
Na/(Na+K)	0.63
(Na+K)/Al	0.94
Fe2O3/FeO	1.50

Whole-rock geochemical analyses – Flinks Dal Formation.

Sample no.	304127	304024	304036	304749	304758	326042	326058
Disc type	Fs.1	Fs.1	Fs.1	Fs.1	Pd.1	Pd.2	Pd.2
Major elements (wt%)							
SiO2	56.14	54.70	55.16	53.83	55.46	57.73	56.24
Al2O3	20.39	19.86	20.55	18.82	21.65	20.63	20.19
Fe2O3T	5.42	5.45	5.05	6.61	5.87	4.19	4.74
MgO	0.37	0.48	0.46	0.88	0.85	0.52	0.46
CaO	1.37	1.49	1.29	2.09	1.63	1.37	1.11
Na2O	8.00	8.51	9.06	6.74	6.99	6.55	8.65
K2O	5.49	5.88	6.10	5.66	6.15	6.14	5.63
TiO2	0.49	0.56	0.46	0.79	0.44	0.42	0.38
MnO	0.27	0.26	0.26	0.29	0.24	0.19	0.23
P2O5	0.18	0.21	0.14	0.43	0.12	0.14	0.16
Total	98.12	97.41	98.53	96.14	99.40	97.88	97.79
Trace elements (p.p.m)							
Ba	671	966	664	1219	687	350	571
Nb	237	213	193	226	206	185	194
Zr	714	795	771	963	812	673	763
Y	72	67	65	73	66	60	77
Sr	339	452	354	809	541	207	284
Rb	170	180	189	176	195	178	197
Zn	139	167	156	174	165	123	141
Pb	13	15	12	13	14	10	0
U	2	8	6	8	6	2	6
Th	10	7	5	6	7	7	4
Ga	35	35	34	34	35	32	34
La	136	112	117	125	111	115	128
Ce	245	236	234	245	233	218	261
C.I.P.W. norms							
Quartz	0.0	0.0	0.0	0.0	0.0	0.0	0.0
Zircon	0.1	0.2	0.2	0.2	0.2	0.1	0.2
Orthoclase	33.1	35.7	36.7	34.8	36.6	37.1	34.1
Albite	36.4	26.4	22.1	32.8	30.2	40.1	34.1
Anorthite	3.6	0.0	0.0	4.6	7.5	6.1	0.0
Nepheline	17.7	24.3	27.5	14.4	15.9	9.0	21.8
Acmite	0.0	2.3	4.4	0.0	0.0	0.0	0.6
Diopside	2.0	5.5	4.9	3.0	0.0	0.0	4.0
Corundum	0.0	0.0	0.0	0.0	0.8	1.1	0.0
Hypersthene	0.0	0.0	0.0	0.0	0.0	0.0	0.0
Olivine	2.3	1.8	2.1	3.8	4.0	2.9	1.5
Magnetite	3.8	2.7	1.3	4.7	4.1	2.9	3.0
Hematite	0.0	0.0	0.0	0.0	0.0	0.0	0.0
Ilmenite	0.5	0.5	0.5	0.6	0.5	0.4	0.4
Apatite	0.4	0.5	0.3	1.1	0.3	0.3	0.4
Lith. code	511	514	514	514	514	514	514
Camp site	Cmp.07	Cmp.02	Cmp.02	Cmp.02	Cmp.02	Cmp.12	Cmp.12
Colour index	9.10	11.00	9.20	13.20	8.80	6.50	9.30
Frac. index	87.20	88.83	90.77	82.10	82.80	86.20	90.50
Diff. index	87.20	86.50	86.30	82.10	82.70	86.20	89.90
Na/(Na+K)	0.69	0.69	0.69	0.64	0.63	0.62	0.70
(Na+K)/Al	0.94	1.03	1.05	0.91	0.84	0.84	1.01
Fe2O3/FeO	1.00	1.00	1.00	1.00	1.00	1.00	1.00

Whole-rock geochemical analyses – Flinks Dal Formation.

Sample no.	326069	326074	326077	326078	326146	326173	304751
Disc type	Pd.2	Pd.2	Pd.2	Pd.2	Pd.2	Pd.2	Fs.1
Major elements (wt%)							
SiO2	54.79	56.54	56.38	55.51	57.14	56.16	54.02
Al2O3	17.86	19.96	19.62	19.74	21.42	19.29	18.76
Fe2O3T	7.16	4.68	4.85	5.23	4.50	4.83	7.11
MgO	0.71	0.56	0.58	0.55	0.60	0.65	0.26
CaO	1.60	1.18	1.15	1.21	1.35	1.25	1.24
Na2O	9.05	8.09	8.62	9.03	6.20	8.46	7.88
K2O	4.89	5.91	5.64	5.46	5.97	6.06	5.33
TiO2	0.60	0.46	0.44	0.50	0.44	0.47	0.42
MnO	0.32	0.21	0.23	0.25	0.22	0.24	0.46
P2O5	0.34	0.17	0.17	0.19	0.15	0.18	0.07
Total	97.32	97.76	97.68	97.67	97.99	97.59	95.54
Trace elements (p.p.m)							
Ba	1010	806	730	616	877	764	358
Nb	310	168	232	243	165	174	596
Zr	1098	657	948	1022	656	739	2814
Y	95	66	69	69	57	71	148
Sr	483	356	404	339	655	393	348
Rb	215	188	183	183	175	177	264
Zn	241	144	174	186	138	170	359
Pb	12	9	16	13	8	14	39
U	10	6	7	10	5	5	19
Th	10	5	10	6	2	17	37
Ga	45	34	36	34	32	33	46
La	-1	113	127	132	102	129	277
Ce	-1	227	237	252	207	255	536
C.I.P.W. norms							
Corundum	0.0	0.0	0.0	0.0	2.7	0.0	0.0
Sod. metasil.	0.2	0.0	0.0	0.0	0.0	0.0	0.0
Zircon	0.2	0.1	0.2	0.2	0.1	0.2	0.6
Orthoclase	29.7	35.8	34.2	33.1	36.0	36.7	33.0
Albite	26.9	34.6	32.3	28.7	41.5	26.8	35.3
Anorthite	0.0	0.7	0.0	0.0	6.0	0.0	0.1
Nepheline	21.5	19.2	21.1	23.9	6.5	21.9	18.6
Acmite	10.1	0.0	3.1	4.8	0.0	5.5	0.0
Diopside	5.3	3.7	4.1	4.3	0.0	4.5	5.2
Wollastonite	0.0	0.0	0.0	0.0	0.0	0.0	0.0
Hypersthene	0.0	0.0	0.0	0.0	0.0	0.0	0.0
Olivine	4.6	1.8	2.3	2.8	3.1	2.8	0.6
Magnetite	0.0	3.3	1.9	1.3	3.2	0.6	5.6
Hematite	0.0	0.0	0.0	0.0	0.0	0.0	0.0
Ilmenite	0.6	0.4	0.4	0.5	0.4	0.5	0.9
Apatite	0.8	0.4	0.4	0.5	0.4	0.4	0.2
Lith. code	514	514	514	514	514	514	521
Camp site	Cmp.12	Cmp.02	Cmp.02	Cmp.02	Cmp.14	Cmp.15	Cmp.07
Colour index	11.40	9.60	9.20	9.30	7.10	8.90	12.41
Frac. index	88.40	89.60	90.60	90.50	84.10	90.90	86.90
Diff. index	78.10	89.60	87.50	85.70	84.10	85.40	86.90
Na/(Na+K)	0.74	0.68	0.70	0.72	0.61	0.68	0.69
(Na+K)/Al	1.13	0.99	1.03	1.05	0.78	1.06	1.00
Fe2O3/FeO	1.00	1.00	1.00	1.00	1.00	1.00	1.20

Whole-rock geochemical analyses – Flinks Dal Formation.

Sample no.	326129	304005	304010	326081	326104	326105	326113
Disc type	Pd.2	Fs.1	Fs.1	Pd.2	Pd.2	Pd.2	Pd.2
Major elements (wt%)							
SiO2	54.04	54.59	57.95	55.23	56.20	57.50	53.81
Al203	20.10	21.84	19.99	19.86	22.24	20.27	21.19
Fe203T	6.67	5.04	5.95	5.50	5.31	4.59	6.93
MgO	0.32	0.17	0.35	0.47	0.61	0.45	0.23
CaO	1.26	0.93	0.63	1.26	1.28	0.91	1.20
Na20	9.17	6.63	6.56	9.39	5.87	7.30	8.52
K20	5.43	5.92	4.90	5.23	5.83	6.22	4.96
TiO2	0.25	0.26	0.35	0.33	0.37	0.24	0.66
MnO	0.33	0.25	0.29	0.29	0.25	0.24	0.28
P205	0.06	0.05	0.05	0.09	0.07	0.07	0.06
Total	97.63	95.68	97.01	97.65	98.03	97.79	97.84
Trace elements (p.p.m)							
Ba	16	208	424	105	376	400	62
Nb	330	202	195	342	185	251	388
Zr	1144	1038	867	1360	627	1055	603
Y	149	106	-1	95	55	74	151
Sr	36	386	213	142	397	324	86
Rb	277	206	150	224	202	228	290
Zn	195	170	185	209	137	164	249
Pb	22	16	11	21	6	12	22
U	4	2	4	9	3	5	7
Th	29	12	0	19	1	6	21
Ga	43	43	37	41	37	38	51
La	261	91	181	206	88	134	262
Ce	518	148	315	421	185	269	634
C.I.P.W. norms							
Corundum	0.0	3.1	2.9	0.0	4.2	0.0	0.0
Zircon	0.2	0.2	0.2	0.3	0.1	0.2	0.1
Orthoclase	32.9	36.6	29.9	31.7	35.2	37.6	30.0
Albite	25.6	37.8	55.0	27.7	42.2	37.8	33.5
Anorthite	0.0	4.5	3.0	0.0	6.1	4.2	5.0
Nepheline	26.8	11.3	1.3	25.5	4.6	13.7	21.8
Acmite	4.0	0.0	0.0	5.8	0.0	0.0	0.0
Diopside	5.2	0.0	0.0	5.0	0.0	0.0	0.6
Wollastonite	0.0	0.0	0.0	0.0	0.0	0.0	0.0
Hypersthene	0.0	0.0	0.0	0.0	0.0	0.0	0.0
Olivine	1.3	1.9	2.5	1.9	2.8	2.2	2.8
Magnetite	3.1	4.0	4.6	1.3	4.1	3.5	5.3
Hematite	0.0	0.0	0.0	0.0	0.0	0.0	0.0
Ilmenite	0.6	0.5	0.6	0.6	0.5	0.5	0.5
Apatite	0.1	0.1	0.1	0.2	0.2	0.2	0.1
Lith. code	521	522	522	524	524	524	524
Camp site	Cmp.13	Cmp.02	Cmp.02	Cmp.02	Cmp.02	Cmp.02	Cmp.13
Colour index	10.20	6.50	7.80	9.00	7.60	6.30	9.40
Frac. index	89.50	85.80	86.10	90.70	80.00	89.20	85.40
Diff. index	85.30	85.70	86.10	84.90	82.00	89.20	85.40
Na/(Na+K)	0.72	0.63	0.67	0.73	0.60	0.64	0.72
(Na+K)/Al	1.04	0.79	0.80	1.06	0.72	0.92	0.91
Fe203/FeO	1.20	1.20	1.20	1.20	1.20	1.20	1.20

Whole-rock geochemical analyses - Flinks Dal Formation.

Sample no.	326114	326133	326147	326195	326196	304106	304107
Disc type	Pd.2	Pd.2	Pd.2	Pd.2	Pd.2	Fs.1	Fs.1
Major elements (wt%)							
SiO2	51.74	56.05	55.61	60.46	56.37	55.92	54.24
Al2O3	20.13	20.15	20.42	14.26	19.66	18.56	18.83
Fe2O3T	9.98	5.20	6.19	7.89	4.99	8.53	4.36
MgO	0.60	0.34	0.26	0.32	0.59	0.32	0.72
CaO	2.06	1.17	1.15	1.34	1.10	1.68	1.58
Na2O	8.05	8.53	8.06	6.80	8.34	5.64	6.32
K2O	4.05	5.81	5.50	5.02	5.85	5.64	6.94
TiO2	0.63	0.23	0.25	0.53	0.39	0.71	0.68
MnO	0.35	0.19	0.24	0.25	0.24	0.23	0.16
P2O5	0.07	0.06	0.07	0.09	0.16	0.10	0.28
Total	97.66	97.73	97.75	96.96	97.69	97.33	94.11
Trace elements (p.p.m)							
Ba	55	24	22	47	638	365	1108
Nb	267	193	156	245	211	185	125
Zr	1385	743	789	1196	814	738	552
Y	79	59	66	103	70	50	44
Sr	130	24	23	39	219	448	215
Rb	243	237	251	202	208	151	140
Zn	310	149	156	242	171	123	67
Pb	16	13	6	21	12	13	9
U	9	2	2	8	4	2	4
Th	9	5	0	22	10	7	4
Ga	50	39	43	41	36	39	26
La	123	69	79	270	129	105	63
Ce	233	136	168	496	256	185	118
C.I.P.W. norms							
Corundum	0.0	0.0	0.0	0.0	0.0	0.3	0.0
Zircon	0.3	0.2	0.2	0.2	0.2	0.2	0.1
Orthoclase	24.6	35.2	33.3	30.7	35.4	34.4	43.6
Albite	34.1	32.4	36.0	46.9	33.0	41.3	27.2
Anorthite	7.0	0.0	3.4	0.0	0.0	8.0	2.7
Nepheline	19.4	22.0	18.4	0.0	20.2	4.3	16.1
Acmite	0.0	0.8	0.0	11.1	1.8	0.0	0.0
Diopside	2.6	4.7	1.7	5.5	3.9	0.0	3.4
Wollastonite	0.0	0.0	0.0	0.0	0.0	0.0	0.0
Hypersthene	0.0	0.0	0.0	3.1	0.0	0.0	0.0
Olivine	3.4	0.6	1.6	1.2	1.7	5.5	3.1
Magnetite	7.7	3.6	4.8	0.6	2.9	5.3	2.8
Hematite	0.0	0.0	0.0	0.0	0.0	0.0	0.0
Ilmenite	0.7	0.4	0.5	0.5	0.5	0.5	0.3
Apatite	0.2	0.1	0.2	0.2	0.4	0.2	0.7
Lith. code	524	524	524	521	524	531	531
Camp site	Cmp.13	Cmp.14	Cmp.14	Cmp.15	Cmp.15	Cmp.07	Cmp.07
Colour index	14.60	9.40	8.80	11.10	9.40	11.50	10.30
Frac. index	78.10	90.40	87.70	88.60	90.40	80.00	86.90
Diff. index	78.10	89.60	87.70	77.60	88.60	80.00	86.90
Na/(Na+K)	0.75	0.69	0.69	0.67	0.68	0.60	0.58
(Na+K)/Al	0.88	1.01	0.94	1.17	1.02	0.83	0.95
Fe2O3/FeO	1.20	1.20	1.20	1.20	1.20	0.80	0.80

Whole-rock geochemical analyses – Flinks Dal Formation.

Sample no.	304125	304131	272491	272510	304113
Disc type	Pd.1	Pd.1	Pd.1	Pd.3	Fs.1
Major elements (wt%)					
SiO2	55.40	54.37	55.27	57.24	56.60
Al2O3	18.78	18.34	22.04	20.22	21.18
Fe2O3T	5.95	7.32	4.01	4.77	4.17
MgO	0.96	0.93	0.60	0.44	0.30
CaO	2.13	2.14	1.15	1.03	0.90
Na2O	6.90	7.63	9.58	9.11	5.80
K2O	5.89	5.53	5.74	5.80	6.48
TiO2	0.62	1.07	0.43	0.34	0.42
MnO	0.24	0.33	0.14	0.20	0.17
P2O5	0.26	0.51	0.14	0.14	0.21
Total	97.13	98.17	99.10	99.29	96.22
Trace elements (p.p.m)					
Ba	779	408	725	450	1264
Nb	187	313	160	282	185
Zr	775	648	634	1365	747
Y	63	77	49	68	59
Sr	405	239	405	244	691
Rb	147	168	168	219	210
Zn	135	145	107	108	115
Pb	9	16	9	9	11
U	3	4	4	6	5
Th	7	10	10	0	7
Ga	30	24	38	40	31
La	122	185	71	84	81
Ce	235	429	136	170	155
C.I.P.W. norms					
Corundum	0.0	0.0	0.0	0.0	3.5
Zircon	0.2	0.1	0.1	0.3	0.2
Orthoclase	35.9	33.4	34.3	34.5	39.8
Albite	32.6	30.4	26.3	29.2	41.2
Anorthite	3.0	0.0	0.2	0.0	3.5
Nepheline	15.0	18.7	30.1	23.3	5.3
Acmite	0.0	0.9	0.0	4.8	0.0
Diopside	5.4	6.4	4.1	3.7	0.0
Wollastonite	0.0	0.0	0.0	0.0	0.0
Hypersthene	0.0	0.0	0.0	0.0	0.0
Olivine	3.2	4.1	1.9	2.9	3.0
Magnetite	3.7	4.1	2.5	0.5	2.6
Hematite	0.0	0.0	0.0	0.0	0.0
Ilmenite	0.5	0.6	0.3	0.4	0.3
Apatite	0.6	1.2	0.3	0.3	0.5
Lith. code	531	531	534	534	534
Camp site	Cmp.07	Cmp.07	Cmp.12	Cmp.12	Cmp.07
Colour index	13.40	16.50	9.00	7.90	6.50
Frac. index	83.50	83.40	90.70	91.90	86.40
Diff. index	83.50	82.50	90.70	87.10	86.40
Na/(Na+K)	0.64	0.68	0.72	0.70	0.58
(Na+K)/Al	0.94	1.01	1.00	1.05	0.78
Fe2O3/FeO	0.80	0.80	0.80	0.80	0.80

Whole-rock geochemical analyses – Alkali-gabbro dyke.

Sample no.	58083	58116	59631	59602	272493	272513	272527
Disc type	Pd.3	Pd.3	Pd.3	Pd.3	Pd.3	Pd.3	Pd.3
Major elements (wt%)							
SiO2	52.12	47.02	48.34	48.38	47.11	47.01	45.61
Al2O3	16.08	16.36	18.10	18.64	16.46	16.50	16.40
Fe2O3T	9.66	13.84	11.59	11.47	13.30	13.83	14.82
MgO	3.03	5.31	3.74	3.52	4.07	4.20	4.51
CaO	4.77	7.54	9.06	9.15	8.16	7.96	8.25
Na2O	4.82	3.85	3.99	3.99	4.39	3.98	3.91
K2O	4.58	1.99	1.51	1.36	1.95	1.94	1.83
TiO2	2.92	2.83	2.54	2.28	2.83	2.77	3.16
MnO	0.26	0.17	0.13	0.12	0.16	0.16	0.17
P2O5	1.76	1.49	1.27	1.10	1.91	1.74	1.84
Total	100.00	100.40	100.27	100.01	100.34	100.09	100.50
Trace elements (p.p.m)							
Ba	4965	1520	1263	1292	1555	1665	1551
Nb	97	30	21	19	30	31	29
Zr	634	272	279	275	272	246	259
Y	44	26	20	18	29	29	-1
Sr	3280	1191	1572	1603	1108	1099	1136
Rb	84	27	18	17	29	24	25
Zn	156	75	61	61	77	73	85
Pb	3	2	0	1	6	0	0
U	19	5	10	8	7	7	7
Th	0	0	0	0	0	0	0
Ga	23	19	17	19	20	20	18
La	97	32	22	18	35	40	36
Ce	168	57	57	44	68	68	61
C.I.P.W. norms							
Quartz	0.0	0.0	0.0	0.0	0.0	0.0	0.0
Zircon	0.1	0.1	0.1	0.1	0.1	0.0	0.1
Orthoclase	27.2	11.8	9.0	8.1	11.6	11.6	10.9
Albite	30.2	25.1	28.0	28.5	25.9	26.5	22.5
Anorthite	8.7	21.6	27.2	29.2	19.6	21.6	21.9
Nepheline	5.8	4.2	3.2	3.0	6.2	4.0	5.8
Acmite	0.0	0.0	0.0	0.0	0.0	0.0	0.0
Diopside	3.8	5.5	8.4	8.2	7.6	6.0	6.3
Wollastonite	0.0	0.0	0.0	0.0	0.0	0.0	0.0
Hypersthene	0.0	0.0	0.0	0.0	0.0	0.0	0.0
Olivine	17.3	24.8	18.3	17.6	21.3	22.6	24.5
Magnetite	2.1	3.1	2.6	2.6	3.0	3.1	3.3
Hematite	0.0	0.0	0.0	0.0	0.0	0.0	0.0
Ilmenite	0.5	0.3	0.2	0.2	0.3	0.3	0.3
Apatite	4.2	3.5	3.0	2.6	4.5	4.2	4.4
Lith. code	611	611	611	614	614	614	614
Camp site	Cmp.12	Cmp.12	Cmp.12	Cmp.12	Cmp.12	Cmp.12	Cmp.12
Colour index	23.90	37.30	32.60	31.20	36.70	36.20	38.80
Frac. index	63.20	41.10	40.20	39.60	43.70	42.10	39.20
Diff. index	63.20	41.10	40.20	39.60	43.70	42.10	39.20
Na/(Na+K)	0.62	0.75	0.80	0.82	0.77	0.76	0.76
(Na+K)/Al	0.80	0.52	0.45	0.43	0.57	0.52	0.51
Fe2O3/FeO	0.20	0.20	0.20	0.20	0.20	0.20	0.20

Whole-rock geochemical analyses - Larvikite ring-dyke.

Sample no.	58036	58062	272429
Disc type	Pd.3	Pd.3	Pd.3
Major elements (wt%)			
SiO2	51.10	53.87	54.22
Al2O3	15.82	16.51	17.25
Fe2O3T	12.07	11.19	8.92
MgO	2.72	1.41	2.04
CaO	5.65	4.25	4.92
Na2O	4.38	4.85	4.47
K2O	3.92	4.56	4.54
TiO2	2.47	1.95	2.07
MnO	0.29	0.30	0.18
P2O5	1.89	1.24	1.24
Total	100.31	100.13	99.85
Trace elements (p.p.m)			
Ba	4596	3216	4006
Nb	49	108	68
Zr	334	467	429
Y	35	52	37
Sr	1362	1072	1841
Rb	43	110	84
Zn	141	173	97
Pb	2	8	2
U	5	6	11
Th	0	0	0
Ga	20	28	24
La	64	87	47
Ce	115	138	99
C.I.P.W. norms			
Quartz	0.0	0.0	0.0
Zircon	0.1	0.1	0.1
Orthoclase	23.2	27.1	27.0
Albite	32.5	37.0	36.2
Anorthite	12.0	9.9	13.7
Nepheline	2.5	2.3	1.0
Acmite	0.0	0.0	0.0
Diopside	4.0	3.3	3.0
Wollastonite	0.0	0.0	0.0
Hypersthene	0.0	0.0	0.0
Olivine	16.9	13.4	13.0
Magnetite	3.7	3.5	2.8
Hematite	0.0	0.0	0.0
Ilmenite	0.6	0.6	0.3
Apatite	4.5	3.0	3.0
Lith. code	624	624	624
Camp site	Cmp.17	Cmp.17	Cmp.17
Colour index	29.70	23.70	22.10
Frac. index	58.30	66.40	63.40
Diff. index	58.30	66.40	64.20
Na/(Na+K)	0.63	0.62	0.60
(Na+K)/Al	0.72	0.78	0.71
Fe2O3/FeO	0.30	0.30	0.30

Whole-rock geochemical analyses - Laminated alkali syenite.

Sample no.	63720	304735	58399	58400	304078	304085	304089
Disc type	Pd.3	Pd.1	Pd.3	Pd.3	Fs.1	Fs.1	Fs.1
Major elements (wt%)							
SiO2	61.05	57.31	60.86	60.27	59.72	60.25	59.94
Al2O3	15.91	13.98	16.02	15.65	16.02	15.77	15.55
Fe2O3T	8.52	10.37	8.26	9.16	7.42	7.85	8.04
MgO	0.34	1.17	0.61	0.53	0.13	0.30	0.31
CaO	1.75	2.09	2.15	2.20	1.95	2.02	2.05
Na2O	6.00	5.04	5.52	5.57	6.72	6.17	6.22
K2O	5.29	5.41	5.56	5.24	5.07	5.39	5.18
TiO2	0.70	0.87	0.53	0.89	0.46	0.65	0.79
MnO	0.25	0.31	0.21	0.31	0.19	0.27	0.29
P2O5	0.09	0.12	0.16	0.17	0.01	0.07	0.09
Total	99.90	96.67	99.88	99.99	97.70	98.76	98.46
Trace elements (p.p.m)							
Ba	160	466	515	648	61	102	213
Nb	177	225	222	202	537	106	176
Zr	631	922	503	595	1487	259	378
Y	74	97	88	79	163	53	-1
Sr	35	80	98	77	37	35	47
Rb	217	227	231	202	433	169	174
Zn	202	257	202	235	211	152	162
Pb	17	22	21	29	17	4	11
U	0	5	3	3	11	0	5
Th	3	13	22	8	25	2	0
Ga	40	40	38	35	45	34	38
La	146	169	205	150	288	119	130
Ce	322	342	384	278	541	267	280
C.I.P.W. norms							
Quartz	0.0	0.0	0.0	0.0	0.0	0.0	0.0
Zircon	0.1	0.2	0.1	0.1	0.3	0.1	0.1
Orthoclase	31.5	33.3	33.1	31.1	30.8	32.4	31.2
Albite	51.1	43.5	47.0	47.4	47.9	49.0	49.5
Anorthite	0.9	0.0	2.5	2.2	0.0	0.0	0.0
Nepheline	0.0	0.0	0.0	0.0	4.2	1.7	1.5
Acmite	0.0	0.8	0.0	0.0	2.5	1.0	1.3
Diopside	6.4	8.7	6.3	6.8	8.8	8.6	8.6
Wollastonite	0.0	0.0	0.0	0.0	0.0	0.0	0.0
Hypersthene	3.2	3.3	6.5	6.7	0.0	0.0	0.0
Olivine	2.8	5.6	0.5	1.0	3.5	4.0	4.5
Magnetite	3.3	3.7	3.2	3.5	1.7	2.6	2.5
Hematite	0.0	0.0	0.0	0.0	0.0	0.0	0.0
Ilmenite	0.5	0.6	0.4	0.6	0.4	0.5	0.6
Apatite	0.2	0.3	0.4	0.4	0.0	0.2	0.2
Lith. code	631	632	634	634	634	634	634
Camp site	Cmp.06	Cmp.10	Cmp.06	Cmp.06	Cmp.06	Cmp.06	Cmp.06
Colour index	16.50	22.20	17.03	19.10	14.40	15.90	16.40
Frac. index	82.60	77.60	80.10	78.50	75.30	84.00	83.60
Diff. index	82.50	76.80	80.10	78.50	82.90	83.10	82.20
Na/(Na+K)	0.63	0.59	0.60	0.62	0.67	0.64	0.65
(Na+K)/Al	0.98	1.01	0.94	0.95	1.03	1.01	1.02
Fe2O3/FeO	0.40	0.40	0.40	0.40	0.40	0.40	0.40

Whole-rock geochemical analyses – Laminated alkali syenite.

Sample no.	304717	304718	304738
Disc type	Fs.1	Fs.1	Fs.1
Major elements (wt%)			
SiO2	59.00	60.73	60.03
Al203	15.18	15.81	15.37
Fe203T	9.00	6.25	8.10
MgO	0.43	0.26	0.40
CaO	2.04	2.05	1.95
Na20	6.44	6.38	6.43
K20	4.93	5.47	5.09
TiO2	0.83	0.37	0.75
MnO	0.30	0.21	0.26
P205	0.13	0.04	0.15
Total	98.27	97.57	98.54
Trace elements (p.p.m)			
Ba	467	298	240
Nb	382	178	280
Zr	1123	1695	763
Y	120	89	91
Sr	71	74	43
Rb	221	251	194
Zn	288	201	217
Pb	30	41	20
U	8	4	6
Th	46	27	20
Ga	35	35	32
La	302	183	194
Ce	576	348	345
C.I.P.W. norms			
Quartz	0.0	0.0	0.0
Zircon	0.2	0.3	0.2
Orthoclase	29.8	33.2	30.7
Albite	46.6	48.2	48.5
Anorthite	0.0	0.0	0.0
Nepheline	2.8	2.2	1.8
Acmite	3.4	2.8	3.3
Diopside	8.4	9.0	7.8
Wollastonite	0.0	0.0	0.0
Hypersthene	0.0	0.0	0.0
Olivine	6.0	2.7	5.4
Magnetite	1.8	1.0	1.5
Hematite	0.0	0.0	0.0
Ilmenite	0.6	0.4	0.5
Apatite	0.3	0.1	0.4
Lith. code	634	634	634
Camp site	Cmp.10	Cmp.10	Cmp.10
Colour index	17.20	13.20	15.60
Frac. index	82.60	86.40	84.20
Diff. index	79.20	83.60	80.90
Na/(Na+K)	0.67	0.64	0.66
(Na+K)/Al	1.05	1.04	1.05
Fe203/FeO	0.40	0.40	0.40

Whole-rock geochemical analyses - Laminated porphyritic syenite.

Sample no.	54161	63793	242241	304028	304093	326097	326098
Disc type	Pd.3	Pd.3	Fs.2	Fs.1	Pd.2	Pd.2	Pd.2
Major elements (wt%)							
SiO2	62.64	61.39	59.96	60.41	60.30	61.23	60.45
Al2O3	15.70	15.31	14.33	14.15	13.72	14.05	13.97
Fe2O3T	8.48	9.91	9.24	9.34	8.79	7.80	8.81
MgO	0.16	0.19	0.31	0.23	0.26	0.28	0.37
CaO	0.85	1.15	1.63	1.32	1.39	1.05	1.13
Na2O	5.94	6.09	6.87	6.91	7.05	6.57	6.18
K2O	5.17	5.00	5.01	5.01	4.47	5.04	4.90
TiO2	0.60	0.65	0.68	0.62	0.55	0.56	0.74
MnO	0.30	0.32	0.29	0.32	0.32	0.26	0.33
P2O5	0.08	0.08	0.0	0.07	0.10	0.08	0.10
Total	99.92	100.09	98.32	98.39	96.95	96.92	96.98
Trace elements (p.p.m)							
Ba	158	94	44	124	23	101	153
Nb	336	273	332	361	475	239	330
Zr	1443	999	1475	1714	1619	1221	911
Y	116	130	130	155	154	102	106
Sr	67	25	72	37	34	36	56
Rb	197	230	231	220	255	178	170
Zn	341	345	309	312	555	292	306
Pb	26	44	37	61	91	37	34
U	11	6	12	14	17	9	8
Th	32	27	25	52	81	20	33
Ga	46	46	44	41	47	38	34
La	475	473	263	327	551	282	325
Ce	785	587	538	600	888	488	616
C.I.P.W. norms							
Quartz	5.3	3.5	0.0	0.0	0.3	2.0	3.2
Zircon	0.3	0.2	0.3	0.4	0.3	0.3	0.2
Orthoclase	30.6	29.6	30.2	30.1	27.3	30.8	29.9
Albite	50.4	51.0	44.6	45.7	47.2	45.7	46.1
Anorthite	0.9	0.0	0.0	0.0	0.0	0.0	0.0
Nepheline	0.0	0.0	1.2	0.0	0.0	0.0	0.0
Acmite	0.0	0.5	11.1	12.2	12.7	10.4	7.0
Diopside	2.5	4.6	7.2	5.5	5.7	4.3	4.5
Wollastonite	0.0	0.0	0.0	0.0	0.0	0.0	0.0
Hypersthene	2.8	2.5	0.0	0.8	5.1	5.0	4.8
Olivine	0.0	0.0	3.4	3.4	0.0	0.0	0.0
Magnetite	6.4	7.2	1.5	1.1	0.5	0.9	3.3
Hematite	0.0	0.0	0.0	0.0	0.0	0.0	0.0
Ilmenite	0.6	0.6	0.6	0.6	0.6	0.5	0.6
Apatite	0.2	0.2	0.0	0.2	0.2	0.2	0.2
Lith. code	641	641	641	641	641	641	641
Camp site	Cmp.02	Cmp.05	Cmp.06	Cmp.02	Cmp.06	Cmp.02	Cmp.02
Colour index	12.50	15.10	12.70	11.60	12.20	10.80	13.50
Frac. index	86.30	84.70	87.00	88.10	87.50	88.90	86.30
Diff. index	86.30	84.10	75.90	75.90	74.80	78.50	79.30
Na/(Na+K)	0.64	0.65	0.68	0.68	0.71	0.66	0.66
(Na+K)/Al	0.98	1.01	1.17	1.19	1.20	1.16	1.11
Fe2O3/FeO	1.20	1.20	1.20	1.20	1.20	1.20	1.20

Whole-rock geochemical analyses – Laminated porphyritic syenite.

Sample no.	54234	54240	304032	304195	326013	326087	326140
Disc type	Fs.1	Pd.3	Fs.1	Fs.1	Pd.2	Pd.2	Pd.2
Major elements (wt%)							
SiO2	61.65	61.41	61.19	59.98	60.73	60.75	59.72
Al2O3	15.16	15.41	14.52	14.36	14.45	14.62	13.76
Fe2O3T	8.10	9.98	8.18	8.97	7.40	7.46	9.33
MgO	0.11	0.16	0.10	0.19	0.29	0.33	0.30
CaO	0.68	1.11	1.37	1.61	1.43	1.25	1.66
Na2O	6.40	5.76	7.08	7.06	6.81	6.65	6.41
K2O	5.27	5.10	5.01	4.98	5.10	5.08	4.75
TiO2	0.62	0.82	0.51	0.54	0.46	0.47	0.65
MnO	0.29	0.23	0.31	0.26	0.21	0.27	0.32
P2O5	0.05	0.08	0.04	0.06	0.08	0.08	0.09
Total	98.33	100.06	98.31	98.01	96.96	96.96	96.99
Trace elements (p.p.m)							
Ba	91	70	50	79	52	72	38
Nb	202	282	351	218	351	219	512
Zr	938	1070	1596	741	1361	861	2292
Y	92	115	139	85	140	84	223
Sr	27	31	24	41	52	30	50
Rb	201	230	226	209	243	196	171
Zn	261	286	311	338	313	276	346
Pb	34	42	52	56	50	33	61
U	6	5	9	5	9	10	22
Th	21	27	36	26	19	20	47
Ga	42	47	37	43	41	36	38
La	246	376	312	210	440	214	636
Ce	381	574	598	418	849	407	1234
C.I.P.W. norms							
Quartz	2.4	4.6	0.0	0.0	0.0	0.5	1.3
Zircon	0.2	0.2	0.3	0.2	0.3	0.2	0.5
Orthoclase	31.7	30.2	30.1	30.1	31.1	31.0	29.0
Albite	49.6	48.9	47.7	44.2	47.5	48.5	45.8
Anorthite	0.0	1.1	0.0	0.0	0.0	0.0	0.0
Nepheline	0.0	0.0	0.0	1.6	0.0	0.0	0.0
Acmite	5.0	0.0	11.8	12.3	10.6	8.5	9.0
Diopside	2.8	3.4	5.9	6.9	6.0	5.1	6.9
Wollastonite	0.0	0.0	0.0	0.0	0.0	0.0	0.0
Hypersthene	3.9	3.4	0.1	0.0	1.9	3.9	3.9
Olivine	0.0	0.0	3.0	3.3	1.6	0.0	0.0
Magnetite	3.7	7.5	0.4	0.8	0.4	1.5	2.7
Hematite	0.0	0.0	0.0	0.0	0.0	0.0	0.0
Ilmenite	0.6	0.4	0.6	0.5	0.4	0.5	0.6
Apatite	0.1	0.2	0.1	0.1	0.2	0.2	0.2
Lith. code	644	644	644	644	644	644	644
Camp site	Cmp.02	Cmp.02	Cmp.02	Cmp.10	Cmp.10	Cmp.02	Cmp.06
Colour index	11.10	15.00	10.10	11.60	10.50	11.30	14.40
Frac. index	88.70	83.70	89.60	88.20	89.20	88.60	85.10
Diff. index	83.70	83.70	77.80	76.00	78.60	80.00	76.10
Na/(Na+K)	0.65	0.63	0.68	0.68	0.67	0.67	0.67
(Na+K)/Al	1.07	0.97	1.18	1.18	1.16	1.12	1.14
Fe2O3/FeO	1.20	1.20	1.20	1.20	1.20	1.20	1.20

Whole-rock analyses; Peralkaline Microsyenite Suite – Lujavrite from SW Motzfeldt.

Sample no.	272537	272538	272539	272540	46261	46268
Disc type	Pd.3	Pd.3	Pd.3	Pd.3	Pd.3	Pd.3
Major elements (wt%)						
SiO2	57.43	56.92	54.90	58.67	56.97	57.11
Al203	19.94	19.92	16.91	21.51	18.72	19.25
Fe203T	6.60	6.55	12.01	2.59	8.40	9.97
MgO	0.03	0.04	0.48	0.18	0.01	0.03
CaO	0.94	0.50	1.00	0.35	0.75	0.99
Na20	9.64	10.33	11.02	10.81	10.55	6.96
K20	5.28	5.10	3.61	4.90	3.96	5.23
TiO2	0.16	0.14	0.37	0.07	0.02	0.04
MnO	0.28	0.21	0.37	0.30	0.17	0.25
P205	0.11	0.03	0.04	0.03	0.02	0.03
Total	100.41	99.74	100.71	99.41	99.57	99.86
Trace elements (p.p.m)						
Ba	242	279	175	274	0	3
Nb	789	460	675	661	542	527
Zr	1153	2350	2161	2656	4655	4679
Y	167	168	133	-1	-1	-1
Sr	80	41	54	61	29	167
Rb	515	486	319	548	359	502
Zn	1055	299	675	729	110	167
Pb	68	10	55	56	13	20
U	65	14	36	26	4	5
Th	254	16	28	31	0	0
Ga	88	90	81	107	66	69
La	319	315	287	255	368	346
Ce	594	496	568	482	668	633
C.I.P.W. norms						
Corundum	0.0	0.0	0.0	0.0	0.0	0.4
Zircon	0.2	0.5	0.4	0.5	0.9	0.9
Orthoclase	31.1	30.1	21.2	29.0	23.4	30.8
Albite	33.9	29.3	24.5	36.1	36.7	46.2
Anorthite	0.0	0.0	0.0	0.0	0.0	4.7
Nepheline	21.1	24.3	22.7	25.7	20.3	6.8
Acmite	7.4	11.8	23.0	6.3	13.2	0.0
Diopside	0.2	1.0	3.9	1.3	0.1	0.0
Wollastonite	1.6	0.5	0.0	0.0	1.5	0.0
Sod. metasil.	0.0	0.0	0.0	0.2	0.0	0.0
Olivine	0.0	0.0	0.5	0.1	0.0	0.1
Magnetite	2.7	2.1	3.0	0.0	3.4	3.9
Hematite	1.1	0.0	0.0	0.0	0.2	5.7
Ilmenite	0.5	0.4	0.7	0.6	0.3	0.5
Apatite	0.3	0.1	0.1	0.1	0.0	0.1
Lith. code	711	711	711	711	714	714
Camp site	Cmp.19	Cmp.19	Cmp.19	Cmp.19	Cmp.20	Cmp.20
Colour index	3.60	3.60	8.20	2.00	3.80	4.50
Frac. index	93.40	95.50	91.40	97.40	93.60	83.80
Diff. index	86.10	83.70	68.30	90.90	80.40	83.80
Na/(Na+K)	0.74	0.75	0.82	0.77	0.80	0.67
(Na+K)/Al	1.08	1.13	1.30	1.07	1.16	0.89
Fe203/FeO	6.00	6.00	6.00	6.00	6.00	6.00

Whole-rock geochemical analyses – Poikilitic arfvedsonite microsyenite.

Sample no.	63789	63795	297681	304065	242313	54239	304033
Disc type	Fs.1	Pd.3	Fs.2	Fs.1	Fs.2	Pd.3	Fs.1
Major elements (wt%)							
SiO2	60.50	61.97	59.45	61.38	59.15	61.62	61.27
Al2O3	13.86	16.04	13.81	13.39	14.32	15.87	14.33
Fe2O3T	9.37	8.50	9.77	11.08	9.09	8.91	8.26
MgO	0.07	0.13	0.27	0.10	0.36	0.14	0.10
CaO	1.16	0.99	1.21	0.59	2.32	1.10	1.22
Na2O	7.30	7.04	6.79	6.78	7.80	6.67	7.26
K2O	4.72	4.48	4.66	4.29	5.03	4.74	4.89
TiO2	0.56	0.47	0.68	0.59	0.67	0.61	0.51
MnO	0.31	0.23	0.29	0.33	0.28	0.22	0.29
P2O5	0.06	0.26	0.15	0.05	0.06	0.06	0.05
Total	97.93	100.11	97.08	98.56	99.08	99.94	98.17
Trace elements (p.p.m)							
Ba	124	47	124	19	35	63	874
Nb	420	317	471	564	357	296	274
Zr	2113	1514	2219	216	1802	1824	1122
Y	173	155	200	208	146	139	74
Sr	29	25	40	15	25	19	493
Rb	274	268	278	252	313	283	248
Zn	299	262	349	449	302	222	151
Pb	53	38	70	164	49	28	9
U	13	7	16	18	16	3	7
Th	41	23	59	58	96	12	12
Ga	47	57	46	46	45	59	40
La	464	337	550	632	314	259	85
Ce	774	586	896	1065	575	407	176
C.I.P.W. norms							
Quartz	0.0	1.0	0.0	3.6	0.0	1.1	0.0
Zircon	0.4	0.3	0.5	0.0	0.4	0.4	0.2
Orthoclase	28.6	26.5	28.4	25.8	30.1	28.1	29.5
Albite	46.0	57.6	46.5	45.9	35.9	55.4	47.5
Anorthite	0.0	0.0	0.0	0.0	0.0	0.0	0.0
Nepheline	0.0	0.0	0.0	0.0	5.6	0.0	0.0
Acmite	13.1	1.8	11.2	11.1	12.6	1.1	11.6
Diopside	4.9	2.8	4.6	2.4	9.9	4.5	5.4
Sod. metasil.	0.0	0.5	0.0	0.0	1.5	0.0	0.5
Hypersthene	2.9	3.9	4.5	8.1	0.0	3.3	3.0
Olivine	2.7	0.0	2.0	0.0	3.5	0.0	1.7
Magnetite	0.0	5.0	1.3	2.2	0.0	5.6	0.0
Hematite	0.0	0.0	0.0	0.0	0.0	0.0	0.0
Ilmenite	0.6	0.4	0.6	0.6	0.5	0.4	0.6
Apatite	0.2	0.6	0.4	0.1	0.1	0.1	0.1
Lith. code	721	721	721	721	723	724	724
Camp site	Cmp.02	Cmp.02	Cmp.02	Cmp.02	Cmp.02	Cmp.02	Cmp.02
Colour index	11.31	12.80	13.30	13.50	14.00	14.00	10.80
Frac. index	88.26	85.20	86.20	86.50	84.60	85.60	89.00
Diff. index	74.60	85.20	75.00	75.40	71.60	84.60	77.00
Na/(Na+K)	0.70	0.70	0.69	0.71	0.70	0.68	0.69
(Na+K)/Al	1.24	1.02	1.17	1.18	1.28	1.01	1.20
Fe2O3/FeO	1.00	1.00	1.00	1.00	1.00	1.00	1.00

Whole-rock analyses; Peralkaline Microsyenite Suite - Unaltered.

Sample no.	240532	242213	242236	304151	304162
Disc type	Fs.2	Fs.2	Fs.2	Pd.1	Fs.1
Major elements (wt%)					
SiO2	61.05	55.78	58.62	65.23	58.64
Al2O3	14.54	13.84	14.38	18.34	15.27
Fe2O3T	10.22	8.40	10.90	0.61	8.35
MgO	0.66	0.57	0.55	0.03	0.24
CaO	1.82	4.39	2.16	0.80	2.14
Na2O	9.60	7.16	7.44	5.76	8.11
K2O	3.68	4.97	4.75	7.47	2.55
TiO2	0.66	0.57	0.83	0.01	0.67
MnO	0.40	0.31	0.31	0.01	0.35
P2O5	0.09	0.10	0.12	0.0	0.07
Total	102.72	96.09	100.06	98.26	96.39
Trace elements (p.p.m)					
Ba	243	87	277	179	125
Nb	603	596	401	9	476
Zr	2863	1759	801	42	2525
Y	203	148	102	102	154
Sr	108	42	37	32	190
Rb	443	370	337	664	242
Zn	382	344	296	14	339
Pb	46	20	11	2	41
U	30	32	29	0	24
Th	5	14	18	0	18
Ga	52	45	42	65	46
La	332	254	296	6	302
Ce	601	458	548	8	567
C.I.P.W. norms					
Quartz	0.0	0.0	0.0	1.6	0.0
Zircon	0.6	0.4	0.2	0.0	0.5
Orthoclase	21.2	30.7	28.2	44.9	15.7
Albite	45.4	27.2	37.0	49.6	60.4
Anorthite	0.0	0.0	0.0	2.2	0.0
Nepheline	4.1	9.9	5.8	0.0	3.5
Acmite	10.1	8.9	11.1	0.0	3.9
Diopside	7.2	19.3	8.8	1.1	9.3
Wollastonite	0.0	0.0	0.0	0.3	0.0
Sod. metasil.	3.4	1.8	0.7	0.0	0.0
Olivine	6.9	1.1	7.3	0.0	3.3
Magnetite	0.0	0.0	0.0	0.3	2.5
Hematite	0.0	0.0	0.0	0.0	0.0
Ilmenite	0.7	0.6	0.6	0.0	0.7
Apatite	0.2	0.2	0.3	0.0	0.2
Lith. code	731	731	731	731	731
Camp site	Cmp.10	Cmp.10	Cmp.10	Cmp.10	Cmp.10
Colour index	15.10	21.20	17.00	1.40	16.00
Frac. index	84.30	78.40	82.80	96.10	83.50
Diff. index	70.80	67.70	71.10	96.10	79.60
Na/(Na+K)	0.80	0.69	0.70	0.54	0.83
(Na+K)/Al	1.36	1.24	1.21	0.96	1.05
Fe2O3/FeO	0.60	0.60	0.60	0.60	0.60

Whole-rock analyses; Peralkaline Microsyenite Suite – Mineralised.

Sample no.	304067	304068	304157	304158	304169	304170	304173
Disc type	Fs.1	Fs.1	Fs.1	Pd.1	Fs.1	Pd.1	Fs.1
Major elements (wt%)							
SiO2	63.53	69.81	61.13	59.99	61.82	59.16	63.11
Al2O3	10.63	9.48	15.99	16.41	12.86	12.28	11.48
Fe2O3T	10.73	2.47	6.85	7.50	9.85	13.00	10.97
MgO	0.00	0.15	0.01	0.66	0.06	1.17	0.0
CaO	0.54	2.20	0.65	1.01	0.27	1.25	0.21
Na2O	4.96	5.58	8.74	5.13	5.60	5.96	4.80
K2O	1.84	0.02	2.97	6.60	3.16	1.98	2.92
TiO2	0.35	3.16	0.13	0.13	0.29	0.33	0.29
MnO	0.46	0.16	0.25	0.31	0.61	0.79	0.45
P2O5	0.01	1.49	0.0	0.0	0.0	0.01	0.0
Total	93.05	94.52	96.72	97.74	94.51	95.93	94.24
Trace elements (p.p.m)							
Ba	133	20	38	151	83	50	48
Nb	5503	0	779	645	214	2922	3440
Zr	7792	736	5286	5714	724	11382	8040
Y	533	33	318	372	83	569	430
Sr	99	388	67	87	40	115	68
Rb	216	0	336	625	207	187	221
Zn	1293	1236	448	322	333	776	66
Pb	329	539	37	21	55	614	580
U	291	56	37	11	6	294	471
Th	207	10975	13	10	26	80	39
Ga	73	122	74	65	40	79	52
La	2050	2010	582	518	221	1494	1381
Ce	3233	2301	1068	948	414	2554	2310
C.I.P.W. norms							
Quartz	28.0	36.0	0.0	2.0	17.6	13.3	24.2
Zircon	1.7	0.2	1.1	1.2	0.2	2.4	1.7
Orthoclase	11.6	0.1	18.0	39.7	19.8	12.1	18.2
Albite	44.8	49.9	65.6	44.2	50.2	52.0	42.8
Anorthite	1.4	0.8	0.0	2.3	0.7	0.9	1.1
Nepheline	0.0	0.0	1.1	0.0	0.0	0.0	0.0
Acmite	0.0	0.0	7.5	0.0	0.0	0.0	0.0
Diopside	0.0	0.4	2.9	2.2	0.3	4.2	0.0
Wollastonite	0.6	0.0	0.0	0.0	0.1	0.0	0.0
Hypersthene	0.0	6.0	0.0	0.6	0.0	1.1	0.0
Olivine	0.0	0.0	0.0	0.0	0.0	0.0	0.0
Magnetite	10.0	2.6	3.3	6.3	8.4	10.7	9.9
Hematite	1.0	0.0	0.0	0.9	1.4	1.9	1.2
Ilmenite	0.9	0.3	0.5	0.6	1.2	1.5	0.9
Apatite	0.0	3.7	0.0	0.0	0.0	0.0	0.0
Lith. code	733	733	733	733	733	733	733
Camp site	Cmp.05	Cmp.05	Cmp.10	Cmp.10	Cmp.10	Cmp.10	Cmp.10
Colour index	11.00	13.00	6.70	9.80	10.00	17.50	10.80
Frac. index	84.40	86.00	92.20	85.80	87.60	77.30	85.20
Diff. index	84.40	86.00	84.70	85.80	87.60	77.30	85.20
Na/(Na+K)	0.80	1.00	0.82	0.54	0.73	0.82	0.71
(Na+K)/Al	0.96	0.97	1.10	0.95	0.98	0.97	0.96
Fe2O3/FeO	2.50	2.50	2.50	2.50	2.50	2.50	2.50

Whole-rock analyses; Peralkaline Microsyenite Suite - Mineralised.

Sample no.	304174	304175	304188	304191
Disc type	Fs.1	Fs.1	Pd.1	Pd.1
Major elements (wt%)				
SiO2	55.87	56.52	49.00	54.71
Al2O3	12.43	11.96	10.90	11.06
Fe2O3T	13.22	12.74	9.42	15.37
MgO	0.0	0.0	1.57	1.38
CaO	0.44	0.35	5.51	1.15
Na2O	9.45	9.70	2.53	3.20
K2O	1.14	1.43	4.89	4.74
TiO2	0.30	0.27	0.29	0.33
MnO	0.63	0.62	0.66	0.89
P2O5	0.0	0.0	0.01	0.01
Total	93.46	93.60	84.78	92.84
Trace elements (p.p.m)				
Ba	263	0	15	0
Nb	297	2176	2875	3139
Zr	810	12922	22437	14893
Y	98	625	1247	785
Sr	47	91	325	91
Rb	207	95	370	445
Zn	228	1401	5434	1929
Pb	22	844	1367	703
U	7	173	100	61
Th	19	83	147	102
Ga	35	57	36	53
La	187	1999	2211	4865
Ce	335	3513	4025	8330
C.I.P.W. norms				
Quartz	0.0	0.0	5.7	14.1
Zircon	0.2	2.7	5.2	3.2
Orthoclase	7.2	8.9	33.0	29.7
Albite	61.6	52.7	24.5	28.7
Anorthite	0.0	0.0	4.5	1.9
Nepheline	0.1	2.0	0.0	0.0
Acmite	21.1	26.5	0.0	0.0
Diopside	2.2	1.6	9.6	3.2
Wollastonite	0.0	0.0	6.0	0.0
Hypersthene	0.0	0.0	0.0	2.2
Olivine	2.7	4.1	0.0	0.0
Magnetite	3.6	0.2	8.5	12.9
Hematite	0.0	0.0	1.6	2.4
Ilmenite	1.3	1.2	1.4	1.8
Apatite	0.0	0.0	0.0	0.0
Lith. code	733	733	733	733
Camp site	Cmp.10	Cmp.10	Cmp.10	Cmp.10
Colour index	9.80	7.20	19.60	20.10
Frac. index	90.10	90.10	63.20	72.50
Diff. index	68.90	63.60	63.20	72.50
Na/(Na+K)	0.93	0.91	0.44	0.51
(Na+K)/Al	1.35	1.46	0.87	0.94
Fe2O3/FeO	2.50	2.50	2.50	2.50

Whole-rock analyses; Peralkaline Microsyenite Suite - Pegmatitic.

Sample no.	304178	304179	304182	304183
Disc type	Fs.1	Pd.1	Fs.1	Fs.1
Major elements (wt%)				
SiO2	54.41	44.54	58.13	58.10
Al2O3	20.55	8.16	16.99	15.74
Fe2O3T	4.31	27.37	7.38	8.58
MgO	0.03	2.68	0.11	0.14
CaO	0.73	3.53	0.68	0.72
Na2O	9.65	6.04	7.25	7.35
K2O	3.72	2.37	5.03	5.31
TiO2	0.11	0.74	0.18	0.43
MnO	0.20	0.87	0.26	0.33
P2O5	0.0	0.02	0.0	0.0
Total	93.70	96.32	96.01	96.70
Trace elements (p.p.m)				
Ba	66	49	165	128
Nb	735	867	416	576
Zr	4485	5589	2565	3552
Y	294	287	179	246
Sr	70	71	48	87
Rb	266	202	336	398
Zn	177	1129	268	279
Pb	46	61	23	29
U	8	23	1	4
Th	12	11	1	0
Ga	61	44	57	56
La	507	459	242	353
Ce	900	777	461	626
C.I.P.W. norms				
Quartz	0.0	0.0	0.0	0.0
Zircon	1.0	1.2	0.5	0.7
Orthoclase	23.3	14.6	31.0	32.4
Albite	44.9	14.6	50.3	40.5
Anorthite	1.9	0.0	0.0	0.0
Nepheline	22.7	8.4	6.3	6.9
Acmite	0.0	20.6	1.8	9.8
Diopside	1.7	15.6	3.1	3.3
Wollastonite	0.0	0.0	0.0	0.0
Hypersthene	0.0	0.0	0.0	0.0
Olivine	0.9	14.0	2.1	4.6
Magnetite	3.1	9.3	4.4	1.2
Hematite	0.0	0.0	0.0	0.0
Ilmenite	0.4	1.7	0.5	0.7
Apatite	0.0	0.0	0.0	0.0
Lith. code	735	735	735	735
Camp site	Cmp.10	Cmp.10	Cmp.10	Cmp.10
Colour index	6.20	40.60	10.10	9.70
Frac. index	90.90	58.20	89.40	90.60
Diff. index	90.90	37.60	87.50	79.80
Na/(Na+K)	0.80	0.79	0.69	0.68
(Na+K)/Al	0.97	1.53	1.02	1.13
Fe2O3/FeO	1.00	1.00	1.00	1.00

Rare-earth element analyses - All Samples.

Sample no.	304160	304160	304740	58352	326161	326161	326161	304051	58368	304052	304055	58363
Cryst/rock	rock	rock	rock	rock	rock	amph	feld	rock	rock	rock	rock	rock
REE elements (p.p.m)												
La	50.60	48.50	45.60	59.80	64.10	214.00	29.80	65.50	53.70	396.00	73.00	287.00
Ce	108.00	109.00	92.20	124.00	125.00	579.00	39.00	134.00	116.00	593.00	148.00	445.00
Nd	56.30	54.00	43.00	66.00	75.70	368.00	-1.00	64.00	56.00	241.00	58.00	236.00
Sm	8.64	8.39	6.41	8.04	8.80	61.90	1.36	10.90	8.46	40.00	9.85	35.90
Eu	3.89	3.79	3.70	2.67	3.39	3.15	2.83	3.18	1.56	2.94	1.74	3.66
Tb	0.85	0.95	0.83	1.04	0.93	6.76	-1.00	1.21	1.04	4.26	1.19	3.87
Yb	1.75	1.80	8.00	2.19	1.94	9.69	0.60	1.89	1.91	12.00	1.90	6.20
Lu	0.58	0.28	0.22	0.31	0.35	1.55	-1.00	0.34	0.34	2.59	0.23	1.06
Ta	4.07	3.27	2.75	5.25	5.53	33.30	1.40	5.36	4.71	14.70	6.01	13.80
Lith. code	314	314	314	324	324	324	324	324	334	414	334	423

Sample no.	304040	304723	304115	304115	304115	304115	287157	304747	304753	304755	304755	304755
Cryst/rock	rock	rock	rock	biot	feld	albite	rock	rock	rock	rock	feld	amph
REE elements (p.p.m)												
La	856.00	864.00	419.00	103.00	123.00	1.88	76.80	90.50	107.00	82.10	24.30	209.00
Ce	1430.00	1690.00	758.00	177.00	200.00	-1.00	175.00	179.00	221.00	162.00	45.70	496.00
Nd	427.00	590.00	316.00	62.30	72.00	-1.00	54.00	66.80	112.00	76.50	26.10	266.00
Sm	75.40	89.10	43.70	13.00	12.00	0.54	8.90	10.20	14.20	9.60	2.60	41.20
Eu	4.53	5.73	3.16	1.01	0.96	-1.00	2.26	1.69	2.46	1.75	1.12	4.09
Tb	9.71	10.40	11.00	3.23	1.91	-1.00	0.88	1.36	1.87	1.52	0.34	4.65
Yb	19.00	14.00	43.50	60.00	6.70	-1.00	2.59	4.30	5.27	3.78	0.90	13.40
Lu	2.89	2.19	6.20	2.08	0.91	-1.00	0.43	0.69	0.79	0.59	0.09	2.46
Ta	29.70	13.90	61.20	25.00	17.10	-1.00	9.21	13.00	16.90	11.60	3.20	39.50
Lith. code	423	423	425	425	425	425	431	431	431	431	431	431

Table A3.3

Rare-earth element analyses – All Samples.

Sample no.	304755	54132	304003	304009	304009	304009	326091	326091	326091	326091	54132	54132
Cryst/rock	neph	rock	rock	rock	feld	neph	rock	feld	amph	neph	feld	mafics
REE elements (p.p.m)												
La	15.70	82.80	57.60	93.60	26.50	19.60	78.00	20.90	187.00	4.24	13.50	180.00
Ce	26.20	177.00	121.00	202.00	47.90	34.90	153.00	35.20	402.00	7.00	22.00	431.00
Nd	-1.00	52.90	55.10	101.00	20.40	-1.00	73.30	-1.00	213.00	-1.00	-1.00	190.00
Sm	1.36	10.80	7.90	12.70	2.57	1.93	9.50	1.44	32.90	0.25	1.16	36.00
Eu	0.32	2.81	2.80	1.71	0.49	0.28	2.67	1.21	4.51	0.14	1.48	4.61
Tb	-1.00	1.25	1.05	1.90	0.32	0.38	1.19	0.15	3.73	-1.00	-1.00	3.70
Yb	-1.00	3.75	2.35	5.27	0.74	1.50	2.88	0.50	6.19	-1.00	-1.00	9.40
Lu	-1.00	0.62	0.38	0.89	0.11	-1.00	0.42	-1.00	1.03	-1.00	-1.00	0.15
Ta	1.18	14.20	8.36	16.10	0.91	0.61	11.80	1.45	32.90	0.44	1.42	39.30
Lith. code	431	434	434	434	434	434	434	434	434	434	434	434

Sample no.	304026	304026	304092	54138	54181	304127	304752	304024	304101	304758	326154	304750
Cryst/rock	pyrox	feld	rock	rock	rock	rock	rock	rock	rock	rock	rock	rock
REE elements (p.p.m)												
La	47.70	193.00	1060.00	134.00	60.00	143.00	96.40	124.00	151.00	118.00	33.20	104.00
Ce	91.80	356.00	1860.00	284.00	131.00	308.00	204.00	266.00	312.00	247.00	68.00	204.00
Nd	51.00	168.00	722.00	107.00	-1.00	105.00	90.10	93.00	110.00	91.00	36.30	71.00
Sm	9.82	26.80	121.00	18.10	9.00	19.10	13.50	17.50	20.50	16.30	3.74	11.40
Eu	1.49	3.14	7.93	1.93	1.05	2.23	1.36	2.28	2.28	2.09	0.30	1.46
Tb	2.29	2.88	23.20	2.12	1.04	2.39	1.56	1.86	2.42	1.83	0.44	1.28
Yb	12.70	1.50	75.00	6.71	4.29	4.60	4.20	4.00	5.50	4.50	2.70	4.50
Lu	2.11	0.15	11.40	0.83	0.63	0.78	0.61	0.61	0.88	0.63	0.45	0.67
Ta	3.82	0.41	148.00	15.00	9.39	14.70	12.60	11.30	16.20	12.30	6.71	13.10
Lith. code	435	435	493	511	511	511	514	514	514	514	521	521

Rare-earth element analyses – All Samples.

Sample no.	304107	304131	58085	58085	326066	58085	326066	63720	304078	304738	54161	326087
Cryst/rock	rock	rock	rock	mafics	rock	feld	feld	rock	rock	rock	rock	rock
REE elements (p.p.m)												
La	67.50	142.00	113.00	158.00	36.20	116.00	26.50	132.00	412.00	221.00	416.00	234.00
Ce	141.00	311.00	231.00	418.00	76.70	196.00	50.40	309.00	793.00	447.00	791.00	483.00
Nd	49.30	124.00	86.20	205.00	45.40	-1.00	27.00	130.00	268.00	158.00	268.00	237.00
Sm	9.79	20.90	13.80	30.80	4.71	11.30	2.90	19.70	45.60	25.40	36.60	32.60
Eu	5.68	4.80	3.34	5.18	1.89	3.03	1.72	1.96	2.75	3.68	2.73	2.61
Tb	1.12	2.50	1.66	3.70	0.77	1.06	0.32	2.17	5.10	3.36	4.24	4.22
Yb	3.40	5.00	3.79	8.30	2.29	2.10	-1.00	4.80	15.00	7.00	11.50	8.50
Lu	0.37	0.88	0.54	1.60	0.36	0.16	-1.00	0.84	2.12	0.11	1.53	1.28
Ta	7.00	17.10	10.60	44.60	8.75	3.00	1.68	9.15	34.60	9.05	20.50	14.70
Lith. code	531	531	534	534	534	534	534	631	634	634	641	644

Sample no.	326087	326087	304033	304157	304186	326135	326135	304073
Cryst/rock	feld	amph	rock	rock	rock	rock	feld	rock
REE elements (p.p.m)								
La	20.50	107.00	386.00	253.00	235.00	82.80	34.70	264.00
Ce	35.70	265.00	792.00	500.00	440.00	163.00	54.00	542.00
Nd	18.00	168.00	272.00	160.00	140.00	80.70	-1.00	207.00
Sm	2.74	22.80	54.60	30.20	26.10	11.20	2.55	30.90
Eu	0.87	1.33	3.31	1.87	1.81	5.18	3.95	1.29
Tb	0.30	1.99	7.12	4.94	4.92	1.55	-1.00	3.45
Yb	0.50	10.10	14.40	14.90	18.00	3.91	0.70	5.50
Lu	-1.00	1.99	2.13	1.66	2.47	0.55	-1.00	0.82
Ta	0.82	14.40	26.50	21.70	23.10	8.00	1.23	5.96
Lith. code	644	644	721	733	735	911	911	921

APPENDIX FOUR

MINERAL CHEMISTRY

APPENDIX FOUR - MINERAL CHEMISTRY

4.1 Electron-Probe Microanalysis

4.1.1 Preparation and operating conditions

The mineral analyses obtained by the author (Tables A4.2, A4.3, A4.4, A4.5) were derived exclusively from the EDS-Microprobe at the University of Manchester. This machine is a Modified Cambridge Instrument Company Geoscan and uses only energy dispersive spectrometer (E.D.S.) analysis. The E.D.S. comprises a Kevek Detector, a Harwell 2010 pulse processor and Link Systems 290 Electronics. Link Systems ZAF-4/FLS software is used to convert x-ray spectra obtained from the specimen into chemical analysis.

The following operating conditions were used:

15KV Electron Beam Accelerating Voltage

75 Deg X-ray Take-Off Angle

3nA Specimen Current on Cobalt Metal

2.5 KCPS Output Count rate from Cobalt metal with 18% detection system dead time.

The ZAF- 4/FLS software deconvolutes overlapping X-ray peaks and subtracts a background radiation by reference to a previously obtained library of standard peak profiles. X-ray intensities are automatically Z.A.F. corrected using a procedure based on TIM1 programme of Duncomb and Jones (1969). The atomic number correction described by Duncomb and Reed (1968) is used together with Reed's (1965) fluorescence correction. The absorption effects are calculated using, Philbert's equation with Heinrich's, and as calculated by Yakowitz et al., (1973).

The samples for analysis were prepared as polished thin sections and carbon coated. The following elements were analysed by the author Si, Ti, Al, Fe, Mn, Ca, Na, K, Zr.

The probe-analyses labelled APJ are taken from Jones (1980), who used a Cambridge instrument Company Geoscan at the University of Durham (Jones Ibid, p. 245-288).

4.1.2 Mineral calculations

a. Pyroxene

Pyroxenes are recalculated on the basis of 4 cations and 6 oxygens. The following elements were determined; Si, Ti, Al, Fe, Mn, Mg, Ca, Na, K and occasionally Zr. Unfortunately Zr 'caused problems' on the EDS and the results obtained are approximate. Because only total iron can be determined from the microprobe, determination of Fe_2O_3/FeO was undertaken by assuming stoichiometry in 4 cations and 6 oxygens per formula unit using the following steps (eg, Table A4.1).

1. The Wt% of oxides are divided by their molecular weights to give their molecular proportions.

2. The molecular proportion (mp) is multiplied by the cation number of the respective element. To give the cation proportion (cp) (ie, for Na_2O = mp x 2).

3. The cation proportions of all the elements are totalled and then divided into the chosen cation recalculation (ie, 4 in pyroxene) to give a cation factor (X).

4. The cation proportions are then individually multiplied by this factor X to give the cation proportion to the sum of X.

5. Each individual cation proportion to sum of X (Table A4.1: col. 5) is multiplied by the number of oxygens in the original oxide to give the atomic proportion of equivalent oxygens (ie, SiO_2 = cp x 2).

6. The sum of the equivalent oxygens (Table A4.1: col. 6) should be 6 assuming stoichiometry. If the sum is less than 6 then the lack of oxygen can be assigned to Fe_2O_3 in the mineral, (ie, Fe^3 = 2 x oxygen deficiency).

7. This number can then be included in the column of cation proportions to 4 cations (Table A4.1: col. 2) by subtraction from the total FeO proportion in that column. The difference being the true FeO proportion. Thus the Fe_2O_3/FeO ratio is determined.

8. These values are easily worked back to give the oxide percentages if required.

This method, shown to the author by Dr. L.M. Larsen (GGU), proves simple and very effective (see also Larsen, 1976). However, because the Fe_2O_3 is calculated as a remainder problems can arise due to incomplete analyses, particularly if ZrO_2 is missing (especially in aegirine analysis, see Jones, 1982).

b. Amphibole

The amphiboles of Motzfeldt range from hastingsite to arvedsonite in composition. Where amphibole nomenclature has been used in this work it is that of Leake (1978). To use this nomenclature it is necessary to determine the Fe_2O_3 ratio of the mineral. This has been undertaken with a method analogous to that used in the pyroxene recalculation (Table A4.1). The method uses essentially charge-balance criteria. However, the crystal chemistry of amphiboles is complex, but while many cation substitutions are possible there are crystal-chemical limits. "It may look utterly ridiculous from the point of view of crystal chemistry, but the charge will balance!" from Robinson et al. (1982).

The standard amphibole formula is summarised;

$A_{0-1}\ B_2\ C_5\ {}^{vi}T_8\ {}^{iv}O_{22}\ (OH,F,Cl)_2$

and a list of reasonable chemical limits might be:

K = A-site only	Mg = C-site and B-site
Na = A-site or B-site	Fe^3 = C-site only
Ca = B-site only	Ti = C-site only
Mn = C-site or B-site	Al = C-site or T-site
Fe^2 = C-site or B-site	Si = T-site only

With these parameters in mind it is usually possible to recalculate and find the max. and min. values of Fe_2O_3 and keep within the chemical and crystal limits. For the recalculations used in this work 16 cations to 23 oxygens were used.

4.1.3 Notes on electron-microprobe data tables

Cryst & Posn : (crystal number and position)

Rim = Rim
Cor = Core
Int = Intermediate between core and rim
GS = Data from Gitte Schwartz (pers comm.)
APJ = data from Jones (1980)

Not analysed: = -1.00

Colour Key:

V = Very	g = green	y = yellow
D = Deep	r = red	bl = blue
P = Pale	b = brown	

eg, Drb-yb = Deep red-brown to yellow-brown

Name Key: Amphiboles

MHas = Magnesian hastingsite
Has = Hastingsite
H-Hb = Hastingsitic hornblende
MH-Hb = Magnesian hastngsitic hornblende
EdHb = Edenitic-hornblende
FEdHb = Ferro-edenitic hornblende
FEd = Ferro-edenite
Kat = Katophorite
FRh = Ferro-richterite
FEk = Ferro-eckermannite
Arf = Arfvedsonite

Name Key: Pyroxenes

Sal = Salite
Fsal = Ferrosalite
H = Hedenbergite
A-A = Aegirine-augite
A-H = Aegirine-hedenbergite
Aeg = Aegirine

Example Aegirine-augite (AM82 from Jones 1980.)

(1)	(2) Wt % oxides	(3) mol. props of oxides	(4) cation props	(5) cation props to sum of 4	(6) equivalent oxygens
SiO_2	51.35	0.855 (x1)	0.855	1.980 (x2)	3.960
TiO_2	0.51	0.006 (x1)	0.006	0.014 (x2)	0.029
Al_2O_3	0.75	0.007 (x2)	0.014	0.032 (x1.5)	0.048
FeO_1	24.59	0.342 (x1)	0.342	0.792 (x1)	0.792
MnO	1.09	0.015 (x1)	0.015	0.035 (x1)	0.035
MgO	2.27	0.056 (x1)	0.056	0.130 (x1)	0.130
CaO	9.87	0.176 (x)	0.176	0.408 (x1)	0.408
Na_2O	7.96	0.129 (x2)	0.258	0.598 (x0.5)	0.299
K_2O	0.00	0.000 (x2)	0.000	0.000 (x0.5)	0.000
ZrO_2	0.60	0.005 (x1)	0.005	0.012 (x2)	0.024
	98.98		1.727	4	5.724

4/1.747 = 2.290 factor (X)

6 - 5.724 = 0.276 (ox. deficiency)

Fe^{3+} = 2 x 0.276 = 0.552

Fe^{2+} = 0.240

Thus giving,

SiO_2	51.35
TiO_2	0.51
Al_2O_3	0.75
Fe_2O_3	19.03
FeO	7.44
MnO	1.09
MgO	2.27
CaO	9.87
Na_2O	7.96
K_2O	0.00
ZrO_2	0.60
Total	100.86
*FeO	24.59

Number of ions on the basis of 6 oxygens -

Si	1.980	2
Al	0.020	
Al	0.012	1
Ti	0.014	
Fe^{3+}	0.552	
Mg	0.130	
Fe^{2+}	0.240	
Mn	0.035	
Zr	0.012	
Ca	0.408	1
Na	0.598	
K	0.000	

Table A4.1

Microprobe analyses – Pyroxene. Geologfjeld Formation.

Sample no. Cryst & posn	304160 2.cor	304160 2.int	304160 2.rim	304160 3.cor	304160 3.rim	304160 5.int	304160 6.cor	304160 6.rim	304160 7.cor	304160 8.cor	304160 9.cor	304160 9.int
Major elements (wt%)												
SiO2	50.97	50.78	50.77	50.31	50.05	50.67	51.38	51.26	50.87	51.83	51.24	51.36
TiO2	0.41	0.56	0.37	0.38	0.46	0.32	0.39	0.48	0.39	0.45	0.56	0.67
Al2O3	0.72	1.15	1.02	1.37	1.12	1.12	0.97	1.39	1.45	0.84	1.10	0.95
Fe2O3	3.30	3.57	3.75	3.13	2.97	1.99	2.53	1.90	1.70	1.35	2.07	2.30
FeO	11.35	12.40	11.69	15.19	16.60	15.86	13.01	13.93	16.13	14.10	12.20	13.20
MnO	1.12	1.07	1.05	1.28	1.30	1.25	1.09	1.09	1.18	1.14	0.99	1.23
MgO	9.16	8.34	8.41	6.15	5.43	6.28	8.42	7.82	6.19	8.67	9.38	8.97
CaO	21.48	21.96	22.04	21.61	21.34	21.47	21.54	21.70	21.81	21.77	21.65	21.77
Na2O	1.07	1.02	1.09	1.16	1.15	1.08	1.09	1.07	1.05	0.82	0.89	0.79
K2O	0.00	0.00	0.00	0.00	0.00	0.00	0.00	0.00	0.00	0.00	0.00	0.0
ZrO2	0.00	0.00	0.00	0.00	0.00	0.00	0.00	0.00	0.00	0.00	0.00	0.0
Total	99.59	100.86	100.19	100.58	100.42	100.05	100.42	100.64	100.76	100.98	100.09	101.25
FeOT	14.32	15.62	15.06	18.01	19.28	17.65	15.29	15.64	17.66	15.31	14.07	15.27
4 cations to 6 oxygens												
Si	1.964	1.944	1.953	1.955	1.960	1.977	1.971	1.967	1.970	1.979	1.962	1.956
Al	0.033	0.052	0.046	0.063	0.052	0.052	0.044	0.063	0.066	0.038	0.050	0.043
Ti	0.012	0.016	0.011	0.011	0.013	0.009	0.011	0.014	0.011	0.013	0.016	0.019
Zr	0.00	0.00	0.00	0.00	0.00	0.00	0.00	0.00	0.00	0.00	0.00	0.0
Fe3	0.096	0.103	0.108	0.092	0.088	0.058	0.073	0.055	0.049	0.039	0.060	0.066
Mg	0.526	0.476	0.482	0.356	0.317	0.365	0.481	0.447	0.357	0.494	0.535	0.509
Fe2	0.366	0.397	0.376	0.494	0.544	0.518	0.417	0.447	0.523	0.450	0.391	0.420
Mn	0.037	0.035	0.034	0.042	0.043	0.041	0.035	0.035	0.039	0.037	0.032	0.040
Ca	0.887	0.901	0.908	0.900	0.896	0.898	0.885	0.892	0.905	0.891	0.Fsal	0.Fsal
Na	0.080	0.076	0.081	0.087	0.087	0.082	0.081	0.079	0.079	0.060	0.066	0.059
K	0.00	0.00	0.00	0.00	0.00	0.00	0.00	0.00	0.00	0.00	0.00	0.0
Atomic percentages												
Na	7.9	7.7	8.3	8.9	8.8	8.2	8.0	7.8	7.9	5.8	6.4	5.7
Fe2+Mn	39.9	43.9	42.1	54.7	59.2	55.6	44.6	47.8	56.3	46.8	41.3	44.7
Mg	52.1	48.4	49.5	36.4	32.0	36.3	47.4	44.3	35.8	47.5	52.2	49.5
Lith. code	314	314	314	314	314	314	314	314	314	314	314	314
Spot no.	2	7	3	4	5	20	23	24	26	28	31	33
Name	Sal	Sal	Sal	Fsal	Fsal	Fsal	Sal	Fsal	Fsal	Sal	Sal	Sal

Table A4.2

Microprobe analyses – Pyroxene. Geologfjeld Formation.

Sample no.	304160	304160	304160	304160	304160	304160	304160	304159	304159	304159	304159	304159
Cryst & posn	9.rim	11.cor	11.int	11.rim	12.cor	12.int	12.rim	21.int	21.rim	22.cor	22.rim	23.cor
Major elements (wt%)												
SiO2	51.31	51.14	51.32	50.80	51.16	49.90	49.91	50.48	49.78	50.66	50.77	49.14
TiO2	0.51	0.30	0.30	0.49	0.38	0.30	0.33	0.48	0.39	0.78	0.56	0.31
Al2O3	1.12	0.93	1.34	1.14	1.37	1.31	1.14	0.95	0.95	0.87	0.91	1.26
Fe2O3	0.52	2.90	1.20	2.12	1.93	3.93	0.06	4.25	4.79	4.25	3.77	5.03
FeO	17.01	12.29	15.22	15.16	14.02	16.25	19.90	11.65	13.80	11.08	11.81	15.44
MnO	1.09	1.10	1.27	1.05	1.18	1.60	1.37	1.01	1.23	1.01	0.92	1.08
MgO	6.93	8.97	6.96	7.15	7.79	5.09	4.57	8.62	6.56	9.79	9.63	5.59
CaO	21.64	21.81	21.77	21.79	21.79	21.40	21.26	21.46	21.38	21.42	21.46	21.46
Na2O	0.78	0.88	1.04	0.93	0.97	1.20	0.71	1.13	1.24	0.92	0.82	1.09
K2O	0.00	0.00	0.00	0.00	0.00	0.00	0.00	0.00	0.00	0.00	0.00	0.0
ZrO2	0.00	0.00	0.00	0.00	0.00	0.00	0.00	0.00	0.00	0.00	0.00	0.0
Total	100.91	100.33	100.44	100.65	100.59	100.99	99.27	100.02	100.12	100.79	100.66	100.39
FeOT	17.48	14.91	16.30	17.07	15.76	19.79	19.95	15.47	18.12	14.91	15.21	19.97
4 cations to 6 oxygens												
Si	1.981	1.961	1.982	1.964	1.966	1.949	1.990	1.945	1.943	1.931	1.940	1.929
Al	0.051	0.042	0.061	0.052	0.062	0.060	0.054	0.043	0.044	0.039	0.041	0.058
Ti	0.015	0.009	0.009	0.014	0.011	0.009	0.010	0.014	0.011	0.022	0.016	0.009
Zr	0.00	0.00	0.00	0.00	0.00	0.00	0.00	0.00	0.00	0.00	0.00	0.0
Fe3	0.015	0.084	0.035	0.062	0.056	0.116	0.002	0.123	0.141	0.122	0.108	0.149
Mg	0.399	0.513	0.401	0.412	0.446	0.296	0.271	0.495	0.382	0.556	0.548	0.327
Fe2	0.549	0.394	0.491	0.490	0.451	0.531	0.663	0.375	0.451	0.353	0.377	0.507
Mn	0.036	0.036	0.042	0.034	0.038	0.053	0.046	0.033	0.041	0.033	0.030	0.036
Ca	0.896	0.896	0.901	0.902	0.897	0.896	0.908	0.886	0.894	0.875	0.879	0.902
Na	0.058	0.065	0.078	0.070	0.072	0.091	0.055	0.085	0.094	0.068	0.061	0.083
K	0.00	0.00	0.00	0.00	0.00	0.00	0.00	0.00	0.00	0.00	0.00	0.0
Atomic percentages												
Na	5.6	6.4	7.7	7.0	7.1	9.4	5.3	8.6	9.7	6.7	6.0	8.7
Fe2+Mn	56.1	42.7	52.7	52.1	48.6	60.1	68.5	41.3	50.8	38.2	40.1	57.0
Mg	38.3	50.9	39.6	41.0	44.3	30.5	26.2	50.1	39.5	55.0	53.9	34.3
Lith. code	314	314	314	314	314	314	314	314	314	314	314	314
Spot no.	32	38	41	45	49	53	51	82	81	83	84	85
Name	Fsal	Sal	Fsal	Fsal	Fsal	Fsal	Fsal	Sal	Fsal	Sal	Sal	Fsal

Microprobe analyses – Pyroxene. Geologfjeld Formation.on.

Sample no.	304159	304159	304159	304051	304051	304051	326161	326161	326161	58352	58352	58352
Cryst & posn	23.rim	24.cor	24.rim	89.cor	89.int	89.rim	99.cor	99.int	99.rim	103.cor	103.rim	104.cor
Major elements (wt%)												
SiO2	49.17	50.23	49.74	50.13	50.22	50.30	49.99	50.31	50.12	49.52	48.61	48.89
TiO2	0.43	0.45	0.00	0.59	0.58	0.48	0.64	0.72	0.80	0.60	0.44	0.61
Al2O3	1.10	0.96	0.69	1.57	1.51	1.39	1.50	1.55	1.99	1.37	1.15	1.42
Fe2O3	4.74	5.62	8.98	1.54	2.77	1.22	2.16	1.83	1.07	3.65	4.33	4.11
FeO	15.53	10.82	13.61	12.52	12.27	13.35	12.06	11.89	11.26	13.18	16.22	13.59
MnO	1.42	1.06	1.76	0.61	0.43	0.76	0.58	0.52	0.56	0.69	0.77	0.72
MgO	5.38	8.49	4.06	9.54	8.93	8.77	9.38	9.88	10.62	8.53	5.35	7.22
CaO	21.20	21.67	19.90	21.97	21.76	21.97	21.58	21.60	21.41	21.70	22.12	22.48
Na2O	1.18	1.23	2.45	0.47	0.91	0.61	0.76	0.70	0.56	0.66	0.82	0.69
K2O	0.00	0.00	0.00	0.00	0.00	0.00	0.00	0.00	0.00	0.00	0.00	0.0
ZrO2	0.00	0.00	0.00	0.00	0.26	0.27	0.26	0.26	0.24	0.28	0.29	0.31
Total	100.13	100.53	101.20	98.94	99.65	99.12	98.91	99.26	98.64	100.18	100.11	100.07
FeOT	19.79	15.88	21.69	13.91	14.77	14.45	14.00	13.53	12.22	16.46	20.12	17.30
4 cations to 6 oxygens												
Si	1.937	1.930	1.945	1.942	1.938	1.954	1.939	1.939	1.933	1.917	1.921	1.909
Al	0.051	0.044	0.032	0.072	0.069	0.064	0.069	0.071	0.090	0.063	0.054	0.065
Ti	0.013	0.013	0.00	0.017	0.017	0.014	0.019	0.021	0.023	0.017	0.013	0.018
Zr	0.00	0.00	0.00	0.00	0.005	0.005	0.005	0.005	0.005	0.005	0.006	0.006
Fe3	0.140	0.163	0.264	0.045	0.081	0.036	0.063	0.053	0.031	0.106	0.129	0.121
Mg	0.316	0.486	0.237	0.551	0.513	0.508	0.542	0.567	0.610	0.492	0.315	0.420
Fe2	0.511	0.348	0.445	0.406	0.396	0.434	0.391	0.383	0.363	0.427	0.536	0.444
Mn	0.047	0.034	0.058	0.020	0.014	0.025	0.019	0.017	0.018	0.023	0.026	0.024
Ca	0.895	0.892	0.834	0.912	0.900	0.914	0.897	0.892	0.885	0.900	0.937	0.940
Na	0.090	0.091	0.185	0.035	0.068	0.046	0.057	0.053	0.042	0.049	0.063	0.052
K	0.00	0.00	0.00	0.00	0.00	0.00	0.00	0.00	0.00	0.00	0.00	0.0
Atomic percentages												
Na	9.3	9.5	20.0	3.5	6.9	4.5	5.6	5.2	4.1	4.9	6.7	5.5
Fe2+Mn	57.9	39.8	54.4	42.1	41.4	45.3	40.6	39.2	36.9	45.4	59.8	49.8
Mg	32.8	50.7	25.6	54.4	51.8	50.1	53.7	55.6	59.1	49.6	33.5	44.7
Lith. code	314	314	314	324	324	324	324	324	324	324	324	324
Spot no.	86	87	88	263	264	265	283	284	285	293	294	295
Name	Fsal	Sal	A–A	Sal	Sal	Sal	Sal	Sal	Sal	Sal	Fsal	Fsal

Microprobe analyses - Pyroxene. Geologfjeld Formation.

Sample no.	58352	58352	304055	304055	304055
Cryst & posn	108.cor	108.rim	25.cor	26.cor	26.rim
Major elements (wt%)					
SiO2	48.84	48.43	51.40	50.76	50.82
TiO2	0.47	0.27	0.96	0.00	0.25
Al2O3	1.32	1.36	0.49	0.60	1.96
Fe2O3	2.67	4.11	22.75	13.00	17.98
FeO	13.22	14.49	5.50	14.00	8.15
MnO	0.66	0.72	1.17	1.17	1.11
MgO	8.41	5.82	0.56	1.58	1.05
CaO	21.81	21.89	6.30	14.79	11.46
Na2O	0.47	1.01	10.22	5.19	7.63
K2O	0.00	0.00	0.00	0.00	0.0
ZrO2	0.34	0.30	1.40	0.52	0.40
Total	98.24	98.41	100.75	101.60	100.83
FeOT	15.63	18.19	25.97	25.70	24.33
4 cations to 6 oxygens					
Si	1.927	1.932	1.987	1.982	1.965
Al	0.062	0.064	0.022	0.028	0.090
Ti	0.014	0.008	0.028	0.00	0.007
Zr	0.006	0.006	0.026	0.010	0.008
Fe3	0.079	0.123	0.662	0.382	0.523
Mg	0.494	0.346	0.032	0.092	0.061
Fe2	0.436	0.483	0.178	0.457	0.264
Mn	0.022	0.024	0.038	0.039	0.036
Ca	0.922	0.936	0.261	0.619	0.475
Na	0.036	0.078	0.766	0.393	0.572
K	0.00	0.00	0.00	0.00	0.0
Atomic percentages					
Na	3.6	8.4	75.5	40.1	61.3
Fe2+Mn	46.4	54.5	21.3	50.6	32.2
Mg	50.0	37.2	3.2	9.4	6.5
Lith. code	324	324	334	334	334
Spot no.	301	302	89	91	92
Name	Sal	Fsal	A-H	A-H	AH

Microprobe analyses – Pyroxene. Motzfeldt So Formation.

Sample no.	54132	304009	304009	304003	304003	304003	304003	304009	304009	304009	304009	304009
Cryst & posn	APJ	15.cor	15.rim	16.cor	16.int	16.rim	17.cor	18.cor	18.int	18.rim	19.cor	19.rim
Major elements (wt%)												
SiO2	51.15	50.81	50.59	50.90	50.79	50.57	51.19	50.90	50.57	51.45	51.90	51.53
TiO2	0.72	0.75	0.60	0.57	0.30	0.51	1.78	0.30	0.50	0.00	0.00	0.0
Al2O3	1.47	0.46	0.51	1.09	0.86	1.08	0.40	0.57	0.68	0.72	0.39	0.69
Fe2O3	4.21	22.94	23.29	4.54	9.05	12.53	29.26	27.93	25.94	28.93	26.13	24.99
FeO	7.89	5.90	5.43	8.10	7.87	9.67	0.00	2.11	4.19	1.12	3.49	4.20
MnO	0.67	0.79	0.65	0.61	0.99	1.06	0.70	0.94	0.79	1.07	1.08	0.88
MgO	10.55	0.79	0.73	10.85	7.54	4.05	0.00	0.57	0.25	0.36	0.64	0.46
CaO	23.09	8.13	7.73	21.97	18.83	15.41	1.75	5.96	5.39	4.37	6.06	6.65
Na2O	1.04	9.40	9.59	1.11	3.18	5.07	13.31	10.71	10.61	11.59	10.52	10.23
K2O	0.02	0.00	0.00	0.00	0.00	0.00	0.11	0.00	0.00	0.00	0.00	0.0
ZrO2	0.05	1.18	1.28	0.00	0.31	0.48	2.68	0.40	1,04	1.13	0.41	0.40
Total	100.86	101.16	100.42	99.75	99.72	100.44	100.56	100.40	99.98	100.73	100.64	100.04
FeOT	11.68	26.55	26.39	12.19	16.02	20.95	25.70	27.25	27.53	27.15	27.01	26.69
4 cations to 6 oxygens												
Si	1.925	1.964	1.967	1.935	1.954	1.959	1.965	1.966	1.970	1.976	1.998	1.996
Al	0.065	0.021	0.024	0.049	0.039	0.050	0.018	0.026	0.031	0.032	0.018	0.032
Ti	0.020	0.022	0.018	0.016	0.009	0.015	0.051	0.009	0.015	0.00	0.00	0.0
Zr	0.001	0.022	0.024	0.00	0.006	0.009	0.050	0.007	0.020	0.021	0.008	0.008
Fe3	0.119	0.667	0.682	0.130	0.262	0.365	0.845	0.812	0.761	0.836	0.757	0.729
Mg	0.592	0.045	0.042	0.615	0.432	0.234	0.00	0.033	0.014	0.021	0.037	0.027
Fe2	0.248	0.191	0.177	0.258	0.253	0.313	0.00	0.068	0.136	0.036	0.112	0.136
Mn	0.021	0.026	0.022	0.020	0.032	0.035	0.023	0.031	0.026	0.035	0.035	0.029
Ca	0.931	0.337	0.322	0.895	0.776	0.640	0.072	0.246	0.225	0.180	0.250	0.276
Na	0.076	0.704	0.723	0.082	0.237	0.381	0.990	0.802	0.801	0.863	0.785	0.768
K	0.001	0.00	0.00	0.00	0.00	0.00	0.006	0.00	0.00	0.00	0.00	0.0
Atomic percentages												
Na	8.1	72.9	75.0	8.4	24.8	39.6	97.7	85.9	82.0	90.4	81.0	80.0
Fe2+Mn	28.7	22.5	20.6	28.5	29.9	36.1	2.3	10.6	16.6	7.4	15.2	17.2
Mg	63.2	4.7	4.4	63.1	45.3	24.3	0.00	3.5	1.4	2.2	3.8	2.8
Lith. code	432	434	434	434	434	434	434	434	434	434	434	434
Spot no.	–	63	64	65	67	66	68	69	71	70	74	73
Name	Sal	A–H	A–H	Sal	A–A	A–A	Aeg	Aeg	Aeg	Aeg	Aeg	Aeg

Microprobe analyses - Pyroxene. Motzfeldt So Formation.

Sample no. Cryst & posn	304009 20.cor	304009 20.rim	304009 84.cor	326091 112.cor	326091 112.rim	326091 117.cor	326091 117.int	326091 121.cor	326091 121.cor
Major elements (wt%)									
SiO2	51.25	51.43	51.75	48.71	48.41	50.57	50.73	50.20	50.15
TiO2	0.22	0.31	0.45	0.51	0.58	0.61	0.64	0.42	0.93
Al2O3	0.74	0.75	0.52	1.15	0.86	1.29	1.20	0.73	0.84
Fe2O3	25.49	28.20	21.39	5.24	14.28	2.37	2.69	26.12	22.11
FeO	3.81	1.63	8.17	8.29	11.47	10.89	10.45	4.13	6.49
MnO	0.90	1.05	0.48	0.63	0.71	0.71	0.76	0.60	0.70
MgO	0.61	0.50	0.64	8.90	1.96	9.54	9.58	0.72	0.84
CaO	7.59	5.20	8.53	21.75	12.99	22.24	21.92	4.05	5.56
Na2O	10.00	11.17	8.96	1.36	5.73	0.87	1.08	10.76	9.87
K2O	0.00	0.00	0.00	0.00	0.00	0.00	0.00	0.00	0.0
ZrO2	0.70	0.48	-1.00	0.45	0.88	0.25	0.23	1.20	1.38
Total	101.31	100.73	100.90	97.00	97.86	99.34	99.29	98.93	98.87
FeOT	26.74	27.00	27.42	13.00	24.32	13.02	12.87	27.64	26.39
4 cations to 6 oxygens									
Si	1.967	1.974	2.000	1.924	1.952	1.947	1.951	1.971	1.976
Al	0.034	0.034	0.024	0.053	0.041	0.059	0.055	0.034	0.039
Ti	0.006	0.009	0.013	0.015	0.018	0.018	0.019	0.012	0.027
Zr	0.013	0.009	0.00	0.009	0.017	0.005	0.004	0.023	0.026
Fe3	0.736	0.814	0.622	0.156	0.433	0.069	0.078	0.772	0.656
Mg	0.035	0.029	0.037	0.524	0.118	0.548	0.549	0.042	0.049
Fe2	0.122	0.052	0.264	0.274	0.387	0.351	0.336	0.136	0.214
Mn	0.029	0.034	0.016	0.021	0.024	0.023	0.025	0.020	0.024
Ca	0.312	0.214	0.353	0.920	0.561	0.917	0.903	0.171	0.235
Na	0.744	0.831	0.671	0.104	0.448	0.065	0.081	0.819	0.754
K	0.00	0.00	0.00	0.00	0.00	0.00	0.00	0.00	0.0
Atomic percentages									
Na	80.0	87.8	67.9	11.3	45.9	6.6	8.2	80.5	72.4
Fe2+Mn	16.2	9.1	28.3	32.0	42.1	37.9	36.4	15.3	22.9
Mg	3.8	3.1	3.7	56.8	12.1	55.5	55.4	4.1	4.7
Lith. code	434	434	434	434	434	434	434	434	434
Spot no.	75	77	253	308	309	318	317	323	324
Name	Aeg	Aeg	A-H	Sal	A-H	Sal	Sal	Aeg	A-H

Microprobe analyses – Pyroxene. Flinks Dal Formation.

Sample no.	304752	304752	304752	304752	304752	304752	304752	304752	304752	304752	304752	304752
Cryst & posn	45.cor	45.int	45.rim	46.cor	47.cor	48.cor	48.int	48.rim	50.cor	50.int	50.rim	50.rim
Major elements (wt%)												
SiO2	50.11	50.11	50.84	52.23	52.28	50.17	51.49	52.64	51.65	50.53	50.41	50.73
TiO2	0.38	0.34	0.30	1.66	1.29	0.41	0.37	0.43	0.47	0.33	0.41	0.36
Al2O3	0.72	0.68	0.81	0.34	0.22	0.84	0.30	0.63	1.00	0.81	0.42	1.01
Fe2O3	8.02	8.54	5.18	28.54	26.79	4.44	14.68	21.91	2.46	4.12	15.83	2.97
FeO	16.08	15.80	16.20	1.62	2.38	16.70	12.75	7.58	14.34	13.52	10.62	13.18
MnO	1.55	1.64	1.60	1.05	1.08	1.34	1.28	0.76	1.10	1.15	0.86	1.16
MgO	3.18	3.20	4.88	0.64	0.71	4.75	1.65	0.83	7.83	6.54	1.67	7.65
CaO	19.69	19.80	21.40	4.74	4.61	20.27	13.70	8.60	21.99	21.24	12.29	21.59
Na2O	2.53	2.52	1.54	11.65	11.44	1.69	5.90	9.16	0.99	1.55	6.56	1.15
K2O	0.00	0.00	0.00	0.00	0.00	0.00	0.00	0.00	0.00	0.00	0.00	0.0
ZrO2	-1.00	-1.00	-1.00	-1.00	-1.00	-1.00	-1.00	-1.00	-1.00	-1.00	-1.00	-1.00
Total	102.25	102.63	102.74	102.47	100.79	100.62	102.14	102.54	101.83	99.78	99.07	99.81
FeOT	23.29	23.49	20.86	27.30	26.48	20.69	25.97	27.29	16.56	17.23	24.87	15.85
4 cations to 6 oxygens												
Si	1.950	1.945	1.955	1.967	1.996	1.967	1.990	1.998	1.965	1.970	1.994	1.966
Al	0.033	0.031	0.037	0.015	0.010	0.039	0.014	0.028	0.045	0.037	0.020	0.046
Ti	0.011	0.010	0.009	0.047	0.037	0.012	0.011	0.012	0.014	0.010	0.012	0.011
Zr	0.00	0.00	0.00	0.00	0.00	0.00	0.00	0.00	0.00	0.00	0.00	0.0
Fe3	0.235	0.249	0.150	0.809	0.770	0.131	0.427	0.626	0.070	0.121	0.471	0.087
Mg	0.185	0.185	0.280	0.036	0.040	0.278	0.095	0.047	0.444	0.380	0.098	0.442
Fe2	0.523	0.513	0.521	0.051	0.076	0.548	0.412	0.241	0.456	0.441	0.351	0.427
Mn	0.051	0.054	0.052	0.033	0.035	0.044	0.042	0.025	0.035	0.038	0.029	0.038
Ca	0.821	0.823	0.882	0.191	0.188	0.852	0.567	0.350	0.896	0.887	0.521	0.897
Na	0.191	0.190	0.115	0.851	0.847	0.129	0.442	0.674	0.073	0.117	0.503	0.087
K	0.00	0.00	0.00	0.00	0.00	0.00	0.00	0.00	0.00	0.00	0.00	0.0
Atomic percentages												
Na	20.1	20.2	11.9	87.6	84.9	12.9	44.6	68.3	7.2	12.0	51.3	8.8
Fe2+Mn	60.4	60.2	59.2	8.7	11.1	59.3	45.8	27.0	48.7	49.1	38.7	46.8
Mg	19.5	19.6	28.9	3.7	4.0	27.8	9.6	4.8	44.0	38.9	10.0	44.5
Lith. code	514	514	514	514	514	514	514	514	514	514	514	514
Spot no.	164	165	166	167	168	169	170	171	175	176	177	178
Name	A-A	A-A	A-A	Aeg	Aeg	Aeg	A-H	A-H	Fsal	A-A	A-H	Fsal

Microprobe analyses – Pyroxene. Flinks Dal Formation.

Sample no.	304752	304752	304752	304752	304752	304752	304758	304758
Cryst & posn	51.cor	51.rim	51.rim	52.cor	52.int	52.rim	163.cor	164.rim
Major elements (wt%)								
SiO2	49.88	50.28	50.98	49.46	49.94	50.78	50.56	50.70
TiO2	0.38	0.34	0.20	0.35	0.41	0.26	0.34	0.36
Al2O3	0.82	0.73	0.79	0.79	0.79	0.52	0.75	0.71
Fe2O3	6.07	4.66	7.19	6.90	6.25	13.02	6.19	6.17
FeO	15.07	15.85	12.47	17.75	18.39	12.88	11.67	11.96
MnO	1.49	1.45	1.08	1.53	1.49	1.35	1.25	1.16
MgO	4.61	4.80	5.54	2.60	2.67	1.85	6.57	6.90
CaO	20.14	20.35	19.65	19.11	19.11	14.41	20.14	20.14
Na2O	2.02	1.83	2.70	2.38	2.36	5.38	2.22	2.09
K2O	0.00	0.00	0.00	0.00	0.00	0.00	0.00	0.0
ZrO2	-1.00	-1.00	-1.00	-1.00	-1.00	-1.00	-1.00	-1.00
Total	100.48	100.30	100.61	100.87	101.41	100.44	99.69	100.20
FeOT	20.53	20.05	18.94	23.96	24.01	24.60	17.24	17.51
4 cations to 6 oxygens								
Si	1.957	1.974	1.973	1.960	1.967	1.993	1.966	1.962
Al	0.038	0.034	0.036	0.037	0.037	0.024	0.034	0.032
Ti	0.011	0.010	0.006	0.010	0.012	0.008	0.010	0.011
Zr	0.00	0.00	0.00	0.00	0.00	0.00	0.00	0.0
Fe3	0.179	0.138	0.209	0.206	0.185	0.385	0.181	0.180
Mg	0.270	0.281	0.320	0.154	0.157	0.108	0.381	0.398
Fe2	0.495	0.520	0.404	0.588	0.606	0.423	0.380	0.387
Mn	0.049	0.048	0.035	0.051	0.050	0.045	0.041	0.038
Ca	0.847	0.856	0.815	0.811	0.806	0.606	0.839	0.835
Na	0.154	0.139	0.203	0.183	0.180	0.409	0.167	0.157
K	0.00	0.00	0.00	0.00	0.00	0.00	0.00	0.0
Atomic percentages								
Na	15.9	14.1	21.1	18.8	18.1	41.5	17.2	16.0
Fe2+Mn	56.2	57.5	45.6	65.5	66.1	47.5	43.4	43.4
Mg	27.9	28.4	33.3	15.8	15.8	11.0	39.3	40.6
Lith. code	514	514	514	514	514	514	514	514
Spot no.	179	180	181	182	183	184	399	400
Name	A-A	A-A	A-A	A-A	A-A	A-A	A-A	A-A

Microprobe analyses – Pyroxene. Alkali gabbro & Larvikite.

Sample no.	272549	272549	272549	272455	58037	58062
Cryst & posn	APJ	APJ	APJ	APJ	APJ	APJ
Major elements (wt%)						
SiO2	49.79	51.38	51.28	51.81	50.85	50.87
TiO2	1.75	1.10	1.65	0.89	1.06	1.19
Al2O3	3.10	1.77	3.10	1.78	1.90	1.88
Fe2O3	3.72	1.53	0.00	0.00	2.77	0.47
FeO	7.33	8.86	9.94	13.20	8.76	11.54
MnO	0.28	0.32	0.36	0.55	0.56	0.62
MgO	12.28	12.61	11.82	10.22	11.73	10.73
CaO	22.41	22.39	20.78	21.59	22.39	21.77
Na2O	0.63	0.45	0.84	0.68	0.62	0.59
K2O	0.00	0.00	0.02	0.00	0.00	0.0
ZrO2	0.03	0.00	0.00	0.06	0.06	0.03
Total	101.31	100.40	99.79	100.78	100.70	99.69
FeOT	10.67	10.23	9.94	13.20	11.25	11.96
4 cations to 6 oxygens						
Si	1.853	1.925	1.929	1.959	1.910	1.938
Al	0.136	0.078	0.137	0.079	0.084	0.084
Ti	0.049	0.031	0.047	0.025	0.030	0.034
Zr	0.001	0.00	0.00	0.001	0.001	0.001
Fe3	0.104	0.043	0.00	0.00	0.078	0.013
Mg	0.681	0.704	0.663	0.576	0.657	0.609
Fe2	0.228	0.277	0.313	0.417	0.275	0.368
Mn	0.009	0.010	0.011	0.018	0.018	0.020
Ca	0.894	0.899	0.838	0.875	0.901	0.889
Na	0.045	0.033	0.061	0.050	0.045	0.044
K	0.00	0.00	0.001	0.00	0.00	0.0
Atomic percentages						
Na	4.7	3.2	5.8	4.7	4.5	4.2
Fe2+Mn	24.6	28.0	30.9	41.0	29.4	37.3
Mg	70.7	68.8	63.3	54.3	66.0	58.5
Lith. code	614	614	614	621	621	621
Spot no.	0	0	0	0	0	0
Name	Sal	Sal	Sal	Sal	Sal	Sal

Microprobe analyses – Pyroxene. Laminated alkali syenite.

Sample no.	304718	304718	304718	304718
Cryst & posn	38.cor	38.int	38.rim	39.cor
Major elements (wt%)				
SiO2	48.93	50.52	50.93	48.74
TiO2	0.50	0.27	0.45	0.50
Al2O3	0.69	0.54	0.39	0.54
Fe2O3	14.24	14.08	12.99	10.00
FeO	14.06	13.98	14.73	14.28
MnO	0.95	0.93	0.89	0.98
MgO	0.89	0.90	0.78	2.87
CaO	15.13	14.45	13.96	17.29
Na2O	4.95	5.52	5.69	3.49
K2O	0.00	0.00	0.00	0.0
ZrO2	-1.00	-1.00	-1.00	-1.00
Total	100.34	101.22	100.82	98.70
FeOT	26.87	26.66	26.42	23.28
4 cations to 6 oxygens				
Si	1.947	1.982	2.002	1.957
Al	0.032	0.025	0.018	0.025
Ti	0.015	0.008	0.013	0.015
Zr	0.00	0.00	0.00	0.0
Fe3	0.426	0.416	0.384	0.302
Mg	0.053	0.052	0.046	0.172
Fe2	0.468	0.459	0.484	0.480
Mn	0.032	0.031	0.030	0.033
Ca	0.645	0.607	0.588	0.744
Na	0.382	0.420	0.434	0.272
K	0.00	0.00	0.00	0.0
Atomic percentages				
Na	40.9	43.7	43.7	28.4
Fe2+Mn	53.5	50.9	51.7	53.6
Mg	5.7	5.4	4.6	18.0
Lith. code	634	634	634	634
Spot no.	138	140	139	141
Name	A-H	A-H	A-H	A-H

Microprobe analyses - Pyroxene. Laminated porphyritic syenite.

Sample no.	54232	304032	304032
Cryst & posn	29.cor	137.cor	139.cor
Major elements (wt%)			
SiO2	52.26	49.77	52.52
TiO2	0.71	0.00	0.70
Al2O3	0.00	0.00	0.79
Fe2O3	32.54	14.96	27.71
FeO	0.55	14.27	4.20
MnO	0.00	0.83	0.41
MgO	0.00	0.49	0.0
CaO	0.80	12.86	3.79
Na2O	13.34	5.83	11.64
K2O	0.00	0.00	0.0
ZrO2	0.55	-1.00	-1.00
Total	100.76	99.02	101.75
FeOT	29.83	27.73	29.13
4 cations to 6 oxygens			
Si	1.996	2.001	1.995
Al	0.00	0.00	0.035
Ti	0.020	0.00	0.020
Zr	0.010	0.00	0.0
Fe3	0.935	0.453	0.792
Mg	0.00	0.029	0.0
Fe2	0.018	0.480	0.133
Mn	0.00	0.028	0.013
Ca	0.033	0.554	0.154
Na	0.988	0.455	0.857
K	0.00	0.00	0.0
Atomic percentages			
Na	98.2	45.9	85.4
Fe2+Mn	1.8	51.2	14.6
Mg	0.00	2.9	0.0
Lith. code	641	644	644
Spot no.	107	362	365
Name	Aeg	A-H	Aeg

Microprobe analyses – Pyroxene. Peralkaline microsyenite.

Sample no.	258372	258372	258372	304185	304185	304185	304185
Cryst & posn	GS.cor	GS.cor	GS.rim	130.cor	130.cor	134.cor	134.cor
Major elements (wt%)							
SiO2	52.86	52.94	52.45	52.30	52.88	52.76	53.23
TiO2	0.81	0.96	0.61	1.02	0.92	0.68	1.04
Al2O3	1.11	0.71	1.16	0.40	0.89	1.71	1.12
Fe2O3	30.17	33.02	29.18	30.93	30.98	29.64	30.21
FeO	1.40	0.00	1.61	2.03	1.59	2.19	1.24
MnO	0.48	0.00	0.44	0.34	0.00	0.00	0.41
MgO	0.00	0.00	0.00	0.32	0.00	0.00	0.0
CaO	0.77	0.69	0.69	1.09	1.24	0.18	0.64
Na2O	13.16	13.84	13.01	12.84	13.23	13.31	13.46
K2O	0.00	0.00	0.00	0.00	0.00	0.00	0.0
ZrO2	-1.00	-1.00	-1.00	0.75	0.86	0.78	0.54
Total	100.78	101.24	98.16	102.03	102.58	101.25	101.90
FeOT	28.55	28.80	27.87	29.87	29.47	28.85	28.42
4 cations to 6 oxygens							
Si	2.006	1.995	2.019	1.979	1.983	1.994	1.999
Al	0.050	0.031	0.053	0.018	0.039	0.076	0.050
Ti	0.023	0.027	0.018	0.029	0.026	0.019	0.029
Zr	0.00	0.00	0.00	0.014	0.016	0.014	0.010
Fe3	0.861	0.936	0.845	0.881	0.874	0.843	0.854
Mg	0.00	0.00	0.00	0.018	0.00	0.00	0.0
Fe2	0.045	0.00	0.052	0.064	0.050	0.069	0.039
Mn	0.016	0.00	0.014	0.011	0.00	0.00	0.013
Ca	0.032	0.028	0.028	0.044	0.050	0.007	0.026
Na	0.969	1.011	0.971	0.942	0.962	0.976	0.980
K	0.00	0.00	0.00	0.00	0.00	0.00	0.0
Atomic percentages							
Na	94.1	100.0	93.6	91.0	95.1	93.4	95.0
Fe2+Mn	5.9	0.00	6.4	7.2	4.9	6.6	5.0
Mg	0.00	0.00	0.00	1.7	0.00	0.00	0.0
Lith. code	731	731	731	731	731	731	731
Spot no.	0	0	0	337	338	342	343
Name	Aeg	Aeg	Aeg	Aeg	Aeg	Aeg	Aeg

Microprobe analyses - Pyroxene. Undiff.

Sample no.	304074	304074	304074	304074	304074	304074	304074
Cryst & posn	59.cor	59.int	59.rim	60.cor	60.rim	65.cor	65.rim
Major elements (wt%)							
SiO2	49.69	49.07	49.46	50.58	50.97	49.97	50.16
TiO2	0.00	0.00	0.00	0.19	0.27	0.00	0.0
Al2O3	0.76	0.56	0.68	0.94	0.86	0.55	0.43
Fe2O3	12.48	13.40	14.71	21.47	18.88	17.12	14.73
FeO	16.70	16.16	14.39	9.16	10.75	12.54	14.31
MnO	0.93	1.00	0.94	0.58	0.53	0.80	0.89
MgO	0.00	0.00	0.00	0.00	0.00	0.00	0.0
CaO	15.18	14.88	13.09	8.86	9.78	11.63	12.10
Na2O	4.81	4.84	5.83	8.53	8.06	6.80	6.31
K2O	0.00	0.00	0.00	0.00	0.00	0.00	0.0
ZrO2	-1.00	-1.00	-1.00	-1.00	-1.00	-1.00	-1.00
Total	100.56	99.92	99.11	100.31	100.11	99.40	98.93
FeOT	27.93	28.22	27.63	28.48	27.74	27.94	27.56
4 cations to 6 oxygens							
Si	1.981	1.973	1.988	1.980	2.000	1.993	2.013
Al	0.036	0.027	0.032	0.043	0.040	0.026	0.021
Ti	0.00	0.00	0.00	0.006	0.008	0.00	0.0
Zr	0.00	0.00	0.00	0.00	0.00	0.00	0.0
Fe3	0.374	0.405	0.445	0.633	0.557	0.514	0.445
Mg	0.00	0.00	0.00	0.00	0.00	0.00	0.0
Fe2	0.557	0.543	0.484	0.300	0.353	0.418	0.480
Mn	0.032	0.034	0.032	0.019	0.018	0.027	0.030
Ca	0.648	0.641	0.564	0.372	0.411	0.497	0.520
Na	0.372	0.377	0.454	0.647	0.613	0.526	0.491
K	0.00	0.00	0.00	0.00	0.00	0.00	0.0
Atomic percentages							
Na	38.7	39.5	46.8	67.0	62.3	54.2	49.1
Fe2+Mn	61.3	60.5	53.2	33.0	37.7	45.8	50.9
Mg	0.00	0.00	0.00	0.00	0.00	0.00	0.0
Lith. code	921	921	921	921	921	921	921
Spot no.	200	201	202	203	204	210	211
Name	A-H	A-H	A-H	A-H	A-H	A-H	A-H

Microprobe analyses – Amphibole.

Sample no.	304160	304160	304160	304160	304160	304160	304160	304160	304160	304160	304160	304160
Cryst & posn	2.cor	2.int	2.rim	5.cor	5.int	5.rim	27.cor	27.int	27.rim	28.cor	28.int	28.rim
Major elements (wt%)												
SiO2	41.08	41.53	38.64	39.88	39.57	39.01	39.32	37.33	37.94	40.61	39.08	39.77
TiO2	2.87	2.85	2.60	2.85	2.72	2.75	2.82	2.65	2.46	2.89	2.54	2.70
Al2O3	9.15	9.30	9.82	9.48	9.33	9.34	9.36	9.93	10.00	9.08	9.74	9.43
Fe2O3	0.59	0.16	2.22	2.23	0.70	0.70	0.30	4.72	1.88	0.0	2.64	2.40
FeO	20.66	20.92	26.00	21.73	23.48	26.28	24.23	24.55	26.79	21.76	22.56	23.60
MnO	0.90	0.54	1.27	0.99	1.09	1.30	1.26	1.39	1.28	0.93	1.17	1.40
MgO	7.10	7.37	2.31	5.17	4.88	2.64	4.22	1.73	1.77	6.19	4.38	3.78
CaO	10.83	10.94	10.40	10.52	10.33	10.33	10.56	10.32	10.11	10.59	10.40	10.32
Na2O	3.10	3.17	2.93	3.40	2.95	3.00	2.87	3.15	2.90	3.07	3.09	3.32
K2O	1.50	1.43	1.70	1.36	1.50	1.48	1.54	1.65	1.57	1.53	1.55	1.53
ZrO2	0.0	0.0	0.24	0.0	0.18	0.19	0.28	0.36	0.38	0.0	0.0	0.0
Total	97.79	98.20	98.14	97.62	96.73	97.02	96.75	97.79	97.07	96.65	97.15	98.27
FeOT	21.20	21.07	28.00	23.74	24.11	26.91	24.50	28.80	28.48	21.76	24.93	25.77
16 cations to 23 oxygens												
Si	6.405	6.427	6.231	6.304	6.346	6.338	6.336	6.074	6.211	6.436	6.255	6.316
Al	1.682	1.697	1.868	1.767	1.764	1.789	1.779	1.906	1.929	1.696	1.837	1.766
Ti	0.337	0.331	0.315	0.339	0.328	0.335	0.341	0.324	0.302	0.345	0.305	0.323
Zr	0.0	0.0	0.019	0.0	0.014	0.015	0.022	0.028	0.030	0.0	0.0	0.0
Fe3	0.070	0.019	0.269	0.266	0.084	0.085	0.036	0.578	0.231	0.0	0.318	0.287
Mg	1.649	1.700	0.556	1.219	1.165	0.640	1.013	0.421	0.432	1.463	1.046	0.896
Fe2	2.694	2.708	3.507	2.873	3.150	3.570	3.266	3.341	3.668	2.884	3.020	3.135
Mn	0.120	0.071	0.174	0.132	0.148	0.179	0.172	0.191	0.177	0.125	0.159	0.189
Ca	1.809	1.814	1.797	1.783	1.776	1.798	1.823	1.800	1.773	1.798	1.784	1.757
Na	0.936	0.951	0.916	1.043	0.918	0.945	0.896	0.995	0.919	0.944	0.959	1.021
K	0.299	0.282	0.349	0.275	0.307	0.306	0.317	0.342	0.327	0.309	0.317	0.310
Atomic percentages												
Na	21.3	21.3	28.0	25.8	23.8	27.9	24.0	30.9	29.4	22.4	25.3	27.8
Ca	41.2	40.6	55.0	44.1	46.0	53.1	48.8	56.0	56.8	42.8	47.1	47.8
Mg	37.5	38.1	17.0	30.1	30.2	18.9	27.1	13.1	13.8	34.8	27.6	24.4
Lith. code	314	314	314	314	314	314	314	314	314	314	314	314
Spot no.	104	105	106	95	94	96	97	98	99	100	101	102
Colour	Drb-yb	Drb-yb	Dgb-yb	Drb-b	Drb-b	Dgb-gb	Db-b	Dgb-gb	Dgb-gb	Drb-b	Drb-b	Dgb-gb
Name	H-Hb	H-Hb	Has	H-Hb	H-Hb	H-Hb	H-Hb	Has	Has	H-Hb	H-Hb	H-Hb

Table A4.3

Microprobe analyses – Amphibole.

Sample no.	304159	304159	304159	304159	304159	304159	304159	304159	326189	326189	326189	326189
Cryst & posn	86.cor	86.rim	87.cor	87.int	87.rim	88.cor	88.int	88.rim	157.rim	158.rim	160.cor	160.rim
Major elements (wt%)												
SiO2	40.49	38.98	41.00	41.11	40.81	40.50	39.92	39.50	38.10	37.90	40.02	37.63
TiO2	2.83	2.46	2.89	3.06	2.12	2.86	2.76	2.47	2.37	2.16	3.78	2.11
Al2O3	10.09	10.81	9.76	9.73	9.76	10.08	10.40	10.29	11.19	11.75	10.43	11.08
Fe2O3	1.87	2.48	0.41	0.0	1.42	0.50	0.0	2.59	4.22	3.77	0.0	2.95
FeO	23.95	26.72	22.90	23.79	25.04	25.77	26.90	27.60	26.18	27.68	24.66	27.83
MnO	1.03	1.28	0.79	1.10	1.22	1.05	1.18	1.21	1.26	1.17	0.56	1.06
MgO	4.11	1.73	5.49	5.09	4.06	3.75	2.79	1.35	1.37	0.86	4.42	0.74
CaO	11.01	10.55	10.89	11.06	10.99	11.04	10.77	10.64	11.08	10.90	11.06	10.86
Na2O	3.24	3.08	3.23	3.15	2.90	2.92	2.88	3.16	2.94	2.68	2.65	2.63
K2O	1.62	1.63	1.50	1.43	1.63	1.67	1.64	1.65	1.66	1.81	1.65	1.75
ZrO2	-1.00	-1.00	-1.00	-1.00	-1.00	-1.00	-1.00	-1.00	-1.00	-1.00	-1.00	-1.00
Total	100.24	99.73	98.85	99.50	99.94	100.16	99.25	100.45	100.36	100.70	99.24	98.64
FeOT	25.63	28.95	23.26	23.79	26.31	26.22	26.90	29.93	29.97	31.07	24.66	30.48
16 cations to 23 oxygens												
Si	6.285	6.186	6.379	6.383	6.372	6.317	6.315	6.245	6.040	6.014	6.281	6.098
Al	1.847	2.023	1.791	1.780	1.796	1.854	1.940	1.918	2.091	2.199	1.929	2.116
Ti	0.330	0.294	0.338	0.357	0.248	0.335	0.328	0.293	0.282	0.258	0.446	0.258
Zr	0.0	0.0	0.0	0.0	0.0	0.0	0.0	0.0	0.0	0.0	0.0	0.0
Fe3	0.219	0.297	0.048	0.0	0.166	0.059	0.0	0.308	0.503	0.450	0.0	0.359
Mg	0.950	0.410	1.274	1.177	0.944	0.873	0.659	0.319	0.324	0.203	1.035	0.179
Fe2	3.109	3.546	2.980	3.089	3.270	3.361	3.559	3.650	3.470	3.673	3.236	3.771
Mn	0.135	0.172	0.104	0.144	0.161	0.139	0.158	0.162	0.169	0.157	0.075	0.146
Ca	1.831	1.794	1.815	1.840	1.838	1.845	1.826	1.803	1.882	1.854	1.860	1.885
Na	0.974	0.949	0.975	0.948	0.879	0.884	0.883	0.970	0.902	0.825	0.807	0.825
K	0.322	0.330	0.297	0.283	0.324	0.332	0.331	0.332	0.336	0.367	0.331	0.362
Atomic percentages												
Na	25.9	30.1	24.0	23.9	24.0	24.5	26.2	31.4	29.0	28.6	21.8	28.6
Ca	48.8	56.9	44.7	46.4	50.2	51.2	54.2	58.3	60.6	64.3	50.2	65.2
Mg	25.3	13.0	31.3	29.7	25.8	24.2	19.6	10.3	10.4	7.0	28.0	6.2
Lith. code	314	314	314	314	314	314	314	314	324	324	324	324
Spot no.	255	256	257	258	259	260	261	262	388	390	393	394
Colour	Drb-yb	Dgb-yb	Drb-yb	Drb-yb	Dgb-yb	Drb-yb	Drb-yb	Dgb-yb	Dgb-yb	Dgb-yb	Drb-yb	Dgb-yb
Name	H-Hb	Has	H-Hb	H-Hb	H-Hb	H-Hb	H-Hb	H-Hb	Has	Has	H-Hb	Has

Microprobe analyses - Amphibole.

Sample no. Cryst & posn	304051 90.cor	304051 90.int	304051 90.rim	304051 91.cor	304051 91.int	305051 91.rim	304051 92.cor	304051 92.int	304051 92.rim	326161 98.cor	326161 98.int	326161 98.rim
Major elements (wt%)												
SiO2	39.25	39.46	37.05	39.56	38.79	36.67	39.28	38.57	37.40	38.67	37.83	36.60
TiO2	3.77	3.68	1.63	3.66	3.65	2.25	3.60	3.36	2.55	3.66	3.05	2.07
Al2O3	10.44	10.36	11.06	10.29	10.66	11.37	10.59	10.61	11.41	10.31	10.84	11.43
Fe2O3	0.00	0.00	3.78	0.00	0.00	3.72	0.0	0.0	0.50	0.0	0.0	2.45
FeO	21.71	22.13	26.40	22.24	25.11	27.11	23.65	25.32	28.01	22.81	26.41	26.34
MnO	0.45	0.54	1.08	0.55	0.68	1.11	0.61	0.59	0.83	0.55	0.83	1.21
MgO	5.78	5.52	1.09	5.60	3.65	0.62	4.25	3.65	1.50	5.00	2.29	1.29
CaO	10.93	11.15	10.05	11.14	11.11	10.82	11.07	10.97	10.70	10.98	10.78	10.56
Na2O	2.96	2.91	2.80	2.89	2.57	2.71	2.74	2.67	2.57	2.84	2.78	2.60
K2O	1.53	1.42	1.79	1.59	1.68	1.71	1.63	1.68	1.62	1.51	1.52	1.69
ZrO2	0.31	0.28	0.69	0.26	0.63	0.68	0.24	0.47	0.64	0.14	0.38	0.76
Total	97.12	97.46	97.42	97.80	98.52	98.77	97.67	97.89	97.73	96.48	96.70	97.00
FeOT	21.71	22.13	29.80	22.24	25.11	30.46	23.65	25.32	28.46	22.81	26.41	28.54
16 cations to 23 oxygens												
Si	6.212	6.240	6.074	6.232	6.179	5.959	6.255	6.171	6.086	6.197	6.166	6.016
Al	1.947	1.932	2.138	1.912	2.001	2.178	1.988	2.001	2.188	1.948	2.082	2.214
Ti	0.448	0.437	0.201	0.434	0.437	0.275	0.431	0.404	0.312	0.441	0.374	0.256
Zr	0.024	0.022	0.055	0.020	0.049	0.054	0.019	0.037	0.051	0.011	0.030	0.061
Fe3	0.0	0.0	0.466	0.0	0.0	0.455	0.0	0.0	0.061	0.0	0.0	0.303
Mg	1.362	1.300	0.267	1.316	0.866	0.151	1.010	0.870	0.363	1.195	0.556	0.317
Fe2	2.874	2.927	3.620	2.930	3.345	3.684	3.150	3.387	3.811	3.057	3.600	3.620
Mn	0.060	0.073	0.150	0.073	0.091	0.153	0.082	0.080	0.115	0.075	0.114	0.168
Ca	1.854	1.889	1.766	1.881	1.896	1.884	1.888	1.881	1.865	1.885	1.883	1.859
Na	0.907	0.893	0.890	0.883	0.793	0.854	0.846	0.827	0.811	0.882	0.878	0.830
K	0.310	0.287	0.374	0.320	0.341	0.354	0.332	0.342	0.336	0.309	0.316	0.354
Atomic percentages												
Na	22.0	21.9	30.4	21.6	22.3	29.6	22.6	23.1	26.7	22.3	26.5	27.6
Ca	45.0	46.3	60.4	46.1	53.3	65.2	50.4	52.6	61.4	47.6	56.8	61.8
Mg	33.0	31.8	9.1	32.3	24.4	5.2	27.0	24.3	11.9	30.2	16.8	10.5
Lith. code	324	324	324	324	324	324	324	324	324	324	324	324
Spot no.	266	267	268	269	270	271	272	273	274	280	281	282
Colour	Drb-rb	Drb-rb	Dg-g	Drb-yb	Drb-yb	Dgb-g	Drb-yb	Drb-yb	Dgb-yb	Drb-rb	Dgb-rb	Dgb-g
Name	MHas	MHas	Has	Has	Has	Has	H-Hb	Has	Has	Has	Has	Has

Microprobe analyses – Amphibole.

Sample no.	326161	326161	58352	58352	58352	58352	58352	58352
Cryst & posn	100.rim	101.cor	106.cor	106.int	106.rim	110.cor	110.int	110.rim
Major elements (wt%)								
SiO2	36.23	38.37	37.06	37.36	36.91	37.88	37.58	36.47
TiO2	2.05	3.62	2.66	3.22	2.47	3.45	3.16	1.62
Al2O3	11.00	10.58	10.47	9.85	9.88	9.42	9.83	9.26
Fe2O3	3.78	0.08	4.61	2.43	2.32	0.78	0.99	5.84
FeO	26.76	23.16	24.75	25.38	27.21	25.21	25.92	26.60
MnO	1.21	0.68	0.76	0.56	1.05	0.52	0.75	1.27
MgO	0.73	4.92	2.24	3.04	1.33	3.51	2.86	0.29
CaO	10.43	10.84	10.62	10.68	10.52	10.59	10.59	9.54
Na2O	2.65	2.68	2.97	2.76	2.69	2.84	2.80	3.10
K2O	1.61	1.69	1.60	1.53	1.39	1.48	1.42	1.63
ZrO2	0.43	0.03	0.50	0.45	0.22	0.38	0.45	1.05
Total	96.88	96.66	98.25	97.27	96.00	96.05	96.34	96.66
FeOT	30.16	23.24	28.89	27.57	29.30	25.91	26.81	31.85
16 cations to 23 oxygens								
Si	5.997	6.146	5.990	6.073	6.141	6.194	6.157	6.105
Al	2.147	1.998	1.995	1.887	1.938	1.816	1.898	1.828
Ti	0.255	0.437	0.324	0.394	0.309	0.425	0.390	0.204
Zr	0.034	0.002	0.039	0.035	0.018	0.030	0.036	0.086
Fe3	0.471	0.010	0.560	0.297	0.290	0.096	0.122	0.736
Mg	0.180	1.175	0.540	0.737	0.331	0.856	0.697	0.071
Fe2	3.705	3.103	3.345	3.451	3.786	3.448	3.552	3.724
Mn	0.169	0.092	0.104	0.078	0.147	0.071	0.104	0.180
Ca	1.850	1.860	1.840	1.860	1.876	1.856	1.859	1.711
Na	0.850	0.832	0.931	0.871	0.868	0.899	0.889	1.006
K	0.341	0.345	0.331	0.318	0.295	0.309	0.296	0.348
Atomic percentages								
Na	29.5	21.5	28.1	25.1	28.2	24.9	25.8	36.1
Ca	64.2	48.1	55.6	53.6	61.0	51.4	54.0	61.4
Mg	6.3	30.4	16.3	21.3	10.8	23.7	20.2	2.5
Lith. code	324	324	324	324	324	324	324	324
Spot no.	288	289	297	298	299	304	305	306
Colour	Dg-g	Drb-rb	VDrb-rb	VDrb-rb	VDgb-gb	Drb-yb	Drb-yb	VDg-yb
Name	Has	Has	Has	Has	Has	Has	Has	Has

Microprobe analyses – Amphibole.

Sample no.	304055	304055	304055	304055	304055	304055	304055	304055	304055	304055
Cryst & posn	68.cor	68.rim	69.cor	69.rim	70.cor	70.rim	71.cor	71.rim	72.cor	72.rim
Major elements (wt%)										
SiO2	42.19	43.10	42.18	43.88	43.17	43.69	40.45	41.77	40.05	42.20
TiO2	1.37	1.65	1.89	1.48	1.50	1.40	1.80	1.58	3.00	1.69
Al2O3	5.28	5.41	6.37	5.09	6.22	5.16	6.94	6.21	10.07	6.61
Fe2O3	6.98	5.82	4.13	7.79	5.16	5.55	6.41	7.80	0.0	7.52
FeO	23.29	25.25	24.36	23.19	26.17	25.79	25.05	23.61	23.59	23.61
MnO	1.35	1.40	1.21	1.33	1.17	1.38	1.40	1.25	0.58	1.28
MgO	2.26	2.14	3.27	2.04	1.76	2.08	1.69	1.85	5.26	2.03
CaO	6.66	6.43	8.09	4.59	5.81	6.77	7.80	6.44	10.38	6.06
Na2O	5.16	5.20	4.33	6.36	5.43	5.16	4.33	5.30	3.01	5.46
K2O	1.69	1.67	1.69	1.69	1.56	1.64	1.69	1.70	1.58	1.74
ZrO2	-1.00	-1.00	-1.00	-1.00	-1.00	-1.00	-1.00	-1.00	-1.00	-1.00
Total	96.23	98.07	97.53	97.43	97.96	98.62	97.56	97.51	97.53	98.22
FeOT	29.57	30.48	28.08	30.20	30.82	30.78	30.82	30.63	23.59	30.38
16 cations to 23 oxygens										
Si	6.889	6.917	6.767	7.033	6.923	6.977	6.579	6.747	6.331	6.745
Al	1.016	1.024	1.205	0.961	1.176	0.971	1.332	1.183	1.878	1.246
Ti	0.168	0.199	0.228	0.178	0.181	0.169	0.220	0.192	0.357	0.203
Zr	0.0	0.0	0.0	0.0	0.0	0.0	0.0	0.0	0.0	0.0
Fe3	0.857	0.703	0.498	0.939	0.623	0.667	0.785	0.948	0.0	0.904
Mg	0.549	0.512	0.782	0.488	0.421	0.494	0.409	0.445	1.238	0.483
Fe2	3.181	3.388	3.269	3.109	3.511	3.444	3.407	3.190	3.119	3.157
Mn	0.186	0.190	0.165	0.181	0.159	0.187	0.193	0.171	0.078	0.173
Ca	1.166	1.107	1.390	0.789	0.999	1.159	1.359	1.114	1.758	1.039
Na	1.635	1.618	1.348	1.977	1.688	1.598	1.365	1.660	0.922	1.693
K	0.353	0.341	0.346	0.345	0.319	0.333	0.351	0.350	0.319	0.355
Atomic percentages										
Na	48.8	50.0	38.3	60.8	54.3	49.2	43.6	51.6	23.5	52.7
Ca	34.8	34.2	39.5	24.2	32.1	35.7	43.4	34.6	44.9	32.3
Mg	16.4	15.8	22.2	15.0	13.5	15.2	13.1	13.8	31.6	15.0
Lith. code	334	334	334	334	334	334	334	334	334	334
Spot no.	217	218	219	220	221	222	223	224	225	226
Colour	VDg-g	VDg-g	VDg-bg	VDg-g	VDg-g	VDg-g	VDg-bg	VDg-g	VDbg-bg	VDg-g
Name	Kat	Kat	FEd	Kat	Kat	Kat	FEdHb	Kat	H-Hb	Kat

Microprobe analyses - Amphibole.

Sample no.	304710	304710	304710	304710	304710	304710	304052	304052	304052	304052	304052	304052
Cryst & posn	42.cor	42.int	42.rim	43.cor	43.int	43.rim	56.cor	56.int	56.rim	57.cor	57.cor	57.int
Major elements (wt%)												
SiO2	49.17	49.46	48.88	49.58	48.36	48.65	48.55	48.76	49.04	47.95	47.93	48.16
TiO2	0.79	0.76	0.80	0.92	0.94	0.90	0.63	0.73	0.57	1.42	1.58	1.40
Al2O3	1.63	1.17	1.56	1.71	1.78	1.52	1.54	1.62	1.45	1.76	1.76	1.98
Fe2O3	9.36	8.93	9.97	9.19	11.13	8.81	6.86	5.15	7.08	5.79	6.39	6.21
FeO	25.14	25.50	24.40	25.87	24.37	26.45	25.23	26.35	24.23	26.04	26.20	25.61
MnO	1.23	1.13	1.21	1.02	1.02	1.22	1.31	1.04	1.24	1.26	1.12	1.14
MgO	0.44	0.51	0.40	0.54	0.43	0.25	2.07	1.98	2.01	1.88	1.94	1.94
CaO	0.99	0.79	0.60	0.91	0.80	0.49	2.93	2.88	2.66	3.21	3.15	3.12
Na2O	8.96	9.01	9.12	9.00	9.00	8.69	7.49	7.44	7.89	7.39	7.44	7.53
K2O	1.55	1.52	1.60	1.54	1.62	1.63	1.63	1.59	1.70	1.52	1.50	1.60
ZrO2	-1.00	-1.00	-1.00	-1.00	-1.00	-1.00	-1.00	-1.00	-1.00	-1.00	-1.00	-1.00
Total	99.29	98.78	98.55	100.28	99.46	98.61	98.25	97.54	97.88	98.23	99.00	98.70
FeOT	33.57	33.53	33.37	34.14	34.38	34.38	31.41	30.98	30.60	31.26	31.94	31.20
16 cations to 23 oxygens												
Si	7.722	7.802	7.726	7.708	7.600	7.727	7.687	7.762	7.758	7.611	7.558	7.593
Al	0.302	0.217	0.291	0.314	0.330	0.286	0.287	0.305	0.270	0.329	0.327	0.368
Ti	0.094	0.090	0.095	0.108	0.111	0.107	0.075	0.088	0.068	0.169	0.187	0.166
Zr	0.0	0.0	0.0	0.0	0.0	0.0	0.0	0.0	0.0	0.0	0.0	0.0
Fe3	1.106	1.060	1.186	1.075	1.316	1.053	0.818	0.617	0.843	0.692	0.758	0.737
Mg	0.103	0.121	0.094	0.125	0.100	0.058	0.488	0.471	0.474	0.445	0.456	0.456
Fe2	3.302	3.364	3.225	3.363	3.203	3.514	3.341	3.507	3.206	3.457	3.455	3.377
Mn	0.164	0.150	0.162	0.135	0.136	0.164	0.175	0.140	0.167	0.169	0.150	0.153
Ca	0.167	0.134	0.102	0.151	0.135	0.083	0.497	0.491	0.451	0.547	0.532	0.527
Na	2.730	2.755	2.796	2.714	2.744	2.677	2.301	2.298	2.421	2.273	2.275	2.301
K	0.310	0.306	0.323	0.306	0.325	0.331	0.330	0.322	0.343	0.308	0.302	0.321
Atomic percentages												
Na	91.0	91.5	93.4	90.8	92.1	95.0	70.0	70.5	72.4	69.6	69.7	70.1
Ca	5.6	4.5	3.4	5.1	4.5	2.9	15.1	15.1	13.5	16.8	16.3	16.0
Mg	3.4	4.0	3.1	4.2	3.4	2.1	14.9	14.4	14.2	13.6	14.0	13.9
Lith. code	415	415	415	415	415	415	414	414	414	414	414	414
Spot no.	152	153	154	155	156	157	191	192	193	194	196	195
Colour	VDgbl-g	VDgbl-g	VDgbl-g	VDgbl-g	VDgbl-g	VDgbl-g	Dg-yg	Dg-yg	Dg-yg	Dg-yg	Dg-yg	Dg-yg
Name	Arf	Arf	Arf	Arf	Arf	Arf	Arf	Arf	Arf	Arf	Arf	Arf

Microprobe analyses – Amphibole.

Sample no. Cryst & posn	304052 57.rim	304165 148.cor	304165 148.rim	304165 149.cor	304165 150.cor	304003 75.cor	304003 75.int	304003 75.rim	304003 77.cor	304003 77.cor	304003 77.int	304003 77.rim
Major elements (wt%)												
SiO2	48.25	48.57	50.38	48.72	47.67	44.18	45.45	45.97	45.40	45.35	44.59	44.54
TiO2	1.35	1.08	0.88	1.25	1.47	2.05	2.69	2.72	2.47	2.04	2.04	2.10
Al2O3	1.79	1.80	1.36	1.72	2.61	5.68	4.48	4.44	5.20	5.51	5.31	5.00
Fe2O3	5.61	10.11	8.32	7.93	10.22	5.29	7.50	8.82	5.71	4.44	6.03	7.16
FeO	26.89	23.45	21.25	25.23	22.83	21.03	23.30	22.66	21.04	22.02	21.04	21.82
MnO	1.18	1.25	1.88	1.12	1.41	1.46	1.31	1.56	1.37	1.38	1.47	1.54
MgO	1.96	1.46	3.09	1.57	2.05	5.29	2.49	1.91	5.42	5.20	4.99	3.93
CaO	3.45	0.73	0.34	0.62	0.98	7.64	4.35	3.53	6.75	6.71	6.56	6.56
Na2O	7.22	8.67	8.95	8.40	8.32	5.05	6.98	7.64	5.69	5.53	5.62	5.76
K2O	1.51	1.90	1.91	1.84	1.93	1.63	1.69	1.74	1.66	1.54	1.53	1.65
ZrO2	-1.00	-1.00	-1.00	-1.00	-1.00	-1.00	-1.00	-1.00	-1.00	-1.00	-1.00	-1.00
Total	99.22	99.03	98.36	98.42	99.49	99.29	100.25	101.00	100.71	99.70	99.19	100.07
FeOT	31.93	32.55	28.73	32.37	32.03	25.79	30.05	30.60	26.18	26.01	26.47	28.26
16 cations to 23 oxygens												
Si	7.595	7.619	7.823	7.691	7.439	6.852	7.056	7.083	6.924	6.983	6.921	6.911
Al	0.333	0.333	0.249	0.320	0.480	1.038	0.821	0.807	0.935	1.000	0.972	0.914
Ti	0.160	0.128	0.103	0.149	0.172	0.240	0.315	0.315	0.284	0.236	0.238	0.245
Zr	0.0	0.0	0.0	0.0	0.0	0.0	0.0	0.0	0.0	0.0	0.0	0.0
Fe3	0.664	1.194	0.972	0.943	1.201	0.617	0.876	1.023	0.655	0.514	0.705	0.836
Mg	0.461	0.341	0.715	0.370	0.478	1.223	0.576	0.440	1.231	1.192	1.154	0.909
Fe2	3.540	3.076	2.760	3.331	2.979	2.729	3.025	2.920	2.684	2.835	2.731	2.831
Mn	0.158	0.166	0.247	0.150	0.186	0.192	0.172	0.204	0.177	0.179	0.194	0.203
Ca	0.581	0.123	0.057	0.105	0.164	1.269	0.724	0.583	1.104	1.107	1.091	1.091
Na	2.204	2.639	2.695	2.570	2.517	1.518	2.101	2.283	1.684	1.650	1.691	1.733
K	0.304	0.381	0.379	0.371	0.385	0.322	0.335	0.343	0.322	0.303	0.303	0.328
Atomic percentages												
Na	67.9	85.0	77.7	84.4	79.7	37.9	61.8	69.1	41.9	41.8	43.0	46.4
Ca	17.9	4.0	1.6	3.4	5.2	31.6	21.3	17.6	27.5	28.0	27.7	29.2
Mg	14.2	11.0	20.6	12.2	15.1	30.5	16.9	13.3	30.6	30.2	29.3	24.4
Lith. code	414	414	414	414	414	434	434	434	434	434	434	434
Spot no.	197	375	376	377	378	231	232	233	235	236	238	239
Colour	Dg-yg	VDblg-g	VDblg-g	VDblg-g	VDblg-g	g-b	Dg-b	Vdg-Db	g-gb	g-gb	g-gb	Dg-gb
Name	Arf	Arf	Arf	Arf	Arf	Kat	Kat	Arf	Kat	Kat	Kat	Kat

Microprobe analyses - Amphibole.

Sample no.	304003	304003	304003	304003	304003	304003	304003	304003	304003	304003	304003	304003
Cryst & posn	79.cor	79.int	79.rim	81.cor	81.int	81.rim	82.cor	82.int	82.rim	83.cor	83.int	83.rim
Major elements (wt%)												
SiO2	44.12	45.22	44.83	44.54	44.37	44.85	45.40	46.12	44.80	45.11	45.32	45.27
TiO2	2.09	2.63	2.62	3.14	2.15	2.15	1.99	1.95	2.60	2.01	2.02	2.91
Al2O3	5.69	4.64	4.38	7.64	5.60	5.16	5.70	5.03	4.86	5.61	5.52	4.27
Fe2O3	4.57	10.14	8.36	0.0	3.98	6.51	3.23	6.02	6.74	4.45	4.60	6.13
FeO	21.96	20.46	21.51	17.86	22.28	22.73	22.46	21.74	23.83	20.25	21.36	24.62
MnO	1.48	1.41	1.30	0.68	1.30	1.45	1.22	1.26	1.46	1.40	1.44	1.48
MgO	5.06	2.83	2.76	9.56	4.94	3.52	5.66	4.87	2.78	6.18	5.84	1.94
CaO	7.50	4.28	4.24	10.70	7.76	5.95	7.56	5.54	5.13	7.82	7.56	4.16
Na2O	4.94	7.41	7.14	3.48	4.93	6.09	5.01	6.23	6.39	5.05	5.15	6.95
K2O	1.63	1.71	1.62	1.49	1.68	1.51	1.63	1.60	1,58	1.70	1.58	1.58
ZrO2	-1.00	-1.00	-1.00	-1.00	-1.00	-1.00	-1.00	-1.00	-1.00	-1.00	-1.00	-1.00
Total	99.05	100.74	98.76	99.09	99.01	99.93	99.87	100.36	100.16	99.59	100.40	99.32
FeOT	26.07	29.59	29.03	17.86	25.87	28.59	25.37	27.16	29.89	24.26	25.49	30.14
16 cations to 23 oxygens												
Si	6.873	6.959	7.039	6.736	6.911	6.963	6.972	7.055	6.976	6.921	6.925	7.115
Al	1.045	0.842	0.811	1.362	1.028	0.944	1.033	0.906	0.893	1.016	0.995	0.791
Ti	0.245	0.305	0.310	0.357	0.252	0.252	0.230	0.225	0.304	0.232	0.232	0.344
Zr	0.0	0.0	0.0	0.0	0.0	0.0	0.0	0.0	0.0	0.0	0.0	0.0
Fe3	0.536	1.174	0.987	0.0	0.467	0.761	0.373	0.693	0.790	0.514	0.528	0.726
Mg	1.175	0.650	0.645	2.156	1.148	0.815	1.295	1.110	0.644	1.414	1.331	0.455
Fe2	2.861	2.634	2.824	2.260	2.903	2.951	2.884	2.781	3.103	2.599	2.730	3.236
Mn	0.195	0.184	0.174	0.088	0.172	0.191	0.159	0.164	0.193	0.182	0.187	0.197
Ca	1.253	0.706	0.713	1.734	1.295	0.990	1.244	0.908	0.855	1.285	1.238	0.701
Na	1.494	2.210	2.173	1.021	1.489	1.835	1.491	1.847	1.928	1.503	1.527	2.118
K	0.324	0.335	0.324	0.287	0.334	0.299	0.319	0.311	0.314	0.333	0.309	0.317
Atomic percentages												
Na	38.1	62.0	61.5	20.8	37.9	50.4	37.0	47.8	56.3	35.8	37.3	64.7
Ca	31.9	19.8	20.2	35.3	32.9	27.2	30.9	23.5	24.9	30.6	30.2	21.4
Mg	30.0	18.2	18.3	43.9	29.2	22.4	32.1	28.7	18.8	33.7	32.5	13.9
Lith. code	434	434	434	434	434	434	434	434	434	434	434	434
Spot no.	240	241	242	244	245	246	247	248	249	250	251	252
Colour	g-b	Dg-b	Dg-b	rb-Pb	Dg-b	Dg-b	Db-g	g-Db	Dg-VDb	Dg-Db	Dg-Db	VDg-VDb
Name	Kat	Kat	Kat	FEdHb	Kat	Kat	Kat	Kat	Kat	Kat	Kat	Kat

Microprobe analyses – Amphibole.

Sample no.	326091	326091	326091
Cryst & posn	113.cor	113.int	116.cor
Major elements (wt%)			
SiO2	42.13	42.02	44.03
TiO2	2.76	2.62	3.02
Al2O3	6.50	6.73	7.08
Fe2O3	0.30	2.97	1.56
FeO	21.16	19.39	18.12
MnO	0.81	0.99	0.87
MgO	7.32	6.57	9.13
CaO	9.59	7.52	10.15
Na2O	3.52	4.58	4.00
K2O	1.47	1.53	1.49
ZrO2	0.40	0.19	0.27
Total	95.96	95.13	99.72
FeOT	21.43	22.06	19.53
16 cations to 23 oxygens			
Si	6.703	6.723	6.648
Al	1.219	1.270	1.261
Ti	0.331	0.315	0.342
Zr	0.031	0.015	0.020
Fe3	0.036	0.358	0.177
Mg	1.736	1.567	2.053
Fe2	2.816	2.594	2.288
Mn	0.109	0.135	0.111
Ca	1.635	1.289	1.642
Na	1.086	1.422	1.171
K	0.299	0.311	0.287
Atomic percentages			
Na	24.4	33.2	24.1
Ca	36.7	30.1	33.7
Mg	38.9	36.6	42.2
Lith. code	434	434	434
Spot no.	310	311	315
Colour	g-Prb	g-Prb	Drb-yg
Name	FEdhb	FEdhb	FEdhb

Microprobe analyses - Amphibole.

Sample no.	326091	326092	326092	326092	326092	326092
Cryst & posn	121.cor	151.cor	152.rim	153.cor	153.rim	154.cor
Major elements (wt%)						
SiO2	41.96	43.13	42.94	44.16	43.83	42.97
TiO2	2.96	2.72	3.01	2.87	2.56	2.89
Al2O3	6.89	7.21	6.22	7.50	5.99	5.97
Fe2O3	1.07	0.0	4.60	0.08	3.26	2.27
FeO	17.23	22.30	24.48	20.71	23.00	27.22
MnO	0.80	0.82	1.12	0.67	1.22	1.18
MgO	9.00	6.55	2.68	8.35	4.99	2.64
CaO	10.00	10.48	6.23	10.51	8.07	8.33
Na2O	3.57	3.43	5.46	3.53	4.65	4.29
K2O	1.53	1.53	1.78	1.66	1.65	1.77
ZrO2	0.22	-1.00	-1.00	-1.00	-1.00	-1.00
Total	95.24	98.19	98.53	100.05	99.22	99.54
FeOT	18.20	22.30	28.62	20.79	25.94	29.27
16 cations to 23 oxygens						
Si	6.627	6.724	6.805	6.678	6.826	6.800
Al	1.283	1.326	1.162	1.337	1.100	1.113
Ti	0.351	0.319	0.359	0.327	0.299	0.344
Zr	0.017	0.0	0.0	0.0	0.0	0.0
Fe3	0.128	0.0	0.548	0.009	0.383	0.271
Mg	2.118	1.522	0.634	1.883	1.158	0.624
Fe2	2.276	2.908	3.245	2.620	2.996	3.603
Mn	0.107	0.108	0.151	0.086	0.160	0.159
Ca	1.692	1.751	1.058	1.704	1.346	1.413
Na	1.093	1.037	1.678	1.036	1.405	1.316
K	0.309	0.305	0.360	0.320	0.327	0.357
Atomic percentages						
Na	22.3	24.1	49.8	22.4	35.9	39.2
Ca	34.5	40.6	31.4	36.9	34.4	42.1
Mg	43.2	35.3	18.8	40.7	29.6	18.6
Lith. code	434	434	434	434	434	434
Spot no.	322	380	381	382	383	384
Colour	Db-Yb	Db-gb	Db-Dg	Db-yb	Dgb-Pgb	Db-gb
Name	FEdHb	FEdHb	Kat	FEdHb	FEd	FEd

Microprobe analyses - Amphibole.

Sample no.	304752	304752	304752	304752	304752	304758	304758	326103	326103	326103	326103	272438
Cryst & posn	49.cor	49.int	49.rim	54.cor	55.cor	165.cor	166.cor	161.cor	161.rim	162.cor	162.rim	APJ
Major elements (wt%)												
SiO2	42.59	42.85	42.87	46.01	46.61	47.97	48.63	41.33	42.27	41.71	42.08	41.61
TiO2	2.10	1.94	2.19	1.75	1.54	0.96	0.90	1.99	1.91	1.81	1.90	3.83
Al2O3	6.88	7.14	6.88	4.24	3.53	2.18	1.89	6.62	6.83	6.52	6.99	8.80
Fe2O3	3.46	2.35	2.15	4.11	4.12	7.48	4.72	3.46	2.61	1.94	3.47	0.0
FeO	23.97	25.06	25.16	21.65	24.01	20.16	23.01	23.23	22.25	21.68	22.33	15.15
MnO	1.45	1.36	1.43	1.42	1.52	1.46	1.46	1.40	1.20	1.10	1.36	0.55
MgO	4.38	4.35	4.19	5.60	4.03	4.64	4.44	4.33	5.51	5.87	5.42	9.18
CaO	9.13	9.50	9.25	6.65	5.59	3.25	3.33	9.24	9.49	9.11	9.49	12.12
Na2O	3.93	3.71	3.83	5.55	5.93	7.46	7.08	3.66	3.66	3.56	3.65	3.44
K2O	1.61	1.56	1.58	1.53	1.61	1.58	1.51	1.60	1,61	1.58	1.55	1.53
ZrO2	-1.00	-1.00	-1.00	-1.00	-1.00	-1.00	-1.00	-1.00	-1.00	-1.00	-1.00	0.02
Total	99.50	99.82	99.52	98.51	98.51	97.14	96.96	96.87	97.34	94.89	98.26	96.23
FeOT	27.09	27.17	27.09	25.35	27.72	26.89	27.26	26.34	24.60	23.43	25.46	15.15
16 cations to 23 oxygens												
Si	6.671	6.692	6.719	7.154	7.313	7.536	7.673	6.656	6.704	6.761	6.633	6.445
Al	1.271	1.315	1.271	0.777	0.653	0.405	0.351	1.257	1.277	1.246	1.298	1.607
Ti	0.247	0.228	0.258	0.205	0.181	0.114	0.107	0.241	0.228	0.220	0.226	0.446
Zr	0.0	0.0	0.0	0.0	0.0	0.0	0.0	0.0	0.0	0.0	0.0	0.002
Fe3	0.408	0.276	0.253	0.481	0.486	0.884	0.561	0.419	0.311	0.237	0.412	0.0
Mg	1.023	1.012	0.978	1.297	0.943	1.086	1.043	1.040	1.302	1.419	1.274	2.119
Fe2	3.141	3.273	3.298	2.815	3.151	2.648	3.037	3.129	2.952	2.939	2.944	1.962
Mn	0.192	0.181	0.190	0.186	0.202	0.195	0.195	0.191	0.161	0.151	0.181	0.072
Ca	1.532	1.590	1.554	1.108	0.941	0.547	0.563	1.595	1.613	1.582	1.603	2.011
Na	1.193	1.122	1.163	1.672	1.806	2.271	2.167	1.142	1.126	1.118	1.116	1.033
K	0.323	0.310	0.315	0.304	0.323	0.316	0.303	0.329	0.326	0.327	0.312	0.302
Atomic percentages												
Na	31.8	30.1	31.5	41.0	48.9	58.2	57.4	30.2	27.9	27.1	27.9	20.0
Ca	40.9	42.7	42.1	27.2	25.5	14.0	14.9	42.2	39.9	38.4	40.1	39.0
Mg	27.3	27.2	26.5	31.8	25.6	27.8	27.6	27.5	32.2	34.5	31.9	41.0
Lith. code	514	514	514	514	514	514	514	524	524	524	524	531
Spot no.	172	173	174	188	190	401	402	395	396	397	398	0
Colour	Dg-gb	Dg-gb	Dg-gb	Dg-b	Dblg-g	Dgbl-g	Dgbl-g	Dgb-rb	Dgd-rb	gb-yb	Dgb-yb	-
Name	FEdHb	FEdHb	FEdHb	Kat	Kat	Arf	Arf	FEdHb	FEdHb	FEd	FEdHb	MH-Hb

Microprobe analyses - Amphibole.

Sample no.	272439	272443	272443	272477	272482	272485	58020	58025	272510
Cryst & posn	APJ	APJ	APJ	APJ	APJ	APJ	APJ	APJ	APJ
Major elements (wt%)									
SiO2	42.08	46.48	44.44	43.37	43.40	44.05	45.02	43.83	44.90
TiO2	2.53	1.38	2.41	2.33	2.32	2.45	0.88	2.53	2.09
Al2O3	9.02	3.12	6.72	4.22	7.30	5.88	3.64	7.53	4.85
Fe2O3	0.33	7.85	0.0	4.57	2.36	2.60	9.47	0.0	4.08
FeO	20.53	22.60	20.59	25.67	20.59	25.50	16.23	17.28	22.16
MnO	0.65	1.50	0.86	1.25	0.76	1.35	1.14	0.79	1.36
MgO	8.72	2.61	8.36	2.88	7.04	3.48	6.48	10.19	4.99
CaO	10.26	2.63	9.71	6.94	9.12	7.44	6.31	8.34	6.78
Na2O	2.97	7.70	3.42	4.90	4.32	5.03	6.13	3.45	5.48
K2O	1.50	1.38	1.37	1.71	1.26	1.37	1.44	1.49	1.43
ZrO2	0.08	0.29	0.0	0.12	0.0	0.0	0.0	0.0	0.09
Total	98.67	97.54	97.88	97.96	98.48	99.15	96.74	95.43	98.21
FeOT	20.83	29.66	20.59	29.78	22.72	27.84	24.75	17.28	25.83
16 cations to 23 oxygens									
Si	6.456	7.377	6.879	6.972	6.700	6.916	7.077	6.845	7.034
Al	1.631	0.584	1.226	0.800	1.329	1.088	0.675	1.386	0.896
Ti	0.292	0.165	0.281	0.282	0.269	0.289	0.104	0.297	0.246
Zr	0.006	0.022	0.0	0.009	0.0	0.0	0.0	0.0	0.007
Fe3	0.038	0.937	0.0	0.552	0.274	0.307	1.120	0.0	0.481
Mg	1.994	0.617	1.929	0.690	1.620	0.814	1.518	2.372	1.165
Fe2	2.635	3.000	2.665	3.451	2.659	3.348	2.134	2.257	2.903
Mn	0.084	0.202	0.113	0.170	0.099	0.180	0.152	0.105	0.180
Ca	1.687	0.447	1.610	1.195	1.509	1.252	1.063	1.396	1.138
Na	0.884	2.370	1.026	1.527	1.293	1.531	1.868	1.045	1.664
K	0.294	0.279	0.271	0.351	0.248	0.274	0.289	0.297	0.286
Atomic percentages									
Na	19.4	69.0	22.5	44.8	29.2	42.6	42.0	21.7	41.9
Ca	37.0	13.0	35.3	35.0	34.1	34.8	23.9	29.0	28.7
Mg	43.7	18.0	42.3	20.2	36.6	22.6	34.1	49.3	29.4
Lith. code	531	531	531	531	531	531	531	531	534
Spot no.	0	0	0	0	0	0	0	0	0
Colour	-	-	-	-	-	-	-	-	-
Name	H-Hb	Arf	FEd	Kat	FEdHb	Kat	Kat	Ed	Kat

Microprobe analyses – Amphibole.

Sample no.	272455	58062
Cryst & posn	APJ	APJ
Major elements (wt%)		
SiO2	42.82	42.69
TiO2	2.95	4.14
Al2O3	10.94	9.25
Fe2O3	0.0	0.0
FeO	18.98	14.85
MnO	0.47	0.51
MgO	6.66	10.73
CaO	9.78	11.44
Na2O	3.77	2.75
K2O	1.50	1.41
ZrO2	0.27	0.09
Total	98.14	97.86
FeOT	18.98	14.85
16 cations to 23 oxygens		
Si	6.590	6.506
Al	1.985	1.662
Ti	0.341	0.475
Zr	0.020	0.007
Fe3	0.0	0.0
Mg	1.527	2.437
Fe2	2.443	1.893
Mn	0.061	0.066
Ca	1.613	1.868
Na	1.125	0.813
K	0.295	0.274
Atomic percentages		
Na	26.4	15.9
Ca	37.8	36.5
Mg	35.8	47.6
Lith. code	624	624
Spot no.	0	0
Colour	–	–
Name	FEdHb	FedHb

Microprobe analyses - Amphibole.

Sample no.	63721	58400	304718	304718	304718	304718	304718	304718	304718	304718	304718	304718
Cryst & posn	APJ	APJ	35.cor	36.cor	37.cor	39.cor	39.rim	40.cor	40.int	40.rim	41.cor	41.int
Major elements (wt%)												
SiO2	43.06	42.45	40.93	42.63	43.95	43.26	43.30	42.16	42.23	43.40	42.16	42.34
TiO2	2.54	2.66	2.31	1.80	2.16	2.40	1.88	2.70	2.69	2.69	2.70	2.65
Al2O3	5.06	5.88	6.43	4.32	4.38	5.33	4.87	6.45	6.05	5.36	6.05	6.36
Fe2O3	0.41	0.29	4.58	2.75	4.24	4.43	3.89	3.56	2.40	3.40	4.49	4.95
FeO	30.13	28.80	24.47	27.44	27.73	26.99	26.98	27.34	28.50	27.63	27.06	26.21
MnO	0.92	1.63	0.79	1.21	1.27	1.22	1.08	1.09	1.08	1.11	0.99	1.09
MgO	2.67	2.51	2.77	1.53	1.78	1.64	1.69	2.29	1.91	2.05	1.83	2.06
CaO	8.39	8.27	8.25	7.52	7.00	7.11	6.37	8.80	8.08	7.17	8.08	7.71
Na2O	3.89	3.93	4.43	4.66	5.06	5.18	5.28	4.28	4.29	4.94	4.71	4.85
K2O	1.35	1.42	1.45	1.43	1.59	1.51	1.44	1.42	1.49	1.59	1.41	1.57
ZrO2	0.14	0.17	0.04	-1.00	-1.00	-1.00	-1.00	-1.00	-1.00	-1.00	-1.00	-1.00
Total	98.56	98.01	96.43	95.28	99.15	99.06	96.78	100.08	98.73	99.34	99.50	99.80
FeOT	30.50	29.06	28.58	29.91	31.55	30.97	30.48	30.54	30.66	30.69	31.10	30.66
16 cations to 23 oxygens												
Si	6.922	6.848	6.666	7.082	7.019	6.900	7.049	6.666	6.779	6.896	6.712	6.698
Al	0.959	1.118	1.235	0.845	0.824	1.002	0.934	1.202	1.144	1.003	1.135	1.187
Ti	0.307	0.323	0.282	0.225	0.260	0.288	0.230	0.321	0.324	0.322	0.323	0.315
Zr	0.011	0.013	0.003	0.0	0.0	0.0	0.0	0.0	0.0	0.0	0.0	0.0
Fe3	0.049	0.035	0.561	0.344	0.510	0.532	0.477	0.423	0.289	0.407	0.538	0.590
Mg	0.640	0.603	0.673	0.379	0.423	0.389	0.411	0.540	0.458	0.486	0.435	0.486
Fe2	4.051	3.885	3.333	3.813	3.704	3.600	3.673	3.614	3.827	3.671	3.603	3.467
Mn	0.125	0.223	0.109	0.170	0.171	0.164	0.149	0.146	0.147	0.149	0.133	0.146
Ca	1.445	1.429	1.439	1.339	1.198	1.216	1.111	1.490	1.391	1.221	1.379	1.307
Na	1.213	1.229	1.398	1.501	1.566	1.603	1.668	1.311	1.335	1.522	1.455	1.488
K	0.277	0.292	0.301	0.302	0.325	0.306	0.299	0.287	0.306	0.323	0.287	0.316
Atomic percentages												
Na	36.8	37.7	39.8	46.6	49.1	50.0	52.3	39.2	41.9	47.1	44.5	45.4
Ca	43.8	43.8	41.0	41.6	37.6	37.9	34.8	44.6	43.7	37.8	42.2	39.8
Mg	19.4	18.5	19.2	11.8	13.3	12.1	12.9	16.2	14.4	15.1	13.3	14.8
Lith. code	631	634	634	634	634	634	634	634	634	634	634	634
Spot no.	0	0	133	134	137	142	144	145	146	147	148	149
Colour	-	-	VDb-Dg	VDg-b	VDg-b	VDg-VDb	VDg-VDb	VDbg-b	VDbg-b	VDg-b	VDg-b	VDg-b
Name	FEd	FEd	FEdHb	Kat	Kat	Kat	Kat	FEdHb	FEd	Kat	FEdHb	Kat

Microprobe analyses - Amphibole.

Sample no.	304718	304718
Cryst & posn	41.rim	41.rim
Major elements (wt%)		
SiO2	42.75	42.50
TiO2	2.68	2.77
Al2O3	6.09	6.07
Fe2O3	3.89	3.58
FeO	27.42	28.17
MnO	0.93	0.92
MgO	1.82	1.79
CaO	7.47	7.52
Na2O	4.92	4.67
K2O	1.50	1.55
ZrO2	-1.00	-1.00
Total	99.48	99.54
FeOT	30.92	31.39
16 cations to 23 oxygens		
Si	6.787	6.763
Al	1.141	1.138
Ti	0.320	0.332
Zr	0.0	0.0
Fe3	0.465	0.429
Mg	0.431	0.425
Fe2	3.641	3.750
Mn	0.126	0.125
Ca	1.270	1.282
Na	1.515	1.443
K	0.304	0.314
Atomic percentages		
Na	47.1	45.8
Ca	39.5	40.7
Mg	13.4	13.5
Lith. code	634	634
Spot no.	150	151
Colour	VDg-b	VDg-b
Name	Kat	Kat

Microprobe analyses – Amphibole.

Sample no.	54232	54232	54232	54232	54232	54232	54232	54232	54232	54232	54232	54232
Cryst & posn	29.cor	29.int	29.rim	30.cor	30.cor	30.int	30.int	30.rim	31.cor	31.int	31.rim	32.cor
Major elements (wt%)												
SiO2	50.24	49.48	49.33	46.28	46.66	45.91	46.06	49.74	45.22	45.97	45.95	45.19
TiO2	0.45	0.47	0.40	2.47	2.68	2.55	1.93	0.63	1.30	1.18	1.12	2.06
Al2O3	1.13	0.89	0.72	2.62	2.58	2.30	2.82	2.04	2.41	2.35	2.14	2.42
Fe2O3	0.52	2.26	1.55	0.22	0.19	1.00	3.94	0.0	0.19	1.83	0.0	1.94
FeO	33.38	31.58	30.95	30.54	31.84	30.26	29.46	33.36	33.29	32.02	33.88	29.37
MnO	1.87	2.04	2.15	0.98	0.88	0.97	1.16	1.36	1.28	1.28	1.28	1.27
MgO	0.66	0.70	0.74	2.27	2.11	2.03	1.24	0.99	0.55	0.58	0.51	1.73
CaO	0.24	1.02	1.01	6.50	6.47	6.40	6.09	0.80	5.07	5.09	5.18	6.08
Na2O	7.31	6.93	7.07	5.29	5.25	5.32	5.76	6.56	5.04	5.43	4.95	5.34
K2O	1.60	1.97	1.81	1.34	1.42	1.41	1.47	1.50	1.41	1.50	1.46	1.44
ZrO2	0.39	0.0	0.20	0.05	0.16	0.0	0.0	0.0	0.24	0.0	0.10	0.23
Total	97.80	97.34	95.94	98.58	100.24	98.15	99.96	96.98	95.98	97.23	96.58	97.07
FeOT	33.85	33.61	32.35	30.74	32.01	31.16	33.01	33.36	33.46	33.67	33.88	31.11
16 cations to 23 oxygens												
Si	8.081	8.012	8.082	7.396	7.364	7.388	7.306	8.068	7.534	7.534	7.614	7.372
Al	0.214	0.170	0.140	0.494	0.481	0.436	0.528	0.390	0.473	0.454	0.418	0.465
Ti	0.055	0.057	0.049	0.296	0.318	0.308	0.230	0.077	0.163	0.145	0.140	0.253
Zr	0.030	0.0	0.016	0.004	0.012	0.0	0.0	0.0	0.019	0.0	0.008	0.019
Fe3	0.063	0.275	0.192	0.027	0.022	0.121	0.471	0.0	0.023	0.226	0.0	0.238
Mg	0.159	0.170	0.181	0.542	0.496	0.488	0.293	0.239	0.136	0.143	0.125	0.420
Fe2	4.491	4.277	4.240	4.082	4.202	4.073	3.908	4.526	4.638	4.388	4.696	4.007
Mn	0.255	0.280	0.299	0.133	0.118	0.133	0.156	0.186	0.180	0.178	0.180	0.176
Ca	0.042	0.177	0.177	1.113	1.095	1.103	1.036	0.139	0.905	0.893	0.920	1.063
Na	2.281	2.175	2.245	1.640	1.606	1.661	1.773	2.065	1.629	1.724	1.590	1.688
K	0.329	0.407	0.379	0.274	0.285	0.289	0.298	0.310	0.299	0.314	0.308	0.301
Atomic percentages												
Na	91.9	86.2	86.2	49.8	50.2	51.1	57.2	84.5	61.0	62.5	60.3	53.2
Ca	1.7	7.0	6.8	33.8	34.3	33.9	33.4	5.7	33.9	32.4	34.9	33.5
Mg	6.4	6.7	7.0	16.4	15.5	15.0	9.4	9.8	5.1	5.2	4.7	13.2
Lith. code	644	644	644	644	644	644	644	644	644	644	644	644
Spot no.	108	109	118	110	114	111	113	112	119	120	121	122
Colour Name	FEk	Arf	Arf	Kat	Kat	Kat	Kat	Arf(FEk)	FRh	FRh	FRh	Kat

Microprobe analyses – Amphibole.

Sample no.	54232	54232	304032	304032	304032	304032	304032	304087	304087	304087	304087
Cryst & posn	32.int	32.rim	138.cor	138.rim	140.cor	140.rim	142.cor	144.cor	145.cor	146.cor	147.cor
Major elements (wt%)											
SiO2	45.47	46.92	48.13	48.17	48.25	48.17	49.98	48.94	46.08	45.36	46.05
TiO2	2.32	1.18	0.93	0.78	2.24	2.38	0.25	0.64	2.50	1.86	2.65
Al2O3	2.61	2.10	1.38	1.34	1.28	1.63	0.27	1.16	2.88	2.91	2.68
Fe2O3	2.91	0.0	5.74	4.63	0.0	2.08	8.00	7.25	3.21	3.48	1.41
FeO	28.28	32.75	26.84	27.45	30.19	28.38	27.42	28.21	30.42	30.23	30.75
MnO	1.11	0.91	1.25	1.28	0.80	0.75	1.55	1.52	1.05	1.32	1.32
MgO	1.96	1.23	2.71	2.16	3.03	3.31	0.28	0.0	1.17	1.05	1.10
CaO	6.16	2.85	4.47	4.50	5.03	5.57	1.64	1.48	6.08	5.96	6.15
Na2O	5.60	6.16	6.53	6.62	5.92	6.17	8.18	8.12	5.72	5.40	5.69
K2O	1.55	1.14	1.52	1.40	1.46	1.40	1.83	1.58	1.51	1.53	1.34
ZrO2	0.23	0.21	-1.00	-1.00	-1.00	-1.00	-1.00	-1.00	-1.00	-1.00	-1.00
Total	98.21	95.45	99.50	98.33	98.21	99.84	99.41	98.92	100.63	99.10	99.13
FeOT	30.89	32.75	32.01	31.62	30.19	30.25	34.62	34.74	33.31	33.36	32.02
16 cations to 23 oxygens											
Si	7.309	7.752	7.570	7.668	7.672	7.521	7.908	7.793	7.272	7.287	7.363
Al	0.495	0.409	0.256	0.251	0.241	0.300	0.051	0.218	0.536	0.551	0.505
Ti	0.280	0.147	0.110	0.093	0.268	0.280	0.030	0.077	0.297	0.224	0.319
Zr	0.018	0.017	0.0	0.0	0.0	0.0	0.0	0.0	0.0	0.0	0.0
Fe3	0.352	0.0	0.680	0.555	0.0	0.245	0.952	0.869	0.381	0.421	0.170
Mg	0.469	0.302	0.635	0.513	0.717	0.770	0.067	0.0	0.276	0.252	0.262
Fe2	3.801	4.526	3.531	3.654	4.015	3.706	3.628	3.757	4.015	4.062	4.112
Mn	0.152	0.127	0.166	0.172	0.108	0.099	0.208	0.205	0.141	0.179	0.178
Ca	1.061	0.504	0.753	0.767	0.857	0.933	0.278	0.253	1.028	1.026	1.055
Na	1.745	1.975	1.992	2.043	1.825	1.867	2.508	2.506	1.750	1.683	1.765
K	0.318	0.241	0.305	0.285	0.296	0.280	0.370	0.321	0.305	0.313	0.273
Atomic percentages											
Na	53.3	71.0	58.9	61.5	53.7	52.3	87.9	90.8	57.3	56.8	57.3
Ca	32.4	18.1	22.3	23.1	25.2	26.1	9.7	9.2	33.7	34.7	34.2
Mg	14.3	10.9	18.8	15.4	21.1	21.6	2.3	0.0	9.0	8.5	8.5
Lith. code	644	644	644	644	644	644	644	644	644	644	644
Spot no.	123	125	363	364	366	367	368	370	371	372	374
Colour			gb-rb	gb-rb	gb-rb	gb-rb	Dbg-Pg	Dbg-Pg	Db-g	Db-g	Db-g
Name	Kat	Arf	FRh	FRh	FRh	FRh	Arf	Arf	Kat	Kat	Kat

Microprobe analyses – Amphibole.

Sample no.	258350	258350	304185	304185	304185	304185	304185
Cryst & posn	GS	GS	126.cor	126.int	126.rim	128.cor	129.cor
Major elements (wt%)							
SiO2	50.56	50.63	46.99	46.20	48.14	47.04	47.05
TiO2	1.28	0.59	0.81	1.00	0.86	0.77	0.69
Al2O3	1.79	1.71	3.09	3.06	2.57	2.57	2.47
Fe2O3	4.47	7.80	8.04	7.66	8.05	9.38	8.72
FeO	29.94	26.83	26.11	27.03	26.94	25.90	26.51
MnO	1.42	1.19	1.14	1.13	1.00	1.23	1.06
MgO	0.0	0.0	0.91	0.79	0.91	0.88	0.81
CaO	0.80	0.87	2.69	2.54	1.91	2.15	2.09
Na2O	8.59	9.18	7.64	7.47	8.09	7.86	7.73
K2O	1.55	1.56	1.55	1.43	1.55	1.52	1.58
ZrO2	-1.00	-1.00	0.74	1.12	0.98	0.76	0.71
Total	100.40	100.35	99.71	99.44	100.99	100.05	99.43
FeOT	33.97	33.85	33.34	33.92	34.18	34.34	34.36
16 cations to 23 oxygens							
Si	7.875	7.855	7.407	7.344	7.493	7.410	7.460
Al	0.328	0.312	0.574	0.574	0.472	0.477	0.461
Ti	0.150	0.069	0.096	0.119	0.101	0.091	0.082
Zr	0.0	0.0	0.057	0.087	0.074	0.058	0.055
Fe3	0.524	0.911	0.954	0.916	0.942	1.112	1.041
Mg	0.0	0.0	0.214	0.188	0.210	0.207	0.192
Fe2	3.900	3.481	3.442	3.593	3.506	3.412	3.515
Mn	0.188	0.156	0.152	0.153	0.132	0.164	0.143
Ca	0.133	0.145	0.455	0.433	0.319	0.362	0.355
Na	2.594	2.763	2.337	2.301	2.442	2.401	2.375
K	0.308	0.308	0.312	0.290	0.308	0.306	0.320
Atomic percentages							
Na	95.1	95.0	77.7	78.7	82.2	80.8	81.3
Ca	4.9	5.0	15.1	14.8	10.7	12.2	12.1
Mg	0.0	0.0	7.1	6.4	7.1	7.0	6.6
Lith. code	731	731	731	731	731	731	731
Spot no.	–	–	331	322	333	335	336
Colour			VDgbl-yg	VDgbl-yg	VDgbl-yg	VDgbl-yg	D-VDbl
Name	Arf	Arf	Arf	Arf	Arf	Arf	Arf

Microprobe analyses – Amphibole.

Sample no.	304074	304074	304074	304074	304074	304074	304074
Cryst & posn	63.cor	64.cor	64.rim	66.cor	66.rim	67.cor	67.rim
Major elements (wt%)							
SiO2	39.78	41.59	39.97	36.86	37.99	41.15	40.18
TiO2	0.39	0.49	0.47	0.74	0.0	0.49	0.45
Al2O3	7.38	6.01	7.45	10.29	8.69	6.19	7.81
Fe2O3	8.63	8.96	9.96	5.99	7.99	10.65	9.70
FeO	26.53	26.99	25.77	27.35	27.13	24.98	24.79
MnO	0.93	1.00	0.99	0.77	0.82	0.95	0.95
MgO	0.0	0.0	0.0	0.0	0.0	0.0	0.0
CaO	7.97	6.03	7.51	10.05	9.33	5.98	6.11
Na2O	4.13	5.16	4.48	2.68	2.99	5.51	5.09
K2O	1.82	1.69	1.88	1.85	1.96	1.67	1.91
ZrO2	-1.00	-1.00	-1.00	-1.00	-1.00	-1.00	-1.00
Total	97.57	97.92	98.48	96.58	96.89	97.58	96.99
FeOT	34.30	35.05	34.74	32.74	34.32	34.57	33.52
16 cations to 23 oxygens							
Si	6.552	6.802	6.518	6.149	6.336	6.735	6.599
Al	1.434	1.159	1.432	2.024	1.709	1.194	1.513
Ti	0.048	0.061	0.058	0.093	0.0	0.061	0.055
Zr	0.0	0.0	0.0	0.0	0.0	0.0	0.0
Fe3	1.070	1.103	1.222	0.752	1.003	1.312	1.199
Mg	0.0	0.0	0.0	0.0	0.0	0.0	0.0
Fe2	3.655	3.692	3.515	3.817	3.785	3.420	3.406
Mn	0.130	0.139	0.136	0.109	0.116	0.132	0.132
Ca	1.408	1.058	1.313	1.796	1.667	1.049	1.075
Na	1.321	1.635	1.416	0.867	0.968	1.749	1.621
K	0.383	0.352	0.390	0.393	0.416	0.349	0.400
Atomic percentages							
Na	48.4	60.7	51.9	32.6	36.7	62.5	60.1
Ca	51.6	39.3	48.1	67.4	63.3	37.5	39.9
Mg	0.0	0.0	0.0	0.0	0.0	0.0	0.0
Lith. code	921	921	921	921	921	921	921
Spot no.	207	208	209	212	213	214	215
Colour	D-Dbl	D-Dblg	D-Dblg	VDgbl-g	Dblg-blg	D-Dblg	D-Dblg
Name	FEdHb	Kat	Kat	Has	H-Hb	Kat	Kat

Microprobe analyses – Feldspar. All samples normalised to 100%.

Sample no.	304159	326189	326189	326189	304009	304009	304009	304009	304003	304003	304003	304003
Cryst & posn	85.cor	155.cor	159.cor	159.cor	16.cor	17.cor	18.cor	19.cor	74.cor	74.cor	74.cor	76.cor
Major elements (wt%)												
SiO2	67.23	66.23	66.68	66.56	66.14	65.57	69.26	69.58	66.45	66.72	65.08	65.49
Al2O3	18.66	19.30	19.24	19.39	18.17	17.91	18.96	18.68	18.50	18.36	18.56	18.30
FeOT	0.0	0.0	0.0	0.0	0.29	0.0	0.0	0.0	0.0	0.25	0.0	0.0
CaO	0.0	0.67	0.53	0.57	0.0	0.0	0.0	0.0	0.0	0.0	0.0	0.0
Na2O	5.83	5.81	6.02	6.01	4.05	0.61	11.53	11.57	5.07	5.94	0.81	1.29
K2O	8.27	7.99	7.51	7.46	11.35	15.91	0.25	0.16	9.98	8.25	15.55	14.92
Total	100.00	100.00	100.00	100.00	100.00	100.00	100.00	100.00	100.00	100.00	100.00	100.00
cations to 8 oxygens												
Si	3.015	2.976	2.987	2.981	3.009	3.022	3.021	3.033	3.005	3.013	2.998	3.009
Al	0.987	1.023	1.016	1.024	0.975	0.973	0.975	0.960	0.986	0.977	1.008	0.991
FeT	0.0	0.0	0.0	0.0	0.011	0.0	0.0	0.0	0.0	0.010	0.0	0.0
Ca	0.0	0.032	0.026	0.027	0.0	0.0	0.0	0.0	0.0	0.0	0.0	0.0
Na	0.507	0.506	0.523	0.522	0.358	0.055	0.975	0.978	0.444	0.520	0.072	0.115
K	0.473	0.458	0.429	0.426	0.659	0.936	0.014	0.009	0.576	0.476	0.914	0.875
Atomic percentages												
K	48.3	46.0	43.9	43.7	64.8	94.5	1.4	0.9	56.5	47.8	92.7	88.4
Na	51.7	50.8	53.5	53.5	35.2	5.5	98.6	99.1	43.5	52.2	7.3	11.6
Ca	0.0	3.2	2.7	2.8	0.0	0.0	0.0	0.0	0.0	0.0	0.0	0.0
Lith. code	314	324	324	324	434	434	434	434	434	434	434	434
Spot no.	254	385	391	392	58	59	61	62	228	229	230	234

Table A4.4

Microprobe analyses – Feldspar. All samples normalised to 100%.

Sample no.	326091	326091	326092	304752	304752	304752	304752	304752	304752	304718	304718	304718
Cryst & posn	pf40.cor	114.cor	151.cor	44.cor	44.cor	44.cor	44.cor	44.cor	44.cor	34.cor	34.cor	34.cor
Major elements (wt%)												
SiO2	69.16	68.66	69.06	66.08	67.01	66.96	67.12	66.96	66.79	67.22	67.14	67.60
Al2O3	19.05	19.24	18.96	18.66	18.36	18.54	18.64	18.75	18.52	18.67	18.86	18.65
FeOT	0.26	0.33	0.27	0.0	0.0	0.0	0.0	0.0	0.32	0.23	0.0	0.23
CaO	0.0	0.0	0.0	0.0	0.0	0.0	0.0	0.0	0.0	0.0	0.17	0.0
Na2O	10.90	11.05	11.50	5.75	5.48	5.94	5.85	6.04	5.83	7.73	7.70	7.54
K2O	0.33	0.31	0.21	8.80	9.16	8.56	8.39	8.24	8.53	5.64	5.68	5.94
Total	100.00	100.00	100.00	100.00	100.00	100.00	100.00	100.00	100.00	100.00	100.00	100.00
cations to 8 oxygens												
Si	3.023	3.009	3.016	2.998	3.018	3.011	3.013	3.006	3.007	3.009	3.002	3.013
Al	0.982	0.994	0.976	0.998	0.975	0.983	0.986	0.993	0.983	0.985	0.994	0.980
FeT	0.009	0.012	0.010	0.0	0.0	0.0	0.0	0.0	0.012	0.009	0.0	0.009
Ca	0.0	0.0	0.0	0.0	0.0	0.0	0.0	0.0	0.0	0.0	0.008	0.0
Na	0.924	0.939	0.974	0.506	0.478	0.518	0.509	0.526	0.509	0.671	0.667	0.651
K	0.018	0.017	0.012	0.509	0.526	0.491	0.480	0.472	0.490	0.322	0.324	0.338
Atomic percentages												
K	1.9	1.8	1.2	50.1	52.4	48.7	48.5	47.3	49.0	32.4	32.4	34.2
Na	98.1	98.2	98.8	49.9	47.6	51.3	1.5	52.7	51.0	67.6	66.8	65.8
Ca	0.0	0.0	0.0	0.0	0.0	0.0	0.0	0.0	0.0	0.0	0.8	0.0
Lith. code	434	434	434	514	514	514	514	514	514	634	634	634
Spot no.	312	313	379	158	159	160	161	162	163	131	132	135

Microprobe analyses - Feldspar. All samples normalised to 100%.

Sample no.	304718	304087	304185	304185	304185	304185	304185	304185	304185	304074	304074	304074
Cryst & posnpf	5034.cor	143.cor	122.cor	122.cor	123.cor	124.cor	125.cor	128.cor	131.cor	58.cor	58.cor	62.cor
Major elements (wt%)												
SiO2	67.40	67.81	68.67	68.89	68.95	65.71	69.19	69.40	68.90	69.18	68.89	69.35
Al2O3	18.99	18.69	19.22	19.03	18.85	18.15	18.86	18.90	18.93	19.29	19.30	19.13
FeOT	0.28	0.0	0.38	0.0	0.41	0.0	0.36	0.25	0.25	0.0	0.0	0.0
CaO	0.0	0.0	0.0	0.0	0.0	0.0	0.0	0.0	0.0	0.18	0.18	0.0
Na2O	8.08	6.91	11.14	11.51	11.40	3.12	11.06	11.24	11.36	11.35	11.64	11.41
K2O	5.25	6.59	0.28	0.11	0.12	12.45	0.19	0.22	0.19	0.0	0.0	0.11
Total	100.00	100.00	100.00	100.00	100.00	100.00	100.00	100.00	100.00	100.00	100.00	100.00
cations to 8 oxygens												
Si	2.999	3.021	3.008	3.017	3.019	3.013	3.027	3.026	3.018	3.013	3.005	3.021
Al	0.996	0.981	0.992	0.983	0.973	0.981	0.973	0.972	0.978	0.991	0.992	0.982
FeT	0.010	0.0	0.014	0.0	0.015	0.0	0.013	0.009	0.009	0.0	0.0	0.0
Ca	0.0	0.0	0.0	0.0	0.0	0.0	0.0	0.0	0.0	0.008	0.008	0.0
Na	0.697	0.597	0.947	0.978	0.968	0.278	0.938	0.950	0.965	0.959	0.984	0.964
K	0.298	0.374	0.016	0.006	0.007	0.728	0.011	0.012	0.011	0.0	0.0	0.006
Atomic percentages												
K	29.9	38.5	1.7	0.6	0.7	72.4	1.2	1.2	1.1	0.0	0.0	0.6
Na	70.1	61.5	98.3	99.4	99.3	27.6	98.8	98.8	98.9	99.2	99.2	99.4
Ca	0.0	0.0	0.0	0.0	0.0	0.0	0.0	0.0	0.0	0.8	0.8	0.0
Lith. code	634	644	731	731	731	731	731	731	731	921	921	921
Spot no.	136	369	325	326	327	328	329	334	339	198	199	206

Microprobe analyses – Biotite.

Sample no.	304003	304003	326091	326091	304752	304752	304752	304752
Cryst & posn	78.cor	80.cor	118.cor	120.cor	53.cor	53.int	53.rim	55.cor
Major elements (wt%)								
SiO2	37.80	37.37	35.42	35.85	36.30	35.89	37.87	36.03
TiO2	3.27	3.60	3.32	3.24	4.26	4.42	2.85	4.43
Al2O3	10.36	10.69	10.02	10.35	11.36	10.98	10.09	11.51
FEOT	26.64	28.11	31.43	30.12	28.78	28.91	29.35	29.31
MnO	0.87	0.84	1.57	1.51	0.98	1.24	1.51	1.14
MgO	7.84	7.04	4.46	4.12	5.28	4.83	5.13	5.48
CaO	0.0	0.0	0.0	0.0	0.0	0.0	0.0	0.0
Na2O	0.53	0.63	0.37	0.39	0.74	0.60	0.43	0.93
K2O	9.01	8.74	9.07	9.10	8.54	8.73	8.96	8.62
Total	96.31	97.04	96.35	95.19	96.24	95.62	96.20	97.45
cations to 22 oxygens								
Si	5.949	5.874	5.817	5.900	5.786	5.787	6.060	5.697
Al	1.922	1.981	1.940	2.008	2.135	2.088	1.904	2.146
Ti	0.387	0.425	0.410	0.402	0.510	0.536	0.343	0.527
FeT	3.506	3.695	4.317	4.145	3.836	3.898	3.927	3.876
Mg	1.839	1.649	1.092	1.011	1.253	1.162	1.225	1.291
Mn	0.116	0.112	0.218	0.210	0.133	0.170	0.204	0.153
Ca	0.0	0.0	0.0	0.0	0.0	0.0	0.0	0.0
Na	0.161	0.193	0.118	0.126	0.228	0.188	0.134	0.285
K	1.809	1.754	1.900	1.911	1.737	1.796	1.829	1.739
Lith. code	434	434	434	434	514	514	514	514
Spot no.	237	243	319	321	185	186	187	189

Table A4.5

References

Abbey, S. 1983. Studies in standard samples of silicate rocks and minerals. *Geol. Surv. Canada. paper* 83-15.

Allaart, J.H., 1973. Geological map of Greenland 1:100,000, Narssarssuaq, 60 v. 2 Syd. Copenhagen. Geol. Surv. Greenland (also Meddr Grønland 192,4) 41pp.

Allart, J.H. 1976. Ketilidian mobile belt in South Greenland. In: A. Escher and W.S. Watt (eds), *Geology of Greenland.* The Geological Survey of Greenland, Copenhagen.

Anderson, E.M. 1951. *The Dynamics of faulting and dyke formation with applications to Britain.* Edingburgh, Oliver and Boyd, 2nd edition. 206 pp.

Anderson, S.L., & Burke, K., 1983. A Wilson Cycle approach to some Proterozoic problems in eastern North America. In L.G. Medaris, C.W, Byers, D.M. Mickelson & W.C. Shanks (Eds), Proterozoic Geology: Selected Papers from an International Proterozoic Symposium. *Geol Soc. Am. Mem.* 161, 75-93.

Armour-Brown, A., Tukiainen, T., & Wallin, B., 1980. The South Greenland Uranium Exploration Project. *Rapp. Grønlands geol. Unders.* 100, 83-86.

Armour-Brown, A., Tukiainen, T. & Wallin, B., 1981. Uranium districts in South Greenland. *Rapp. Grønlands geol. Unders.* 105, 51-55.

Armour-Brown, A., Tukiainen, T. & Wallin, B., 1982. The South Greenland Uranium Exploration Programme Final Report. Unpubl. intern. GGU rep., 92 pp.

Armour-Brown, A., Tukiainen, T., Wallin, B., Bradshaw, C., & Emeleus, C.H., 1983. Uranium exploration in South Greenland. *Rapp. Grønlands. Geol. Unders.* 115, 68-75.

Badgley, C.P., 1965. *Structural and Tectonic Principles,* New York and London, Harper & Row Ltd.

Bailey, D.K., 1964. Crustal warping -a possible tectonic control of alkaline magmatism. *J. Geophys. Res.* 69.

Bailey, D.K., 1970. Volatile flux, heat focussing and the generation of magma. *Geol. Jour. Spec. Issue,* 2, 177-186.

Bailey, D.K., 1972. Uplift, rifting and magmatism in continental plates. *J. Earth Sci.,* 8, 225-240.

Bailey, D.K., 1974a. Continental rifting and alkaline magmatism, In; Sørensen, H., ed., *The alkaline rocks.* London, Wiley, 148-159.

Bailey, D.K., 1974b. Origin of alkaline magmas as a result of anatexis, b) crustal anatexis, In; Sørensen, H., ed., *The alkaline rocks.* London, Wiley, 436-442.

Bailey, D.K., 1977. Lithosphere control of continental rift magmatism. *J. Geol. Soc. London,* 133, 103-106.

Bailey, D.K. 1980. Volcanism, earth degassing and replenished lithosphere mantle. *Phil. Trans. Royal Society London* A297, 309-322.

Bailey, D.K. 1982. Mantle metasomatism - continuing chemical change within the earth. Nature, 296, 525-530.



Bailey, D.K., & McDonald, R., 1975. Fluorine & Chlorine in peralkaline liquids and the need for magma generation in a open system. *Min. Mag.* 40, 405-414.

Bailey, J.C., Rose-Hansen, J., Lovborg, L. & Sørensen, H., 1981. Evolution of Th and U whole-rock contents in the Ilimaussaq intrusion. In: The Ilimaussaq Intrusion, South Greenland. A Progress Report on Geology, Mineralogy, Geochemistry and Economic Geology. (J.C. Bailey, L.M. Larsen & H. Sørenson, eds.). *Rapp. Grønlands Geol. Unders.* 113, 87-98.

Bailey, D.K. & Schairer, J.F., 1964. Feldspar - liquid equilibration in peralkaline liquids - The Orthoclase Effect. Amer. J. of Science. 62, 1198 - 1206.

Bailey, D.K. & Schairer, J.F., 1966. System Na_2O-Al_2O_3-Fe_2O_3-SiO_2 and petrogenesis of alkaline rocks. *J. Petrol.* 7, 114-70.

Bailey, J. & Sørenson, I. 1976. Trace element techniques in the Institute for Petrology, University of Copenhagen: With an appendix on major element X-ray fluorscence techniques in the greenland Geological Survey, Copenhagen. Unpubl. Report. University of Copenhagen.

Baker, B.H., Goles, G.G., Leeman, W.P. & Lindstrom, M.M., 1977. Geochemistry and petrogenesis of a Basalt-Benmoreite-Trachyte suite from the southern part of the Gregory Rift, Kenya. *Contrib. Mineral. Petrol.* 64, 303-332.

Balashov, Y.A. 1966. Differentaition of rare-earth elements during magmatic process. In: *Chemistry of the earth crust.* Vinogradov, A.P. (Ed). Vol I. Acad Sci. of USSR: Israel prog. for Sci. pubs. Jerusalem.

Balk, R., 1937. Structural Behaviour of Igneous Rocks. 177.

Baragar, W.R.A., 1977. Volcanism of the Stable Crust. In: *Volcanic Regimes in Canada.* Geol. Ass. Canada. Spec. Paper no. 16, 377-405

Benkhelil, J. & Robineau, B. 1986. *Le Fossé de la Bénué est-il un rift?* Bulletin des Centres des Recherches Exploration-production. Elf-Aquitaine, 7, 315-321.

Bennett, J.N., Turner, D.C., Ike, E.C. & Bowden, P. 1984. The geology of some northern Nigerian anorogenic ring complexes. *B.G.S.-Overseas Geology and Mineral Resources.* London HMSO.

Berthelsen, A., & Heinriksen, N., 1975. Geological Map of Greenland. 1:100,000, Ivigtut 61 v. 1 Syd. The Orogenic and Cratogenic Geology of a Precambrian Shield Area. Descriptive text, 169 pp., Geological Survey of Greenland, Copenhagen.

Blaxland, A.B., van Breemen, O., Emeleus, C.H. & Anderson, J.G., 1978. Age and origin of the major syenite centers in the Gardar province of South Greenland: Rb-Sr studies. *Geol. Soc. Am. Bull.*, 89, 231-244.

Blaxland, A.B., van Breemen, O., & Steenfeldt, A., 1976. Age and origin of agpaitic magmatism at Ilimaussaq, South Greenland: Rb- Sr study. *Lithos.* 9, 31-38.

Blundell, D.J. 1978. A gravity survey across the Gardar Igneous Province, S.W. Greenland. *Quart. J. Geol. Soc. Lond.* 135, 545-554.

Bohse, H., Brooks, C.K. & Kunzendorf, K. 1971. Field observations on the kakortokites of the Ilimaussaq intrusion, South Grrenland. Rapp. *Grønlands geol. Unders.* 38, 43pp.

Bott, M.H.P. 1981. Crustal doming and the mechanism of continental rifting. In: Illies, J.H. (Ed) Mechanism in graben formation. *Tectonophysics* 73, 1-8.

Bowen, N.L., 1945. Phase equilibria bearing on the origin and differentiation of alkaline rocks. *Am. J. Sci.*, 243A.

Bradshaw, C., 1985. The alkaline rocks of the Motzfeldt Centre; progress report on the 1984 field season. *Rapp. Grønlands geol. Unders.*, 125, 62-64.

Bradshaw, C., & Tukiainen, T., 1983. Geological and radiometric mapping of the Motzfeldt Centre of the Igaliko Complex, South Greenland. Unpubl. intern. GGU rep., 35 pp.

Bridgwater, D., 1967. Feldspathic inclusions in the Gardar Igneous Rocks of South Greenland and their relevance to the formation of Major Anorthosites in the Canadian Shield. *Can. J. Earth Sci.*, 4, 995-1014.

Bridgwater, D. & Harry, W.T. 1968. Anorthosite xenoliths and plagioclase megacrysts in Precambrian intrusions in South Greenland. *Bull. Grønlands geol. Unders.* 77 (also Meddr. Grønland, 186, 2)2

Bridgwater, D. & Gormsen, K. 1969. Geological reconnaissance of the Precambrian rocks of South-East Greenland. *Rapp. Grønlands geol. Unders.* 19, 43-50

Bridgwater, D. & Coe, K., 1970. The role of stoping in the emplacement of the giant dykes of Isortoq, South Greenland. *Geol. J. spec. Issue,* 2, 67-78.

Bridgwater, D., Keto, L., McGregor, V.R. & Myers, J.S. 1976. Archean gneiss complex of Greenland. In: A. Escher & W.S. Watt (eds). *Geology of Greenland.* The Greenland geological Survey, Copenhagen.

Brown, W.L., Becker, S.M. & Parsons, I., 1983. Cryptoperthites and cooling rate in a layered syenite pluton. *Contrib. Mineral. Petrol.*, 82, 13-25.

Brown, G.C., Hughes, D.J. and Esson, J. 1973. New XRF data retrieval techniques and their application to U.S.G.S. standard rocks.

Buddington, A.F., 1959. Granite emplacement with special reference to North America, *Bull. Geol. Soc., Am.*, 70, 671-747.

Burke, K. 1978. Evolution of continental rift systems in the light of plate tectonics. In: I.B. Ramberg & E.R. Neuman. *Tectonics and geophysics of continental rifts.* 1-9.

Burke, K., 1980. Intracontinental rifts and aulacogens. In: *Continental Tectonics.* National Acad. Sci., 42-49.

Burke, K. & Dewey, J.D. 1973. Plume generated triple junctions, key indicators in applying plate tectonics to old rocks. *J. Geol.* 81, 406-433.

Burke, K., Dewey, J.F. & Kidd, W.S.F., 1977. World distribution of sutures- The sites of former oceans. *Tectonophysics* 40, 69-99.

Burnham, C.W. 1979. Magmas and Hydrothermal deposits. In: H.L. Barnes (ed), *Geochemistry of hydrothermal ore deposits*, John Wiley & Sons, Inc. New York.

Bussell, M.A., Pitcher, W.S. and Wilson, P.A., 1976. Ring Complexes of the Peruvian Coastal batholith, a long standing Subvolcanic regime. *Can. J. Earth Sci.*, 13, 1020-1030.

Butler, J.R. and Smith, A.Z. 1962. Zirconium, niobium and certain other trace elements in some alkali igneous rocks. *Geochim. Cosmochim. Acta,* 26: 945-953.

Chambers, A.D., 1976. The Petrology and Geochemistry of North Qôroq Centre, Igaliko Complex, South Greenland. Unpubl. Ph.D. thesis, University of Durham.

Chapman, C.A., 1966. Paucity of mafic ring-dykes - Evidence for floored polymagmatic chambers. *Amer. Jour. Sci.*, 264, 66-77.

Chapman, C.A., 1967. Magmatic central complexes and tectonic evolution of certain orogenic belts. In; *Etages Tectoniques.*

Chase, C.G., & Gilmar, T.H., 1973. Precambrian plate tectonics: The midcontinental gravity high. *Earth Planet. Sci. Lett.* 21, 70-78.

Chase, J.W., Winchester, J.W. and Coryell, C.D. 1962. Lanthanum, europium and dysoprosium distributions in igneous rocks and minerals. *Trans. Amer. Geophys. Union.*, 68, 567.

Christie-Blick, N. & Biddle, K.T., 1985. Deformation and basin formation along strike slip faults. In: Biddle, K.T. & Christie-Blick, N. (Eds) *Strike slip deformation, Basin Formation, and sedimentation.* 1-34. Society of Economic Palaeontologists and Mineralogists. Spec. Publication. No. 37, Tulsa, USA.

Cloos, E., 1955. Experimental analysis of fracture patterns. *Bull. Geol. Soc. Am.*, 66, 241-256.

Cobbing, E.J., Pitcher, W.S., Wilson, J.J., Baldock, J.W., Taylor, W.P., McCourt, W. & Snelling, N.J., 1981. The geology of the Western Cordillera of northern Peru. *I.G.S.-Overseas Memoir* 5. London HMSO.

Collerson, K.D., 1982. Geochemistry and Rb-Sr geochronology of associated Proterozoic Peralkaline and Subalkaline Anorogenic Granites from Labrador. *Contrib. Mineral. Petrol.*, 81, 126-147.

Collins, W.J., Beams, S.D., White, A.J.R. & Chappell, B.W. 1982. Nature & origin of A-type granites with particular reference to southeastern Australia. *Contr. Mineral. Pet.* 80, 189-200.

Coombs, D.S., 1963. Trends and affinities of basaltic magmas and pyroxenes as illustrated on the diopside-olivine-silica diagram. *Min. Soc. Am. Spec. Pap.* 1, 227-250.

Coombs, D.S. & Wilkinson, J.F.G., 1969. Lineages and fractionation trends in undersaturated volcanic rocks from the East Otago province (N. Zealand) and related rocks. *J. Petrol.* 10, 440-500.

Cox, K.G., Bell, J.D., & Pankhurst, R.J., 1979. *The Interpretation of Igneous Rocks.* Allen & Unwin publ. London.

Dewey, J.F., & Burke, K., 1974. Hot spots and continental break up. *Geology* 2, 57-60.

Dietrich, R.V., 1968. Behaviour of Zr in artificial magmas with diverse P.T. *Lithos*, 1, 20-29.

Doig, R., 1970. An Alkaline Province rock linking Europe & N. America. *Can. J. Earth Sci.*, 7, 22-28.

Donaldson, J.A. & Irving, E., 1972. Grenville front and rifting of the Canadian Shield. *Nature Phys. Sci.*, 237.

Drummond, S.E. & Ohmoto, H. 1985. Chemical evolution and mineral deposition in boiling hydrothermal systems. *Economic Geology.* 80, 126-147.

Drysdall, A.R., Jackson. N,J., Ramsay, C.R., Douch, C.J. & Hackett, D. 1984. Rare element mineralisation related to Precambrian alkali granites in the Arabian Shield. *Economic Geology.* 79, 1366- 1377.

Duncomb, P. and Jones, E.M. 1969. Tube investments Company Report. No. 260.

Duncomb, P. and Reed, S.J.B. 1968. Quantitative Electron Probe Microanalysis. *N.B.S. Spec. Pub.* 298, 133-154.

Ebdon, D. 1985. *Statistics in Geography*, 2nd edition. Basil Blackwell Ltd, Oxford.

Emeleus, C.H., 1964. The Grønnedal-Ika Alkaline Complex, South Greenland. The structure and Geological History of the Complex *Bull. Grønlands geol. Unders.*, 45, (also Meddr. Grønland, 172, 3) 75pp.

Emeleus, C.H. & Harry, W.T., 1970. The Igaliko nepheline syenite complex. General description. *Bull. Grønlands geol. Unders.*, 85 (also Meddr. Grønland, 186, 3) 116 pp.

Emeleus, C.H. & Upton, B.G.J., 1976. The Gardar period in Southern Greenland. In; A. Escher & W.S. Watt, (eds), *The Geology of Greenland.* 153-181. The Geological Survey of greenland, Copenhagen.

Emslie, R.F., 1978. Anorthosite Massifs, Rapakivi Granites, and Late Proterozoic Rifting of North America. *Precambrian Res.*, 7, 61-98.

Ewart, A. 1981. The meineralogy and chemistry of the anorogenic Tertiary silic volcanics of SE queensland and NE New South Wales, Australia. *J. Geophysics Res.*, 86, 10242-10256.

Ferguson, J. 1964. Geology of the Ilimaussaq alkaline intrusion, South greenland. *Bull. Grønlands geol. Unders.* 89, 193pp. (also Meddr om Grønland. 172)

Ferguson, J., 1969. The differentiation of Agpaitic Magmas: The Ilimaussaq intrusion, S. Greenland. *Canadian Mineralogist* 10, Part 3, 335-349.

Fitton, J.G. & Gill, R.C.O. 1970. The oxidation of ferrous iron in rocks during mechanical grinding. *Geochim. Cosmochim. Acta*, 34. 518-524.

Fitton, J.G. & James, D. X-ray fluorescence spectroscopy at the University of Edinburgh. Unpubl. XRF guide. University of Edinburgh.

Fletcher, C.J.N. & Litherland, M., 1981. The geology and tectonic setting of the Velasco Alkaline province, eastern Bolivia. *J. Geol. Soc. London.* 138, 541-548.

Gabelman, J.W., 1984. Magmatic Rocks vs Rest Fluids as sources of Uranium Ore Fluids. In: *Syngenesis and Epigenesis in the formation of Mineral Deposits.* Eds: Wauschkuhn, A., Kluth, C. and Zimmerman, R.A.. Part IV, 519-536. Springer-Verlag. Berlin.

Galakhov, A.V., 1967. Chemical composition of rocks in the Khibiny alkalic massif. *Dokl. Acad. Sci.* (English translation), 171, 225-8.

Gast, P.W. 1968. Trace element fractionation and the origin of tholeiitic and alkaline magma types. *Geochem. Cosmochim. Acta* 32, 1057-1086.

Gerasimovsky, V.I. 1966. Geochemical features of agpaitic nepheline syenites. In: *Chemistry of the earths crust.* Vol I. A.P.Vinogradov, (Ed). Acad Sci. of USSR: Israel prog. for Sci. pubs. Jerusalem.

Gerasimovsky, V.I., 1969. Geochemistry of the Ilimaussaq Alkaline massif. (In Russian). Izd. 'Nauka', Moskva, 1-74.

Gerasimovsky, V.I., 1974. Trace elements in selected groups of alkaline rocks. In: H. Sørenson (ed), *The Alkaline Rocks*, 402-412. New York. Wiley. Izd. 'Nauka', Moskva, 1-74.

Gill, R.C.O., 1973. Mechanism for the salic magma bias of continental alkaline provinces. *Nature Phys. Sci.*, 242, 41-42.

Gordon, M.B., & Hempton, M.R., 1986. Collision induced rifting: The Grenville orogeny and the Keweenawan rift of North America. *Tectonophysics,* 127, 1-25.

Green, J.C., 1983. Geologic and geochemical evidence for the nature and development of the middle proterozoic (Keweenawan) midcontinent rift of North America. *Tectonophysics,* 94, 413-437.

Halls, H.C., 1978. Late Precambrian central North American rift system -a survey of recent geological and geophysical investigations. In: I.B. Ramberg, and E.R. Newman, (Eds). *Tectonics and geophysics of continental rifts.* 111-123.

Hamilton, E.I., 1964. The geochemistry of the northern part of the Ilimaussaq intrusion, S.W. Greenland. *Bull. Grønlands geol. Unders.,* 42, 104pp. (also Meddr. Grønland, Bd. 162, No. 10).

Harding, T.P., Vierbuchen, R.C. & Christie-Blick, N., 1985. Structural styles, plate tectonic setting and hydrocarbon traps of divergent (transtensional) wrench faults. In: Biddle, K.T. & Christie-Blick, N., (Eds) *Strike slip deformation, basin formation, and sedimentation.* Society of Economic Palaeontologists and Mineralogists. Spec. publication No.37, Tulsa, USA.

Harris, P.G., 1969. Basalt type and African rift valley tectonism. *Tectonophysics,* 8, 427-436.

Harry, W.T. & Pulvertaft, C.T.R., 1963. The Nunarssuit intrusive complex, South Greenland. *Bull. Grønlands geol. Unders.,* 36, (also Meddr. Grønland 169, 1) 136 pp.

Harry, W.T. & Richey, J.E., 1963. Magmatic pulses in the emplacement of plutons. *Lpool Manchr. geol. J.,* 3, 254-268.

Heinrich, K.F.J. 1966. X-ray absorption uncertainty. In: T.D. McKingley, K.F.J. Heinrich and D.B. Wittry (Editors), *The Electron Microprobe.* Wiley, New York, N.Y., pp. 296-377.

Helgeson, H.C. 1964. *Complexing and hydrothermal Ore deposition.* International Series of Monographs on Earth Sciences. Pergamon Press. 1964. pp128.

Henderson, P. 1980. General geochemical properties and abundances of the rare earth elements. In: *Rare earth element geochemistry* Ed: P. Henderson. Elsevier. Netherlannds.

Henriksen, N. 1960. Structural analysis of a fault in South-West Greenland. *Bull. Grønlands Geol. Unders.* 26. (also Meddr. Grønland, 162).

Hess, P.C., 1980. Polymerization Model for Silicate Melts. In: *Physics of Magmatic Processes.* Hargreaves, R.B., (Ed) Princeton University Press, N.J. USA.

Hills, E.S., 1963. *Elements of Structural Geology,* 2nd ed., London, Chapman and Hall Ltd.

Holland, J.G. and Brindle, D.W. 1966. A self consistant mass absorption correction for silicate analysis by x-ray fluorescence. *Spectrochim Acta,* 22. 2083-2093.

Holmes, A., 1931. The problem of the association of acid and basic rock in central complexes. *Geol. Mag.,* 68, 241-245.

Hawthorne, F.C. 1981. Crystal Chemistry of the Amphiboles. In: Veblen, D.R. (ed). *Review in Mineralogy, Amphiboles and other hydrous pyriboles - mineralogy.* Vol. 9a. 1-95. Min. Soc. Am. Bookcrafters Inc. Michigan.

Illes, J.H. (Ed). 1981. Mechanism for graben formation. *Tectonophysics* 73, 249-266.

Irvine, T.N., Baragar, W.R.A., 1971. A guide to the chemical classification of the common volcanic rocks. *Can. J. Earth Sci.* 8, 523-548.

Jacobsen, R.R.E., MacLeod, W.N. and Black, R., 1958. Ring complexes in the younger Granite Province of Northern Nigeria. *Geol. Soc. London, Mem.* no. 1, 77 pp.

Jahns & Burnham, 1969. Experimental studies of pegmatite genesis: I. A model for the derivation and crystallisation of granitic pegmatites. *Econ. Geol.*, 64, 843-863.

Jones, A.P., 1980. The petrology and structure of the Motzfeldt Centre, Igaliko, South Greenland. Unpubl. Ph.D. thesis. Univ. of Durham.

Jones, A.P & Larsen, L.M. 1985. Geochemistry and REE minerals of nepheline syenites from the Motzfeldt Centre, South Greenland. *Am. Mineral.* 70, 1087-1100.

Keller, G.R., Lidiak, E.G., Hinze, W.J. & Braile, L.W., 1983. The role of rifting in the tectonic development of the Midcontinent, USA. *Tectonophysics* 94, 391-412.

Knox, G.J., 1974. The structure and emplacement of the Rio Fortaleza Central Acid Complex, Ancash, Peru. *J. Geol. Soc. London.* 130, 295-308.

Kogarko, L.N., 1974. Role of volatiles. In Sørensen, H. (ed.) 1974, *The Alkaline Rocks.* John Wiley & Sons Ltd., 474-487.

Kogarko, L.N. 1979. Microcomponents as indicators of the differentiation of Alkaline Magmatic Series. In: *Origin and Distribution of the elements.* Arhens, L.H. (Ed), 212-222. Pergamon Press, Oxford.

Konnerup-Madsen, J., 1984. Compositions of fluid inclusions in granites and quartz syenites from the Gardar continental rift province (South Greenland). *Bull. Mineral.*, 107, 327-340.

Konnerup-Madsen, J., Rose-Hansen, J. & Larsen, E., 1981. Hydrocarbon gases associated with alkaline igneous activity: evidence from compositions of fluid inclusions. In: the Ilimaussaq Intrusion, South Greenland. A Progress on Geology, Mineralogy, Geochemistry and Economic Geology. (J.C. Bailey, L.M. Larsen & H. Sørenson, eds.) *Rapp. Grønlands Geol. Unders.* 103, 99-108.

Kumorapeli, P.S. & Saull, V.A., 1966. The St Lawrence valley system: a North American equivalent of the East African Rift Valley system, *Can. J. Earth Sci.* 3, 639-658. **Kuno, H. 1967.** Igneous rock series. In: *Chemistry of the earths crust.* Vol II. A.P. Vinogradov (Ed). Acad Sci. of USSR: Israel prog. for Sci. pubs. Jerusalem.

Larsen, J.G., 1973. Petrochemical work on the Precambrian Lavas, Eriksfjord Formation, South Greenland. *Rapp. Grønlands Geol. Unders.* 55, 40-41.

Larsen, J.G., 1977. Petrology of the late lavas of the Eriksfjord Formation, Gardar Province, South Greenland. *Bull. Grønlands. Geol. Unders.*, 125, 31 pp.

Larsen, L.M. 1976. Clinopyroxenes and coexisting mafic minerals from the Alkaline Ilimaussaq Intrusion, South Greenland. *J. of Petrology.* Vol. 17, no. 2. 258-290.

Larsen, L.M., 1977. Aenigmatites from the Ilimaussaq intrusion, south Greenland. Chemistry and petrological implications. *Lithos,* 10, 257-70.

Larsen, L.M. 1979. Distribution of REE and other traces between phenocrysts and peralkaline undersated magmas. *Lithos* 12, 303-315.

Larsen, L.M. & Sørensen, H., 1985. The Ilimaussaq intrusion - progressive crystallisation and formation of layering in an agpaitic magma. *Geol. Soc. Lond. Spec. Publ.*

Larsen, L.M. & Steenfelt, A., 1974. Alkali loss and retention in an iron-rich peralkaline phonolite dyke from the Gardar province, South Greenland. *Lithos,* 7, 81-90.

Larsen, L.M. & Tukiainen, T., 1985. New observations on the easternmost extension of the Gardar supracrustals (Eriksfjord Formation), South Greenland. *Rapp. Grønlands. geol. Unders.*, 125, 64-66.

Laznicka, P., 1985. *Empirical Metallogeny: Depositional Environments, Lithologic Associations and Metallic Ores. Vol 1: Phanerozoic Environments, Associations and Deposits, Part B. Developments in economic geology,* 19, Elsevier, Amsterdam.

Leake, B.E. Nomenclature of amphiboles. Amer. Mineral., 63, 1023-1052.

LeBas, M.J., LeMaitre, R.W., Streckeisen, A. and Zanetin, B. 1986. A chemical classification of the volcanic rocks based on the total Alkali- Silica diagram. *J. of Petrology.* Vol 27, No.3, 745-750.

Le Maitre, R.W., 1976a. The chemical variability of some common igneous rocks. *J. Petrol.* 17, 589-637.

Le Maitre, R.W., 1976b. Some problems of the projection of chemical data in mineralogical classifications. *Contrib. Mineral. Petrol.*, 56, 181-189.

Lloyd, F.E. & Bailey, D.K. 1975. Light element metasomatism of the continental mantle the evidence and the consequences. *Phys. Chem. Earth*, 9, 389-416.

MacDonald, R. 1968. Composition amd origin of Hawaiian lavas. *Geol. Soc. Amer. Min., 116, 477-522.*

MacDonald, R. 1974. Tectonic settings and magma associations. *Bull. Volcanol.* 38, 575-593.

MacDonald, R. & Edge, R.A. 1970. Trace element distribution in alkali from the Tugtutøq region, South Greenland.*Bull. Geol. Soc.* Denmark, 20, 64-66.

MacDonald, R., Upton, B.G.J. & Thomas, J.E., 1973. Potassium- and fluorine-rich hydrous phase coexisting with peralkaline granite in South Greenland. *Earth Planet. Sci. Lett.*, 18, 217-222.

McMillan, W.J., & Panteleyev, A. 1980. Ore deposit models - 1, Porphyry copper deposits, *Geoscience, Canada*, 7(2), 52-63.

Marsh, J.S., 1973. Relationships between transform directions and alkaline igneous rock lineaments in Africa and South America. *Earth. Planet. Sci. Lett.* 18, 317-323.

Marsh, J.S. 1987. Evolution of a strongly differentiated suite of phonolites from the Khinghardt mountains, Namibia. *Lithos.* 20, No.1,41-58.

Maurin, J.E., Benkhelil, J. & Robineau, B. 1986. Fault rocks of the Kaltongo Lineament, NE Nigeria and their relationship with Benue Trough tectonics. *J. Geol. Soc. London*, 143, 587-599.

McKenzie, D. 1978. Some remarks on the development of sedimentary basins. *Earth and Planetary Sci. Letters*, 40, 25-32.

McKenzie, D. 1985. The extraction of magma from the crust and mantle. *Earth and Planetary Science letters*, 74, 81-91.

Möller, P. & Muecke, G.K. 1984. Significance of Eu anomalies in silicate melts and crystal-melt equilibria: a re-evaluation. *Contrib. Mineral. Petrol.* 87, 242-250.

Morgan, P. 1983. Constraints on rift thermal processes from heat-flow and uplift. *Tectonpophysics.* 277-298.

Morris, R.V. & Haskins, L.A., 1974. EPR measurement of the effect of glass composition on the oxidation state of europium. *Geochim. Cosmochim. Acta*, 38, 1447-1459.

Morse, S.A., 1982. A partisan review of Proterozoic anorthosites. *Am. Mineral.*, 67, 1087-1100.

Myers, J.S., 1975. Cauldron subsidence and fluidisation: mechanisms of intrusion of the Coastal Batholith of Peru into its own volcanic ejecta. *Bull. Geol. Soc. Am.* 86, 1209-20.

Nakurama, N. 1974. Determination of REE, BA, Fe, Na and K in carbonaceous chondrites. *Geochim. Cosmochim. Acta*, 38, 757-775.

Nathan, H.D. & Van Kirk, C.K. 1978. A model for magmatic crystallisation. *J. of Petrology.* 19, 66-94.

Neumann, H. 1948 On hydrothermal differentiation. *Economic Geology.* 43, 77-83.

Neumann, E-R. 1980. Petrogenesis of the Oslo region larvikites and associated rocks. *Journal of Petrology*, 21, 499-531.

Norrish, K. and Chappell, B.W. 1967. X-ray fluorescence spetography. In: J. Zussman (Editor), *Physical Methods in Determinative Mineralogy.* Academic Press, London, pp. 161-214.

Norrish, K. and Hutton, J.T. 1969. An accurate x-ray spectrographic method for the analysis of a wide range of geological samples. *Geochim. Cosmochim. Acta*, 33. 431-453.

Parsons, I., 1978. Feldspars and fluids in cooling plutons. *Mineral. Mag.* 42, 1-18.

Parsons, I., 1979. The Klokken Gabbro-Syenite Complex, South Greenland: Cryptic Variation and Origin of Inversely Graded Layering. *J. Petrol.*, 20, 653-694.

Parsons, I., 1980. Alkali-feldspar and Fe-Ti oxide exsolution textures as indicators of the distribution and subsolidus effects of magmatic water in the Klokken layered syenite intrusion, S. Greenland. *Trans. R. Soc. Edin.*, 71, 1-12.

Parsons, I., 1981. The Klokken gabbro-syenite complex, South Greenland: quantitative interpretation of mineral chemistry. *J. Petrol.*, 22, 233-260.

Parsons, I. & Becker, S. M. 1986. High-temperature fluid-rock interactions in a layered syenite pluton. *Nature.* 321, 764-766.

Parsons, I. & Becker, S. M. 1987. Layering, compaction and post-magmatic processe in the Klokken Intrusion. In: I. Parsons (ed), *Origins of Igneous Layering*, 29-92. D. Reidel Publishimg Company.

Parsons, I. & Butterfield, A.W., 1981. Sedimentary features of the Nunarssuit and Klokken syenites, South Greenland. *J. geol. Soc. London*, 138, 289-306.

Pearce, N.J.G. 1988. The Petrology and Geochemistry of the Igaliko Dyke swarm, South Greenland. Unpubl. Ph.D thesis. University of Durham.

Pearce, N.J.G., & Emeleus, C.H., 1985. Geological investigations of the Igaliko dyke swarm, South Greenland. *Rapp. Grønlands geol. Unders.* 125, 60-61.

Petersilie, I.A. & Sørensen, H., 1970. Hydrocarbon gases and bituminous substances in rocks from the Ilimaussaq alkaline intrusions, South Greenland. *Lithos*, 3, 59-76.

Philpotts, J.A. 1970. Redox estimation from a calculation of Eu^{2+} and Eu^{3+} concentrations in natural phases. Earth Planet. Sci. Lett., 9, 256-268.

Piper, J.D.A., 1982. The Precambrian palaeomagnetic record: the case for the Proterozoic supercontinent. *Earth planet. Sci. Lett.*, 59, 61-89.

Pitcher, W.S., 1977. The anatomy of a batholith. *J. Geol. Soc.* 135, 157-182.

Poulsen, V., 1964. The sandstones of the Precambrian Eriksfjord Formation in South Greenland. *Rapp. Grønlands geol. Unders.*, 2, 16pp.

Powell, M., 1976. Theoretical, geochemical and petrological study of the Igdlerfigssalik nepheline syenite intrusion, Greenland. Unpubl. Ph.D thesis. University of Leeds.

Powell, M., 1978. The crystallisation history of the Igdlerfigssalik nepheline syenite intrusion, S. Greenland. *Lithos* 11, 99-120.

Reed, S.J.B. 1965. *Brit. J. Appl. Phys.* 16, 913.

Rhodes, R.C., 1971. Structural geometry of subvolcanic ring complexes as related to pre-Cenozoic motions of continental plate. *Tectonophysics,* 12, 111-117.

Robinson, P., Spear, F.S., Schumacher, J.C., Laird, J., Klein, C., Evans, B.W. and Doolan, B.L. 1982. Phase relations of metamorphic amphiboles: Natural Occurence and Theory. In: Veblen, D.R. & Ribbe, P.H. (Editors).

Rock, N.M.S., & Leake. B.E. 1984. The International Mineralogical Association amphibole nomenclature scheme: computerisation and its consequences. *Mineral Mag.,* 48, 211-217.

Ronenson, B.M., 1966. The origin of miaskites and the associated rare-metal mineralisations. (In Russian). Geologiya mestorozhdeniy redkikh elementor, 28, 1-174. Izd. 'Nedra', Moskva.

Sawkins, F.J., 1976. Widespread continental rifting: some considerations of timing and mechanism. *Geology,* 4, 427-430.

Sengör, A. M. C., Burke, K. & Dewey, J.F. 1978. Rifts in high angles to orogensic belts: Tests for their origin and upper Rhine graben as an example. *Amer. J. Science,* 278, 24-40.

Siedner, G. 1965. Geochemical features of a strongly fractionated alkali igneous suite. *Geochim et Cosmochim. Acta.* 29, 113-137.

Sood, M.K. & Edgar, A.D., 1970. Melting relations of undersaturated alkaline rocks from the Ilimaussaq intrusion and Grønnedal-Ika complex South Greenland, under water vapour and controlled partial oxygen pressure *Meddr. Grønland.* 181. 12, 1-41.

Sørensen, H. 1969. On the magmatic evolution of the Alkaline Igneous Province of South Greenland. In: *Problems of Geochemistry.* Khitarov, N.I. (Ed). Acad Sci. of USSR: Israel prog. for Sci. pubs. Jerusalem.

Sørensen, H., 1970. Internal structures and geological setting of the 3 agpaitic intrusions Khbiha and Lovozero of the Kola peninsula and Ilimaussaq, S. Greenland. *Canadian Mineralogist,* 10, Part 3, 299-334.

Sørensen, H. & Larsen, L.M., 1978. Aspects of the crystallization of volatile-rich peralkaline undersaturated magmas - exemplified by the Ilimaussaq intrusion, South Greenland. *J. Mineralogie Recife* (vol. Djalma Guimaraes) 7, 135-142.

Sørensen, H. & Larsen, L.M., 1987. Layering in the Ilimaussaq alkaline intrusion, South Greenland. In: I. Parsons (ed), *Origins of Igneous layering,* 1-28. D. Reidel Publishing Company.

Sørensen, H., Rose-Hansen, J., & Petersen, O.V., 1981. The mineralogy of the Ilimaussaq intrusion. In: The Ilimaussaq Intrusion, South Greenland. A Progress Report on Geology, Mineralogy, Geochemistry and Economic Geology (J.C. Bailey, L.M. Larsen & H. Sørenson, eds.) *Rapp. Grønlands Geol. Unders.* 103, 19-24.

Stephenson, D., 1972. Alkali clinopyroxenes from nepheline syenites of the South Qôroq Centre, South Greenland. *Lithos,* 5, 187-201.

Stephenson, D. 1973 The petrology and mineralogy of the South Qôroq Centre, Igaliko Complex, South Greenland. Unpubl. Ph.D thesis, University of Durham.

Stephenson, D., 1974. Mn and Ca enriched olivines from nepheline syenites of the South Qôroq Centre, South Greenland. *Mineralog. Mag. London,* 46, 283-300.

Stephenson, D., 1976a. A simple-shear model for the ductile deformation of high-level intrusions in South Greenland. *J. geol. Soc. London,* 132, 307-318.

Stephenson, D., 1976b. The South Qôroq nepheline syenites, South Greenland: petrology, felsic mineralogy and petrogenesis. *Bull. Grønlands geol. Unders.,* 118, 55 pp.

Stephenson, D., & Upton, B.G.J., 1982. Ferromagnesian silicates in a differentiated alkaline complex: Kûngnât Fjeld, South Greenland. *Mineralog. Mag. London,* 46, 283-300.

Stewart, J.H. 1976. Late Precambrian evolution of North America. *Geology* 4, No.1, 11-15.

Stewart, J.W. 1964. The earlier Gardar igneous rocks of the Ilimaussaq area, South Greenland. Unpub. Ph.D thesis. University of Durham, England.

Stewart, J.W., 1970. Precambrian alkaline ultramafic carbonatite volcanism, at Qagssiarssuk, South Greenland. *Bull. Grønlands Geol. Unders.,* 84 (also Meddr. Grønland 186, 4) 70pp.

Sun, S.S., 1980. Lead isotope study of young volcanic rocks from mid- ocean ridges, ocean islands and island arcs. *Phil. Trans. R. Soc. Lond.,* A297, 409-445.

Sykes, L.R., 1978. Intraplate seismicity, reactivation of pre-existing zones of weakness alkaline magmatism and other tectonism post-dating continental framentation. *Rev. Geophys. Space Phys.* 16, 621-688.

Taylor, H.P Jr. 1974. The application of oxygen and hydrogen isotope studies to problems of hrydrothermal aletration and ore deposition. *Economic Geol.,* 69, 843-883.

Taylor, H.P Jr. 1977. Water-rock interactions and the origin of H_2O in granitic batholiths. *J. Geol. Soc.,* 133, 509-558.

Taylor, H.P Jr. 1980. The effects of assimilation of country rocks by magmas on $^{18}O/^{16}O$ and $^{87}Sr/^{86}Sr$ systematics in igneous rocks. *Earth Planet. Sci. Lett,* 47, 243-254.

Taylor, R.P., Strong, D.F. and Fryer, B.F. 1981. Volatile control of contrasting trace element distributions in peralkaline granitic and volcanic rocks. *Contr. Mineral. Pet.* 77, 267-271.

Taylor, S.R. 1965. The application of trace element data to problems in petrology. *Phys. Chem. Earth,* 6, 133-213.

Taylor, S.R., Campbell, I.H., McCulloch, M.T. & McLenan, S.M., 1983. A Lower Crustal Origin for Massif-Type Anorthosites. *Nature, London,* 311, 372-374.

Taylor, S.R., Emeleus, C.H. & Exley, C.S., 1956. Some anomalous K/Rb ratios in igneous rocks and their petrologic significance. *Geochim. Cosmochim. Acta,* 10, 224-229.

Theisen, R. and Vollach, D. 1967. *Tables of x-ray mass absorption coefficients.* Verlag Stahleisen M.B.H., Dusseldorf.

Thirlwall, M.F. 1969. The petrochemistry of the British Old Red Sandstone Volcanic Province. Unpubl. Ph.D. thesis, Univ. of Edinburgh.

Thompson, R.N. 1982. Magmatism of the British Tertiary Volcanic Province, *Scot. J. Geol.* 18, 49-107.

Thompson, R.N., Morrison, M.A., Dickin, A.P. and Hendry, G.L. 1983. Continental flood basalts ...Arachnids rule OK? In: C.J. Hawksworth and M.J. Norry (eds) *Continental Basalts and Mantle Xenoliths.* Shiva, Cheshire.

Thompson, R.N., Morrison, M.A., Hendry, G.L. & Parry, S., 1984. An assessment of the relative roles of crust and mantle in magma genesis: an elemental approach. *Philos. Trans. R. Soc. London,* A310, 549-590.

Thorning, L., & Boserup, M., 1985. Geophysical field work in relation to mineral exploration programmes in South Greenland. *Rapp. Grønlands geol. Unders.* 125, 78-79.

Tukiainen, T., 1981. Preliminary results of the geological and radiometric reconnaissance in the Motzfeldt Centre of the Igaliko Complex. Unpubl. intern. GGU rep., 27 pp.

Tukiainen, T., 1985a. Geological mapping and mineral exploration in the Motzfeldt Centre of the Igaliko nepheline syenite complex, South Greenland. *Rapp. Grønlands geol. Unders.* 125, 56-60.

Tukiainen, T. 1985b Pyrochlore in alkaline intrusions of Greeland. Interim report No. 2, Unpubl. report, Greeland Geological Survey, Copenhagen.

Tukiainen, T. 1985c Pyrochlore in alkaline intrusions of Greeland. Interim report No. 3, Unpubl. report, Greeland Geological Survey, Copenhagen.

Tukiainen, T. 1986a Excursion guide: Motzfeldt Centre of the Igaliko Nepheline Syenite Complex, South Greenland. Unpubl. report, Greenland Geological Survey, Copenhagen.

Tukiainen, T. 1986b Pyrochlore in alkaline intrusions of Greeland: Supplementary material for the excursion to the Motzfeldt Centre of the Igaliko Nepheline Syenite Complex, South Greenland. Unpubl. report, Greeland Geological Survey, Copenhagen.

Tukiainen, T. 1986c GGU-Pyrochlore Project. Final Report. Unpubl. report, Greeland Geological Survey, Copenhagen and Commision of Economic European Communities.

Tukiainen, T., Bradshaw, C., & Emeleus, C.H. 1984. Geological and radiometric mapping of the Motzfeldt Centre of the Igaliko Complex, South Greenland. *Rapp. Grønlands Geol. Unders.* 120, 78-83.

Tukiainen, T., Bradshaw, C., Carle, C., & Olesen, L.B., 1984. New extensive Th-Zr-Nb-REE mineralisation in the Motzfeldt Centre, S. Greenland, as outlined by an airborne gamma-spectrometric survey. 16th Nordiska Geologiska Vintermotet, Stockholm.

Tuttle, O.F. & Bowen, N.L. 1958. *Mem. Geol. Soc. Am.* 74.

Upton, B.G.J., 1960. The alkaline complex of Kûngnât Fjeld, South Greenland. *Bull. Grønlands geol. Unders.,* 27, (Also Meddr. Grønland 123), 145 pp.

Upton, B.G.J., 1961. Textural features of some contrasted igneous cumulates from South Greenland. *Bull. Grønlands geol. Unders.* 29. (also Meddr Grønland 123, 6), 1-32.

Upton, B.G.J. 1962. Geology of Tugtutôq and neighbouring Islands, South Greenland. Part 1. *Meddr om Grønland* 169, No.8, 59pp.

Upton, B.G.J. 1964. The geology of Tugtutôq and neighbouring Islands, South Greenland. Part II: Nordmarkite syenites and related alkaline rocks. *Meddr. om. Grønland* 169, No.2, 62pp.

Upton, B.G.J. 1964b The geology of Tugtutôq and neighbouring Islands, South Greenland. Part IV: The nepheline syenites of the Hviddal Composite dyke. *Meddr. om. Grønland* 169, No.3, 50-88. (also Bull. Grønlands geol. Unders. 48)

Upton, B.G.J., 1971.b Chemical variation within 3 alkaline complexes in S. Greenland. *Lithos,* 4, 163-184.

Upton, B.G.J., 1974. The alkaline province of South-West Greenland. In Sørensen, H. (ed.), *The alkaline rocks.,* 221-238. New York: Wiley.

Upton, B.G.J., & Blundell, D.J., 1978. The Gardar igneous province: evidence for Proterozoic continental rifting. In: E.R. Neumann & I.B. Ramberg, (eds), *Petrology and Geochemistry of Continental Rifts.* 163-172. Riedel, Dordrecht.

Upton, B.G.J & Emeleus, C.H.E. 1987. Mid-Proterozoic alkaline magmatism in southern Greenland: the Gardar province. In: J.G. Fitton & B.G.J. Upton (eds) *The Alkaline rocks*, Geol. Soc. Lond. Spec. Pub. No. 30, 11, 449-471.

Upton, B.G.J., & Fitton, J.G. 1985. Gardar dykes north of the Igaliko Syenite Complex, southern Greenland. *Rapp. Grønlands Geol. Unders.*

Upton, B.G.J., & Thomas, J.E. 1980. The Tugtutôq younger giant dyke complex, fractional crystallisation of transitional olivine basalt magma. *J. Petrol.,* 21, 167-198.

Upton, B.G.J., Stephenson, D. & Martin, A.R., 1985. The Tugtutôq older giant dyke complex: mineralogy and geochemistry of an alkali-gabbro - augite-syenite - foyaite association in the Gardar province of South Greenland. *Mineral. Mag.* 49, 623-642.

Ussing, N.V., 1912. Geology of the country around Julianehåb, Greenland. *Meddr. Grønland* 38, 376.

Vlasov, K.A (ed). 1966. *Geochemistry and mineralogy of rare elements and genetic types of their deposits. Vol 1: Geochemistry of Rare Elements.* Israel Program for Scientific Translations. Jerusalem, 1966.

Watson, E.B. 1979. Zirconium saturation in felsic liquids; experimental results and applications to trace element geochemistry. *Contr. Mineral. Pet.* 70, 407-419.

Weaver, S.D., Sceal, J.S.C., & Gibson, I.L., 1972. Trace-element data relevent to the origin of trachytic and pantelleritic lavas in the East African rift system. *Contrib. Min. Pet.* 36, 181-194.

Weill, D.F. & McKay, G.A. 1975. The partitioning of Mg, Fe, Sr, Ce, Sm, Eu and Yb inlunar igneous systems and a possible origin of KREEP by equilibrium partial melting. *Proc. 6th Lunar Sci. Conf.*, 1143-1158.

Wiebe, R.A., 1985. Proterozoic Basalt Dike in the Nain Anorthosite Complex, Labrador. *Can. J. Earth Sci.,* 22, 1149-1157.

Wilcox, R.E., Harding, T.P. & Seely, D.R. 1973. Basic Wrench Tectonics. *Am. Assoc. Petrol. Geol. Bull.* 57, 74-96.

Wolff, J.A. 1987. Crystallisation of nepheline syenite in a subvolcanic magma system; Tenerife, Canary Islands. *Lithos.* 20, No.3, 207-224.

Wright, J.B., 1971. The phonolite-trachyte spectrum. *Lithos,* 4, 1-5.

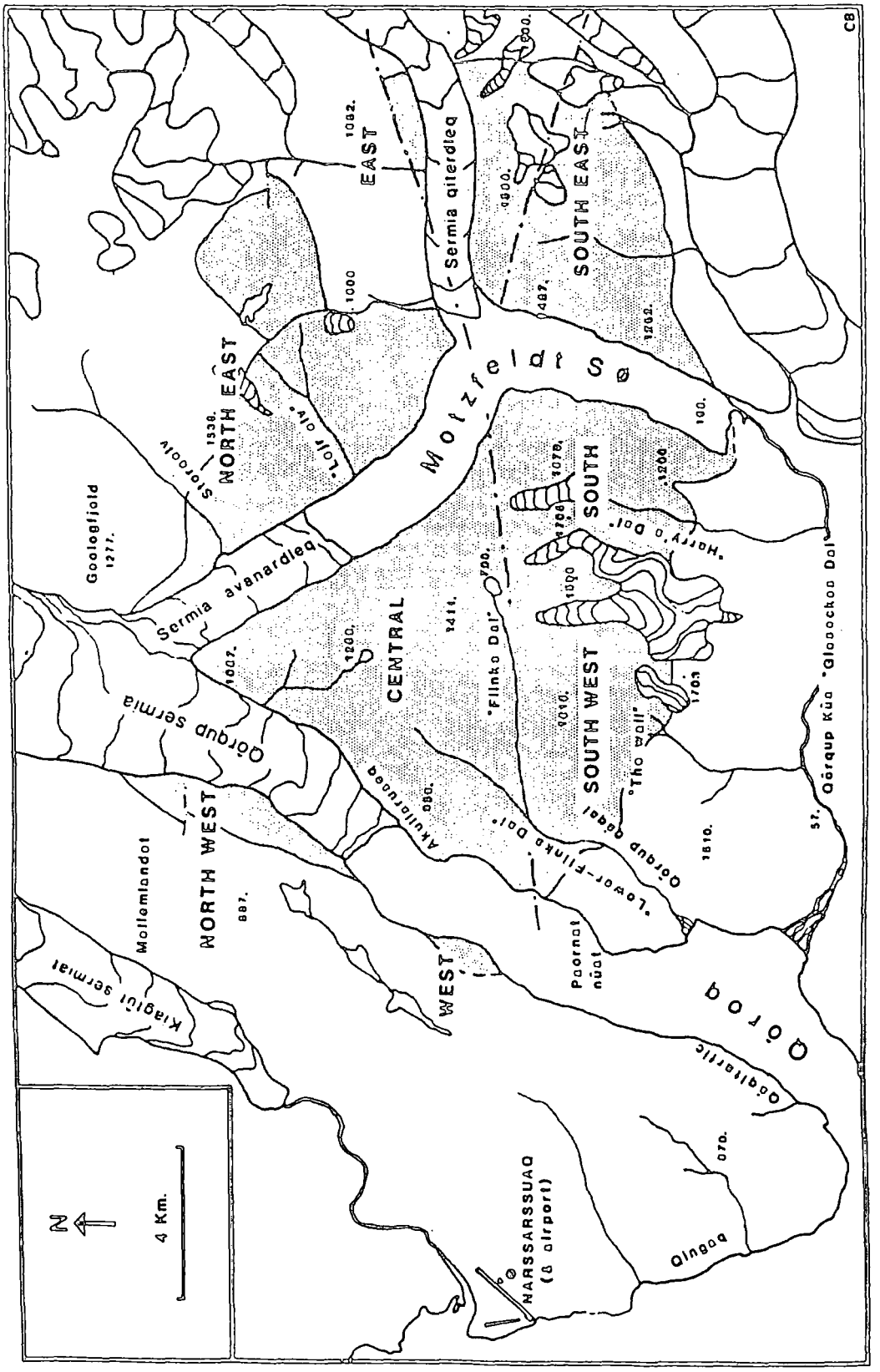
Wyllie, P.J., 1979. Magmas and Volatile components. *Am. Min.,* 64, 469-500.

Wyllie, P.J., 1981. Plate-tectonics and magma genesis. *Geol. Rundschau,* 70, 128-153, Stuttgart.

Yakowitz, H., Myklebust, R.L. and Heinrich, K.F.J. 1973. Frame: An on line correction procedure for quantitative electron probe microanalysis. *N.B.S. Tech. Note.* 796.



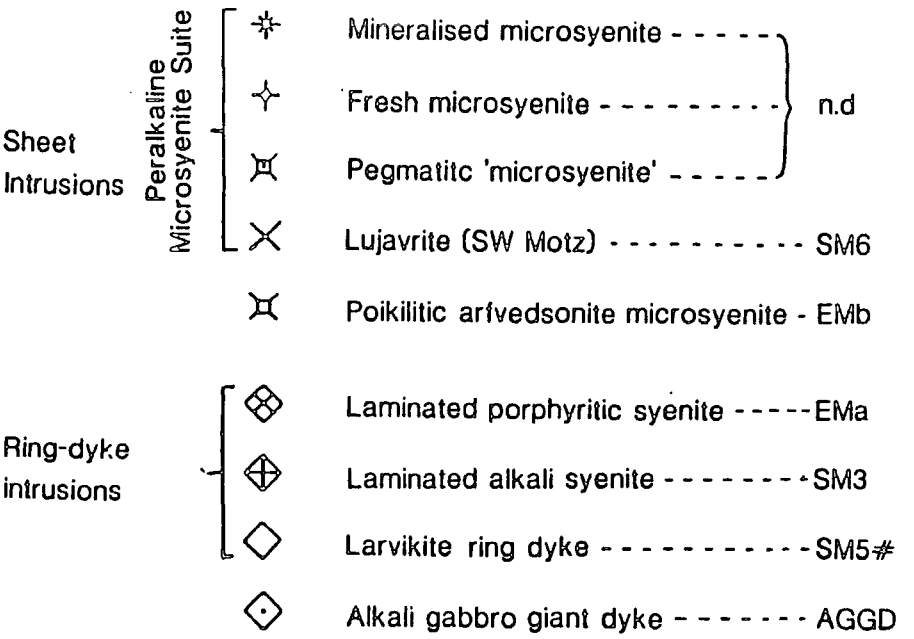
MOTZFELDT - SHOWING REGIONAL DIVISIONS AND LOCALITY NAMES.

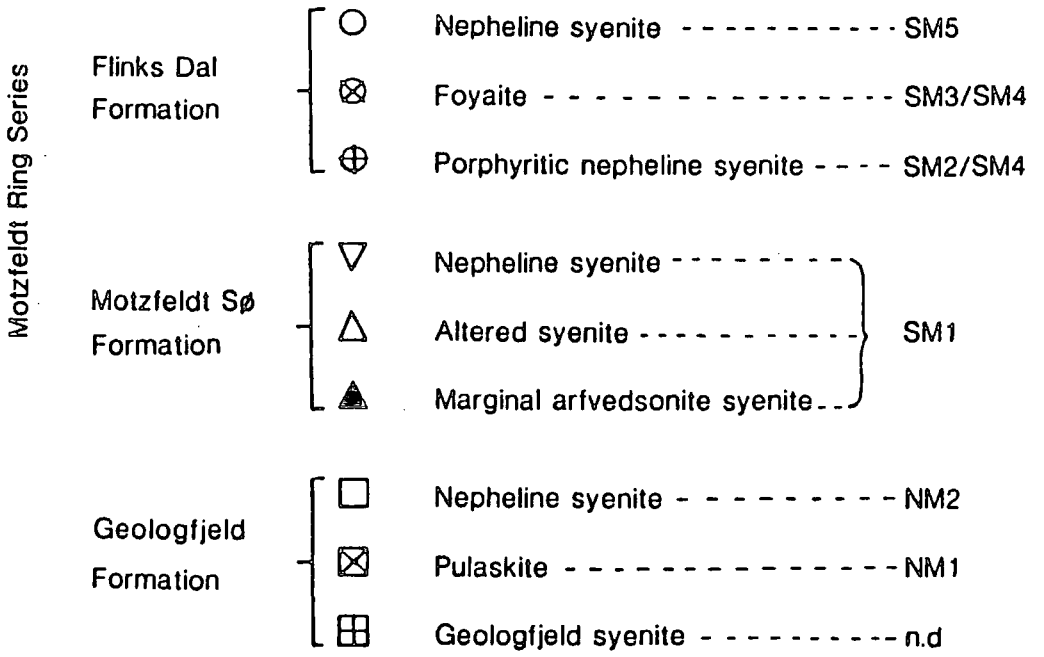


Topography and regional divisions of the Motzfeldt Centre.

ENC 4

Guide to symbols used thoughout this thesis





The previous nomenclature of Emeleus & Harry (1970) and Jones (1980) is shown for reference.

CB

ENC. 3

-45°15' -45°10' -45°05' -45°00' -44°55' -44°50' -44°45'

61°15'

61°10'

61°05'

SCALE 1:50000

SAMPLELOCATIONS
MOTZFELDT CENTRE
* = C.H.EMELEUS ▲ = A.P.JONES
□ = C.BRADSHAW

TT/I

PROJECTION: LAMBERT'S CONICAL ORTHOMORPHIC.
ELLIPSOID: INTERNATIONAL. a = 6378388M. F = 1/297.
STANDARD PARALLEL: 61G 30' 00" N

ENC.2

Geological Map

of

The Motzfeldt Centre, Igaliko Complex, S. Greenland.

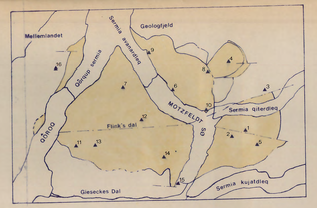
Colin Bradshaw

Scale 1:50 000

0 1 2 3 4 5 6 Km



Compilation of the map is based mainly on surveys by C. Bradshaw, University of Durham and T. Tukiainen of the Greenland Geological Survey (GGU). The mapping programme commenced in 1982 as part of the GGU-Syduran project (Armour Brown et al., 1983) and continued with the GGU-Pyrochlore project in 1984. Incorporated in the work are aspects of the earlier surveys by C.H. Emeleus and W.T. Harry (1970) and A.P. Jones (1980).



C. Bradshaw - Camp site locations



ENC. 1

LEGEND

Gardar Geology

Intrusive units of the Motzfeldt Centre

Motzfeldt Ring Series

			eg.
Hypabyssal Series*	Poikilitic arfvedsonite syenite	20	304033
	Laminated porphyritic syenite	19	304032
	Laminated alkali syenite	18	304717
Flinks Dal Formation	FDF-Larvikite	17	272429
	FDF-Nepheline syenite	16	272491
	FDF-Foyaite (transgressive)	15	326102
	FDF-Foyaite (central)	14	326113
	FDF-Lujavrite	SW 13	272539
	FDF-Porphyritic neph. syenite	12	304024
Motzfeldt Sø Formation	MSF-Nepheline syenite	10	304003
	MSF-Peralkaline Microsyenite	NE SE 9	304157
	MSF-Altered syenite	8	304722
	MSF-Marginal syenite	7	304165
Geologfjeld Formation	GF-Nepheline syenite	6	304055
	GF-Pulaskite	5	326161
	GF-Geologfjeld syenite	4	304160

Other intrusions (various ages)

Also of the Igaliko Complex	Alkali-gabbro	3	59602
	South Qôroq	2	58231
	North Qôroq	1	155135

Pre-Motzfeldt

Supracrustal units

Eriksfjord Formation	Sediments, mainly quartzite		304049
	Intermediate lava, tuff & agglom.	11	54126
	Basic lava, tuff & agglomerate		63758

*possibly younger than the Flinks Dal Formation

Pre-Gardar Geology

Ketilidian mobile belt (basement)

Julianehab Formation	Gneiss, granite, diorite etc.	54159

Geological Symbols

- Geological boundary
- Geological boundary, uncertain
- Geological boundary, gradational
- Fault, movement if known
- Strike & dip of sediments
- Strike & dip of igneous lamination
- Superficial deposits
- Conjectural ?
- Volcanic plug
- Hybrid syenite HY
- Pegmatite P
- Sodalite syenite S

Topographical Symbols

- Contour at 100m intervals 100
- Spot height in metres 802
- Lake
- Snow-field
- Glacier
- River/stream